NCAT Report 21-03

September 2021

National Center for Asphalt Technology
NCAT
at AUBURN UNIVERSITY

Phase VII (2018-2021) NCAT Test Track Findings

Randy West, David Timm, Buzz Powell, Nam Tran, Fan Yin, Benjamin Bowers, Carolina Rodezno, Fabricio Leiva, Adriana Vargas, Fan Gu, Raquel Moraes, Mostafa Nakhaei

NCAT Report 21-03
Phase VII (2018-2021) NCAT Test Track Findings

By

Randy West, PhD, PE
David Timm, PhD, PE
Buzz Powell, PhD, PE
Nam Tran, Ph.D., P.E., LEED GA, MBA
Fan Yin, PhD
Carolina Rodezno, PhD
Benjamin Bowers, PhD, PE
Fabricio Leiva, PhD, PE
Adriana Vargas, PhD
Fan Gu, PhD, PE
Raquel Moraes, PhD
Mostafa Nakhaei

Sponsored by

Alabama Department of Transportation
Arkansas Department of Transportation
Cargill
Collaborative Aggregates, LLC
Colorado Department of Transportation
Federal Highway Administration
Florida Department of Transportation
FP2
Georgia Department of Transportation
Illinois Department of Transportation
Kansas Department of Transportation
Kentucky Transportation Cabinet
Maryland State Highway Agency
Michigan Department of Transportation
Minnesota Department of Transportation
Mississippi Department of Transportation
Missouri Department of Transportation
New York State Department of Transportation
North Carolina Department of Transportation
Oklahoma Department of Transportation
Pennsylvania Department of Transportation
South Carolina Department of Transportation
Tennessee Department of Transportation
Texas Department of Transportation
United Soybean Board
Virginia Department of Transportation
West Virginia Division of Highways
Wisconsin Department of Transportation

September 2021

DISCLAIMER

The contents of this report reflect the views of the authors who are responsible for the facts and accuracy of the data presented herein. The contents do not necessarily reflect the official views or policies of Test Track sponsors, the National Center for Asphalt Technology, or Auburn University. This report does not constitute a standard, specification, or regulation. Comments contained in this paper related to specific testing equipment and materials should not be considered endorsement of any commercial product or service; no such endorsement is intended or implied.

ACKNOWLEDGMENTS

This project was sponsored by Alabama DOT, Arkansas DOT, Cargill, Collaborative Aggregates, LLC, Colorado DOT, Federal Highway Administration, Florida DOT, FP2, Georgia DOT, Illinois DOT, Kansas DOT, Kentucky Transportation Cabinet, Maryland SHA, Michigan DOT, Minnesota DOT, Mississippi DOT, Missouri DOT, New York State DOT, North Carolina DOT, Oklahoma DOT, Pennsylvania DOT, South Carolina DOT, Tennessee DOT, Texas DOT, United Soybean Board, Virginia DOT, West Virginia DOH, and Wisconsin DOT.

The authors also wish to thank ASTEC, East Alabama Paving and Trucking, Blacklidge Emulsions, Vulcan Materials Co., Wiregrass Construction / Lambert Materials, Martin Marietta Aggregates, Ingevity, InfraTest USA, and Road Science.

The authors gratefully acknowledge the following members of the NCAT Applications Steering Committee for their review of this technical report: Jennifer Albert, James Anderson, Tim Aschenbrener, Nathan Awwad, Shane Buchanan, Trenton Clark, Dale Decker, Stacey Diefenderfer, Gary Fitts, Jean-Paul Fort, Stacy Glidden, Heather Hall, Steve Jackson, Sam Johnson, Chris Jones, Tim Kowalski, Mike Law, Cheng Ling, Nathan Maack, Joe Mahoney, Todd Mansell, Leslie McCarthy, Robert McGennis, Kevin McGhee, Marty McNamara, David Mensching, Chuck Mills, Mel Monk, Nathan Morian, Tim Murphy, Scott Nazar, Derek Nener-Plante, Jared Nix, Bill Pine, Kim Schofield, Debbie Schwerman, Todd Thomas, Dave Vanderweele, Chris Wagner, Brett Williams, and Chris Winiecki.

TABLE OF CONTENTS

1. INTRODUCTION

1.1 NCAT Test Track Background

The National Center for Asphalt Technology (NCAT) Test Track is a successful pavement proving ground originally constructed in 2000. The 1.7-mile oval track is a unique accelerated pavement testing facility combining full-scale test section construction with heavy trafficking at highway speeds to evaluate pavement response and performance in a drastically shortened time frame. The Test Track allows sponsors to realistically evaluate innovative asphalt technologies, allowing rapid implementation of materials and design methods that advance safe, durable, and sustainable asphalt pavements.

Figure 1. Aerial Photograph of the NCAT Test Track

The Test Track has 46 main test sections, each nominally 200 ft. in length. Some are divided into subsections depending on the objective of the experiment. Twenty-six sections are located on the straight segments and the remaining 20 sections are equally divided between the two curves.

Experiments are sponsored over a three-year research cycle. Each cycle begins with the construction phase. Building and replacing test sections typically takes about six months including material acquisition, mix design, pavement design, mix production, and construction. The second phase involves trafficking the sections, collecting field performance and pavement response data, as well as laboratory testing plant-produced mixtures sampled during construction. During this two-year period, five heavily loaded tractor trailer rigs with legally loaded axles provide approximately 10 million 18,000-pound equivalent single-axle loads (ESALs). The final phase of the cycle involves forensic analyses of damaged sections to determine contributing factors to pavement distress.

Individual research needs can be evaluated in single or dual test sections, while broader research needs across the asphalt pavement community are addressed in groups of test sections with multiple sponsors. Experimental results are usually evident in test section performance, allowing findings to be easily interpreted and implemented. This gives sponsor agencies confidence in making specification decisions regarding materials, construction practices, and design methods that can improve pavement performance in their states. Industry sponsors can use Test Track results to effectively demonstrate the value of their product or technology to the asphalt pavement community.

Twenty-six highway agencies and private sector partners funded experiments in the seventh cycle of the Test Track from 2018 to 2021. This record number includes agencies in both northern and southern climates as a result of an ongoing partnership with the Minnesota Road Research Facility (MnROAD) focusing on pavement preservation and cracking test validation.

1.2 Research Cycles

The inaugural Test Track research cycle began in 2000. The first experimental sections focused primarily on surface mixtures, including Superpave, stone matrix asphalt (SMA), and Hveem designs using a wide range of aggregate types, gradations, and asphalt binders. The underlying pavement structure was substantial—approximately 20 inches of asphalt mix over a granular base layer and a stiff subgrade—to ensure that pavement damage was isolated to the surface layers only.

The second research cycle began in 2003. Twenty-four of the original test sections remained in place for continued evaluation. New experiments included 14 surface mix performance test sections as well as eight “structural” sections rebuilt from the subgrade up. These structural experiments analyzed the entire pavement structure rather than only the surface layers. Construction of these sections involved removing the original thick pavement structure and rebuilding the subgrade, aggregate base, and asphalt layers so that the sections had varying asphalt layer thickness (5, 7, and 9 inches). Strain gauges, pressure plates, and temperature probes were installed to monitor pavement structural response to traffic loading and temperature changes.

The third cycle, which began in 2006, included 22 newly built test sections consisting of 15 new surface mix performance sections, four new structural sections, and three reconstructed structural sections. Of the original test sections constructed in 2000, eight remained in place, accumulating 30 million ESALs by the end of the third cycle. Sixteen sections remained in place from the second cycle, accruing a total of 20 million ESALs.

During construction of the fourth cycle in 2009, 25 new test sections (12 surface mix and 13 structural) were built. Three mix performance sections from the first cycle remained in place and accumulated 40 million ESALs by the end of the fourth cycle. Nine sections from the second cycle remained, accumulating 30 million ESALs, as well as nine sections from the third cycle, which accumulated 20 million ESALs by the end of the fourth cycle. In total, there were 16 structural sections and 30 surface mix performance sections in the fourth cycle.

The fifth cycle, beginning in 2012, included 21 new experimental sections. The remaining 25 sections were left in place for continued evaluation from previous cycles: two from 2000, three

from 2003, six from 2006, and 14 from 2009. With a focus on recycled materials, porous friction course (PFC) mixes, and pavement preservation, the fifth cycle encompassed more complex experiments than previous cycles. Additionally, pavement preservation sections were placed both on the Test Track and on a local county road, Lee Road 159.

In 2015, the sixth cycle expanded the scope of Test Track research through a new partnership with the Minnesota Department of Transportation's MnROAD facility. The NCAT-MnROAD partnership featured a collaboration addressing two national research needs: (1) validating asphalt mixture cracking tests for routine use in mix design and quality assurance and (2) quantifying the life-extending benefits of pavement preservation treatments. The Cracking Group Experiment included seven sections on the Test Track and eight sections on MnROAD's mainline test road. The Preservation Group Experiment expanded the efforts that began in the fifth cycle on Lee Road 159 with 34 additional sections placed on U.S. Highway 280 near the Test Track. As a complement, the same treatments were placed on low- and high-volume roadways in Minnesota. The sixth cycle at the Test Track also included 13 other new sections (11 surface mix performance and 2 structural) as well as 17 sections that remained in place for continued evaluation.

The seventh cycle began in 2018 with continued focus on pavement preservation and cracking tests in collaboration with MnROAD, as well as additional experiments focused on balanced mix design (BMD) and rejuvenators. The goal of the Preservation Group study is to discretely quantify both life-extending and condition-improving benefits of different preservation treatments applied at various stages of pavement life on low- and high-volume roadways in both southern and northern climates. The field performance data will also aid in the development of specifications and quality assurance guidelines for preservation treatments. The continued goal of the Cracking Group experiment is to validate laboratory cracking tests by correlating lab results with field performance. This will aid agencies in establishing appropriate cracking test methods and performance criteria and in making implementation decisions based on practicality, sensitivity to mix design variables, and test variability, among others. Another focus in the 2018 cycle is BMD. One state conducted a field performance comparison of BMD versus Superpave volumetric mix design, while another state sought to establish performance-based test criteria for BMD implementation. Field performance of various rejuvenators for both hot mix recycling and spray-on applications was also evaluated. A total of 18 sections were resurfaced or rebuilt for new experiments, while 28 sections remained in place for continued evaluation, including two sections that have been in service since the original construction of the Test Track in 2000.

1.3 Seventh Cycle Sponsors

Sponsors of the continued Cracking Group Experiment include FHWA and the following Departments of Transportation: Alabama, Florida, Illinois, Maryland, Michigan, Minnesota, Mississippi, New York, North Carolina, Oklahoma, and Wisconsin.

Sponsors of the extended Preservation Group Experiment include FP^2 Inc., the Federal Highway Administration (FHWA), and the following Departments of Transportation: Alabama, Arkansas, Colorado, Georgia, Illinois, Kansas, Kentucky, Maryland, Michigan, Minnesota, Missouri,

Mississippi, New York, North Carolina, Oklahoma, Pennsylvania, South Carolina, Tennessee, Texas, West Virginia, and Wisconsin.

Individual sponsors for the 2018 research cycle are listed below in alphabetical order.

1.3.1 Alabama Department of Transportation (ALDOT)

Alabama DOT funded the continued evaluation of three open-graded friction course (OGFC) sections placed in 2012. The objective of the study was to evaluate potential changes in ALDOT's mix design procedure for OGFC to improve the durability of these mixtures in the field. These potential changes were evaluated in three test sections (E9A, E9B, and E10) on the NCAT Test Track.

Alabama also sponsored two new sections to assess the field performance of two thinlay mixes to provide ALDOT with thinner overlay alternatives that would be more suitable options for pavement preservation on high volume roads. Section N10 had an SMA thinlay with an NMAS of 4.75 mm and PG 76-22 binder placed at a thickness of 0.8 in. Section N11 used a 4.75 mm dense-graded thinlay mix with PG 67-22 placed 0.5 in. thick. In order to assess the performance of the thinlays without being impacted by the performance of the underlying layers, a 7-inch asphalt base layer produced with a highly modified binder (H_iMA) binder was placed and compacted in one lift beneath the thinlays.

1.3.2 Cargill, Inc.

Cargill sponsored companion sections at NCAT and MnROAD to evaluate balanced mix design procedures for designing high RAP mixtures with rejuvenators. The rejuvenators are utilized to restore some performance properties of RAP binder, reducing the effect of high recycled binder contents on the mixture's long-term performance. A 45% RAP mixture was designed with Cargill's Anova™ asphalt rejuvenator for comparing with a control mixture containing 30% RAP without rejuvenator. Both mixtures were placed on the NCAT Test Track for a field evaluation. Similar sections were placed at MnROAD to evaluate performance of the mixes in both northern and southern climates.

1.3.3 Collaborative Aggregates LLC

Collaborative Aggregates sponsored continued evaluation of Section N7, which was placed in 2015. This experiment was designed to determine the effectiveness of their bio-based Delta S® rejuvenator by comparing the field performance of two 9.5 mm surface mixtures. The first mixture placed in Section N7 was produced with 35% RAP and a PG 67-22 binder. The binder was dosed with Delta S rejuvenator at a rate of 5% by weight of the recycled binder in the RAP. The second (control) mixture was placed in Section N1, which was the control section of the Cracking Group Experiment. It was produced with a PG 67-22 virgin binder and 20% RAP, which is a typical RAP content allowed for use in surface mixtures in the United States.

1.3.4 Florida Department of Transportation (FDOT)

Florida DOT sponsored two new sections to evaluate the effects of different in-place densities on mixture durability. A secondary objective of this work was to characterize the mixtures' properties and performance in the laboratory utilizing the same density level achieved in the field. To complete this research, one asphalt mixture containing 20% reclaimed asphalt

pavement (RAP) and a polymer modified binder was placed and compacted in four 100-foot test strips in Sections E5 and E6 during the 2018 reconstruction of the NCAT Test Track. Each section was divided into two segments, resulting in four 100-ft. subsections compacted to varying levels of density (94%, 92%, 90%, and 88%).

FDOT also sponsored continued evaluation of Sections E7 and E8 from the 2015 cycle. The objective of this experiment was to evaluate different amounts of RAP on cracking performance and the use of a softer polymer modified binder. A secondary objective of this work was to characterize the mixtures' properties in the laboratory to determine which tests might successfully predict cracking resistance. To complete this research, four mixtures were placed that varied in terms of binder type (PG grade) and recycled material content. Both sections were divided into 100-ft. subsections containing a total of four 9.5 mm NMAS surface mixes with RAP percentages varying from 20-30%. Three of the mixes contain PG 76-22 SBS-modified binder with 20, 25, and 30% RAP, while the fourth mix contains PG 64-28 SBS-modified binder and 30% RAP. Load application was extended for one more cycle to achieve the level of damage suitable for comparisons and statistical analyses.

1.3.5 Georgia Department of Transportation (GDOT)

Georgia DOT sponsored two sections to evaluate reflection cracking mitigation treatments. Each section was divided into three subsections for a total of six treatment methods. GDOT placed similar sections in 2012 and continued to evaluate them through the 2015 cycle. The same saw cut pattern and surface overlay mix used in previous cycles was used in 2018 so that the only factors influencing reflective cracking would be the treatment methods. The six treatments included PETROMAT® fabric interlayer, GlasGrid® interlayer, chip seal with No. 7 stone, chip seal with fractionated coarse RAP, open-graded interlayer with Ultrafuse® tack coat, and rubber-modified asphalt interlayer with Ultrafuse®.

1.3.6 Kentucky Transportation Cabinet (KYTC)

Kentucky sponsored continued evaluation of Section N7 placed in 2015. The objective of this study was to construct two 100-foot-long test sections: one with an approved KYTC mix (S7A) and one with a finer mix designed by NCAT with a lower number of gyrations (S7B). The goal was to improve the performance of longitudinal joint and overall mix durability without compromising rutting performance. Both mixtures were Superpave 9.5 mm nominal maximum aggregate size (NMAS) with a PG 76-22 polymer modified binder and contained similar aggregate components, with the second mix having a modified aggregate blend to achieve a finer gradation. The surface layers were placed on both the inside and outside lanes of the track to facilitate evaluation of longitudinal joint performance.

1.3.7 Mississippi Department of Transportation (MDOT)

Mississippi DOT sponsored a new structural section, S2, with lime and cement stabilization of poor unbound foundation materials to provide structural response data for mechanistic-empirical (M-E) pavement design. The section was excavated and filled with 48 in. of high-plasticity Mississippi clay, with the upper 6 in. treated with lime. Above that was a 6-in. layer of cement-treated dirty-sand base. The section was fully instrumented with strain gauges, pressure cells, and temperature probes. The short-term goal of the section was to

fundamentally characterize the structural characteristics of the stabilized foundation pavement, measure its response to environmental changes, and track surface performance. The long-term goal is to gather the necessary M-E properties to perform transfer function calibration that will provide more accurate distress predictions for this pavement type.

MDOT also funded Section S3 to evaluate spray-on rejuvenators, with these products being applied on the existing asphalt pavement surface alone or in combination with emulsified asphalt binders (to produce rejuvenating fog seals) and/or other materials (e.g., polymers). NCAT conducted a preliminary study of seven products to assist MDOT in screening the various spray-on rejuvenator products available on the market. The screening process included conducting Federal Aviation Administration (FAA) procedure P-632 (Bituminous Pavement Rejuvenation) on binders extracted two and four weeks after application, as well as determining pavement surface friction characteristics before and after treatment application. S3 was divided into two subsections, one with a proprietary age-regenerating surface treatment and one with a plant-based topical rejuvenating seal. The spray-on rejuvenator products were applied to an experimental mix placed in 2012. The hot mix asphalt of Section S3 was a dense-graded mix with sand and gravel containing 25% RAP and an asphalt content of 6.8%. The asphalt binder used in the design was a neat binder with PG 67-22.

1.3.8 Oklahoma Department of Transportation (ODOT)

Oklahoma DOT sponsored two sections to acquire data in support of implementing performance tests and criteria for balanced mix design. Oklahoma's previous BMD approach evaluated rutting resistance using the Hamburg wheel tracking test and cracking resistance using the Illinois Flexibility Index test, but ODOT decided to switch to the Indirect Tensile Asphalt Cracking Test (IDEAL-CT) for cracking evaluation in 2019. Section N9 is a 1.5-in. mill-and-inlay with a 9.5 mm NMAS mix containing PG 76-28 modified binder and 15% RAP. Section S1 is a 5.0-in. mill-and-inlay. The surface mix is a 12.5 mm NMAS mix with PG 70-28 modified binder and 12% RAP, while the 19 mm NMAS base course contains PG 64-28 modified binder with 30% RAP and a rejuvenator.

1.3.9 South Carolina Department of Transportation (SCDOT)

South Carolina DOT sponsored Section S9, the so-called "thick-lift" section in the 2018 Test Track research cycle. The section was paved 8 inches thick in one pass and was meant to answer determine if thick-lift AC could be adequately compacted during construction, determine the required cooling time after paving, perform well under heavy trafficking, and if it would behave like conventional multi-lift pavement in terms of pavement response (i.e., stress, strain, deflection) under loading. S9 was fully instrumented with pressure plates and strain gauges to measure pavement response to loading over time. During construction, embedded thermocouples were used to measure in situ temperatures while thermal imaging was used to capture surface cooling.

1.3.10 Tennessee Department of Transportation (TDOT)

Tennessee DOT funded Section S4, which was divided into two subsections to evaluate spray-on rejuvenator products [alone or in combination with emulsified asphalt binders (to produce rejuvenating fog seals) and/or other materials (e.g., polymers)]. Following NCAT's preliminary

study of seven spray-on rejuvenator products to assist in the selection process, TDOT chose Reclamite® (Ergon) and CMS-1PF (e-Fog). Both spray-on rejuvenator products were applied to a thinlay preservation mix that was placed in 2015. The hot mix asphalt was a dense-graded mix with sand and limestone containing 15% fine RAP with an asphalt content of 6.2%. The asphalt binder used in the design was a neat binder PG 67-22.

1.3.11 Texas Department of Transportation (TxDOT)

Texas DOT sponsored Sections S10 and S11 to evaluate the field performance of mixes designed using a BMD approach versus the Superpave volumetric approach. TxDOT's provisional specification for BMD incorporates the Hamburg wheel tracking test for the evaluation of rutting resistance and the overlay test for cracking resistance evaluation. Both sections were 2.5-in. mill-and-inlays, and the two 9.5 NMAS mixes had the same PG 70-22 modified binder and 20% RAP binder replacement but different gradations and volumetric properties. The BMD mix had 5.5% total binder content, a 0.8% increase over that of the Superpave mix from mix design.

1.3.12 United Soybean Board (USB)

The United Soybean Board sponsored Section W10 to evaluate a surface mix produced with a PG 76-22 binder modified with a biopolymer derived from soybean oil. This product was developed through research conducted at Iowa State University. Field performance of W10 was compared with a similar surface mix produced with a conventional polymer-modified PG 76-22 binder in Section E5A. Both sections were 1.75-in. mill-and-inlays, and both mixes were produced using the same 12.5 mm NMAS mix design with 20% RAP except for the different binders to evaluate the effect of the biopolymer.

1.3.13 Virginia Department of Transportation (VDOT)

Virginia DOT sponsored continued evaluation of Sections N4 and S12, both placed in 2012 to study the use of cold central plant recycled (CCPR) asphalt mix as a base course in a flexible pavement cross section. The original experiment featured three test sections and complimented a study that began in 2011 on I-81 in Virginia featuring a range of recycling techniques. The sections constructed at the Test Track used reclaimed asphalt obtained from the I-81 project and were meant to characterize the field performance and quantify the structural characteristics under accelerated trafficking.

1.3.14 West Virginia Department of Highways (WVDOH)

WVDOH sponsored Sections W4 and W5 to evaluate a local dolomite aggregate source and determine its appropriate limit in surface mixes to provide good friction characteristics. Section W4 used a surface mixture containing 70% dolomite and 30% sandstone as coarse aggregates, and W5 had 90% dolomite and 10% sandstone as coarse aggregates. Both sections had a 50 mm thick (2-inch) surface course.

1.4 Seventh Cycle Donations

Numerous companies provided generous donations of equipment, materials, and labor in helping build the 2018 test sections. This support helps minimize costs and ensures that the highest quality is achieved. As in previous cycles, ASTEC provided personnel and equipment to

assist in mix production and test section construction. Roadtec and East Alabama Paving and Trucking provided construction equipment. Significant donations to the Test Track were made by Blacklidge Emulsions, Vulcan Materials Co., Wiregrass Construction / Lambert Materials, Martin Marietta Aggregates, Ingevity, InfraTest USA, and Road Science. Donations specific to test sections included Adfors Saint-Gobain, Appalachian Aggregates, Cedar Mountain Stone / Chemung Contracting, CRH Americas Materials, Lehman-Roberts, Liberty Tire Recycling, Mulzer Stone, Propex Geosolutions, Silver Star Construction, Valero, and West Virginia Paving.

1.5 Construction

New test sections were milled by Roadtec Inc. who generously provided milling machines and highly skilled operators at no cost to the track's budget. The Test Track manager coordinated milling locations and depths. East Alabama Paving Company provided dump trucks and drivers to collect and haul millings.

The instrumentation system developed through previous Test Track cycles was used to measure pavement responses in all structural sections, including the Cracking Group Experiment. Instrumentation includes horizontal strain gauges, pressure plates, and temperature probes. The instrumentation plan and analysis routines used to gather data for mechanistic pavement analyses are fully described in NCAT Report 09-01.

East Alabama Paving Company was awarded contracts to produce the asphalt mixtures and construct test sections through a competitive bidding process administered through Auburn University. Due to space limitations on the contractor's yard, some materials were temporarily stored on paved surfaces on Test Track property before they were moved to the plant site for mix production.

A special sequence was used to produce each mix. The plant's cold feed bins were calibrated for each unique stockpile. Production began with running the aggregate through the drum without the addition of asphalt binder to achieve a consistent gradation and temperature. This uncoated material was discharged and wasted. Liquid asphalt was then turned on and the mix was discharged at the slat conveyor bypass chute until the aggregates were well coated. The bypass chute was then closed, and the mixture was conveyed into the storage silo until the plant controls indicated that approximately one truckload had accumulated. This mix was loaded into a truck and then dumped into a stockpile for future recycling. At this point, the plant was assumed to have reached steady state conditions and subsequent mix run into the silo would be uniform in terms of aggregate gradation, asphalt content, and temperature. After the desired quantity of mix had been produced, the aggregate and asphalt flows were stopped, the remaining materials in the dryer and mixer were discharged at the bypass chute, and the plant was shut down. The cold feed bins were unloaded, and the plant was readied for the next test mix.

Prior to placement of mixes on each test section, a trial mix was produced to evaluate the quality control requirements of the sponsor. Trial mixes were hauled to the Test Track and sampled by NCAT personnel for laboratory testing and evaluation. Test results of the trial mixes were presented to each sponsor to determine appropriate adjustments in plant settings for the subsequent production of mix for placement.

Mix produced for placement on the test sections followed the same production sequence described above. Mix production continued until a sufficient quantity of material was available for placement. The contractor was responsible for hauling mixes to the track, and the paving equipment and crew were staged at the track.

Figure 2. Paving a Test Section for the 2018-2021 Research Cycle

Before placing mixes on the test sections, the contractor tacked the underlying asphalt pavement with a PG 67-22 binder, NTSS-1HM emulsion, or other tack material depending on the sponsor's preference. Target application rates were generally between 0.04 to 0.07 gallons per square yard (residual for emulsion) unless otherwise directed.

Mixes were dumped from end-dump haul trucks into a Roadtec SB2500D material transfer machine operated from the Track's inside lane so that only the paving machine operated on the actual test sections. Compaction was accomplished by at least three passes of a steel-wheeled roller. The roller was capable of vibrating during compaction depending on the sponsor's preference. After the steel-wheeled roller was removed from the pavement mat, the contractor continued rolling the mat with a rubber tire roller until the desired in-place density was achieved.

1.6 Trafficking Operations

Trafficking for the 2018 Test Track was applied in the same manner as with previous cycles. Two shifts of professional drivers operated five trucks pulling triple flatbed trailers (Figure 3) and one truck pulling a triple box trailer from 5 a.m. until approximately 10:40 p.m. Tuesday

through Saturday. Trafficking began on November 26, 2018, and ended February 27, 2021. The total traffic applied to the test sections during this cycle was 10,023,907 ESALs.

Figure 3. Heavily Loaded Triple-Trailer used for Accelerated Loading on the Test Track

Axle weights for each of the five trucks are shown in Table 1. On some occasions, either due to a specialized study or mechanical malfunction, trailers were removed from the operation. This left the truck pulling either a single flatbed trailer or a combination of double flatbeds.

Table 1. Axle Weights (lb) for the 2018 Truck Fleet

Truck ID	Steer	Tandem		Single				
	Axle 1	Axle 2	Axle 3	Axle 4	Axle 5	Axle 6	Axle 7	Axle 8
1	10,150	19,200	18,550	21,650	20,300	21,850	21,100	19,966
2	11,000	20,950	20,400	20,950	21,200	21,000	20,900	20,900
3	10,550	20,550	21,050	21,000	21,150	21,150	21,350	20,850
4	10,550	21,050	20,700	21,100	21,050	21,050	20,900	21,050
5	11,200	19,850	20,750	20,350	20,100	21,500	19,500	20300
Avg.	10,680	20,320	20,290	20,760	20,760	21,310	20,550	20,613
COV, %	3.9	3.9	4.9	2.2	2.5	1.7	3.6	2.2

1.7 Performance Monitoring

Test section performance was evaluated with a comprehensive range of surface measurements. Additionally, the health and response of the structural sections were routinely evaluated using embedded stress and strain gauges and falling weight deflectometer (FWD) testing. Table 2 summarizes the performance monitoring plan. Rut depths, International Roughness Index (IRI), mean texture depth, and cracking results were reported on the Test Track website.

Table 2. NCAT Test Track Performance Monitoring Plan

Activity	Sections	Frequency	Method
Rut depth	all	weekly	ARAN van, AASHTO R 48
Mean texture depth	all	weekly	ARAN van, ASTM E1845
Mean texture depth	selected	quarterly	CTM, ASTM E2157-09
International Roughness Index	all	weekly	ASTM E950, AASHTO R 43
Automated crack mapping	sponsored	weekly	PathRunner 3D Pavement Collection Vehicle, digital video recording
FWD	structural	3 times/mo.	AASHTO T 256-01
Stress/strain response to live traffic	structural	weekly	NCAT method
Pavement temperature at four depths	all	hourly	Campbell Sci. 108 thermistors
Pavement reflectivity/albedo	sponsored	quarterly	ASTM E 1918-06
Field permeability	OGFC/PFCs	quarterly	NCAT method
Core density	sponsored	quarterly	ASTM D979, AASHTO T 166
Friction	all	monthly	ASTM E274, AASHTO T 242
Friction	selected	quarterly	DFT, ASTM E1911
Tire-pavement noise	all	quarterly	OBSI, AASHTO TP 76-11, CPX, ISO 11819-2, Absorption, ASTM E1050-10

1.8 Laboratory Testing

Samples of plant-produced mix for quality assurance (QA) testing were obtained from the beds of haul trucks using a sampling stand located at the Test track (Figure 4). Typical QA tests were conducted immediately on the hot samples. Table 3 lists the test methods used for QA testing. Test results were reviewed by respective section sponsors for acceptance. In cases where the QA results did not meet sponsor approval, the mixture was removed, adjustments were made at the plant, and another production run was made until mix properties were satisfactory. QA test results and mix designs for each layer were reported for all test sections on the Test Track website.

Table 3. Tests Used for Quality Assurance of Mixes

Test Description	Test Method	Replicates
Splitting samples	AASHTO T 328-05	as needed
Asphalt content	AASHTO T 308-10	2
Gradation of recovered aggregate	AASHTO T 30-10	2
Laboratory compaction of samples	AASHTO T 312-12	2
Maximum theoretical specific gravity	AASHTO T 209-12	2
Bulk specific gravity of compacted specimens	AASHTO T 166-12	2
Mix moisture content	AASHTO T 329-15	2

Figure 4. Sampling Plant-Produced Mix for Quality Assurance Testing

NCAT staff obtained large representative samples of each experimental mix placed on the Test Track for additional testing. Mix was diverted from the conveyor of the material transfer vehicle (MTV) ahead of the paver into a flatbed truck. The truck then hauled the mix to the rear of the track's laboratory where the mix was shoveled into five-gallon buckets and labeled. A total of 1,283 buckets of mix were sampled for additional testing to accomplish the research objectives of the experiment. Asphalt binder samples were also obtained at the plant for characterization.

A testing plan for advanced characterization of the experimental mixes was established to meet section-specific and general Test Track research objectives. Test results are maintained in a database at NCAT. Evaluation of rejuvenators was somewhat different than the standard binder recovery and testing process in that only the top 3/8 in. of cores were extracted for binder evaluation. Cores were cut after four weeks of curing, then at six months, one year, one and a half years, and two years. Extensive laboratory evaluation of the recovered binders included multiple stress creep recovery (MSCR), PG grading (high, intermediate, and low temperature), rotational viscosity, complex shear modulus, dynamic viscosity, phase angle, ΔT_c, and Glover-Rowe Parameter. The testing plan for mixes with rejuvenators also included friction testing at 20, 40, and 60 km/h using the Dynamic Friction Test (DFT) according to ASTM E1911 at selected intervals after surface treatment application: 72–96 hours, 2 weeks, 4 weeks, 6 months, 1 year, 1 1/2 years, and 2 years.

1.9 Key Findings from Previous Cycles

Many highway agencies have used Test Track findings to refine their materials specifications, construction practices, and pavement design procedures for asphalt pavements. This section summarizes key Test Track research findings resulting in more cost-effective asphalt mixtures,

refined specifications, and improved pavement designs for the sponsoring agencies. Some of the findings have already been implemented by several states and have the potential for broader implementation. These key findings are organized into nine areas:

1. Mix design,
2. Aggregate properties,
3. Binder characteristics,
4. Structural pavement design and analysis,
5. Tack coat applications,
6. Relationships between laboratory results and field performance,
7. Interlayers,
8. Foundation support, and
9. Tire-pavement interaction.

1.9.1 Mix Design

Fine-Graded vs. Coarse-Graded Mixtures. In the early years of Superpave implementation, there was an emphasis on coarse-graded mixtures to improve rutting resistance. However, that notion was called into question when the results of WesTrack showed that a coarse-graded gravel mix was less resistant to rutting and fatigue cracking than a fine-graded mix with the same aggregate. In the first cycle of the NCAT Test Track, this issue was examined more completely. Twenty-seven sections were built with a wide range of aggregate types to compare coarse-, intermediate-, and fine-graded mixtures. Results demonstrated that fine-graded Superpave mixes perform as well as coarse-graded and intermediate-graded mixes under heavy traffic and tend to be easier to compact, less prone to segregation, and less permeable (*1*). Based on these findings, many state highway agencies revised their specifications to allow the use of more fine-graded mix designs.

Warm-Mix Asphalt (WMA). An early version of MeadWestvaco's (now Ingevity) Evotherm® WMA technology was used in overlays to repair two test sections with extensive damage near the end of the 2003 research cycle. These two sections were opened to heavy traffic immediately after construction and remained in service throughout the 2006 cycle with rutting performance comparable to a companion HMA section for 10.5 million ESALs and no cracking. One section was left in place at the start of the 2009 cycle and endured more than 16 million ESALs before the test section was used for a different experiment. The performance of those sections was early evidence that WMA could hold up to extremely heavy traffic. Additional WMA test sections built in 2009 also performed very well (*2*) and helped agencies gain confidence to implement WMA despite concerns of increased rutting potential raised by laboratory tests.

High Reclaimed Asphalt Pavement (RAP) Content Mixtures. Six test sections built in the 2006 cycle and trafficked through the 2009 cycle were devoted to evaluating the performance of pavements containing moderate (20%) and high (45%) RAP contents. After approximately 20 million ESALs, the sections had practically no rutting, very little raveling, and small amounts of low severity surface cracking. The use of a softer virgin binder was shown to provide better resistance to raveling and cracking of the 45% RAP mixes. No rutting or cracking benefit was observed for using polymer-modified virgin binder in the mixes with 20% or 45% RAP (*2*).

Additional test sections built in 2009 with 50% RAP in each pavement layer performed better than a companion virgin test section in all performance measures including fatigue cracking. The improved fatigue cracking is partly attributed to higher stiffness of the 50% RAP mixes, which resulted in substantially lower tensile strains at the bottom of the test sections compared to sections with all virgin mixtures (*2*).

Design Gyrations. The Test Track, along with data from field projects across the U.S. collected as part of NCHRP Project 9-29 (*3*), showed that the gyratory compaction effort specified in AASHTO standards was too high. The lab compaction effort was not representative of what actually occurs in pavements since high N_{design} numbers tend to grind aggregate particles and break them down much more than what occurs during construction or under traffic. Mix designers were typically using coarse-graded mixes to meet the volumetric mix design criteria, but those mixes are more challenging to compact in the field and tend to be more permeable, making the pavements less durable (*4*). Numerous mixes on the Test Track designed with 50 to 70 gyrations in the Superpave gyratory compactor held up to the heavy loading with great performance (*1*). As a result, many states significantly reduced their N_{design} levels for Superpave mix design.

The durability of longitudinal joints in asphalt pavements is a major concern of the Kentucky Transportation Cabinet (KYTC) and many other state DOTs. While poor compaction of the mix at a longitudinal joint is often considered the main cause leading to its deterioration, coarse-graded asphalt mixtures can also make compaction more challenging at the joint. For this reason, KYTC evaluated a fine-graded mixture designed with an N_{design} of 65 gyrations against a KYTC-approved coarse-graded mixture designed with an N_{design} of 100 gyrations in two adjacent sections following standard practices for constructing the longitudinal joints. Field permeability tests on the longitudinal joints showed that the fine-graded mixture was 20% less permeable, making the joint less susceptible to moisture damage (*5*).

Stone-Matrix Asphalt (SMA) Mixtures. Through the first three cycles of the Test Track, 19 SMA sections (eight on the 2000 track, eight on the 2003 track, and three on the 2006 track) were put to the test. Excellent performance of these sections in the first cycle prompted several states to adopt this premium mix type for heavy traffic highways. Mississippi, Missouri, and Georgia then used the Test Track to evaluate lower-cost aggregates which have helped make SMA mixtures more economical. An SMA mixture containing 12% GTR by weight of binder and an SMA with 5% recycled asphalt shingles (RAS) was successfully used in the 2012 Group Experiment. These two mixes did not contain added fibers as typically used with SMA but had no issues with binder draindown (*6*).

Thin Lift Overlays. Thin HMA overlays (less than 1¼-in. thick) are a common treatment for pavement preservation; about half of U.S. states currently use 4.75 mm NMAS mixtures in thin overlay applications. An advantage of these mixtures is that they can be placed as thin as ½-inch, covering a much larger area than thicker overlays.

In 2003, the Mississippi DOT sponsored a test section with a 4.75 mm surface mix containing limestone screenings, fine crushed gravel, and a native sand with a polymer-modified asphalt. That section has carried more than 60 million ESALs with only 7 mm of rutting and minimal cracking. This section is proof that well-designed 4.75 mm mixes are a durable option for

pavement preservation. In 2012, the same 4.75 mm NMAS mix was redesigned by adding RAP, changing from polymer-modified to neat asphalt, eliminating imported stone screenings, and relying completely on locally available surplus sand stockpiles in Mississippi. After 20 million ESALs, no cracking, rutting, roughness, raveling, or friction deficiencies were noted for the redesigned mix (*5*).

The Tennessee DOT (TDOT) has used 5/8-in. NMAS mixes for thin-lift surfaces for many years. TDOT wanted to evaluate 4.75 mm mixes in thicker lifts (e.g. 1¼ in.) to achieve better in-place density but wanted to make sure this would not lead to a rutting problem. In 2015, TDOT evaluated a 4.75 mm mix placed in a 1½-in. lift to assess its rutting resistance. The mix was designed with PG 64-22 virgin binder, 16% fine RAP, and a total binder content of 6.8% with 0.13 RAP binder ratio. The mixture showed excellent performance with no cracking, less than 2.0 mm rutting, and good smoothness. The mixture also maintained a stable friction value and had a slight increase in macrotexture under traffic (*5*).

New Generation Open-Graded Friction Course (OGFC) Mixes. OGFC mixtures have been used in the southern states for many years as a method for reducing wet-weather accidents on the highway. However, its use has declined in recent years due to premature raveling issues occurring after approximately six or seven years in service.

In 2012, the Alabama DOT sponsored three test sections to evaluate potential changes in its mix design procedure to improve the durability of OGFC mixtures. The first potential change is the use of a finer gradation of 9.5 mm NMAS, the second is the use of synthetic fiber instead of cellulose fiber, and the final change considered is to use GTR-modified binder and cellulose fiber. These changes were incorporated in three OGFC designs. The three mixtures had no cracking or raveling, and very minimal rutting after 20 million ESALs were applied over two research cycles (*5*). These proposed changes are being considered in an updated OGFC mix design procedure.

1.9.2 Aggregate Properties

Flat and Elongated. The Georgia DOT led the way in using SMA in the early 1990s and soon after began to modify their OGFC mixes toward a coarser and thicker European porous mix. Georgia established strict aggregate shape limits for these premium mixes based on European experience; however, these strict specifications limited the available aggregate sources in Georgia and resulted in prices that were more than four times the price of conventional coarse aggregates. Georgia DOT used the Track to evaluate the effect of using aggregates with a less strict flat and elongated requirement for their OGFC mixes. Test Track performance showed that the lower cost aggregates actually improved drainage characteristics (*2*).

Toughness. The South Carolina DOT used the Test Track to evaluate an aggregate with an LA abrasion loss that exceeded their specification limit. Aggregate degradation was assessed through plant production, construction, and under traffic. Although the aggregate did break down more than other aggregates through the plant, the test section performed very well. Rutting performance was similar to other sections on the track and there were no signs of raveling according to texture measurements (*1*). Based on these results, the agency revised its specifications to allow this aggregate source.

Polishing and Friction. In the 2003 cycle, the South Carolina DOT evaluated a surface mix containing a new aggregate source to assess its polishing characteristics. Friction tests conducted at regular intervals showed a sharp decline in results, indicating that the aggregate was not suitable for use in surface mixes. This enabled South Carolina to make an assessment in less than two years without putting the driving public at risk (*1*). Mississippi and Tennessee DOTs followed with similar experiments to assess blends of limestone and gravel on mix performance and friction. Both states concluded that mixes containing crushed gravel provided satisfactory performance and revised their specifications to allow more gravel in their surface mixes (*6*). Test sections sponsored by the Florida DOT used a limestone aggregate source with a known history of polishing issues. When the sections became unsafe for the NCAT fleet, a high friction surface treatment containing an epoxy binder and calcined bauxite aggregate was evaluated. The treatment provided excellent friction results for over 30 million ESALs.

Elimination of the Restricted Zone. Part of the original Superpave mix design procedure included a restricted zone within the gradation band for each NMAS. In the first cycle of the Test Track, sections with a variety of aggregate types proved that mixtures with gradations passing through the restricted zone were not necessarily susceptible to rutting (*1*). The restricted zone was subsequently removed from Superpave specifications.

1.9.3 Binder Characteristics

Effect of Binder Grade on Rutting. Superpave guidelines have recommended using a higher PG grade for high-traffic volume roadways to minimize rutting. Results from the first cycle showed that permanent deformation was reduced by an average of 50% when the high-temperature grade was increased from PG 64 to PG 76 (*7*). This two-grade bump is typical for heavy traffic projects, and these results validated one of the key benefits of modified asphalt binders.

The Alabama DOT also sponsored test sections in the first cycle to evaluate surface mixes designed with 0.5% more asphalt binder, and results showed that increasing the asphalt content of mixes containing modified binders did not adversely affect rutting resistance; however, mixes produced with neat binders were more sensitive to changes in asphalt content (*7*).

Comparison of Different Types of Binder Modification. Experiments with paired test sections in the first cycle compared mixes containing PG 76-22 polymer-modified asphalt binders using styrene butadiene styrene (SBS) and styrene butadiene rubber (SBR). Sections included dense-graded Superpave, SMA, and porous friction course (PFC) mixes. Excellent performance was observed in all mixes produced with modified binders regardless of the type of modifier used (*7*). In 2009, a similar experiment sponsored by the Missouri DOT and Seneca Petroleum comparing the performance of surface mixes containing an SBS-modified binder and a GTR-modified binder demonstrated that a GTR-modified binder can provide the same performance as traditional polymer modification (*2, 8*).

Evaluation of Alternative Binders. Three test sections were built in 2009 to evaluate Trinidad Lake Asphalt (TLA) and Thiopave® pellets for use in asphalt mixtures. TLA pellets are made from a naturally occurring asphalt binder source in Trinidad, while Thiopave® pellets are produced based on a sulfur-modified asphalt formulation. Thiopave® pellets must be used in combination

with a warm mix additive to lower the mixing temperature to 275°F or less to reduce hydrogen sulfide emissions to an acceptable level. All three asphalt layers of the TLA section were modified with 25% TLA based on weight of total binder. For the two Thiopave® sections, the base and intermediate mixes were modified with 30% and 40% Thiopave®, respectiviely, while the surface mixes were not modified with Thiopave®.

The field performance of the three test sections was compared with that of a conventional asphalt control section. Pavement response measurements indicated that all the test sections were structurally sound throughout the research cycle. No cracking was found, rutting was acceptable, and ride quality in each section was deemed excellent after 10 million ESALs. (*2*).

1.9.4 Structural Pavement Design and Analysis

Asphalt Layer Coefficient for Pavement Design. Although many highway agencies are preparing for implementation of a mechanistic-based pavement design method, thousands of projects are still designed using the empirical pavement design method, which was largely based on the AASHTO Road Test in the late 1950s. In simplified terms, the empirical method relates pavement serviceability to expected traffic and the structural capacity of the pavement structure. The pavement structural capacity is calculated by summing the products of the thickness and the layer coefficient of each layer.

A study funded by the Alabama DOT re-examined the asphalt layer coefficient using the performance and loading history of all structural sections from the second and third Test Track cycles. These test sections included broad ranges of asphalt thickness, mix types, bases, and subgrades. The analysis indicated that the asphalt layer coefficient should be increased from 0.44 to 0.54 (*9*). This 18% increase translates directly to an 18% reduction in the design thickness for new pavements and overlays. Alabama estimates a yearly savings of $25 to $50 million in construction costs since implementing the new layer coefficient in 2010 (*10*).

Strain Threshold for Perpetual Pavement Design. The perpetual pavement design concept has been validated using several Test Track sections. This design approach is based on engineering each pavement layer to withstand critical stresses so that damage does not occur in lower layers of the structure. On a life-cycle cost basis, perpetual pavements are more economical than traditional pavement designs and are less disruptive to traffic since roadway maintenance is minimized.

Two of the original 2003 structural sections were deemed perpetual as they carried more than three times their “design traffic” based on the 1993 AASHTO guide with only minor surface damage before the sections were replaced for another experiment. In the 2006 cycle, Oklahoma sponsored two sections to further validate the concept for pavements built on a very soft subgrade. One section was designed using the 1993 AASHTO guide, and the other section was designed using the PerRoad Perpetual Design program. The conventional design resulted in a 10-inch asphalt cross-section, whereas the perpetual design was 14 inches thick. Results validated the concept of limiting critical strains to eliminate bottom-up fatigue cracking (*6*). Economic analysis of the two pavement design alternatives demonstrated that perpetual pavement is more cost effective in a life-cycle cost comparison (*11*). The three perpetual pavement sections and nine other structural test sections that experienced bottom-up fatigue

cracking in the 2003, 2006, and 2009 research cycles were later used to develop a limiting strain distribution that clearly separated the perpetual pavement sections from the others. The limiting strain distribution has been implemented in PerRoad for future perpetual pavement design that can sustain the heaviest loads and provide an indefinite structural life without being overly conservative (*12*).

Measured Performance versus Pavement ME Predicted Performance. Fifteen structural study test sections were analyzed with the MEPDG using the default national calibration coefficients (*13, 14*). For virtually all sections, the MEPDG over-predicted rutting, generally with errors in the range of 70 to 100%. The rutting predictions for most sections were significantly improved after calibrating the model coefficients. MEPDG fatigue cracking predictions with the default coefficients were also poor for most of the sections. In about half of the cases, the MEPDG significantly under-predicted fatigue cracking, but in a few cases, it over-predicted the amount of fatigue cracking. Attempts to adjust the fatigue model coefficients in the MEPDG did not improve the overall correlation of predicted versus measured fatigue cracking.

Dynamic Modulus Prediction. In mechanistic-based pavement design methods, dynamic modulus (E*) is a primary input for asphalt pavement layers since this property characterizes the effects of loading rate and temperature on asphalt concrete. Three predictive dynamic modulus models and laboratory-measured E* values were compared to determine which model most accurately reflected E* values determined in laboratory testing. The Hirsch model proved to be the most reliable model for predicting the E* of an asphalt mixture (6).

1.9.5 Tack Coat Applications

Methods for Improving OGFC Performance. Delamination can significantly affect the longevity of OGFC mixtures and is due largely to construction practices and tack coat applications. Due to its high air voids content, an OGFC mix has less contact area with the underlying receiving surface, so a heavier tack coat is needed for an OGFC mix than for a dense-graded mix to form an adequate bond.

Two FDOT tack coat studies conducted in the 2009 and 2012 Test Track cycles evaluated several tack methods for improving OGFC performance. The same OGFC mix, which used PG 76-22 and 15% RAP, was placed at a thickness of 0.75 in. in each test section after a tack coat was applied. Results of these studies found that a thick polymer-modified tack coat (CRS-2P) applied with a spray paver at a target rate of 0.20 gal-yd^2 significantly improved OGFC performance. In addition, a non-tracking hot-applied polymer tack applied with a conventional distributor at a target residual rate of 0.15 gal/yd^2 can be considered an alternative to CRS-2P applied with a spray paver, depending on paving conditions (*2, 8*).

1.9.6 Relationships between Laboratory Results and Field Performance

Cracking Tests. Due to increasing concerns that volumetric properties are not sufficient to ensure the long-term durability of asphalt mixtures, especially those with higher recycled contents, the Cracking Group experiment was planned and built in the sixth cycle to help DOTs select asphalt mixture cracking tests. Sections remained in place for continued evaluation during the seventh cycle. The experiment includes seven new sections built on the Test Track to validate tests for top-down cracking and eight rebuilt sections on MnROAD's mainline test road

to validate tests for low-temperature cracking. The seven Test Track sections have the same pavement structure except for the surface mixes, which were designed with a range of recycled materials contents, binder types and grades, and in-place densities to achieve various levels of cracking performance.

The field cracking performance of the Cracking Group experiment at the end of the sixth cycle was used to provide a preliminary evaluation of five cracking tests as follows (*5*):

- While the Energy Ratio test indicated positive results in the previous evaluation at the Test Track, it did not properly identify the surface mixture with a substantial amount of cracking in the Cracking Group experiment.
- The semi-circular bend test and its J_c criteria (Louisiana method) was unable to distinguish mixes with significant cracking from those with no cracking in the test sections.
- The overlay test results (both the Texas method and the NCAT-modified method) ranked the mixtures largely in accordance with their anticipated level of field cracking performance. Both methods appear to appropriately rank the mixtures with different in-place density levels. The mixture with a higher density level had higher cycles to failure than the control mixture with a lower density level.
- Since the Illinois Flexibility Index Test (I-FIT) and the indirect tensile asphalt cracking test (IDEAL-CT) are based on a similar calculation method, their results showed the same trends in most respects and ranked the mixtures largely in accordance with their anticipated cracking performance. However, a concern with both the I-FIT and IDEAL-CT methods is the impact of specimen density. Counter to the expected outcome, higher density specimens have lower FI and CT_{Index} results than lower density specimens for the same mix.

Lab Testing of Friction and Texture Changes. NCAT used Test Track data to validate a method for determining texture and friction changes of any asphalt surface layer subjected to traffic. The procedure involves making slabs of the pavement layer in the laboratory and subjecting the slabs to simulated trafficking in a three-wheel polishing device developed at NCAT. The slabs are periodically tested for friction and texture using ASTM standards for the Dynamic Friction Tester and the Circular Track Meter. Excellent correlations were established between the friction results in the lab and the field (*15*).

Rutting Tests. Although most state DOTs indicate that rutting has been virtually eliminated as a primary distress, there is still interest in identifying reliable laboratory tests that can evaluate rutting performance. Through each cycle, NCAT has conducted several performance tests on the mixtures placed at the track, including dynamic modulus, repeated load tests, and wheel-tracking tests to determine if laboratory test results correlate with actual rutting measured on the track.

Results have shown that dynamic modulus does not correlate well with rutting. However, the Asphalt Pavement Analyzer (APA) has consistently provided reasonable correlations with Test Track rutting performance. Based on a correlation between APA results and rutting on the track in the third cycle, an APA criterion of 5.5 mm was established for heavy traffic surface mixes for tests conducted in accordance with AASHTO T 340-10 (*6*).

The Hamburg wheel tracking test has been increasingly accepted in recent years, and numerous state DOTs now have Hamburg requirements for mix design approval. The test is considered to be a proof test for the evaluation of rutting and moisture susceptibility. Although there is no national consensus on Hamburg test temperature and criteria, many highway agencies set the maximum rut depth of 12.5 mm at 20,000 wheel passes. NCAT conducted the Hamburg test in accordance with AASHTO T 324 at 50°C on 18 mixtures from the 2012 research cycle. Hamburg results correlated reasonably well (R^2 = 0.74) with rutting measurements on the track (*2*), and none of the test sections had any evidence of moisture damage.

The flow number (FN) test is another lab test to evaluate the rutting resistance of asphalt mixes. In the third cycle, NCAT used a confined FN test with 10 psi confining stress and a repeated axial stress of 70 psi. A strong correlation was found between the results of the FN test using these conditions and rutting on the track. Using this method, a minimum FN of 800 cycles was recommended for heavy traffic pavements (*6*). More recently, NCHRP Report 673, A Manual for Design of Hot Mix Asphalt with Commentary, and NCHRP Report 691, Mix Design Practices for Warm Mix Asphalt, both recommended the FN test for assessing the rutting resistance of mix designs. The testing criteria and traffic level performance thresholds from these reports have been adopted in AASHTO TP 79-13. FN tests conducted on surface mixes from the fourth cycle did not correlate well with measured rutting. However, all results met the FN criteria in AASHTO TP 79-13 for 3 to 10 million ESALs of traffic (*2*).

Air Voids. Air voids in laboratory-compacted specimens is a common pay factor for asphalt pavements. The Indiana DOT sponsored Test Track research to identify an appropriate lower limit for this acceptance parameter. Surface mixes were intentionally produced with air voids between 1.0 and 3.5% by adjusting the aggregate gradation and increasing the asphalt contents. Results showed that rutting increased significantly when the air voids were less than 2.75% (*6*). When test results with a target air voids of 4.0% are below that value and the roadway is to be subjected to heavy traffic, removal and replacement of the surface layer is appropriate. It is important to note that the experiment used only mixes with neat (unmodified) asphalt binder and without recycled materials. Other surface mixes on the track containing modified binders or high recycled asphalt binder ratios that were produced with air voids below 2.5% have held up very well under the extreme traffic on the track.

1.9.7 Interlayers

Alternative Interlayers. Several state agencies have used cracking relief interlayers to provide a discontinuity between the existing surfaces and new overlays so that existing cracks are not as easily reflected to the overlays. In Georgia, the most specified interlayer is a single chip seal treatment placed on the existing surface. An asphalt leveling course is placed over the chip seal at 75 to 80 lbs/sy before placing an overlay. This method, however, has not been as effective as desired.

The Georgia DOT sponsored a study at the Test Track beginning in 2012 to evaluate two alternative interlayers. To simulate cracking, deep saw cuts were made in two test sections and filled with sand to avoid self-healing after placement of interlayers. One section was then treated with a double chip seal treatment with a sand seal top layer, and the other with a 9.5 mm open-graded interlayer (OGI). Both sections were then covered with a 9.5 mm NMAS

dense-graded overlay. Cracking began to develop in both sections after 10 million ESALs. The amount of cracking in the OGI section increased significantly in the second cycle with 50% of the saw cuts having reflected through to the surface after 20 million ESALs. For the other section, reflective cracking was observed in only 6% of the saw cuts. Cracks in both sections remained at low severity (≤ 6 mm). The maximum rut depth in the surface treatment interlayer section was 0.75 in. (21 mm) while it was only 0.25 in. (6 mm) in the OGI section (*5*).

1.9.8 Foundation Support

Engineered RAP Base. Cold Central Plant Recycling (CCPR) is a highly sustainable method of combining RAP with foamed or emulsified asphalt and additives in a central recycling plant without the application of heat, which has been used for rehabilitating low- and medium-volume roadways. This method was evaluated in three test sections beginning in 2012, complementing an existing project on I-81 in Virginia for use on heavily loaded roadways. Two sections were designed to evaluate the difference between 6 and 4 in. of asphalt built over 5 in. of CCPR materials and 6 in. of aggregate base. In a third test section, the 6-in. aggregate base was replaced with an 8-in. cement-stabilized base (CSB) followed by 5 in. of CCPR materials and 4 in. of asphalt mix. Through two research cycles and over 20 million ESALs, all three sections have performed extremely well with no cracking, minimal rutting, and no appreciable change in ride quality (*5*). Two of these sections remained in place for continued evaluation during the seventh cycle. Based on measured strains, the CSB section is expected to be perpetual, while the section with aggregate base could develop bottom-up fatigue cracking.

1.9.9 Tire-Pavement Interaction

Noise and Pavement Surface Characteristics. Noise generated from tire-pavement interaction is substantially influenced by the macrotexture and porosity of the surface layer. Tire-pavement noise testing on the track has indicated that the degree to which these factors influence noise levels is related to the weight of the vehicle and tire pressure. For lighter passenger vehicles, the porosity of the surface, which relates to the degree of noise attenuation, is the dominant factor. For heavier vehicles (with higher tire pressures), the macrotexture of the surface and the positive texture presented at the tire-pavement interface has a greater influence (*6*).

Quiet Pavements. Each cycle of the Test Track has included new-generation OGFC mixtures featuring a variety of aggregate types. Testing has shown that these surfaces, also known as porous friction courses, eliminate water spray and provide excellent skid resistance as well as noise reduction benefits.

High-Precision Diamond Grinding. Smoothness is the most important pavement characteristic from the perspective of users. Occasionally, pavement maintenance or rehabilitation results in a bump in the roadway surface that needs to be removed. Precision diamond grinding has been used on the Test Track in each cycle to smooth out transitions between some test sections. None of the areas leveled with the grinding equipment have exhibited any performance issues and some were in service for up to 10 years with no performance problems. No sealing was applied to these treated surfaces.

High Friction Surface Treatment (HFST). A good friction surface is needed in critical braking and cornering locations for safe driving. While the current standard HFST has shown the highest

friction and high macrotexture characteristics for skid resistance, it requires premium thermosetting polymer resin and imported calcined bauxite aggregate, making it an expensive surface treatment. Therefore, state highway agencies are interested in finding an alternative.

An FHWA-sponsored friction study conducted on the Test Track from 2012 to 2014 used regionally available friction aggregates to replace calcined bauxite. The results showed that polymer resin bound surfaces with other regionally available friction aggregate sources did not provide the same level of surface friction as those with the calcined bauxite (*16*). A follow-up study in 2015 was then conducted on the track to evaluate asphalt (instead of polymer resin) bound surfaces with calcined bauxite as the primary friction aggregate. These surfaces included two micro-surfacing treatments, one with a 50-50 aggregate blend of calcined bauxite and limestone sand and the other with a 100% sandstone blend, as well as one thin overlay using a 4.75 mm SMA mixture with 40% calcined bauxite, 59% granite, and 1% filler. They were placed using conventional asphalt construction equipment and methods instead of the specialized application equipment required to place the standard HFST. Both micro-surfacing sections maintained good friction and macrotexture through 10 million ESALs. For the micro-surfaced sections, the average friction values (SN40R) were 55 for the calcined bauxite/limestone blend and 50 for the sandstone. Macrotexture (Mean Profile Depth, MPD) measurements were 0.70 mm and 0.90 mm for the calcined bauxite/limestone blend and the sandstone treatments, respectively. The SMA section was placed later, so it received only 3.4 million ESALs of traffic. This surface also had good friction (SN40R = 55), but its macrotexture was lower (MPD = 0.35 mm) than those of the micro-surfacing treatments (*5*). The friction measurements for the three surfaces are lower than that of the standard HFST surface (SN40R = 65), which has been tested for five years with over 23 million ESALs on the track.

In 2015, the Oklahoma DOT sponsored a study to find a high friction asphalt surface mixture produced with aggregates available in Oklahoma. The surface mixture selected for evaluation was OGFC as it had the best macrotexture. Sandstone aggregate was selected for the mixture as it had the best friction characteristics among four locally available aggregates tested in a prior laboratory study. After 10 million ESALs of heavy truck traffic, no rutting or noticeable cracking was observed. The ride quality of the two sections did not change during the traffic period. The highest SN40R value of 57 was measured a few months after construction, and the final SN40R value of 53 was taken in the last three month of truck traffic. The measured friction values were higher than the typical SN40R of 45 to 35 for other dense-graded asphalt surfaces placed on the track but lower than the SN40R for the standard HFST placed in 2011, which were above 65 at the end of the same cycle. The OGFC surface had very good macrotexture with MPD of approximately 1.2 mm over the two years of truck traffic (*5*).

1.10 References

1. Timm, D., R. West, A. Priest, B. Powell, I. Selvaraj, J. Zhang, and R. Brown. *Phase II NCAT Test Track Results*. NCAT Report 06-05. National Center for Asphalt Technology at Auburn University, Auburn, Ala., 2006.
2. West, R., D. Timm, R. Willis, B. Powell, N. Tran, M. Sakhaeifar, R. Brown, M. Robbins, A. Vargas-Nordcbeck, F. Leiva Villacorta, X. Guo, and J. Nelson. *Phase IV NCAT Pavement Test*

Track Findings. NCAT Report 12-10. National Center for Asphalt Technology at Auburn University, Auburn, Ala., 2012.
3. Prowell, B., and E. R. Brown. *NCHRP Report 573: Superpave Mix Design: Verifying Gyration Levels in the Ndesign Table*. Transportation Research Board of the National Academies, Washington, D.C., 2009.
4. Leiva-Villacorta, F. and R. West. Analysis of Field Compactability Using Accumulated Compaction Pressure Concept. *Transportation Research Record: Journal of the Transportation Research Board, No. 2057*, Transportation Research Board of the National Academies, Washington, D.C., 2008, pp 89-98.
5. West, R., D. Timm, B. Powell, M. Heitzman, N. Tran, C. Rodezno, D. Watson, F. Leiva, A. Vargas. *Phase VI (2015-2017) NCAT Test Track Findings*. NCAT Report 18-04. National Center for Asphalt Technology at Auburn University, Auburn, Ala., 2019.
6. Willis, R., D. Timm, R. West, B. Powell, M. Robbins, A. Taylor, A. Smit, N. Tran, M. Heitzman, and A. Bianchini. *Phase III NCAT Test Track Findings*. NCAT Report 09-08. National Center for Asphalt Technology at Auburn University, Auburn, Ala., 2009.
7. Brown, E. R., L. A. Cooley, Jr., D. Hanson, C. Lynn, B. Powell, B. Prowell, and D. Watson. *NCAT Test Track Design, Construction, and Performance*. NCAT Report 02-12. National Center for Asphalt Technology at Auburn University, Auburn, Ala., 2002.
8. West, R., D. Timm, B. Powell, M. Heitzman, N. Tran, C. Rodezno, D. Watson, F. Leiva, A. Vargas, R. Willis, M. Vrtis, and M. Diaz. *Phase V (2012-2014) NCAT Test Track Findings*. NCAT Report 16-04. National Center for Asphalt Technology at Auburn University, Auburn, Ala., 2018.
9. Peters-Davis, K., and D. Timm. *Recalibration of the Asphalt Layer Coefficient*. NCAT Report 09-03. National Center for Asphalt Technology at Auburn University, Auburn, Ala., 2009.
10. Timm, D., and K. Davis. Are We Underestimating the Strength of Asphalt? *Hot Mix Asphalt Technology*, Vol. 15, No. 1, National Asphalt Pavement Association, 2010.
11. Sakhaeifar, M., R. Brown, N. Tran, and J. Dean. Evaluation of Long-Lasting Perpetual Asphalt Pavement with Life-Cycle Cost Analysis. *Transportation Research Record: Journal of the Transportation Research Board, No. 2368*, Transportation Research Board of the National Academies, Washington, D.C., 2013, pp. 3-11.
12. Tran, N., M. Robbins, D. Timm, R. Willis, and C. Rodezno. *Refined Limiting Strain Criteria and Approximate Ranges of Maximum Thicknesses for Designing Long-Life Asphalt Pavements.* NCAT Report 15-05R. National Center for Asphalt Technology at Auburn University, Auburn, Ala., 2016.
13. Guo, X. *Local Calibration of the MEPDG Using Test Track Data*. MS thesis. Auburn University, Auburn, Ala., 2013.
14. Guo, X., and D. Timm. Local Calibration of MEPDG Using National Center for Asphalt Technology Test Track Data. *TRB 94th Annual Meeting Compendium of Papers*, Paper 15-1032, Transportation Research Board 94th Annual Meeting, Washington, D.C., 2015.
15. Erukulla, S. *Refining a Laboratory Procedure to Characterize Change in Hot-Mix Asphalt Surface Friction.* MS Thesis. Auburn University, Auburn, Ala., 2011.
16. Heitzman, M., P. Turner, and M. Greer. *High Friction Surface Treatment Alternative Aggregates Study.* NCAT Report 15-04. National Center for Asphalt Technology at Auburn University, Auburn, Ala., 2015.

2. CRACKING GROUP EXPERIMENT: VALIDATION OF TOP-DOWN CRACKING TESTS FOR BALANCED MIX DESIGN

Dr. Randy West, Dr. David Timm

2.1 Background

As interest in balanced mix design (BMD) began to grow six years ago, the FHWA and state departments of transportation in Alabama, Florida, Illinois, Maryland, Michigan, Minnesota, Mississippi, New York, North Carolina, Oklahoma, and Wisconsin worked with NCAT and MnROAD to develop an experiment to evaluate numerous cracking tests. The primary objective of the experiment was to determine which laboratory cracking tests had the best correlation with field performance. Two complimentary experiments were planned and built; the experiment at the NCAT Test Track focused on validating tests for top-down cracking, and the experiment at MnROAD focused on validating tests for thermal cracking. This chapter describes the findings of the NCAT Test Track top-down cracking experiment. The findings of the MnROAD thermal cracking test validation will be provided later in a separate report.

The NCAT Test Track Cracking Group experiment included seven test sections, each with a different surface mix. The seven mixtures were intentionally designed to yield a range of field top-down cracking performance. Six of the seven mixtures (i.e. N1, N2, N5, N8, S5, and S6) were designed in accordance with the conventional Superpave requirements of AASHTO M 323 using an N_{design} of 80 gyrations. The mix design for Section S13 was unique in that it was a gap-graded, asphalt rubber mixture designed using the Marshall method using 75 blows per side. Table 1 summarizes the general mix descriptions, virgin binders, recycled materials contents, and continuous grades of the extracted and recovered binders from plant mix samples. For Section S5, the requested binder grade was a PG 58-28 to use with the higher RAP content mixture. However, the "softer" binder supplied for the section actually graded as a PG 64-28, which was verified to contain polymer modification.

Table 1. Summary of Surface Mixtures Used in the NCAT Top-Down Cracking Experiment

Test Track Section	Mixture Description	NMAS[a] (mm)	Virgin Binder Grade	RAP Content	RAS Content	Recovered Binder Cont. Grade
N1	Control (20% RAP)	9.5	PG 67 -22	20%	0%	88.6 -16.6
N2	Control, Higher Density	9.5	PG 67 -22	20%	0%	89.9 -15.9
N5	Control, Low Density, Low AC[b]	9.5	PG 67 -22	20%	0%	88.0 -18.5
N8	Control + 5% RAS	9.5	PG 67 -22	20%	5%	107.3 -5.4
S5	35% RAP, PG 58-28	9.5	PG 64 -28	35%	0%	82.8 -23.0
S6	Control, HiMA[c] Binder	9.5	PG 94 -28	20%	0%	101.4 -21.5
S13	Gap-graded, asphalt-rubber	12.5	Not tested	15%	0%	Not tested

[a] Nominal Maximum Aggregate Size; [b] asphalt content; [c] Highly Modified Asphalt

The test sections were built relatively thin for the heavy loading on the Test Track so that the surface layers would experience significant deflections. To avoid bottom-up fatigue cracking, the intermediate and base layers contained the same highly modified binder used in S6. The same mix design was used for the lower two layers; it was a 19.0 mm NMAS Superpave mix containing 17% RAP (19% RAP binder ratio) with an N_{design} of 60 gyrations. The surface mixtures

were constructed as a 1.5-inch lift over the highly polymer-modified intermediate and base layers, which were 2.25 inches each.

The as-constructed cross-sections of the test sections are illustrated in Figure 1. Some variations in thicknesses of the layers were identified from construction surveys and later verified with cores.

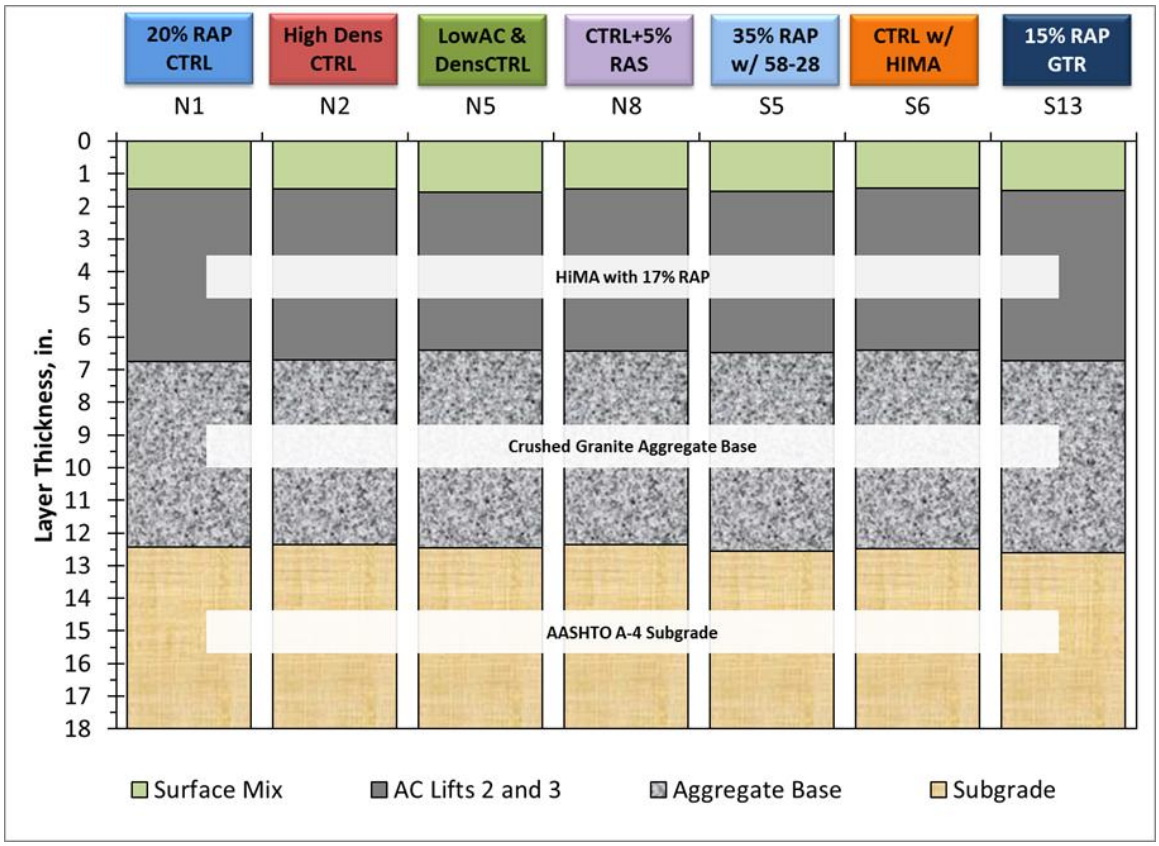

Figure 1. Cross-section of Cracking Group Test Sections on the NCAT Test Track

2.2 As-Constructed Mixture Properties

Table 2 summarizes traditional quality control results for the surface layer mixtures. As noted previously, all of the mixtures except for S13 were dense-graded Superpave mixtures that would be classified as fine-graded by AASHTO M 323. The gap-graded, asphalt-rubber surface mixture for S13 was unique, with a binder content at least 1.6% higher than each of the Superpave mixtures. The as-constructed density levels for two of the sections (N2 and N5) were also intentionally variable for the experiment. Section N2 was compacted to a higher relative density target of 96%, and N5 was constructed to a lower relatively density target of 90%. The other six sections had a target density of 92 to 93% of their respective maximum theoretical densities.

Table 2. Traditional Quality Control Properties of the NCAT Top-Down Cracking Group Experiment Test Sections

	N1 Control	N2 Control w/ High Density	N5 Control w/ Low Dens. & AC	N8 Control w/ 5% RAS	S5 35% RAP PG 58-28	S6 Control w/ HiMA	S13 Gap-Graded Asphalt-Rubber*
Sieve Size							
12.5 mm (1/2")	99	100	100	99	99	100	96
9.5 mm (3/8")	97	98	99	98	96	98	85
4.75 mm (#4)	67	70	73	66	73	67	35
2.36 mm (#8)	52	54	54	51	56	52	22
1.18 mm (#16)	41	43	42	41	44	42	19
0.60 mm (#30)	28	28	28	30	29	28	14
0.30 mm (#50)	15	15	15	17	16	15	8
0.15 mm (#100)	9	9	9	11	10	9	5
0.075 mm (#200)	5.4	5.6	5.7	7.1	6.3	5.4	3.6
Total Binder Content (P_b)	5.4	5.4	5.1	5.3	5.8	5.8	7.4
Eff. Binder Content (P_{be})	4.7	4.7	4.4	4.8	5.1	5.0	6.6
RAP Binder Ratio	0.18	0.18	0.19	0.18	0.29	0.17	0.08
RAS Binder Ratio	--	--	--	0.19	--	--	--
Dust/Binder Ratio	1.1	1.2	1.3	1.5	1.2	1.1	0.5
Rice Sp. Gravity (G_{mm})	2.469	2.468	2.478	2.492	2.472	2.459	2.402
Avg. Bulk Sp. Gravity (G_{mb})	2.375	2.372	2.348	2.415	2.393	2.384	2.319
Lab Compaction Temp.	290°F	290°F	290°F	290°F	285°F	325°F	350°F
Air Voids (V_a)	3.8	3.9	5.3	3.1	3.2	3.1	3.4
Agg. Bulk Gravity (G_{sb})	2.634	2.631	2.633	2.672	2.656	2.634	2.631
Avg. VMA	14.7	14.7	15.4	14.4	15.1	14.7	18.4
Avg. VFA	74	73	66	79	79	79	81
Mat Density (%G_{mm})	93.6	96.1	90.3	91.5	92.2	91.8	92.7

*75-blow Marshall hammer compaction used for mix design and QC.

2.3 Laboratory Testing Plan

The five laboratory cracking tests initially selected by the sponsors of the NCAT Test Track Cracking Group Experiment were the energy ratio (ER), the Texas overlay (OT-TX) test, the NCAT modified overlay test (OT-NCAT), the Louisiana semi-circular bend test (SCB-LA), and the Illinois flexibility index test (I-FIT). The Indirect Tensile Cracking Test (i.e., IDEAL-CT) was added to the experimental plan after the experiment was under way based on discussions with the sponsors. The Asphalt Mixture Performance Tester (AMPT) cyclic fatigue test was also added to the experiment later in the project. Table 3 summarizes the cracking tests conducted in the experiment. Further details of the tests were provided in the end-of-cycle report from the 2015 Test Track, (*1*) and Chen (*2*).

Table 3. Top-Down Cracking Tests Analyzed in this Experiment

Test	Test Method	Primary Output	Key Reference
Energy Ratio	No standard	ER	Roque et al. (*3*)
Texas Overlay Test	Tex-248-F	β	Garcia et al. (*4,5*)
NCAT Overlay Test	Tex-248-F*	β	Ma (*6*), Garcia et al. (*4*)
Louisiana SCB	ASTM D8044-16	J_c	Cooper III et al. (*7*)
Illinois Flexibility Index Test	AASHTO TP 124	FI	Ozer et al. (*8*)
IDEAL Cracking Test	ASTM D8225-19	CT Index	Zhou et al. (*9*)
AMPT Cyclic Fatigue	AASHTO TP 133-19	S_{app}	Wang et al. (*10*)

*With change of frequency, gap, and definition of failure

Each of the cracking tests, except cyclic fatigue, were conducted on samples prepared and conditioned in four ways:

1. Lab-mixed, lab-compacted (LMLC) specimens after short-term oven aging (STOA) according to AASHTO R 30, abbreviated as LMLC-STOA.
2. LMLC-STOA plus an additional eight hours of aging at 135°C in a loose mix condition prior to compaction. The additional eight hours of aging at 135°C is referred to by NCAT as the "critical aging" procedure as described in Chen et al. (*10, 11*), abbreviated as LMLC-CA.
3. Plant-mixed, lab-compacted (PMLC) specimens reheated (RH) to the compaction temperature, abbreviated as PMLC-RH.
4. PMLC specimens reheated then "critically-aged" prior to compaction, abbreviated as PMLC-CA.

Lab-mixed, lab-compacted specimens were prepared to match the gradations and asphalt contents for the respective mixes obtained from quality control testing as shown in Table 2. The plant-produced mixtures were sampled at the time of construction and placed in five-gallon buckets. The mixtures were later reheated to 150°C for two hours, quartered into appropriate masses for specimens, heated to the respective compaction temperature for one hour, and then compacted using a Superpave gyratory compactor (SGC). For plant-produced mixture samples subject to the critical aging procedure, the buckets of mix were reheated to 150°C for two hours to allow for the mixtures to be quartered and placed in pans in a thin layer less than approximately 20 mm thick, then put in an oven equipped with a timer to condition the loose mixtures for eight hours at 135°C. The eight-hour critical aging protocol was conducted

overnight so that the next morning, the mixtures could be immediately brought to the compaction temperature and then compacted with an SGC. The lab compacted specimens were compacted to 7.0±0.5% air voids, except for mixture N2 which used a target air void content of 4.0±0.5% and N5 which used a target air void content of 10.0±0.5%. After the laboratory experimental plan had been completed, it was found that the flexibility index and CT_{Index} were sensitive to the effect of specimen air void content in a counterintuitive way. Therefore, additional specimens were prepared at 7.0±0.5% air voids for the N2 and N5 mixtures and tested in the I-FIT and IDEAL-CT.

The cyclic fatigue test was added to the experimental plan after the preparation of laboratory mixture samples had been completed. Therefore, the AMPT tests were only conducted on PMLC specimens (reheated and critically-aged).

2.4 Field Performance Results

From October 2015 to February 2021, the Cracking Group Experiment test sections accumulated 20 million ESALs. Their field performance at the end of the second three-year research cycle is summarized in Table 4. It should be noted that when cracking began to appear in any test section, a few cores were taken on cracks to determine if the cracking was confined only to the surface layer or if the cracks extended deeper. Those cores always confirmed that the cracks originated at the surface and there was no evidence of debonding or segregation. Figure 3 shows examples of cores taken to evaluate the cracking; the yellow line highlights the crack and the yellow arrow indicated the direction of traffic. The cracks were typically noticed first as hairline cracks in the outer parts of the wheelpaths and would grow in the direction of traffic and transverse to the direction of traffic in the wheelpaths.

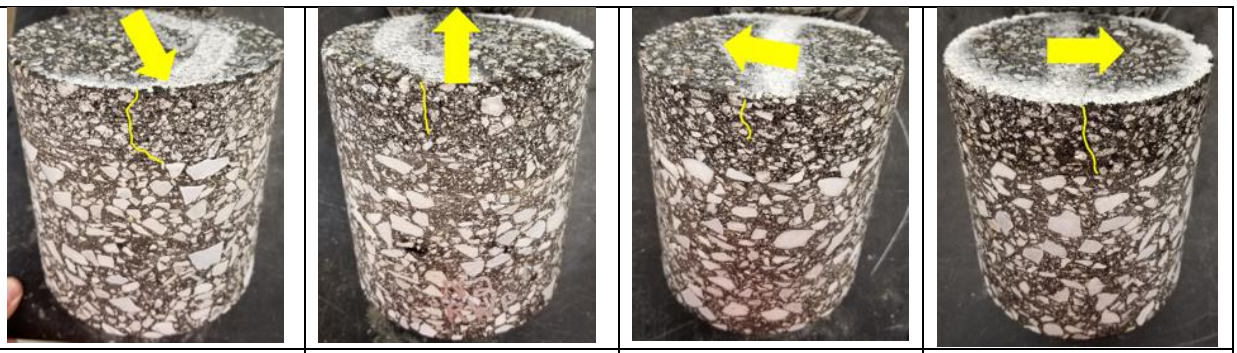

N1 – left wheelpath	N2 – right wheelpath	N5 – right wheelpath	N8 – left wheelpath

Figure 3. Cores Showing Top-Down Cracking

Sections N5 and N8 reached terminal serviceability in February 2020, at which time the surface layers were milled and an overlay was constructed on the test sections to enable the trucks to continue to operate without diverting around those sections. After milling, it was noted only a small area of about 12 feet in length of section N8 had any deterioration in the lower layers, again confirming that the observed cracking was almost entirely top-down.

Table 4. Performance of NCAT Cracking Group Test Sections after 20 Million ESALs

Test Track Section	Mixture Description	Rutting (mm)	Change in IRI (in./mi)	Change in Mean Texture Depth (mm)	Cracking (% of lane area)	
					Feb. 2020	Feb 2021
N1	Control	4.9	5	0.60	11.2	44.5
N2	Control, Higher Density	4.4	11	0.60	7.7	12.5
N5*	Control, Low Density, Low AC	1.4	30	0.61	21.1	47.4*
N8*	Control + 5% RAS	1.8	50	0.76	70.8	99.3*
S5	35% RAP, PG 58-28	3.5	5	0.66	0.2	1.1
S6	Control, HiMA binder	3.3	8	0.78	0	0.9
S13	Gap-graded, asphalt-rubber	5.6	9	0.20	0	0

*Rutting, IRI, and MTD data are from Feb. 2020 at 16 Million ESALs prior to mill and overlay of the section. Cracking results reported for Feb 2021 for these sections are projected.

The cracking data in Table 4 are shown for two dates. February 2020 was the last month that all of the sections were still in service and represents the conditions after approximately four and a half years and 16 million ESALs had been applied to the test sections. February 2021 represents the completion of the experiment. After N5 and N8 were milled and overlaid in February 2020, the cracking data for these two sections had to be projected forward based on data prior to their removal from the experiment. A sigmoidal function was fit to the cracking versus ESALs data for these sections using the form of equation 1.

$$Cracking = 1 - e^{(-\theta_1 \times MESALs^{\theta_2})} \quad (1)$$

Where θ_1 *and* θ_2 are curve fitting coefficients and MESALs are millions of ESALs.

This approach to estimating the amount of cracking beyond 16 million ESALs was found to be reasonable based on comparisons of measured versus predicted data for N1 and N2. This projection of cracking for these two sections was necessary to develop correlations between lab results and field performance using all of the test sections. Figure 4 shows the progression of cracking for the test sections over the two cycles.

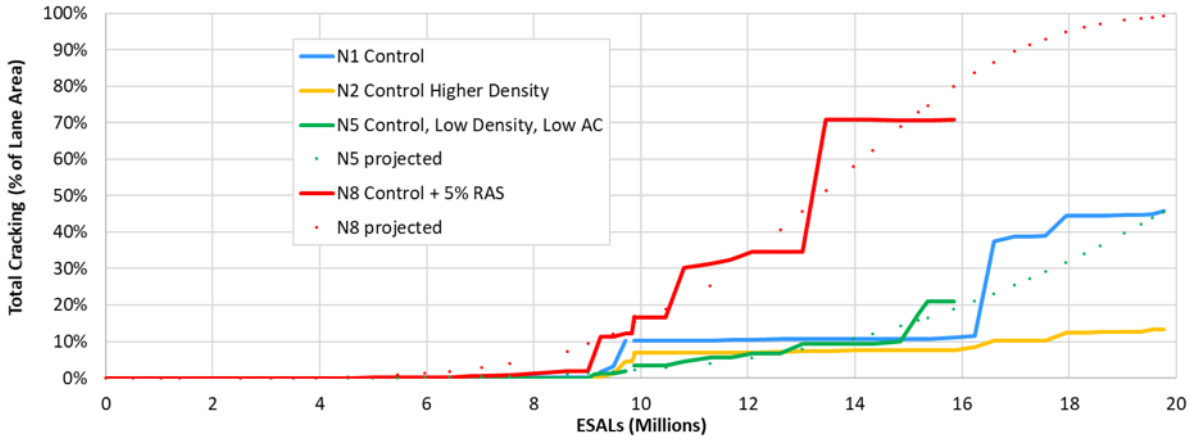

Figure 4. Cracking versus ESALs for the Four Test Sections with Significant Cracking

The field performance of the Cracking Group Experiment test sections satisfied the primary objective of the study, which was to generate a wide range in the extent and severity of top-down cracking. As can be seen in Table 4, each of the test sections performed very well with regard to rutting and change in texture, which is an indicator of raveling. After 20 million ESALs of trafficking, three of the test sections (S5, S6, and S13) had little to no cracking, one section (N2) had a low amount of low severity cracking, two sections (N1 and N5) had a moderate extent of cracking, about 45% – although their severity levels were quite different, and one section (N8) had extensive, high severity cracking.

The difference in severity level of cracking for N1 (Ctrl) and N5 (Ctrl Low Density & AC) is evident in two ways. Photos from the sections (Figure 5) show that N1 had low severity cracking in January 2021, whereas the cracking in N5 observed on December 19, 2019 had begun to lead to shallow potholes through the surface layer. This is also evident in the change in IRI for these sections. Section N1 had a change of only five inches per mile in roughness over five and a half years, whereas N5 increased in roughness by 30 inches per mile over four and a half years.

	
N1: Moderate Extent but Low Severity Cracking, Jan. 2021	N5: Moderate Extent but High Severity Cracking (and Potholes), Dec. 2019

Figure 5. Cracking in N1 (Control) and N5 (Control, Low Density, Low AC)

Figure 6 shows a photo of part of N8 (Ctrl +5% RAS) from December 2019. At that point in time, the cracking was about 70% of the lane area with potholes starting to develop.

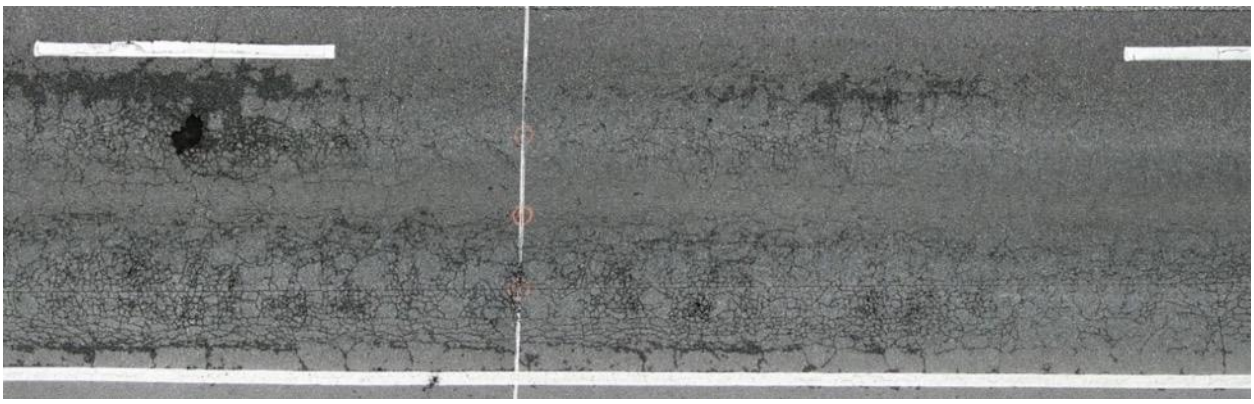

Figure 6. Distress in Part of N8 in December 2019

2.5 Pavement Response Analysis

Part of the field investigation of the Cracking Group sections included measurements made from embedded instrumentation under truck loading along with backcalculation of in-situ material properties from falling weight deflectometer (FWD) testing. The goals with each of these monitoring programs included the following:

- Characterize seasonal temperature effects on pavement responses;
- Evaluate differences in pavement responses driven primarily by surface lift mixture differences; and
- Quantify effects of pavement cracking on measured pavement responses through non-destructive testing.

To that end, each section in the experiment was instrumented with asphalt strain gauges (ASGs), earth pressure cells (EPCs), and temperature probes during the construction process. The ASGs were placed to measure bending-induced tensile strain at the bottom of the asphalt base layer in the direction of traffic while the EPCs were placed at the asphalt concrete/granular base interface and granular base/subgrade interface to measure vertical pressures at those depths, respectively. While 100% of the EPCs survived installation and both research cycles, the ASG survivability was extremely low and did not produce sufficient data to include in the following analyses. Data were collected from the embedded gauges twice per week during the first test cycle followed by weekly in the second test cycle. Data collection alternated mornings and afternoons to capture both the short term (i.e., daily) and long term (i.e., seasonal) temperature fluctuations.

The FWD testing program consisted of testing approximately three times per month along the inside, outside, and between wheelpaths at four random locations in each section. Each set of deflection data at a given location consisting of three replicate drops at three drop heights representing 6, 9, and 12-kip loadings. The measured deflection data were used in EVERCALC 5.0 to back-calculate the layer properties to establish a time history of in situ properties during the two-year test cycle. Only data from the 9-kip load level resulting in backcalculated properties with a root-mean-square-error (RMSE) of less than 3% are presented below.

2.5.1 Measured Pavement Responses

Data collected over both test cycles were normalized to a reference temperature of 68°F and plotted against time in Figures 7 and 8 for base and subgrade pressures, respectively. The temperature normalization process followed a previously-established procedure (*1*) and used data collected from both test cycles. The gap in both data sets corresponds to the reconstruction time between test cycles where traffic was not applied to the sections.

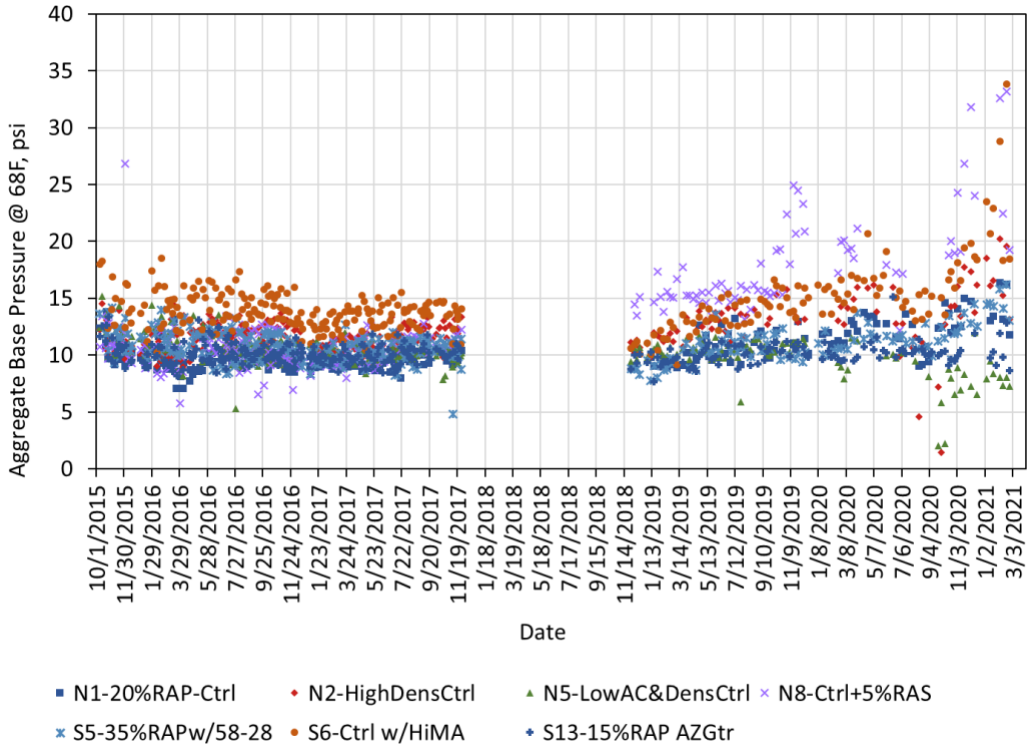

Figure 7. Base Pressure at 68°F Versus Time

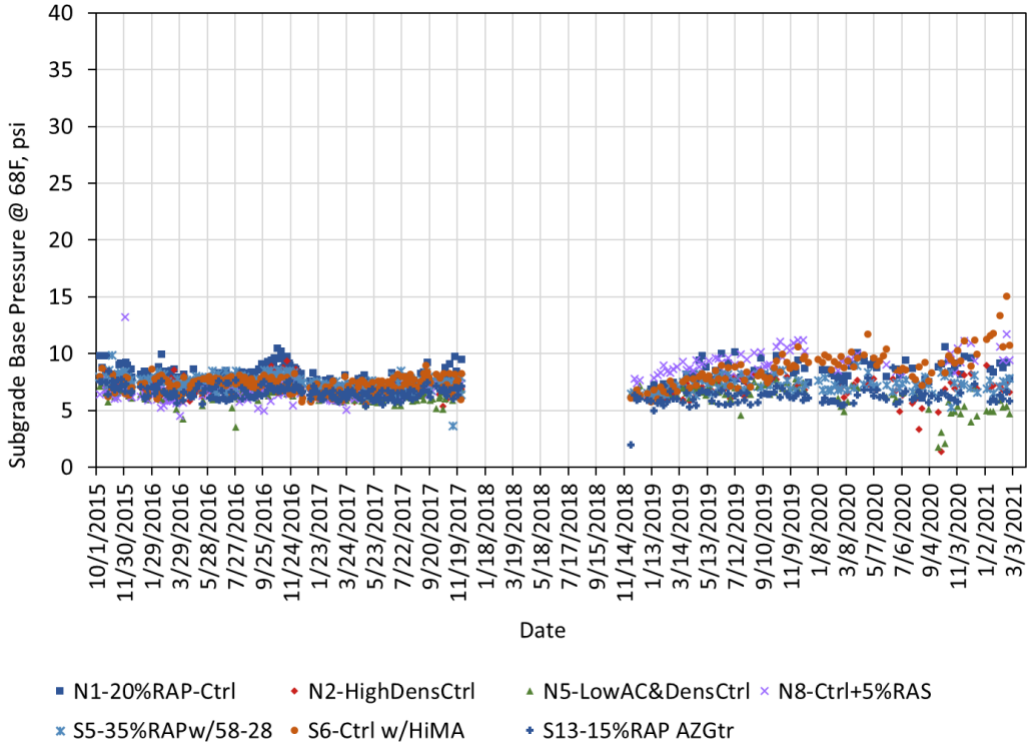

Figure 8. Subgrade Pressure at 68°F Versus Time

As shown in Figures 7 and 8, the data from the first test cycle (2015 through 2017) show no apparent effects of pavement damage as each data set is relatively constant over time, or even decreasing as with S6 (Ctrl w/ HiMA). The damage that had appeared during the first test cycle was not severe enough to increase the base and subgrade pressure readings. However, the effects of pavement damage become much more evident with certain sections in the second test cycle. The most severely damaged section was N8 (Ctrl + 5%RAS) which reached 20% of lane area cracked in mid-February 2019. A sharp increase of 10 psi in the aggregate base pressure (Figure 7) and a more general upward trend of about 4 psi in the subgrade pressure (Figure 8) correspond to this increasing cracking damage. Clearly, though the cracking was top-down, it was severe enough to affect the load carrying capacity of the section resulting in elevated stress levels in the pavement foundation. Section N5 also reached 20% of lane area cracked 11 months later in mid-January 2020. The steadiness of both pressure data sets, and even a slight decline at the end of the second test cycle in Figures 7 and 8, suggest that though there was extensive cracking at the surface, it was not severe enough to affect stress levels deeper in the pavement structure. Both of these sections were milled and inlaid in mid-February 2020.

The remaining sections survived to the end of the second test cycle with no rehabilitation but with varying degrees of cracking across the lane area as noted in Table 4. It is important to emphasize that the measurements shown in Figures 7 and 8 correspond to particular locations in each section and do not represent the overall condition of the pavement, but rather only in close proximity to the particular pressure cells. That may help explain the increasing pressure measurements toward the end of the second test cycle for some of the sections. Notable are N1 (20%RAP-Control), N2 (High Density Control), S5 (35%RAP w/58-28) and S6 (Ctrl w/ HiMA), which all show similar trends with slightly increasing pressure measurements during the second test cycle with a sharper increase in the last few months. This suggests that the cracking in the vicinity of the pressure cells had become severe enough to begin compromising the sections' structural integrity. The exception was S13 (15%RAP GTR), which did not have any observable cracking and no appreciable changes in pressure measurements.

2.5.2 Backcalculated Asphalt Concrete Moduli

Backcalculated AC moduli, normalized to 68°F following procedures similar to normalizing pressure responses, are plotted in Figure 9 for both test cycles. The vertical spread in the respective data series represents spatial variability within each test section and it appears that the modulus was decreasing toward the end of the second cycle as cracking became more widespread and severe. To better visualize the data, the data was subdivided into grouped sections and examined by offset (between wheelpaths, inside wheelpath and outside wheelpath) as shown in Figures 10 through 15.

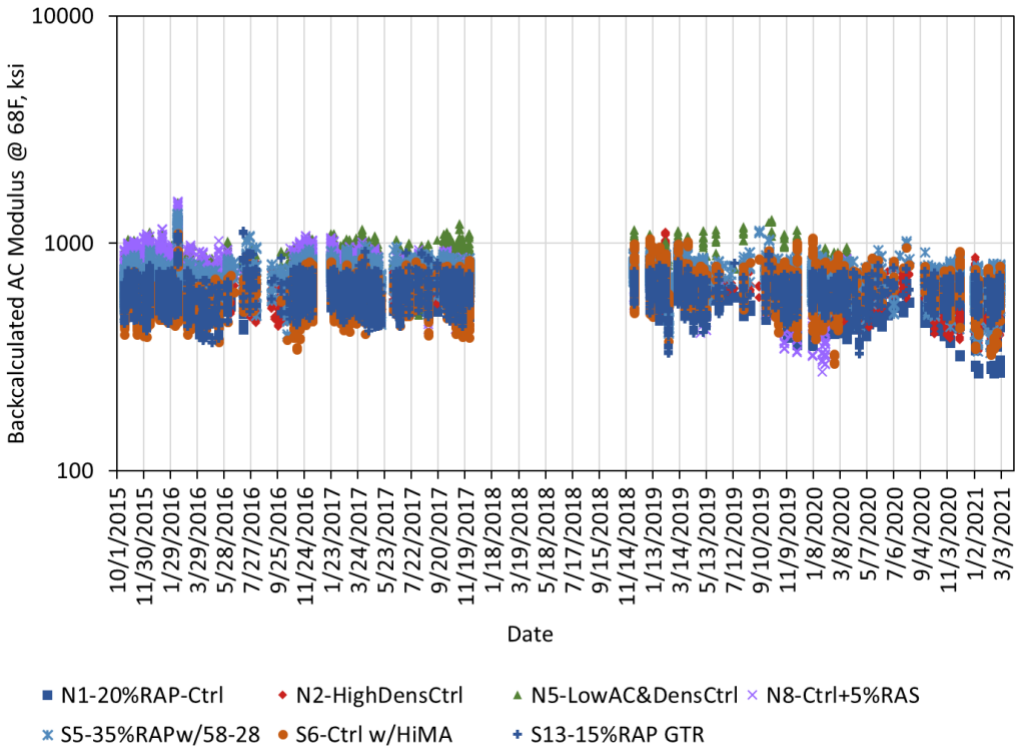

Figure 9. Backcalculated AC Moduli at 68°F for All Test Locations

Sections N5 (LowAC&DensCtrl) and N8 (Ctrl+5%RAS) experienced the most widespread and severe damage and are shown in Figure 10, which contains data from both test cycles and all test locations. It is clear that N8 had a substantial decline in AC modulus during the second test cycle as damage became more severe up until it was milled and overlaid. This trend is not as readily apparent in Section N5, and the data appear more scattered. The trendlines in Figure 10 quantify the decline with an approximate 33% decrease in AC modulus in Section N8 and only an 8% decrease in Section N5.

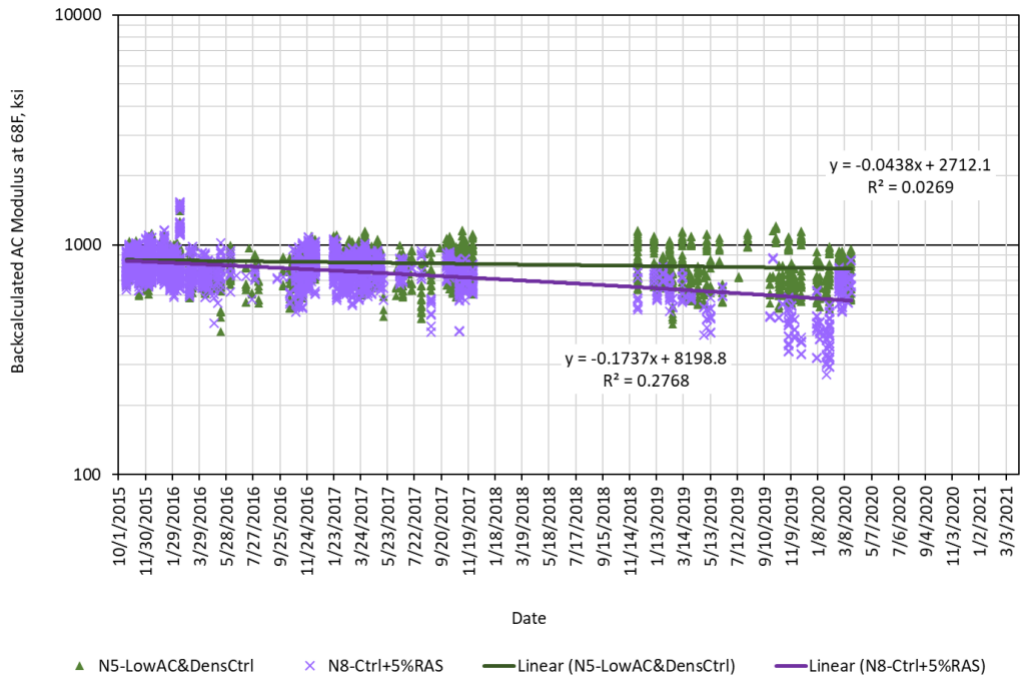

Figure 10. N5 and N8 Backcalculated AC Moduli at 68°F for All Test Locations

To examine the effect of transverse offset more closely in the lane, Figure 11 subdivides the data from Figure 10 into between wheelpaths (Figure 11a), inside wheelpath (Figure 11b) and outside wheelpath (Figure 11c) with linear trendlines fit to the respective data sets. The slopes of the trendlines indicate if cracking at the surface is affecting structural integrity. Larger negative slopes (and corresponding higher R^2) indicate more significant damage while smaller slopes (and corresponding smaller R^2) indicate less damage.

In all three offsets (between, inside, and outside) Section N8 (Ctrl+5%RAS) experienced more pavement damage with a similar order of magnitude between all three. The most severe offset was the outside wheelpath where the AC modulus at 68°F decreased by 39% during the entire experiment. In contrast, N5 (LowAC&DensCtrl) did not appear to suffer structural degradation between the wheelpaths and had a relatively slighter damaging affect in the inside and outside wheelpaths. In the inside wheelpath, N5 experienced a 20% modulus reduction from start to finish. It should be noted that these sections were resurfaced before the others so their degradation should not be directly compared to the others that experienced the full 20 million ESALs.

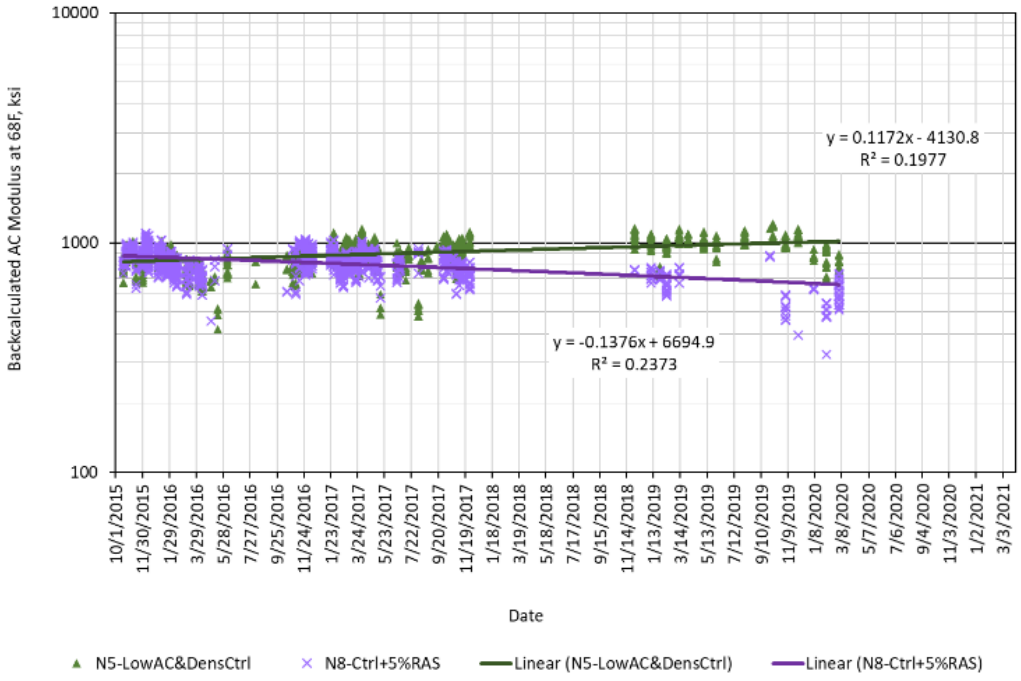

a) Between Wheelpaths

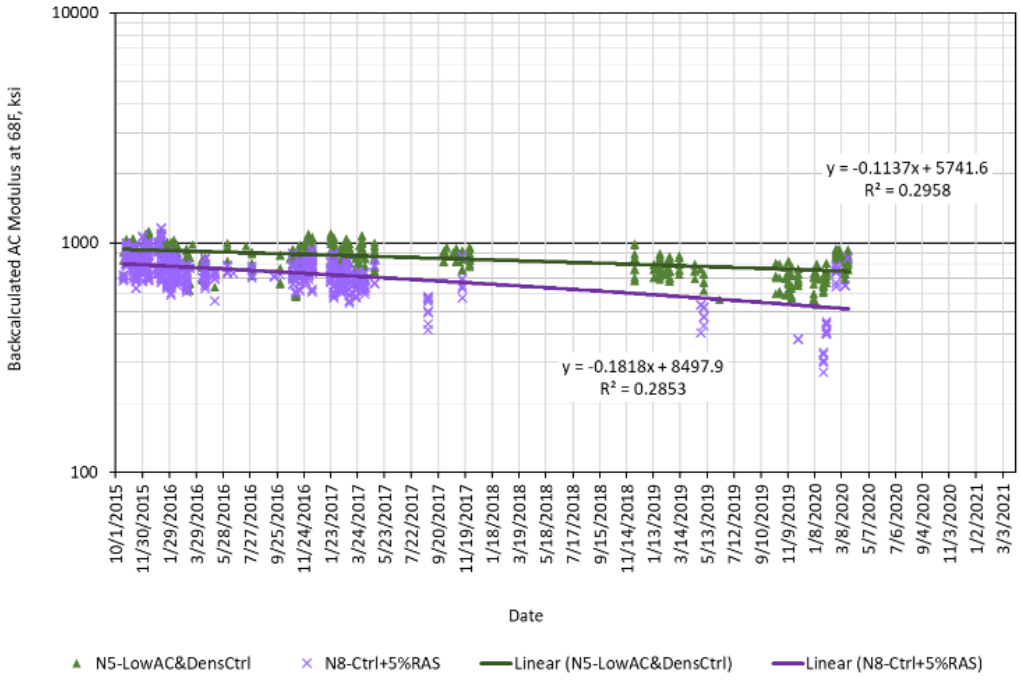

b) Inside Wheelpath

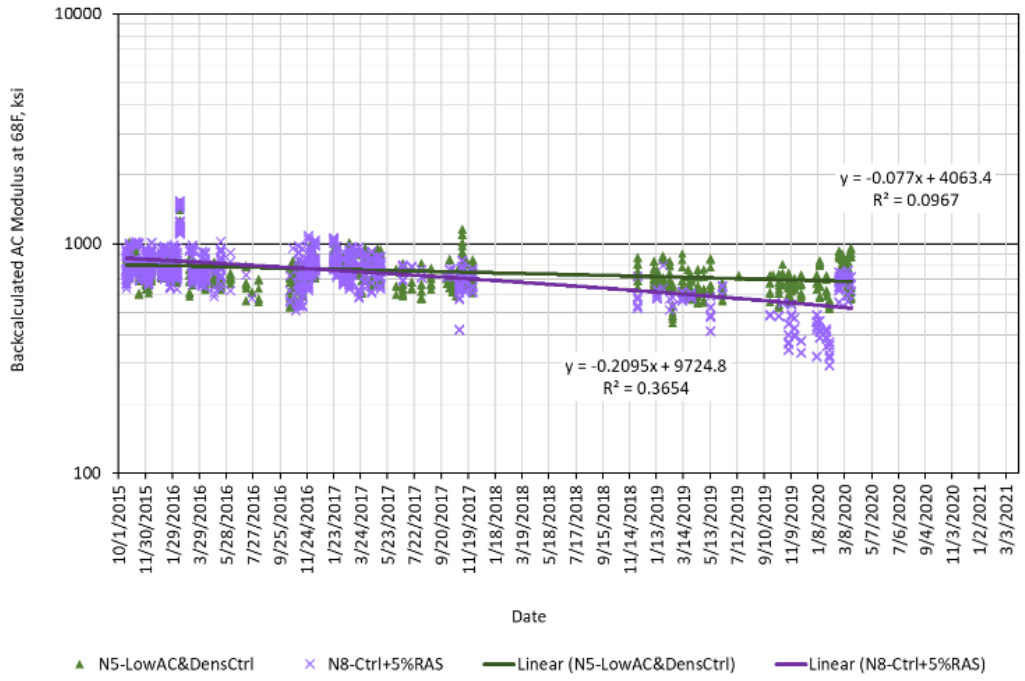

c) Outside Wheelpath

Figure 11. N5 and N8 Backcalculated AC Moduli at 68°F By Wheelpath

Since the other sections did not appear to have changing modulus versus time during the first test cycle, the remaining plots (i.e. Figures 12 through 15) focus only on the second test cycle. Figure 12 contains data for N1 (20%RAP-Control) and N2 (High Density Control) at all locations while Figure 13 subdivides the data by wheelpath. The trendlines in Figure 12 indicate similar behavior from both sections with a decline in modulus of 32% (N1) and 24% (N2) averaged across each section. Similar trends were observed by wheelpath (Figure 13), indicating that the structural degradation was equally experienced throughout the section.

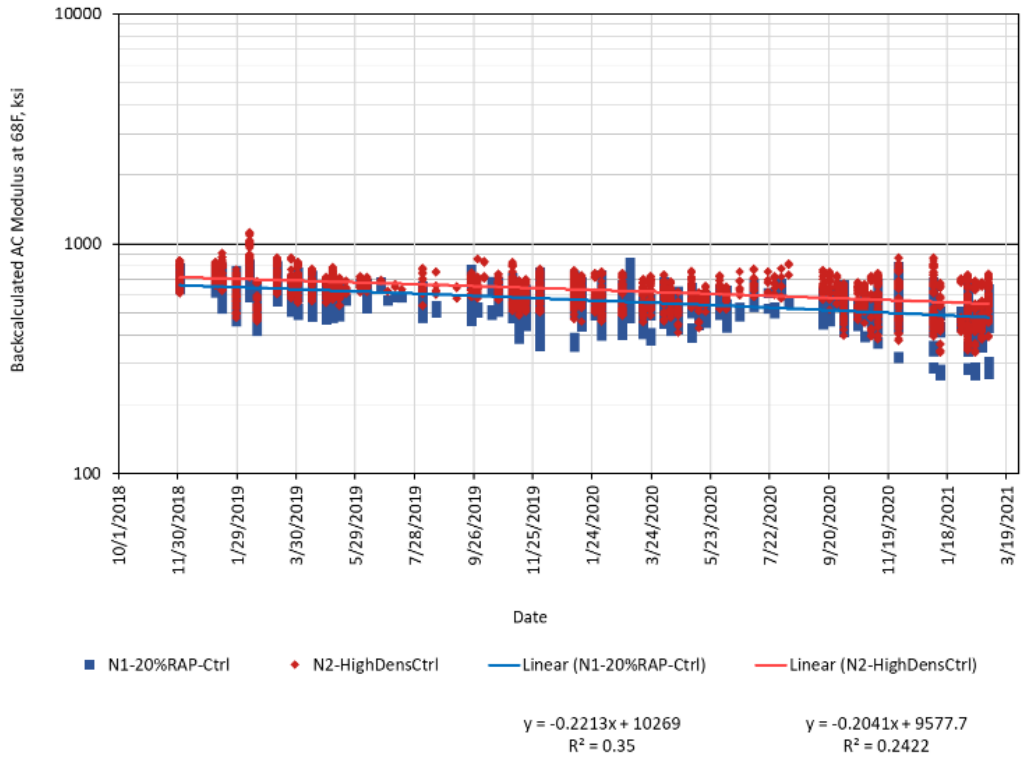

Figure 12. N1 and N2 Backcalculated AC Moduli at 68°F for All Test Locations (Second Test Cycle)

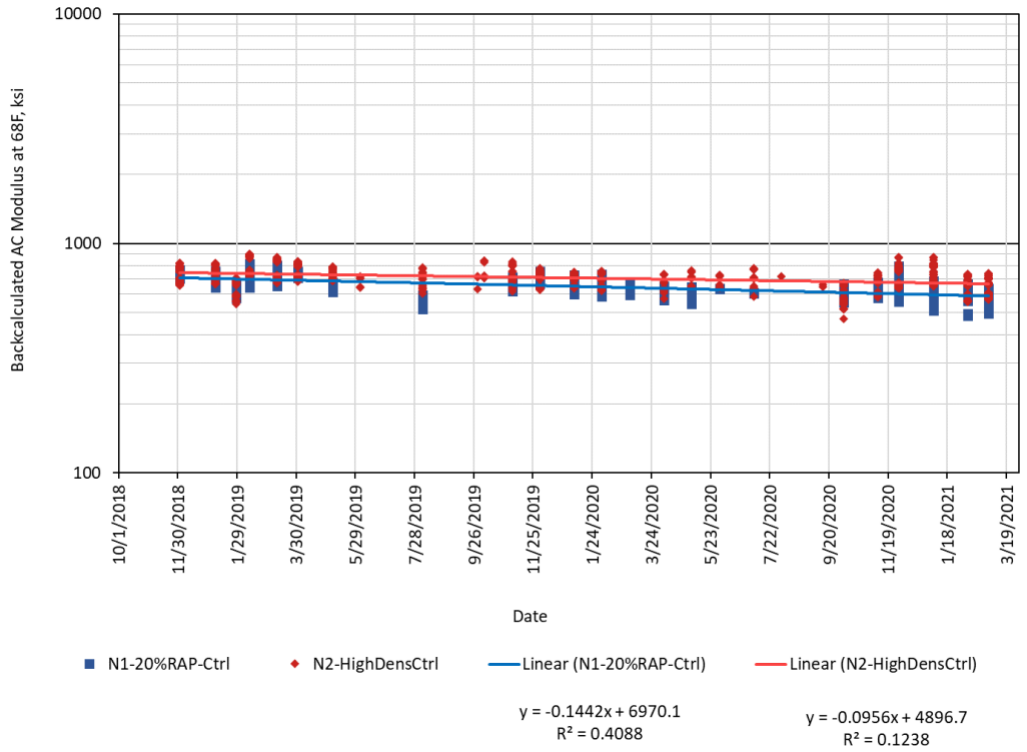

a) Between Wheelpaths

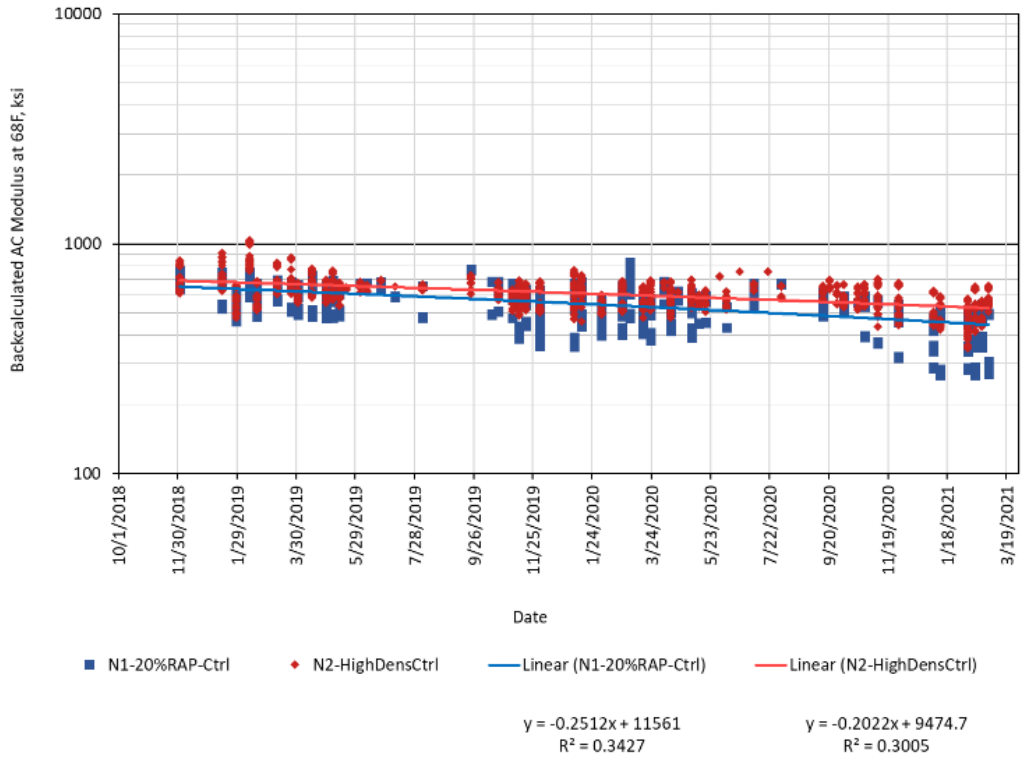

b) Inside Wheelpath

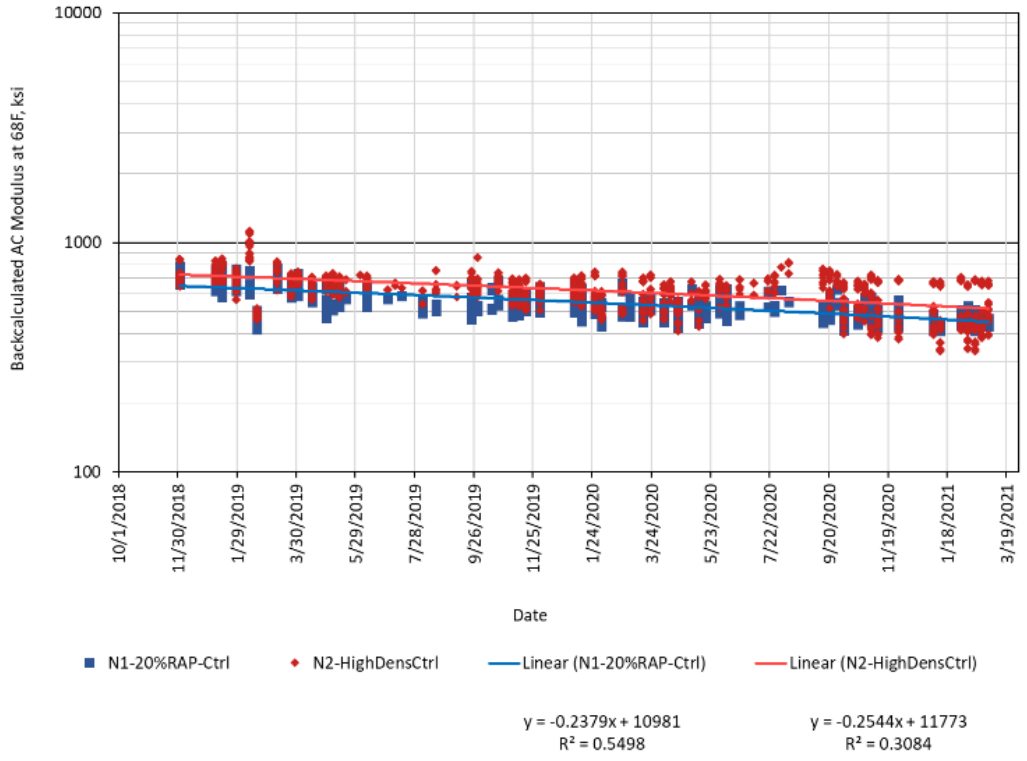

c) Outside Wheelpath

Figure 13. N1 and N2 Backcalculated AC Moduli at 68°F by Wheelpath (Second Test Cycle)

It is evident from Figure 14 that the south tangent sections (S5-35%RAP w/58-28, S6-Ctrl w/ HiMA & S13-15%RAP GTR) did not experience the same level of section-wide structural degradation as the north tangent sections during the second test cycle with nearly flat trendline slopes and low R^2 values. Of these sections, S13 experienced only a 2% decline in modulus while S5 (12% decrease) and S6 (20% decrease) were greater. Recall from the discussion of pressure responses that S13 had essentially no change in pressure at 68°F, which is consistent with no changes in AC modulus. The other sections experienced some increases in pressure, corresponding to their decreasing moduli. Subdividing the data by wheelpath as shown in Figure 15 found similar trends.

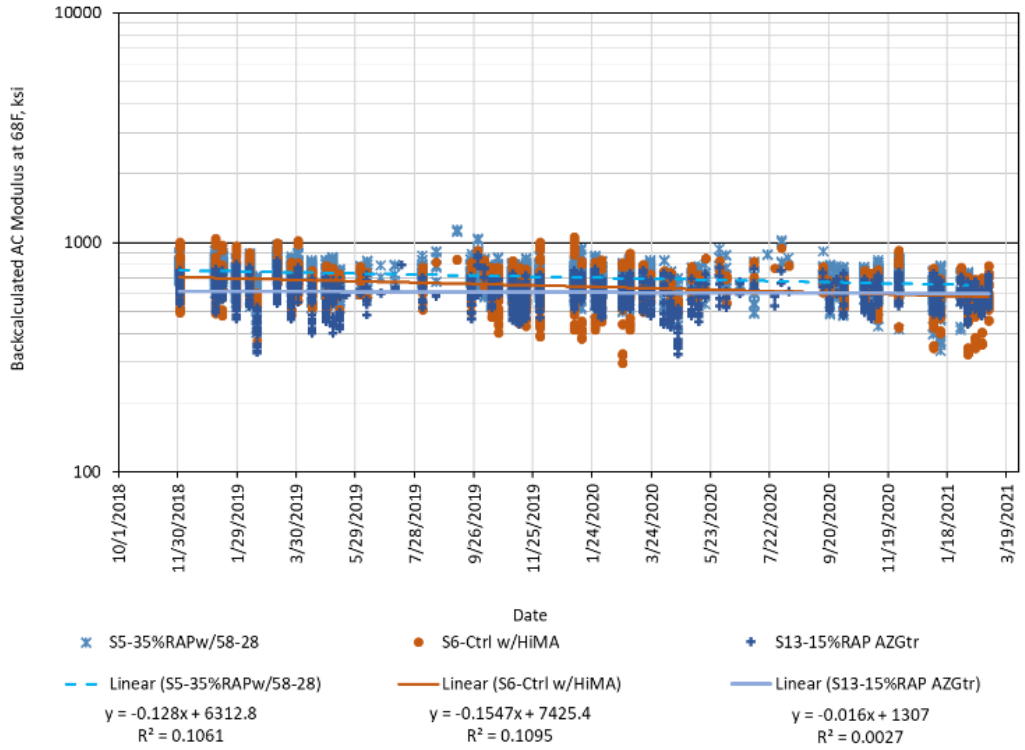

Figure 14. S5, S6, and S13 Backcalculated AC Moduli at 68°F at All Test Locations (Second Test Cycle)

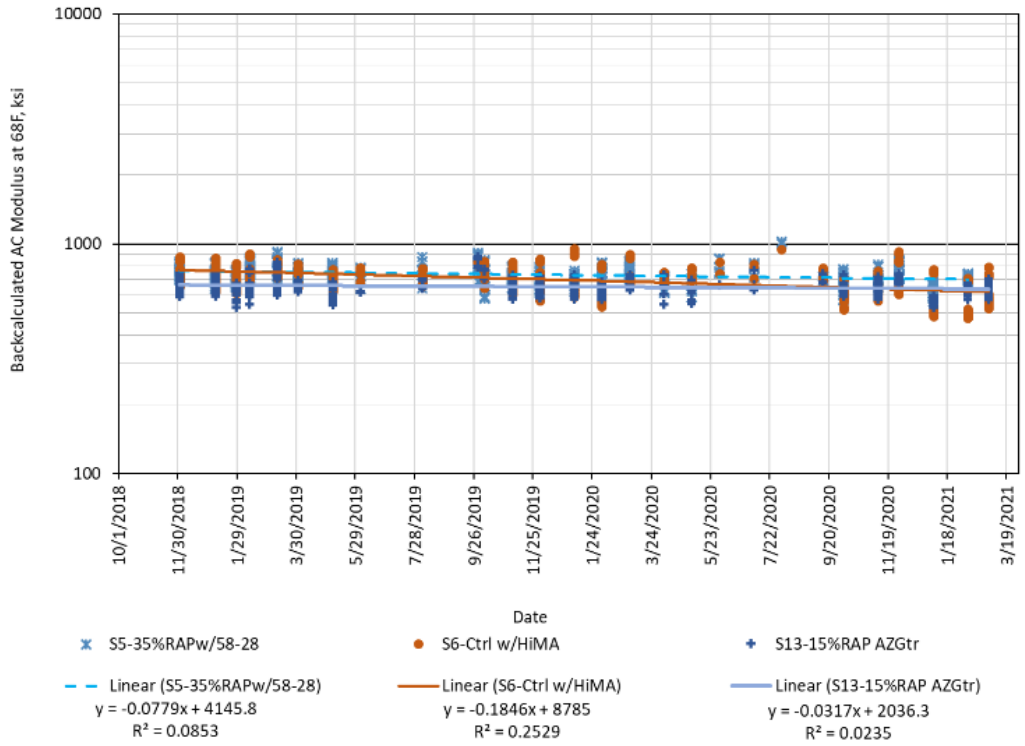

a) Between Wheelpaths

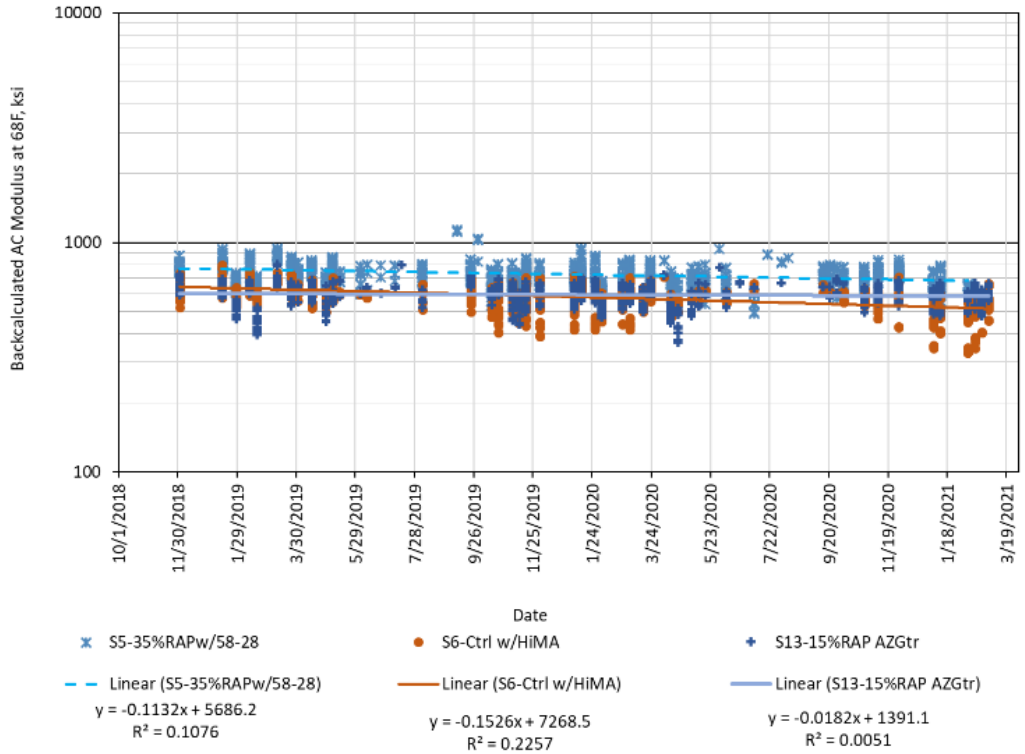

b) Inside Wheelpath

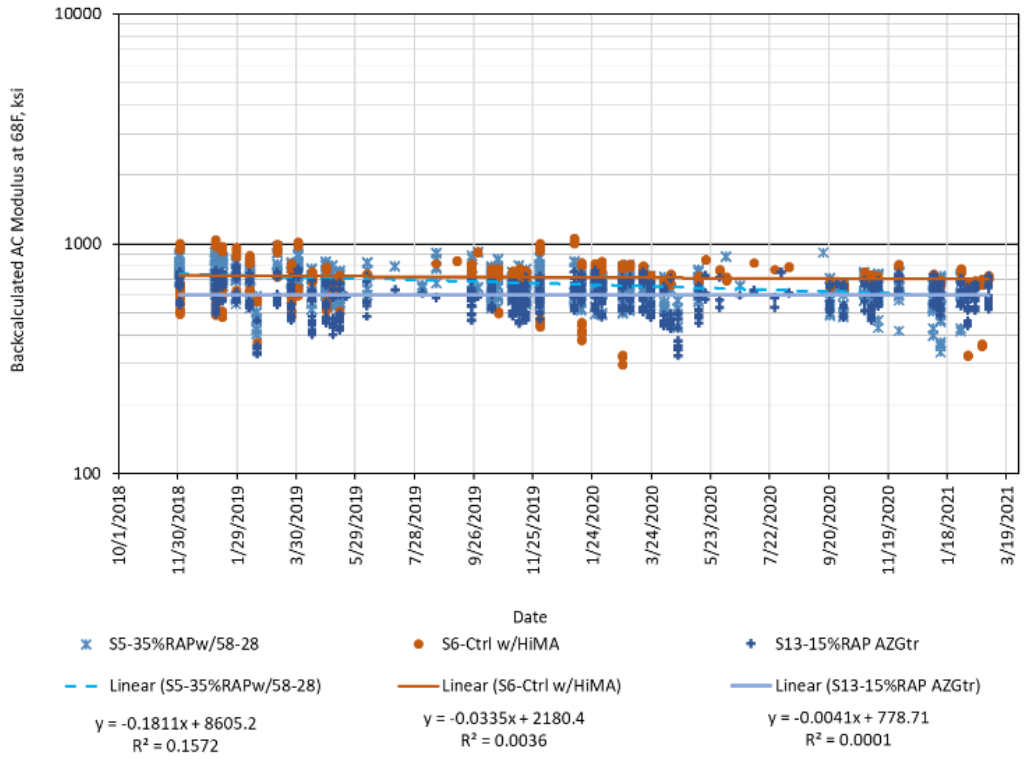

c) Outside Wheelpath

Figure 15. S5, S6, and S13 Backcalculated AC Moduli at 68°F by Wheelpath (Second Test Cycle)

Table 5 summarizes the average decrease in modulus over two research cycles as described above. It is important to emphasize that Sections N5 (LowAC&DensCtrl) and N8 (Ctrl+5%RAS) were milled and inlaid in February 2020 so their respective decreases correspond to 16 million ESALs compared to 20 million ESALs for the other test sections. Of the remaining sections, the best structural performer was S13 (15%RAP GTR) which was also evident from the pressure measurements. The other sections landed between these sets with somewhat similar structural performance.

Table 5. AC Modulus Decrease by Test Section

Section	Average Section-Wide AC Modulus Decrease
N1 (20%RAP-Control)	32%
N2 (High Density Control)	24%
N5 (LowAC&DensCtrl)*	8% (20% in Outside Wheelpath)
N8 (Ctrl+5%RAS)*	33% (39% in Outside Wheelpath)
S5 (35%RAP w/58-28)	12%
S6 (Ctrl w/HiMA)	20%
S13 (15%RAP GTR)	2%

*Taken out of service in February 2020.

2.6 Results of Laboratory Tests and Field Performance Correlations

This section presents the results of the laboratory cracking tests for each of the methods selected by the sponsors of the experiment. For a complete description of the tests, associated

methods of analysis, and aging condition, please see the work by Chen (*2*). The number of replicates per test are noted in the discussion for each method. Outlier analyses were conducted on results for each set of replicates following ASTM E 178 using a 90% confidence level.

As previously noted, all specimens were initially prepared at 7.0±0.5% air voids except for N2 (Control High Density) which used a target air void content of 4.0±0.5% air voids, and N5 (Control Low Density & AC) which used target air void content of 10.0±0.5% air voids, representing the nominal target in-place relative density for each section. Later in the experimental work, additional I-FIT and IDEAL-CT tests were conducted on N2 and N5 mixtures also compacted to 7.0±0.5% air voids to avoid the effect of specimen air voids on the results of these cracking tests. For these two tests, results are reported for the specimens prepared to 7.0±0.5% air voids and at the nominal target in-place air void contents for N2 and N5. However, the correlations of lab results to field performance are presented only for test results of specimens prepared to 7.0±0.5% air voids. The field cracking data used in correlation analyses corresponds to the percent of lane area cracked after 20 million ESALs in Table 2. As previously noted, sections N5 (Control Low Density & AC) and N8 (Control +5% RAS) were milled and inlaid in February 2020; thus, the field cracking data of these two sections was projected to 20 million ESALs based on non-linear extrapolation using Equation 1.

2.6.1 Energy Ratio Results

The Energy Ratio results are summarized in Table 6. ER results are determined from analysis of three tests with the trimmed means of those tests used to calculate the single ER value. Although there were at least three replicates for each component test in the ER procedure, the final ER value does not have replicates, which limits many types of statistical analyses such as Analysis of Variance (ANOVA).

According to Roque et al. (*3*), $DCSE_{HMA}$ is the amount of energy required to initiate cracking. From their testing of cores from pavements at least 10 years old, they proposed a minimum $DCSE_{HMA}$ criteria of 0.75 kJ/m^3 to screen out extremely stiff mixtures and a minimum ER criterion of 1.95 for pavements subject to one million ESALs or more per year. However, the Test Track sections are exposed to about five million ESALs per year, a much higher level of traffic than the ER validated range.

From the results in Table 6, it can be seen that only the critically-aged lab prepared sample (LMLC-CA) for N8 had a mean $DCSE_{HMA}$ result below 0.75 kJ/m^3, indicating that this mixture is very stiff and susceptible to top-down cracking. That is a correct assessment as shown in the field performance results. However, the ER parameter does not correctly identify this mix as being more susceptible to top-down cracking than the other mixes in each set of sample type and mix aging condition. Furthermore, the mix with the best field performance, S13 (Gap-Gr, asphalt-rubber), has the lowest ER in each mix set, which is also an incorrect assessment in terms of top-down cracking resistance.

Table 6. Results of Energy Ratio Tests

Test Section and Mixture Description	Resilient Modulus (GPa)	Creep Compliance Rate	IDT Fracture Energy (kJ/m³)	$DCSE_{HMA}$ (kJ/m³)	Energy Ratio
	Trimmed Means				
LMLC-STOA					
N1: Control	10.41	2.94E-09	3.6	3.30	5.11
N2: Control, Higher Density	15.32	1.85E-09	3.4	3.08	7.38
N5: Control, Low Dens. & AC	10.13	3.50E-09	1.5	1.31	1.85
N8: Control + 5% RAS	12.34	6.77E-10	1.6	1.35	8.06
S5: 35% RAP, PG 58-28	9.70	3.98E-09	2.7	2.48	3.81
S6: Control, HiMA Binder	6.96	3.01E-09	4.9	4.67	6.85
S13: Gap-gr., asphalt-rubber	9.33	4.61E-09	2.1	1.97	2.08
LMLC-CA					
N1: Control	14.12	4.16E-10	2.2	1.90	18.03
N2: Control, Higher Density	15.97	2.62E-10	2.3	1.95	28.69
N5: Control, Low Dens. & AC	10.71	8.68E-10	1.4	1.17	5.55
N8: Control + 5% RAS	15.03	2.07E-10	0.8	0.58	12.46
S5: 35% RAP, PG 58-28	12.87	4.59E-10	2.0	1.74	15.20
S6: Control, HiMA Binder	8.55	9.44E-10	4.0	3.74	16.69
S13: Gap-gr., asphalt-rubber	9.87	2.22E-09	2.2	1.97	3.79
PMLC-RH					
N1: Control	9.94	3.79E-09	4.8	4.52	5.52
N2: Control, Higher Density	12.41	1.98E-09	3.9	3.58	7.43
N5: Control, Low Dens. & AC	7.93	4.31E-09	3.4	3.19	3.57
N8: Control + 5% RAS	12.75	4.98E-10	1.8	1.57	12.82
S5: 35% RAP, PG 58-28	7.38	3.46E-09	6.0	5.76	7.39
S6: Control, HiMA Binder	7.28	2.44E-09	5.4	5.17	9.18
S13: Gap-gr., asphalt-rubber	7.40	5.17E-09	2.7	2.52	2.24
PMLC-CA					
N1: Control	13.08	8.31E-10	2.7	2.43	11.36
N2: Control, Higher Density	16.99	2.16E-10	1.8	1.49	26.42
N5: Control, Low Dens. & AC	11.04	9.13E-10	1.9	1.68	7.60
N8: Control + 5% RAS	17.28	1.93E-10	1.0	0.79	17.16
S5: 35% RAP, PG 58-28	9.89	1.23E-09	3.9	3.67	12.35
S6: Control, HiMA Binder	8.73	1.04E-09	6.8	6.50	25.55
S13: Gap-gr., asphalt-rubber	10.54	1.48E-09	3.2	2.98	8.36

Figure 16 shows a bar chart for the ER results of the critically-aged plant mix samples. The chart is divided into three sections based on the observed field performance. It is clear from this chart that ER does not distinguish the mixtures with different cracking susceptibilities. Since there are no replicates of ER results for each mixture, standard deviations for ER cannot be determined and statistical comparisons are not possible.

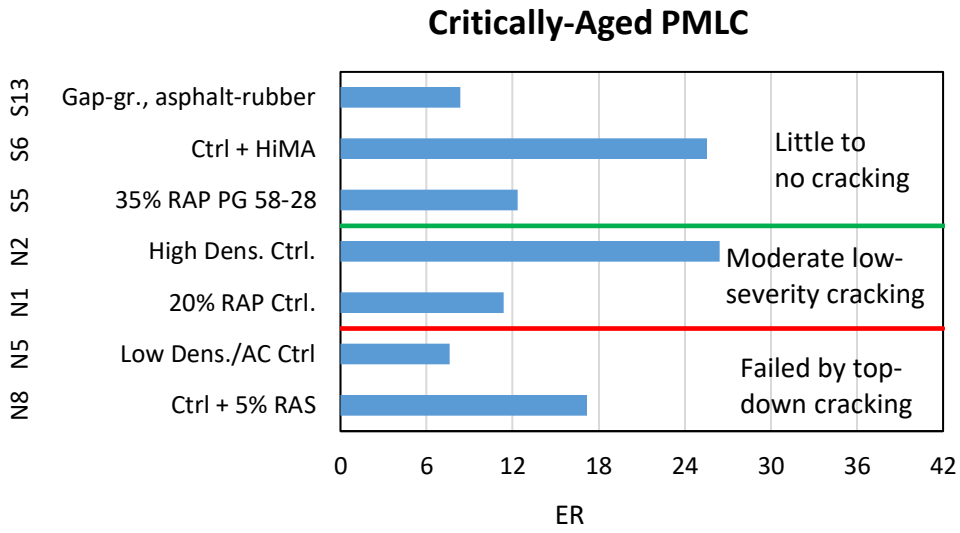

Figure 16. ER Results and Field Performance Groupings

Figure 17 shows correlation plots of Energy Ratio versus the observed cracking data on the Test Track for each of the four sample preparation and mix aging sets. The R^2 values shown are for the best-fit least-squares regressions among linear, exponential, logarithmic, or power functions as determined by Excel. It is evident from each of the four plots that ER is a not a good indicator of top-down cracking resistance for these asphalt mixtures.

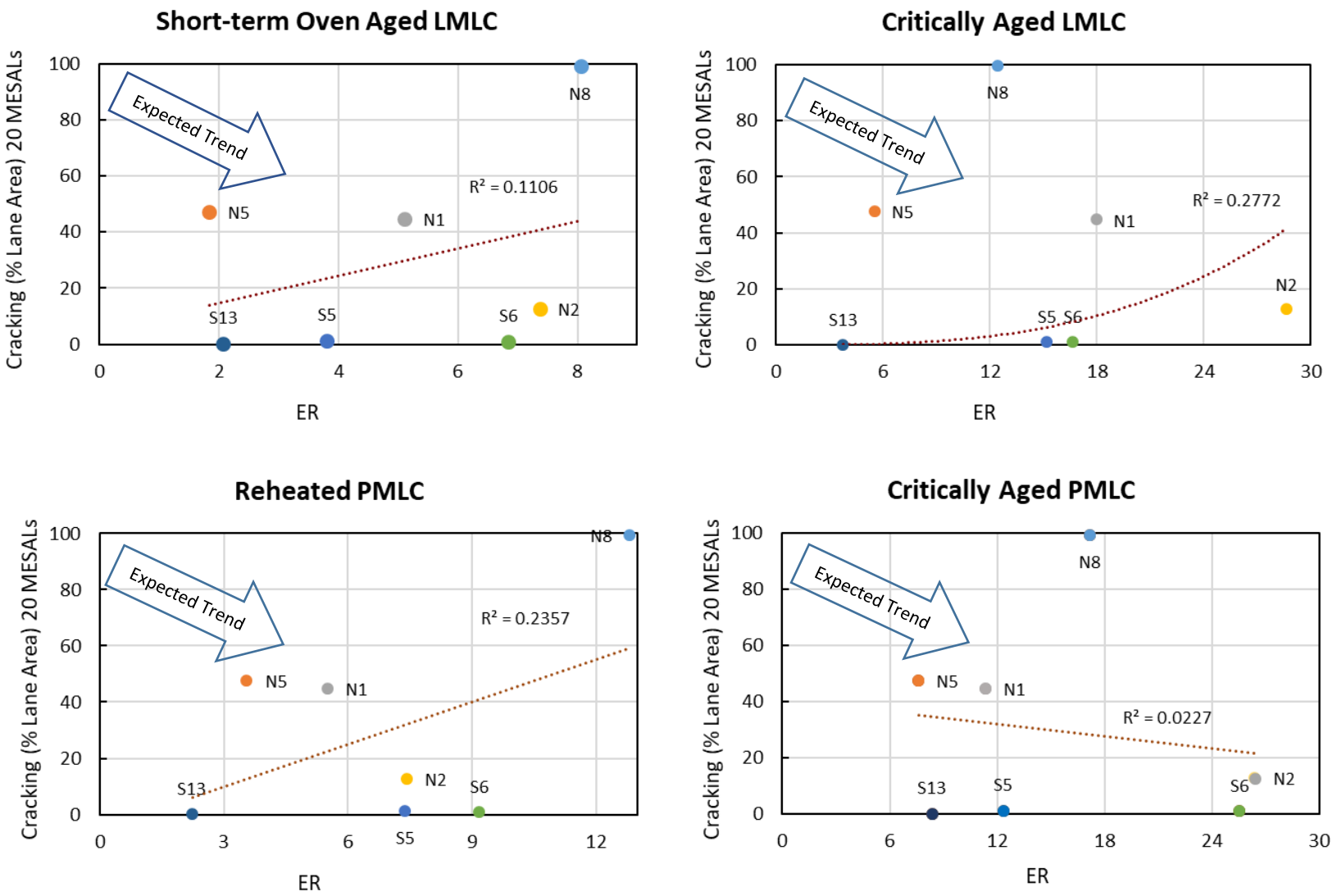

Figure 17. Correlations of ER with Field Performance for the Lab and Plant Samples Subject to Different Aging Conditions

2.6.2 Texas Overlay Results

During the first half of this experiment, the OT-TX results were analyzed and reported as cycles to failure, N_f, according to Texas method in 2018 (*1*). Since that time, the Texas DOT has begun using two other parameters, critical fracture energy (G_c) and the crack progression rate (β) developed by Garcia et al. to assess cracking resistance of asphalt mixtures (*4*). Critical fracture energy has been shown to be a measure of mixture toughness rather than cracking resistance, whereas the crack progression rate parameter has been found to be an excellent indicator of cracking resistance and is less variable than the number of cycles for failure parameter, N_f (*4, 5*). Since the primary purpose of this study is to determine the relationships of the cracking test results to the field performance on the Test Track, this report will focus only on the new crack resistance index parameter, β.

Table 7 summarizes those results for each of the seven mixes prepared and conditioned as outlined previously. The results shown are based on a minimum of four replicates after the outlier analysis. In most cases, five replicates were tested. For the β parameter, a lower number indicates better cracking resistance. Texas DOT recently established a preliminary BMD criterion for maximum cracking progression rate (i.e. β) of 0.45 applicable to most mix types including SMA, Superpave, and certain other dense-graded mixtures. A lower maximum criterion of 0.40 has been proposed for crack attenuating mixtures (CAM) and thin overlay mixtures (TOM). These preliminary criteria are applicable to short-term conditioned lab-produced mix and reheated plant-mix samples.

An examination of the results in Table 7 indicates that the general trends are logical. Within each set of mix sample type and aging condition, the β for mix N8 is the highest and the β for mix S13 is the lowest. For each mixture, the β increased after critical aging, except for the plant mix samples (N8).

Table 7. Results of Texas Overlay Tests Using the β Parameter

Test Section and Mixture Description	LMLC-STOA		LMLC-CA		PMLC-RH		PMLC-CA	
	Avg.	COV	Avg.	COV	Avg.	COV	Avg.	COV
N1: Control	1.00	9%	2.34	29%	0.88	32%	2.08	16%
N2: Control, Higher Density	0.84	28%	2.04	35%	0.60	16%	2.03	11%
N5: Control, Low Dens. & AC	0.90	25%	2.38	20%	0.85	7%	2.96	11%
N8: Control + 5% RAS	2.31	22%	3.25	5%	3.54	10%	3.43	4%
S5: 35% RAP, PG 58-28	0.55	12%	2.04	19%	0.60	14%	1.54	22%
S6: Control, HiMA Binder	0.42	3%	0.89	22%	0.95	38%	1.07	13%
S13: Gap-gr., asphalt-rubber	0.40	20%	0.57	13%	0.32	2%	0.48	9%

Figure 18 shows a bar chart for the OT-TX β results for the critically-aged plant mix samples. The whiskers represent plus and minus one standard deviation of the β parameter from the replicate tests. The chart is divided by the cracking performance of the test sections. It is apparent that the OT-TX β parameter does a very good job of distinguishing the cracking resistance of the mixtures. For this study, a β value of about 1.75 appears to be a good criterion to separate excellent cracking resistance (i.e. little to no cracking on the Test Track) from moderate cracking resistance of the critically-aged PMLC results.

The ANOVA indicated that mixtures had a statistically significant effect on the β parameter. The Games-Howell post-hoc pairwise comparison was then conducted to determine which mixtures were statistically different from one another. The letters (A, B, C, D, E) down the middle of the chart indicate the results of the Games-Howell comparisons. Mixtures that do not share a letter are significantly different at a 95% confidence level. From this analysis, the gap-graded, asphalt rubber mix in S13 was superior to all other mixtures. Statistically, the β parameter separated the mixtures into five groups, although there was overlap among most of the groups. This indicates that the OT-TX β is a powerful test in discerning cracking resistance of asphalt mixtures.

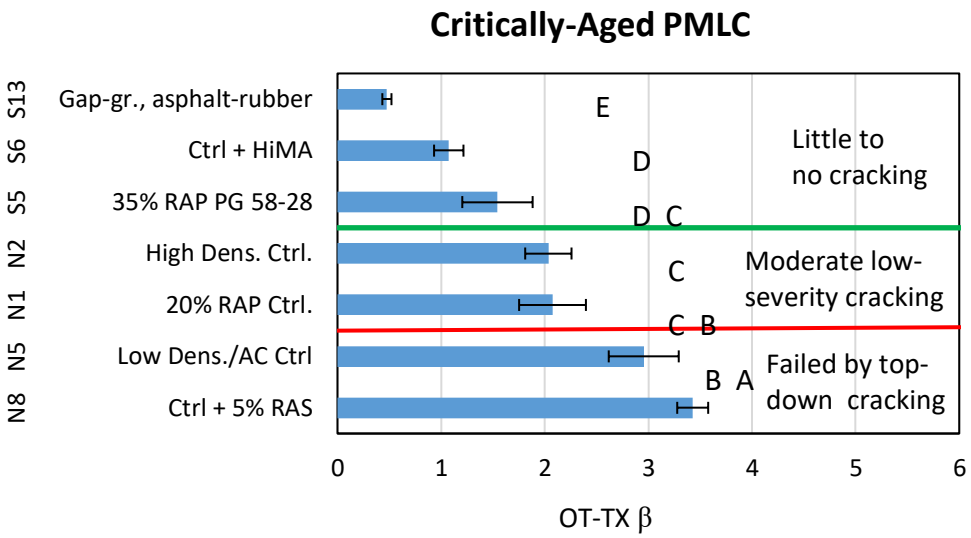

Figure 18. Statistical Comparisons of OT-TX β among Mixtures with Performance Groupings

Figure 19 shows correlation plots of OT-TX β results versus the observed cracking on the Test Track for the lab-prepared and plant-produced samples after the different aging conditions. These relatively high R^2 values for each of the four plots indicate that the OT-TX β is a very good indicator of top-down cracking resistance for asphalt mixtures. It is logical to expect the critically-aged results to better correlate with field performance, since the binders in those samples are aged to represent the condition of the binders after about five years of field aging for surface layers on the Test Track. For this test, the coefficients of determination are similar for the critically-aged samples and the corresponding reheated or STOA samples, which indicates that even the results after reheated plant mix or STOA lab mix correlates as well with the field performances as the critically-aged samples.

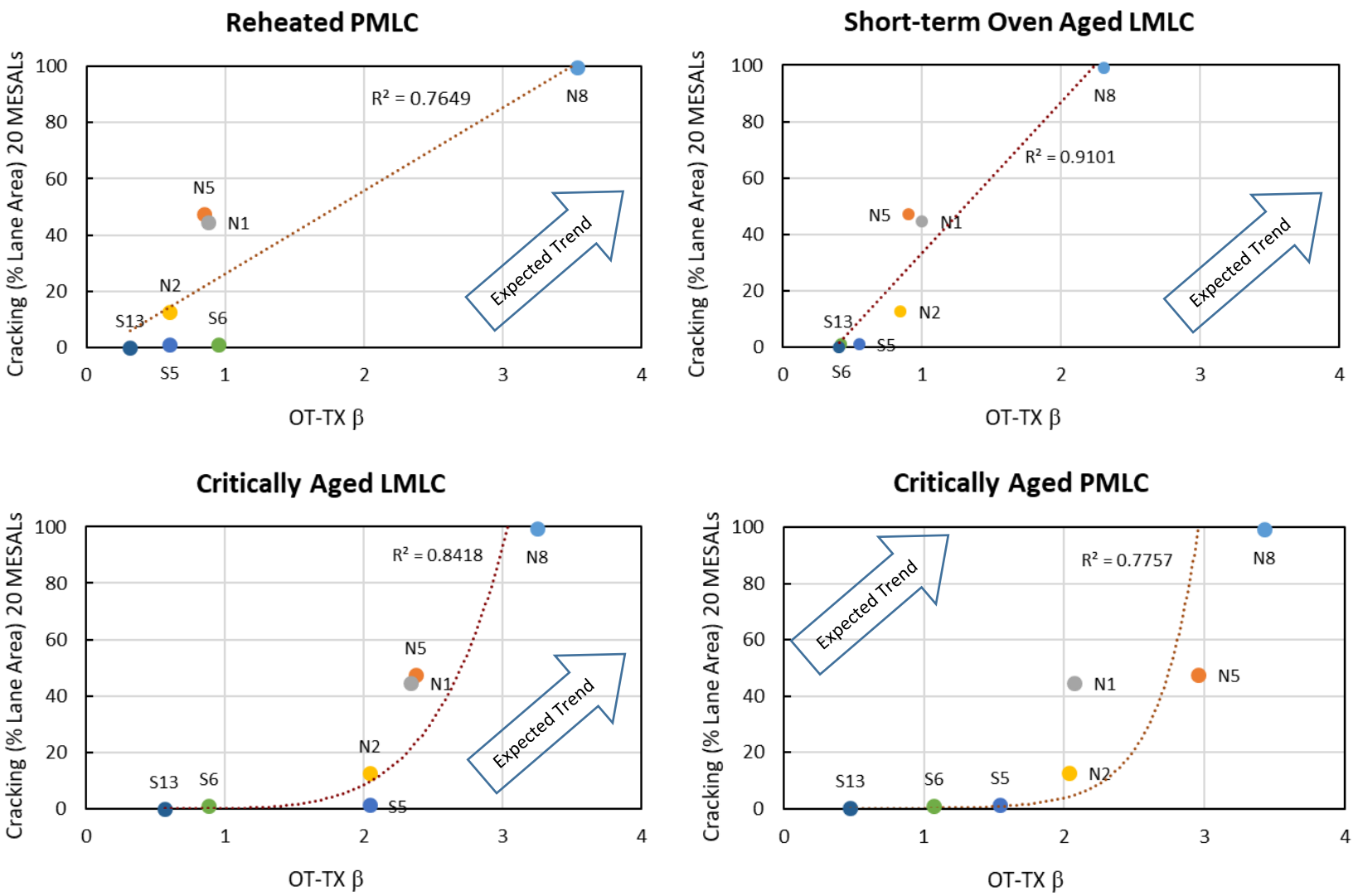

Figure 19. Correlations of OT-TX β with Field Performance for the Lab and Plant Samples Subject to Different Aging Conditions

2.6.3 NCAT Overlay Test Results

Table 8 summarizes the results of the OT-NCAT procedure also using the β parameter. For this test, a minimum of three replicates were tested. The variability of the β values from the OT-NCAT method compared to the OT-TX method is generally lower. The average COVs of the OT-TX results for all four sets ranged from 12 to 20% compared to 6 to 14% for the OT-NCAT method.

For the LMLC-STOA set, very similar OT-NCAT β values were obtained for four mixtures (N2, S5, S6, and S13). The same is true for the PMLC-RH set although the group was a little different (N1, N2, S6, and S13). However, after critical aging, the β values increased and the differences between mixes increased. Thus, for the OT-NCAT β parameter, the critical aging of loose mix is helpful in making distinctions among mixtures with different field performance.

Table 8. Results of the OT-NCAT Tests Using Beta Parameter

Test Section and Mixture Description	LMLC-STOA		LMLC-CA		PMLC-RH		PMLC-CA	
	Avg.	COV	Avg.	COV	Avg.	COV	Avg.	COV
N1: Control	0.27	2%	0.48	18%	0.27	9%	0.50	14%
N2: Control, Higher Density	0.24	9%	0.42	12%	0.24	8%	0.41	9%
N5: Control, Low Dens. & AC	0.33	10%	0.66	9%	0.32	4%	0.60	16%
N8: Control + 5% RAS	0.41	4%	1.15	35%	0.60	8%	0.95	29%
S5: 35% RAP, PG 58-28	0.25	2%	0.52	10%	0.29	4%	0.33	6%
S6: Control, HiMA Binder	0.25	5%	0.29	11%	0.26	12%	0.27	9%
S13: Gap-gr., asphalt-rubber	0.24	8%	0.25	8%	0.24	7%	0.26	6%

Figure 20 shows a bar chart of OT-NCAT β results for the critically-aged plant mix samples. The chart is divided by the cracking performance of the test sections. From this chart, it can be seen that the OT-NCAT β parameter correctly ranked and provided some differentiation among the mixtures that corresponded to their field cracking performance.

As with the OT-TX method, the ANOVA indicated that mixtures had a statistically significant effect on the β parameter. The Games-Howell post-hoc pairwise comparison determined which mixtures were statistically different from one another. The letters in the middle of the chart indicate the results of the Games-Howell comparisons; mixtures that do not share a letter are significantly different at a 95% confidence level. The Games-Howell analysis separated the mixtures into four statistical groups, although there was some overlap among the groups. Although no single mixture was distinct from the others, this analysis indicates that the OT-NCAT β is able to distinguish among the top-down cracking susceptibilities of the mixtures in this study. A β value between 0.41 and 0.33 appears to separate the mixtures with good cracking resistance from those with moderate cracking resistance for the critically-aged plant mix samples. The midpoint of this range is 0.37 and is suggested as a preliminary maximum criterion for β based on critically-aged PMLC results of this experiment. Further research, including benchmarking studies and additional field validation studies, should be considered before implementation of any criteria.

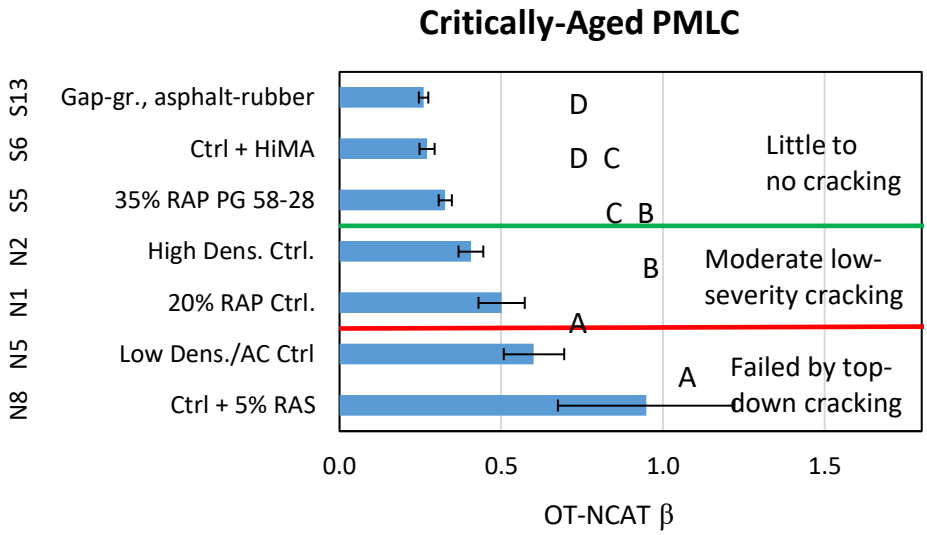

Figure 20. Statistical Comparisons of OT-NCAT β among Mixtures with Performance Groupings

Figure 21 shows correlation plots of OT-NCAT β results versus the observed top-down cracking on the Test Track for the four sample preparation and aging condition sets. As with the OT-TX method, the high R^2 values indicate that the OT-NCAT β is a very good indicator of propensity for top-down cracking. The PMLC-CA correlation to field performance has the highest R^2 value of all tests in this study.

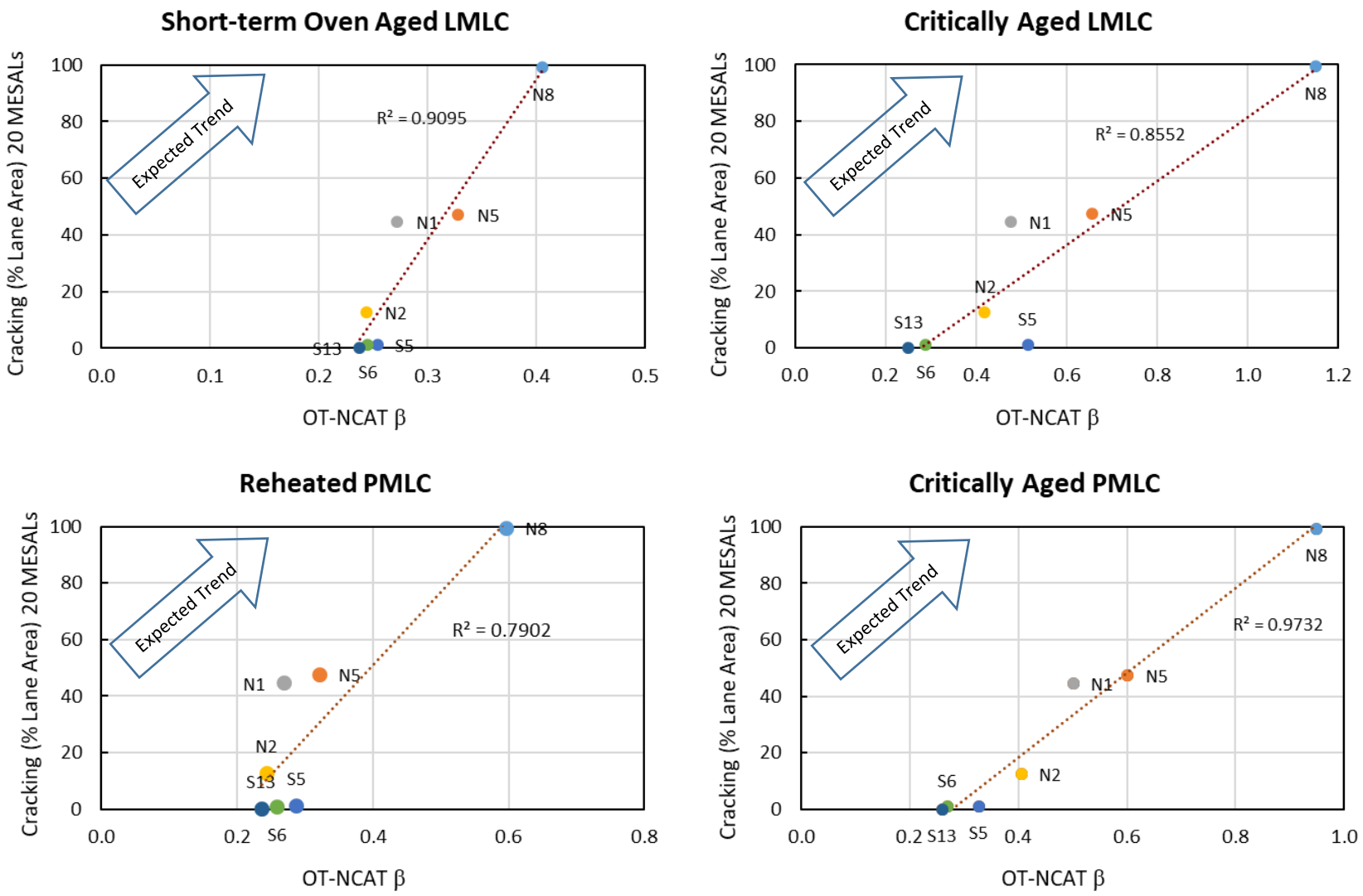

Figure 21. Correlations of OT-NCAT β with Field Performance for the Lab and Plant Samples Subject to Different Aging Conditions

2.6.4 Semi-circular Bend Test (Louisiana Method) Results

Table 9 shows results of the critical strain energy release rate, J_c, the key test output for the Louisiana SCB test. For this test, at least four replicates were tested at each of the three notch depths. The critical strain energy release rate, also referred to as J-integral, is calculated as shown in Equation 2.

$$J_c = -(\frac{1}{b})\frac{dU}{da} \quad (2)$$

Where:

J_c is the critical strain energy release rate (kJ/m^2);
b is the average sample thickness (mm);
a is the notch depth (mm);
U is the strain energy to failure (N-mm); and
dU/da is the change of strain energy with notch depth, or more simply, the slope of the best fit linear regression between notch depth and the strain energy to failure.

Since the regression is fit through all of the data, the standard error of the slope was used to estimate the standard deviation of the slope by dividing the estimate of the total regression error (*Se*) by the sum of squared differences between the x values (*Sxx*); in this case, notch depths. Since the average thickness of specimens is a constant, the slope is the only variable in the J_c equation. Thus, the estimated standard deviation of the slope multiplied by the average thickness was used to estimate the variability of J_c results. A more detailed explanation of this analysis is provided by Moore (*13*). The COVs reported in Table 11 are the estimated standard deviation divided by the average J_c.

Table 9. SCB Critical Strain Energy Release Rate, J_c, and the Estimated COV

Test Section and Mixture Description	LMLC-STOA		LMLC-CA		PMLC-RH		PMLC-CA	
	Avg.	COV	Avg.	COV	Avg.	COV	Avg.	COV
N1: Control	0.29	27%	0.38	6%	0.36	46%	0.34	9%
N2: Control, Higher Density	0.54	10%	0.45	9%	0.61	19%	0.27	12%
N5: Control, Low Dens. & AC	0.32	15%	0.26	13%	0.34	53%	0.22	8%
N8: Control + 5% RAS	0.23	15%	0.23	12%	0.39	33%	0.25	9%
S5: 35% RAP, PG 58-28	0.30	9%	0.27	16%	0.34	50%	0.28	10%
S6: Control, HiMA Binder	0.23	30%	0.34	16%	0.37	21%	0.32	9%
S13: Gap-gr., asphalt-rubber	0.61	17%	0.56	15%	0.51	57%	0.57	25%

As can be seen, critical aging had an inconsistent effect on J_c for lab-prepared mixtures, but generally decreased the J_c results, as expected, for the plant-produced mixtures.

Since 2016, the Louisiana Department of Transportation and Development has required a minimum J_c value of 0.6 kJ/m^2 for high traffic mixtures and 0.5 kJ/m^2 for medium to low traffic mixtures. These criteria are based on compacted specimens that have been long-term oven aged for five days at 85°C in accordance with AASHTO R30. Although the long-term aging in R30 and the critical aging procedure used in this study are likely to provide different aging effects on the mixtures, only the S13 mixture met the lower J_c criteria for the LMLC-CA and PMLC-CA sets.

This mixture, as well as those used in S5 and S6, performed very well under the extremely high traffic loading on the Test Track.

Figure 22 shows a bar chart for the J_c results of the critically-aged plant mix samples. The whiskers in this chart are the estimated standard deviations of J_c as described previously. Since these standard deviations were not determined in the standard way, ANOVA and pairwise comparison analyses were not conducted for these results. From this chart, it appears that J_c is able to distinguish the S13 mixture as superior and the two mixes that failed first from the other mixtures, but the overall rankings are not consistent with the field cracking data from the Test Track.

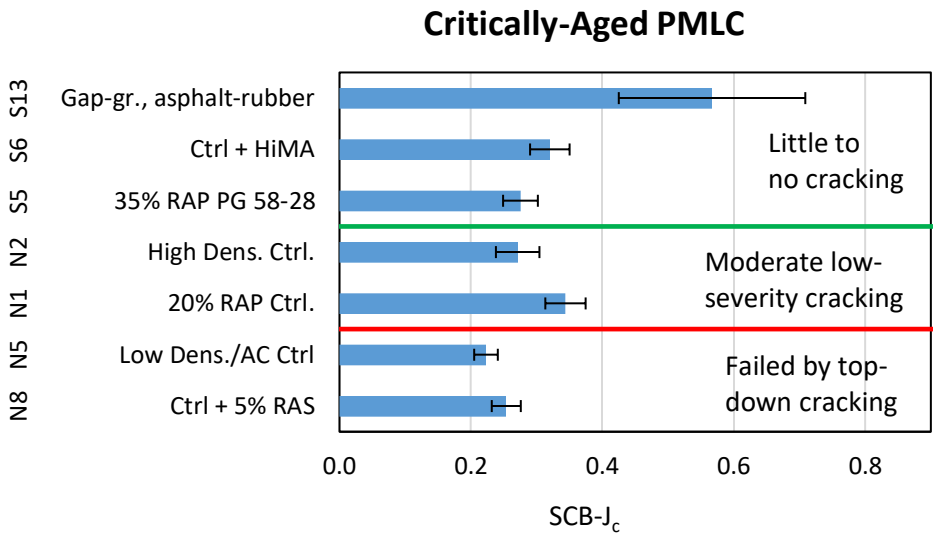

Figure 22. Chart of SCB-J_c Results and Field Performance Groupings

Figure 23 shows correlation plots of J_c results versus the observed top-down cracking for the four sample preparation and aging condition sets. Only the critically-aged PMLC set has a reasonably strong correlation between J_c and field performance. However, even for this set of data, some results are hard to rationalize. For example, N2 and N8 have similar J_c values (0.27 and 0.28, respectively), but these test sections had dramatically different top-down cracking performance on the Test Track.

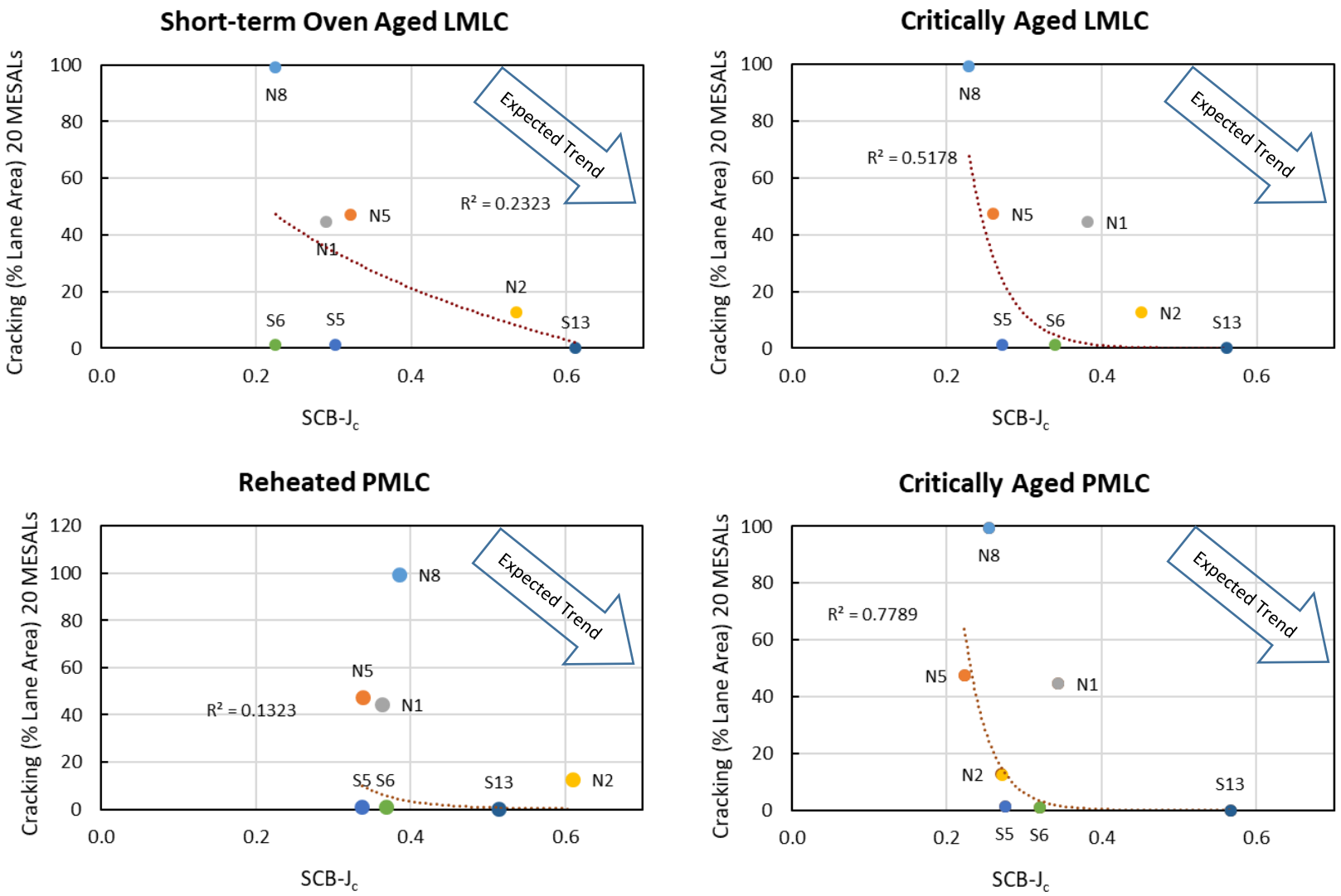

Figure 23. Correlations of SCB-J_c with Field Performance for the Lab and Plant Samples Subject to Different Aging Conditions

2.6.5 Illinois Flexibility Index Test Results

Table 10 summarizes the results of the I-FIT test. These results are based on a minimum of five replicates. According to the test, a higher flexibility index indicates better crack resistance. Overall, these results follow the expected trends within each sample type and conditioning method set. There appears to be a good spread in the average results, but the COVs are high (i.e. above 40%) for some mixtures. As expected, critical aging causes a substantial decrease in FI results. The impact of specimen air void contents in FI results can be seen by comparing the two sets of results for N2 and N5. For N2, FI results were slightly higher for specimens at 4% air voids compared to 7% air voids for STOA and reheated mix samples, but were lower after critical aging. For N5, FI results were substantially higher for specimens at 10% air voids compared to 7% air voids for each sample type and aging condition. Overall, the effect of specimen air void content on FI results is counterintuitive, that is the results seem to indicate that a lower density improves cracking resistance. That is clearly not the case as evident in the field cracking performance of N1 compared to N2.

Table 10. Results of IFIT Tests

Test Section and Mixture Description	LMLC-STOA		LMLC-CA		PMLC-RH		PMLC-CA	
	Avg.	COV	Avg.	COV	Avg.	COV	Avg.	COV
N1: Control	4.16	23%	0.63	50%	3.58	8%	0.59	51%
N2: Ctrl, Higher Dens. 7% Va	2.24	21%	0.25	76%	1.46	25%	1.38	74%
N2: Ctrl, Higher Dens. 4% Va	2.65	31%	0.10	76%	1.86	13%	0.10	67%
N5: Ctrl, Low Dens. & AC 7% Va	1.37	13%	0.21	53%	1.34	16%	0.67	93%
N5: Ctrl, Low Dens. & AC 10% Va	4.02	18%	0.74	34%	2.69	29%	0.80	35%
N8: Control + 5% RAS	0.43	44%	0.03	71%	0.39	18%	0.07	68%
S5: 35% RAP, PG 58-28	5.21	22%	0.70	30%	6.27	10%	1.79	16%
S6: Control, HiMA Binder	14.68	24%	3.43	20%	4.53	6%	3.77	16%
S13: Gap-gr., asphalt-rubber	15.12	34%	5.15	21%	10.40	42%	4.34	18%

The Illinois Department of Transportation (IDOT) currently requires one hour of short-term aging for mixtures containing low absorption aggregates and two hours of short-term aging for mixtures containing high absorption aggregates. Additionally, for surface mixtures only, IDOT uses a long-term aging protocol of three days at 95°C after I-FIT specimens are cut and notched. IDOT's current criteria for FI for dense-graded mixtures is a minimum of 8.0 after short-term aging, and a minimum of 5.0 after long-term aging. For SMA, the minimum FI is 16.0 after short-term aging, and 10.0 after long term aging. IDOT also has a separate criterion for a 4.75 mm mixture used for crack relief layers. Of the LMLC-STOA set of dense-graded Superpave mixtures, only the mixture from S6 exceeds the IDOT minimum criterion of 8.0 after short-term aging, but it does not meet the minimum FI of 5.0 after long-term aging. The mixture from S13 is similar to an SMA but it does not meet IDOT's minimum SMA criterion of 16.0 after short-term aging or the minimum FI of 10.0 after long-term aging. However, comparisons of these results with the Illinois criteria must be taken with caution since the aging procedures are different. A few other states have different preliminary criteria for flexibility index.

Figure 24 shows a bar chart for the FI results of the critically-aged plant mix samples. The whiskers represent plus and minus one standard deviation of FI. It is clear that FI does a good job of ranking the mixtures according to their top-down cracking performance.

The ANOVA indicated that mixtures had statistically different FI results and the Games-Howell post-hoc pairwise comparison determined which mixtures were statistically different from one another. It can be seen from the pairwise comparisons in Figure 24 that FI did not statistically distinguish the moderately performing mixtures from the poor performing mixtures due partly to the relatively high variability of some FI results. Also, the mixture from S5, which performed very well on the Test Track, had FI results that were not statistically grouped with the other good performing mixtures (i.e., S6 and S13). Setting a preliminary FI criterion between the results for S5 and N2 seems reasonable; therefore, a minimum FI threshold of 1.5 for critically-aged PMLC mixtures should provide good resistance to top-down cracking. Further research, including benchmarking studies and additional field validation studies, should be considered before implementation of any criteria.

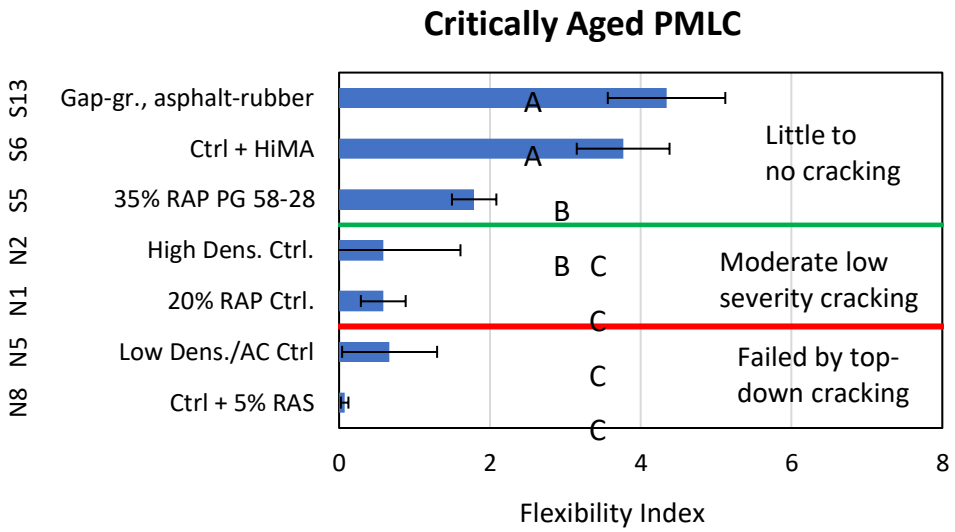

Figure 24. Chart of Statistical Comparisons of FI among Mixtures with Performance Groupings

Figure 25 shows the correlation plots of FI versus the top-down cracking observed on the Test Track for the four sample preparation and aging condition sets. Each chart shows a strong correlation between FI and the amount of top-down cracking at the conclusion of the experiment. These results indicate that FI is a good indicator of top-down cracking resistance.

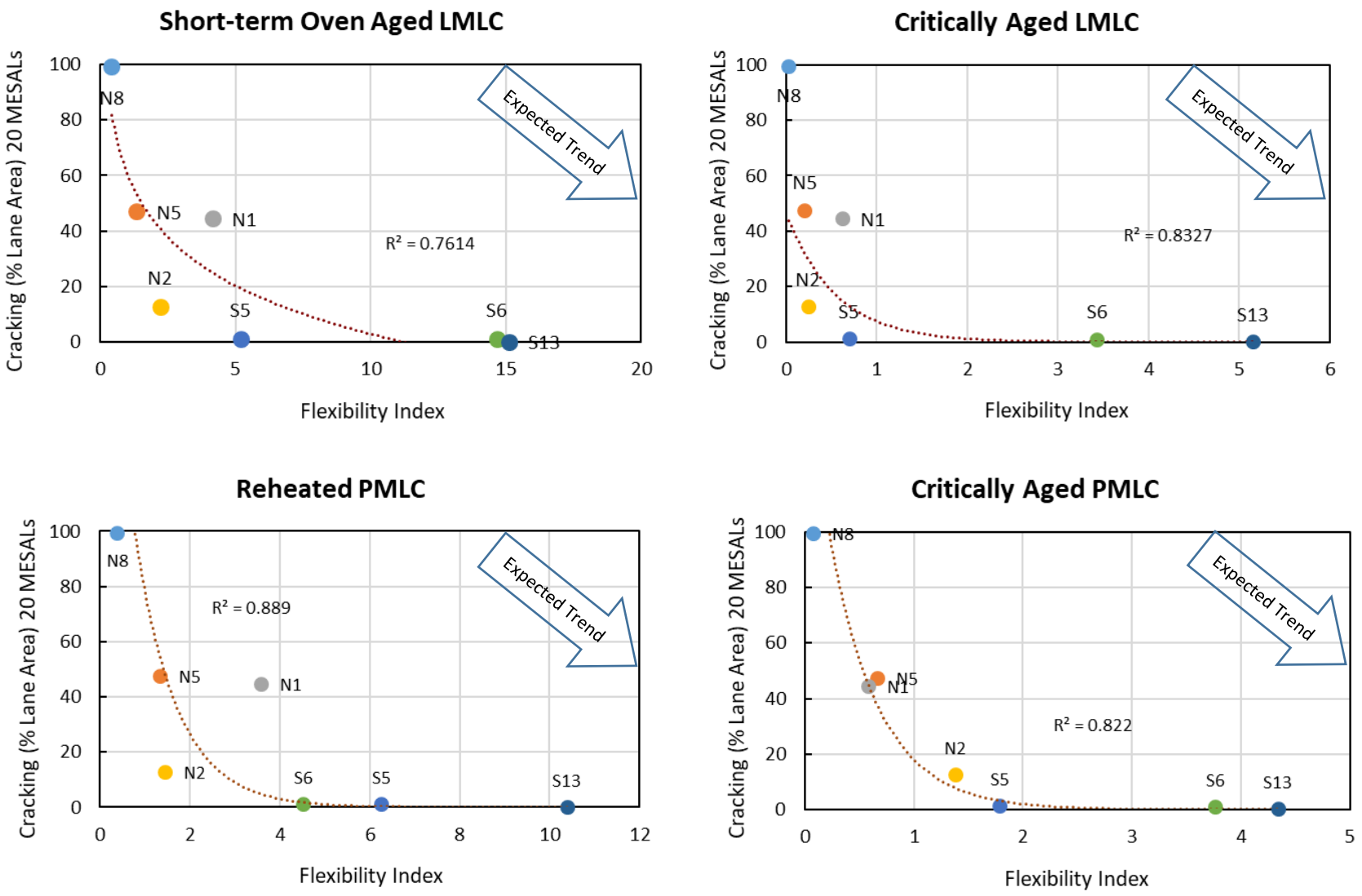

Figure 25. Correlations of FI with Field Performance for the Lab and Plant Samples Subject to Different Aging Conditions

2.6.6 IDEAL Cracking Test Results

Table 11 summarizes the results of the IDEAL-CT. These results are based on a minimum of five replicates. For this test, a high CT_{Index} indicates better crack resistance. As expected, CT_{Index} results for each mixture decreased substantially with the critical aging procedure. It can also be seen that the CT_{Index} results for the LMLC-CA set are similar to the corresponding results of the PMLC-CA, set which indicates that the lab preparation of the mixtures provides similar results as plant-produced mixtures.

As with the FI results, the effect of specimen air void contents on CT_{Index} can be seen by comparing the two sets of results for N2 and N5. For N2, CT_{Index} results were substantially lower for specimens at 4% air voids compared to 7% air voids for each sample type and aging condition. For N5, CT_{Index} were substantially higher for specimens at 10% air voids compared to 7% air voids for. Overall, the effect of specimen air void contents on CT_{Index} results is counterintuitive, that is the results seem to indicate that a lower density improves cracking resistance. However, the field cracking performance of N1 compared to N2 shows that is not true.

Table 11. Summary of CT_{Index} Results

Test Section and Mixture Description	LMLC-STOA		LMLC-CA		PMLC-RH		PMLC-CA	
	Avg.	COV	Avg.	COV	Avg.	COV	Avg.	COV
N1: Control	30.2	10%	7.3	13%	26.2	21%	8.8	9%
N2: Ctrl, Higher Dens. 7% Va	27.2	9%	10.3	17%	20.7	10%	10.8	18%
N2: Ctrl, Higher Dens. 4% Va	13.9	10%	6.1	13%	13.2	14%	5.1	18%
N5: Ctrl, Low Dens. & AC, 7% Va	19.2	7%	6.5	17%	15.9	14%	7.6	12%
N5: Ctrl, Low Dens. & AC, 10% Va	33.2	13%	11.8	11%	23.8	21%	8.6	12%
N8: Control + 5% RAS	10.9	23%	2.8	28%	6.7	30%	2.4	23%
S5: 35% RAP, PG 58-28	41.6	17%	10.7	17%	32.4	15%	16.3	9%
S6: Control, HiMA Binder	80.8	16%	22.2	22%	32.9	11%	18.7	20%
S13: Gap-gr., asphalt-rubber	133.1	27%	63.4	19%	208.1	49%	68.4	19%

Figure 26 shows the bar chart for the CT_{Index} results of the critically-aged plant mix samples. The CT_{Index} ranking of the mixtures is consistent with the field performance of the test sections. For the critically- aged set of PMLC samples, a CT_{Index} criterion of 15 appears to discriminate good performing mixtures from moderately performing mixtures based on their top-down cracking performance on the Test Track.

The ANOVA indicated that some mixtures had statistically different CT_{Index} results. The Games-Howell post-hoc pairwise comparison determined which mixtures were statistically different from one another as indicated by the letters down the middle of the chart. Mixtures that do not share a letter are significantly different at a 95% confidence level. It can be seen that the CT_{Index} result for the mixture from S13 is superior to all other mixtures and that the mixture from N8 is the worst mixture, which is consistent with the top-down cracking performance on the Test Track. The pairwise comparisons of CT_{Index} also statistically distinguished the mixtures with little to no cracking from the mixtures having a moderate amount of low severity cracking. It is important to note that none of the Games-Howell groupings overlapped, which further indicates that CT_{Index} is effective in distinguishing the cracking resistance of mixtures.

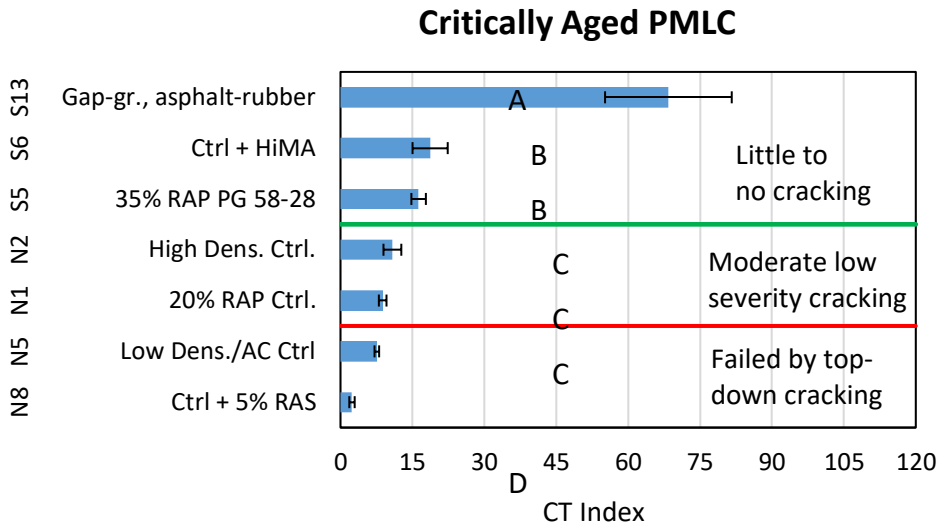

Figure 26. Chart of Statistical Comparisons of CT_{Index} among Mixtures with Performance Groupings

Figure 27 shows the correlations of CT_{Index} with the top-down cracking observed on the Test Track for the four sample preparation and aging condition sets. Each chart shows a strong correlation between the CT_{Index} and top-down cracking at the conclusion of the experiment. These results indicate that CT_{Index} is a good indicator of top-down cracking resistance.

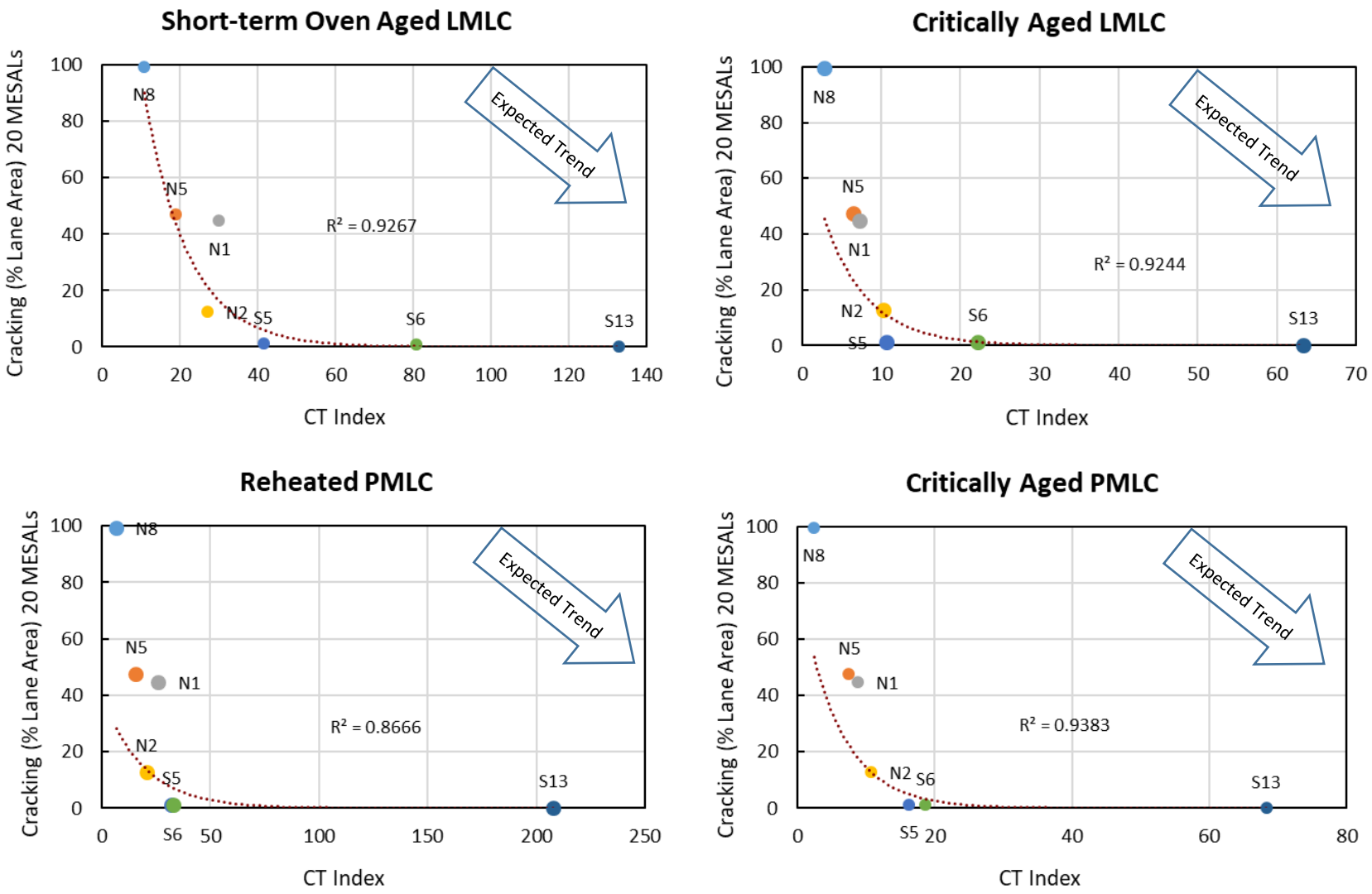

Figure 27. Correlations of CT_{Index} with Field Performance for the Lab and Plant Samples Subject to Different Aging Conditions

2.6.7 AMPT Cyclic Fatigue Test

Table 12 shows the results for the AMPT cyclic fatigue test fatigue cracking index parameter, S_{app}. The cyclic fatigue test was added to the experimental plan after the work on lab-prepared mixtures was completed, so the test was only conducted on plant-produced samples. Three replicates were tested for each of the seven plant-produced mixture at the reheated condition and the critically aged condition.

The S_{app} index parameter was developed by North Carolina State University (NCSU) to include the effects of a mixture's modulus and toughness on the amount of fatigue damage the material can tolerate under loading. The S_{app} value is determined at the average of the high-temperature and low-temperature binder performance grade from LTPPBind Online for the project of interest minus three degrees Celsius. The AMPT test data are processed through the *FlexMAT*™ program to calculate the representative S_{app} value. Higher S_{app} values indicate better fatigue resistance of the mixture.

Table 12. Summary of Fatigue Index Parameter, S_{app}, from AMPT Cyclic Fatigue Tests

Test Section and Mixture Description	PMLC			
	Reheated		Critically-Aged	
	Representative S_{app}	COV of S_{app}	Representative S_{app}	COV of S_{app}
N1: Control	26.46	20%	18.13	15%
N2: Control, Higher Density	35.38	8%	24.83	4%
N5: Control, Low Dens. & AC	26.49	5%	15.29	24%
N8: Control + 5% RAS	7.58	27%	6.90	9%
S5: 35% RAP, PG 58-28	43.95	32%	47.23	10%
S6: Control, HiMA Binder	53.83	38%	52.29	14%
S13: Gap-gr., asphalt-rubber*	32.54	4%	29.20	11%

*Results reported are from NCSU analysis

NCAT conducted the cyclic fatigue tests in accordance with AASHTO TP 107 and analyzed the data using *FlexMAT*™. Results for the S13 mixture were lower than expected, so NCSU analyzed the data and found that the mixture had a second peak in the phase angle vs. C (or modulus) plot. They noted that this was not surprising based on findings in literature that asphalt-rubber mixtures are a two-phase system and exhibit two peaks in the stress-strain plots under tensile loading. None of the other mixtures had the second peak. The results shown in Table 12 for S13 are the S_{app} values determined by NCSU.

Figure 28 shows the bar chart for S_{app} results for the critically-aged set of samples. Note that the order of the mixes in this chart differs from the other bar charts so that the Games-Howell groupings could be shown in a logical way. Results for S13 were moved down in the ranking to third place based on its representative S_{app} value. From this chart, it appears that S_{app} correctly ranks the mixtures in terms of their top-down cracking performance on the Test Track, with the possible exception of the gap-graded, asphalt-rubber mixture in S13 which had no cracking. The five Games-Howell groupings are not consistent with the three field performance groupings.

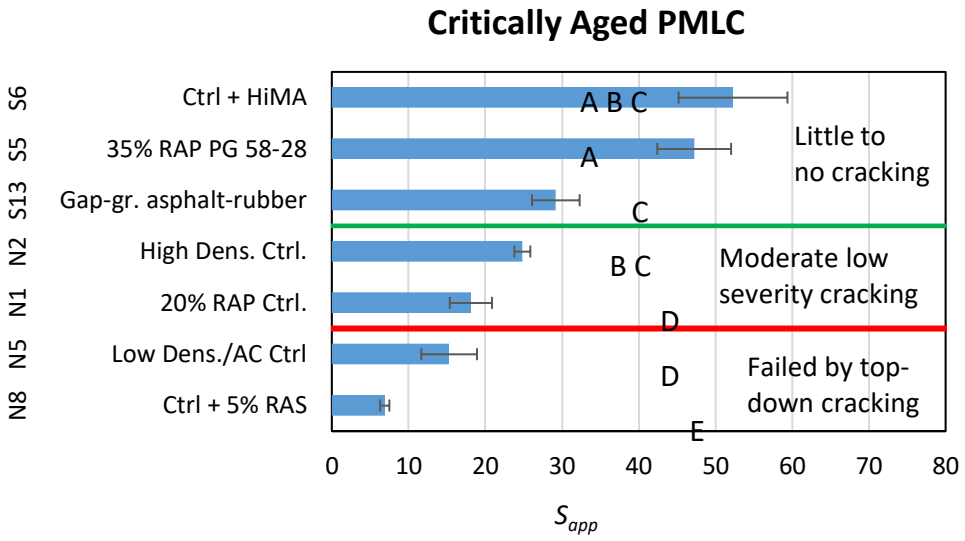

Figure 28. Chart of Comparisons of S_{app} among Mixtures with Performance Groupings

Table 13 shows NCSU's recommended S_{app} criteria for short-term aged mixtures based on the field performance of 105 asphalt mixtures with a range of RAP contents, binder grades, and warm mix asphalt technologies (*12*). The NCAT Test Track would be considered Very Heavy traffic in this table. The field performance of the Test Track Cracking Group Experiment appears to support the recommended criteria for the Very Heavy traffic level as the S_{app} criterion of 30 separates the test sections with little to no cracking from the test sections with moderate low-severity top down-cracking. The exception is the gap-graded, asphalt rubber mixture from S13 with a S_{app} of 29.2 that marginally failed the minimum criterion of 30. This indicates that the Cyclic Fatigue test or its criteria may need to be adjusted for this mixture type.

Table 13. Recommended Criteria for Sapp Fatigue Index Parameter

Traffic (million ESALs)	Traffic Tier	S_{app} Limits
Less than 10	Standard	$S_{app} > 8$
Between 10 and 30	Heavy	$S_{app} > 24$
Greater than 30	Very Heavy	$S_{app} > 30$
Greater than 30 and slow traffic	Extremely Heavy	$S_{app} > 36$

Figure 29 shows the correlation of S_{app} values with the observed top-down cracking from the Test Track. For both the reheated and critically-aged sets, the plots show strong correlations between the cyclic fatigue test index parameter and top-down cracking performance. These results indicate that S_{app} is a good indicator of top-down cracking resistance.

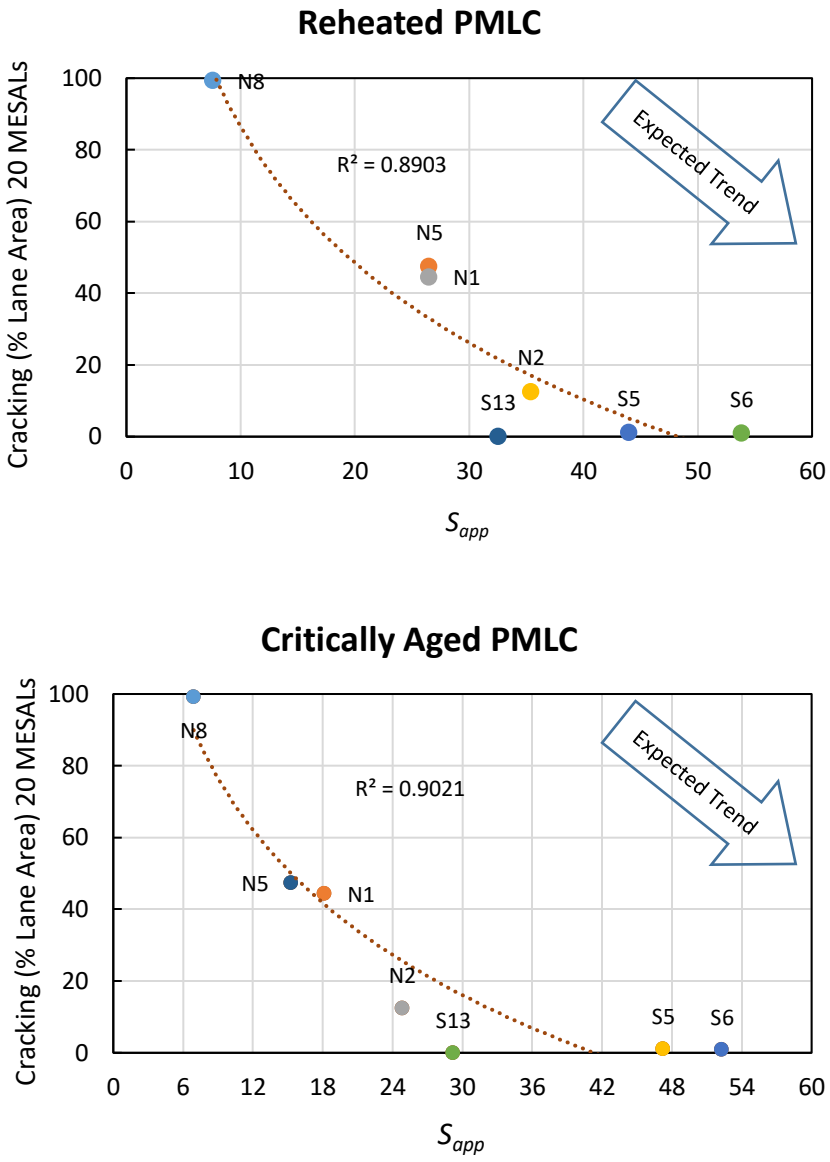

Figure 29. Correlations of S_{app} with Field Performance based on Reheated (Top) and Critically-Aged (Bottom) PMLC Samples

2.7 Summary of Analyses for the Cracking Tests

A summary of important statistical measures from the analyses of the top-down cracking tests evaluated in this study is provided in Table 14. The average COV is the mean within-lab COV from all seven mixtures for each of the four sample preparation and aging condition sets, except for the AMPT cyclic fatigue which only had reheated and critically-aged PMLC results. This is an indication of the within-lab variability, or repeatability, of the tests. All of these COVs are very consistent with those reported in published literature (*13*). The test with the lowest COV is the NCAT version of the overlay test, β parameter. The test with the highest COV is the I-FIT. The second column indicates the number of statistical groupings from the post-hoc Games-

Howell pairwise comparison analysis. A higher number of groupings is an indication of the test's ability to provide statistical distinctions among different mixtures. The Texas-OT method β parameter and the AMPT cyclic fatigue S_{app} parameter have the highest number of groupings. Although, the CT_{Index} had one less grouping than OT-TX β and Cyclic Fatigue S_{app} comparisons, no mixture had CT_{Index} results that belonged to more than one statistical group. This absence of overlapping groupings is also a strong indicator of the ability of the IDEAL-CT to provide results that are discerning among different mixtures. The last column in Table 14 provides the range of coefficients of determination, R^2, for the correlations with top-down cracking field performance for the four sample preparation and conditioning sets. The tests that consistently provided R^2 values above 0.85 were the IDEAL-CT test and the AAMPT Cyclic Fatigue test, with only two correlations available for the Cyclic Fatigue test. Other tests that also provided strong lab to field correlations were the OT-TX, OT-NCAT and I-FIT.

Table 14. Summary of Statistical Measures of Top-Down Cracking Tests

Test and Parameter	Average COV	Games Howell Groups	Range of R^2
Energy Ratio, ER	Not available	Not applicable	0.03 to 0.28
Texas Overlay Test, β	17%	5	0.76 to 0.91
NCAT Overlay Test, β	10%	4	0.79 to 0.97
Louisiana SCB, J_c	20%	Not applicable	0.13 to 0.78
Illinois Flexibility Index Test, FI	34%	3	0.76 to 0.89
IDEAL Cracking Test, CT_{Index}	18%	4	0.87 to 0.94
AMPT Cyclic Fatigue, S_{app}	16%	5	0.89 to 0.90

2.8 Conclusions

After four and a half years of in-service aging and trafficking there was a very good spread in the observed top-down cracking of the seven test sections in the Cracking Group experiment, illustrating that surface mixture properties are a key factor in top-down cracking performance.

Based on the analysis of the seven cracking tests evaluated in this experiment, the following conclusions are provided:

- The energy ratio results failed to match the field performance for top-down cracking. This test also lacks practicality for routine use due to the complexity and time to complete the three parts of the test, so it is not recommended for implementation.
- The Texas overlay test β parameter is a very good indicator of a mixture's resistance to top-down cracking. It is a much more discerning indicator than cycles to failure. The effect of air voids on test results is not counterintuitive as with some other cracking tests. For OT-TX tests on critically-aged mixtures, a β value of about 1.75 appears to separate asphalt mixtures with good from moderate cracking resistance. The key disadvantages of this test are the time required to prepare specimens and cost of the equipment. For these reasons, it is not a practical cracking test for day-to-day use in BMD and testing for quality assurance.
- The NCAT-modified version of the overlay test is also a very good indicator of resistance to top-down cracking. A maximum β value of 0.37 is recommended as a preliminary criterion for critically-aged mixtures based on the PMLC results of this experiment. The NCAT version of the OT has a lower coefficient of variation than the Texas procedure

and the testing time is faster. Like the Texas version, the effect of air voids on the results of the NCAT-OT method is not counterintuitive, but it suffers from the same disadvantages of tedious sample preparation and high equipment cost.

- The results of the Louisiana SCB test did not adequately distinguish the top-down cracking resistance of the mixtures in this experiment. Two of the mixtures that performed very well on the NCAT test Track had J_c results very similar to those of mixtures that had moderate low-severity cracking. Other disadvantages of this test are that it does not lend itself to standard methods of variability analysis, as well as the time and cost of preparing the notched semi-circular specimens.
- The flexibility index from the I-FIT procedure does a fair job of correlating with the top-down cracking field performance of this experiment. However, due to the high variability of FI for several mixtures, the critically-aged PMLC results were not statistically discerning among some good and moderately performing mixtures or between good and poor performing mixtures. Like the Louisiana SCB test, a disadvantage of the I-FIT is the time and cost of preparing the specimens. Another concern about this test is that FI results are affected by specimen air void contents in an incorrect manner. Specimens with lower air voids have lower FI results, which is counter to the field cracking performance as evidenced by the Test Track performance of sections N1 versus N2 in this experiment.
- The CT_{Index} from the IDEAL-CT method is a very good indicator for resistance to top-down cracking. It has strong correlations to the field performance of the NCAT test sections and the results are statistically discernable from mix to mix. For critically-aged samples, a minimum CT_{Index} of 15.0 is recommended as a preliminary criterion for good resistance to top-down cracking. As with the I-FIT procedure, a concern about the IDEAL-CT is that CT_{Index} is affected by specimen air void contents in an incorrect manner. Until this issue is corrected, it is recommended that the test only be conducted on specimens compacted to 7.0±0.5%. The IDEAL-CT method is well suited to everyday use in BMD and testing for quality assurance.
- The AMPT cyclic fatigue test index parameter, S_{app}, correlated very well with the observed top-down cracking in the test sections for this experiment. The results also support NCSU's recommended minimum S_{app} criterion of 30 for short-term aged mixture samples for Very Heavy traffic pavement applications. However, the S_{app} results for the gap-graded, asphalt rubber mixture appear to be lower than what they should be based on excellent field performance on the Test Track and the results of other cracking tests in this study. This may indicate that the cyclic fatigue test or its criteria needs to be adjusted for this mixture type. Significant disadvantages of this test are the time and cost to prepare specimens, cost of the equipment, and complexity of data analysis. For these reasons, it is not well suited for routine use in BMD or quality assurance testing. For further information on equipment costs and time to complete many of the BMD tests, see the Balance Mix Design Resource Guide (*13*).

The NCAT critical-aging procedure was initially developed and further validated as part of this study and has been detailed elsewhere (*2, 13, 14*). Key findings from those studies are as follows:

- Top-down cracking occurs after several years of in-service aging as the asphalt binder in the surface layer stiffens and loses relaxation properties. The rate of aging likely differs based on climatic factors and characteristics of the binders, but information from several national studies indicate that top-down cracking begins to be evident at a critical field aging condition of approximately 70,000 cumulative degree days (CDD).
- To evaluate the resistance of surface mixtures to top-down cracking, it is appropriate to first condition surface mixtures using a laboratory aging protocol that results in binder and mixture properties that are similar to those from field aging of approximately 70,000 CDD. Given that there is a significant aging gradient with depth from the surface, it is not believed to be necessary to further condition non-surface mixtures beyond what occurs during plant production or during the laboratory short-term aging procedure in AASHTO R30 that is intended to simulate aging during production. Ongoing research is further evaluating this assumption.
- A loose-mix aging protocol of five days at 95°C was found to simulate field aging at approximately 70,000 CDD. An alternate loose-mix aging protocol at 135°C was evaluated for periods of 6, 12, and 24 hours. Analysis of the rheological and chemical binder properties indicate loose-mix aging for eight hours at 135°C would be similar to five days at 95°C. No significant difference in the oxidation-hardening relationship was evident for loose-mix aging at 95°C versus 135°C for the limited set of materials in the aging protocol development experiment. NCAT has referred to the loose-mix aging at 135°C for eight hours to simulate 70,000 CDD as the "critical-aging" protocol.
- Statistical analysis comparing cracking tests results of lab-prepared and plant-produced mixtures indicate that after critical-aging there is no statistical difference between lab and plant mixtures for each of the cracking test parameters reported in this chapter. This finding suggests that laboratory prepared mixtures can be used to correctly assess the cracking resistance of surface mixtures as part of a BMD procedure.

2.9 References

1. West, R., D. Timm, B. Powell, M. Heitzman, N. Tran, C. Rodezno, D. Watson, F. Leiva, and A. Vargas. *Phase VI (2015-2018) NCAT Test Track Findings*, NCAT Report 18-04, National Center for Asphalt Technology, Auburn, AL, 2018.
2. Chen, C. *Validation of Laboratory Cracking Tests for Field Top-down Cracking Performance*. Dissertation, Auburn University, Auburn, AL, 2020.
3. Roque, R., B. Birgisson, C. Drakos, and B. Dietrich. Development and Field Evaluation of Energy-based Criteria for Top-down Cracking Performance of Hot Mix Asphalt. *Journal of the Association of Asphalt Paving Technologists*, Vol. 73, 2004, pp. 229-260.
4. Garcia, V. M., A. Miramontes, J. Garibay, I. Abdallah, G. Carrasco, R. Lee, and S. Nazarian. Alternative Methodology for Assessing Cracking Resistance of Hot Mix Asphalt Mixtures with Overlay Tester, *Journal of the Association of Asphalt Paving Technologists*, 2017, pp. 527-548.
5. Garcia, V. M., A. Miramontes, J. Garibay, I. Abdallah, and S. Nazarian. *Improved Overlay Test for Fatigue Resistance of Asphalt Mixtures*, Report 0-6815-1, Center for Transportation Infrastructure Systems, 2016.

6. Ma, W. *Proposed Improvements to Overlay Test for Determining Cracking Resistance of Asphalt Mixtures*. MS thesis. Auburn University, Auburn, Ala., 2014.
7. Cooper III, S. B., W. King, and M. S. Kabir. Testing and Analysis of LWT and SCB Properties of Asphalt Concrete Mixtures. Presented at Louisiana Transportation Conference, Baton Rouge, LA, 2013. http://www.ltrc.lsu.edu/pdf/2016/FR_536.pdf.
8. Ozer, H., I. L. Al-Qadi, J. Lambros, A. El-Khatib, P. Singhvi, and B. Doll. Development of Fracture-based Flexibility Index for Asphalt Concrete Cracking Potential Using Modified Semi-circle Bending Test Parameters. *Construction and Building Materials*, Vol. 115, 2016, pp. 390-401.
9. Zhou, F., S. Im, L. Sun, and T. Scullion. Development of an IDEAL Cracking Test for Asphalt Mix Design and QC/QA, *Journal of the Association of Asphalt Paving Technologist*s, 2017, pp. 549-577.
10. Wang, Y. D., B. S. Underwood, and Y. R. Kim. Development of a Fatigue Index Parameter, S_{app}, for Asphalt Mixes Using Viscoelastic Continuum Damage Theory. *International Journal of Pavement Engineering,* 2020. https://www.tandfonline.com/action/showCitFormats?doi=10.1080/10298436.2020.1751844.
11. Moore, N. *Evaluation of Laboratory Cracking Tests Related to Top-Down Cracking in Asphalt Pavements*. MS thesis. Auburn University, Auburn, AL, 2016.
12. FHWA Tech Brief. *Cyclic Fatigue Index Parameter (S_{app}) for Asphalt Mixture Performance Engineered Mixture Design*, Office of Construction and Pavements, FHWA-HIF-19-091, 2019.
13. Yin, F. and R. West, Balanced Mix Design Resource Guide, Information Series-143, National Asphalt Pavement Association, 2020.
14. Chen, C., F. Yin, P. Turner, R., West, and N. Tran. Selecting a Laboratory Loose Mix Aging Protocol for the NCAT Top Down Cracking Experiment, *Transportation Research Record: Journal of the Transportation Research Board*, Transportation Research Board of the National Academies, Washington, D.C., 2018.
15. Chen, C., F. Yin, A. Andriescu, R. Moraes, D. Mensching, N. Tran, A. Taylor, and R. West. Preliminary Validation of the Critical Aging Protocol for NCAT Top-down Cracking Experiment. *Journal of the Association of Asphalt Paving Technologists*, 2020.

3. ALABAMA LONG-TERM EVALUATION OF OPEN-GRADED FRICTION COURSE MIXTURES

Dr. Fan Gu

3.1. Background

The Alabama Department of Transportation (ALDOT) has used open-graded friction course (OGFC) mixtures for many years. A typical OGFC mix in Alabama consists of a 12.5 mm nominal maximum aggregate size (NMAS), 0.3% cellulose fiber, and 6.0% asphalt binder modified with styrene-butadiene-styrene (SBS) polymer. However, ALDOT has limited its use due to premature raveling issues occurring in the OGFC surface layer after approximately six or seven years in service. Generally, raveling is a problem of material damage rather than structural damage. The raveling distress is a result of wear from the repeated shearing force between tire and pavement surface, moisture damage, or insufficient asphalt-aggregate bonding. One potential solution is to adjust ALDOT's OGFC mix design procedure to improve the durability of OGFC mixtures in Alabama.

3.2. Objective and Scope

The objective of the study was to evaluate potential changes in ALDOT's mix design for OGFC to improve the durability of these mixtures in the field. These potential changes in aggregate NMAS, addition of fiber and asphalt binder were evaluated in the three test sections (E9A, E9B, and E10) on the NCAT Test Track.

3.3. Mix Design

The three experimental OGFC mixtures were designed based on a 12.5 mm OGFC mix design previously approved by ALDOT, which consisted of 91% #78 granite aggregate, 8% M10 granite aggregate, 1% baghouse fines, 0.3% cellulose fiber, and 6% PG 76-22 asphalt binder modified with SBS polymer. While ALDOT determines the optimum asphalt binder content based on a surface constant and oil absorption procedure described in ALDOT-259 procedure, "Open-Graded Asphalt Concrete Friction Course Design Method," most of the OGFC mix designs in Alabama have 6.0% PG 76-22 asphalt binder, which is the minimum asphalt binder content specified by ALDOT for OGFC mixtures. The three experimental OGFC mixtures paved on the NCAT Test Track were as follows:

- For Section E9A, the OGFC mixture was designed with a 9.5 mm NMAS gradation instead of a 12.5 mm NMAS gradation. This mix design consisted of 44% #78 granite aggregate, 50% #89 granite aggregate, 6% M10 granite, 0.3% cellulose fiber, and 6% PG 76-22 asphalt binder modified with polymer. Due to the availability of aggregate materials during the construction, this mixture was produced slightly coarser on 12.5 mm and 9.5 mm sieves, but it was still much finer than the ALDOT-approved 12.5 mm OGFC mixture. Thus, this mix was considered a 9.5 mm mix in this study.
- For Section E9B, the OGFC mixture was designed with a 12.5 mm NMAS gradation similar to the one utilized in the state approved OGFC mix design. It had 91% #78 granite aggregate, 8% M10 granite aggregate, 1% baghouse fines, and 6% PG 76-22 asphalt binder modified with polymer. This mix design also included 0.05% synthetic fiber to prevent draindown of the thick asphalt binder film from aggregate particles.

- The same 12.5 mm NMAS gradation was used in the OGFC mix design for Section E10. However, the mix design had 6.3% recycled tire rubber (RTR) modified asphalt, which consisted of 5.8% base asphalt modified by adding 12% RTR (by weight of asphalt binder). The RTR was a minus No. 30 mesh size, and the base asphalt was a PG 67-22. No fiber was added to the mix in order to determine whether RTR alone could prevent drain-down and provide resistance to raveling.

During mix design, all of the binders were pre-blended with an antistrip agent at a dosage of 0.5% by weight of the base binder. Table 1 shows the component materials of the three experimental mixes as well as one typical OGFC mix approved by ALDOT. Table 2 includes the design gradations for the 9.5 mm and 12.5 mm OGFC mixtures.

Table 1. Mixes Used in the ALDOT OGFC Study

Section ID	NMAS, mm	Fiber Type and Content	Binder PG and Content	Purpose for Selected Mix
--*	12.5	Cellulose, 0.3%	SBS PG76-22, 6.0%	ALDOT Approved Mix
E9A	9.5	Cellulose, 0.3%	SBS PG76-22, 6.0%	Evaluate Effect of Aggregate NMAS
E9B	12.5	Synthetic, 0.05%	SBS PG76-22, 6.0%	Evaluate Effect of Fiber
E10	12.5	No Fiber	RTR PG76-22, 6.3%	Evaluate Effect of Binder and Fiber

*This mix was not paved on the NCAT Test Track.

Table 2. Design Aggregate Gradations for ALDOT OGFC Mixtures

Sieve Size (mm)	Percent Passing	
	9.5 mm OGFC	12.5 mm OGFC
19.0	100.0	100.0
12.5	98.5	95.7
9.5	87.2	56.1
4.75	32.4	15.7
2.36	9.8	9.5
1.18	5.7	7.1
0.6	4.2	5.7
0.3	3.1	4.5
0.075	1.4	2.6

3.4. Field Performance

After the application of 20 million equivalent single axle loads (ESALs) from 2012 to 2017, the three OGFC mixtures still performed well on the track and showed no signs of raveling or cracking. ALDOT decided to continue trafficking these sections in the 2018 Test Track cycle (from 2018 through 2021) in order to evaluate the long-term durability of the three OGFC mixtures. This section presents the field performance of these sections for the three research cycles (from 2012 through 2021) with approximately 30 million ESALs of truck traffic.

3.4.1. Roughness

Roughness is related to pavement construction quality and pavement distresses (e.g., pothole, shoving). Fewer changes and lower values in roughness are indicative of better durability. In this study, roughness was measured in accordance with AASHTO R 57 using an Automatic Road Analyzer (ARAN) Van. Roughness in each wheel path was reported as Mean International

Roughness Index (MIRI) in in/mi. Roughness measurements as a function of traffic loading are shown in Figure 1. Roughness in all of the sections did not change over the past two test cycles from 2015 through 2021, indicating that these three subsections still had excellent smoothness.

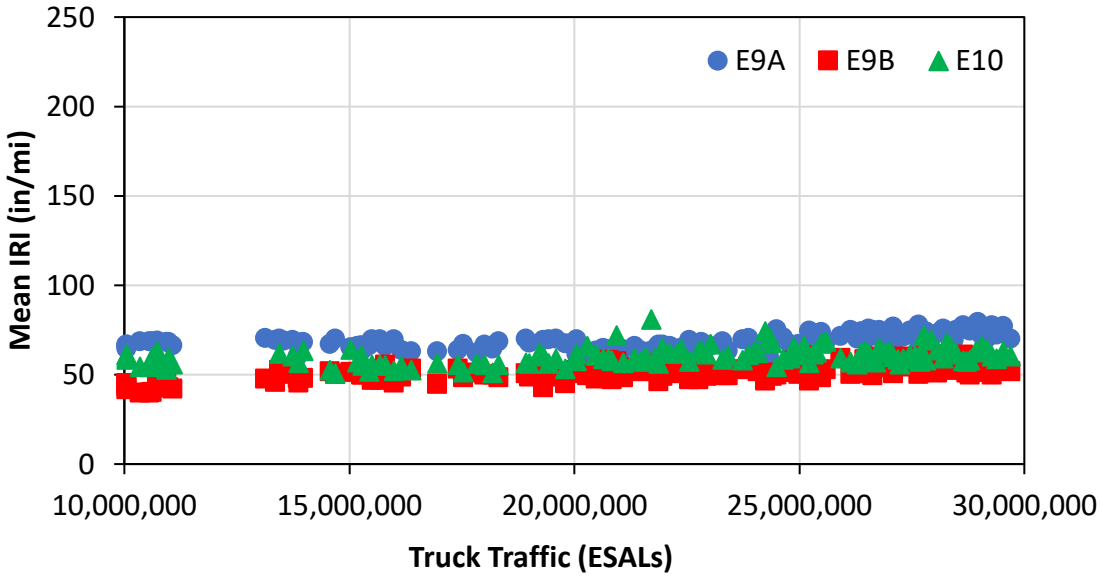

Figure 1. International Roughness Index Performance

3.4.2. Macrotexture

Surface macrotexture is the term used to define short (0.5 to 50 mm) wavelength irregularities in the surface of a pavement and is a function of the gradation of the aggregates in the mix and void structure, among others. Surface macrotexture measurements can provide a good indication of pavement durability, with durable pavements exhibiting smaller changes in surface texture as a function of time and traffic. Macrotexture in the wheelpath is reported using mean texture depth (MTD), which increases with the increase of raveling. Macrotexture performance of the test sections as a function of traffic loading is presented in Figure 2. The mean texture depth of the 9.5 mm mix in Section E9A was approximately the same as that for the 12.5 mm mix with synthetic fiber in Section E9B, and they were both higher than that of the 12.5 mm RTR modified OGFC mix in Section E10. The IRI and MTD levels of three test sections stayed the same over the past two research cycles, indicating that raveling was not occurring in these three test sections.

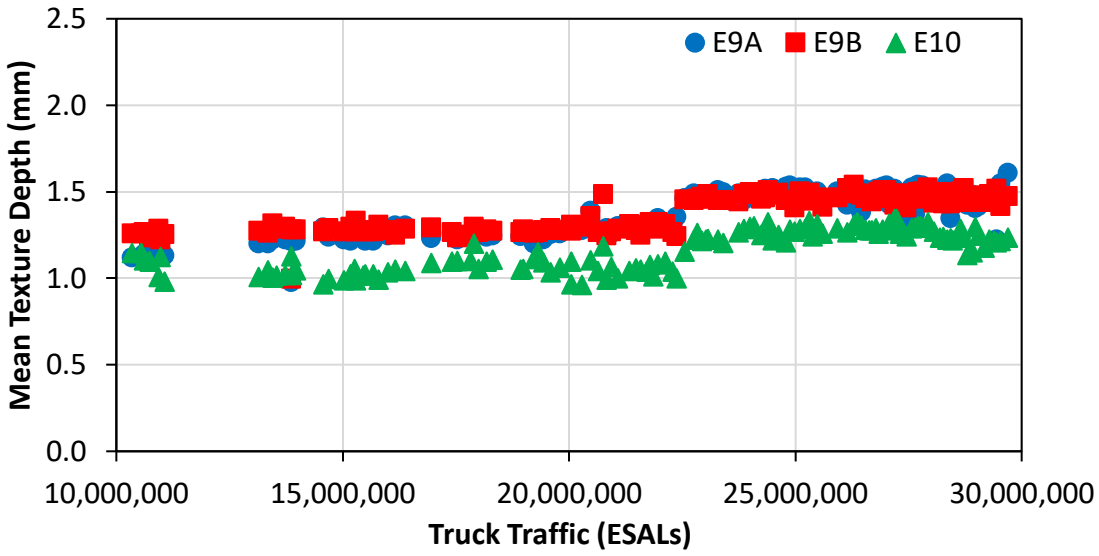

Figure 2. Mean Texture Depth Performance

3.4.3. Permeability

Field permeability in the wheelpath of the test sections was measured using the falling-head field permeameter, which was designed using a standpipe of a constant diameter. The standpipe is then sealed to the pavement using a flexible rubber base and metal base plate to force the sealant into the surface voids. Head loss is then recorded from the standpipes over time. Field permeability as a function of traffic loading is presented in Figure 3. The permeability of the 9.5 mm mix in Section E9A was always higher than both of the 12.5 mm mixes in Section E9B and Section E10. The slope of the permeability degradation curve for the 9.5 mm mix in Section E9A was flatter than those for the other two mixes, indicating that the 9.5 mm mix had a lower rate of permeability degradation over traffic as compared to both 12.5 mm mixes. For the two 12.5 mm mixes, the mix with synthetic fiber in Section E9B exhibited a slightly higher permeability than the RTR modified mix in Section E10. The 9.5 mm mix in Section E9A is still permeable (0.03 cm/sec) after the application of 20 million ESALs.

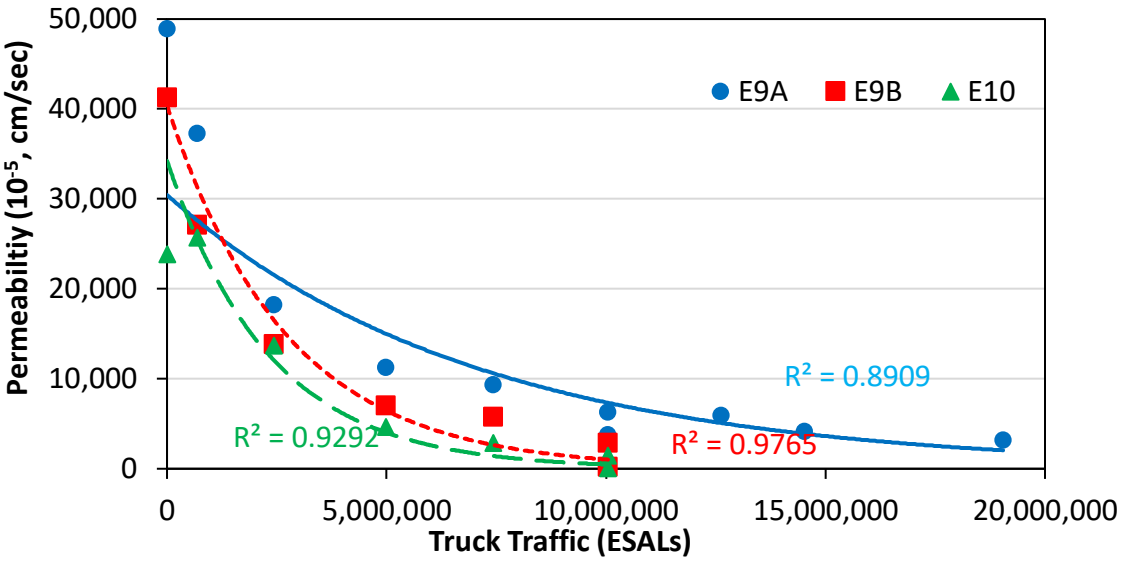

Figure 3. Field Permeability Performance

3.4.4. Rut Depth

As shown in Figure 4, the three test sections showed low rut depth (i.e., less than 0.1 inch) before the accumulated traffic load reached 25 million ESALs. After approximately 30 million ESALs of trafficking, these sections still had rut depths of less than 0.2 inch, indicating that these OGFC mixtures had excellent long-term rutting resistance.

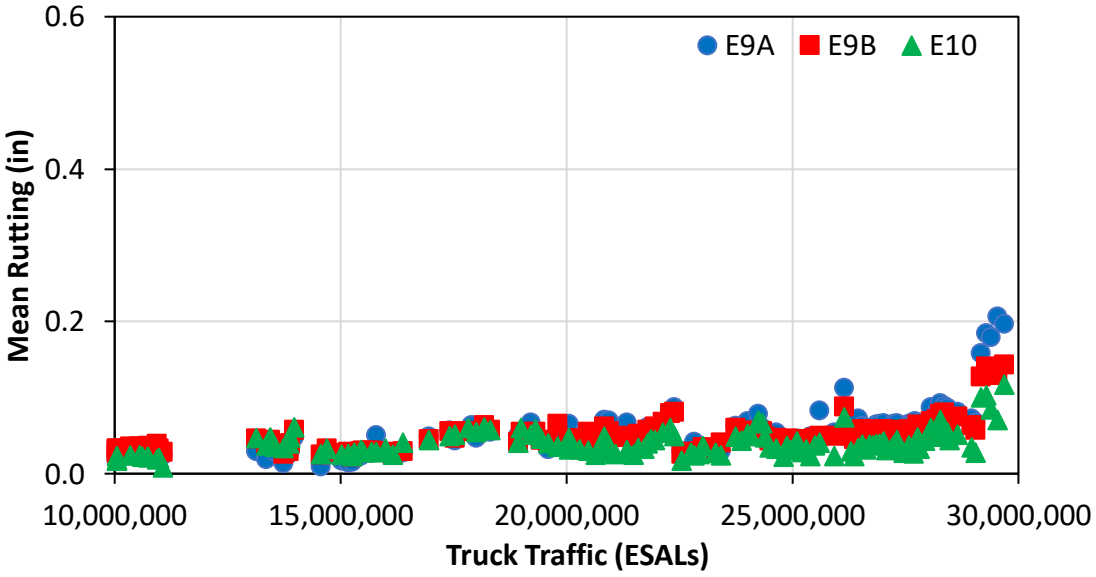

Figure 4. Rutting Performance

3.4.5. Cracking

As shown in Figure 5, Section E9B showed no cracking after approximately 30 million ESALs of truck traffic. Sections E9A and E10 showed no cracking distress before the accumulated traffic load reached 25 million ESALs. After 30 million ESALs of trafficking, Section E9A had about 2.3%

of lane area showing cracks, and Section E10 had about 6.1% of area exhibiting cracks. In general, these three OGFC sections showed excellent long-term cracking resistance. Compared to Section E9A (a 9.5 mm OGFC mixture) and Section E10 (using RTR binder), Section E9B (using synthetic fiber) had the best cracking performance after 30 million ESALs of trafficking.

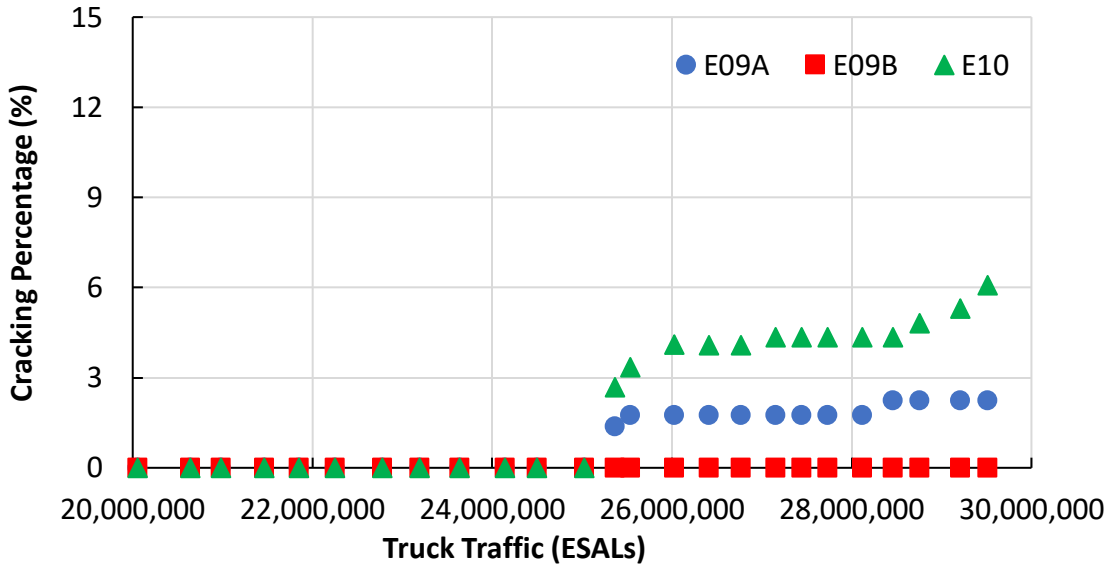

Figure 5. Cracking Performance

3.5. Conclusions

Based on the field performance evaluation at the Test Track from 2012 through 2021, the following conclusions are summarized.

- The roughness of all the test sections was consistent throughout the past three research cycles. The three sections showed excellent rutting and cracking resistance from 2012 through 2021 after approximately 30 million ESALs. Compared to the three experimental OGFC mixtures, the state-approved OGFC mixture was previously paved a few miles away from the NCAT Test Track on I-85 and lasted less than 20 million ESALs.
- The 9.5 mm mixture in Section E9A exhibited a greater field permeability and lower rate of permeability degradation compared to the 12.5 mm mixes in Sections E9B and E10.
- Compared to Sections E9A and E10, Section E9B containing synthetic fiber showed no cracking distress after 30 million ESALs.
- Based on the field evaluation performance, adjustments made in the three modified OGFC mixtures including using smaller NMAS, synthetic fiber and additional asphalt binder can potentially improve the long-term field performance of OGFC mixtures in Alabama.

4. ALABAMA EVALUATION OF HIGH PERFORMANCE THINLAYS

Dr. Carolina Rodezno

4.1 Background

Thinlays are think asphalt overlay mixes typically designed to be placed as thin as 1/2 in. They have been part of the NCAT Test Track since its second research cycle. This research has shown that when properly designed and constructed, thinlays can be both rut and crack resistant, and also provide good ride quality and frictional characteristics.

In 2003, the Mississippi DOT sponsored Section W6, which was paved with a ¾-inch thick, 4.75 mm nominal maximum aggregate size (NMAS) Superpave low volume road mix. The mixture contained 69% Alabama limestone, 30% hard sand, 1% hydrated lime (as an antistrip agent), and a PG 76-22 asphalt binder with a binder content of 6.1%. It was anticipated that the mix would only last 500,000 equivalent single axle loads (ESALs), but to date the section is still in place and has withstood over 60 million ESALs with no cracking, less than 5 mm of rutting, excellent smoothness, and no friction deficiencies.

In 2012, Mississippi sponsored Section S3 to place a redesigned thinlay including 25% RAP and relying on locally available "surplus" sand stockpiles in Mississippi. To date, the section has withstood 30 million ESALs with excellent performance.

In 2015, Tennessee DOT sponsored Section S4 to determine if a thin-lift asphalt overlay would have satisfactory rutting performance when placed as a thicker surface lift (1.5 inches thick). The mix placed was a 4.75-mm 75 blow Marshall mix that included 15% fine RAP, 60% hard limestone, 10% soft limestone, 15% natural sand, and a PG 64-22 asphalt binder with a binder content of 6.4%. The mixture demonstrated excellent performance with respect to rutting not exceeding 1.2 mm, no cracking, and good smoothness after 10 million ESALs.

4.2 Objective and Scope

In the 2018 Test Track research cycle, the Alabama DOT (ALDOT) sponsored Sections N10 and N11 for evaluation. The objective of this experiment was to assess the field performance of two thinlay mixes to provide ALDOT with thinner overlay alternatives that would be suitable options for pavement preservation on high volume roads. Section N10 used a 4.75 mm NMAS Stone Matrix Asphalt (SMA) mix, and Section N11 used a 4.75 mm NMAS dense-graded Superpave mix. In order to assess the performance of the thinlays without being impacted by the performance of the underlying layers, a structurally sound pavement was needed underneath. Therefore, a 7-inch asphalt base layer produced with a highly modified binder (H_iMA) binder was placed and compacted in one lift beneath the thinlays; the thickness of the base was controlled by the necessity of removal of the previous test sections.

4.3 Mix Designs and Construction

Table 1 provides a summary of the mix designs and quality control data of the mixtures. The SMA mix used a blend consisting of 62% limestone, 13% granite, 5% fly ash, and 20% fine fractionated RAP and included a PG 76-22 SBS binder with a total binder content of 6.0%. The dense-graded mix used a blend of 58% limestone, 22% sand, and 20% fine fractionated RAP and used a PG 67-22 binder with a total binder content of 6.1%. Currently, ALDOT does not allow

the use of high percentages of carbonate aggregate on surface mixes due to pavement friction concerns. ALDOT Standard Specification Sections 423 and 424 limit the percentage of carbonate aggregate using the British Pendulum Tester (BPT) on aggregate source samples polished for nine hours. The maximum allowable percentages of carbonate aggregate based on their British Pendulum Number (BPN 9) are presented in Table 2. The limestone source used for the N10 and N11 mixes had a BPN 9 of 26 at the time of construction. For this project a waiver was granted by ALDOT to be able to use higher percentages of limestone than currently allowed since it was desired to use locally available materials.

Table 1. Alabama Thinlay Mix Design Information

Mix Design Parameters	**N10**		**N11**	
Design Method	SMA		Superpave	
Compactive Effort	50 blows		60 gyrations	
Binder Grade	76-22 SBS		67-22	
Sieve	Design	QC	Design	QC
$P_{3/8"}$, %	100	100	100	100
$P_{\#4}$, %	90	81	95	95
$P_{\#8}$, %	54	52	72	76
$P_{\#16}$, %	36	38	53	59
$P_{\#30}$, %	27	29	36	43
$P_{\#50}$, %	19	21	22	27
$P_{\#100}$, %	15	15	14	18
$P_{\#200}$, %	12.4	10.2	9.8	10.5
Total Binder Content (P_b), %	6.1	6.0	6.0	6.1
Eff. Binder Content (P_{be}), %	5.9	5.8	5.9	5.2
Dust/Binder Ratio	2.1	1.8	1.6	2.0
RAP Binder Ratio	0.23	0.24	0.24	0.23
Rice Sp. Gravity (G_{mm})	2.509	2.495	2.513	2.492
Bulk Sp. Gravity (G_{mb})	2.421	2.465	2.429	2.412
VMA	17.8	15	17.5	15.4
VFA	80	82	81	79
Air Voids, %	3.5	3.2	3.3	3.2
Compacted thickness (mm)	19.1	20.3	N/A[1]	12.7
Mat Density (% G_{mm})	94	93.8	94	91.5

[1] Target rate for this mix was 50 PSY

Table 2 ALDOT Allowable Carbonate Aggregate Criteria for SMA and Superpave Mixes

BPN 9 of Aggregate Source	**Maximum Allowable Percentage of Carbonate Stone**
25 ≤	30
26-28	35
29-31	40
32-34	45
≥35	50

Section N10 was constructed on August 29, 2018. The mix was produced at 340°F and had an average in-place density of 93.8%. The as-built lift thickness was 20.3 mm. Figure 5 shows the mix placement and compaction of Section N10. Section N11 was constructed on August 27,

2018. The N11 mix was produced at 325°F and had an average in-place density of 91.5%. The as-built lift thickness was 12.7 mm. Figure 6 shows mix placement and compaction activities on Section N11. The planned thickness/rate of both N10 and N11 were designated by ALDOT, noting that Section N10 was thicker for higher performance preservation and Section N11 was thinner for a treatment with lower cost. Figures 1 and 2 show the milled surface of the inside lane. The outside lane is the research lane, and no changes were made to the base layer prior to placement of the thinlays.

Figure 5. N10 Mix Placement and Compaction

Figure 6. N11 Mix Placement and Compaction

4.4 Laboratory Testing

Plant produced mix was obtained during the construction of the test sections in order to fabricate plant-produced lab-compacted (PMLC) samples for performance testing. No critical aging was performed prior to laboratory performance testing. Reheated (RH) plant mix samples were used for Hamburg Wheel Tracking Tests (HWTT) to assess the rutting resistance of the mixes and the IDEAL-CT and I-FIT tests to evaluate their cracking resistance. In addition, the Cantabro abrasion test was used to assess the durability of the mixes.

4.4.1 HWTT Results

Both mixes were assessed for rutting resistance using the HWTT with testing conducted at 50°C. For each mix, two replicates were tested. The average rut depths at 10,000 passes and 20,000 passes for both mixtures are presented in Table 3. The results show higher rut depths for the

N10 mix (SMA), but both mixes have rut depths well below the typical specification criterion that limit rut depth to a maximum of 12.5 mm for 20,000 passes.

Table 3. Hamburg Wheel Tracking Test Results

Mix ID	Average Rut Depth (mm)	
	10,000 passes	20,000 passes
N10	3.5	5.0
N11	1.6	2.0

4.4.2 IDEAL-CT and I-FIT Test Results

The I-FIT and IDEAL-CT tests were used to assess the intermediate-temperature cracking resistance of both mixes using RH-PMLC samples. Both tests are performed using the indirect tensile mode of loading.

The I-FIT was performed in accordance with AASHTO TP 124. For this test, semi-circular asphalt specimens were trimmed from a larger 160 mm tall by 150 mm diameter gyratory specimen. A notch was then trimmed into each specimen at a target depth of 15 mm and width of 1.5 mm along the center axis of the specimen. The specimens were tested at a target test temperature of 25°C. Specimens were loaded monotonically at a rate of 50 mm/min until the load dropped below 0.1 kN after the peak was recorded. The Flexibility Index (FI) is the area under the load-displacement curve (Fracture Energy) divided by the slope at the curve inflection point post-peak. Mixtures with a higher FI are considered more cracking resistant than mixtures with a lower FI.

The IDEAL-CT was conducted in accordance with ASTM D8225-19. During the test, a monotonic load was applied along gyratory specimens at a constant displacement rate of 50 mm/min. The test was performed at 25°C. The load-displacement curve was analyzed to calculate the cracking tolerance index (CT_{index}) determined from the work of fracture, or the total area under the load displacement curve, and the slope of the curve at 25% reduction from the peak load. Similar to the FI parameter, higher CT_{index} values are desired for better cracking resistance of asphalt mixtures.

Table 4 shows the I-FIT and IDEAL-CT results and the number of replicates for mixes placed on Sections N10 and N11. The number of replicates vary because outlier results were identified per ASTM E 178 and are not included in the average values. The N10 mix exhibited higher FI than the N11 mix, but there is no statistical difference in the results. The Illinois DOT currently recommends a minimum FI criterion of 8 for AC surface mixes, and although state-specific FI criteria are likely needed to represent local climate conditions, the results for both mixes fell below the Illinois DOT requirement. IDEAL-CT results showed significantly higher CT_{index} values for the N10 mix compared to the N11 mix at 50.4, and 12.7, respectively.

Table 4. I-FIT and IDEAL-CT Test Results

Mix ID	I-FIT Results			IDEAL-CT		
	Average FI	Replicates	CV (%)	Average CT_{index}	Replicates	CV (%)
N10	2.4	9	18.4	50.4	5	15.2
N11	1.6	7	20.5	12.7	6	11.0

4.4.3 Cantabro Test Results

Cantabro test results were used to assess the durability potential of the two mixes. The test method followed was AASHTO TP 108-14 where compacted samples are individually placed in the Los Angeles Abrasion machine and tested for 300 revolutions at a rate of 30 to 33 revolutions per minute without the steel charges. The loose material is then discarded and the final specimen weight is recorded. The percent loss is calculated by subtracting the final weight from the original weight. Four replicates of each mix were tested, and the results are presented in Table 5. The results showed relatively low mass loss percentages for both mixes as an indication of adequate durability. In addition, the results were found to be statistically similar.

Table 5. Cantabro Abrasion Results

Mix ID	Average Cantabro Loss (%)	CV (%)
N10	5.8	4.9
N11	6.1	7.8

4.5 Field Performance

Sections were subjected to 10 million ESALs of heavy truck traffic applied over a period of approximately two years. Surface cracking, rutting, and smoothness in terms of international roughness index (IRI) were monitored weekly. In addition, surface friction was measured monthly using a locked-wheel friction test (LWFT) with a ribbed tire under wet conditions. At the end of the cycle, none of the sections had any signs of cracking. Rutting performance was also excellent with Sections N10 and N11 showing rut depths of 2.6 mm and 3.2 mm, respectively. IRI numbers for both sections were high from the beginning of the cycle due in part to the uneven finish of the underlying thick base layers that were placed in one lift. However, as presented in Figure 7, IRI remained stable for the duration of the cycle. Finally, Figure 8 presents the LWFT results of Sections N10 and N11. It can be observed that the friction numbers of both sections remained stable and above the safety threshold of 30 that has been established at the NCAT Test Track. This indicates that for the duration of the test cycle, both thinlays constructed with high percentages of limestone were able to maintain an acceptable friction performance.

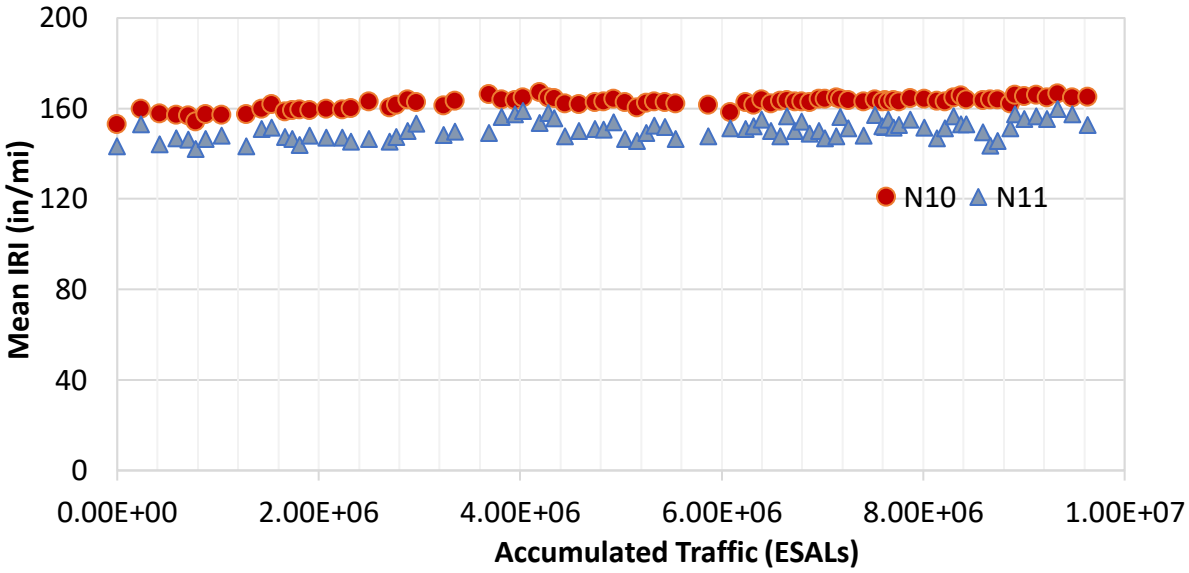

Figure 7. International Roughness Index Values

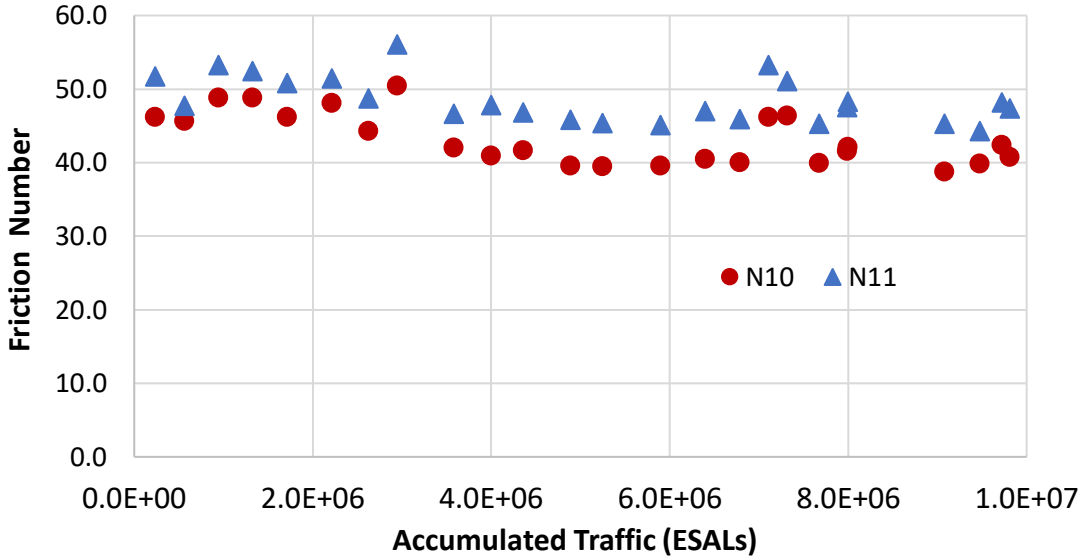

Figure 8. Locked-Wheel Friction Tester Results

4.6 Summary and Conclusions

This study sponsored by ALDOT built upon previous NCAT Test Track successes with thinlays as an alternative pavement preservation treatment for high volume roads. The experiment evaluated the performance of two test sections, N10 and N11, each constructed with 4.75 mm NMAS mixes, one an SMA and the other one a dense-graded Superpave mix. The findings of this study are summarized as follows:

- Both sections performed well after 10 million ESALs with no cracking and minimal rutting.
- Roughness in terms of IRI for both sections was high from the beginning of the test cycle but remained stable over time. This was attributed to the rough base layer placed in a single pass prior to the placement of the surface layers.
- LWFT results showed that both sections had friction values above the NCAT safety threshold value of 30. This indicates that despite the high percentage of limestone used for these mixes, the sections had an adequate friction performance at the end of the cycle as a result of the influence of sand/screenings. It may be possible to utilize the three-wheel polishing device in combination with a Dynamic Friction Tester (DFT) for laboratory mix design and/or approval to blend higher percentages of limestone for thinlays on open roadways. A study including these two tests will be conducted for Kentucky in the eighth Test Track cycle.
- HWTT results indicated that the mixes were not susceptible to rutting, which was supported with minimal field rutting in both sections.
- Cantabro test results suggested that the mixes had adequate and comparable durability performance.
- I-FIT results showed statistically similar FI results for both mixes, however, they were lower than the criterion established for Illinois DOT surface mixes. On the other hand, the IDEAL-CT results showed significantly higher CT_{index} values for mix N10 compared to N11. Despite these results, there was no indication of any field cracking; therefore, it is recommended to continue monitoring these sections to assess their long-term cracking performance.
- The results of this study indicate that it is feasible to construct alternative thinlays on structurally sufficient pavements in Alabama and achieve satisfactory performance.

5. EVALUATION OF BMD MIXTURE WITH HIGH RAP AND ANOVA ASPHALT REJUVENATOR

Dr. Nam Tran

5.1 Introduction

Approximately 100 million tons of asphalt materials are milled off roads each year (*1*), and these materials can be processed for use as reclaimed asphalt pavement (RAP) in new asphalt mixtures to reduce cost of materials as well as conserve natural resources and valuable landfill space. Because of these benefits, the national average RAP content used in new asphalt mixtures has increased over the years with the highest national average level being 21.1% reported for 2019 and 2020 (*2*, *3*). However, state departments of transportation (DOTs) are reluctant to allow higher RAP contents to be used in their projects because of the concern that adding more RAP without other improvements in the mixture would potentially reduce the performance of asphalt pavements, causing higher pavement maintenance and rehabilitation costs. Therefore, before allowing higher RAP contents in asphalt mixtures, DOTs want to ensure these mixtures will provide satisfactory performance.

One of the concerns for high RAP mixtures is related to the recycled asphalt binder. It is often oxidized and stiffer than the virgin binder used in the asphalt mixture. Increasing the RAP content may make the asphalt mixture stiffer and more susceptible to various modes of cracking (i.e., fatigue, thermal, and reflective cracking). To minimize the effect of oxidized asphalt binder on the quality of asphalt mixtures produced with high RAP contents, especially their resistance to cracking, several approaches have been evaluated over the years. One of these approaches is to use a rejuvenator to help achieve a desired performance grade (PG) of the total binder blend. In addition, the optimum contents of rejuvenator and virgin binder can be determined based on a balanced mix design (BMD) approach to improve the overall mixture resistance to both rutting and cracking.

Based on this concept, a high RAP mixture was designed with Cargill's Anova™ asphalt rejuvenator following the BMD approach and constructed on the NCAT Test Track for a field evaluation. In this mixture, the Anova asphalt rejuvenator was utilized to restore the performance properties of RAP binder, reducing the effect of a high RAP content on the mixture's long-term performance. This chapter provides a summary of this research effort and its key findings.

5.2 Research Objectives and Scope

The objective of this study was to determine the effectiveness of Anova asphalt rejuvenator in balancing cracking and rutting performance of high RAP mixtures within the BMD framework. The experiment was conducted by comparing the field performance of two surface mixtures under the same pavement structure as well as traffic and climatic conditions as follows:

- The control mixture was a 30% RAP mixture produced with a PG 64-22 binder. It was placed in Section N3A (hereafter referred to as N3A mixture).
- The experimental mixture was a 45% RAP mixture produced with a PG 64-22 binder and Anova asphalt rejuvenator. It was placed in Section N3B (hereafter referred to as N3B mixture).

- A third mixture was produced based on the same mix design as the experimental (N3B) mixture with 45% RAP but without the rejuvenator for laboratory testing only (hereafter referred to as N3B-NR mixture).

Prior to Test Track construction, two asphalt mix designs were conducted following the Virginia Department of Transportation (VDOT) BMD provisional specification. The provisional BMD specification comprises of three laboratory tests, including Asphalt Pavement Analyzer (APA), Indirect Tensile Asphalt Cracking Test (IDEAL-CT), and Cantabro abrasion test, to evaluate asphalt mixture susceptibility to rutting, cracking, and raveling, respectively.

The control asphalt mixture had 30% RAP with no rejuvenator, and it was placed in the surface layer of Section N3A. The experimental asphalt mixture had 45% RAP with Anova asphalt rejuvenator and was paved in the surface layer of Section N3B. Sections N3A and N3B are each 100 feet long. The experimental mixture was also produced without rejuvenator for laboratory testing only. The three plant-produced mixtures were tested using several performance tests, and the data were analyzed to assist the field evaluation at the Test Track.

5.3 Research Methodology

5.3.1 Experimental Plan

This study was divided into four tasks as illustrated in Figure 1, including (1) mix design, (2) mix production and placement, (3) laboratory performance testing, and (4) field performance evaluation. For this study, the mix designs were first conducted to meet the volumetric criteria. The optimum binder contents and rejuvenator dosage were then adjusted to achieve the performance thresholds required in the VDOT provisional BMD specification released in 2018. Table 1 provides a summary of the VDOT provisional BMD specification used in this study.

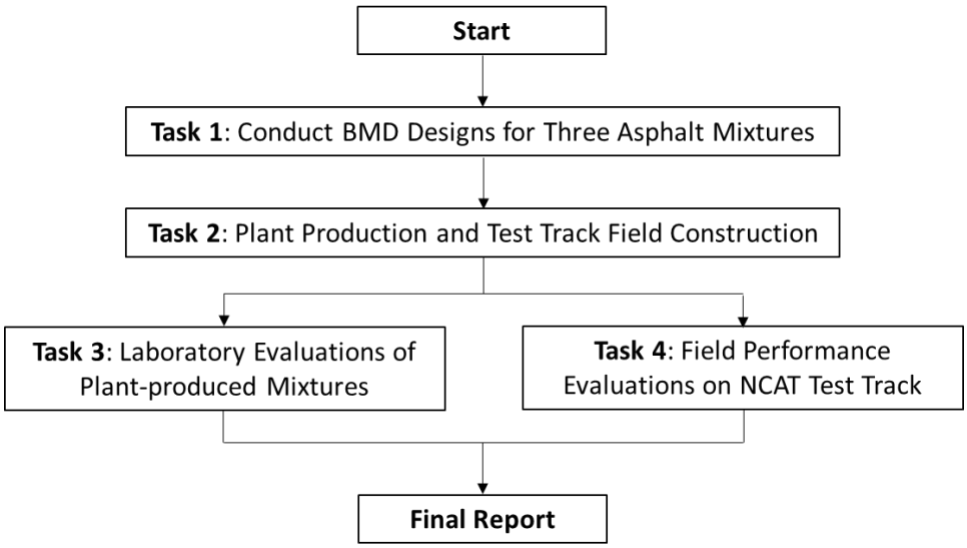

Figure 9. Experimental Plan

Table 6. Performance Testing Requirements in VDOT's BMD Provisional Specification

Test	Procedure	Specimens	Criteria
Asphalt Pavement Analyzer (APA) rutting	Testing is conducted to 8,000 cycles at 64°C with a wheel load of 120 lb and a rubber hose pressure of 120 psi.	Two replicates of two pills (150 mm in diameter by 75 ± 2 mm high) are prepared to achieve target air voids of 7 ± 0.5%. Note: Lab-produced loose mix is short-term aged for two hours at the design compaction temperature.	Rutting depth ≤ 8.0mm
Cantabro Abrasion Test	Testing is conducted to 300 rotations at a speed of 30-33 rotations per minute.	Three replicates (150 mm in diameter by 115 ± 5 mm high) are compacted to N_{design}. Specimen air voids are reported. Note: Lab-produced loose mix is short-term aged for four hours at 135°C prior to compacting.	Mass loss ≤ 7.5%
Indirect Tension Asphalt Cracking Test (IDEAL-CT)	Testing is conducted after specimens are conditioned at 25 ± 1°C for 2 ± 0.5 hours. After a contact load of 0.1 ± 0.02 kN is applied, loading is applied using load-line displacement control at 50 mm/minute.	Three replicates (150 mm in diameter by 62 ± 2 mm high) are compacted to 7 ± 0.5% air voids. Note: Lab-produced loose mix is short-term aged for four hours at 135°C prior to compacting.	CT_{index} ≥ 70

5.3.2 Materials

The component materials utilized in this research study were selected due to their use in an original volumetric mix design approved by VDOT for use in the state of Virginia.

The virgin asphalt binder used in this study was a PG 64–22. The same performance grade was used in the original VDOT-approved volumetric mix design. The asphalt binder was provided by an asphalt supplier that provided all the asphalt binders for the reconstruction of the 2018 Test Track.

Similar to the original VDOT approved volumetric mix design, two trap rock aggregate stockpiles, including #8 and #10, and one source of RAP were used in the mix designs for this study. These materials were provided by Chemung Contracting in Virginia.

The nominal maximum aggregate size (NMAS) of the final design gradation was 9.5 mm for both the control (i.e., N3A) and experimental (i.e., N3B and N3B-NR) mixtures, as summarized in Tables 2 and 3. The 1% baghouse fine was the passing #200 material from the #10 aggregate, and it was added to the design gradation to simulate the potential aggregate breakdown during plant production.

Table 7. Aggregate Gradation of the Control Mix

Sieve Size	Gradation (% Passing)				
	#8	#10	Baghouse Fine	RAP	Design
3/4"	100	100	100	100	100
1/2"	100	100	100	100	100
3/8"	91	100	100	99	97
#4	28	95	100	57	61
#8	8	64	100	38	38
#16	6	43	100	29	27
#30	6	29	100	22	20
#50	5	19	100	16	14
#100	4	10	100	12	10
#200	3.1	2.9	100.0	8.2	5.5
Cold Feed	33%	36%	1%	30%	100%

Table 8. Aggregate Gradation of the Experimental Mix

Sieve Size	Gradation (% Passing)				
	#8	#10	Baghouse Fine	RAP	Design
3/4"	100	100	100	100	100
1/2"	100	100	100	100	100
3/8"	91	100	100	99	97
#4	28	95	100	57	61
#8	8	64	100	38	38
#16	6	43	100	29	28
#30	6	29	100	22	21
#50	5	19	100	16	15
#100	4	10	100	12	10
#200	3.1	2.9	100.0	8.2	6.3
Cold Feed	25%	29%	1%	45%	100%

Two chemical additives were used in this study. The first, Anova 1815 rejuvenator, is a chemically modified vegetable oil-based recycling agent. It was designed to chemically balance and reactivate aged asphalt binder, thereby allowing more recycled materials (RAP and RAS) to be used in asphalt mixtures. In the laboratory, Anova 1815 was added directly to the asphalt binder followed by a low shear blending for three to five minutes to achieve homogeneity. For field production, the rejuvenator can be blended with the asphalt binder at the terminal or injected in-line into the asphalt binder at the asphalt plant (*4*). The Anova 1815 rejuvenator was used in the experimental mixture in this study.

While the control mix had no rejuvenator, it contained a chemical warm-mix additive named Anova 1501. The additive was designed to improve workability, facilitate compaction at lower temperatures, and enhance asphalt mixture resistance to moisture damage. A dosage rate in the range of 0.2 to 0.7% by total weight of the asphalt binder is recommended for this additive (*5*).

5.3.3 Volumetric and BMD Mix Designs

Two mix designs were needed for this study: one for the control mix with 30% RAP with a PG 64-22 binder and Anova 1501 warm-mix additive, and the other for the experimental mixture

with 45% RAP with the same PG 64-22 binder and Anova 1815 rejuvenator. The warm-mix additive and rejuvenator were preblended with the base binder during mix design at dosages recommended by the sponsor.

Based on the VDOT-approved volumetric mix design (N_{des} = 50) provided by Chemung Contracting in Virginia, the control mix design with 30% RAP was first verified to make sure it met all the VDOT volumetric requirements. The aggregate gradation of this mixture was then adjusted to create a design gradation for the experimental mixture with 45% RAP. The experimental mixture was then tested, and the optimum binder content was selected to meet all the VDOT volumetric requirements. The design gradations for the control and experimental mixtures are previously shown in Tables 2 and 3, respectively.

After the volumetric mix designs had been completed, the performance tests required in the VDOT provisional BMD specification were conducted for these mixtures, including APA for rutting, Cantabro for raveling, and IDEAL-CT for cracking. The thresholds for accepting a BMD mix design based on the results of these tests are previously summarized in Table 1.

In the first round of BMD testing, the volumetric mix designs for both mixtures met the APA rutting and Cantabro abrasion test criteria shown in Table 1, but they did not meet the IDEAL-CT cracking threshold. Since the VDOT provisional BMD specification allows the volumetric properties of a BMD mix design to drift outside the VDOT volumetric limits, the binder and rejuvenator contents could be adjusted to meet the IDEAL-CT cracking threshold without changing the design gradations of these mixtures. For the control mixture, the binder content was increased, and for the experimental mixture, both the binder content and rejuvenator content were adjusted. The final BMD mix designs for the control and experimental mixtures met all the requirements in the VDOT provisional BMD specification summarized in Table 1.

5.3.4 Plant Production and Paving at Test Track

Based on the BMD mix designs, the two mixtures were produced and placed on the Test Track on September 6, 2018. The control mixture was produced with Anova 1501 warm-mix additive that was in-line blended, and the mix temperature was approximately 310°F when it left the plant. After the control mix had been produced, the in-line pump was switched to Anova 1815 rejuvenator for producing the experimental mixture, and the temperature of this mixture was approximately 315°F when it left the plant. In addition, a third mixture was also produced based on the same experimental BMD mix design but without the rejuvenator for laboratory testing only.

The control mixture was placed in Section N3A (100 feet long). The paver was then hot-stopped to clean out the mix from the hopper. After that, the paving continued to place the experimental mixture in Section N3B (100 feet long), as shown in Figure 2.

The temperature measured behind the paver for the control mixture was 290°F, and the in-place density was 96.2% of G_{mm} of as-produced mix. Due to an incident at the Test Track, the temperature measured behind the paver for the experimental mixture was lower at 279°F. However, since the rejuvenator was also designed for use as a warm-mix additive, the experimental mixture still compacted well, and the in-place density was 96.8% of G_{mm} of as-produced mix. Table 4 summarizes the design and construction data for the two test sections.

Figure 10. Paving of Section N3A and N3B

Table 9. Design and Construction Data for Control and Experimental Sections

Design Method:	BMD		24 Hour High Temp. (F):	87
Compactive Effort (Ndes):	50 gyrations		24 Hour Low Temp. (F):	74
Binder PG:	64-22		24 Hour Rainfall (in):	0
Paving	**N3A - Control Mix**		**N3B - Experimental Mix**	
As-Built Sublot Lift Thickness(in):	1.5		1.5	
Approx. Underlying AC (in):	9.5		9.5	
Type of Tack Coat Utilized:	NTSS-1HM		NTSS-1HM	
Undilluted Target Tack Rate (gal/sy):	0.1		0.1	
Approx. Avg. Temp. at Plant (F):	310		315	
Avg. Mat Compaction (%Gmm):	96.2		96.8	
Sieve Size	**Design**	**QC**	**Design**	**QC**
25mm (1"):	100	100	100	100
19mm (3/4"):	100	100	100	100
12.5mm (1/2"):	100	100	100	100
9.5mm (3/8"):	97	95	97	96
4.75mm (#4):	61	56	61	56
2.36mm (#8):	38	36	38	38
1.18mm (#16):	27	26	28	27
0.6mm (#30):	20	18	21	20
0.3mm (#50):	14	11	15	13
0.15mm (#100):	9	7	10	9
0.075mm (#200):	5.5	4.9	6.3	6.1
Mix Properties				
Binder Content (Pb):	5.5	6.0	5.8	6.0
Eff. Binder Content (Pbe):	5.2	5.7	5.5	5.7
Dust-to-Eff. Binder Ratio:	1.1	0.9	1.1	1.1
RAP Binder Replacement (%):	24	25	38	38
RAS Binder Replacement (%):	0	0	0	0
Total Binder Replacement (%):	24	25	38	38
Rice Gravity (Gmm):	2.715	2.679	2.691	2.664
Bulk Gravity (Gmb):	2.636	2.608	2.628	2.624
Air Voids (Va):	2.9	2.7	2.3	1.5
Aggregate Gravity (Gsb):	2.973	2.966	2.963	2.949
VMA:	16.2	17.3	16.5	16.3
VFA:	82	85	86	91

5.3.5 Laboratory Evaluation of Plant-Produced Mixtures and Binders

During production, three plant mixtures were sampled for laboratory evaluation to assist the field evaluation, including the control 30% RAP mixture (N3A), the experimental 45% RAP mixture (N3B), and the 45% mixture without rejuvenator (N3B-NR). Table 5 includes the laboratory tests that were conducted to evaluate the following mixture performance properties:

- Cracking and fracture: IDEAL-CT, Overlay Test (OT), Illinois Flexibility Index Test (I-FIT), and Disc-Shaped Compact Tension (DCT) Test
- Rutting: APA and Hamburg Wheel Tracking Test (HWTT)
- Durability/raveling: Cantabro Abrasion Test
- Moisture susceptibility: Tensile Strength Ratio (TSR)

Table 10. Laboratory Evaluation Plan

Test	N3A		N3B		N3B-NR	
	Reheated	Aged[2]	Reheated	Aged	Reheated	Aged
Mixture Tests (by NCAT)						
Virginia Specification						
IDEAL-CT (VDOT)	x	x	x	x	x	x
APA (VDOT)	x		x			
Cantabro	x		x		x	
Other Specifications						
OT (NJDOT B-10)	x	x	x	x	x	x
I-FIT (AASHTO TP 124)	x	x	x	x	x	x
DCT (ASTM D7313)	x	x	x	x	x	x
TSR (AASHTO T283)	x		x			
HWTT (AASHTO T 324)	x		x			
Binder Tests (by Cargill)						
Extract/recovery/PG[1]	x	x	x	x	x	x

[1]Includes RAP and base asphalt binder sampled during construction; [2]Plant mix was reheated and critically aged for eight hours at 135°C prior to compaction (*6*).

During production, the PG 64-22 binder used to produce the asphalt mixtures was also sampled for verifying its performance grade (PG). In addition, asphalt binders were also extracted and recovered from the three plant-produced mixtures for testing. The extraction of the asphalt binder was performed by the ASTM D2172 test procedure (centrifuge method). The extracted asphalt binder was recovered by following the ASTM D1856 test procedure. The recovered asphalt binder was subjected to several levels of aging prior to testing, as summarized in Table 6. The recovered asphalt binder was graded in accordance with ASTM D7643 and the guidelines in the NCHRP 452 report (*7*). All of this testing was conducted at the Cargill laboratory.

Table 11. Aging Procedures

Aging Level	Description
HTPG: As Extracted LTPG: As Extracted + RTFO	Standard aging method, calibrated to correspond to standard M320 grades
HTPG: As Extracted + RTFO + 40-hr PAV LTPG: As Extracted + RTFO + 40-hr PAV	Additional PAV testing, reflecting an extended (2 x PAV) aging of asphalt binder

*HTPG: high temperature performance grade; LTPG: low temperature performance grade; RTFO: rolling thin film oven; PAV: pressurized aging vessel.

5.3.6 Field Performance Evaluation

The control and experimental asphalt mixtures were placed in Sections N3A and N3B as part of the seventh research cycle. Each test section is 100 feet long. Truck trafficking for the seventh research cycle started on November 26, 2018, and approximately 10 million equivalent single axle loads (ESALs) were applied on these test sections by the end of fleet operations on February 28, 2021.

Truck traffic on the Test Track was suspended every Monday to facilitate the collection of rutting, surface cracking, ride quality, and surface texture data. The ride quality and surface texture of each pavement surface were measured based on the international roughness index (IRI) and mean texture depth (MTD) using the Dynatest Mark IV inertial profiler. Rutting in the wheel paths of each test section was measured using the Dynatest Mark IV inertial profiler and the ALDOT beam procedure, as per the ALDOT T-392 standard specification. The ALDOT T-392 method uses a four-foot beam with a dial gauge to measure rut depths along the wheel path at predetermined locations in each test section of the Test Track. The accuracy of the rut depths obtained using the ALDOT beam method is estimated to be ± 2.5 mm.

The surface cracking data were obtained by initially carrying out a visual inspection of the test section, and the observed surface cracks were then mapped and measured. The area of the cracked section was determined by conducting a linear measurement of the cracks within the test section, which was then used to calculate the percent lane area of surface cracking.

5.4 Results and Discussion

5.4.1 Volumetric Mix Design with Performance Verification

The control and experimental mixtures were first designed based on VDOT's volumetric mix design (VMD) criteria. Based on the VDOT-approved volumetric mix design provided by Chemung Contracting in Virginia, the VMD for the control mixture with 30% RAP was verified. The gradation of the control mixture was then adjusted to conduct the VMD for the experimental mixture with 45% RAP. The design gradations for these mixtures are shown in Tables 2 and 3 with their volumetric properties provided in Table 7. Both mixtures met VDOT's volumetric mix design requirements.

Table 12. Results of Volumetric Mix Designs for Control and Experimental Mixtures

Design Method:	VMD		
Compactive Effort (Ndes):	50 gyrations		
Binder PG:	64-22		
Mix Properties	**N3A-Control**	**N3B-Experimental**	**Criteria**
% Total AC (Pb):	5.2	5.2	
Rice Gravity (Gmm):	2.729	2.717	
Bulk Gravity (Gmb):	2.620	2.608	
Design Air Voids (Va):	4.0	4.0	4.0
VMA*:	16.3	16.7	Min. 16.0
VFA:	76	77.3	70 - 85
Dust-to-Eff. Binder Ratio:	1.1	1.2	0.7 - 1.3
Eff. Binder Content (Pbe):	4.89	4.96	
Abs. Binder Content (Pba):	0.31	0.31	
% AC Contribution from RAP:	1.33	2.20	
% Virgin Binder:	3.86	3.04	
% RAP Binder Replacement:	26	42	
Agg. Bulk Gravity (Gsb):	2.973	2.963	
Agg. Effective Gravity (Gse):	3.000	2.989	
Agg. Absorption (Abs):	0.88	0.96	

*VMA was calculated based on G_{se} instead of G_{sb}

After the volumetric mix designs for the control and experimental mixtures were completed, their rutting and cracking resistance was evaluated using the APA and IDEAL-CT at the optimum binder contents. The test specimens for these mixtures were prepared according to the specimen fabrication procedure prescribed in the VDOT provisional BMD specification. Once testing was completed, the results were analyzed in accordance with ASTM E178, *Standard Practice for Dealing with Outlying Observations*, to determine the outliers in the APA and IDEAL–CT test results.

Table 8 summarizes the APA and IDEAL-CT results for the volumetric mix design of the control mixture. The average APA rut depth was 2.7 mm, which was less than the VDOT threshold value of 8.0 mm after 8,000 cycles. However, the CT_{index} results, which were determined from the IDEAL-CT test to evaluate the cracking resistance of asphalt mixture, showed that the control mix failed to meet the minimum CT_{index} criterion of 70.

Table 13. APA and IDEAL-CT Results for Volumetric Mix Design of Control Mixture

APA Rut Depth @ 8,000 Cycles (mm)		**CT_{Index} @ 25°C**	
Average	**Standard Deviation**	**Average**	**Standard Deviation**
2.6	0.36	44.9	8.8

For the experimental mixture, the APA and IDEAL–CT tests were conducted at the volumetric optimum binder content (i.e., 5.2%) with three rejuvenator dosages (referred to as low, medium, and high dosages) as recommended by the sponsor. In addition, the IDEAL-CT test was also conducted without the rejuvenator to evaluate its effect. The APA and IDEAL-CT results for the experimental mixture are shown in Figures 3 and 4, respectively. The following observations can be drawn based on the test results:

- As shown in Figure 3, the average rut depths of the experimental mixture determined at the three rejuvenator dosages were below the maximum threshold of 8.0 mm. Also, while the average rut depths were different amongst the three rejuvenator dosages, the difference was not statistically significant based on a one-way ANOVA statistical test at 5% significance level.
- The CT_{Index} results determined at the three dosages (i.e., low, medium, and high) were all below the minimum CT_{Index} threshold of 70, and they were not statistically different based on a one-way ANOVA statistical test at 5% significance level. However, they were statistically higher than the CT_{Index} for the experimental mixture without the rejuvenator. Also, the medium rejuvenator dosage yielded the highest average CT_{Index} results, so it was selected for further evaluation in this study.

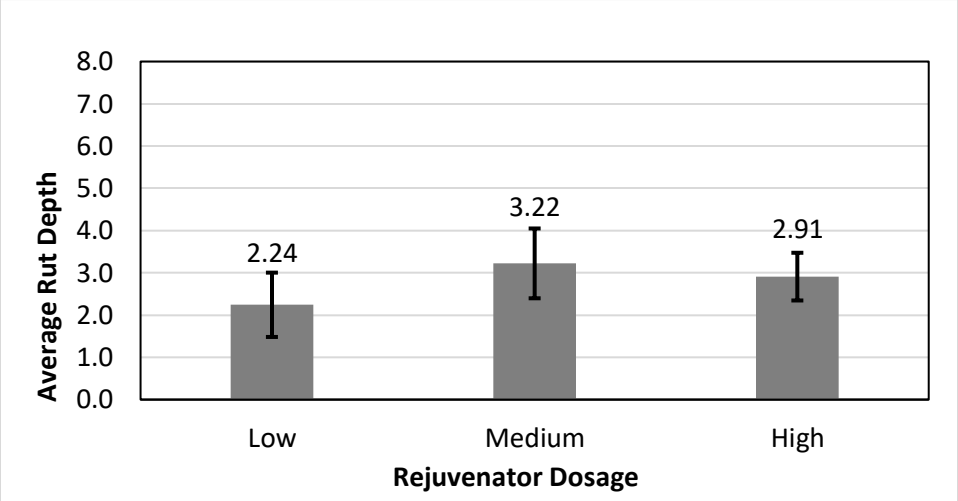

Figure 11. APA Results for Volumetric Mix Design of Experimental Mixture at Three Rejuvenator Dosages

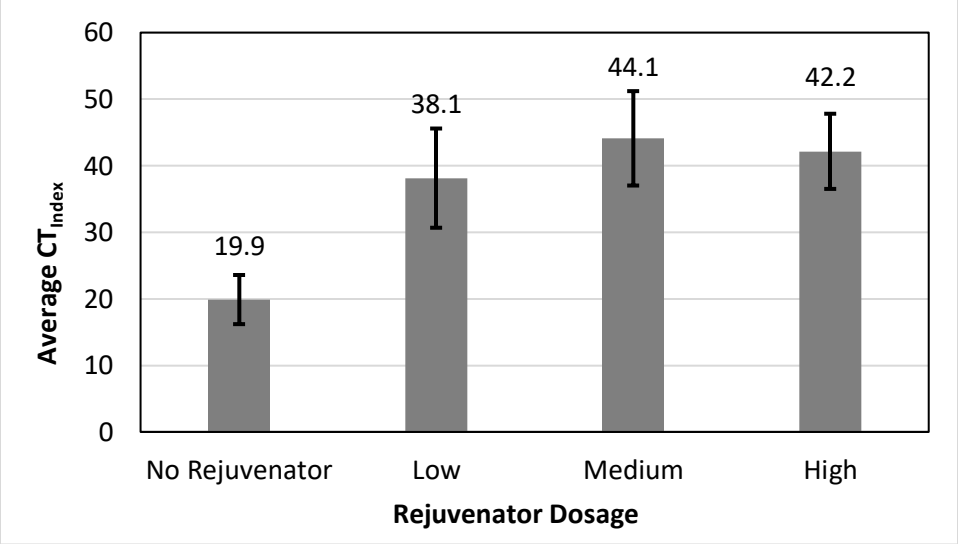

Figure 12. CT_{Index} Results for Volumetric Mix Design of Experimental Mixture at Three Rejuvenator Dosages

In summary, the volumetric mix designs for the control and experimental mixtures met the APA maximum rutting threshold, but they did not meet the minimum CT_{index} requirement. To improve the cracking resistance of these two mixtures, the next step was to increase the virgin binder contents as discussed in the following section.

5.4.2 Balanced Mix Design to Meet Performance Requirements

To select the optimum binder contents at which the cracking resistance of the control and experimental mixtures could meet the VDOT provisional BMD specification without adverse effects on their resistance to rutting and raveling, the APA, IDEAL-CT and Cantabro tests were conducted at multiple binder contents. Results would then be used to develop the correlations between the performance test results and the binder contents for these mixtures, which could then be used to determine the BMD optimum binder contents.

IDEAL – CT Results. Since IDEAL-CT testing was already conducted for the control mixture at 5.2%, additional IDEAL-CT testing was conducted at two higher binder contents, including 5.7% and 6.2%. Based on the correlation between the CT_{Index} results and binder contents, shown in Figure 5, the CT_{index} results would increase for higher binder contents. In addition, it was estimated that the control mixture would meet the minimum CT_{Index} threshold of 70 at approximately 5.5% binder content. An additional set of IDEAL-CT specimens were later tested at 5.5% asphalt content, and the average CT_{Index} for this set was 74.6, as plotted in Figure 5.

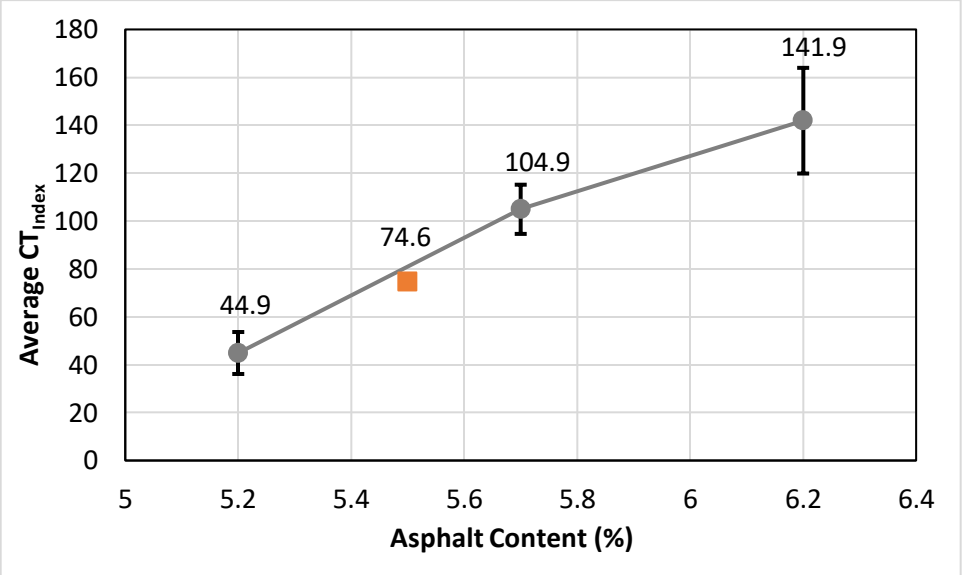

Figure 13. CT_{Index} Results for Control Mixture at Various Asphalt Contents

For the experimental mixture, additional IDEAL-CT testing was conducted at the medium rejuvenator dosage for two other binder contents at 5.7% and 6.2%, and at 5.5% for comparing with the control mixture. The CT_{Index} results were greater for higher binder contents, as shown in Figure 6. Also, based on the CT_{Index} results, it was estimated that the experimental mixture would pass the minimum CT_{Index} threshold of 70 at approximately 5.8% asphalt content. Thus, another set of IDEAL-CT specimens was prepared at 5.8% asphalt content, and the CT_{Index} for this set was 80.5, as plotted in Figure 6.

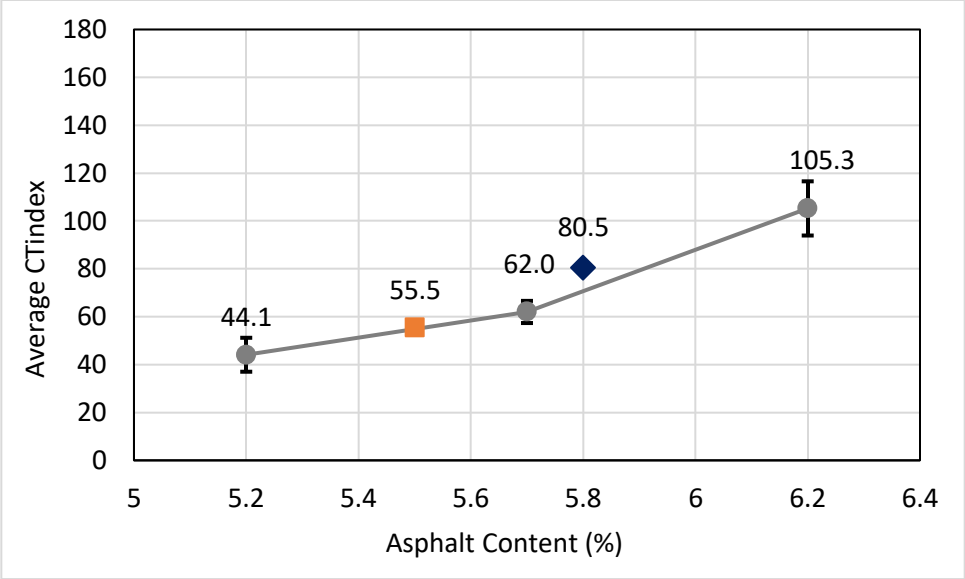

Figure 14. CT_{Index} Results for Experimental Mixture at Various Asphalt Contents

Based on the CT_{Index} results, the selected asphalt contents for the control and experimental mixtures were 5.5% and 5.8%, respectively, for a field evaluation at the Test Track.

APA Test Results. Figure 7 shows the APA test results conducted based on the VDOT provisional BMD specification at the same three binder contents (i.e., 5.2%, 5.7%, and 6.2%) at which the IDEAL-CT testing was performed. The highest average APA rut depth of 4.2 mm was observed for the experimental mixture at 6.2% asphalt content and with the medium rejuvenator dosage. Based on these results, both the control and experimental mixtures passed the maximum APA rut depth requirement of 8.0 mm at 5.5% and 5.8% asphalt contents, respectively.

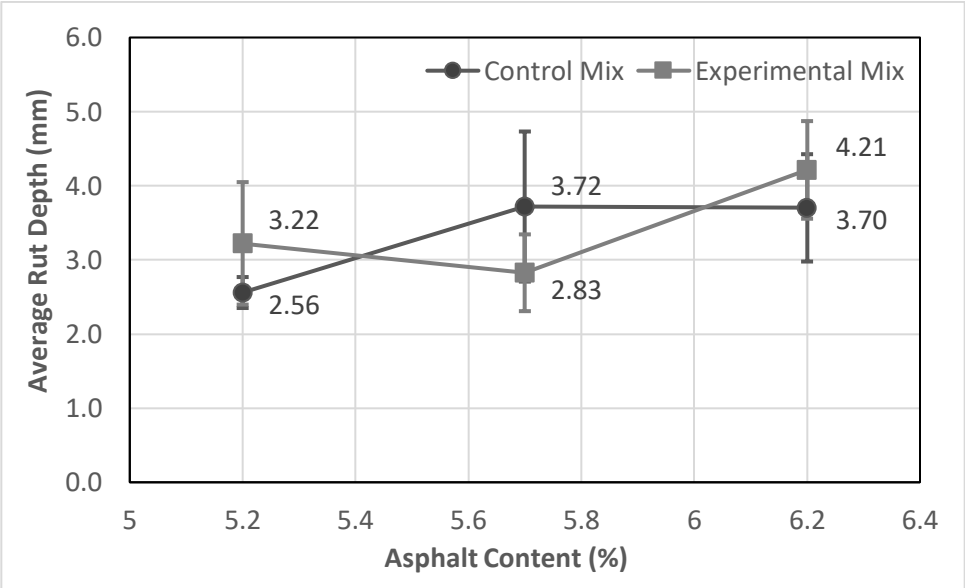

Figure 15. APA Test Results for Control and Experimental Mixtures at Three Asphalt Contents

Cantabro Test Results. In addition to the IDEAL-CT and APA tests, the Cantabro abrasion test was also conducted for the control and experimental mixtures during mix design. Test specimens were compacted to N_{des} (i.e., 50 gyrations) and tested in accordance with the VDOT provisional BMD specification.

Figure 8 shows the Cantabro mass loss percentage and air voids measured at three asphalt contents (i.e., 5.0%, 5.5%, and 6.0%) for the control mix. Both the mass loss and air voids decreased with the increasing of asphalt content. The selected asphalt content of 5.5% with a corresponding average mass loss of 4.7% was below VDOT's maximum mass loss criterion of 7.5%.

For the experimental mix design, the mass loss percentage and air voids were measured at four different asphalt contents, including 4.7%, 5.2%, 5.7%, and 6.2%. However, the Cantabro loss data determined at 5.7% appeared to be variable and inconsistent with the trend shown in Figure 9, so the information was not included in this chapter. The mass loss and air void results for the experimental mix design showed the same trends as those for the control mix. It was estimated that the average mass loss of the experimental mixture at the selected asphalt content of 5.5% would be between 3.3% and 2.6%, which would meet VDOT's maximum mass loss criterion of 7.5%.

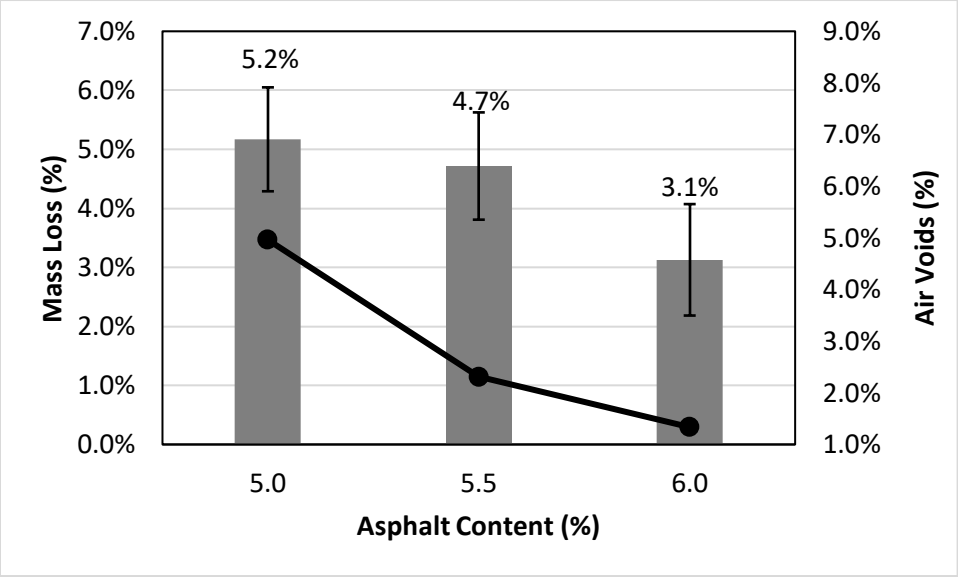

Figure 16. Cantabro Test Results of the Control Mix (BMD)

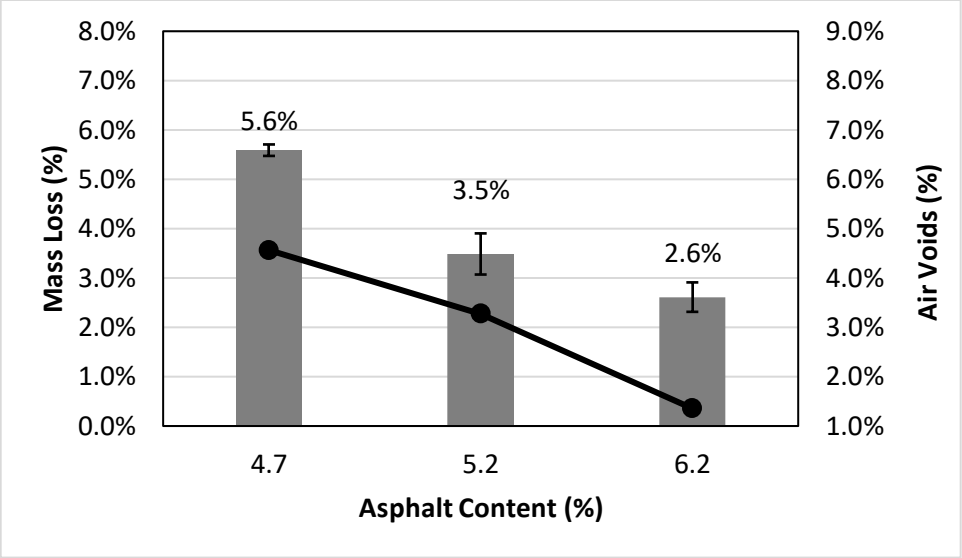

Figure 17. Cantabro Test Results of the Experimental Mix (BMD)

Final Mix Design. Figure 10 compares the APA and IDEAL-CT test results for the volumetric and balanced mix designs. The control mixtures had 30% RAP with no rejuvenator while the experimental mixtures had 45% RAP with rejuvenator at the medium dosage.

The two volumetric mix designs for the control and experimental mixtures had the same binder content of 5.2% and showed similar APA rut depths and CT_{Index} results. Their APA rut depths met the VDOT maximum rut depth threshold of 8 mm, but their CT_{index} values did not meet the VDOT minimum CT_{Index} criterion of 70. To meet the VDOT minimum CT_{Index} threshold, the binder contents of the two volumetric mix designs were increased. The control mixture met the CT_{Index} requirement at a binder content of 5.5% while the experimental mixture met the requirement at 5.8% binder content with their CT_{Index} and APA rut depth results being almost the same, as shown in Figure 10.

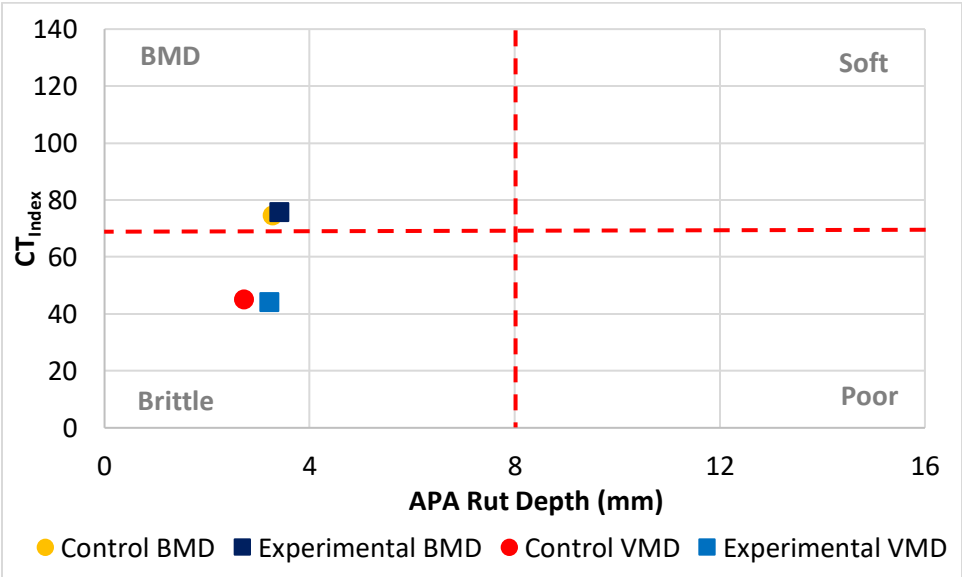

Figure 18. Volumetric Mix Design vs. Balanced Mix Design

5.4.3 Asphalt Binder Test Results

Table 9 provides a summary of binder test results for the three plant-produced mixtures tested in the Cargill laboratory, including (1) control mixture with 30% RAP and a warm mix additive placed in Section N3A (N3A), (2) experimental mixture with 45% RAP and rejuvenator placed in Section N3B (N3B), and (3) experimental mix with 45% RAP and no rejuvenator produced for laboratory testing only (N3B-NR).

Asphalt binders were first extracted and recovered from the three plant-produced mixtures after they had been reheated and reduced to sample size. They were then laboratory aged at two aging levels before testing. The first aging level is the same as the standard aging procedure for extracted binders described in AASHTO M320. The second aging level is an extended binder aging protocol in which the extracted asphalt binder was subjected to twice the standard PAV aging time of 20 hours (2 x PAV aging). The continuous high temperature performance grade (HTPG) was determined based on the extracted binder for the first aging level and based on the RTFO+2PAV aged binder for the second aging level. The continuous low temperature performance grade (LTPG) was determined based on the RTFO aged and RTFO+2PAV aged binders for the first and second aging levels, respectively. Based on the Bending Beam Rheometer results, S-BBR is the temperature where stiffness, *S*, equals 300 MPa, while m-BBR is the temperature where *m* equals 0.300. ΔT_c is the difference between the S-BBR and m-BBR. The following observations can be drawn based on the binder test results:

- The N3B-NR binder appeared to be the stiffest, followed by the N3A binder and then N3B binder based on the HTPG and S-BBR.
- Based on the m-BBR results, the N3B binder was most flexible. The N3B-NR binder appeared to be more flexible than the N3A binder for the first aging level, but they were similar for the extended aging level.
- Since a higher ΔT_c value suggests lower binder susceptibility to non-load related cracking for binders with the same LTPG, the N3A binder would be more susceptible to non-load related cracking, followed by the N3B-NR binder and then the N3B binder.

In summary, based on the test results of the extracted binders, the N3B binder showed improved long-term cracking resistance without an adverse effect on its rutting resistance compared to the other two binders. In addition, the N3A and N3B-NR binders would have similar rutting and long-term cracking performance.

Table 14. Test Results for Asphalt Binders Extracted from Plant-Produced Mixtures

Binder Aging Level	Mix ID	HTPG (°C)	S-BBR (°C)	m-BBR (°C)	ΔTc (°C)	PG
HTPG: As Extracted LTPG: As Extracted + RTFO	N3A	76.7	-23.8	-14.6	-9.2	76 – 10
	N3B	75.9	-24.0	-22.0	-2.0	70 – 22
	N3B-NR	78.8	-21.5	-18.6	-2.9	76 – 16
HTPG: As Extracted + RTFO + 2PAV LTPG: As Extracted + RTFO + 2PAV	N3A	91.2	-20.7	-12.8	-7.9	88 – 10
	N3B	90.5	-22.8	-17.0	-5.9	88 – 16
	N3B-NR	94.3	-18.6	-12.9	-5.7	94 – 10

5.4.4 Lab Performance Test Results for Plant-Produced Mixtures

The plant-produced mixtures sampled during construction were used to prepare plant-mixed, lab-compacted (PMLC) specimens for performance testing in the NCAT laboratory, as shown in Table 5. To compare test specimens, loose mix was reheated and split to sample size. Depending on the loose mix aging condition planned in Table 5 for each performance test, test specimens were compacted after the split samples were either reheated (RH) to the compaction temperature, or they were compacted after the loose mix samples were critically aged (CA) for eight hours at 135°C. The reheated and critically aged specimens were shown with suffix "RH" and "CA", respectively.

Tensile Strength Ratio (TSR) Test Results. The moisture susceptibility of the three mixtures was evaluated in accordance with AASHTO T283 on test specimens compacted using reheated plant mix samples. Results of the moisture susceptibility test are presented in Figure 11. All mixtures met the minimum TSR of 0.80 required for moisture resistance, with the control mix (N3A-RH) having the highest TSR.

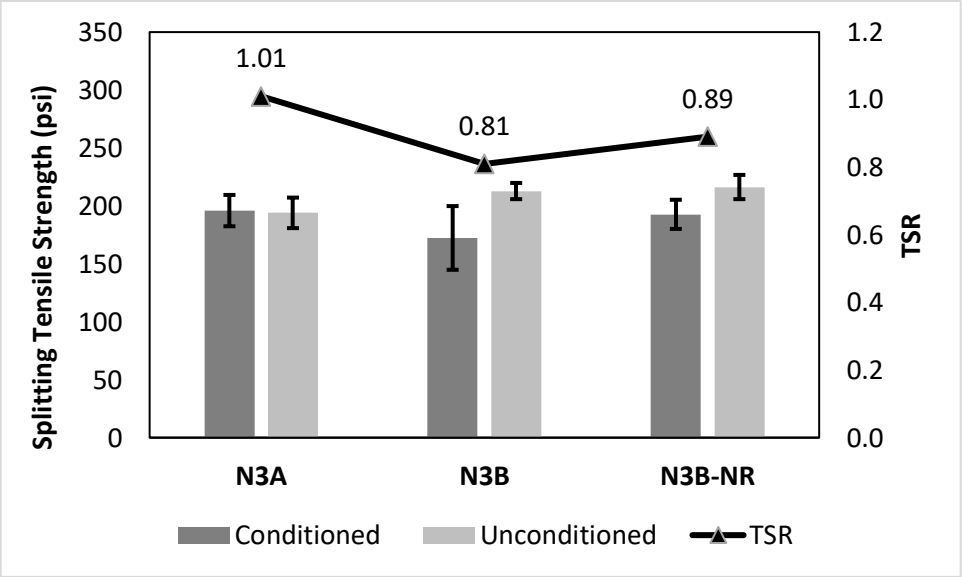

Figure 19. TSR Test Results for Reheated Plant Mixtures

Asphalt Pavement Analyzer (APA) Test Results. The rutting resistance of the plant mixtures was evaluated using both the APA and HWTT. Testing was only conducted for the reheated control mixture (N3A-RH) and the experimental mixture with rejuvenator (N3B-RH). The rutting resistance of the experimental mixture without rejuvenator (N3B-NR) was expected to be similar or better than that of the N3B mixture due to its similar mixture composition and the absence of a rejuvenator in the N3B-NR mixture.

Results of the APA testing are summarized in Table 10. Rut depth was measured using both the manual and automatic methods. Numerically, the N3B mixture recorded a higher rut depth in both methods of measurement. Also, the Coefficient of Variation (COV) was higher for the N3B mixture in both the manual and automated average rut depth measurements. The p-values of the one-way ANOVA statistical test ($\alpha = 0.05$) suggested no significant difference between the

average rut depths of the control and experimental mixes for both methods of rut depth measurement.

Table 15. APA Rutting Test Results for Reheated Plant Mixtures

Parameter	Mix Identifier	Average	COV	P-Value
Manual rut depth (mm)	N3A	2.97	0.22	0.267
	N3B	3.44	0.69	
Automated rut depth (mm)	N3A	2.97	0.23	0.382
	N3B	3.37	0.84	

Hamburg Wheel Tracking Test (HWTT) Results. Table 11 summarizes the HWTT results for evaluating the rutting resistance of reheated N3A and N3B mixtures. The average HWTT rut depths were almost the same for the two mixtures after 10,000 and 20,000 passes, and no stripping inflection points (SIP) were observed for the HWTT specimens. Also, based on the p-values of a one-way ANOVA ($\alpha = 0.05$) test, there was no statistical difference between the average HWTT rut depths of the reheated N3A and N3B mixtures at either 10,000 or 20,000 passes. The HWTT rutting results appeared to agree with the APA rutting results.

Table 16. HWTT Rutting Results for Reheated Plant Mixtures

Parameter	Mix Identifier	Average	COV	P-Value
10,000 Passes	N3A	2.51	0.07	0.760
	N3B	2.55	0.02	
20,000 Passes	N3A	3.15	0.11	0.875
	N3B	3.10	0.03	

Illinois Flexibility Index Test (I-FIT) Results. Table 12 summarizes the flexibility index (FI) results determined from the I-FIT for the reheated N3A, N3B, and N3B-NR mixtures. These results were determined after an outlier analysis was conducted on the replicate FI results at 5% significance level as specified in ASTM E178. After eliminating the outlying observation(s), the descriptive statistics were determined. Numerically, the reheated N3B mixture recorded the highest average FI, suggesting that the N3B mixture had better cracking resistance than the others.

In addition, a one-way ANOVA ($\alpha = 0.05$) statistical test was conducted, and the resulting p-value (0.007) suggested that significant differences existed among the average FI values of the three mixtures. However, the p-value did not specifically indicate where the significant difference lied. Thus, the Tukey-Kramer test was then conducted to determine where the differences occurred between the three mixtures. The grouping results of the Tukey-Kramer test are shown in the last column of Table 12. For the mixtures that shared the same letter, their average flexibility indexes were not statistically different. The Tukey-Kramer statistical groupings of the reheated FI results, as shown in Table 12, suggested that significant differences existed between the average FI of the rejuvenated and unrejuvenated experimental mixes (i.e., N3B and N3B-NR), as they did not share the same letter. However, the reheated N3A mixture shares a letter with both the reheated N3B and N3B-NR mixtures. The higher cracking resistance observed in the reheated N3B mixture was attributed to the effect of the rejuvenator.

Table 17. I-FIT Results with Tukey – Kramer Statistical Groupings (Reheated Mixtures)

Parameter	Mix Identifier	Average FI	COV	P-Value	Groupings
FI	N3A	6.6	0.27	0.007	A, B
	N3B	7.5	0.35		A
	N3B-NR	3.7	0.33		B

Table 13 summarizes the I-FIT results of the critically aged N3A, N3B, and N3B-NR mixtures. The average FI values of the critically aged mixtures were below 0.5, suggesting that cracks may show up in these mixtures after a few years at the Test Track. While the FI results were statistically different, they were considered not practically different in this case.

Table 18. I-FIT Results with Tukey – Kramer Statistical Groupings (Critically Aged Mixtures)

Parameter	Mix Identifier	Average FI	COV	P-Value	Groupings
FI	N3A	0.46	0.70	0.007	A
	N3B	0.31	0.51		A, B
	N3B-NR	0.14	0.66		B

Figure 12 compares the FI results of the reheated and critically aged mixtures. In the reheated condition, the N3B mixture showed the higher FI results. However, the three mixtures aged quickly during the critical aging process, resulting in all the average FI values being below 0.5, which may lead to a concern about the long-term cracking resistance of these mixtures.

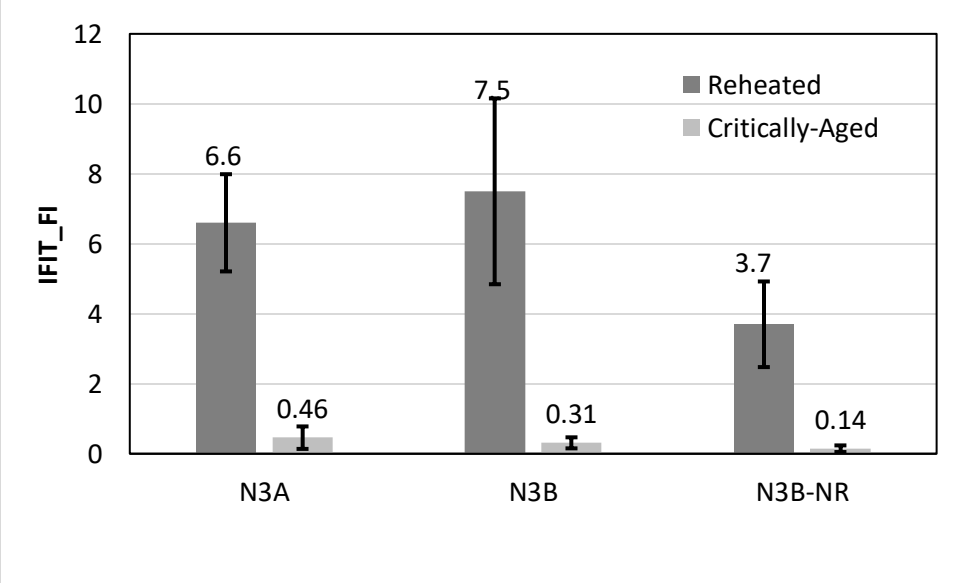

Figure 20. Comparison of Reheated and Critically Aged I-FIT Results

Overlay Test (OT) Results. The Overlay Test was conducted in accordance with NJDOT B-10. According to NJDOT B-10, the number of cycles to failure (N_f) is reported as an index that represents the resistance of an asphalt mixture to reflective cracking. The higher the N_f, the better the resistance of the asphalt mixture to reflective cracking.

The OT results of the reheated mixtures are summarized in Table 14 after an outlier test (ASTM E178) was conducted. The reheated N3B mixture showed higher resistance to reflective

cracking than the other mixtures. Also, the difference in the N_f of the three reheated mixtures was statistically significant at 5% significance level (i.e., $\alpha = 0.05$). The Tukey-Kramer statistical groupings showed that the significant difference was due to the N_f of the reheated N3B-NR mixture.

Table 19. OT Result with Tukey – Kramer Statistical Groupings (Reheated Mixtures)

Parameter	Mix Identifier	Average N_f	COV	P-Value	Groupings
N_f	N3A	297	0.24	0.000	A
	N3B	326	0.09		A
	N3B-NR	73	0.32		B

The OT results of the critically aged mixtures are summarized in Table 15. Similar to the critically aged I-FIT results, the N_f of the three plant-produced mixtures dropped significantly after critical aging, and they were not statistically significant at 5% significance level.

Table 20. OT Results (Critically Aged Mixtures)

Parameter	Mix Identifier	Average N_f	COV	P-Value
N_F	N3A	33	0.27	0.096
	N3B	18	0.18	
	N3B-NR	25	0.49	

Figure 13 compares the OT results for the reheated and critically aged mixtures. As for the I-FIT results, the reheated N3B mixture showed higher resistance to cracking than the other two reheated mixtures. The three mixtures aged significantly during critical aging, leading to similar critically aged cycles to failure.

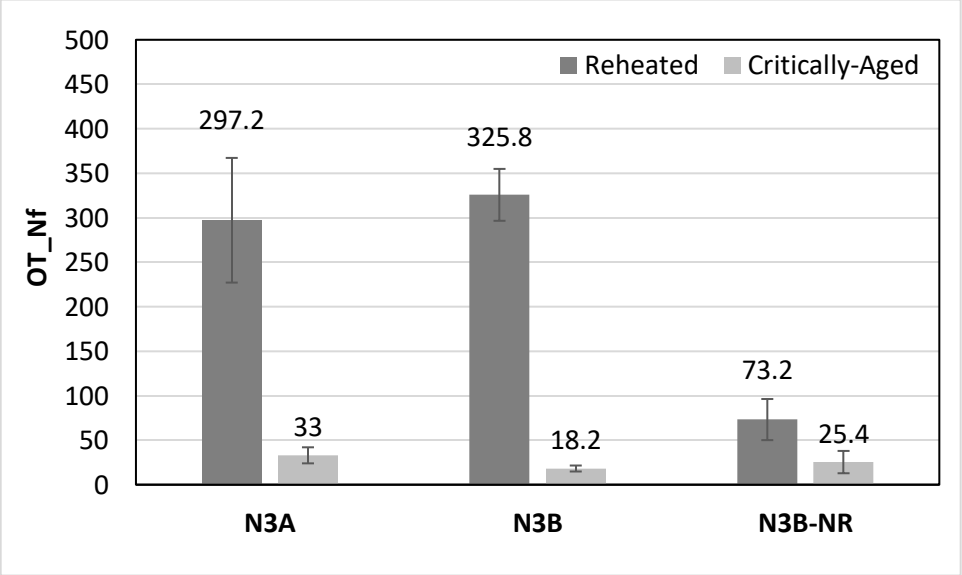

Figure 21. Comparison of Reheated and Critically Aged OT Results

Disc-Shaped Compact Tension (DCT) Test Results. The DCT test was conducted to evaluate resistance of the three plant-produced mixtures to low temperature cracking. The fracture energy (FE) results determined from the DCT testing of the reheated mixtures are summarized

in Table 16 after an outlier analysis (ASTM E178). The reheated N3B mixture had the highest average FE, followed by the reheated N3A mixture and then the reheated N3B-NR mixture. However, the difference was not statistically significant based on a one-way ANOVA statistical test at 5% significance level.

Table 21. DCT Test Results (Reheated Mixtures)

Parameter	Mix Identifier	Average FE	COV	P-Value
FE	N3A	529	0.11	0.136
	N3B	562	0.09	
	N3B-NR	494	0.12	

The DCT results of the critically aged mixtures are presented in Table 17. Similar to the reheated DCT test results, the difference among the average FE of the critically aged mixtures was not statistically significant (though they were very close to being statistically significant) based on a one-way ANOVA at 5% significance level.

Table 22. DCT Test Result (Critically Aged Mixtures)

Parameter	Mix Identifier	Average FE	COV	P-Value
FE	N3A	508	0.11	0.052
	N3B	431	0.16	
	N3B-NR	424	0.11	

The DCT results of the reheated and critically aged mixtures are compared in Figure 14. Unlike the I-FIT and OT test results, critical aging did not appear to significantly affect the DCT results.

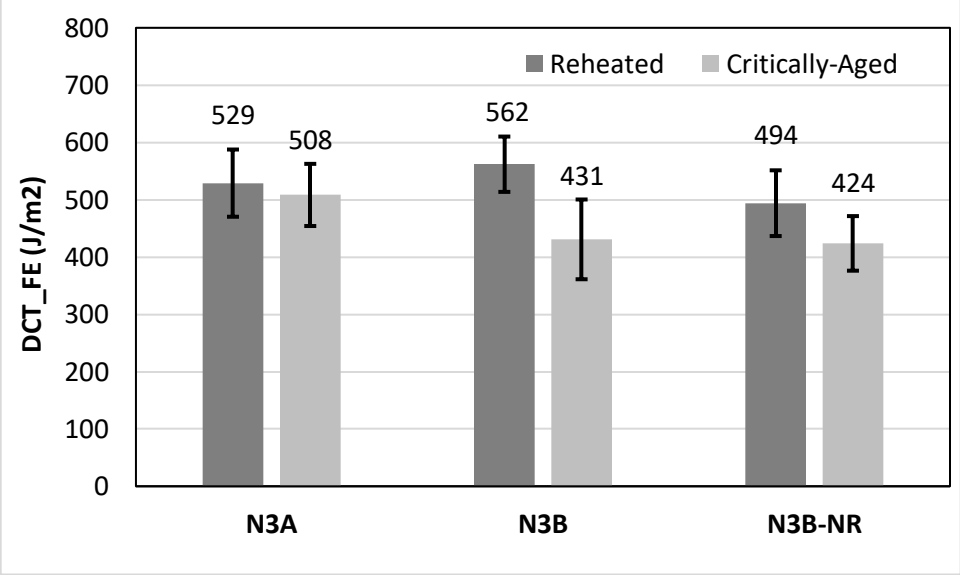

Figure 22. Comparison of Reheated and Critically Aged DCT Test Results

Indirect Tension Asphalt Cracking Test (IDEAL-CT) Results. The cracking resistance of the reheated mixtures was also evaluated based on the CT_{index} determined by the IDEAL-CT, as shown in Table 18. The CT_{Index} results deviated from the other cracking test results with the reheated N3A mixture having the highest average CT_{Index}, followed by the reheated N3B

mixture and then the reheated N3B-NR mixture. The VDOT provisional BMD specification requires a minimum CT_{Index} threshold of 70, and only CT_{Index} of the reheated N3A mixture was higher than the threshold. The p-value of a one-way ANOVA suggested that the difference in the CT_{index} values of the three reheated mixtures was statistically significant. Further, the Tukey-Kramer statistical groupings of the CT_{Index} results showed that significant differences existed among the CT_{index} values of the three reheated plant mixtures.

Table 23. IDEAL–CT Results with Tukey – Kramer Statistical Groupings (Reheated Mixtures)

Parameter	Mix Identifier	Avg. CT_{index}	COV	P-Value	Groupings
CT_{index}	N3A	102	0.15	0.000	A
	N3B	64	0.18		B
	N3B-NR	45	0.20		C

The IDEAL-CT results of the critically aged mixes are summarized in Table 19. The p-value (0.035) of a one-way ANOVA suggested that the CT_{Index} values of the three critically aged mixtures were statistically different at 5% significance level. The Tukey-Kramer statistical groupings showed that the statistical difference only existed between the average CT_{index} of the critically aged N3A and N3B-NR.

Table 24. IDEAL–CT Results with Tukey – Kramer Statistical Groupings (Critically Aged Mixes)

Parameter	Mix Identifier	Avg. CT_{index}	COV	P-Value	Groupings
CT_{index}	N3A	28	0.15	0.035	A, B
	N3B	30	0.13		A
	N3B-NR	23	0.10		B

Figure 15 compares the CT_{Index} results for the reheated and critically aged plant mixtures. While the CT_{Index} values for the reheated plant mixtures were significantly different, they became closer to each other for the critically aged mixtures.

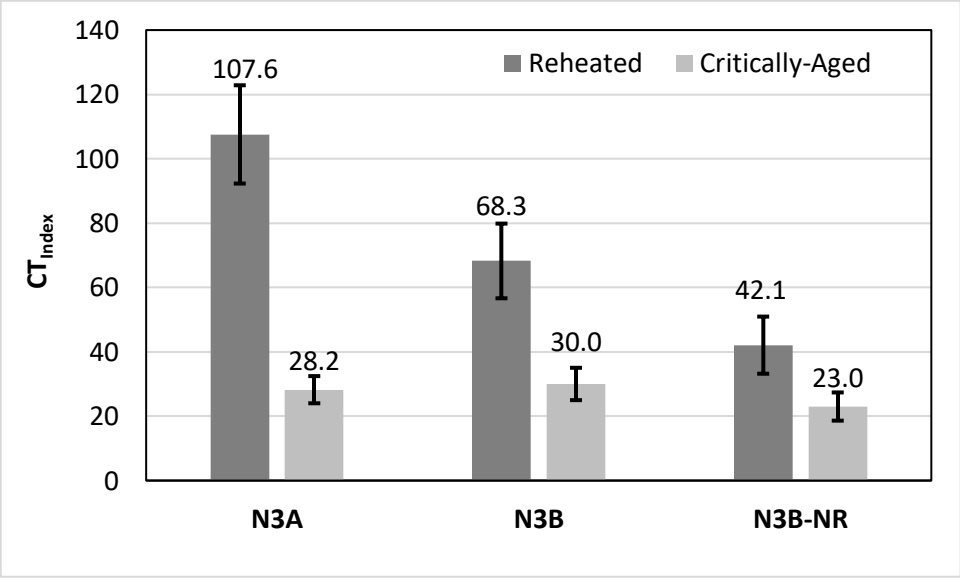

Figure 23. Comparison of Reheated and Critically Aged IDEAL-CT Results

Cantabro Abrasion Test Results. The Cantabro abrasion test was conducted on the reheated plant mixtures compacted to N_{des}, and results are illustrated in Figure 16. The reheated N3B mixture recorded statistically lower mass loss with the other mixtures having statistically the same mass loss values at 5% significance level. All three mixtures showed the average mass losses that were higher than the maximum Cantabro mass loss threshold of 7.5% required in the VDOT provisional BMD specification.

5.4.5 Field Performance Evaluation

Field performance data collected from Sections N3A and N3B of the NCAT Test Track included rutting, cracking, ride quality in terms of International Roughness Index (IRI), and surface macrotexture. At the conclusion of the 2018 research cycle, 10 million ESALs of truck traffic were applied on the test sections.

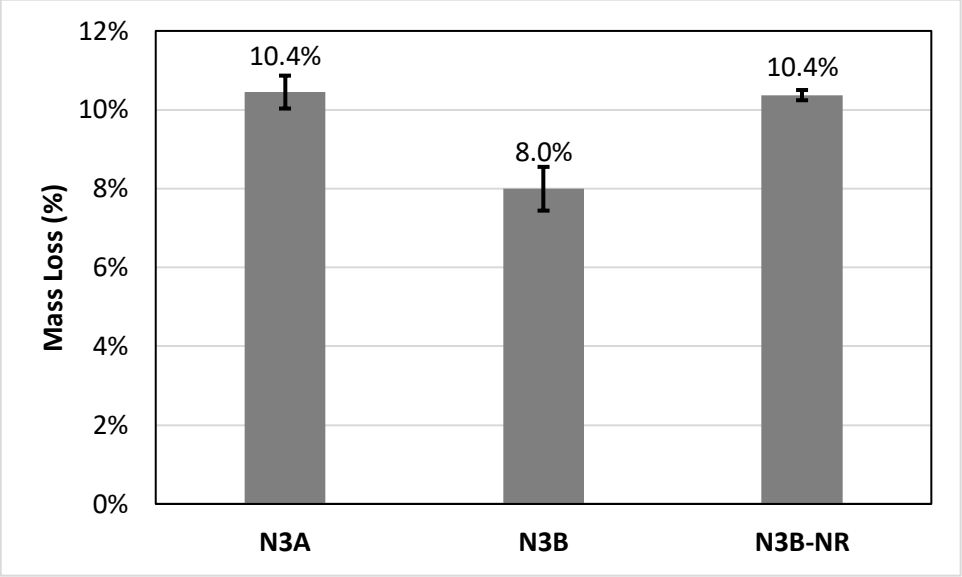

Figure 24. Cantabro Abrasion Test Results for Reheated Plant Mixtures

Rutting. The rutting data for Sections N3A and N3B from the onset to the conclusion of trafficking for the 2018 research cycle are compared in Figure 17. The rut depths were almost identical and below 5.0 mm for both sections. The field rutting performance appeared to agree with the APA and HWTT results for the reheated plant mixtures summarized in Table 20, in which their APA and HWTT results were not statistically different and below the VDOT maximum APA rut depth threshold of 8.0 mm and the commonly used maximum HWTT rut depth criterion of 12.5 mm.

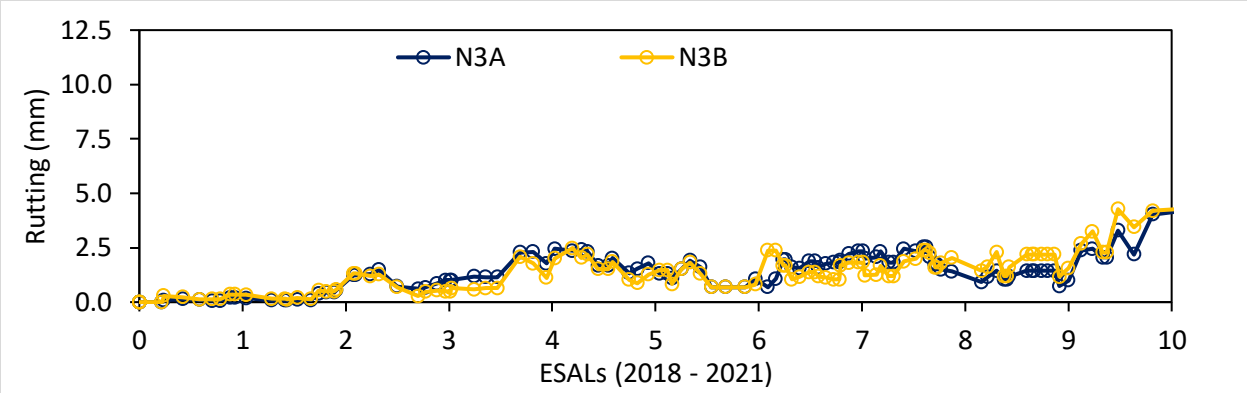

Figure 25. Field Rut Depth Measurements

Table 25. Summary of APA and HWTT Results for Reheated Plant Mixtures

Mix ID	APA Rut Depth (mm)		HWTT Rut Depth (mm)	
	Manual	Automated	10,000 passes	20,000 passes
N3A-RH	2.97	2.97	2.51	3.15
N3B-RH	3.44	3.37	2.55	3.10

*Average results of each measurement sharing the same letter are not statistically different.

Surface Cracking. While there were some signs of near surface cracking initiation observed in the last week of truck trafficking in February of 2021, they may disappear due to the hot summer at the Test Track. Thus, Sections N3A and N3B have performed well with no cracking reported in this research cycle.

Ride Quality. Ride quality, expressed as IRI, was measured for Sections N3A and N3B using the Dynatest inertial profiler, and the results are shown in Figure 18. The rough transition at the beginning of Section N3A affected its overall smoothness. The ride quality of Section N3B stayed in good condition throughout the 2018 research cycle.

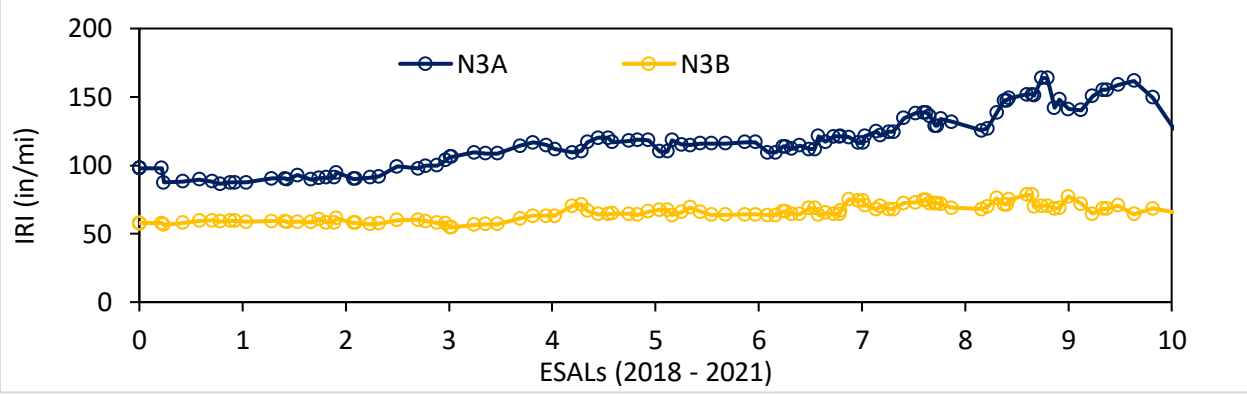

Figure 26. Ride Quality (IRI) Measurements

Surface Macrotexture. Figure 19 compares the mean texture depth (MTD) measurements for Sections N3A and N3B. The results were almost identical for the two test sections. The macrotexture measurements increased due to the removal of asphalt film on the pavement surface at the onset of truck trafficking, and they stayed almost the same throughout the

research cycle. While the Cantabro mass loss results, as summarized in Table 21, were above the VDOT maximum mass loss requirement of 7.5%, there was no sign of raveling observed in the two test sections at the conclusion of the truck trafficking for the 2018 research cycle.

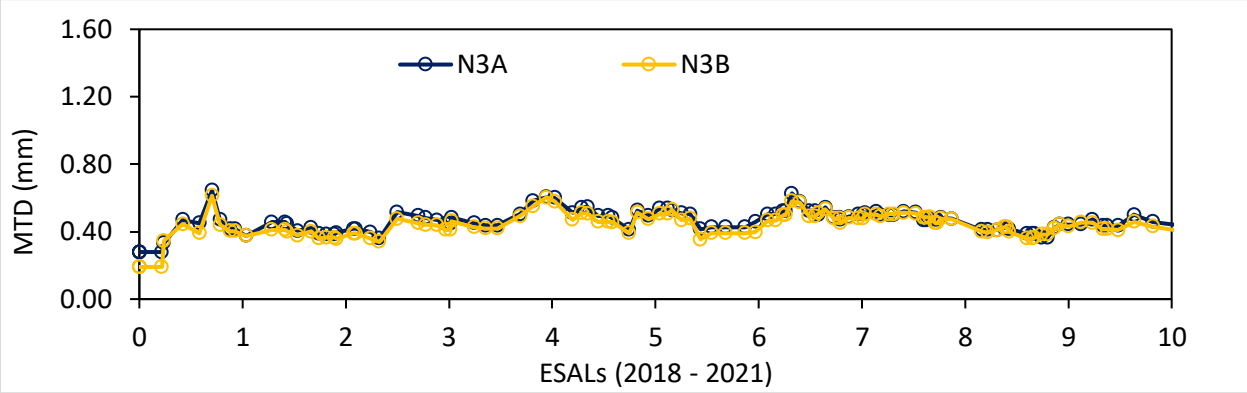

Figure 27. Surface Macrotexture (MTD) Measurements

Table 26. Summary of Cantabro Mass Loss Results for Reheated Plant Mixtures

Mix ID	Cantabro Mass Loss (%)
N3A-RH	10.5 (B)
N3B-RH	8.0 (A)

*Average results with different letters are statistically different.

5.5 Summary And Conclusions

This experiment was conducted to evaluate the effectiveness of Anova asphalt rejuvenator in balancing cracking and rutting performance of high RAP mixtures within the BMD framework. The experiment was conducted by comparing the field performance of two surface mixtures under the same pavement structure, traffic, and climatic conditions. Section N3A was milled and inlaid with the control mixture produced with 30% RAP and a PG 64-22 binder, and Section N3B was inlaid with the experimental mixture that was produced with 45% RAP, a PG 64-22 binder, and Anova asphalt rejuvenator. Both sections were trafficked for 10 million ESALs from November 26, 2018 through February 28, 2021. Their field performance, including rutting, cracking, ride quality, and surface macrotexture, was monitored on a weekly basis.

Both the control and experimental mixtures were designed based on the VDOT provisional BMD specification in which the mixtures were designed and tested to evaluate their resistance to rutting, cracking, and raveling using the APA, IDEAL-CT, and Cantabro tests. The two mixtures were then produced and sampled during construction for laboratory testing. The experimental mixture was also produced without the rejuvenator for laboratory testing only (i.e., without paving on the Test Track). The three mixtures were later evaluated using a battery of laboratory performance tests to support the field evaluation experiment.

Based on the field performance of Sections N3A and N3B and laboratory test results for the BMD mix designs and the three plant-produced mixtures, the following conclusions can be drawn:

- The BMD approach using the APA, IDEAL-CT, and Cantabro abrasion tests can be followed to improve mix resistance to cracking and raveling without causing a detrimental effect to its resistance to rutting. Both the control and experimental mixtures were designed to meet the VDOT provisional BMD specification with similar APA and IDEAL-CT results in their balanced mix designs.
- Both the BMD mixtures were produced, placed, and compacted to achieve good in-place density (i.e., 96.2% of G_{mm} for N3A and 96.8% of G_{mm} for N3B) on the Test Track.
- Both sections showed good and almost identical field rutting performance, which also agreed with the APA and HWTT results for the reheated plant-produced mixtures sampled during construction.
- Both sections exhibited good cracking performance in the 2018 research cycle. However, the laboratory cracking test results suggested a significant decrease in I-FIT, OT, and IDEAL-CT test results after critical aging, which is representative of four to five years of field aging at the Test Track. Thus, it is important to continue monitoring the cracking performance of these test sections in the future.
- The transition area of Section N3A was repaired due to an issue not related to the control mixture, affecting the ride quality measurement for Section N3A. Otherwise, both sections showed good ride quality and almost identical, consistent surface macrotexture measurements throughout the research cycle.
- When comparing the experimental mixtures produced with and without the rejuvenator, the effect of the rejuvenator on the cracking test results was more profound on the reheated plant-produced mixtures and less on the critically aged plant mixes.

In summary, Anova asphalt rejuvenator was used to improve the cracking resistance of a high RAP mixture within the BMD framework without affecting the mixture's resistance to rutting. Section N3A and N3B showed comparable field performance after 10 million ESALs and will be kept in place for traffic continuation in the next research cycle to allow for a thorough field performance evaluation.

5.6 References

1. Boomquist, D., G. Diamond, M. Oden, B. Ruth, and M. Tia. *Engineering and Environmental Aspects of Recycled Materials for Highway Construction*. Report No. FHWA-RD-088, FHWA, Washington, D.C., 1993.
2. NAPA. *Asphalt Pavement Industry Survey on Recycled Materials and Warm-Mix Asphalt Usage: 2018*. National Asphalt Pavement Association, Greenbelt, MD., 2019.
3. NAPA. *Asphalt Pavement Industry Survey on Recycled Materials and Warm-Mix Asphalt Usage: 2019*. National Asphalt Pavement Association, Greenbelt, MD, 2020.
4. Cargill. ANOVA® 1815 Rejuvenator Product Data. Cargill, Incorporated, 2020. https://www.cargill.com/doc/1432177154791/anova-rejuvenator-1815-pds.pdf
5. Cargill. ANOVA® 1501 Warm Mix Additive: Production, Testing and Compaction Details. Cargill, Incorporated, 2020. https://www.dot.ny.gov/divisions/engineering/technical-services/technical-services-repository/details/anova_1501.pdf

6. Chen, C., F. Yin, P. Turner, R. C. West, and N. Tran. Selecting a Laboratory Loose Mix Aging Protocol for the NCAT Top-Down Cracking Experiment. *Transportation Research Record*, *2672*(28), Transportation Research Board of the National Academies, Washington, D.C., 2018, pp. 359-371.
7. McDaniel, R., and M. Anderson. *NCHRP Report 452: Recommended Use of Reclaimed Asphalt Pavement in the Superpave Mix Design Method: Technician's Manual*. Transportation Research Board, National Research Council, Washington, D.C., 2001.

6. EVALUATION OF HIGH RAP MIXTURE WITH DELTA S REJUVENATOR

Dr. Nam Tran

6.1 Introduction

It is a common practice among asphalt producers to use reclaimed asphalt pavement (RAP) as a component in their mixtures. Most state highway agencies allow up to 25% RAP to be used, with the national average RAP content at 21.1% in 2019 (*1*). This amount has not increased significantly over the years, likely due to concerns that using higher proportions of RAP could result in asphalt mixtures that are prone to cracking and/or other durability issues.

Several methods have been investigated to reduce the potential adverse effect of RAP binder on the field performance of asphalt mixtures. One method is to use rejuvenators to restore some rheological properties of oxidized asphalt binders in RAP mixtures. These rejuvenators can be petroleum-based or bio-based materials that have been formulated to restore the balance of maltenes that were lost or transformed to asphaltenes in the oxidized RAP binder.

One of the bio-based rejuvenators commercially available is Delta S, which was developed by the Warner Babcock Institute for Green Chemistry and later commercialized by Collaborative Aggregates, LLC for use in recycled asphalt mixtures. This bio-based rejuvenator was used to produce an asphalt mixture with recycled materials placed in the surface layer of Section N7, and the test section has been trafficked for field performance evaluation on the NCAT Test Track since 2015. The control section for this experiment is Section N1, which is also the control section for the Cracking Group Experiment at the Test Track.

6.2 Experimental Plan

The two surface mixtures were designed to meet the volumetric requirements specified in AASHTO M323 with a design compaction effort (N_{des}) of 80 gyrations. The base and binder asphalt layers in the two sections consisted of the same highly polymer-modified asphalt (HiMA) mixture, which was designed to be resistant to fatigue cracking so that all cracking would occur only in the surface layer. The target combined thickness of the asphalt layers was approximately 6 inches for each section. The asphalt layers were placed on top of an aggregate base consisting of a 6-inch crushed granite layer. The subgrade at the Test Track is classified as an A-4 material according to the AASHTO soil classification system.

6.2.1 Surface Layer of Control Section N1

The surface layer of Section N1 was built using a 9.5 mm NMAS mixture with 20% RAP and a PG 67-22 virgin binder to represent a typical asphalt mixture being used in the United States. This mixture is the control mixture for the Cracking Group experiment, which has been carried out at the NCAT Test Track since 2015.

6.2.2 Surface Layer of Experimental Section N7

As shown in Figure 1, the surface layer of Section N7 was originally built on August 6, 2015, using a 9.5 mm nominal maximum aggregate size (NMAS) mixture with 20% RAP and 5% post-consumer recycled asphalt shingles (RAS). The Delta S rejuvenator was added to the virgin PG 67-22 binder at a dosage of 10% by weight of the recycled binders available in the RAP and RAS materials.

Truck trafficking for the 2015 Test Track research cycle commenced on October 8, 2015. After approximately four months (1.4 million ESALs), cracking in Section N7 was first noted on January 31, 2016. The cores extracted from this section suggested that the cracks were caused by delamination between the surface and intermediate asphalt layers.

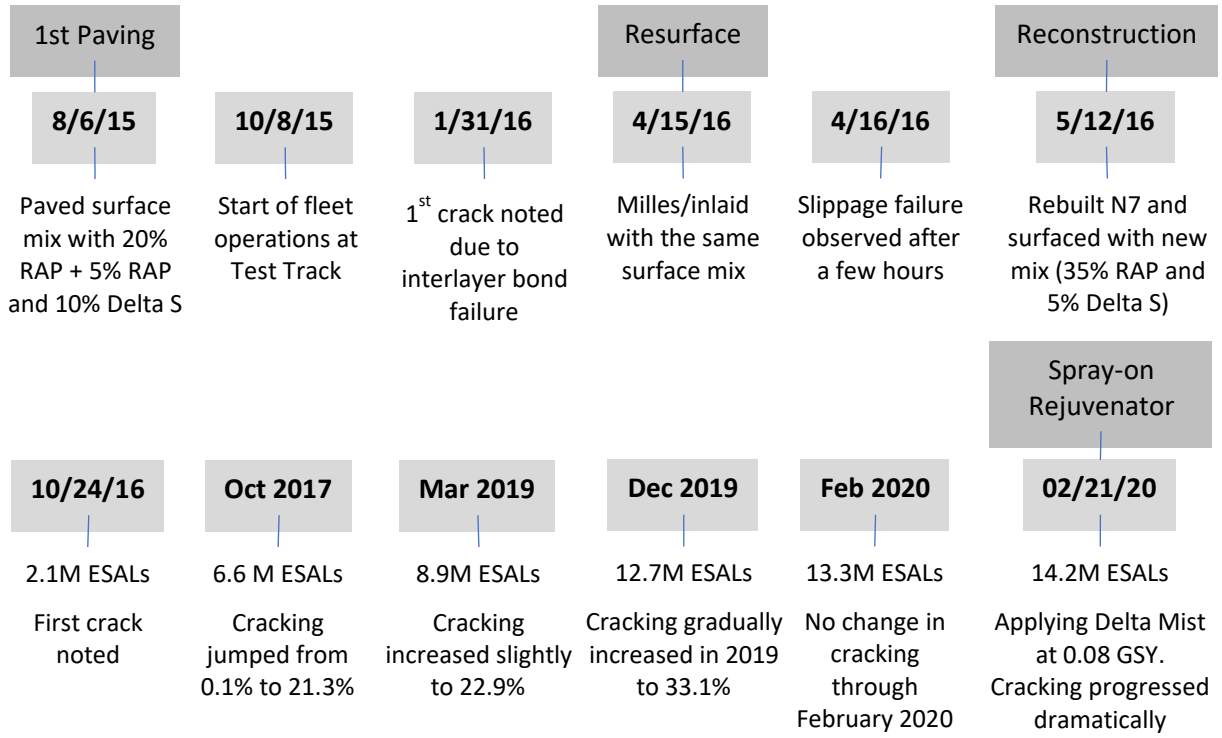

Figure 1. Construction, Rehabilitation and Treatment Activities for Section N7

Section N7 was repaired by milling and repaving the same mixture with an increased tack rate to improve the interlayer bond strength between the surface and underlying layers on April 15, 2016. A slippage failure occurred in Section N7 on April 16, 2016 after just a few hours of fleet operations.

A forensic evaluation of the surface mixture was conducted and later found that the delamination was not caused by an insufficient tack coat (a common cause of delamination), but in fact was due to reduced stiffness and splitting tensile strength of the original surface mixture (*2*). This evaluation included field cores from Sections N7 and N8 as well as specimens prepared using reheated plant mix for Section N7. Results are summarized in Figure 2 and discussed as follows:

- Field cores were extracted from Section N7 (N7 - Cores) right after the slippage failure occurred. In addition, a set of field cores was also extracted from Section N8 (N8 - Cores). The surface mixture in Section N8 was produced based on the same mix design as the surface mix in Section N7 but without Delta S.
- Bucket mix for the surface layer of Section N7 was also reheated in an oven at 295°F for two hours and then split into smaller sample size for the laboratory-compacted specimens. Split samples were then reheated in the oven until they reached 295°F for

compaction; this varied from 45 minutes to an hour. The plant-mixed samples (N7 - PMLC) were then compacted to air voids similar to those measured on the field cores.

- The splitting tensile strength results, shown in Figure 2, were determined at 25°C for all specimens. The results showed that the cores extracted from Section N7 had a lower indirect tensile strength than the field cores extracted from Section N8. In addition, the field cores from Section N7 also had a lower splitting tensile strength than the laboratory specimens compacted from the same plant mix. The reheating of plant mix for compacting laboratory specimens may have improved the interaction of the aged binder and the Delta S rejuvenator in the mixture.

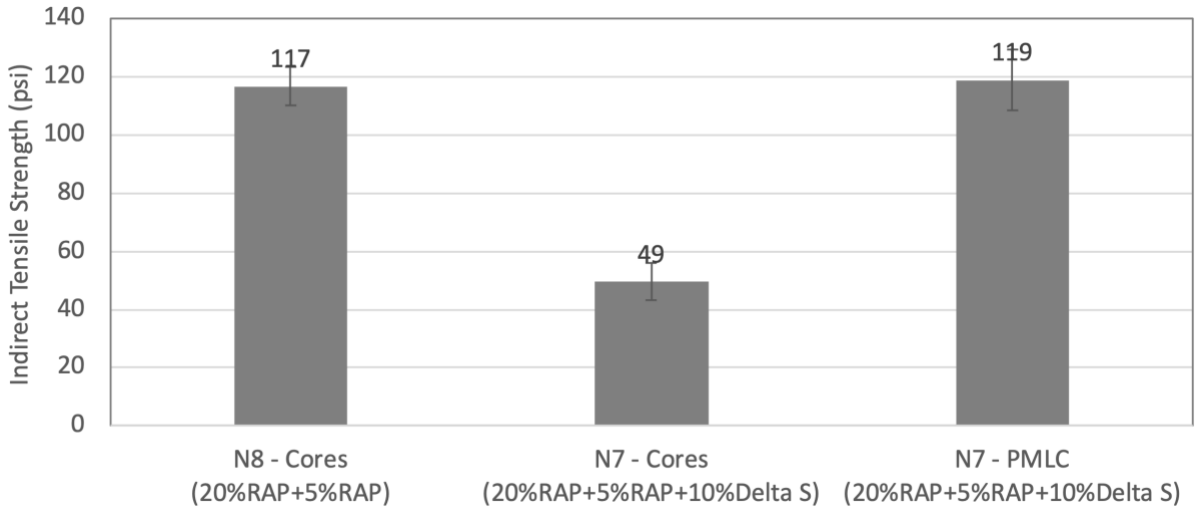

Figure 2. Splitting Tensile Strength Results of Field Cores and Reheated Plant Mixed, Lab Compacted Specimens for 20%RAP+5%RAS Mix with PG 67-22 and 10% Delta S (*2*)

The original and repaved surface mixtures were laid and compacted without any silo storage, as they were produced and hauled to the Test Track (approximately 10 minutes away) for immediate paving. Because of the short haul, the interaction between Delta S (blended with the virgin binder) and the recycled binder, especially in the RAS, may not have been completed, leaving a higher proportion of Delta S in the virgin binder than originally intended. This caused a decrease in stiffness and splitting tensile strength, leading to slippage cracking problems in the original and repaved surface mixture.

While the cause of slippage or surface shearing is similar to that of rutting (resulting from performant deformation of the asphalt surface due to excessive shear stress), the main difference is the direction of deformation, which reflects the direction of the critical stress condition. Due to the reduced level of confinement in the horizontal direction at the pavement surface, horizontal shearing or slippage can occur at lower magnitudes of stress than rutting (*3*).

After careful deliberation, it was decided that the interaction between Delta S and the aged binder in the RAS should be further studied and that the wearing course of Section N7 would be replaced with a mixture containing only RAP materials. This mix would have 35% RAP with a recycled binder ratio similar to that of the original surface mixture in Section N7. Because this mix design did not include RAS (even though it had a similar recycled binder ratio), the Delta S

dosage was reduced to 5% by weight of the aged RAP binder, which was half the dosage originally used in the N7 surface mix. The N7 surface mixture was redesigned to compare directly with the N1 surface mix with 20% RAP, which is the control mix for the Cracking Group experiment. The Delta S dosage was determined to give the 35% RAP mixture in Section N7 a similar flexibility index (FI) determined by the Illinois Flexibility Index Test (I-FIT) to that of the 20% RAP mixture in Section N1 (*2*). Finally, it was determined that the mixture would be kept in a silo for two hours before paving so that the rejuvenator could interact with the RAP binder.

Section N7 was then rebuilt by removing all asphalt layers and repaving from the aggregate base up on May 12, 2016. The redesigned surface layer of Section N7 was built with a 35% RAP surface mixture and only 5% Delta S. To produce the N7 surface mixture, Delta S was in-line injected into the PG 67-22 binder supply at a target rate of 5% by weight of RAP binder. To give Delta S rejuvenator time to interact with the aged binder in the RAP, the mixture was stored in a silo for two hours before being transported to the Test Track.

Figure 3 summarizes the splitting tensile strength results for the lab-mixed and plant-mixed specimens as well as field cores for the 35% RAP mixture with 5% Delta S. The splitting tensile strength of the lab-mixed specimens increased after two and four hours of short-term aging (STA) at 135°C. The splitting tensile strength of the plant-mixed specimens was between the results of the lab-mixed specimens after two and four hours of STA. Finally, the splitting tensile strength of the field cores improved significantly compared with those previously extracted from Section N7 as shown in Figure 2.

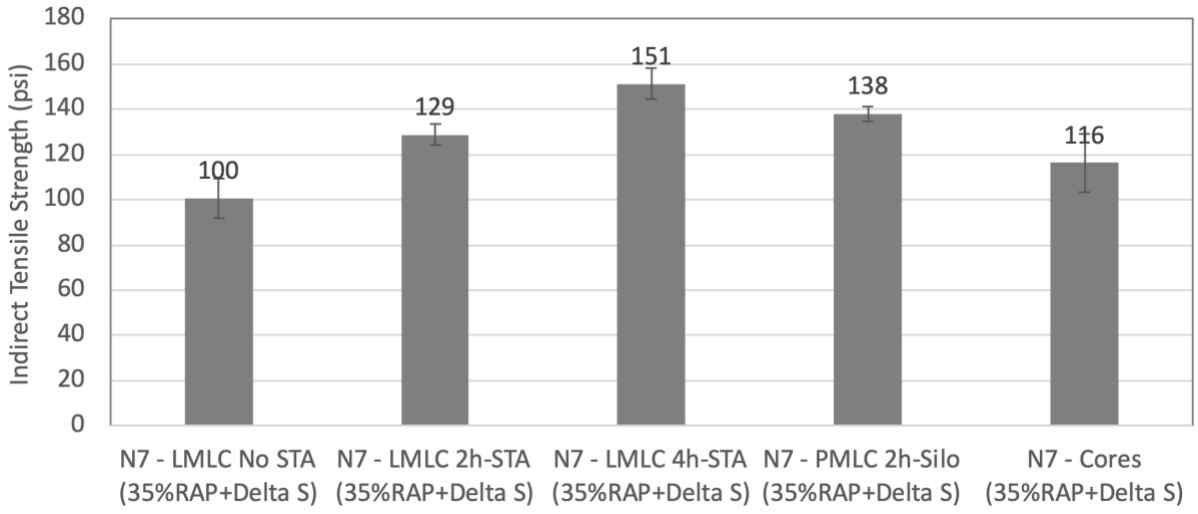

Figure 3. Splitting Tensile Strength Results of Lab-Mixes, Plant-Mixed Specimens, and Field Cores for 35% RAP Mix with PG 67-22 and 5% Delta S

The changes made to the redesigned surface mixture in Section N7 helped address the slippage problems identified in the original surface mixture. A more detailed discussion of the forensic investigation and reconstruction of Section N7 was included in a previous report (*2*).

6.2.3 Field and Lab Evaluations of the Surface Mixtures

The redesigned surface mixture with 35% RAP and 5% Delta S (by weight of the RAP binder) in Section N7 was compared to the surface mixture in Section N1 with 20% RAP. The as-built thicknesses were 1.6 and 1.5 inches for the surface layers of Sections N1 and N7, respectively. Table 1 includes a summary of properties for the two surface mixtures.

Table 1. Surface Mixture Quality Control Properties

Mixture	Pb (%)	Pbe (%)	Recycled Binder Ratio	Va (%)	VMA (%)	In Place % G_{mm}
N1 20% RAP	5.4	4.7	0.177	3.8	15.0	93.6
N7 35% RAP + 5% Delta S	6.0	5.3	0.282	4.3	16.0	92.1

The field performance of the two surface mixtures was evaluated based on weekly measurements of ride quality, rutting, and cracking. In addition, samples of plant mix were taken during construction of Section N1 and reconstruction of Section N7, and they were tested in the laboratory to determine their stiffness, rutting, and cracking resistance to assist the field performance evaluation.

6.3 Field Performance

Figure 3 compares the field performance measurements for Sections N1 (control) and N7 (experimental), including (a) cracking, (b) rutting, (c) International Roughness Index (IRI), and (d) mean texture depth (MTD). A discussion of each field performance characteristic follows.

6.3.1 Traffic

Section N7 was rebuilt when approximately 2.5 million ESALs had been applied to the test sections in the 2015 research cycle. Thus, approximately 7.5 million ESALs were applied to Section N7 while about 10 million ESALs were applied to Section N1 from 2015 - 2018. Both sections were kept in place for traffic continuation from 2018 - 2021. Thus, at the end of the 2018 research cycle, approximately 17.5 and 20 million ESALs were applied to Sections N7 and N1, respectively.

6.3.2 Field Performance in 2015 Research Cycle

Cracking (only 0.1% of the lane area) was first noted in Section N7 on October 24, 2016 after 2.1 million ESALs. For Section N1, cracking (approximately 0.2% of the lane area) was first observed on March 6, 2017 after 6.2 million ESALs.

Cracking then jumped from 0.1% to 21.3% in October of 2017 in Section N7 after approximately 6.6 million ESALs. For Section N1, cracking also increased significantly from 0.2% to 10.2% in October of 2017 after 9.7 million ESALs. Cracking typically grows quickly in spring (around March) and fall (around October) seasons at the Test Track.

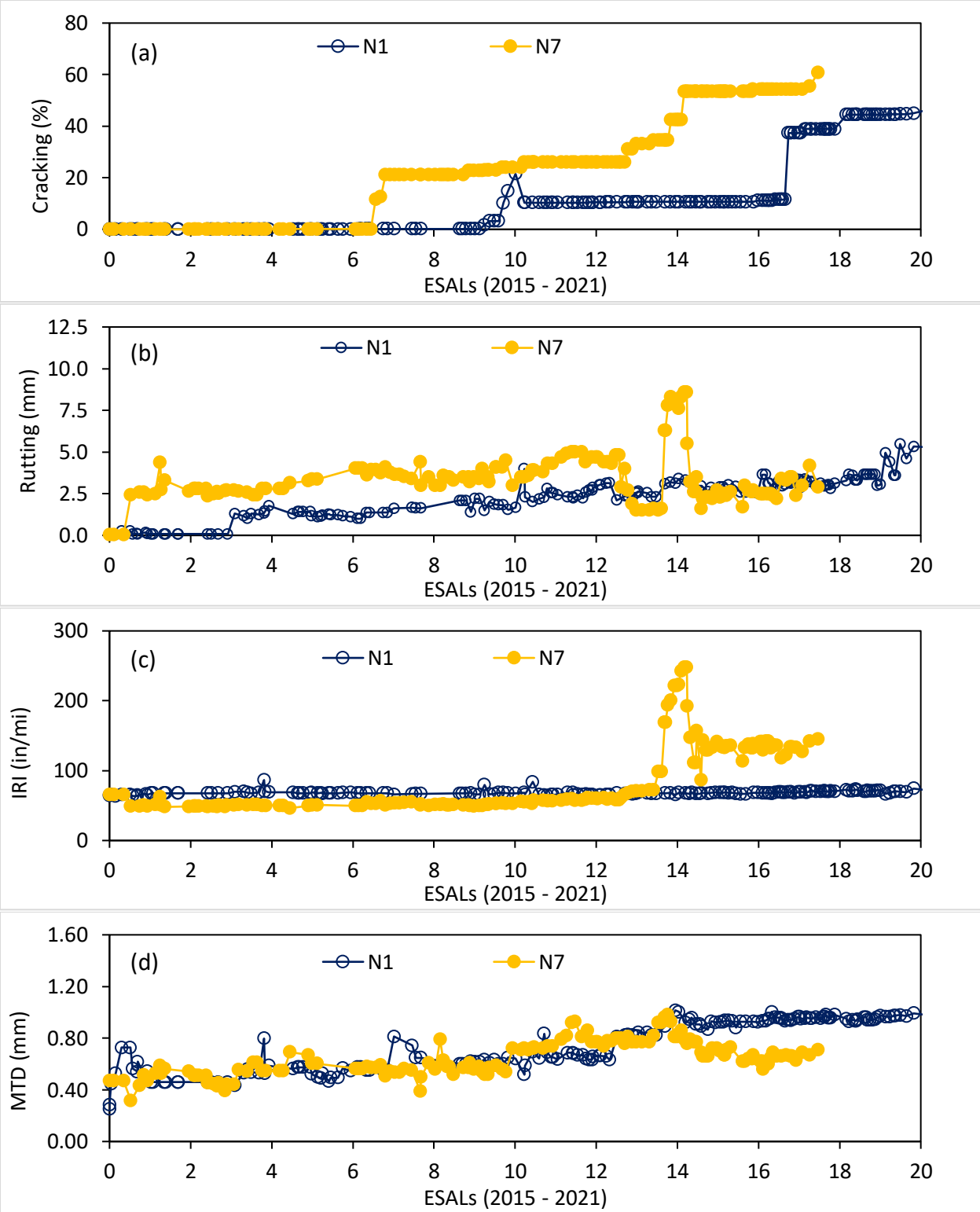

Figure 3. Field Performance of Sections N1 and N7

At the end of fleet operations for the 2015 research cycle in December of 2017, the two surface mixtures in Sections N1 and N7 showed good ride quality and rutting performance. The area of

cracking observed in the surface mixture of Section N7 was higher than that of the surface mixture in Section N1, but the cracks were very tight (less than 1 mm opening) near-surface cracks, as shown in Figure 4. Both sections were kept in place for continued traffic in the 2018 research cycle (2018-2021) to allow for a thorough field performance evaluation.

Figure 4. Close-up of Hairline Cracks in Sections N7 and N1

6.3.3 Field Performance in 2018 Research Cycle

Fleet operations for the 2018 research cycle started in October of 2018. Cracking in Section N1 increased slightly from 10.3% at the beginning of the 2018 research cycle to 11.5% in March of 2020 after 16.6 million ESALs. It then jumped to 37.4% in April of 2020 after 16.9 million ESALs. Cracking then gradually increased up to 45.8% at the end of the 2018 research cycle in February of 2021.

Cracking in Section N7 did not increase again until March of 2019 after 8.9 million ESALs when it increased slightly to 22.9%. Cracking increased gradually in 2019 up to 33.1% in December after approximately 12.7 million ESALs. No increase in cracking was observed between December of 2019 and February of 2020 after 13.3 million ESALs.

The cracks observed in Section N7 in January of 2020 were still in low severity as shown in Figure 5a. In some areas, the cracks became connected, and some fines could be seen along some of the connected cracks (Figure 5b). To further evaluate the cracks observed in Section N7, field cores were extracted from the areas with the connected cracks. As shown in Figure 5c, these cracks appeared to develop from the bottom of Section N7 and propagate to the surface, affecting the performance of the surface layer in this study.

The average rut depths measured in both sections were still below 5.0 mm, indicating good rutting performance. Both sections showed good ride quality (IRI) and good macrotexture.

(a) (b) (c)

Figure 5. (a) Section N7 as of January 8, 2020 (b) Closeup of Hairline Cracks in the Wheel Paths, (c) Field Core Confirming Bottom-Up Cracking

After consulting with the sponsor, Delta Mist spray-on rejuvenator was applied to the distressed surface of Section N7 at a 0.08 GSY rate on February 21, 2020 (Figure 6) to evaluate if the spray-on rejuvenator could help extend the life of asphalt pavements with bottom-up fatigue cracking. Cracking progressed significantly the week after Delta Mist was applied in late February of 2020. Cracking in Section N7 increased from 33.1% right before the Delta Mist application (13.3 million ESALs) to 53.4% in April of 2020 after 14.2 million ESALs. The addition of Delta Mist presumably softened the distressed asphalt structure and accelerated the rate of failure in which the surface layer was then milled and inlaid.

Figure 6. Delta Mist Application on Section N7 in February 2020

The two surface mixtures in Sections N1 and N7 (before the bottom-up cracking failure) showed good ride quality and rutting performance. The bottom-up cracking failure in Section N7 can be observed in rutting and IRI measurements around 14 million ESALs in Figures 3b and 3c. The areas of bottom-up cracking failures (Figure 7) in Section N7 were milled and replaced in May of 2020.

(a) (b)

Figure 7. Section N7 Milled and Inlaid in May of 2020 (a) Milled Surface Showing Bottom-Up Cracking (b) Area of Severe Bottom-Up Cracks

6.4 Laboratory versus Field Cracking Performance

Table 2 summarizes the laboratory test results performed on the plant mixtures and their extracted binders for comparing with the field cracking measurements. The overlay test (OT) was conducted in accordance with the Tex-248F and NCAT-modified procedures while the Illinois Flexibility Index Test (I-FIT) was performed following the AASHTO TP 124-16 procedure. Both tests have been used to evaluate the cracking resistance of asphalt mixtures (*4*-*7*). While the average test results shown in Table 2 were different for the Texas OT and I-FIT tests, they were statistically similar (same letter) when considering the variability of the test results. The NCAT-OT test results were statistically different, and they appeared to agree with the trends shown in the field cracking measurements with Section N7 having a larger area of cracking, which included both top-down and bottom-up fatigue cracking observed in this section.

Table 2. Laboratory and Field Cracking Performance (*2*)

Mixture	ΔT_c	Texas OT (Nf)	NCAT-OT (Nf)	I-FIT (FI)	Field Cracking (%)
N1 20% RAP	-9.4	25 (A)	556 (A)	3.58 (A)	45.8
N7 35% RAP + Delta S	-10.1	10 (A)	73 (B)	3.43 (A)	53.4

*Letters next to Texas OT, NCAT-OT, and I-FIT results represent groupings from statistical analysis.

6.5 Summary and Lessons Learned

This experiment was designed to determine the effectiveness of Delta S rejuvenator by comparing the field performance of two 9.5 mm surface mixtures. The first (control) mixture was placed in Section N1. It was produced with a PG 67-22 virgin binder and 20% RAP, which is a typical RAP content allowed for use in surface mixtures in the United States. The second

(experimental) mixture was placed in Section N7. It was originally produced with 20% RAP, 5% RAP and a PG 67-22 binder blended with 10% Delta S (by weight of the recycled binder). The original mixture was later replaced with a mixture produced with 35% RAP and a PG 67-22 binder. The binder was dosed with Delta S at a rate of 5% by weight of the recycled binder available in the RAP. Lessons learned from the research include the following:

- Delta S should not be used with southeastern post-consumer RAS without an adequate reaction time during production. Without an adequate reaction time with aged binder, Delta S may excessively soften the virgin binder, potentially leading to premature failures.
- The Texas overlay and Illinois flexibility index tests suggested similar cracking performance for the 35% RAP mix with Delta S and the control mix with 20% RAP. However, cracking appeared earlier and progressed slightly quicker for the 35% RAP mix with Delta S at the Test Track. The largest increase in cracking for both sections occurred in October of 2017 for the 2015 research cycle and in April of 2020 for the 2018 research cycle.
- Connected cracks were observed in some locations within Section N7, and the cores extracted from these areas showed these cracks initiated from the bottom layer and propagated to the top, affecting the cracking performance of the surface layer.
- A spray-on rejuvenator is intended to remedy near surface distresses supported by a sound pavement structure. Thus, applying the Delta Mist spray-on rejuvenator to Section N7, when distresses had propagated from the bottom to the asphalt surface, accelerated failure.
- The average rut depths measured in Section N7 were below 5.0 mm, indicating good rutting performance prior to the bottom-up cracking failure. Section N7 also showed good ride quality (IRI) and similar increasing trends in macrotexture compared to Section N1.

6.6 References

1. Williams, B., J.R. Willis, and J. Shacat. *Asphalt Pavement Industry Survey on Recycled Materials and Warm-Mix Asphalt Usage: 2019*. National Asphalt Pavement Association, Lanham, Md., 2020.
2. West, R., D. Timm, B. Powell, M. Heitzman, N. Tran, C. Rodezno, D. Watson, F. Leiva, and A. Vargas. Phase VI (2015-2017) NCAT Test Track Findings, NCAT Report 18-04, 2019, pp. 197.
3. White, G. Shear Stresses in an Asphalt Surface under Various Aircraft Braking Conditions, International Journal of Pavement Research and Technology 9 (2016) 89–101.
4. Zhou, F., S. Hu, D. Chen, and T. Scullion. Overlay Tester: Simple Performance Test for Fatigue Cracking. In T*ransportation Research Record: Journal of the Transportation Research Board, No. 2001*, Transportation Research Board of the National Academies, Washington, D.C., 2007, pp. 1-8.
5. Chen, D. Field Experiences with RDD and Overlay Tester for Concrete Pavement Rehabilitation. *ASCE Journal of Transportation Engineering*, Vol. 134, Issue 1, 2008.
6. Al-Qadi, I., H. Ozer, J. Lambros, A. El Khatib, P. Singhvi, T. Khan, J. Rivera-Perez, and B. Doll. *Testing Protocols to Ensure Performance of High Asphalt Binder Replacement Mixes Using*

RAP and RAS. Illinois Center for Transportation Report FHWA-ICT-15-017. University of Illinois at Urbana-Champaign, 2015.

7. Ozer, H., I. Al-Qadi, J. Lambros, A. El-Khatib, P. Singhvi, and B. Doll. Development of Fracture-Based Flexibility Index for Asphalt Concrete Cracking Potential Using Modified Semi-Circle Bending Test Parameters. *Construction and Building Materials 115*, 2016, pp. 390-401.

7. FLORIDA DEPARTMENT OF TRANSPORTATION DENSITY STUDY

Dr. Fabricio Leiva

7.1 Introduction

Achieving appropriate in-place density is critical to the long-term performance of asphalt pavement, as a small change in in-place density can significantly affect pavement service life. Based on correlations between pavement performance and in-place density, pavement service life is significantly reduced when in-place density is below 93% (%G_{mm}). Linden et al. reported that a 1% decrease in density can result in an approximate 10% loss in pavement life, and Mallela et al. suggested a 35% reduction in service life for pavements with an in-place density between 90.0% and 92.0% when compared with those having an in-place density between 93.0% and 95.0% (*1, 2*).

Water can enter permeable pavements and cause other issues, further reducing service life. To avoid water-induced issues, Terrel et al. suggested that asphalt pavements were relatively impermeable when the in-place density was above 92.0% (*3*). However, the relationship between density and permeability can be greatly influenced by other factors, such as nominal maximum aggregate size (NMAS) and the relative coarseness or fineness of the gradation.

A minimum in-place density has been recommended for various NMAS gradations in previous reports (*4, 5*). Based on historical data, Hughes suggested that realistic target values for density should have an average density of 93.0% and a standard deviation of 1.5 for agencies that started using end-result specifications with density measurements in the late 1980s (*6*). In addition, the Asphalt Institute reported that a target density of less than 92.0% was considered inadequate, and Brown et al. suggested that the initial in-place density for dense graded mixtures should not be less than approximately 92.0% to minimize water permeability and binder aging (*7, 8*). Based on a survey of state highway agencies, Decker reported that 89% of respondents had minimum requirements on in-place density ranging from 91.0% to 93.0%, with 58% of the respondents specifying 92.0% while about 77% of the respondents indicated that maximum requirements were between 97.0% and 98.0%, with 58% specifying 97.0% (*9*). In general, there is consensus in more recent research using various evaluation techniques that the in-place density of the mat should be greater than 92.0%, and 93.0% to 94.0% would be preferred after construction (*10*).

Recognizing the importance of in-place density, a full-scale accelerated pavement test study, sponsored by the Florida DOT (FDOT), was initiated at the NCAT Test Track. Four test sections with thin mill and fill layers (1.5 inches thick) were constructed in 2018 with densities ranging from 88% to 94%. Laboratory characterization and performance tests were also included in the experimental plan.

7.2 Objective and Scope

The objective of this experiment was to evaluate the effect of density level on pavement performance. A secondary objective of this work was to characterize the mixtures' properties and performance in the laboratory utilizing the same density level achieved in the field. To complete this research, one asphalt mixture containing 20% reclaimed asphalt pavement (RAP)

and a polymer modified binder was placed and compacted in four 100-foot test strips in Sections E5 and E6 during the 2018 reconstruction of the NCAT Test Track.

7.3 Background

FDOT has a 93.0% (%G_{mm}) standard target density and corresponding percent within limits (PWL) specification of +3.00 and -1.20. However, this is a relatively new specification. Prior to July 2019, the upper specification limit was +2.00% with the same target density of 93.0%. There is also a 92.0% target density, which is used for areas requiring static compaction and for 1.0" thick lifts regardless of compaction type. Static compaction is typically specified by FDOT for vibration sensitive areas such as urban areas, sinkhole prone geology, underlying utility structures, etc. For static compaction, FDOT sets the target density is 1% higher than for vibratory compaction.

Figure 1 shows the distribution of density results for the previous 10 years (2008 – 2018) for standard compaction projects (93.0% target) in the state of Florida. The average density for this period was 92.92% with a standard deviation of 1.00%. Figure 2 shows the distribution of density results for the previous 10 years (2008 – 2018) when the 92.0% target was applied. The average density for this period was 92.20% with a standard deviation of 1.05%.

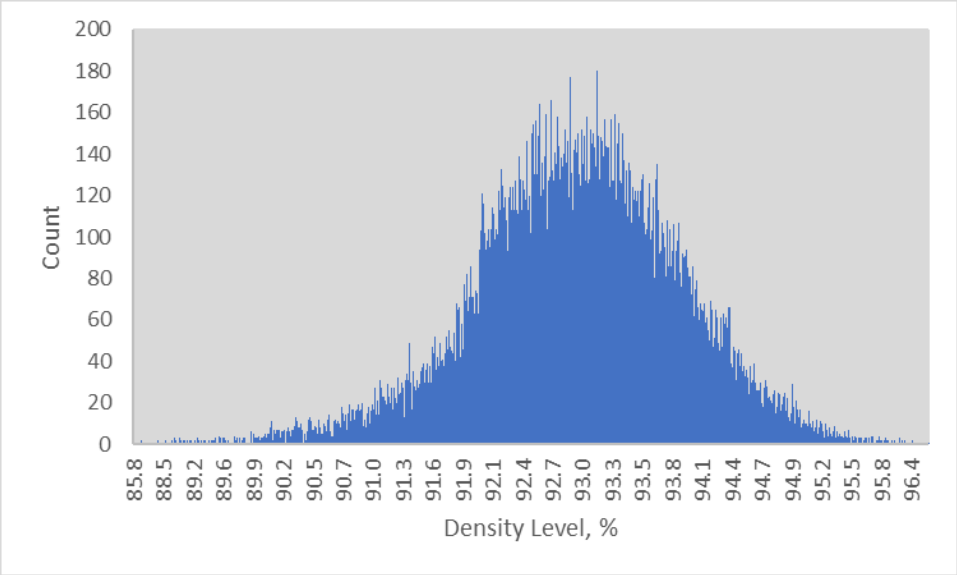

Figure 1. Histogram of 93.0% Target Density (Source Florida DOT)

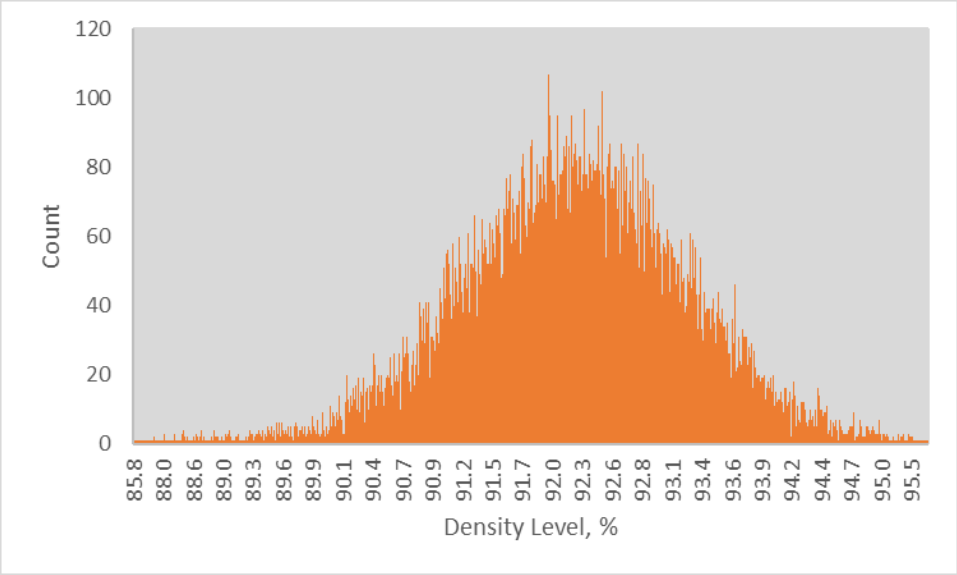

Figure 2. Histogram of 92.0% Target Density (Source Florida DOT)

As shown in Figure 3, lower variability was found in Florida for projects with a target density of 93.0% on almost all of the analyzed years. This effect of reducing density variability as the target density increased was also observed by Aschenbrener et al (*11*). The higher variability observed on projects with the lower target density of 92.0% is likely due to the wider PWL specification, but could also be due to the complexity of the application (vibration sensitive areas). Since density variability can also negatively affect pavement performance, density was monitored periodically in this study with the plan to quantify density variability over time and determine its effect on performance.

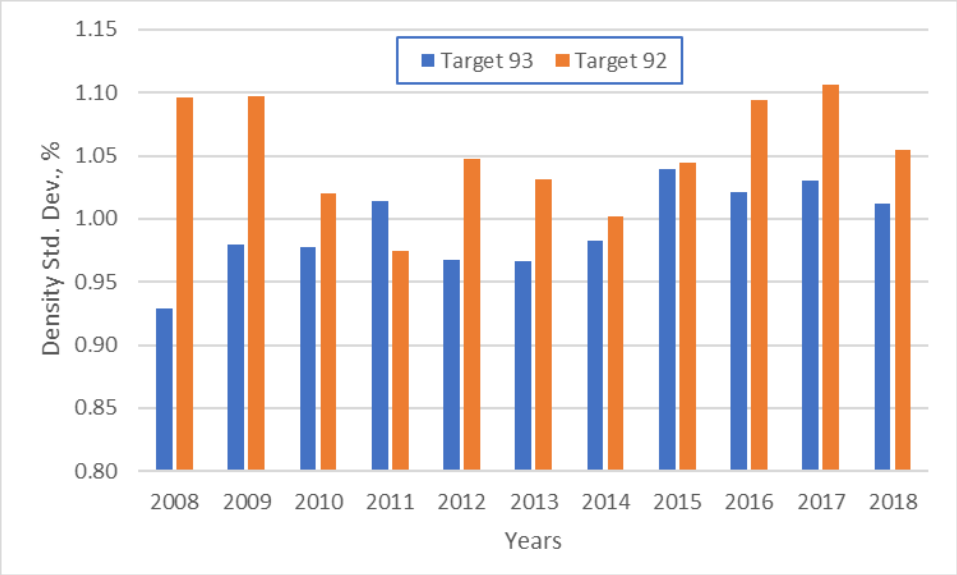

Figure 3. Standard Deviation per Year (Source Florida DOT)

7.4 Mix Design and Construction

One mixture was designed at the NCAT laboratory for this experiment. This mixture utilized a PG 76-22 asphalt binder modified with styrene-butadiene-styrene (SBS). The gradation was a 12.5-mm NMAS blend that was on the fine side of the primary control sieve. The mixture gradation is shown in Table 1. The asphalt mixture design was performed using 100 gyrations with the Superpave gyratory compactor. The mixture was designed with 4.3% air voids and had a VMA of 14.0% and a VFA of 69%. The optimum binder content was 4.8%.

Table 1 shows a summary of the mixture design information and mixture acceptance data for the entire project. A slight increase in binder content and gradation led to a decrease in air voids, decrease in VMA, and increase in VFA values in all four sections. In addition, a slight increase in the material passing the No. 200 sieve on Sections E5-1A and E5-1A resulted in higher dust proportion ratios. Therefore, there is potential impact on the outcomes of some of the performance-type tests that were conducted and field performance.

Table 1. Florida DOT Mixture Characteristics

Mix Design Parameters	**Design Data**	**E5-1A**	**E5-1B**	**E6-1A**	**E6-1B**
Design Method	Superpave				
Compactive Effort	100 Gyrations				
Results	**Design Data**	**Quality Control Data**			
Binder Grade	76-22	76-22	76-22	76-22	2
$P_{3/4"}$, %	100	100	100	100	100
$P_{1/2"}$, %	98	99	99	98	98
$P_{3/8"}$, %	90	89	89	89	87
$P_{\#4}$, %	54	57	57	56	55
$P_{\#8}$, %	40	40	40	38	39
$P_{\#16}$, %	33	32	32	29	31
$P_{\#30}$, %	24	22	22	20	22
$P_{\#50}$, %	13	12	12	10	12
$P_{\#100}$, %	7	8	8	6	7
$P_{\#200}$, %	4.1	5.5	5.5	3.8	3.9
Modifier Type	SBS				
Total Binder Content, %	4.8	5.0	5.0	5.0	5.0
Effective Binder Content, %	4.2	4.3	4.3	4.3	4.3
Dust Proportion	1.0	1.3	1.3	0.9	0.9
% RAP	20	22	22	22	22
Air Voids, %	4.3	3.6	3.6	3.5	3.5
Voids in Mineral Aggregate, %	14.0	13.6	13.6	13.5	13.5
Voids Filled with Asphalt, %	69	74	74	74	74
Production/Construction Data					
Lift Thickness, in	1.5	1.5	1.5	1.5	1.5
Type of Tack Coat		NTSS-1HM			
Undiluted Target Tack Rate/residual, gal/sy		0.1/0.06			
Temperature at Plant, °F		320	320	320	320
Average Mat Compaction, %		93.6	92.0	87.8	89.7

Figure 4 shows the results of the Cantabro test (AASHTO TP 108) conducted on samples that were laboratory produced and compacted at planned field density levels and a sample at the design gyratory compaction level (N_{des}). To assess statistical differences in the Cantabro percent mass loss results, the Tukey-Kramer test ($\alpha = 0.05$) was used to determine where these statistical differences occurred and how the mixtures were grouped. This analysis indicated that the percent mass loss of the mixture compacted for Section E6A-1 compares with E6B-1 but is statistically different (higher) from the rest of the sections. On the other hand, the percent mass loss of Section E5A-1 is statistically different from Sections E6A-1 and E6B-1. Other than these results, there is no evidence of difference between other sets of sections. A good linear correlation between percent mass loss and average air voids of R = 0.92 was obtained. As expected, the Cantabro test showed improved specimen durability with improved density.

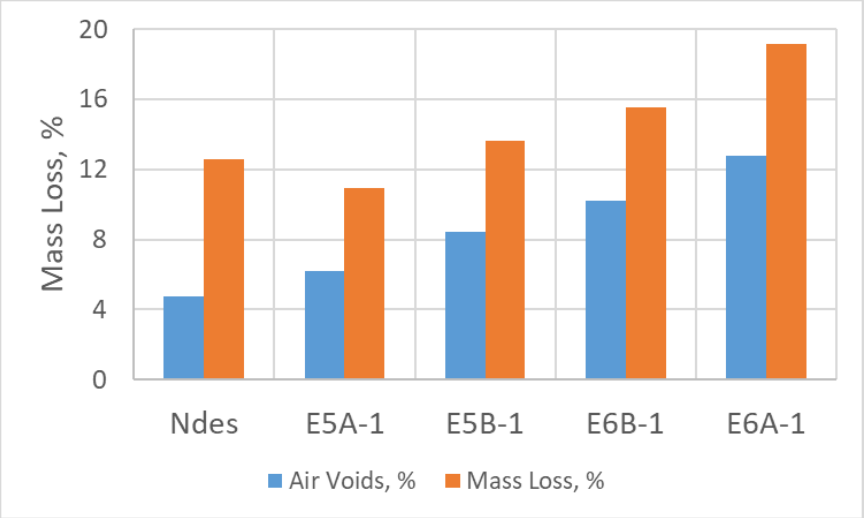

Grouping Information Using the Tukey Method and 95% Confidence

MixID	N	Mean	Grouping		
E6A-1	3	19.2	A		
E6B-1	3	15.5	A	B	
E5B-1	3	13.6		B	C
N_{des}	3	12.6		B	C
E5A-1	3	10.9			C

Means that do not share a letter are significantly different.

Figure 4. Mixture Design Cantabro Test Results Florida DOT Density Study

All four of the test sections for this evaluation were originally constructed on August 29, 2018, and Section E6-1A was repaved on October 4, 2018 since the target density was not met in the field. The asphalt mixture was produced at the East Alabama Paving Company's asphalt plant located approximately five miles from the test track. Travel time from the plant to the site is about 10 minutes and the reported mix temperature at the plant was approximately 320°F. The mixture was delivered to the site using end dump trucks and deposited into a Roadtec SB2500 material transfer vehicle, which transferred the mixture into a Roadtec RP-190e paver (Figure 5). Two rollers were used to compact the mix on this project, a 12-ton Dynapac CC624 as breakdown roller and a Hypac C350D as finish roller. A NTSS-1HM tack was applied at a bar rate of 0.1 gal/yd^2 from the tack truck.

Section E5-1A received the most compactive energy with four vibratory passes and three static passes. This pattern was adjusted on the remaining sections by reducing the number of vibratory passes per section. Densities of the sections were monitored by the contractor with a nuclear density gauge, and 6-inch diameter core samples were taken for acceptance and tested by NCAT personnel.

Figure 5. Equipment Utilized During Construction

7.5 Laboratory Testing

While the field experiment was being conducted, plant-produced loose mix and asphalt binder that had been sampled during construction were taken back to the NCAT laboratory for evaluation. Unless otherwise specified, laboratory performance tests for this study were performed on samples made from re-heated plant-produced mix. Performance testing samples were compacted to the following density targets: 6.5% air voids for E5A, 8.0% air voids for E5B, 12.0% air voids for E6A, and 10.0% air voids for E6B. Target air voids for laboratory specimens after all necessary saw trimming was ±0.5%. The mixtures were evaluated for cracking potential, rutting potential and durability using seven different tests: energy ratio, Illinois Flexibility Index Test (I-FIT), dynamic modulus test (E*), Indirect Tensile Asphalt Cracking Test (IDEAL-CT), Cantabro Mass Loss, Hamburg Wheel Tracking Test (HWTT), and high-temperature indirect tensile (HT-IDT).

7.5.1 Energy Ratio

The energy ratio test procedure was developed to assess an asphalt mixture's resistance to top-down or surface cracking (*12*). This test procedure has been used in past research cycles at the NCAT Test Track as a predictor of whether a mixture might be susceptible to top-down cracking (*13*). Energy ratio is determined using a combination of three tests: resilient modulus, creep

compliance, and indirect tensile strength. These tests are described in greater detail below. These tests were performed at 10°C using an MTS® testing device. The tests were conducted on three specimens 150 mm in diameter and 38 to 50 mm thick, cut from gyratory compacted samples.

The resilient modulus was obtained by applying a repeated haversine waveform load in load control mode. The load was applied for 0.1 seconds and then followed by a 0.9 second rest. The resilient modulus was calculated using the values from the stress-strain curve. The creep compliance test was performed as described in AASHTO T 322-07; however, the temperature of the test was 10°C with a test duration of 1000 seconds. The power function properties of the creep compliance test were determined by curve-fitting the results obtained during constant load control mode. The tensile strength and dissipated creep strain energy (DCSE) at failure were determined from the stress-strain curve of the given mixture during the indirect tensile strength test. Detailed testing procedures and data interpretation methods for the three testing protocols are described elsewhere (*12, 13, 14)*.

The results from these tests were then used to evaluate each mixture's surface cracking resistance using Equation 1. Data analysis was performed using a software package developed at the University of Florida. The details of the software operation are documented elsewhere (*14*). Table 2 lists the recommended thresholds for the energy ratio as a function of ESALs. A higher energy ratio provides more resistance to surface cracking. Additionally, a DCSE at failure of less than 0.75 kJ/m^3 has been used to identify excessively brittle mixes in the field (*11*). The energy ratio criteria in Table 2 are only recommended for mixtures with a DCSE at failure of between 0.75 and 2.50 kJ/m^3 (*12*).

$$ER = \frac{DSCE_f\left[7.294\times10^{-5}\times\sigma^{-3.1}(6.36-S_t)+2.46\times10^{-8}\right]}{m^{2.98}D_1} \quad (1)$$

where

σ = tensile stress at the bottom of the asphalt layer (150 psi),
M_r = resilient modulus,
D_1, m = power function parameters,
S_t = tensile strength,
$DCSE_f$ = dissipated creep strain energy at failure, and
ER = energy ratio.

Table 2. Recommended Energy Ratio Criteria (*12*)

Traffic (ESALs/yr)	Minimum Energy Ratio
Greater than 250,000	1.00
Greater than 500,000	1.30
Greater than 1,000,000	1.95

Note: $DCSE_f$ must be greater than 0.75 kJ/m^3 or the mix is considered brittle.

Table 3 and Figure 6 show the energy ratio results for the mixture with four density levels. When comparing these data, all mixtures had energy ratios above 1.95 and $DCSE_f$ values higher than 0.75 kJ/m^3. Therefore, this mixture is expected to sustain over one million equivalent

single axle loads (ESALs) per year at the four air void levels studied in this project. Resilient modulus was the only parameter that followed a defined trend with respect to the air void contents, and as expected, decreased with an increase in the air void content. Additionally, an excellent linear correlation between resilient modulus and average air voids of R = -0.97 was obtained. A fairly linear correlation between energy ratio and average air voids of R = -0.79 was obtained.

Table 3. Energy Ratio Test Results of Sections E5 and E6

Mix ID	Air Voids (%)	m-value	D_1	S_t (Mpa)	M_R (GPa)	FE (kJ/m³)	$DCSE_{HMA}$ (kJ/m³)	a	$DCSE_{MIN}$ (kJ/m³)	ER
E5A-1	6.3	0.462	3.18E-07	2.44	13.1	3.2	2.97	4.65E-08	0.69	4.33
E5B-1	7.7	0.352	7.21E-07	2.50	10.3	4.0	3.70	4.61E-08	0.69	5.32
E6B-1	10.0	0.408	7.65E-07	2.03	8.6	3.5	3.26	4.87E-08	1.09	3.00
E6A-1	12.0	0.356	9.54E-07	1.78	7.0	2.8	2.57	5.01E-08	0.88	2.93

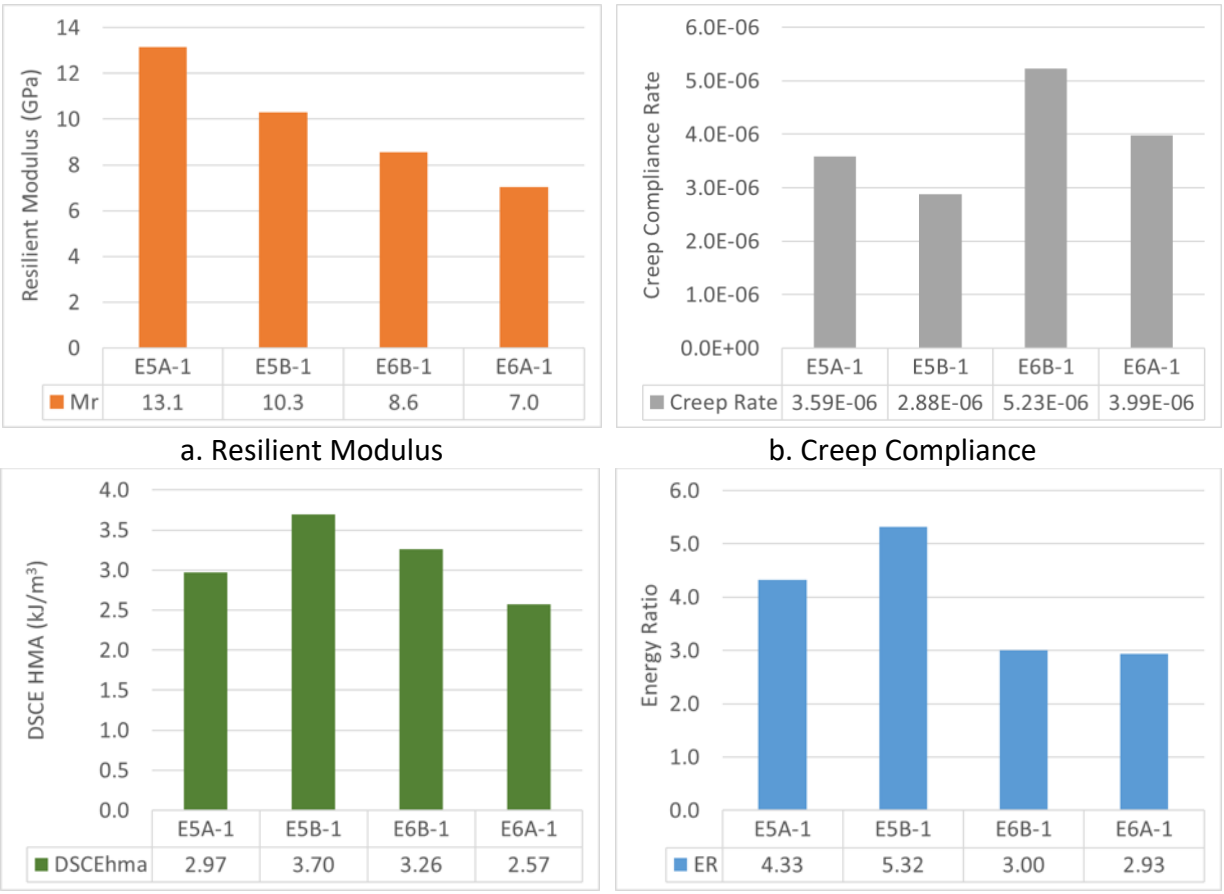

a. Resilient Modulus

b. Creep Compliance

c. DCSE

d. Energy Ratio

Figure 6. Energy Ratio Test Results of Sections E5 and E6

7.5.2 Illinois Flexibility Index Test (I-FIT)

The Illinois Flexibility Index Test (I-FIT) was performed in accordance with AASHTO TP 124-18. Semi-circular asphalt specimens were prepared from a larger 160 mm tall by 150 mm diameter gyratory specimen. Each trimmed slice was cut in half and four replicates were obtained per

specimen. A notch was then trimmed into each specimen at a target depth of 15 mm and width of 1.5 mm along the center axis of the specimen. The specimens were tested at a target test temperature of 25.0 ± 0.5°C after being conditioned in an environmental chamber for two hours. Specimens were loaded monotonically at a rate of 50 mm/min until the load dropped below 0.1 kN after the peak was recorded. Both force and actuator displacement were recorded by the system at a rate of 50 Hz.

The development of flexibility index (FI) threshold values is ongoing, but research conducted for the Illinois Center for Transportation by the University of Illinois at Urbana-Champaign has made some lab to field comparisons between FI and field cracking performance (*15*). Comparisons between the FI results from loose mix samples and mixture performance at FHWA's accelerated loading facility (ALF) showed good agreement between FI and load repetitions to failure of the accelerated sections; the three poor-performing sections had an FI value of less than 2, whereas the control section (which was among the top performers) had an FI value of 10. Additionally, some correlation was seen between the FI and cores obtained from nine different Illinois DOT districts. The FI clearly showed the effects of aging on these cores with a reduction in FI for cores from pavements that were more than 10 years old. Sections with FI less than 4 to 5 on the field cores generally exhibited premature cracking. Currently, a preliminary recommendation of 8.0 has been given for minimum flexibility index.

The test results from all mixtures are provided in Figure 7 and Table 4. All mixtures had FI values below the preliminary Illinois criterion, but significant differences were observed. Section E6B-1 with 10.1% air voids was statistically the top performer, followed by sections E6A-1 and E5A-1 and lastly, as bottom performer, section E5B-1 with 8.1% air voids. Based on past experience, a reversed density trend (increased FI with increased air voids) was expected. However, with this set of I-FIT data there did not appear to be a clear relationship between density and FI.

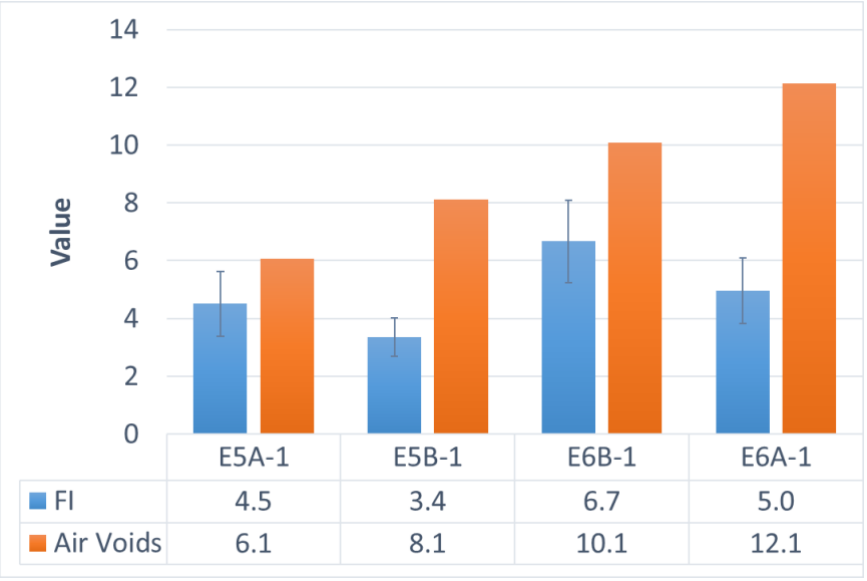

Grouping Information Using the Tukey Method and 95% Confidence

MixID	N	Mean	Grouping		
E6B-1	6	6.7	A		
E6A-1	8	5.0		B	
E5A-1	9	4.5		B	C
E5B-1	8	3.4			C

Means that do not share a letter are significantly different.

Figure 7. Flexibility Index Test Results of Sections E5 and E6

Table 4. I-FIT Test Results of Sections E5 and E6

Mix ID	Specimen Air Voids (%)	FE (J/m2)	Slope (kN/mm)	Strength (kPa)	Flexibility Index		
	Average	*Average*	*Average*	*Average*	*Average*	*St. Dev.*	*CV (%)*
E5A-1	6.1	1,887	-4.40	535.4	4.5	1.1	24.9
E5B-1	8.1	1,796	-5.47	556.7	3.4	0.7	19.9
E6B-1	10.1	1,618	-2.49	363.8	6.7	1.4	21.4
E6A-1	12.1	1,330	-2.79	361.2	5.0	1.1	22.9

7.5.3 Dynamic Modulus (E*)

Dynamic modulus (E*) testing was conducted in accordance with AASHTO T 378 on the four previously described mixtures. This testing was performed using an IPC Global Asphalt Mixture Performance Tester (AMPT). Specimens were produced in accordance with AASHTO R 83. A Pine Instruments gyratory compactor was used to compact specimens to 150 mm in diameter and 180 mm in height. These samples were then cored using a 100 mm diameter core drill and trimmed to 150 mm in height. To provide the necessary information for mechanistic-empirical pavement analyses, the three samples of the mixture compacted at four density levels were tested using three temperatures (4, 20, and 40°C) and three frequencies (10, 1, and 0.1 Hz) in an unconfined state. The mixes were also tested at the 0.01 Hz frequency at the high test temperature. This testing produced a data set for generating master curves for all four mixtures using the procedure outlined in AASHTO R 84.

While the master curves are not direct indicators of performance, they are used in mechanistic pavement design and can give an indication of relative mixture stiffness. This is particularly useful for mixtures containing RAP or recycled asphalt shingles (RAS) where the degree of binder blending is unknown. For the four master curves (Figure 8), the mixture with the lowest air void content (E5A-1) was the “stiffer” mixture at all temperatures and frequencies. Table 5 shows the master curve coefficients and regression parameters for all mixtures.

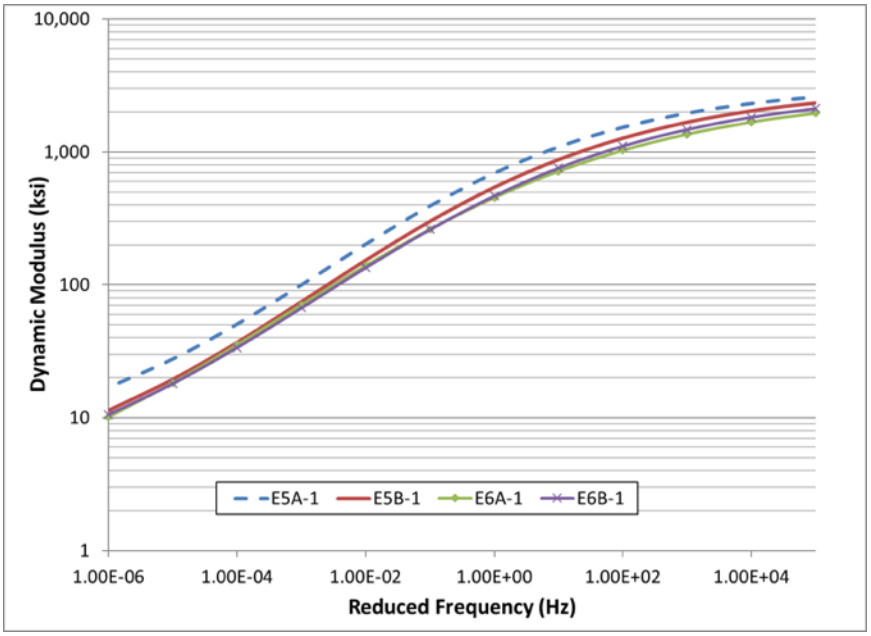

Figure 8. Master Curves of Sections E5 and E6

Table 5 Master Curve Coefficient and Regression Parameters of Sections E5 and E6

Mix	Air Voids,%	Max E* (Ksi)	Min E* (Ksi)	Beta	Gamma	EA	R^2	Se/Sy
E5A-1	6.3	3231.58	5.06	-1.163	-0.438	209640	0.983	0.093
E5B-1	7.9	3126.11	2.50	-1.119	-0.405	217233	0.986	0.085
E6A-1	11.9	2864.30	1.23	-1.163	-0.358	222615	0.985	0.086
E6B-1	10.1	2990.62	2.14	-1.065	-0.388	219100	0.983	0.092

The results of statistical analyses conducted at the tested temperatures and frequencies are shown in Table 6. To assess statistical differences in E* results, the general linear model (α = 0.05) was conducted on the test data measured at a frequency of 10, 1.0, and 0.1 Hz and temperatures of 4, 20, and 40°C. The Tukey-Kramer test (α = 0.05) was used to determine where these statistical differences occurred and how the mixtures were grouped within each project. For each temperature-frequency combination, mixtures with the same letter were not statistically different. The majority of the statistical differences were obtained at low temperatures, and mixtures from Sections E5A-1 and E5B-1 showed higher dynamic moduli than the remaining mixtures. As expected, the mixture from Section E5A-1, with the lowest air voids, had the highest moduli on all temperatures and frequencies. On the other hand, mixtures from Sections E6A-1 and E6B-1 were not statistically different on all temperature-frequency combinations.

Table 6 E* Statistical Grouping (Tukey-Kramer Test at α = 0.05) of Sections E5 and E6

Mix ID	4°C - 10 Hz	4°C - 1 Hz	4°C - 0.1 Hz	
E5A-1	A	A	A	
E5B-1	B	B	B	
E6B-1	C	C	C	
E6A-1	C	C	C	
Mix ID	**20°C - 10 Hz**	**20°C - 1 Hz**	**20°C - 0.1 Hz**	
E5A-1	A	A	A	
E5B-1	B	B	B	
E6A-1	B C	C	B C	
E6B-1	C	C	C	
Mix ID	**40°C - 10 Hz**	**40°C - 1 Hz**	**40°C - 0.1 Hz**	**40°C - 0.01 Hz**
E5A-1	A	A	A	A
E5B-1	B	B	B	B
E6B-1	B C	B	B	B
E6A-1	C	B	B	B

7.5.4 Indirect Tensile Asphalt Cracking Test (IDEAL-CT)

The Indirect Tensile Cracking Test (IDEAL-CT) was performed in accordance with ASTM D 8225-19. The test is performed on SGC specimens compacted to a height of 62 mm and a diameter of 150 mm with no additional specimen preparation. A minimum of three specimens were prepared at each target air void content. Previous research has shown the IDEAL-CT test to have a reversed density trend from the expected behavior (increased density will yield a lower cracking resistance index) (*16*). Therefore, for this study, it was expected that the higher air voids specimens would have higher CT_{Index} values, which is counterintuitive.

Specimens were conditioned for two hours at 25°C in an environmental chamber prior to testing. Testing was performed in a servo-hydraulic indirect tensile load frame using a monotonic loading rate of 50 mm/minute (shown in Figure 9). Specimens are loaded until the load peaks and then drops to less than 0.1 kN. A plot of load versus load-line displacement was then generated (example shown in Figure 10). Equation 2 (from ASTM D 8225-19), is then used to calculate the CT_{Index} for each specimen. A higher CT_{Index} is generally representative of increased mixture cracking resistance.

$$\mathrm{CT_{Index}} = \frac{t}{62} \text{ x } \frac{l_{75}}{D} \; x \; \frac{G_f}{|m_{75}|} \; x \; 10^6 \tag{2}$$

where

CT_{Index} = cracking tolerance index,
G_f = failure energy (J/m^2),
$|m_{75}|$ = absolute value of the post-peak slope m75 (N/m),
l_{75} = displacement at 75% of the peak load post-peak (mm),
D = specimen diameter (mm), and
t = specimen thickness (mm).

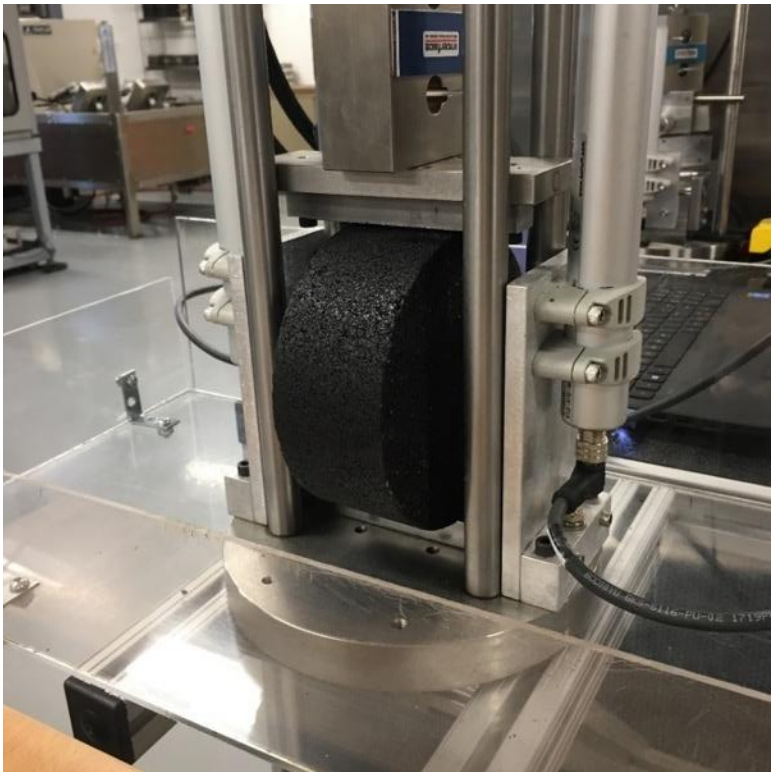

Figure 9. IDEAL-CT Testing Device at NCAT

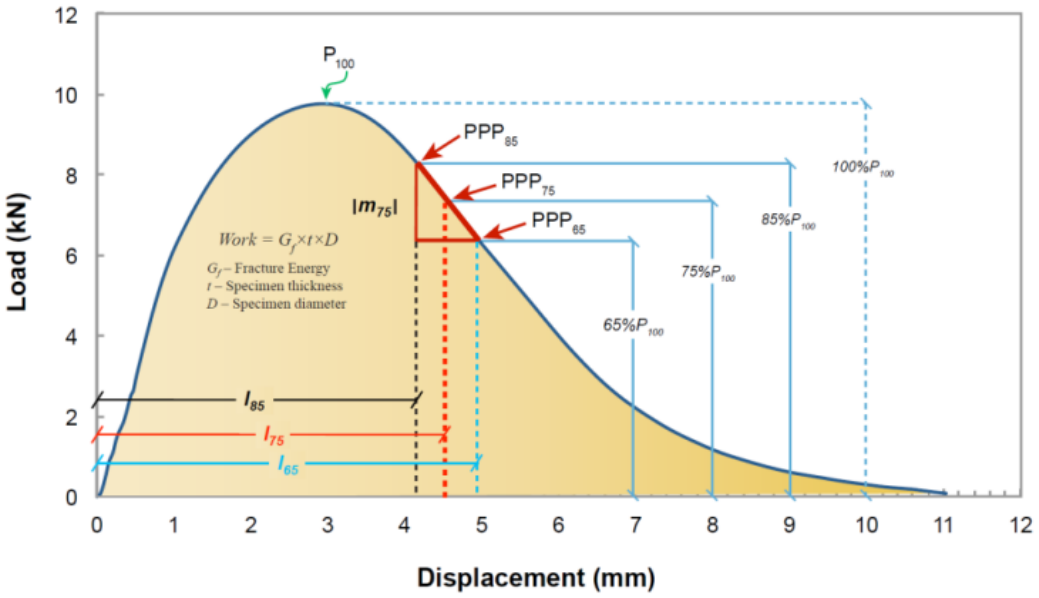

Figure 10. IDEAL-CT Plot of Load Vs. Load Line Displacement (16)

Figure 11 shows that as the air voids content increased the CT_{index} increased. Such behavior has been documented elsewhere (*16*). Statistical analysis indicated that the top performer was Section E6A-1 with 11.9% air voids and the bottom performer was Section E5A-1 with 6.3% air voids. However, no statistical differences between Sections E6A-1 and E6B-1 or between Sections E6B-1 and E5B-1 were obtained. An excellent linear correlation between CT_{Index} and average air voids of R=0.99 was obtained.

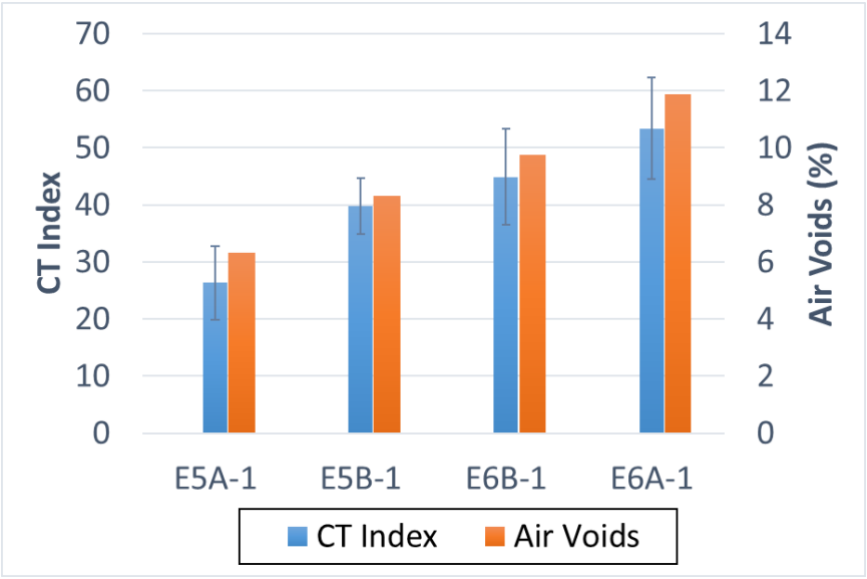

Grouping Information Using the Tukey Method and 95% Confidence

MIxID	N	Mean	Grouping		
E6A-1	5	53.4	A		
E6B-1	6	44.8	A	B	
E5B-1	6	39.8		B	
E5A-1	6	26.3			C

Means that do not share a letter are significantly different.

Figure 11. IDEAL Cracking Test Results of Sections E5 and E6

7.5.5 Cantabro Mass Loss

The Cantabro abrasion test is often used for the design of open-graded friction course (OGFC) mixtures as a measurement of durability and of the potential for aggregate loss (e.g., raveling) from mixtures. A 20% upper limit of aggregate loss for unconditioned OGFC mixture specimens has been recommended (*17*). For this test, standard 150-mm diameter Superpave gyratory compactor (SGC) specimens of nominal 115-mm height are compacted of each mixture. Each specimen is weighed to the nearest 0.1 g, then placed in the drum of an L.A. Abrasion testing machine without the steel charges and subjected to 300 revolutions at 30 to 33 rpm. The specimen is then removed, the loose mix particles are discarded, and the mass is determined again. The loss in specimen mass as a percentage of the original mass during the test is calculated and denoted as mass loss. Doyle and Howard found that mass loss for dense-graded mixtures was less than 15% based on a limited data set and stated that the use of the Cantabro test for dense graded mixtures was promising (*18*).

Figure 12 shows the results of the Cantabro test conducted on the plant produced mixture at the observed levels of density in the field. To assess statistical differences in mass loss results, the Tukey-Kramer test ($\alpha = 0.05$) was used to determine where these statistical differences occurred and how the mixtures grouped within each project. This analysis indicated that mass loss of the mixture compacted for Section E6A-1 was statistically different (higher) from the rest of the sections. On the other hand, mass loss of Section E5A-1 was statistically different from Sections E6B-1 and the N_{des} sample. Section E5B-1 showed the lowest mass loss of all sections. Other than these results, there is no evidence of difference between other sets of sections.

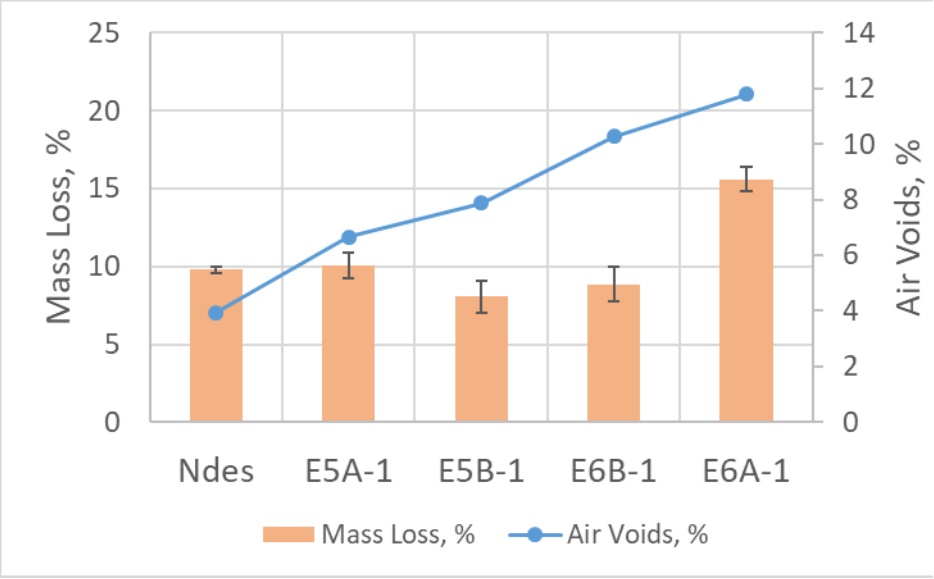

Grouping Information Using the Tukey Method and 95% Confidence

Mixl D	N	Mean	Grouping	
E6A-1	3	15.6	A	
E5A-1	5	10.1		B
Ndes	3	9.8		B C
E6B-1	4	8.8		B C
E5B-1	4	8.0		C

Means that do not share a letter are significantly different.

Figure 12. Cantabro Test Results of Sections E5 and E6

7.5.6 Hamburg Wheel Tracking Test (HWTT)

The Hamburg Wheel Tracking Test was performed to determine the rutting and stripping susceptibility of the four mixtures. Samples were prepared in accordance with AASHTO T 324.

For each mix, four specimens (two replicates) were tested. The specimens were originally compacted to a diameter of 150 mm and a height of 62 mm.

The samples were tested under a 158 ± 1 lb wheel load for 10,000 cycles (20,000 passes) while submerged in a water bath maintained at a temperature of 50°C. During testing, rut depths were measured by a Linear Variable Displacement Transducer (LVDT). After testing, the HWTT data were used to determine the point at which stripping occurred in the mixture under loading and the relative rutting susceptibility of those mixtures. The data shows the progression of rut depth with number of cycles. Two tangents are evident from this curve: the steady-state rutting portion of the curve and the portion of the curve after stripping. The intersection of these two tangents defines the stripping inflection point of the mixture.

Figure 13 shows the rut depths of samples compacted at the observed field air voids contents. The mixtures did not show any signs of stripping; therefore, it is not expected that any of the mixtures will be susceptible to moisture damage. Additionally, all four mixtures showed good resistance to rutting, as 12.5 mm is a common rutting threshold for this test. As expected, an increase in rutting was obtained with an increase in air voids. An excellent linear correlation between the HWT rut depth and average air voids of R = 0.99 was obtained.

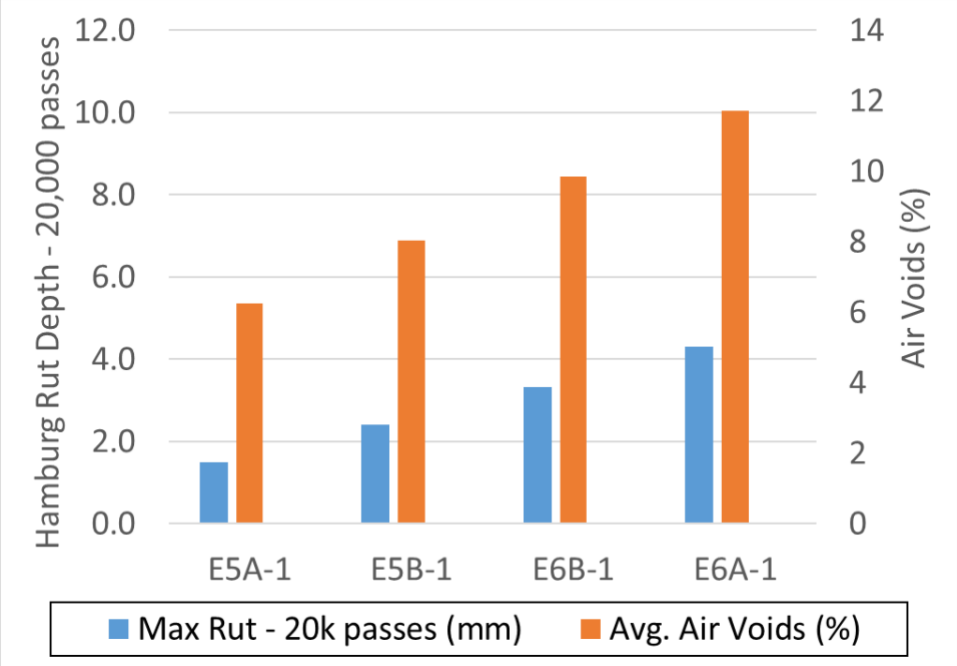

Figure 13. Hamburg Test Results of Sections E5 and E6

7.5.7 High Temperature Indirect Tensile Strength (HT-IDT)

According to the results of work conducted by Christensen et al., IDT strength at a temperature of 20°C below the critical pavement temperature showed an excellent correlation with rutting measured on full-scale pavement sections and tested with the FHWA ALF device (*19*). The results of their study led to preliminary guidelines that can be generated for evaluating rut resistance on the basis of IDT strength tests. In 2007, Christensen and Bonaquist provided revised guidelines for interpreting IDT Strength test results at high temperatures based on field

measured rut depths from pavement sections located at NCAT, MnRoad, and WesTrack (*20*). In a more recent study by Bennert et al., the HT test was evaluated as a potential surrogate for the Asphalt Pavement Analyzer (APA) during quality control testing (*21*). The HT-IDT showed a strong correlation to APA rutting when evaluating asphalt mixtures of varying volumetric properties, asphalt binder grades, and gradations. The study showed that the HT-IDT test was also more repeatable than the APA.

For this study, three replicate specimens were prepared in accordance with AASHTO T 312. Samples were compacted in the gyratory Superpave compactor to a 62 mm height at the measured field air void content of each section. Samples were conditioned in a forced draft oven at the test temperature of 50 °C ± 1°C (122 °F ± 2 °F) for two hours ± 10 minutes prior to testing. Specimens were tested within two minutes of removal from the oven. Specimens were loaded monotonically at 50 mm/minute until the peak load was obtained. The indirect tensile strength (ITS) was then calculated from the peak load and specimen dimensions. Figure 14 shows the results of HT-IDT conducted for all four mixtures. The relationship between HT-IDT and air voids indicates that tensile strength at high temperatures tends to decrease with an increase in air voids. However, for this case, no statistical differences were obtained in tensile strength for Sections E5B-1 and E6B-1 despite the change in air voids of 2.0 %.

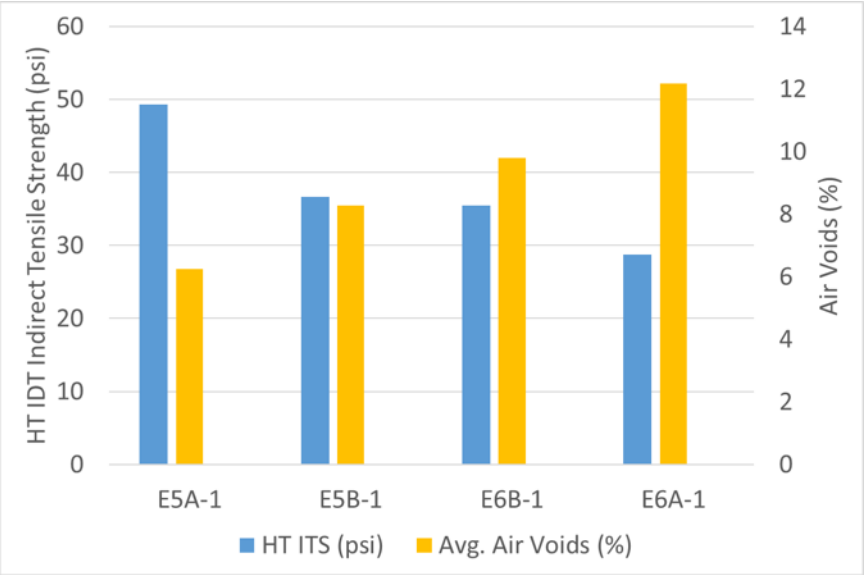

Grouping Information Using the Tukey Method and 95% Confidence

MixID	N	Mean	Grouping		
E5A-1	4	49.2	A		
E5B-1	4	39.4		B	
E6B-1	4	35.5		B	C
E6A-1	5	28.7			C

Means that do not share a letter are significantly different.

Figure 14. HT-IDT Results of Sections E5 and E6

Figure 15 shows the relationship between HT-IDT strength results and rut depths measured with the Hamburg wheel-tracking device. A good correlation was obtained for this dataset and the expected trend was also obtained: an increase in rutting resistance with an increase in tensile strength.

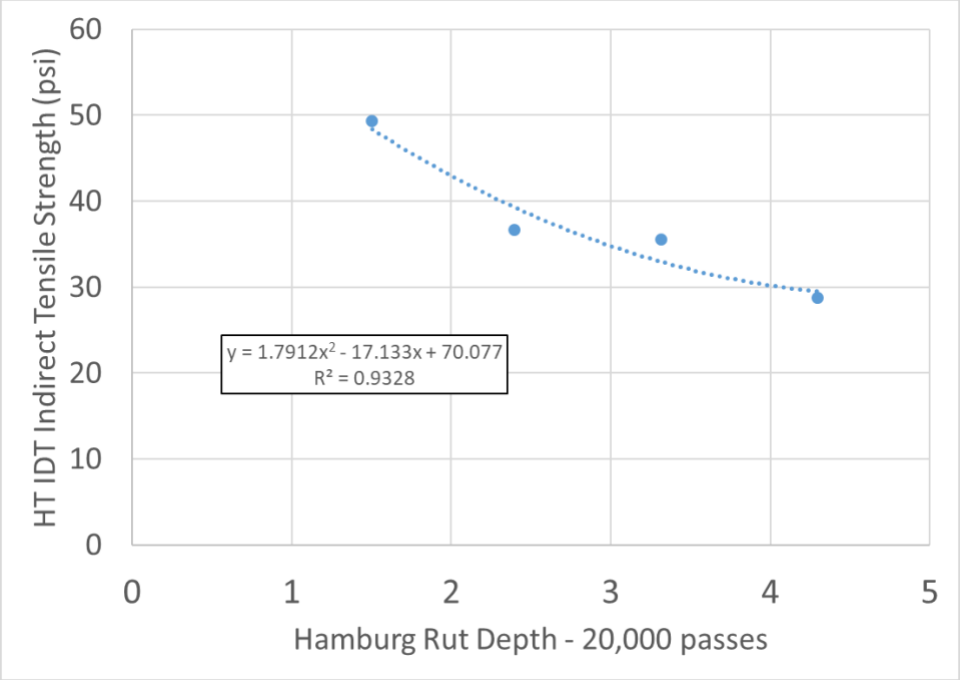

Figure 15. Relationship of HT-IDT Versus HWTT of Sections E5 and E6

7.5.8 Correlation and Ranking Analysis

Pearson correlations were developed between the average laboratory mixture properties, provided in Table 7. R-values close to 1 and -1 show high degrees of correlation. R-values near zero are indicative of non-correlated variables. Laboratory parameters that showed excellent correlation with air void contents to meet field density were CT_{Index}, HWT, HT-IDT and resilient modulus. However, CT_{Index} followed the opposite trend as previously discussed.

Table 7 Laboratory Test Result Pearson Correlation Analysis of Sections E5 and E6

	Air Voids	*FE*	*CT Index*	*HWT*	*HT IDT*	*Mr*	*DSCE*	*ER*
Air Voids	1							
FI	0.43	1						
CT_{Index}	0.99	0.33	1					
HWT	1.00	0.43	0.98	1				
HT IDT	-0.95	-0.21	-0.99	-0.94	1			
Mr	-0.97	-0.41	-1.00	-0.99	0.98	1		
DSCE	-0.52	-0.31	-0.30	-0.46	0.19	0.31	1	
ER	-0.79	-0.85	-0.60	-0.74	0.48	0.66	0.71	1
Mass Loss	0.67	0.09	0.57	0.68	-0.51	-0.55	-0.90	-0.61

Green = excellent correction, Orange = good correlation

Table 8 shows a ranking analysis to organize all four mixtures from one to four with one performing best based on several laboratory performance related parameters. In terms of cracking, there was no consensus on parameters to define a top performer. The Energy Ratio and Cantabro mass loss parameters position Section E5B with 92.0% field density as top performer. In terms of rutting potential, dynamic modulus at 40°C, HWT and HT IDT position Section E5A with 93.6% field density as top performer, and overall there is a good relationship

between field density and rutting potential: the higher the field density the higher the resistance to rutting.

Table 8 Laboratory Test Result Ranking Analysis of Sections E5 and E6

ID	I-FIT FI	CT $_{Index}$	ER	Cantabro Mass Loss	-β/γ (Inflection Point)	E* 40C, 1 Hz (ksi)	HWTT	HT-IDT
E5A	4.5	26.3	4.3	10.1	-2.66	157.7	1.5	49.3
E5B	3.4	39.8	5.3	8.0	-2.76	108.7	2.4	36.6
E6B	6.7	44.9	3.0	8.9	-2.75	95.2	3.3	35.5
E6A	5.0	53.4	2.9	15.6	-3.25	96.1	4.3	28.7
	Individual Ranking							
Field Density (%)	I-FIT FI	CT $_{Index}$	ER	Cantabro Mass Loss	-β/γ (Inflection Point)	E* 40C, 1 Hz (ksi)	HWTT	HT-IDT
93.6	3	4	2	3	1	1	1	1
92.0	4	3	1	1	3	2	2	2
89.7	1	2	3	2	2	4	3	3
87.9	2	1	4	4	4	3	4	4

7.6 Field Performance

Field performance evaluations for roughness (International Roughness Index, IRI), mean texture depth (MTD), rutting (rut depth), and cracking (expressed as a percentage of the lane) are included for all sections from 0 to 10 million ESALs of traffic. Figures 16 to 20 show these field parameters as a function of millions of ESALs. Most sections showed slight variations in IRI values from the beginning, but this value remained almost constant in all cases. On the other hand, a small steady increase in the mean texture depth was observed from when the sections were opened to traffic through 4 million ESALs. After that, the texture has remained almost constant in all cases. Almost no rutting was reported before 9 million ESALs with rut depths below 2.0 mm. At the end of the cycle, a significant increase in rutting has been measured. However, rut depths for all sections were below 5.0 mm (¼ inches) at the conclusion of 10 million ESALs of traffic.

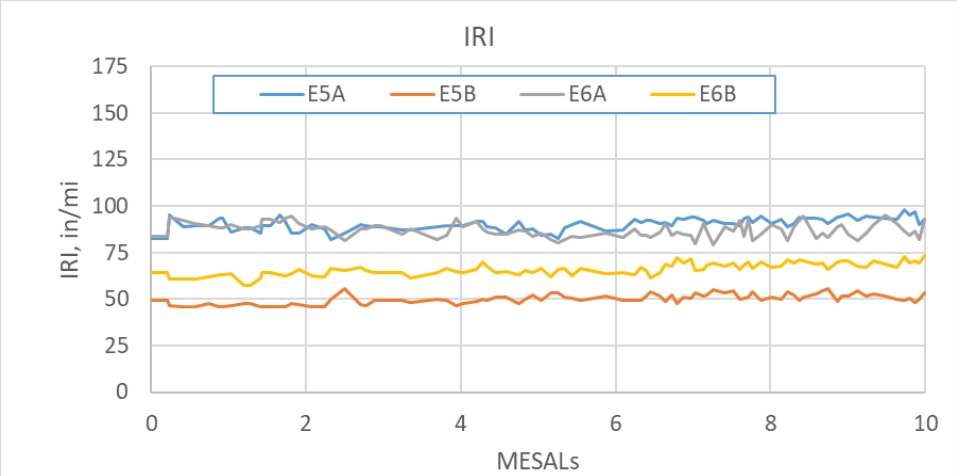

Figure 16. Measured Roughness Results of Sections E5 and E6

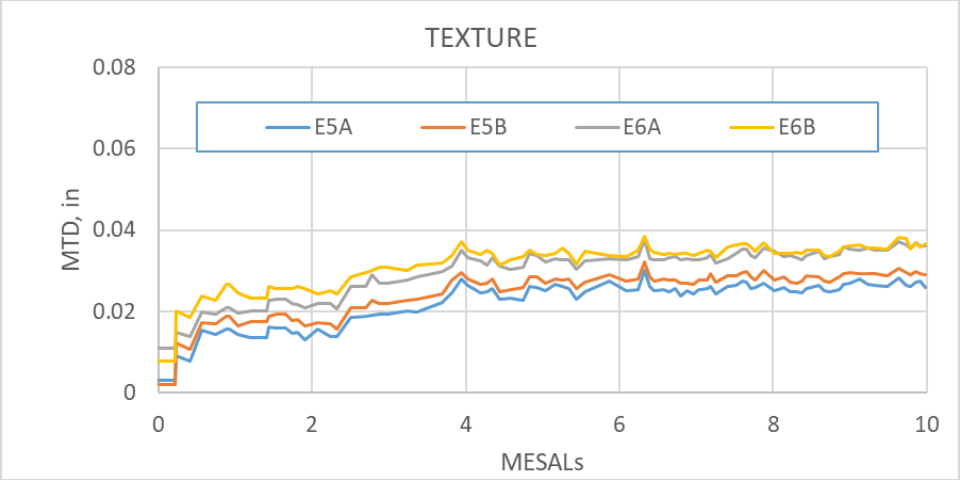

Figure 17. Measured Texture Results of Sections E5 and E6

Figure 18 shows the physical difference in texture between sections E5A and E6A. These are the high and low density levels from the study, and the effect of density is reflected on the surface texture. Despite the low density and potential high permeability of Section E6A, no evidence of moisture damage such as weathering and raveling have been found after 10 million ESALs of trafficking and 2.5 years in place.

a. b.

Figure 18. Difference in Surface Texture of (a) Section E5A (93.6%) and (b) Section E6A (87.9%)

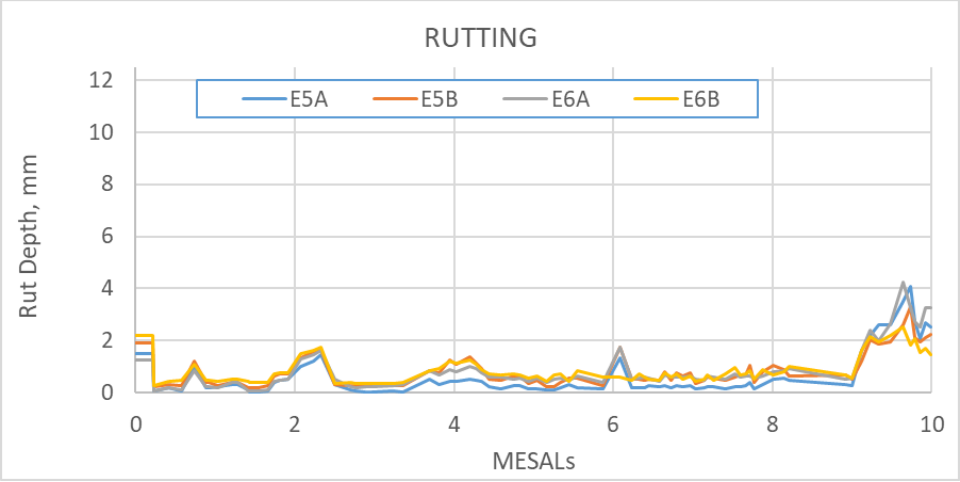

Figure 19. Measured Rutting of Sections E5 and E6

Section E6A, with the lowest overall density, was the first to crack. Section E5A, with the highest overall density, was the last one to crack at around 9 million ESALs. All of the quantified cracks in these sections were low severity cracks at the end of trafficking. Total cracking in all sections was less than 5% of the lane after 10 million ESALs of traffic.

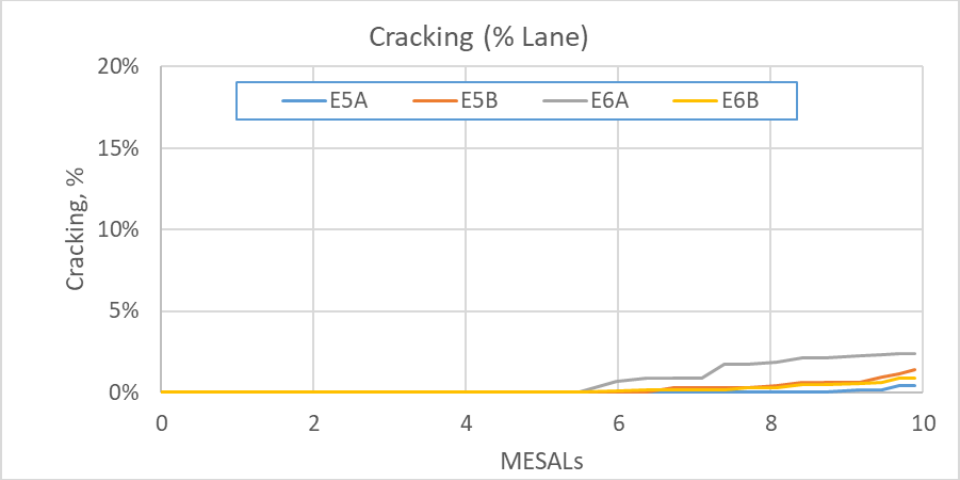

Figure 20. Measured Cracking of Sections E5 and E6

No correlation analyses between laboratory parameters and field performance have been conducted at this time. The relatively low measured distress levels were not adequate to establish any trends. It is expected that the continuation of traffic along with environmental conditions for the next cycle will provide distinctions in performance between the sections that can be statistically analyzed.

7.7 Conclusions

The results of this study support the following conclusions.

- Laboratory cracking test results did not exhibit expected trends in terms of density or air voids. However, a reversed trend for the I-FIT and IDEAL-CT tests with respect to density

was expected based on past experience. There was no consensus among parameters to define a top performer.

- All mixtures, regardless of density level, are expected to sustain over one million equivalent single axle loads (ESALs) per year based on Energy Ratio criteria.
- None of these mixes resulted in considerable amounts of rutting and were considered non susceptible to rutting in the laboratory regardless of the density levels used in this study based on HWTT results and criteria. No evidence of moisture damage was observed in the HWTT. This agrees with the observations of minimal rutting and no moisture damage seen in the field through the first cycle of traffic for these sections.
- Section E5A had dynamic moduli significantly higher than the rest of the sections at all tested temperatures and frequencies. That significant separation from the lower density mixtures was also reflected in the HWTT and HT-IDT rutting test results.
- At the end of trafficking, field performance was good with cracking at less than 5% of the lane in each section, no changes in roughness, little permanent deformation, and no significant changes in texture.
- At the end of trafficking, observed cracking in the test sections was classified as low severity.

7.8 References

1. Linden, R.N., Mahoney, J.P., and Jackson, N.C. (1989). "Effect of Compaction on Asphalt Concrete Performance." *Transportation Research Record 1217*, pp. 20–28, Transportation Research Board of the National Academies, Washington, D.C.
2. Mallela, J., Titus-Glover, L., Sadasivan, S., Bhattacharya, B., Darter, M., and Von Quintas, H. (2013). *Implementation of the AASHTO Mechanistic-Empirical Pavement Design Guide for Colorado*, Colorado Department of Transportation–Research, CDOT-2013-4, Denver, CO.
3. Terrel, R.L., and Al-Swailmi, S. (1994). *Water Sensitivity of Asphalt–Aggregate Mixes: Test Selection*, SHRP Report A-403, Strategic Highway Research Program, National Research Council, Washington, D.C.
4. Cooley, Jr., L.A., Brown, E.R., and Maghsoodloo, S. (2001). *Development of Critical Field Permeability and Pavement Density Values for Coarse-Graded Superpave Pavements*, Report No. 01-03, National Center for Asphalt Technology at Auburn University, Auburn, AL.
5. Brown, E.R., Hainin, M.R., Cooley, A., and Hurley, G. (2004). *Relationship of Air Voids, Lift Thickness, and Permeability in Hot-Mix Asphalt Pavements*, NCHRP Report 531, Transportation Research Board of the National Academies, Washington, D.C.
6. Hughes, C.S. (1989). *Compaction of Asphalt Pavement*, NCHRP Synthesis 152, Transportation Research Board of the National Academies, Washington, D.C.
7. Asphalt Institute. (2007). *The Asphalt Handbook*, Manual Series No. 4 (MS-4), Seventh Edition, Lexington, KY.
8. Brown, E.R., Kandhal, P.S., Roberts, F.L., Kim, Y.R., Lee, D., and Kennedy, T.W. (2009). *Hot Mix Asphalt Materials, Mixture Design and Construction*, Third Edition, NAPA Research and Education Foundation, Lanham, MD.

9. Decker, D. (2017). *Specifying and Measuring Asphalt Pavement Density to Ensure Pavement Performance*, NCHRP Research Report 856, Transportation Research Board of the National Academies, Washington, D.C.
10. McDaniel, R.S. (2018). "Impact of Asphalt Materials Lift Thickness on Pavement Quality." NCHRP Synthesis 20-05/Topic 49-05, Draft Final Report, Transportation Research Board of the National Academies, Washington, D.C.
11. Aschenbrener T., Leiva F., Tran N., *FHWA Demonstration Project for Enhanced Durability of Asphalt Pavements Through Increased In-Place Pavement Density, Phase 2*. NCAT Report 19-02, 2019.
12. Roque, R., B. Birgisson, C. Drakos, and B. Dietrich. Development and Field Evaluation of Energy-Based Criteria for Top-Down Cracking Performance of Hot Mix Asphalt. Journal of the Association of Asphalt Paving Technologists, Vol. 73, 2004, pp. 229-260.
13. Timm D. H., G. A. Sholar, J. Kim, and J. R. Willis. Forensic Investigation and Validation of Energy Ratio Concept. In Transportation Research Record: Journal of the Transportation Research Board, No. 2127, Transportation Research Board of the National Academies, Washington, D.C., 2009, pp. 43-51.
14. Roque, R., W. G. Buttlar, B. E. Ruth, M. Tia, S. W. Dickison, and B. Reid. Evaluation of SHRP Indirect Tension Tester to Mitigate Cracking in Asphalt Concrete Pavements and Overlays. Final Report FDOT B-9885. University of Florida, Gainesville, Fla., 1997.
15. Al-Qadi, I., H. Ozer, J. Lambros, A. El Khatib, P. Singhvi, T. Khan, J. Rivera Pérez, and B. Doll. Testing Protocols to Ensure Performance of High Asphalt Binder Replacement Mixes using RAP and RAS. Illinois Center for Transportation Series No. 15-017, Illinois Center for Transportation, University of Illinois at Urbana-Champaign, 2015.
16. Zhou, F., Im, S., Sun, L., & Scullion, T. (2017). Development of an IDEAL Cracking Test for Asphalt Mix Design and QC/QA. Journal of the Association of Asphalt Paving Technologists, pp 549-577.
17. Watson, D. E., Cooley, L. A., Jr., Moore, K. A., and Williams, K., "Laboratory Performance Testing of Open-Graded Friction Course Mixtures,"Transp. Res. Rec., Vol.1891, 2004, pp. 40–47.
18. Doyle, J. D. and Howard, I. L., "Evaluation of the Cantabro Durability Test for Dense Graded Asphalt," Proceedings of Geo-Frontiers 2011,Advances in Geotechnical Engineering-Geotechnical Special Publication No. 211, ASCE, Reston, VA, 2011, pp. 4563–4572.
19. D. W. Christensen, R. Bonaquist, D. A. Anderson, S. Gokhale, "Indirect tension strength as a simple performance test", Transportation Research Circular, number E-C068, pp. 44 – 57, Washington, 2004.
20. D. W. Christensen, R. Bonaquist "Using the Indirect Tension Test to Evaluate Rut Resistance in Developing Hot-Mix Asphalt Designs", Transportation Research Circular, number E-C124, pp. 62 – 77, Washington, 2007.
21. Bennert T., Haas E., Wass E., Indirect Tensile Test (IDT) to Determine Asphalt Mixture Performance Indicators during Quality Control Testing in New Jersey. Transportation Research Record: Journal of the Transportation Research Board. 2018. https://doi.org/10.1177/0361198118793276

8. FLORIDA DEPARTMENT OF TRANSPORTATION CRACKING STUDY (Phase II)

Dr. Fabricio Leiva

8.1 Introduction

As many state agencies have successfully mitigated rutting as a primary cause of pavement deterioration, more emphasis has been placed on identifying properties of mixtures that may influence the overall durability of a pavement structure. One such distress that affects durability is top-down cracking, which has been documented worldwide. The Florida DOT and the University of Florida were some of the first to recognize the widespread nature of this distress with over 90% of cracking in the state of Florida categorized as top-down (*1*).

As the name implies, these cracks form at the top of the pavement structure and are load-related, as they tend to originate in the wheel paths. However, Roque et al. noted the complex interaction of load, thermal, and aging effects as contributing to top-down cracking. They further explain that after studying a wide variety of material characteristics, there is not one single mixture property that could reliably discern between acceptable and poor cracking performance (*2*).

This report includes mostly results of Phase II of the experiment that started in 2015. For this second cycle there was no additional laboratory testing and the main focus of this report is field performance. Some of the laboratory test results were utilized to establish a lab-field correlation and also to explain some of the field results.

8.2 Objective and Scope

The objective of this experiment was to evaluate different amounts of RAP on cracking performance (three sections) and the use of a softer-polymer modified binder. A secondary objective of this work was to characterize the mixtures' properties in the laboratory to determine which tests might successfully predict cracking resistance. To complete this research, four mixtures were placed in 100-foot test strips in Sections E7 and E8 during the reconstruction of the 2015 Test Track cycle. The mixtures varied in terms of binder type (PG grade) and recycled material content. Load application was extended for one more cycle to complete 20 million equivalent single axle loads (ESALs) to achieve the level of damage suitable for comparisons and statistical analyses.

8.3 Mix Design and Construction

Prior to the 2015 Test Track cycle, four mixtures were designed at the NCAT laboratory for this experiment. All mixtures utilized asphalt binder modified with styrene-butadiene-styrene (SBS) and used a similar aggregate skeleton. The main difference among the four mixtures was the amount of reclaimed asphalt pavement (RAP), which varied from 20% to 30% and also had an impact on the combined gradation (see the No. 8 sieve in Table 1). Mixture gradations, base binder grades, volumetrics, and construction data for all four mixtures are provided in Table 1. The performance grade of the binder for Section E8B was originally intended to be a polymer modified PG 58-28 binder. However, following modification, the final product was a PG 64-28.

Mixtures from Sections E8A and E8B had the same aggregate structure with a different binder. In this study, volumetric design was performed on E8-1A using the PG 76-22 only. The design

with the PG 58-28 binder was not verified in the lab since the binder was not available to NCAT prior to construction. The Cantabro test (ASTM D7064) was performed on design samples at three binder contents (5.0, 5.5, and 6.0%) and quality control samples. Table 1 shows the calculated Cantabro percent of weight loss at optimum binder content for the design samples.

Table 1. Florida DOT Mixture Characteristics

Mix Design Parameters	E7A	E7B	E8A	E8B	E7A	E7B	E8A	E8B
Design Method	Superpave							
Compactive Effort	100 Gyrations							
Results	Design Data				Quality Control Data			
Binder Grade	76-22	76-22	76-22	58-28	76-22	76-22	76-22	64-28
$P_{3/4"}$, %	100	100	100	100	100	100	100	100
$P_{1/2"}$, %	97	97	97	97	98	98	95	97
$P_{3/8"}$, %	85	86	86	86	90	92	87	91
$P_{\#4}$, %	56	58	60	60	54	58	56	63
$P_{\#8}$, %	42	45	48	48	40	44	44	50
$P_{\#16}$, %	33	35	38	38	33	36	37	40
$P_{\#30}$, %	21	23	24	24	24	25	26	27
$P_{\#50}$, %	11	12	13	13	13	13	14	13
$P_{\#100}$, %	7.0	7.0	8	8	7.0	7.0	8.0	8.0
$P_{\#200}$, %	4.5	4.9	5.4	5.4	4.1	4.3	4.6	5.1
Modifier Type	SBS							
Total Binder Content, %	5.2	5.2	5.1	5.1	4.8	5.0	5.0	5.0
Effective Binder Content, %	4.6	4.5	4.4	4.4	4.2	4.4	4.3	4.3
% RAP	20.9	26.4	31.8	31.8	20.0	23.9	28.9	28.8
Air Voids, %	4.0	4.0	4.0	4.0	4.3	4.0	3.5	4.5
Voids in Mineral Aggregate, %	14.6	14.5	14.4	14.4	14.0	14.0	14.0	14.0
Voids Filled with Asphalt, %	73	72	72	72	69	72	74	69
Cantabro % Loss	5.89	6.59	6.30	NA	5.41	5.45	4.55	3.49
Tensile Strength Ratio, %	96.3	97.8	92.4	NA				
Production/Construction Data								
Lift Thickness, in	1.5				1.8	1.9	1.8	1.7
Type of Tack Coat					NTSS-1HM			
Undiluted Target Tack Rate/residual, gal/sy					0.08/0.05			
Temperature at Plant, °F					340	340	340	340
Average Mat Compaction, %					93.9	91.6	92.5	93.5

8.4 Laboratory Testing Conducted in Phase I

Materials (plant-produced loose mix and asphalt binder) that had been sampled during construction were taken back to the NCAT laboratory for evaluation. The binder was tested using the performance grade, multiple stress creep recovery (MSCR) specifications, and frequency sweeps. The mixtures were evaluated for cracking potential and samples were produced following the standard procedure (at standard air void content of 7.0%) of five different tests that followed the same aging treatment as the mixtures of the Cracking Group experiment:

- Semi-circular bend test (SCB-LTRC), Louisiana Method;

- Illinois flexibility index test (I-FIT), Illinois Method;
- Energy ratio, Florida – Draft;
- Overlay test (OT) – Tex-248-F; and
- Overlay test (OT) – NCAT modified.

Additional laboratory performance evaluations included rutting using the Hamburg Wheel Tracking Test (HWTT) and the dynamic modulus (E*) test. The Hamburg test also gives a measure of the moisture resistance of these mixes. The results of these tests were presented and discussed in the previous Test Track findings report (*3*). A summary of the results and ranking analysis is provided in Table 2. Most parameters put the 30% RAP, PG 64-28 mixture (Section E8B) as the most resistant to cracking and the mixture with 25% RAP, PG 76-22 (Section E7B) as the least resistant based on the laboratory performance test results. Fitting parameters used to describe the shape of the mastercurve sigmoidal function and the E* value obtained at 20°C and 10 Hz from dynamic modulus testing were also incorporated in this analysis. The inflection point frequency parameter $-\beta/\gamma$ is being studied as a potential cracking susceptibility indicator (*4, 5*). The lower this parameter, the more susceptible the mixture could be to fatigue cracking. The stiffness of the mixture at intermediate temperatures could also be used as a cracking indicator (E* at 20°C and 10 Hz). Finally, the Cantabro test has provided strong relationships to fatigue cracking in the field and seems to be able to detect differences among common mixture variables (*6*). In this case, Cantabro percentage loss was able to identify the top performer and the bottom performer similarly to other laboratory performance tests.

Table 2. Laboratory Test Results Ranking Analysis

Mix ID	PG Grade	ER	OT-NCAT	FI	SCB - J_c	Cantabro %Loss	$-\beta/\gamma$ (Inflection Point)	E* 20C, 10 Hz (ksi)	Combined Ranking
E7A	94-16	5.1	782	3.5	0.43	5.41	-1.95	986	
E7B	94-16	1.3	212	1.8	0.42	5.45	-2.66	1154	
E8A	94-16	6.1	591	1.9	0.36	4.55	-2.09	1042	
E8B	88-16	5.3	816	5.6	0.30	3.49	-1.87	795	
Mix ID	**%RAP**		**Individual Ranking**						
E7A	20	3	2	2	1	3	2	2	2
E7B	25	4	4	4	2	4	4	4	4
E8A	30	1	3	3	3	2	3	3	3
E8B	30	2	1	1	4	1	1	1	1

8.5 Field Performance

The final phase of this study included field performance evaluations and correlation with laboratory performance test results. Figures 1 through 4 show field performance parameters including roughness (International Roughness Index, IRI), mean texture depth (MTD), rutting (rut depth), and cracking (expressed as a percentage of the lane) for all sections from 0 to 20 million ESALs of traffic. It is important to mention that the methodology used to collect cracking data changed from the first cycle to the second cycle. This change created a slight decrease in the reported percent cracking for the second cycle.

All sections showed slight variations in IRI values from the beginning up to 10 million ESALs, and after this point three sections grouped at a similar IRI level (100 to 125 in/mi), while one section (E8B) showed a small increase at the beginning of the second cycle and stayed constant until the end of trafficking. On the other hand, a small steady increase in the mean texture depth can be observed after 5 million ESALs. Almost no rutting was reported between 0 and 18 million ESALs with rut depths below 2 mm. After 18M ESALs, a sharp increase in rutting was measured in all sections. However, all field sections had less than ¼" total rutting after 20 million ESALs of traffic. A change in the measuring equipment was perform after 18 million ESALs, which may be the cause of the elevated results at the end of the cycle.

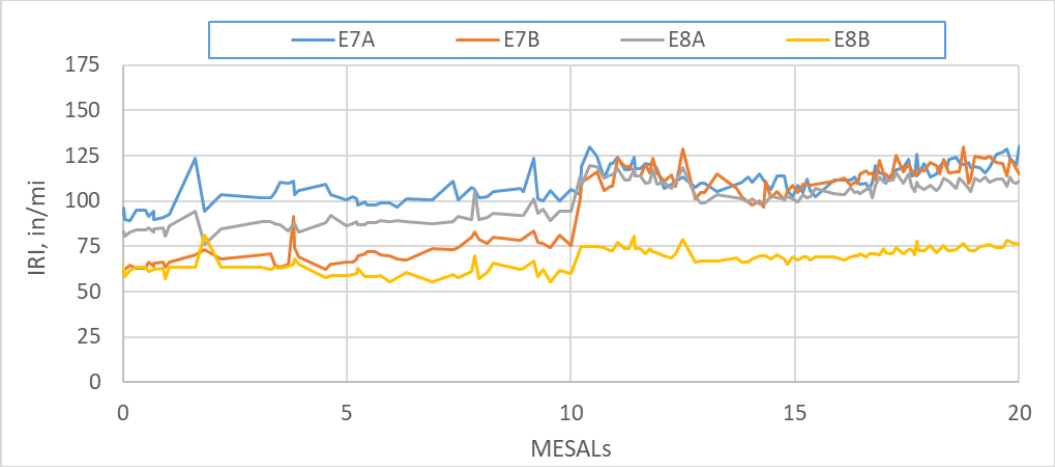

Figure 1. Measured Roughness of Sections E7 and E8

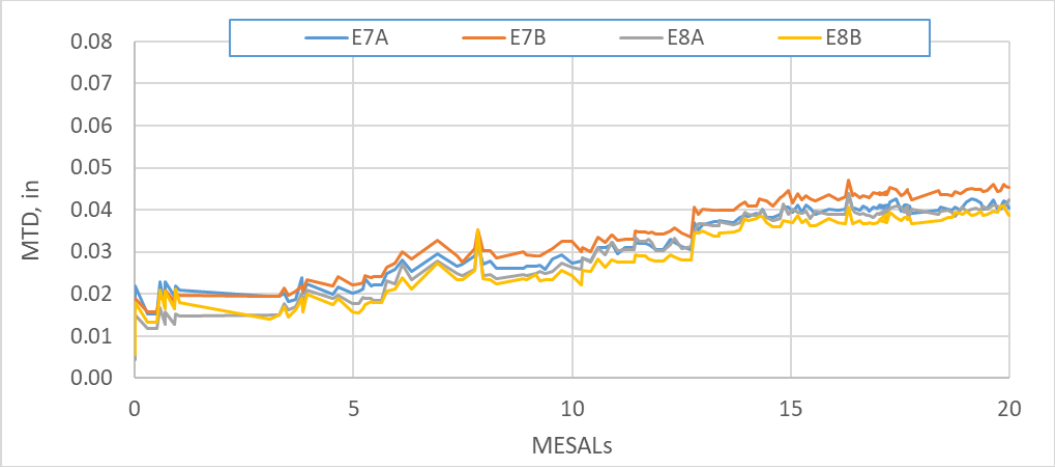

Figure 2. Measured Texture of Sections E7 and E8

The 25% RAP, PG 76-22 mixture was the first to crack in the field (E7B). However, cracking after 10 million ESALs was the highest for the 20% RAP, PG 76-22 mixture (E7A) and the lowest cracking was reported for the 30% RAP, PG 76-22 mixture (E8A), which also was the last mix to crack. At the end of the study, Section E7A showed 19.3% cracking followed by Section E7B with 19.2% cracking. Cracking severity stayed low until the end of the study for all sections. It was observed that after 5 million ESALs, cracks did not change much in length but increased in width

(from approximately 3 to 5 mm) for Sections E7A and E7B. Figure 5 shows a comparison of cracking severity for sections E8A (low) and E7A (low but marginal – 5 mm).

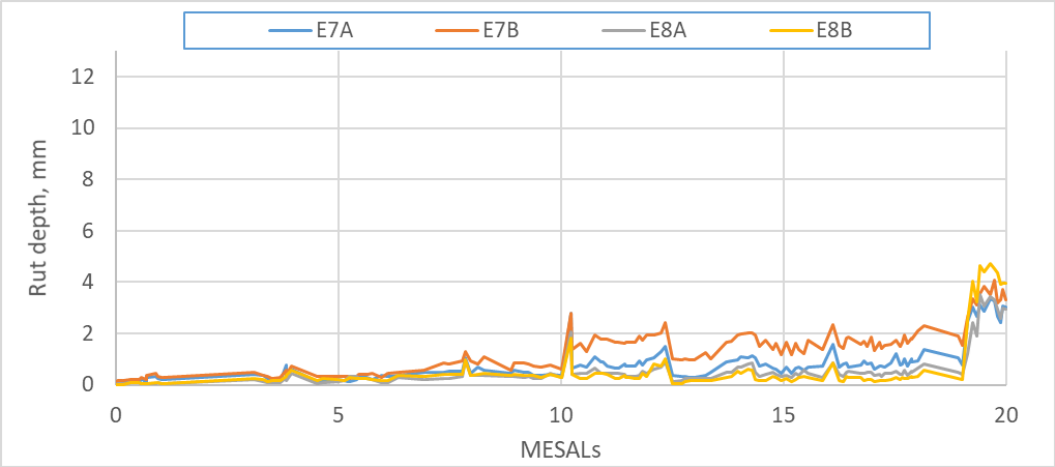

Figure 3. Measured Rutting of Sections E7 and E8

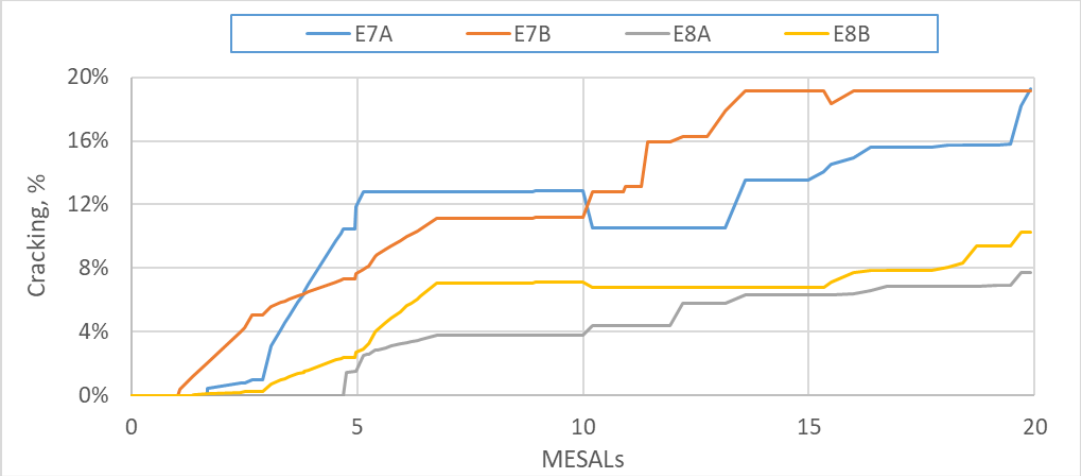

Figure 4. Measured Cracking of Sections E7 and E8

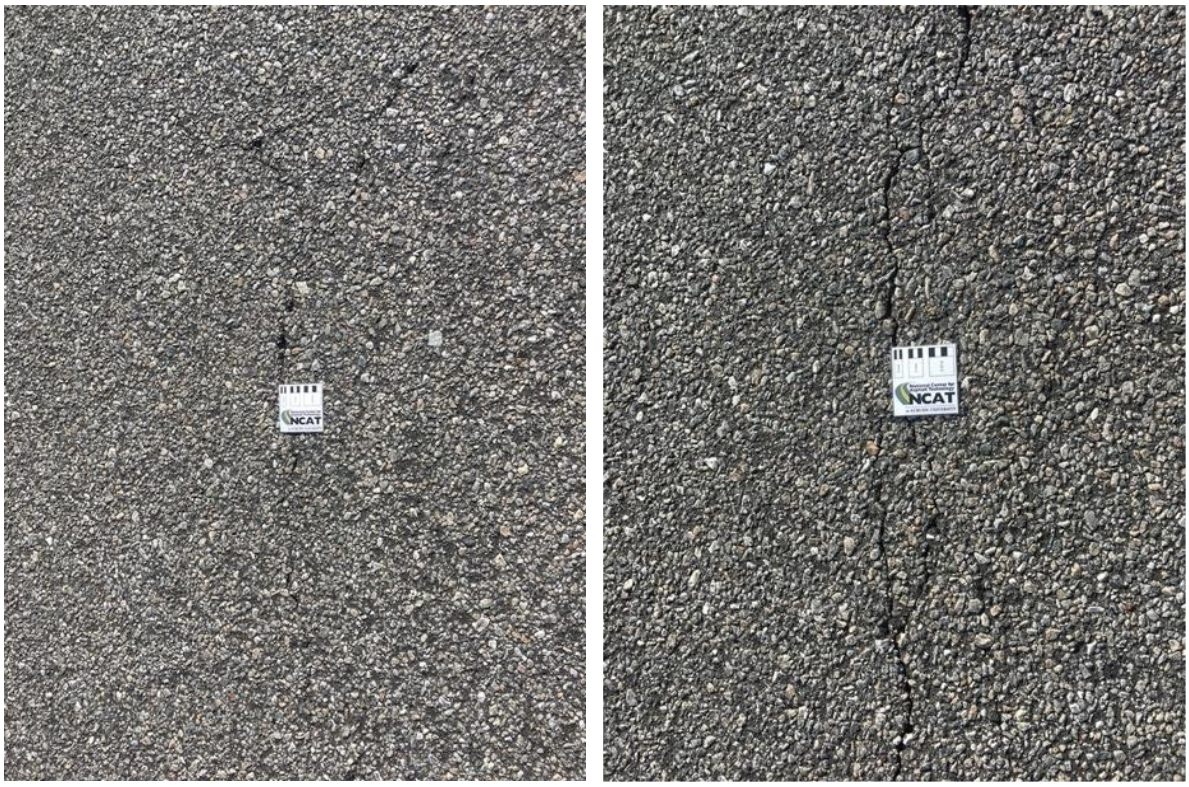

E8A E7A

Figure 5. Example of Measured Cracking Severity Levels

Pearson correlations were developed among field performance results at the end of the cycle and the results are provided in Table 3. R-values close to 1 and -1 show high degrees of correlation. R-values near zero are indicative of non-correlated variables. Blue and green highlighted cells indicate excellent and good correlation, respectively. In this case, rutting and IRI followed a reversed trend while texture and cracking followed the expected trend.

Table 3. Pearson Correlation Analysis among Field Results

	Rutting	IRI	Texture	Cracking
Rutting	1			
IRI	-0.97	1		
Texture	-0.58	0.66	1	
Cracking	-0.43	0.62	0.74	1

Pearson correlations were also developed between the average laboratory mixture properties/results and the percent cracking in the field at 10 and 20 million ESALs with results provided in Table 4. Despite some good correlations among laboratory parameters, percent field cracking showed a good correlation with Cantabro mass loss (percent) only. The Energy Ratio, crack initiation, and propagation parameters from the OT-TX results and the inflection point from the dynamic modulus mastercurves showed fair correlation (tan highlighted fields) with field cracking, as shown in Table 4. These correlations correspond to linear relationships between variables. Other best fit trend lines were analyzed (exponential and polynomial), but no improvement in the correlation coefficient was observed.

Table 4. Pearson Correlation Analysis of Laboratory vs. Field Results

Cracking, % Lane	10 Million ESALs	20 Million ESALs
OT-TX, cycles	0.15	-0.05
OT-NCAT, cycles	-0.15	-0.36
St (MPa)	-0.07	-0.12
MR (GPa)	-0.40	-0.19
DCSEf (kJ/m3)	-0.23	-0.44
ER	-0.55	-0.68
FI	0.01	-0.20
OT-TX-PRO	0.29	0.44
OT-TX-INI	0.30	0.50
beta/gamma (Inflection Point)	-0.27	-0.47
E* 20C, 10 Hz (ksi)	0.24	0.45
Cantabro %Loss	0.66	0.79

As shown in Table 1, the average mat compaction for all four sections ranged from 91.6 to 93.9% (of G_{mm}). These different levels of compaction could have added variability to the results. In practice, higher levels of density tend to improve stability and durability of the asphalt concrete layer. For a future project it would help reduce any potential confounding effect from different density levels by establishing same density targets for all the sections.

All sections had roadway core samples taken (from the wheel paths) every three months during the first 10 million ESALs and one or two samples taken during the second cycle. Figure 6 shows that density tended to increase over time during the first cycle and reached a maximum density near the end of the cycle. This was expected due to additional consolidation under traffic loading. On all the sections but E8B, a decrease in density was observed during traffic loading of the second cycle. This could be due to cracking and loss of fines/binder in the wheel paths, which was seen by the steady increase in texture (Figure 2). No correlations between field performance measurements and density were obtained. However, it can be seen that Section E7B, with the lowest (91.6% of G_{mm}) initial density, had the most cracking of all four sections at 20 million ESALs.

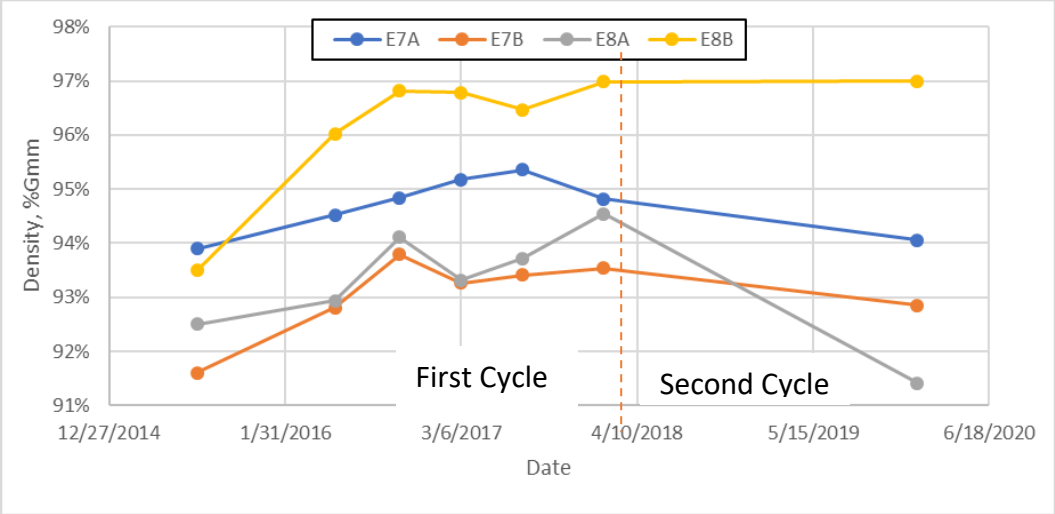

Figure 6. Progression of Density Over Time for Sections E7 and E8

Figures 7 to 10 show cracking maps for all four sections prior to construction and at the end of this study. The amount and variability of in-place cracking prior to construction could also be considered a confounding factor. Section E7A had the lowest cracking extension but at the end of the study it was one of the two sections with the highest cracking percentage. On the other hand, section E8B was significantly damaged with extensive fatigue cracking, but at the end of the study this section showed the lowest cracking percentage.

For Section E7A, the majority of cracking seems to be newly developed and not reflective cracking since there are only a few cracks that can be matched (indicated by red ovals). For the remaining sections, these maps do not provide enough evidence to conclude that this can be categorized as reflective cracking. For Section E7B, there were small differences in the location of the cracks on both longitudinal and transverse directions, but overall cracking shapes and patterns match well enough to be considered reflective cracking. This is the only case where reflective cracking was identified.

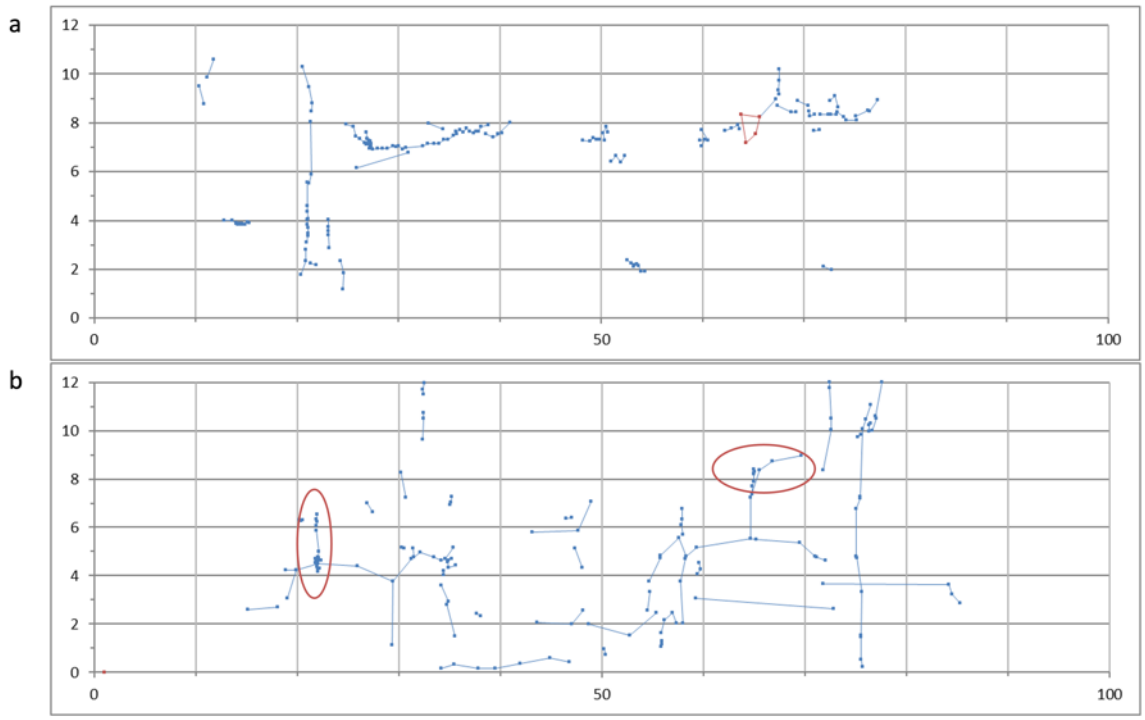

Figure 7. Section E7A Cracking Results (a) Prior to Construction (b) After Loading

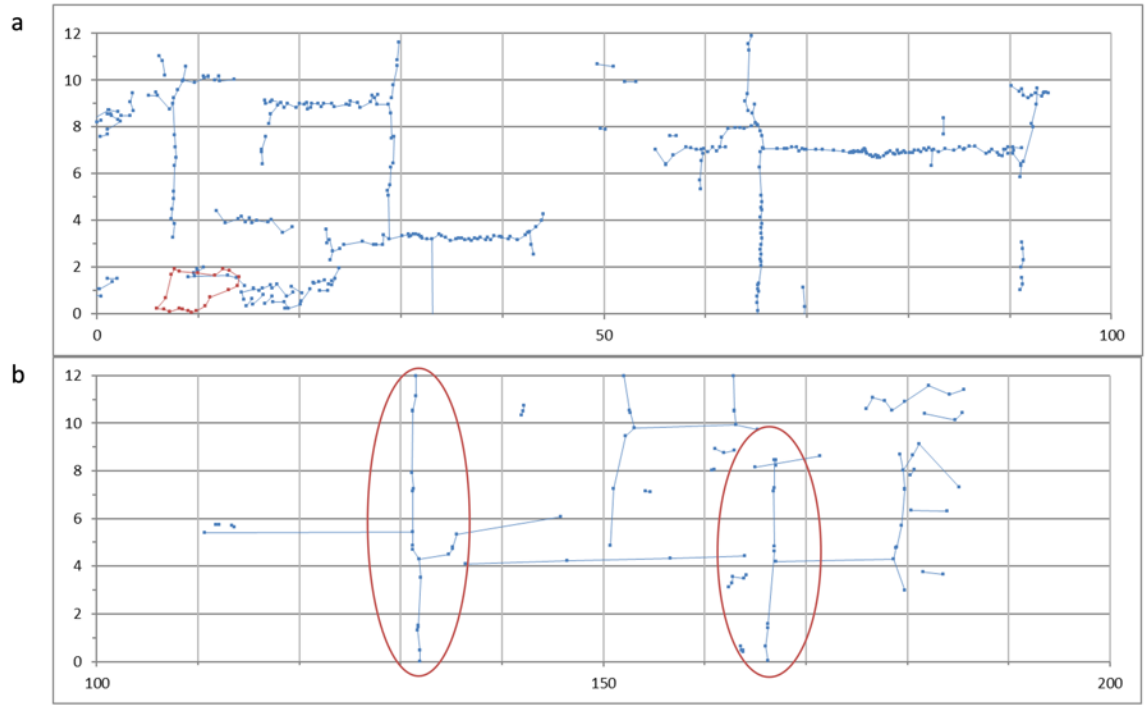

Figure 8. Section E7B Cracking Results (a) Prior to Construction (b) After Loading

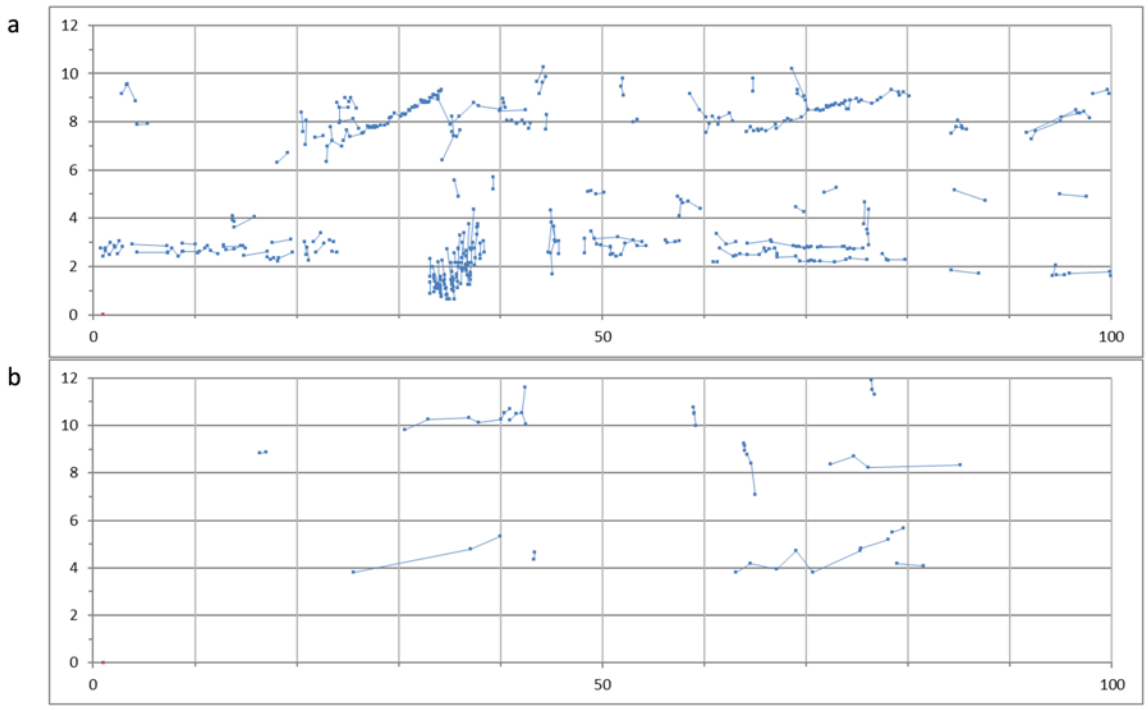

Figure 9. Section E8A Cracking Results (a) Prior to Construction and (b) After Loading

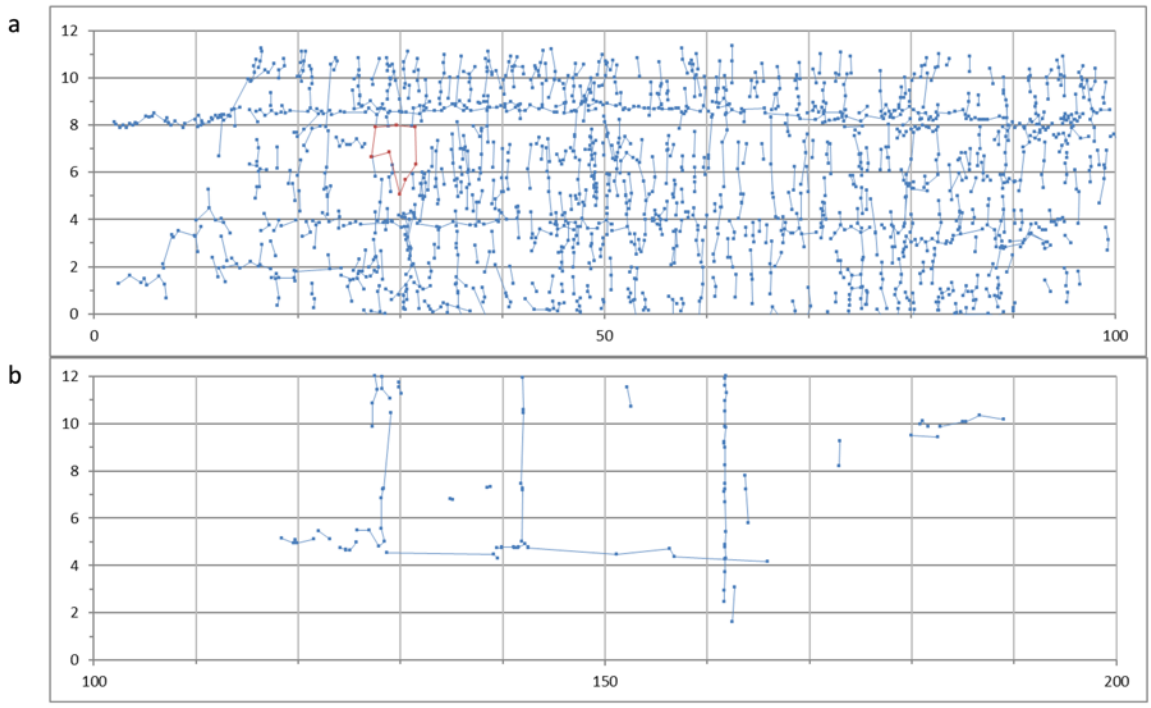

Figure 10. Section E8B Cracking Results (a) Prior to Construction and (b) After Loading

Since there was still uncertainty on the origin or type of cracking observed in these sections, four cores were taken on different locations with cracks. Figure 11 shows pictures of representative cores from each section. The same cracking pattern was observed on all the cores, where the cracks were found throughout the entire thickness of the core which includes the 1.5 in lift built for this experiment and about 8 to 10 inches from the previous cycles. At this point, the most likely cause of these cracks was new bottom-up and reflective cracking. However, top-down cracking can still be a possibility for the observed samples since these sections were in place for 20 million ESALs and over five years such that the top lifts could have cracked first due to high amounts of RAP used in this study (stiffer and more susceptible to cracking mixes).

E7A E7B

E8A E8B

Figure 11. Extracted Samples for Cracking Origin Evaluation

8.6 Conclusions

The results of this study support the following conclusions.

- Field cracking did not follow the expected trend with regards to RAP content. Sections E7A and E7B with the 20 and 25% RAP, respectively, showed the highest amount of cracking compared to the other sections with 30% RAP.
- The use of a softer modified binder did not show significant differences in field performance (Section E8B with a softer binder compared to E8A).
- After 20 million ESALs of traffic, percent field cracking showed good correlation with Cantabro loss and fair correlation with Energy Ratio.
- At the end of trafficking, cracking was classified as low severity for Sections E8A and E8B with low cracking percentage (below 10%) and medium severity for Sections E7A and E7B with a higher cracking percentage (above 10%).
- After visual inspection of the crack maps, it seems that a great number of measured cracks for these sections can be characterized as reflective for Section E7B. For the remaining sections there is not enough evidence to conclude if the measure cracks are reflective or not. However, visual inspection of extracted samples indicates that the most likely cause of these cracks was bottom-up and reflective cracking.
- After 20 million ESALs of traffic, field performance for these sections was good overall in terms of roughness (relatively constant through the study and below 125 in/mi) and permanent deformation (below 5 mm).

8.7 References

1. Wang, J., B. Birgisson, and R. Roque. Windows-Based Top-Down Cracking Design Tool for Florida Using Energy Ratio Concept. In *Transportation Research Record: Journal of the Transportation Research Board, No. 2037*, Transportation Research Board of the National Academies, Washington, D.C., 2007, pp. 86-96.

2. Roque, R., B. Birgisson, C. Drakos, and B. Dietrich. Development and Field Evaluation of Energy-Based Criteria for Top-Down Cracking Performance of Hot Mix Asphalt. *Journal of the Association of Asphalt Paving Technologists*, Vol. 73, 2004, pp. 229-260.
3. West R., Timm D., Powell B., Heitzman M., Tran N., Rodezno C., Watson D., Leiva F., Vargas A. Phase VI (2015-2017) NCAT Test Track Findings. NCAT Report 18-04, 2018.
4. Rastegar, R. *Plant versus Laboratory Production: Impact on Measure Properties of Mixtures with RAP and RAS.* Presented at Transportation Research Board 2016 Annual Meeting, Washington D.C., 2016.
5. Leiva-Villacorta F., A. Taylor, and J. Fort. Analysis of High-Modulus Asphalt Concrete (HMAC) Mixtures Design Methodology Containing Recycle Material. Presented at Transportation Research Board 2018 Annual Meeting, Washington D.C., 2016.
6. West R., C. Van Winkle, S. Maghsoodloo, and S. Dixon. Relationships Between Simple Asphalt Mixture Cracking Tests Using N design Specimens and Fatigue Cracking at FHWA's Accelerated Loading Facility. *Road Materials and Pavement Design,* 18(sup4), 2017, pp. 1-19.

9. GEORGIA INTERLAYER STUDY FOR REFLECTIVE CRACK PREVENTION

Dr. Fan Gu

9.1. Background

The Georgia Department of Transportation (GDOT) aims to find a cost-effective approach to mitigate reflective cracking. The agency's current approaches are to place a single surface treatment application of No. 7 stone with an approximate 85 lbs/yd^2 asphaltic concrete leveling mix overlay or open-graded interlayer (OGI) over the existing surface before overlaying. It is believed that the open texture of the asphalt interlayer provides a disconnect plane between the existing surface and overlay so that underlying cracks are dissipated rather than reflected through to the surface. This approach, however, has not been as effective as desired.

In 2012, GDOT placed two test sections (N12 and N13) at the NCAT Test Track to evaluate two potential methods for reducing reflective cracking. This included 1) double surface treatment with sand seal coat, and 2) OGI. After two years of heavy truck trafficking (approximately 10 million equivalent single axle loads [ESALs]), these two test sections showed an insignificant amount of surface cracking, which was no more than 2% of the total area. In 2015, GDOT decided to sponsor these sections for continual trafficking. After another two years of heavy truck trafficking (approximately 20 million ESALs in total), only 6% of the saw cuts in the double surface treatment section reflected through to the surface, while 50.5% of the saw cuts reflected through to the surface in the OGI. Meanwhile, the OGI section had less rut depth than the double surface treatment section (3 mm and 7.8 mm, respectively).

In 2018, GDOT continued sponsoring sections N12 and N13 to evaluate six potential methods for mitigating reflective cracking. The methods include PETROMAT fabric interlayer, GlasGrid interlayer, chip seal with No. 7 stone, chip seal with reclaimed asphalt pavement, OGI, and rubber modified asphalt interlayer. Compared to the 2012 cycle, Sections N12 and N13 in the 2018 cycle have the same saw cut pattern and the same surface overlay mix design. Therefore, the factor affecting the reflective cracking performance is only the treatment method.

9.2. Section Preparation and Construction

In this research cycle, 1/8-inch wide deep saw cuts were made in the existing pavement for the full depth of the structural layer to simulate cracking in the pavement structure. As shown in Figure 1, the saw cuts were made in a longitudinal direction at 3-foot intervals across the width of the lane and at 15-foot intervals in a transverse direction. Therefore, the saw cut area represented about one-third of the total test section surface area when using 6 inches on each side of the crack as the potential area of influence. The cuts were then filled with sand to keep the cracks from healing back together during warm weather. Note that the saw cut pattern and the sand filling approach in this cycle are the same as those made in the last research cycle.

Figure 1. Deep Saw Cuts to Simulate Pavement Cracks

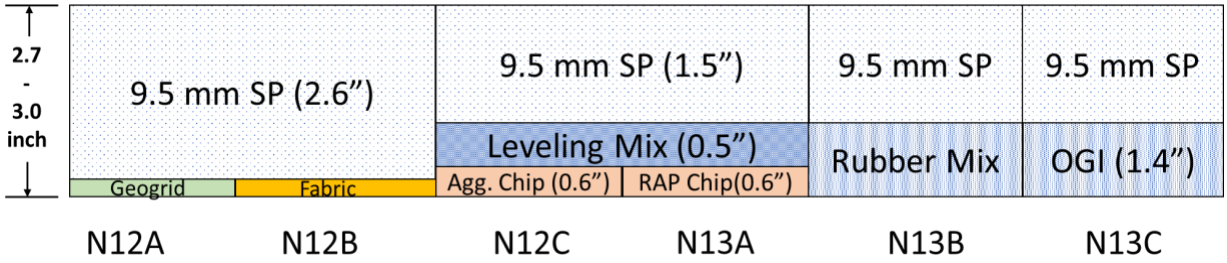

Figure 2. Layer Thickness of Each Section

Figure 2 presents the layer thicknesses of each section. As illustrated, Section N12 was divided into three subsections for different treatment methods, which included N12A (GlasGrid), N12B (PETROMAT fabric) (Figure 3), and N12C (chip seal with No. 7 stone and leveling) (Figure 4). PG 64-22 asphalt binder was used as tack coat for N12A and N12B with an application rate of 0.30 and 0.27 gallon/sq. yard, respectively. GlasGrid and PETROMAT fabric were placed directly on the milled surface following the manufacturers' requirements. Note that the manufacturers performed the installation of geosynthetic interlayers in this study. CRS-2h emulsion tack was applied onto the existing pavement of N12C with a residue rate of 0.23 gallon/sq. yard. The thicknesses of GlasGrid and PETROMAT fabric were 0.08 inches, and the thickness of chip seal with No. 7 stone was 0.6 inches. A 2.6-inch thick 3/8-inch (9.5 mm, Type 2) nominal maximum aggregate size (NMAS) Superpave mix was placed as the single-lift surface layer for subsections N12A and N12B, and a 1.5-inch thick 3/8-inch NMAS Superpave mix was placed as the single-lift surface layer for subsection N12C. Note that no leveling mix was used in subsections N12A and N12B, and 0.5 inch leveling mix (9.5 mm, Type A) was placed on subsection N12C.

Section N13 was also divided into three subsections for different treatment methods, which included N13A (chip seal with 100% fractionated coarse reclaimed asphalt pavement) (Figure

4), N13B (rubber modified asphalt interlayer), and N13C (OGI). Based on the GDOT specification for bituminous tack coat, CRS-2h emulsion tack was applied onto the existing pavement of N13A with a residue rate of 0.23 gallons/sq. yard. To compare with the NTSS-1HM used in the 2012 research cycle, the UltraFuse trackless tack was used for N13B and N13C with an application rate of 0.25 gallons/sq. yard. The thickness of chip seal with reclaimed asphalt pavement was 0.6 inches, and the rubber modified asphalt interlayer and OGI were approximately 1.1 inches thick. The NMAS 9.5 mm Superpave mix was used as the surface layer with a thickness of 1.5 inches for subsections N13A, N13B, and N13C. Note that no leveling mix was used in subsections N13B and N13C, and 0.5-inch leveling mix was placed on subsection N13A.

Figure 3. Geosynthetic Interlayers

Figure 4. Chip Seal with No. 7 Stone (12C) and Reclaimed Asphalt Pavement (13A)

The rubber modified asphalt interlayer, shown in Figure 5a, was a 1/2-inch NMAS gap-graded interlayer with granite aggregate and 7.4% PG 76-22 binder modified with ground tire rubber. The OGI mix, shown in Figure 5b, was a 1/2-inch NMAS porous friction course (PFC) mixture that was designed with a lower asphalt content than a typical PFC surface mix and used PG 64-22 binder grade. It also omitted fiber stabilizer for economic reasons, and instead used a reduced mix temperature of 250°F ± 20°F to resist drain-down. The purpose of these two mixes is to provide a discontinuity between the existing surface and overlay (to relieve stresses from loading and thermal forces) so stresses are dissipated and cracks are not as easily reflected.

PG 64-22 was used in the 9.5 mm Type 2 surface mix for both N12 and N13, and the layer was compacted to 93.8% of maximum theoretical density. Optimum asphalt content for Superpave mixes in Georgia is based on 65 gyrations with a Superpave gyratory compactor. Note that GDOT specifications contain two 9.5 mm mixes: the 9.5 mm Type 1 mix has a finer gradation generally used for leveling courses and thin overlays; the 9.5 mm Type 2 mix is generally used as a surface course on more heavily traveled routes. Mixture properties for the rubber modified asphalt interlayer, OGI, and 9.5 mm mixes are shown in Table 1.


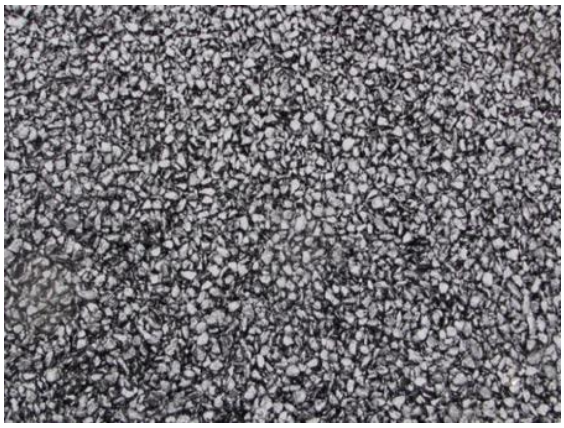

a. Rubber Modified Asphalt Interlayer b. Open Graded Interlayer

Figure 5. Rubber Modified Asphalt and Open Graded Asphalt Interlayers

Table 1. OGI and 9.5 mm Gradation and Mixture Properties

Sieve Size	Rubber Mix	OGI	9.5 mm, Type 2
	Passing Percentage		
3/4”	100	100	100
1/2”	96	96	100
3/8”	79	59	95
No. 4	40	14	64
No. 8	24	8	44
No. 200	3.4	2.0	5.9
Mixture Properties			
Asphalt Content (AC), %	7.4	4.5	5.6
Air Voids, %	6.0	22.2	4.1
Voids in Mineral Aggregate (VMA), %	19.9	30.8	15.4

9.3. Field Performance

Field performance including ride quality, rut depth, surface texture, and cracking was monitored on a weekly basis. Figure 6 shows the change of international roughness index (IRI) based on ESALs. As shown, subsection N12A has much higher IRI than the other five subsections. This was attributed to the interference from the adjacent Section N11 that has an IRI greater than 150 inch/mile, and the influence of the transverse joint. Note that subsection N13C shows a high variability in IRI, which might be also attributed to the interference from the adjacent Section W1 that has a much greater IRI. In general, none of these six subsections shows noticeable change of IRI after 10 million equivalent ESALs of trafficking.

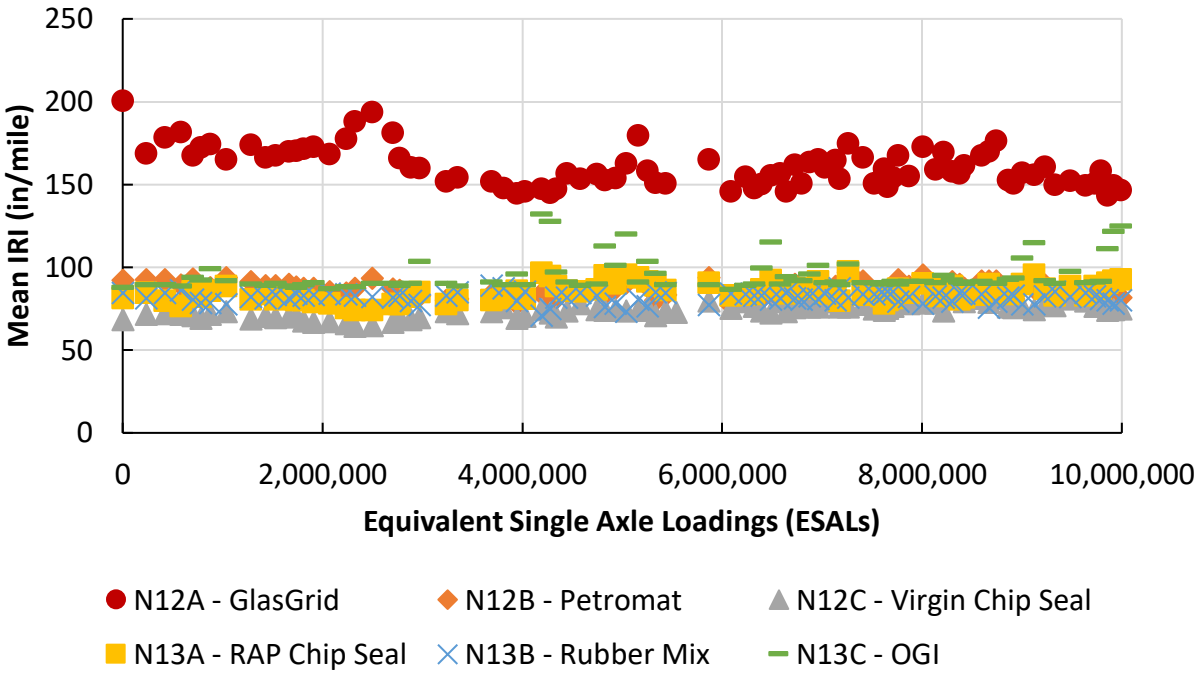

Figure 6. International Roughness Index Comparison of N12 and N13

Figure 7 presents the change in rut depth based on ESALs. It is shown that all of the six subsections have noticeable increase of rut depth starting from 2.7 million ESALs, and subsection N13A (RAP chip seal) has much greater rut depth than others. After 10 million ESALs, the rut depth of subsection N13A is close to 0.40 inches, while the other subsections have rut depths varying from 0.15 to 0.30 inches. Note that subsections N12C and N13A both utilized the chip seal treatment, but subsection N12C had a much lower rut depth that subsection N13A. This might indicate that RAP chip was more likely to rotate under traffic loading compared to virgin aggregate, which results in noticeable rut depth.

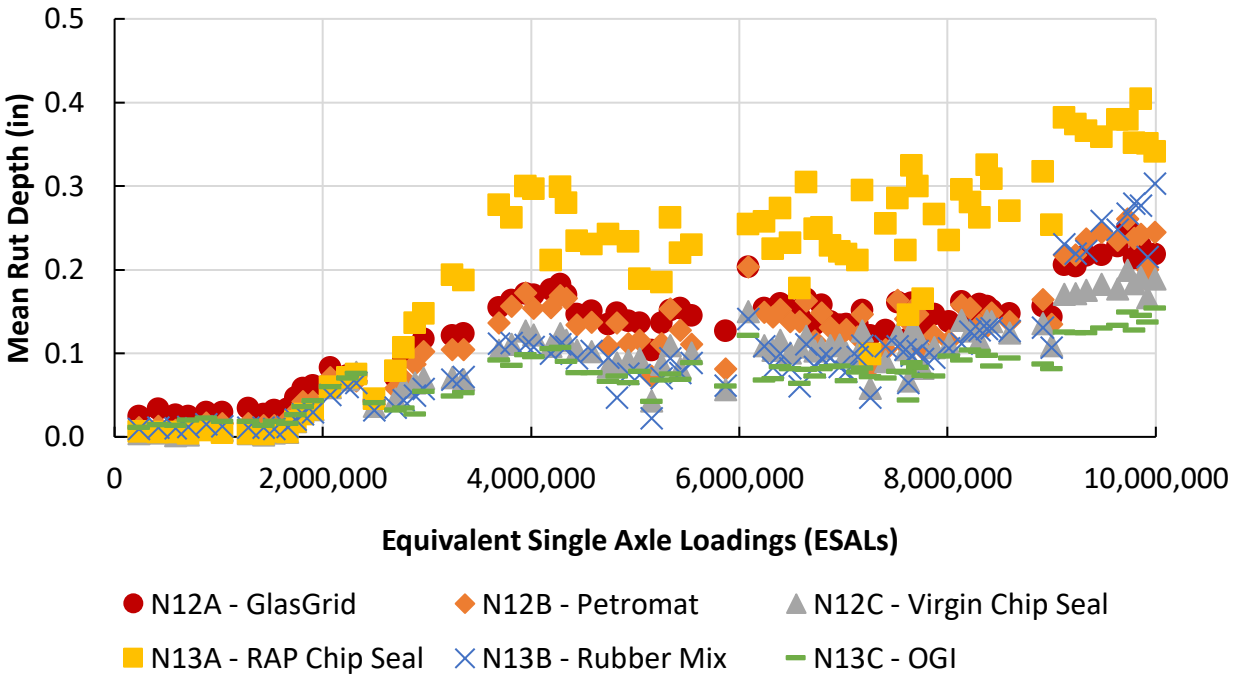

Figure 7. Rut Depth Comparison of N12 and N13

Figure 8 indicates the change of surface texture over time. As illustrated, all of the six subsections have comparable mean texture depth values. The increase in traffic loading marginally increases the mean texture depth of these sections, and the field observation demonstrates that there is no raveling found in any of these sections.

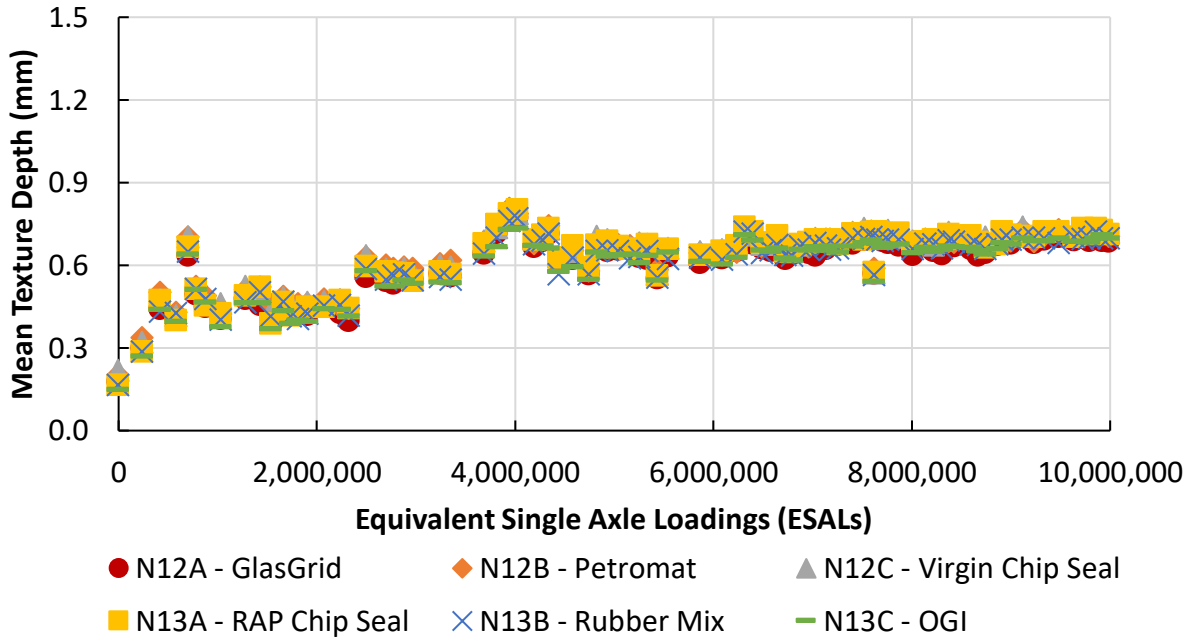

Figure 8. Mean Texture Depth Comparison of N12 and N13

After 10 million ESALs of traffic, there is no cracking distress observed in any of the subsections. This is slightly different from the findings of Sections N12 and N13 in the 2012 research cycle, both of which exhibited minor reflective cracking distresses (less than 2% of crack area) after 10 million ESALs. This might be because the N12 and N13 sections built in 2018 have a slightly thicker asphalt overlay than those built in 2012. Another potential reason is that tack application is heavier in the 2018 research cycle, which may have sealed the cracks and created a better bond.

9.4. Findings

This study aimed to evaluate the long-term performance of six different reflective cracking treatments including two geosynthetic interlayers, two chip seal systems, OGI, and rubber modified asphalt interlayer. After 10 million ESALs of trafficking, the field performance of these sections was as follows:

- The surface roughness of these six subsections do not have any substantial changes.
- The RAP chip seal subsection (N13A) has a greater rut depth than other subsections. After 10 million ESALs of trafficking, the RAP chip seal subsection (N13A) has a rut depth close to 0.4 inches.
- All six subsections exhibited comparable surface macrotexture, which increased with the increasing ESALs. The field observation demonstrates that there is no raveling issue found in any of these sections.
- There is still no reflective cracking distress that could be observed on any surface of these subsections.

Traffic continuation will be performed on these sections and their field performance will be monitored in the next research cycle.

10. KENTUCKY EVALUATION OF LONGITUDINAL JOINTS, MIX DESIGN, AND FRICTION

Dr. Carolina Rodezno

10.1. Background

In the 2015 Test Track research cycle, the Kentucky Transportation Cabinet (KYTC) sponsored Section S7 for evaluation on the NCAT Test Track. The objective of this study was to construct two 100-foot long test sections: one with an approved KYTC mix (S7A) and one with a finer mix designed by NCAT with a lower number of gyrations (S7B). The goal was to improve the performance of longitudinal joint and overall mix durability without compromising rutting performance.

Both mixtures were Superpave 9.5 mm nominal maximum aggregate size (NMAS) with a PG 76-22 polymer modified binder and contained similar aggregate components, with the second mix having a modified aggregate blend to achieve a finer gradation.

Table 1 summarizes the aggregate percentages used for both mixes. As can be observed, the prevalent aggregate was limestone. Table 2 summarizes the mix designs and quality control data of the mixtures. Section S7A mix was a 100-gyration mix, while S7B mix was a 75-gyration mix.

Table 27. Section S7A and S7B Aggregate Percentages

Aggregate Type	% of Total Aggregate	
	S7A	S7B
Limestone #9	43	
Limestone sand	25	49
Washed friction sand	20	25
Natural sand		16
RAP	12	10

Table 2. Kentucky Mix Design Information

Mix Design Parameters	S7A		S7B	
Compactive Effort, gyrations	100		65	
Binder Grade	PG 76-22		PG 76-22	
Sieve (% passing)	Design	QC	Design	QC
12.5mm	100	100	100	100
9.5mm	95	93	93	100
4.75mm	63	51	51	79
2.36mm	35	26	26	46
1.18mm	22	16	16	32
0.60mm	15	12	12	24
0.30mm	10	9	9	12
0.15mm	7	7	7	7
0.075mm	4.8	5.3	5.3	5.1
Total Binder Content (P_b), %	5.9	5.8	5.8	6.0
Eff. Binder Content (P_{be}), %	4.9	4.7	4.7	4.9
Dust/Binder Ratio	1.0	1.1	1.1	1.0
RAP Binder Ratio	0.09	0.13	0.13	0.10
Rice Sp. Gravity (G_{mm})	2.487	2.476	2.476	2.434
Bulk Sp. Gravity (G_{mb})	2.388	2.403	2.403	2.370
VMA	15.7	14	13.9	14
VFA	73	79	79	81
Air Voids, %	4.0	3.0	3.0	2.6
Compacted thickness (mm)	38	33	38	36
Mat Density (% G_{mm})	94	92.1	94	95.1

Approximately 10 million equivalent single axle loads (ESALs) were applied to both sections. At the end of the cycle, neither section showed any signs of cracking, and rutting for both was less than 5 mm. In addition, field permeability on the longitudinal joint showed that the permeability value measured on Section S7B was less than 20% of that measured on Section 7A, which should translate into better joint performance, particularly in the freeze-thaw climate typical of Kentucky. The average values measured for Section S7A and S7B at the end of the cycle were 1,294x10^{-5} cm/s and 243 x10^{-5} cm/s, respectively. Additional information regarding laboratory and field performance of these sections was documented in NCAT Report 18-04: Phase VI NCAT Test Track Findings (*1*).

The good short-term performance of the test sections after one research cycle prompted the KYTC to sponsor traffic continuation on the sections during the Test Track's seventh cycle to assess their long- term performance.

10.2. Objective

The objective of this study was to assess the long- term performance of sections S7A and S7B after enduring two cycles of trafficking, which corresponds to 20 million ESALs.

10.3. Field Performance Monitoring

The field performance of the sections was routinely assessed. Every week, sections were inspected for signs of cracking, rutting, and smoothness in terms of international roughness index (IRI), and surface texture. In addition, surface friction was measured monthly using a locked-wheel skid trailer (LWST). After 11.2 million ESALS into the research cycle, the friction

numbers for both sections started to drop below the minimum safety threshold that has been established at the NCAT Test Track (i.e, skid number =30). Figure 1 presents the LWST results for Sections S7A and S7B. At a traffic level of approximately 11.4 million ESALs, the skid resistance of both sections had dropped to 25.3 for Section S7A, and 26.8 for Section S7B.

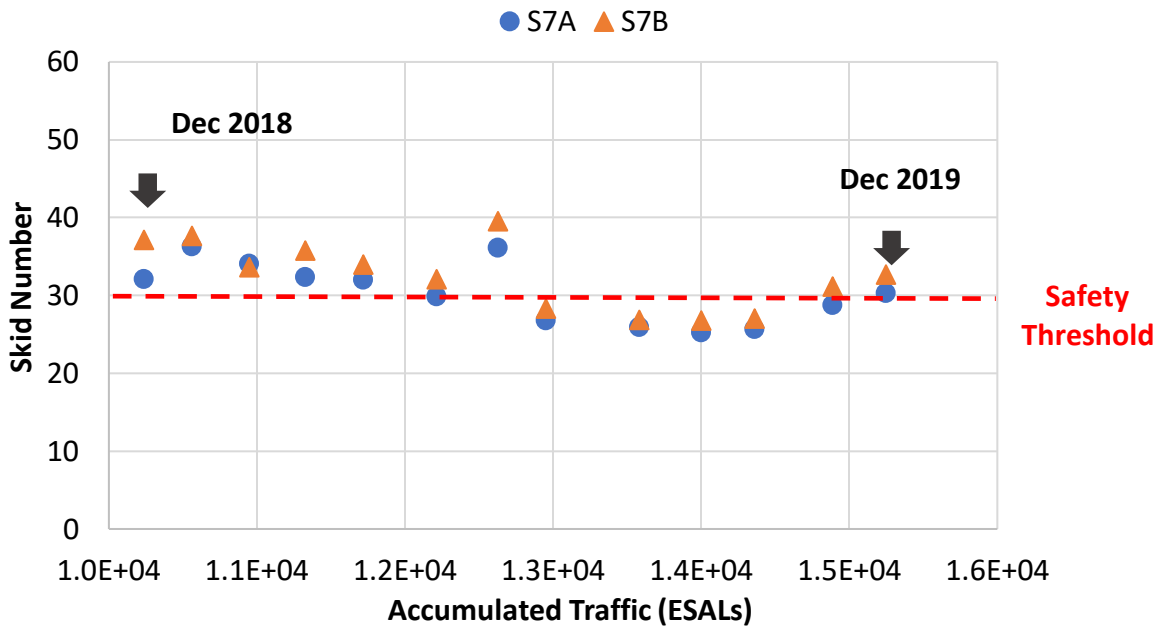

Figure 28. LWST Skid Number for Sections S7A and S7B

10.3.1. Shotblasting Treatment to Improve Surface Friction

The low friction numbers shown for Sections S7A and S7B urged the decision to apply a friction treatment to improve the friction characteristics of the sections. In consultation with the KYTC, a shotblasting treatment was selected and applied to the test sections after approximately 15.3 million ESALs of trafficking. Figure 2 illustrates the shotblasting treatment being applied to the sections and a close up of the steel shots used to abrade the sections.

Figure 29. Application of Shotblasting Treatment to S7A and S7B and Close up of Steel Shots

10.3.2. Field Performance at the Completion of the Test Track Cycle

Figure 32 shows the skid numbers for both sections after shotblasting treatment and through the duration of the cycle. As shown in this figure, the shotblasting treatment accomplished a significant improvement in the friction numbers. Moreover, at the end of the cycle, friction numbers remained above the safety threshold. These results clearly indicate the effectiveness of the shotblasting treatment to restore the friction characteristics of the pavement surfaces.

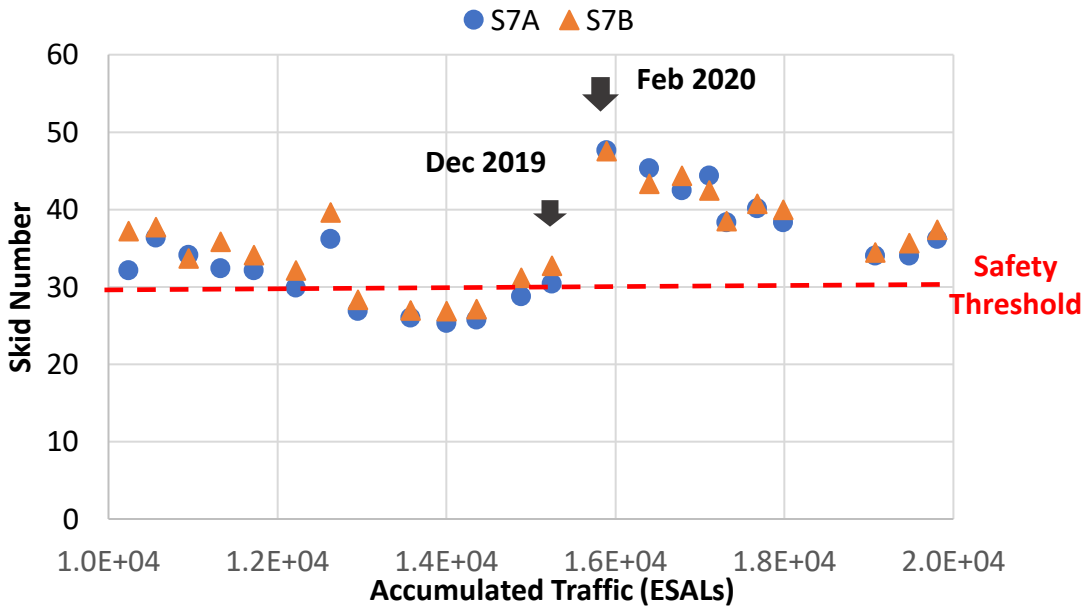

Figure 30. LWST Skid Number for Sections S7A and S7B after Shotblasting

During the summer of 2020, the sections started to show low severity cracking directly at the longitudinal joints as shown in Figure 4. By September 2020, Section S7A had 100% cracking at

the joint, while Section S7B had 49%. At the end of the cycle, Section S7B had 64% of the joint cracked, but still had low severity cracking. Considering that the majority of the joint length of the sections was cracked, it was not meaningful to measure permeability of the cracked joints.

Despite the low severity cracking at the joints, the sections did not experience any cracking. The rutting, roughness, and texture performance measurements of the sections are presented in Figures 5, 6, and 7. From Figure 5, Sections S7A and S7B had average rut depths of 5.4mm and 3.5mm, respectively. The higher rutting values shown for the last six readings are attributed to a change in the measuring profiler. Regardless of the differences in the final readings, rutting has remained relatively low, with Section S7A slightly higher. IRI results remained stable for the duration of the cycle, with Section S7B having lower values, as an indication of improved smoothness for the finer mix (Figure 5). Finally, mean texture depth remained relatively constant with Section S7A showing higher values as compared to Section S7B.

a) b)

Figure 31. Close-up of Cracks at the Longitudinal Joints: a) Section S7A; b) Section S7B.

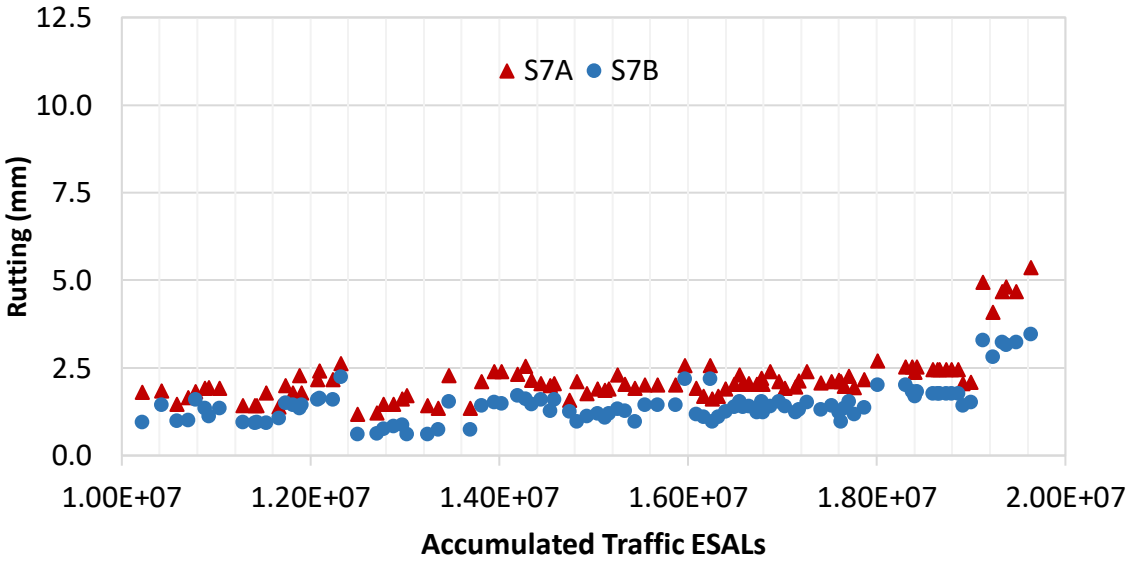

Figure 32. Measured Rut Depth of Sections S7A and S7B

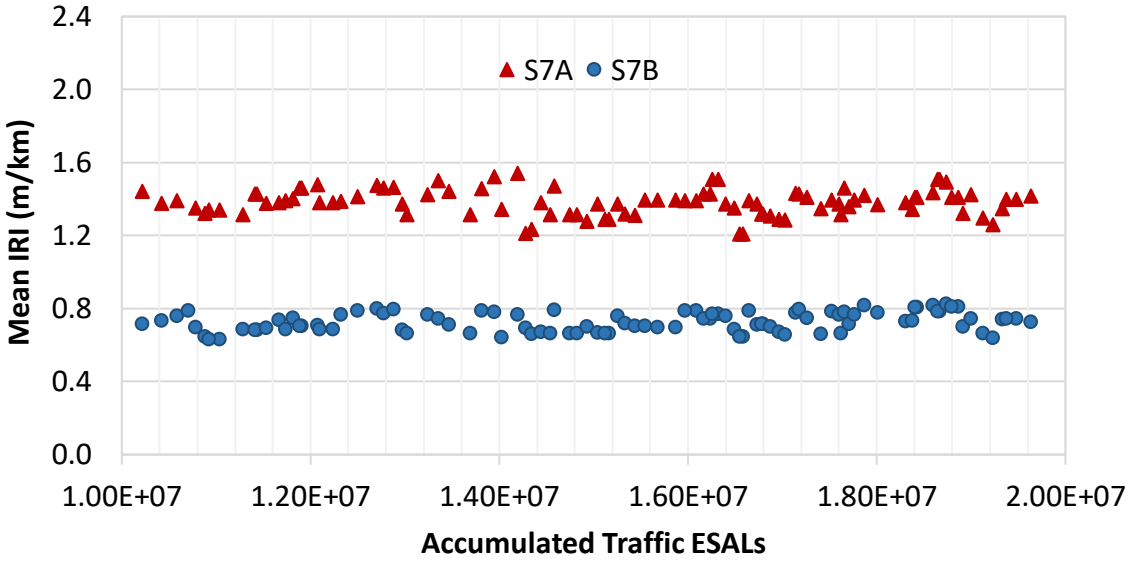

Figure 33. Measured IRI for Sections S7A and S7B

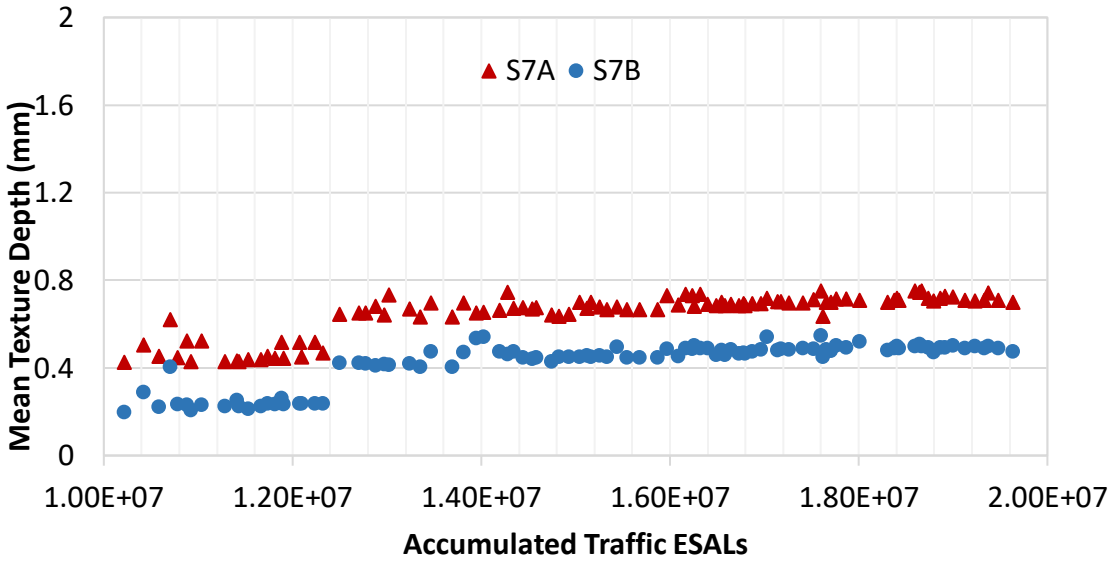

Figure 34. Measured Texture for Sections S7A and S7B

10.4. Summary of Findings

The long-term field performance of the sections is summarized as follows:

- After 20 million ESALs of trafficking, no cracking was observed in the sections, but low severity cracking directly at the joints was observed. At the end of the test track cycle, Section S7A had 100% cracking at the joint, while Section S7B had 64%.
- Rut depths were 5.4 mm and 3.5 mm for Sections S7A and S7B, respectively, indicating that the mixes were not susceptible to rutting. The increase in rut depth towards the end of the cycle was attributed to a change in the measuring profiler.
- IRI and surface texture remained constant through the research cycle, with Section S7B having lower values compared to Section S7A.
- The shotblasting treatment applied to both sections demonstrated an effective solution to improve the friction characteristics of asphalt pavements when polishable aggregates are utilized.

10.5. References

1. West, R. et al. *Phase VI NCAT Pavement Test Track Findings*. NCAT Report 18-04, National Center for Asphalt Technology, Auburn, Ala., 2019.

11. MISSISSIPPI DOT STABILIZED FOUNDATION PAVEMENT

Dr. David Timm

11.1 Introduction

Challenging soil conditions are sometimes mitigated through stabilizing with cementitious material to improve load carrying capacity of flexible pavements. The Mississippi DOT (MDOT) routinely uses this strategy by cement- or lime-stabilization of soils and other granular materials. Though often used by MDOT and other state agencies, there is little data available to support mechanistic-empirical (M-E) analysis and design of these stabilized foundation pavements.

To expand the knowledge base of stabilized foundation pavements, MDOT sponsored Section S2 for the 2018 NCAT Test Track research cycle. This section features materials local to Mississippi that were hauled to and placed at the Test Track and stabilized in place with lime and cement over which asphalt concrete (AC) layers were constructed. The materials are representative of those often stabilized in Mississippi due to their relatively low quality for roadbuilding. Pavement response sensors were embedded during construction to enable direct mechanistic response measurement under live truck traffic and falling weight deflectometer loading. The short-term goal of the section was to fundamentally characterize the structural characteristics of the stabilized foundation pavement, measure its response to environmental changes, and track surface performance. These aspects are covered in this chapter. The long-term goal is to gather the necessary M-E properties to perform transfer function calibration that will provide more accurate distress predictions for this pavement type. As will be described in this chapter, the pavement has not yet experienced any distress or performance deterioration during the first test cycle (two years and 10 million ESALs), so additional trafficking is recommended into the next test cycle.

11.2 Construction and Instrumentation of Section S2

The cross-section and instrumentation plan for Section S2 are shown in Figures 1 and 2, respectively. The section is approximately 200 ft long, with the first 25 and last 25 feet used as transition zones into and out of the section. The thicknesses shown in Figure 1 are based on averaged as-built surveyed depths across the section and the locations of instrumentation are meant to show the depth, not the x-y-locations. The pavement cross section includes four AC layers over a cement treated base (CTB) over lime treated soil (LTS) on top of a Mississippi subgrade (MS Subgrade). Figure 2 shows the instruments in plan view. The asphalt strain gauges (ASGs) were installed to measure bending strain at the bottom of the AC in the direction of travel, while the earth pressure cells (EPCs) measure vertical compressive stresses at critical depths (AC/CTB interface; CTB/LTS interface; LTS/MS subgrade interface). Traffic moves from left to right in Figure 2 where the point of the traffic arrow aligns with the center of the outside wheelpath positioned 36 inches from the outside edge of the edge stripe. The temperature probes were installed vertically to measure the top, middle, and bottom of the AC and 3 inches into the cement treated layer. The following narrative details the construction of the section, starting with subgrade construction, followed by discussion of the sensor installation sequenced with the construction of particular pavement layers.

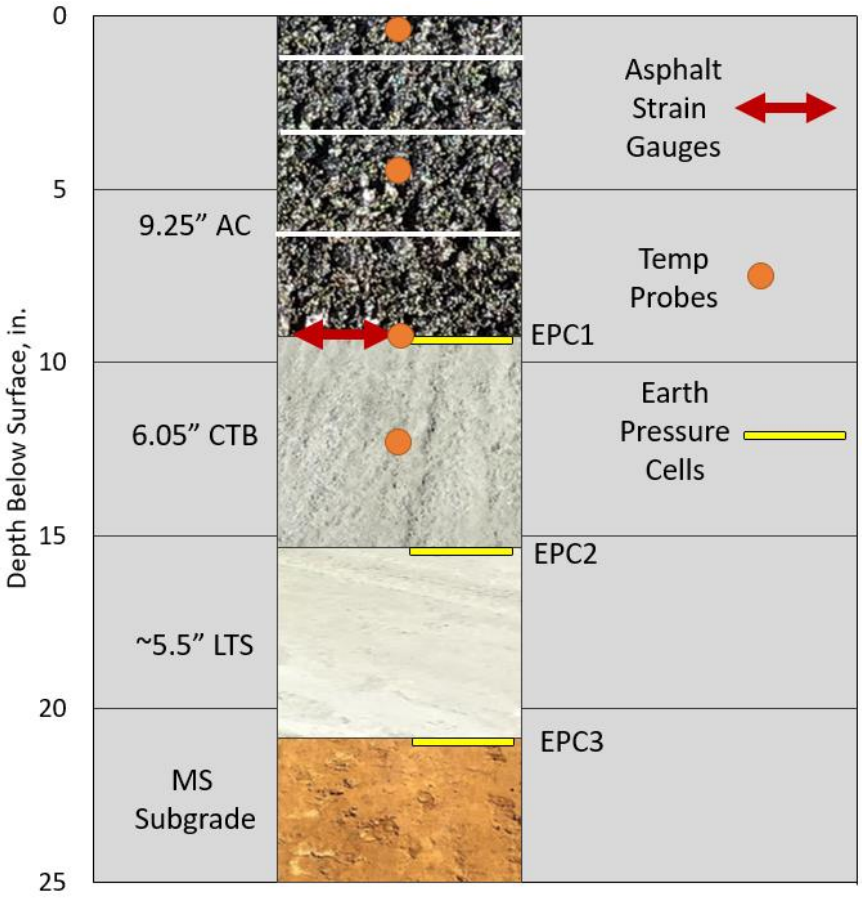

Figure 1. Section S2 Cross Section

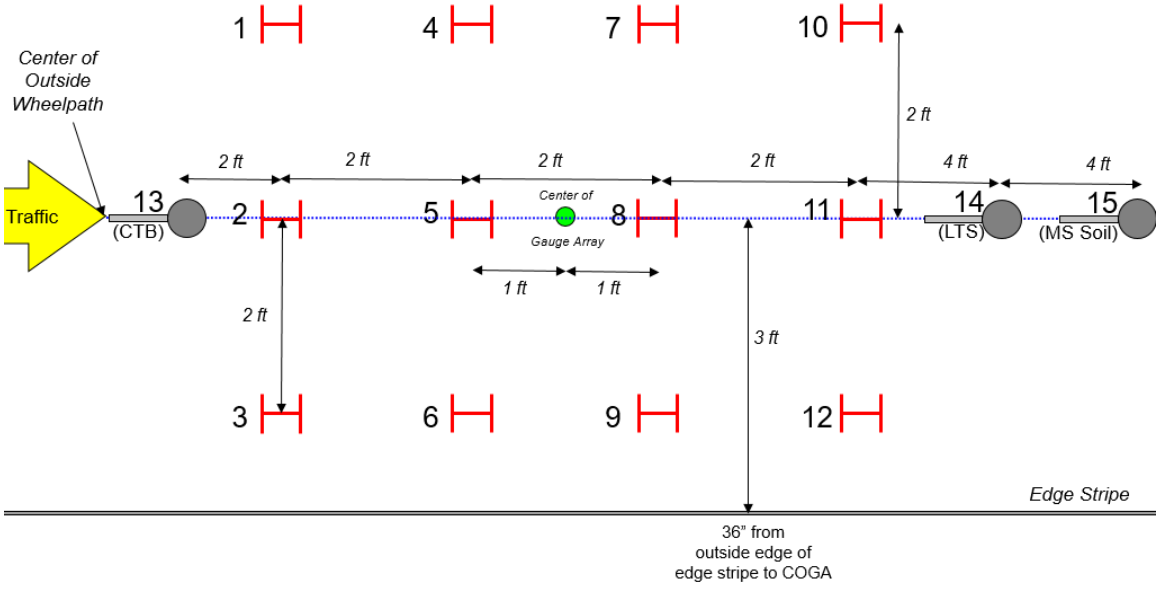

Figure 2. Section S2 Instrumentation Plan View

11.2.1 Excavation, Subgrade Installation and Lime Treatment

Preparing Section S2 for the stabilized foundation pavement required substantial removal of existing materials to facilitate installation of foundation layers from Mississippi. This process began on April 30, 2018, with milling and excavation of the existing pavement and soil to a depth of almost 6 feet as shown in Figure 3. This depth was similar to that excavated for another section built in 2006 for the Oklahoma DOT where soil was imported to the Test Track which demonstrated the depth was sufficient to replicate their local soil conditions. The remaining soil foundation was native to the Test Track, originally placed as part of the construction of the 2000 Test Track and was classified as an AASHTO A-4(0) soil. Soil from Mississippi was hauled to the Test Track and was placed and compacted in eight lifts to a depth of approximately 56 inches. This was done in accordance with provisions described in the 2017 Mississippi Standard Specifications for Road and Bridge Construction. The soil was classified as an AASHTO A6 (20) with 93% passing the #200 sieve (See Table 1). The optimum unit weight was determined to be 107.8 pcf for the soil with 98% of optimum required for layers in the top 36 inches and 95% of optimum for the deeper layers. Table 2 shows the in-place unit weight and moisture contents of all eight soil layers.

Figure 3. Section S2 Excavation

Table 1. Section S2 Mississippi Soil Properties

Soil Property	Value
Liquid Limit	39
Plastic Limit	18
Plasticity Index	21
% Passing No. 4	99
% Passing No. 10	98
% Passing No. 40	98
% Passing No. 60	97
% Passing No. 200	93
AASHTO T88 % Silt	68
AASHTO T88 % Clay	24
AASHTO M145 Classification	A6(20)
ASTM D2487 Classification	CL
Untreated Max γ_d (g/cm^3)[a]	1.73
Untreated OMC (%)[a]	16
Design L_w or C_w[b]	4.0
Treated Max γ_d (g/cm^3)[c]	1.62
Treated OMC (%)[c]	17

Note: Max γd = maximum dry density; OMC = optimum moisture content

[a] Determined by AASHTO T 99.

[b] Determined by Mississippi Test Method 27 and 25, respectively.

[c] Determined by AASHTO T134 with soil-lime mixture tested in the same manner.

Table 2. Section S2 Mississippi Soil As-Built Unit Weight and Moisture Content

Lift No.	Optimum Unit Weight, pcf	Target Unit Weight, pcf	As-Built Unit Weight, pcf	As-Built Moisture Content, %
Lift 1 (Bottom)	107.8	102.4	111.2	15.3
Lift 2	107.8	102.4	111.1	15.7
Lift 3	107.8	105.6	109.6	17.4
Lift 4	107.8	105.6	110.3	17.5
Lift 5	107.8	105.6	111.8	16.5
Lift 6	107.8	105.6	110.1	16.6
Lift 7	107.8	105.6	110.0	16.1
Lift 8 (top)	107.8	105.6	110.7	15.1

Once the soil was placed and compacted (Figure 4a), lime treatment to a target depth of 6 inches began on September 7, 2018. Dry hydrated lime, applied with a drop-spreader (Figure 4b) at 4% by dry weight of the soil, was mixed to depth using a milling machine with the conveyor system turned off (Figure 4c). The lime treated soil (LTS) was designed to obtain a soaked California Bearing Ratio (CBR) of 20% after seven days of protected curing.

a) Mississippi Soil Ready for Lime Treatment

b) Lime Applied by Drop Spreader

c) Lime Mixing with Milling Machine

Figure 4. Lime Treatment of Section S2

While the lime-treated Mississippi soil was still in a relatively loose, uncompacted state, the location of the first EPC was determined, and a small area was excavated in which to place the EPC (Figure 5a). The depth was set as just below the lime-treated/MS soil interface. Following previously-established Test Track sensor installation procedures (*1*), a shallow cavity was created and then filled with a thin layer of -#8 and then -#16 fines sieved from the lime treated soil to create a smooth and stable bed for the EPC. The EPC was laid in place, leveled, and a surveyed depth was determined (Figure 5a). The EPC was then covered with another thin layer of -#16 and -#8 fines over which the disturbed lime treated soil was backfilled and hand compacted. The entire cavity and cable trench were then backfilled and hand compacted to restore the surface of the lime-treated soil with the EPC now buried under approximately 6 inches of material.

Figure 5. Installation of First EPC Below Lime Treated Soil in Section S2

After the sensor was installed, the LTS was compacted with a steel-wheel roller and brought to grade and cross-slope with a motor grader. After density (100.1 pcf) and moisture content (15.8%) were achieved, a prime coat (NTSS-1HM anionic asphalt emulsion) sealed the layer to prevent possible loss of moisture. The prime coat was sprayed at the rate of 0.2 gal/sy. The LTS was given a 10-day mellowing period after which placement of the silty-sand base began on September 17, 2018 (Figure 6). Note that the panorama image in Figure 6 gives the appearance of curvature, but the section is straight, located on the south tangent of the Test Track.

Figure 6. Placement of Silty-Sand Base on Prime Coated LTS in Section S2 (Panorama Image)

11.2.2 Silty-Sand Base Placement and Cement Treatment

The silty-sand base, which would become the cement-treated base (CTB), was also imported from Mississippi. The base material was classified as an AASHTO A2-4 material (see Table 3). Following the same process as the lime treatment, a drop spreader applied 5.1% cement by dry weight of the silty sand to achieve a target compressive strength of 300 psi at 14 days of curing. The milling machine was again used for mixing and another pressure plate was installed following the process described above at the CTB/LTS interface. The CTB was then compacted and graded followed by application of a cationic emulsion prime coat (0.2 gal/sy of Blacklidge® EPR-1). The cement treated material was allowed to cure with no traffic on it until asphalt paving began 17 days later on October 4, 2018. Figure 7 shows the finished CTB surface shortly after application of the prime coat.

Table 3. Section S2 Silty-Sand Base Properties

Base Property	Value
Liquid Limit	---
Plastic Limit	---
Plasticity Index	Non-Plastic
% Passing No. 4	100
% Passing No. 10	99
% Passing No. 40	91
% Passing No. 60	72
% Passing No. 200	16
AASHTO T88 % Silt	7
AASHTO T88 % Clay	8
AASHTO M145 Classification	A2-4
ASTM D2487 Classification	SM
Untreated Max γ_d (g/cm^3)[a]	1.76
Untreated OMC (%)[a]	13
Design L_w or C_w[b]	5.1
Treated Max γ_d (g/cm^3)[c]	1.83
Treated OMC (%)[c]	13

Note: Max γ_d = maximum dry density; OMC = optimum moisture content

[a] *Determined by AASHTO T 99.*

[b] *Determined by Mississippi Test Method 27 and 25, respectively.*

[c] *Determined by AASHTO T134 with soil-lime mixture tested in the same manner.*

Figure 7. Completed CTB in Section S2 Shortly After Tack Coat Application

11.2.3 Asphalt Paving

Before paving the first lift of AC on the CTB, the ASGs and another pressure plate were prepared for installation. Normally, when installing these sensors on unbound granular base layers, a shallow cavity would be dug for the EPC and trenches cutting through the granular base to accommodate the cables. However, it was quickly discovered that the CTB layer was much too hard for this type of installation and it was decided to place the sensors on top of the CTB to minimize disturbance to the CTB.

Other than placing the gauges and cables on top of the CTB, the process of preparing the gauges for paving followed well-established Test Track procedures (*1*). Figure 8a shows an ASG tacked in place while Figure 8b shows the array of 12 ASGs laid out prior to paving. As shown in Figure 8c, all the gauges were covered with mix sieved through a #4 screen and hand compacted to provide minimal protection during the paving and compaction process. Paving operations over the gauge array were identical to elsewhere in the section except that rollers were not allowed to stop or change direction over the gauge array. All three pressure plates survived the paving process while 11 of 12 ASGs were functional after paving. The loss of the ASG was deemed non-critical since redundancy had been built into the system (i.e., three other ASGs were position in the same relative offset as the lost gauge to make the same measurement.

a) ASG Tacked in Place with Sand/Asphalt Mixture

b) ASGs Positioned for Paving

c) ASGs covered with Sieved Mix Prior to Paving

Figure 8. Placement of ASGs in Section S2

The bottom two layers were placed on October 4, 2018 with the next two layers being placed on October 8, 2018. Table 4 shows the plant settings for the mix produced for each layer with each mix using an unmodified PG 67-22 binder designed at 85 gyrations to a target air void content of 4%. These mixtures were representative of designs often used by MDOT for high traffic applications. Figure 9 shows the gradations of each aggregate blend in each layer while Table 5 shows the as-produced quality control properties of each AC layer. Finally, Table 6 lists the as-built in situ compacted densities of each layer. It should also be noted that AC interfaces were tacked with Blacklidge® NTSS-1HM non-tracking tack coat at a target rate of 0.70 gal/sy.

Table 4. Section S2 Asphalt Plant Settings

Material	Layer 1 (bottom)	Layer 2	Layer 3	Layer 4 (top)
Date Produced	10/4/2018	10/4/2018	10/8/2018	10/8/2018
Binder Content, %	4.5	4.5	4.9	5.1
MS Coarse Sand, %	10.0	7.0	6.0	6.0
MS -5/8" Crushed Gravel, %	25.0	40.0	44.0	52.0
MS #67 Fullen Dock Limestone, %	15.0	16.0	0.0	0.0
MS #10 Fullen Dock Limestone, %	19.0	6.0	0.0	0.0
MS #8 Vulcan Limestone, %	0.0	0.0	12.0	12.0
MS #10 Vulcan Limestone, %	0.0	0.0	7.0	9.0
MS Coarse RAP, %	20.0	20.0	10.0	0.0
MS Fine RAP, %	10.0	10.0	20.0	20.0
Hydrated Lime, %	1.0	1.0	1.0	1.0

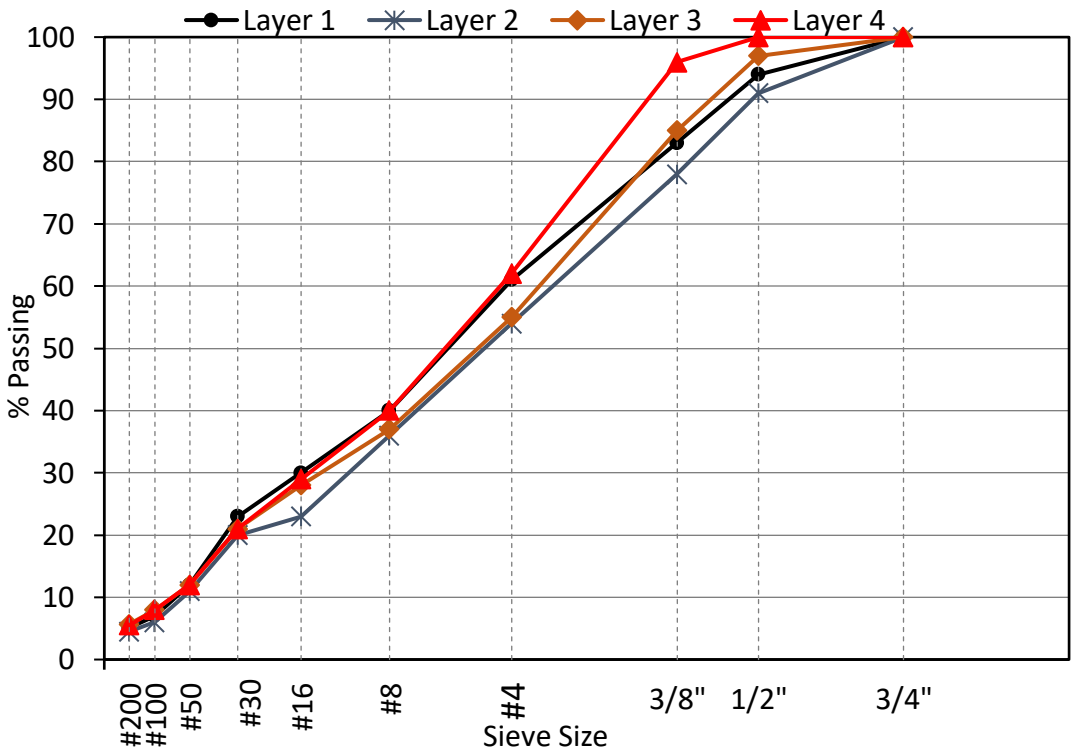

Figure 9. Section S2 AC Aggregate Gradations

Table 5. Section S2 Plant-Produced, Lab Compacted AC QC Results

Properties	Layer 1 (bottom)	Layer 2	Layer 3	Layer 4 (top)
Binder Content, %	4.5	4.5	4.9	5.1
Effective Binder Content (Pbe), %	4.1	4.0	4.4	4.5
Dust-to-Effective Binder Ratio	1.2	1.1	1.3	1.2
RAP Binder Replacement, %	30	31	33	22
Rice Gravity (Gmm)	2.453	2.438	2.436	2.414
Bulk Gravity (Gmb)	3.387	2.381	2.377	2.349
Air Voids (Va), %	2.7	2.3	2.4	2.7
VMA, %	12	12	12	13
VFA, %	78	80	81	79

Table 6. Average Compacted In Situ Density

	Layer 1 (bottom)	Layer 2	Layer 3	Layer 4 (top)
Compaction level, % G_{mm}	93.7	95.6	93.2	92.3

The final sensor installation occurred after paving was completed. To monitor in situ temperatures, a bundle of four thermocouples were installed to measure temperatures at the top, middle, and bottom of the AC and 3 inches into the CTB. A vertical hole was drilled into the pavement just outside the edge stripe that was deep and wide enough to accommodate the four thermocouples with the top one flush to the pavement surface. Figure 10 shows the installation with a slotted trench containing the thermocouple cables running to the shoulder before everything was covered and sealed with roofing asphalt (Figure 11).

Figure 10. Installed Thermocouple Bundle Prior to Covering with Roofing Asphalt

Figure 11. Covering Thermocouple Bundle with Roofing Asphalt

11.3 Field Performance

As with all the other Test Track sections, this section was measured frequently for rutting and roughness and was inspected for cracking during the research cycle. Figure 12 shows the section on February 8, 2021 near the end of the two-year trafficking cycle. The following sections document the field performance in terms of both time and traffic application expressed as equivalent single axle loads (ESALs).

Figure 12. Section S2 Near the End of Trafficking

11.3.1 Rutting

Rutting progression for the stabilized foundation section is presented in Figure 13 where rut depths are on the left vertical axis and cumulative ESALs are on the right vertical axis. Rutting increased primarily during the first spring/summer (April 2019 through September 2019) up to about 0.10 inches. At that point, it leveled off and did not experience increased rutting through the second summer, maintaining rut depths around 0.10 inches. The increase at the very end of the test cycle from 0.10” to 0.15” is believed to be related to a change in the data acquisition software rather than a true increase in rutting, as this jump was not evident in manual methods of rut depth measurement. In either case, rutting did not exceed 0.20” after the application of 10 million ESALs and most likely leveled off at 0.10” after primary rutting occurred during the first summer. Since the Test Track defines rutting failure at 0.5”, and MDOT would not address rutting until it exceeded 0.2” on interstate sections and 0.25” on non-interstate sections, rutting performance of the section through the first 10 million ESALs was excellent. This is not unexpected since rutting is not a primary concern with a stabilized foundation pavement.

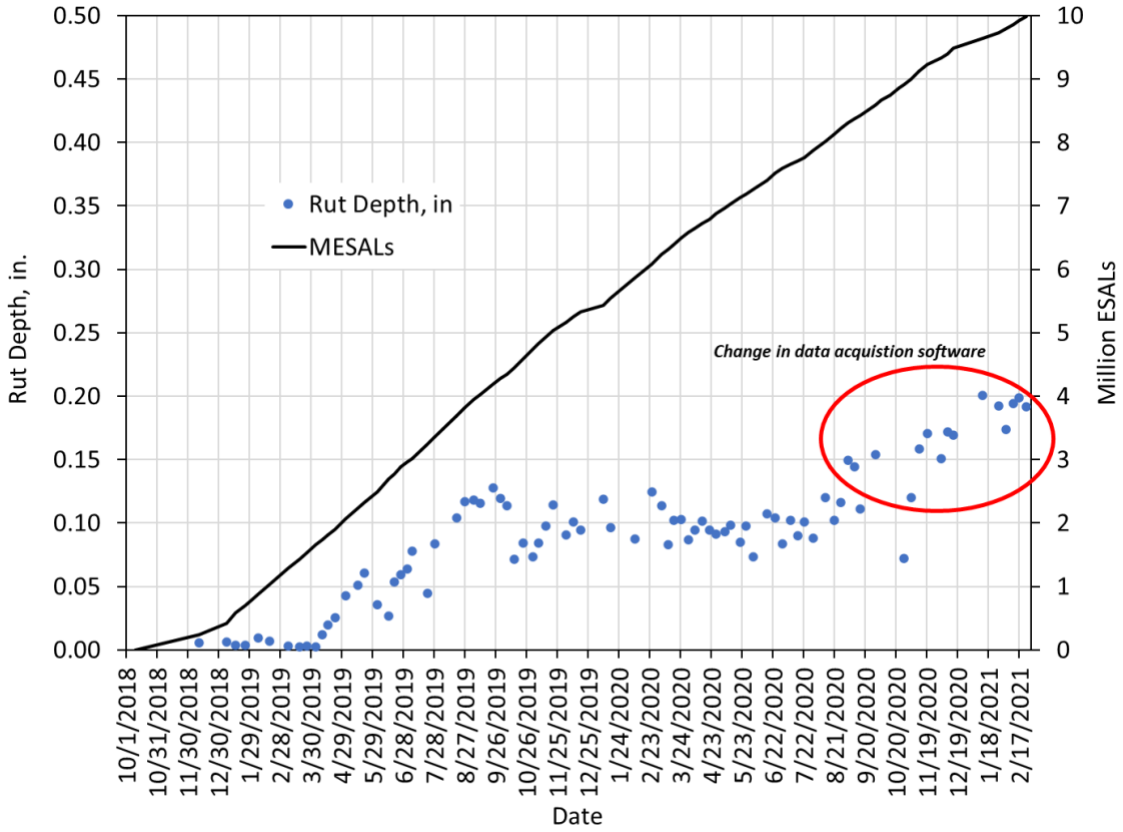

Figure 13. Section S2 Rutting Performance

11.3.2 Cracking

No cracking was observed anywhere in the section after the full two years and 10 million ESALs. There were, however, a few pop outs randomly located in the section. Figure 14 shows one of the largest. Exactly when this pop out occurred is not known but it was not deemed detrimental to the structural integrity of the section.

Figure 14. Pop Out in Section S2

11.3.3 Ride Quality

Ride quality was nearly constant over the application of traffic (Figure 15) where IRI is plotted on the left vertical axis and cumulative ESALs on the right vertical axis. The net increase was less than 10 inches/mile from start to finish, which was within the testing variability and was not deemed significant. Overall, the section exhibited excellent ride quality.

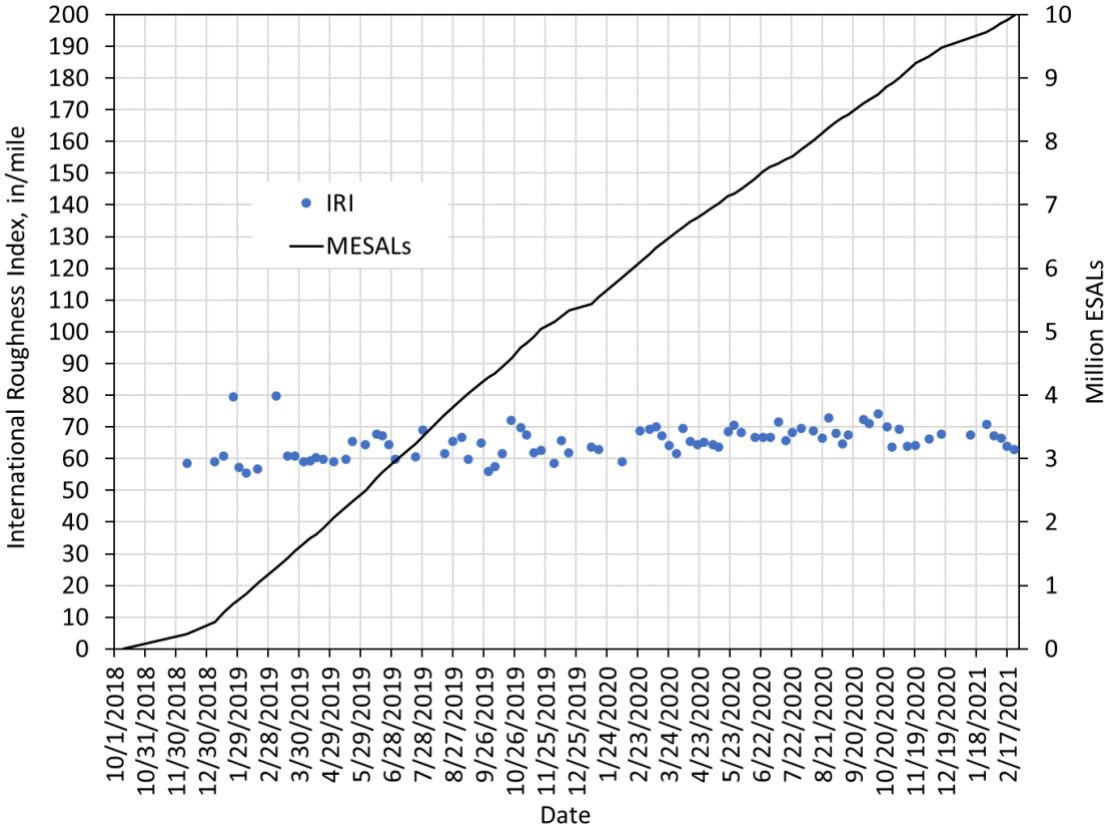

Figure 15. Section S2 Smoothness Data

11.4 Structural Response Characterization

The construction and performance data indicated a well-constructed stabilized foundation pavement with excellent performance through 10 million ESALs. The next portion of this investigation was to characterize the structural response through direct measurement under truck loading and falling weight deflectometer testing.

11.4.1 Structural Responses Measured with Embedded Instrumentation

Structural response measurements were made on a weekly basis during the experiment using the ASGs and EPCs embedded during construction. Response measurements consisted of at least 15 truck passes from which the 95th percentile highest measurement was used to represent the “best hit” on that collection day. Trucks were traveling at approximately 45 mph during each measurement and though all axles were measured, only single axle responses are presented herein for brevity. There was some variation among all the single axles, but they typically weighed approximately 20,000 lbs with dual tires.

Pressure Measurements. Recall from Figure 1 that three earth pressure cells were installed to measure the vertical pressure profile at the top of the cement treated base (CTB), at the top of the lime treated soil (LTS), and at the top of the Mississippi subgrade (Subgrade), respectively. Figure 16 shows the best hit vertical pressure at each depth from each day of data collection during the two-year trafficking cycle. As expected, the highest pressures were measured at shallower depths (i.e., CTB) and the lowest pressures were measured at the bottom of the cross-section (i.e., Subgrade). Cycling due to seasonal temperature changes is clearly evident in the CTB and LTS measurements and less so in the Subgrade measurement. The shorter-term cycling resulted from alternating data collection between morning and afternoons on a week-to-week basis. The cycling in pressure measurements is a direct result of the AC modulus changing with temperature where the highest pressures are measured when the AC is softest (i.e., summer and afternoons). As described above, this effect is most pronounced at the bottom of the AC where the pressure is primarily a function of the overlying AC layers but is mitigated deeper in the structure where the cement- and lime-treated layers are not sensitive to temperature changes.

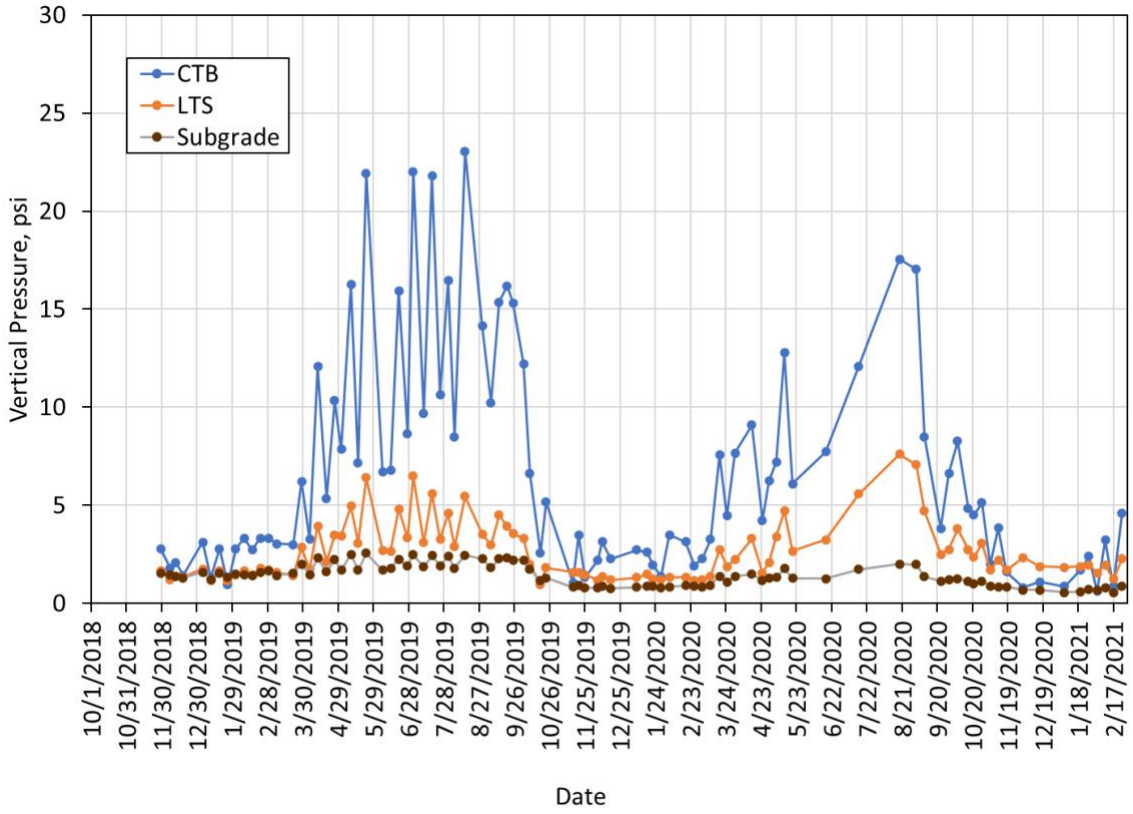

Figure 16. Section S2 Vertical Pressure versus Time

The pressure measurements from Figure 16 were plotted against the mid-depth AC temperature at the time of measurement, as shown in Figure 17. An exponential trendline was fit to each data series and the relative influence of temperature is seen in the shape of the series and the corresponding R^2 of each trendline. Again, the CTB pressure is most affected by changes in AC temperature while subgrade pressure is least affected.

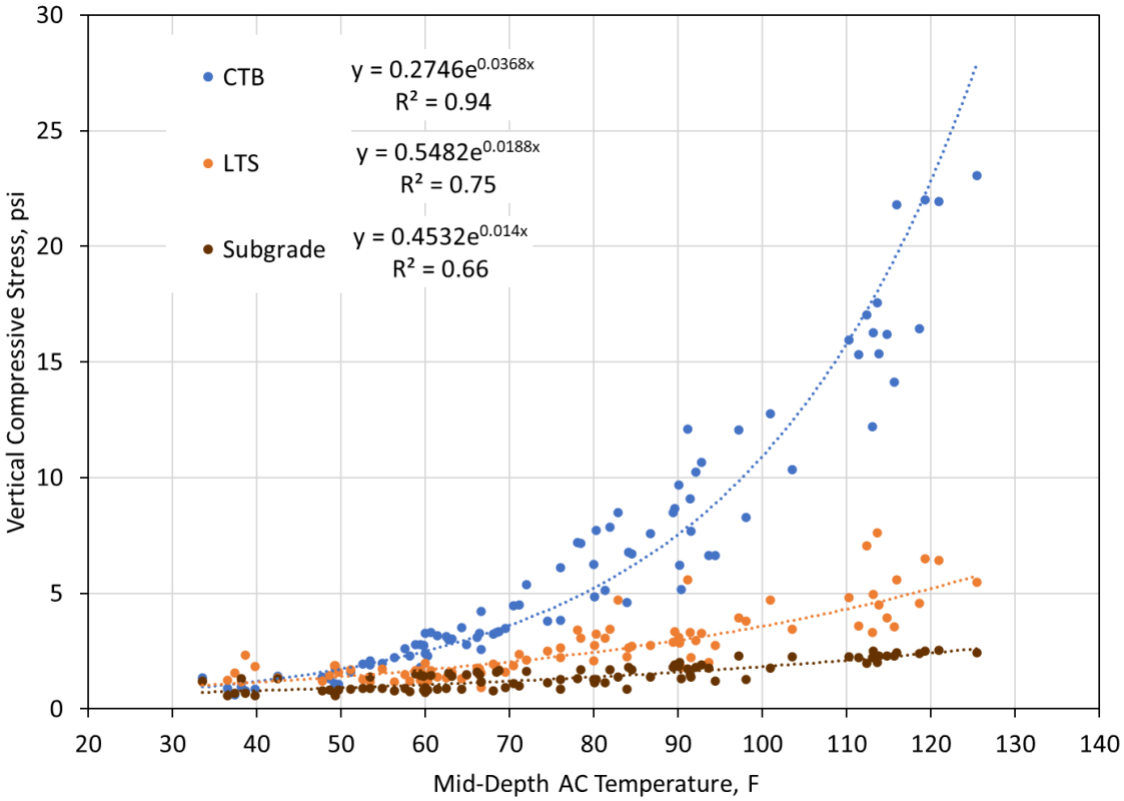

Figure 17. Section S2 Vertical Pressure versus Mid-Depth AC Temperature

The regression equations from Figure 17 were used to normalize the pressure data to a reference temperature following well-established Test Track procedures as documented by McCarty (*2*). The normalized pressure at 68°F is plotted versus time in Figure 18. Relatively flat or decreasing normalized pressures indicate good structural health consistent with the excellent performance measured at the pavement surface. Interestingly, the trendline fit to the subgrade pressure data, with an R^2 of 0.72, indicates a decrease over time, which could be indicative of curing of the overlying lime- and cement-treated materials.

The measurements and observations regarding vertical pressures in this stabilized foundation section were entirely expected. Decreasing pressure and decreasing temperature sensitivity with depth are consistent with conventional understanding of this pavement type, and also consistent with pavements having unbound foundation layers. However, as will be detailed in the next subsection, the strain measurements were unexpected and provide new insights regarding stabilized foundation flexible pavements.

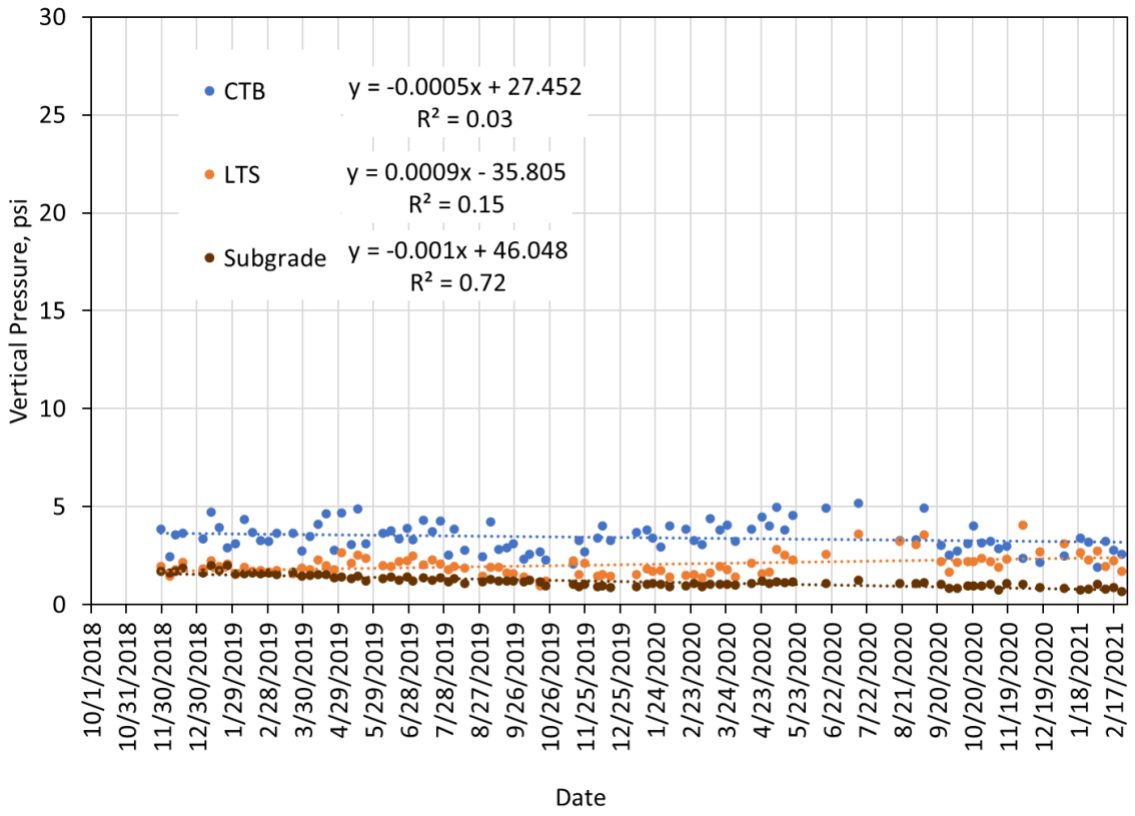

Figure 18. Section S2 Vertical Pressure at 68ºF versus Date

Strain Measurements. Following the approach presented above for the stress measurements, the maximum horizontal tensile strains measured at the bottom of the AC are plotted versus test date in Figure 19. The first critical observation is that the strain levels are quite low with all but one observation below 100 microstrain, a common threshold for perpetual pavement design. At these tensile strain levels, it is unlikely that bottom-up cracking would occur due to flexural bending of the AC. The low tensile strain levels are likely due to the restraint provided by the stabilized foundation layers. The second critical observation is that the strain levels appear to decrease during the warmer parts of the year and increase during the colder months. This is opposite of what is expected in that softening AC during warmer months should cause bending to increase accompanied by higher measured tensile strain. This expectation comes from many other flexible pavements studied at the Test Track (see Chapter 15 for a relative comparison) and elsewhere having unbound foundation layers. Understanding this opposite trend is key to understanding mechanistic responses of stabilized foundation pavements and is explored further below.

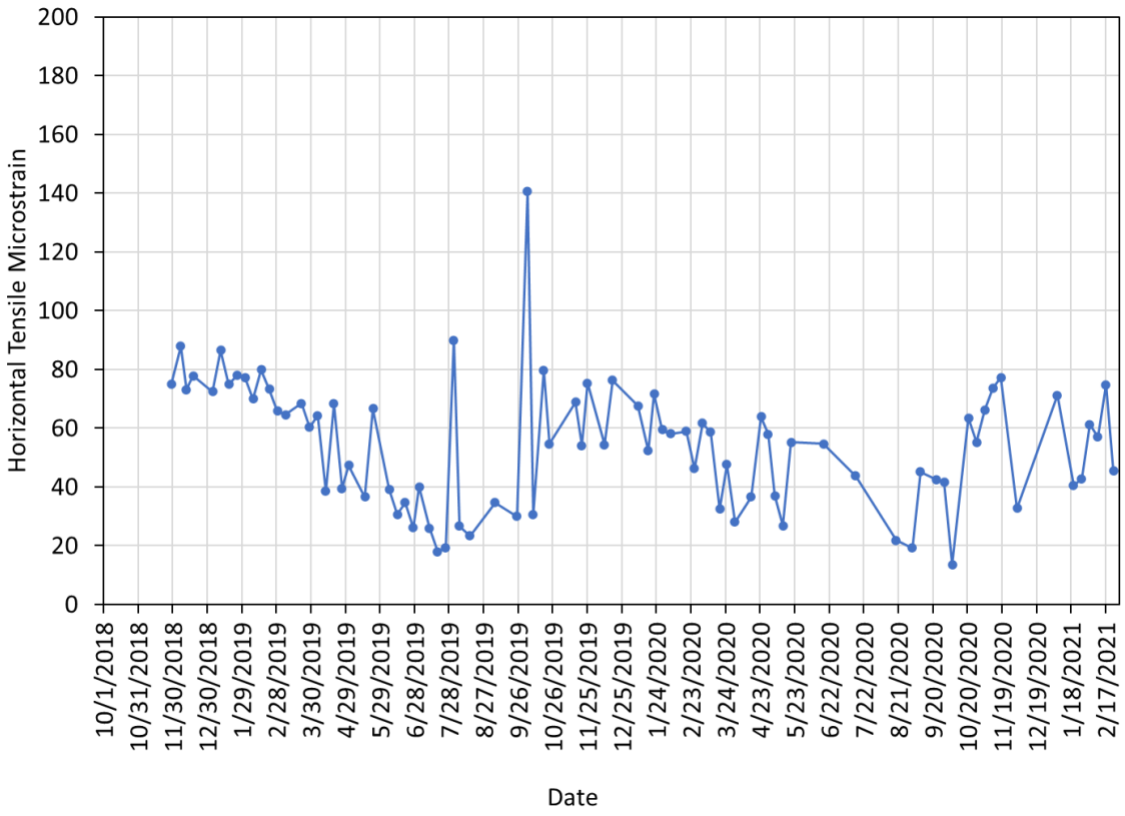

Figure 19. Section S2 Maximum Horizontal Tensile Strain at Bottom of AC versus Date

The strain measurements in Figure 19 were plotted against their corresponding mid-depth AC temperatures to better quantify the influence of temperature, as shown in Figure 20. Data from an unbound granular base section built at the same time (Section S9, 8" thick lift – see Chapter 15) is included in the figure for comparison. There is clearly a downward trend in the stabilized foundation tensile strain response. Evidently, as the AC softens due to increasing temperatures, the section experiences less tensile strain. Conversely, as expected, the conventional flexible pavement shows the strong positive increase in tensile strain with increasing temperature.

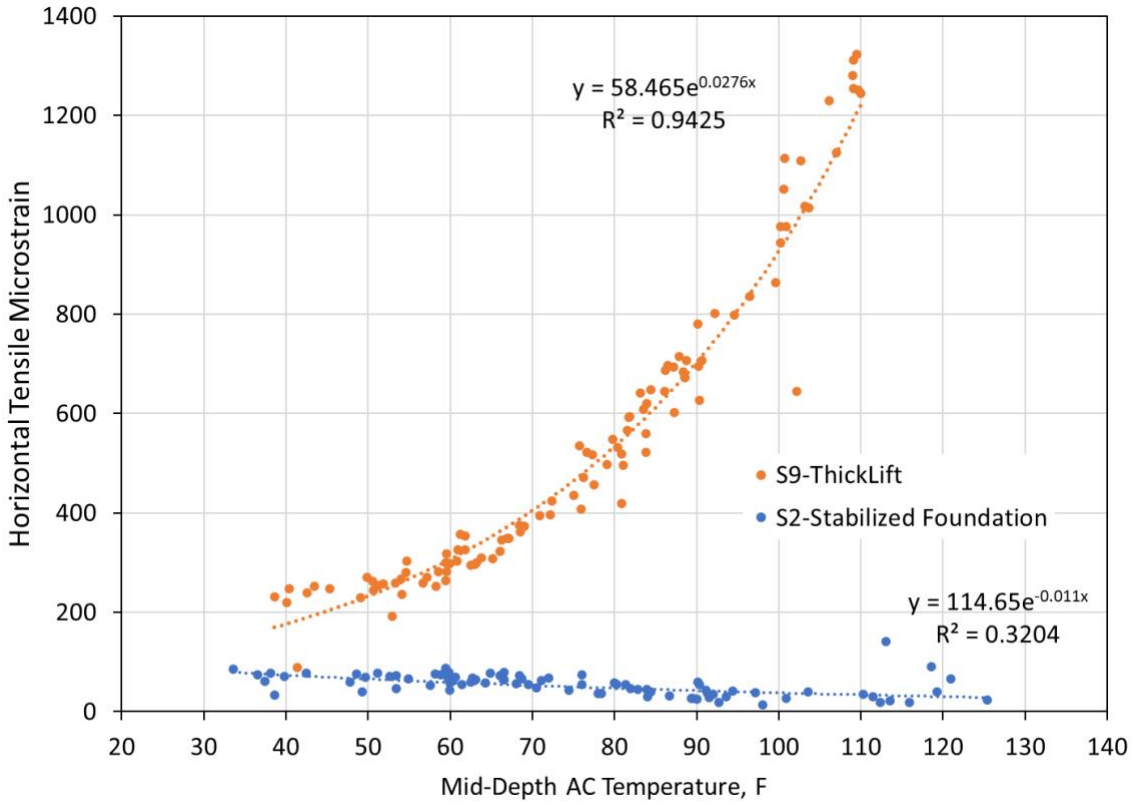

Figure 20. Section S2 Maximum Horizontal Tensile Strain at Bottom of AC versus Mid-Depth AC Temperature

The observation of decreasing tensile strain with increasing temperature was at first confounding and opposite of expected trends. Further investigation by Nakhaei and Timm examined both tensile *and* compressive strains, which revealed an important finding (*3*). Figure 21 plots peak measured tensile strain and peak measured compressive strain versus mid-depth AC temperature. In this data set, the tensile strain was fitted with a linear trendline while the compressive strain was fitted with an exponential trendline. The compressive strain in S2 follows a negative exponential trend that resembles the S9 tensile strain trend (Figure 20) but with a reversed sign. Even the exponential power for the trendlines of both sections are similar with high coefficients of determination (*3*). As explained by Nakhaei and Timm (*3*), Figure 21 also suggests that the stabilized foundation section experiences two different strain modes depending on pavement temperature. At lower temperatures (less than 75°F), the pavement strain response at the bottom of AC is predominantly tensile (i.e., tensile absolute magnitude exceeds compressive absolute magnitude). However, the strain response converted to dominantly compressive mode at higher temperatures (above 75°F). In other words, 75°F is the critical temperature at which the strain readings changes from dominantly tensile mode to dominantly compressive mode for this section.

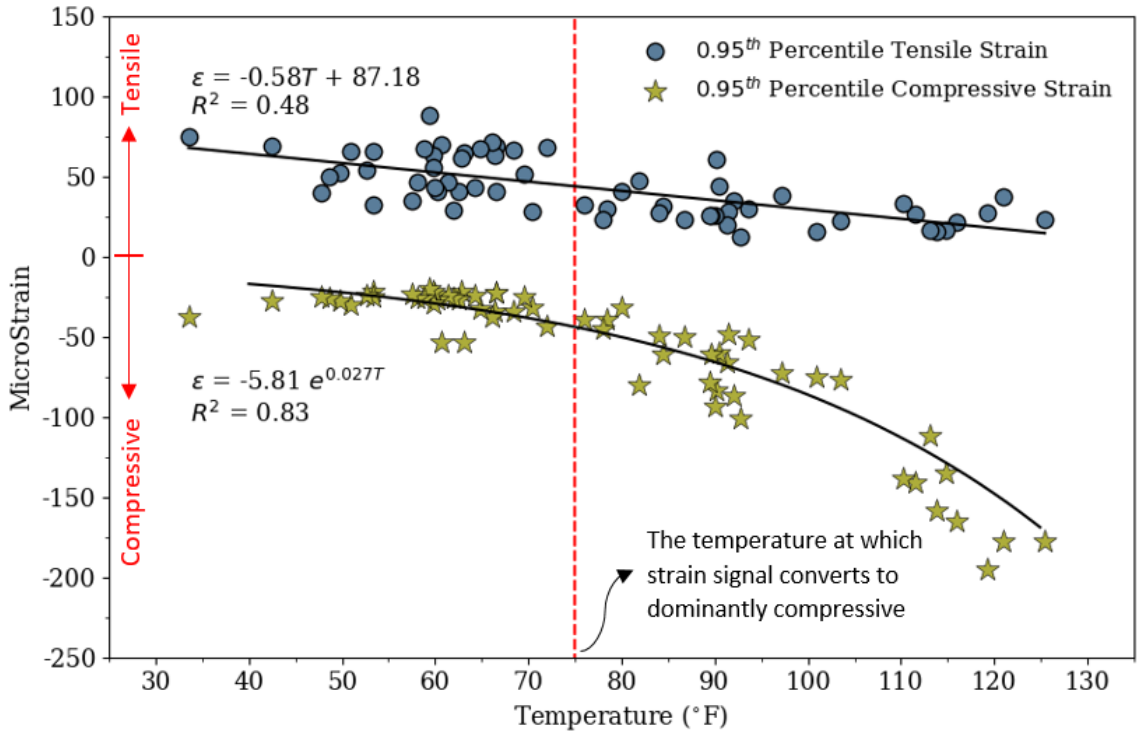

Figure 21. Section S2 Tensile and Compressive Strain at Bottom of AC versus Mid-Depth AC Temperature (*3*)

To illustrate the difference in strain modes for the two sections, Figure 22 shows actual strain traces measured under truck loading for two different conditions (summer and winter). The upper plot in Figure 22 pertains to the conventional section and the strain traces look very similar just having smaller magnitude for winter compared to summer. However, the lower plot for the stabilized foundation section shows a mode reversal where winter is primarily tensile response but summer, when the AC is soft, causes primarily compressive pavement response.

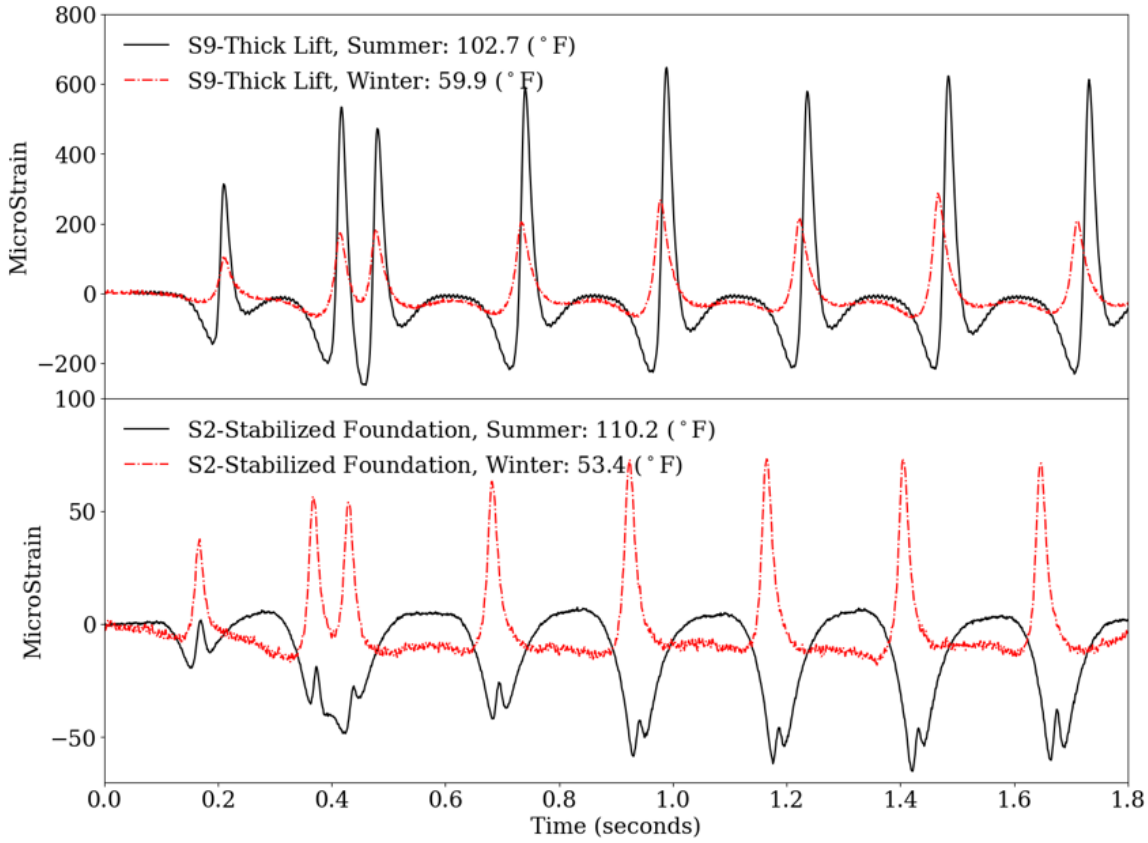

Figure 22. Sections S2 and S9 Measured Strain Responses under Truck Loading (*3*)

Similar observations were made under falling weight deflectometer (FWD) loading as shown in Figures 23 and 24 for winter and summer conditions, respectively. These measurements were from a particular strain gauge in the section, but are representative of all the gauge-specific measurements made under FWD loading. Gauge locations were previously determined using a total station during construction which enabled precise marking of the pavement surface over which to center the FWD load plate. Again, as shown in Figures 23 and 24, the primary mode of response switches from tension to compression with increasing pavement temperature.

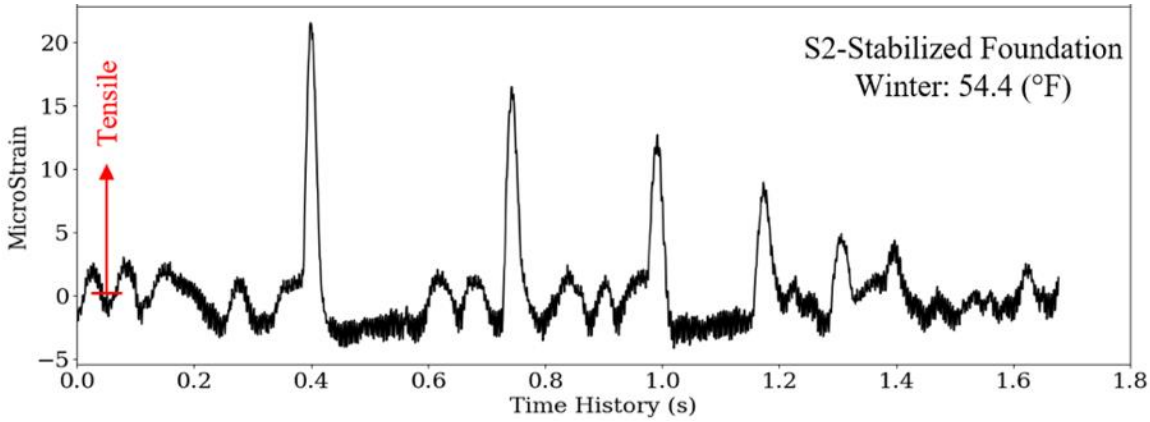

Figure 23. Section S2 Strain Response under FWD Loading during Winter (*3*)

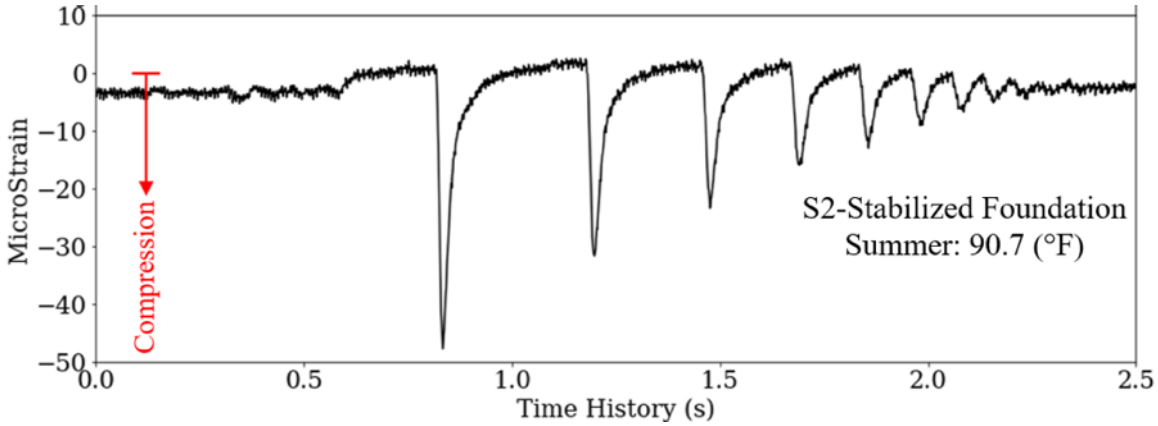

Figure 24. Section S2 Strain Response under FWD Loading during Summer (*3*)

The measured strain responses were unexpected but were consistent under both truck and FWD loading. The next question was whether layered elastic theory, commonly used for mechanistic-empirical pavement design, would predict similar behavior. To conduct this part of the investigation, a customized computer program called MASTIC was developed following layered elastic theory (*4*). The name stands for **MA**TLAB-Ela**stic** which represent the original programming language and mode of computation. The program was checked against other existing programs such as WESLEA and was found to give nearly identical pavement response predictions. Both the stabilized foundation and conventional pavement cross section were simulated with representative layer properties, as listed in Table 7, to determine the horizontal strain distributions versus pavement depth as described below. It is important to emphasize that the layer properties were not necessarily meant to perfectly replicate in situ conditions but rather serve as representative of what could be expected in each section. The unexpectedly high value of the Mississippi subgrade was obtained through computing resilient modulus from the AASHTO two-layer backcalculation approach. It's currently theorized that the relatively low stress levels reaching that layer, due to the very stiff layers above, produced a relatively high modulus. The aggregate base modulus in S9 was consistent with previous studies using the same material at the Test Track (*5, 6*).

Table 7. Simulated Section Properties (*4*)

Section Name	Layers	Elastic Modulus (ksi)	Poison's Ratio	Thickness (in.)
Stabilized Foundation (S2)	Asphalt Concrete	2000 (winter) 300 (summer)	0.35	9.2
	Cement Treated Base	2000	0.2	6.1
	Lime Treated Soil	100	0.4	5.5
	Mississippi Subgrade	30	0.45	infinite
Thick-Lift (S9)	Asphalt Concrete	2000 (winter) 100 (summer)	0.35	8.1
	Aggregate Base	10	0.4	5.5
	Test Track Subgrade	30	0.45	infinite

Figure 25 shows horizontal strain versus depth for the conventional pavement section (S9) where, regardless of season or AC modulus, the maximum tensile strain occurs at the bottom of the AC. This is expected behavior and was observed in strain measurements under truck and

FWD loading. In contrast, Figure 26 shows the theoretical prediction for Section S2 where the winter condition (E1 = 2,000 ksi) produces maximum tension at the bottom of the AC, but the summer condition (E1 = 300 ksi) yields compression at the bottom of the AC. These predictions are consistent with the measurements made under both FWD and truck loading. More interestingly, Figure 26 also shows that peak tensile strain in the AC layer occurs near the mid-depth of the AC. This is another unexpected result and has important ramifications for flexible pavement design and instrumentation. Pavement designers typically focus on the bottom of the AC to predict bottom-up cracking but maximum tension, as shown in Figure 26, could occur at shallower depths and lead to middle-up cracking. Also, researchers typically place asphalt strain gauges at the bottom of the AC to measure maximum tensile strain but, again, the model suggests it could occur at shallower depths.

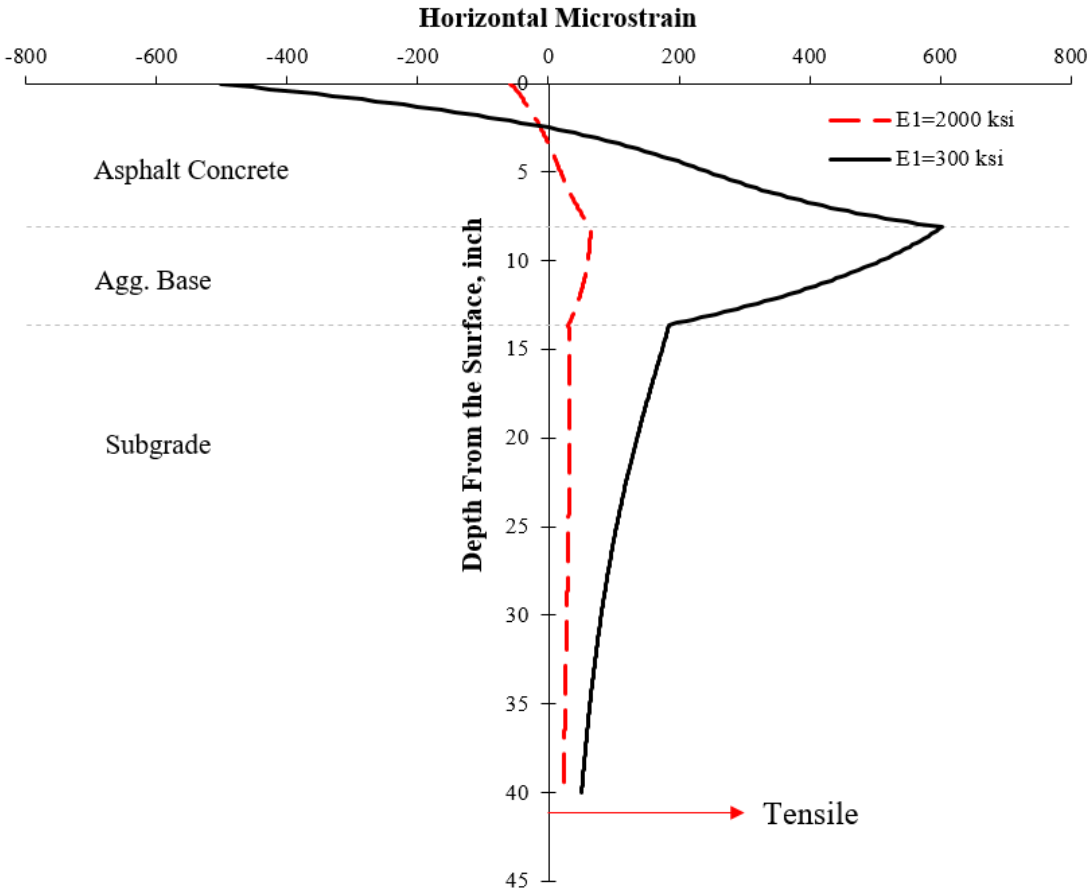

Figure 25. Strain Distribution of the Simulated Thick-Lift Pavement Section (*4*)

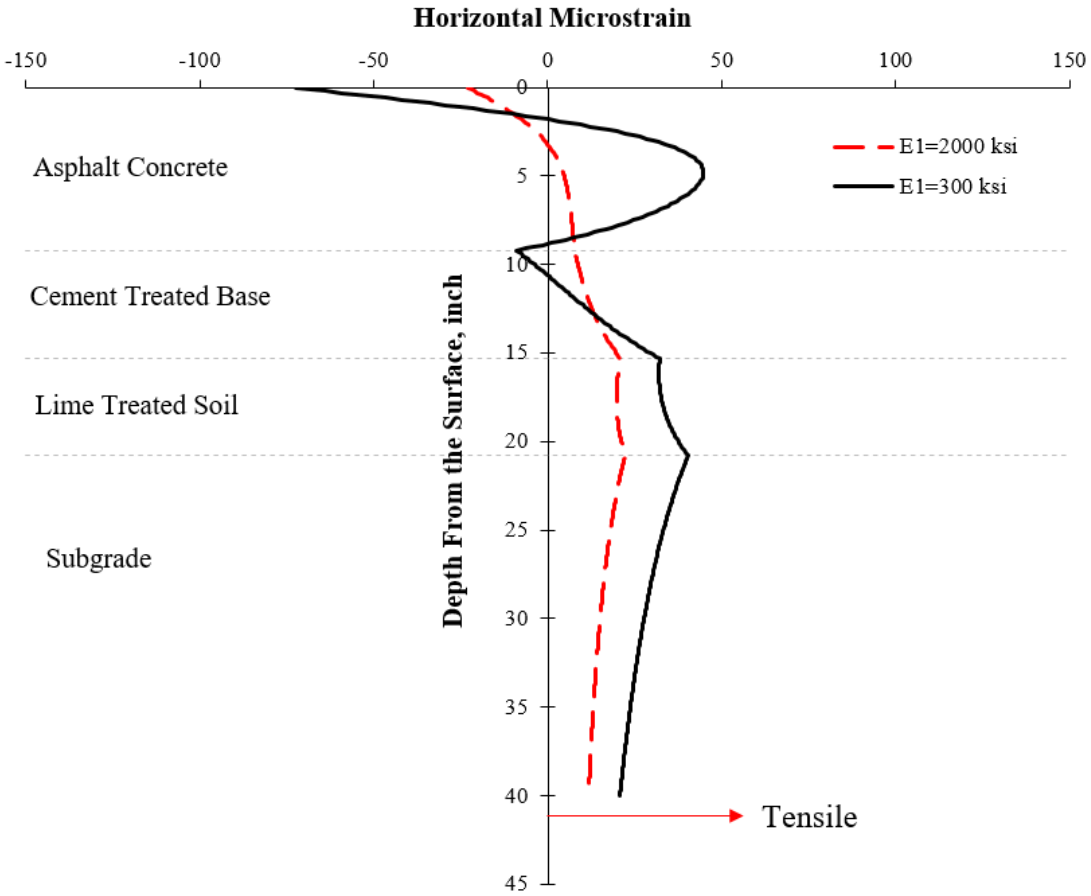

Figure 26. Strain Distribution of the Simulated Stabilized Foundation Pavement Section (*4*)

Despite the important finding that tensile strain is inversely affected by increasing temperature in a stabilized foundation section, the strain levels are relatively low (less than 100 microstrain) and bottom-up cracking is not expected to occur in this section. However, additional trafficking could reveal middle-up cracking over time from peak tension occurring at shallower depths in the AC.

11.4.2 Falling Weight Deflectometer Testing and Backcalculation

FWD testing was conducted three times per month with a Dynatest 8000 FWD during the two-year trafficking cycle. The FWD has nine sensors with standard spacing of 0, 8, 12, 18, 24, 36, 48, 60, and 72 inches from the load center. Testing was conducted at four longitudinal stations in the section with three lateral offsets (inside wheelpath, outside wheelpath, and between wheelpath) at each station. The four stations represented each of three 50 ft subsections and the middle of the gauge array, respectively. Stations 1, 2 and 3 represent the subsections and Station 4 was in the gauge array. Stations 1, 2 and 3 were originally determined by random number generation in the 50 ft subsections at the time of construction but then held fixed during the two years of trafficking. Each FWD test consisted of two seating drops followed by three replicate drops at 6,000, 9,000 and 12,000 lb, respectively.

Backcalculation was originally attempted with EVERCALC 5.0 following well-established procedures used at the Test Track. However, it was quickly discovered that conventional techniques would not apply to a flexible pavement with a stabilized foundation. Therefore, an in-depth investigation that attempted hundreds of different cross sections, boundary conditions, and optimization techniques was undertaken using an in-house customized program called MASTIC. The combination of stiff base and subbase materials and the complex pavement structure with AC, CTB, LTS, MS soil, and Test Track subgrade, all with different material properties, made the backcalculation process a complex and difficult task. The main problem for all backcalculation tasks was high variability in elastic modulus of CTB and LTS. While the majority of backcalculation software packages such as EVERCALC assume a fully bonded interface condition with no ability to change the setting, it was found that changing the friction bonding to partially bonded condition is the key to obtain better results. This effort was extensively documented by Nakhaei (*4*) while only the final results and key findings are presented here for brevity.

Through the course of Nakhaei's investigation (*4*), it was determined that the first and last random locations in the test section (numbers 1 and 3) did not provide reliable backcalculated moduli. Results from these locations tended to have highly erratic and sometimes extremely high or low modulus values, which appeared to stem from a compensating effect in the backcalculation process. Investigation of the raw deflection basins normalized for temperature and load level determined that the deflection basins at these random locations are much smaller than the other two random locations (locations 2 and 4), which may be misinterpreted as a rigid foundation in the backcalculation process leading to erratic backcalculated moduli. Exclusion of the deflection basins at random locations 1 and 3 greatly improved the results, presented below. For practical purposes, a methodology was proposed to automatically identify and remove erroneous deflection basins in flexible pavements with stabilized foundation sections (*4)*. Furthermore, it is suggested that testing at higher load levels (e.g., 16 kips) could potentially provide meaningful deflection data from which backcalculation would be successful, without the confounding compensating effects.

It is currently unclear why locations 1 and 3 had smaller deflection basins, but this could have resulted from the challenge of constructing a pavement section of such complexity (i.e., multiple stabilized lifts) over a relatively short length (200 ft). Further forensic investigation is warranted when the section is eventually taken out of service to better understand the results at these two random locations.

The backcalculation cross-section that yielded the best results, after omitting random locations 1 and 3, was a four-layer system comprised of asphalt concrete over the cement treated base layer over the lime treated soil over the MS subgrade. Full bonding was set between the AC and CTB with nearly full slip between the remaining layers as described by Nakhaei (*4*). The backcalculated moduli for this cross section are shown in Figures 28, 29, 30 and 31 for the AC, CTB, LTS and MS subgrade, respectively. Each figure shows the moduli versus temperature in the left graph and moduli versus date in the right graph. The red lines in the moduli versus temperature plots are best-fit trendlines while the red lines in the modulus versus date graphs are 30-point moving averages to smooth out the raw data.

The strong influence of temperature on AC modulus is clearly evident in Figure 27 where the modulus versus temperature trendline has an R^2 of 0.90 and seasonal cycling is easily identified. This behavior is consistent with modulus versus temperature trends in other, more conventional test sections. Also, the relatively tight grouping of the data around the best-fit trendline indicates a section in good health, which is consistent with performance monitoring of the section.

Figure 28 shows very little dependence of CTB modulus on temperature with most of the data between 1,000 to 2,000 ksi. It is important to note that modulus testing conducted by Mississippi State University on lab-fabricated lab tested CTB materials determined an average elastic modulus of 1,012.5 ksi so the backcalculated values appear reasonable (*7*). The values are also in the correct range to generate the strain reversal phenomenon discussed previously in this chapter (i.e., for the reversal to occur, there must be some evidence of CTB modulus exceeding the AC modulus, which is the case).

Figure 29, depicting the LTS moduli versus temperature and date, also shows very little influence of temperature with values ranging between 300 and 700 ksi. Again, laboratory testing from Mississippi State University on lab-fabricated lab tested samples provides a basis of comparison with an average value of 366.6 ksi (*7*).

Figure 30 shows the MS Subgrade modulus values versus temperature and date. The downward trend versus temperature may be indicative of stress softening behavior. As the temperature increases and the AC modulus decreases, higher stress levels are imposed on the unstablized subgrade, which exhibits lower modulus values. This behavior may also highlight the benefit of protecting this particular subgrade with a substantial cross section above it to keep stress levels relatively low and the apparent modulus reasonably high.

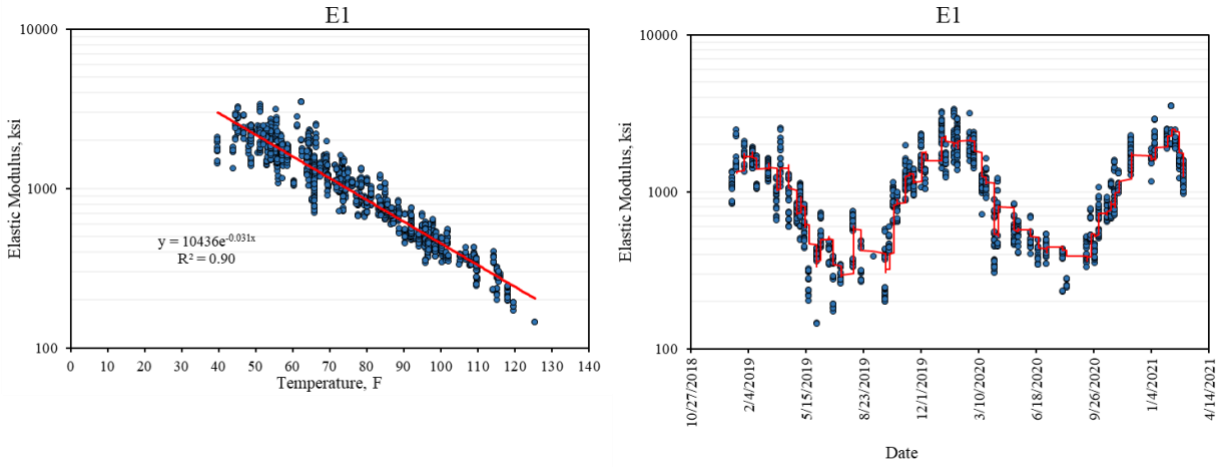

Figure 27. Backcalculated AC Moduli in S2 (*4*)

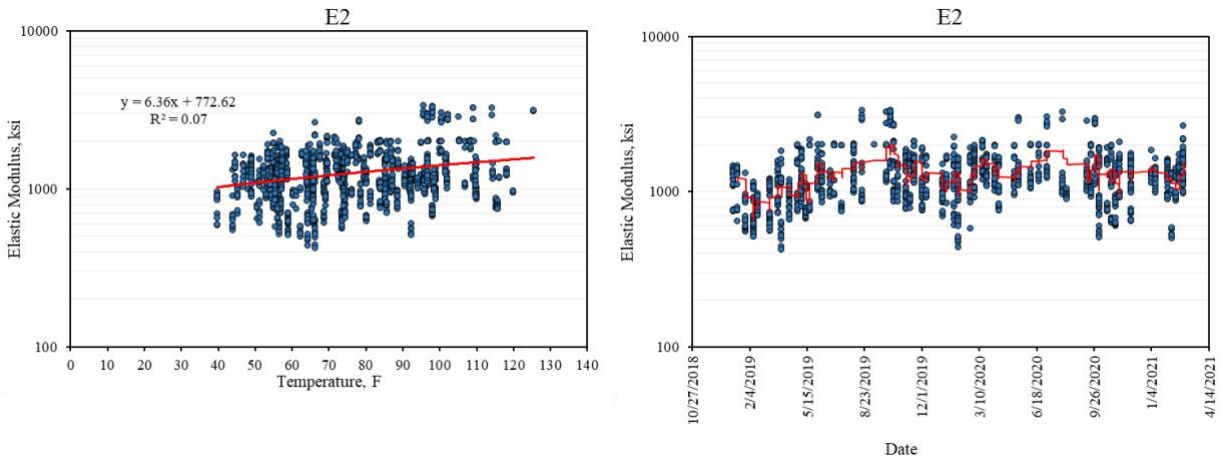

Figure 28. Backcalculated CTB Moduli in S2 (*4*)

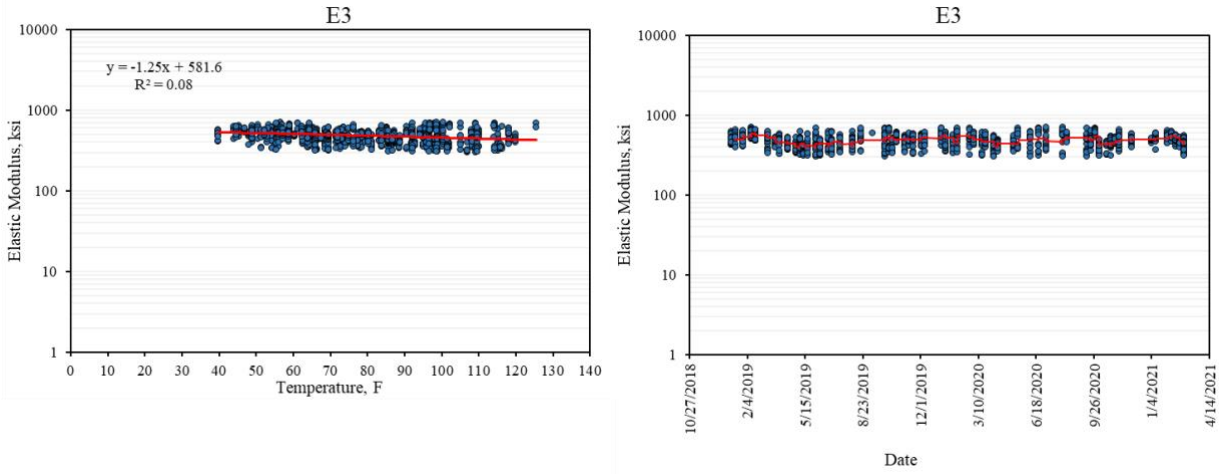

Figure 29. Backcalculated LTS Moduli in S2 (*4*)

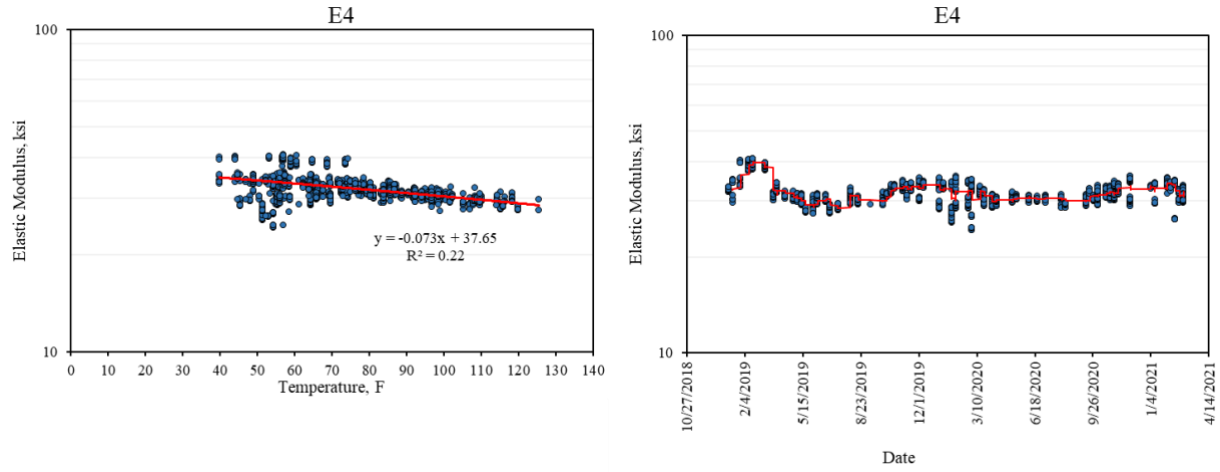

Figure 30. Backcalculated MS Subgrade Moduli in S2 (*4*)

11.5 Laboratory Testing

Fundamental material property and performance tests were conducted on plant-produced, lab-compacted specimens as part of routine testing conducted on Test Track structural sections. The following sections present the test results from dynamic modulus, fatigue (both bending beam and cyclic), IDEAL-CT and Hamburg wheel tracking test.

11.5.1 Dynamic Modulus

Small geometry dynamic modulus (E*) specimens were prepared according to AASHTO PP 99-19 and tested according to AASHTO TP 132-19. Specimens were compacted to a target air void content of 7%. Table 8 tabulates the data at the three temperatures and frequencies used in the testing while Figure 31 illustrates the master curves at a reference temperature of 20°C (68°F) generated from the test data following AASHTO R 84-17. While a direct comparison between backcalculated AC moduli (Figure 27) and |E*| data (Table 8 and Figure 31) is difficult due to fundamental differences in testing and grouping all AC layers together in backcalculation, the |E*| data are consistent with the trend observed in backcalculation with respect orders of magnitude.

Table 8. S2 Dynamic Modulus Test Data

			E Avg (MPa)*				*E* Avg (ksi)*			
Temp (°C)	*Temp (°F)*	*Freq (Hz)*	*S2-4 (Surface)*	*S2-3*	*S2-2*	*S2-1 (Base Mix)*	*S2-4 (Surface)*	*S2-3*	*S2-2*	*S2-1 (Base Mix)*
4	39.2	10	18,012	19,927	19,342	18,049	2,612	2,890	2,805	2,618
4	39.2	1	14,775	16,939	16,327	14,929	2,143	2,457	2,368	2,165
4	39.2	0.1	11,442	13,680	13,130	11,656	1,660	1,984	1,904	1,691
20	68	10	10,638	12,400	11,878	10,770	1,543	1,798	1,723	1,562
20	68	1	7,192	8,823	8,436	7,399	1,043	1,280	1,224	1,073
20	68	0.1	4,276	5,580	5,404	4,514	620	809	784	655
40	104	10	3,459	4,139	4,165	3,709	502	600	604	538
40	104	1	1,605	1,985	2,156	1,810	233	288	313	263
40	104	0.1	647	815	987	778	94	118	143	113

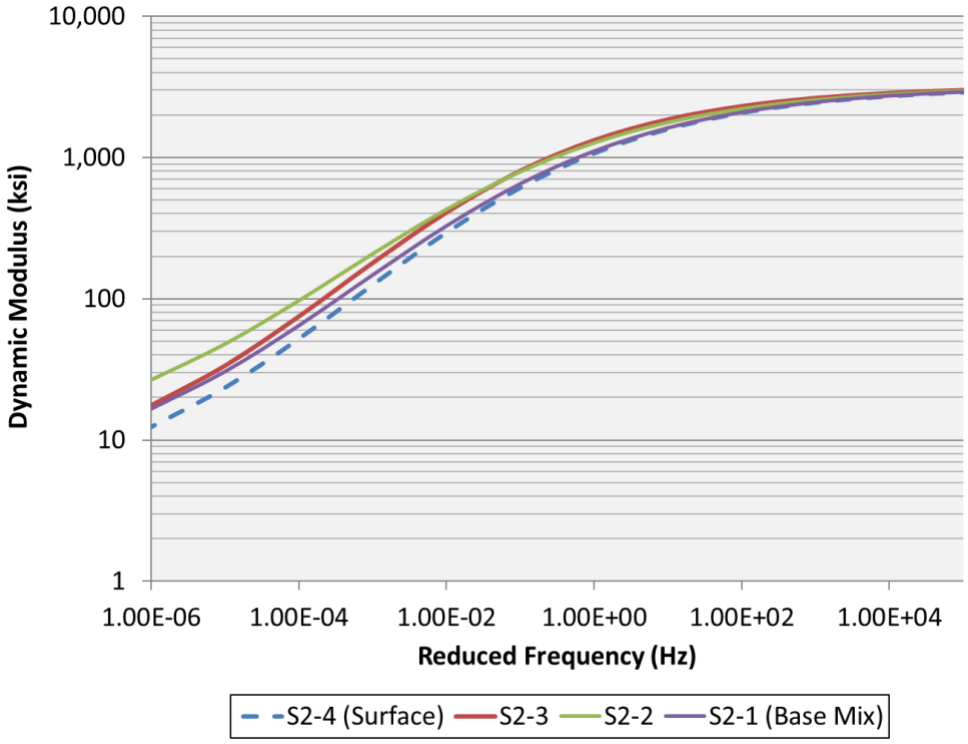

Figure 31. Section S2 Dynamic Modulus Master Curves

11.5.2 Fatigue Testing

Bending beam fatigue testing (BBFT) of the base mix (S2-1) followed AASHTO T 321-17 with specimens again compacted with target air voids of 7% and three target strain levels (300, 400, and 600 microstrain). The results, with three replicates at three strain levels, are shown in Table 9 and Figure 32. It is difficult to derive meaning from the transfer functions without control mixtures for comparison. Additionally, since the section has experienced 10 million ESALs during the research cycle with no apparent bottom-up cracking, the transfer functions need calibration once or if bottom-up fatigue occurs, which is unlikely due to the very low strain levels at the bottom of the AC. However, as discussed previously, further trafficking may initiate middle-up cracking in the section.

Table 9. Section S2 Base Mix Bending Beam Fatigue Test Data

Sample ID	Sample Air Voids (%)	Initial Beam Stiffness (MPa)	Initial Beam Stiffness (ksi)	Cycles to Failure (Peak Mod x Cycles)	Peak-to-Peak On-Specimen Microstrain
12	7.4	7,888	1,144	891,250	300
14	7.3	7,536	1,093	940,444	300
15	7.3	7,821	1,134	607,202	300
7	7.6	10,613	1,539	38,904	400
9	6.8	7,942	1,152	141,796	400
10	7.1	8,283	1,201	49,545	400
2	7.1	7,724	1,120	12,956	600
5	7.0	7,642	1,108	8,175	600
8	7.0	7,988	1,159	3,905	600

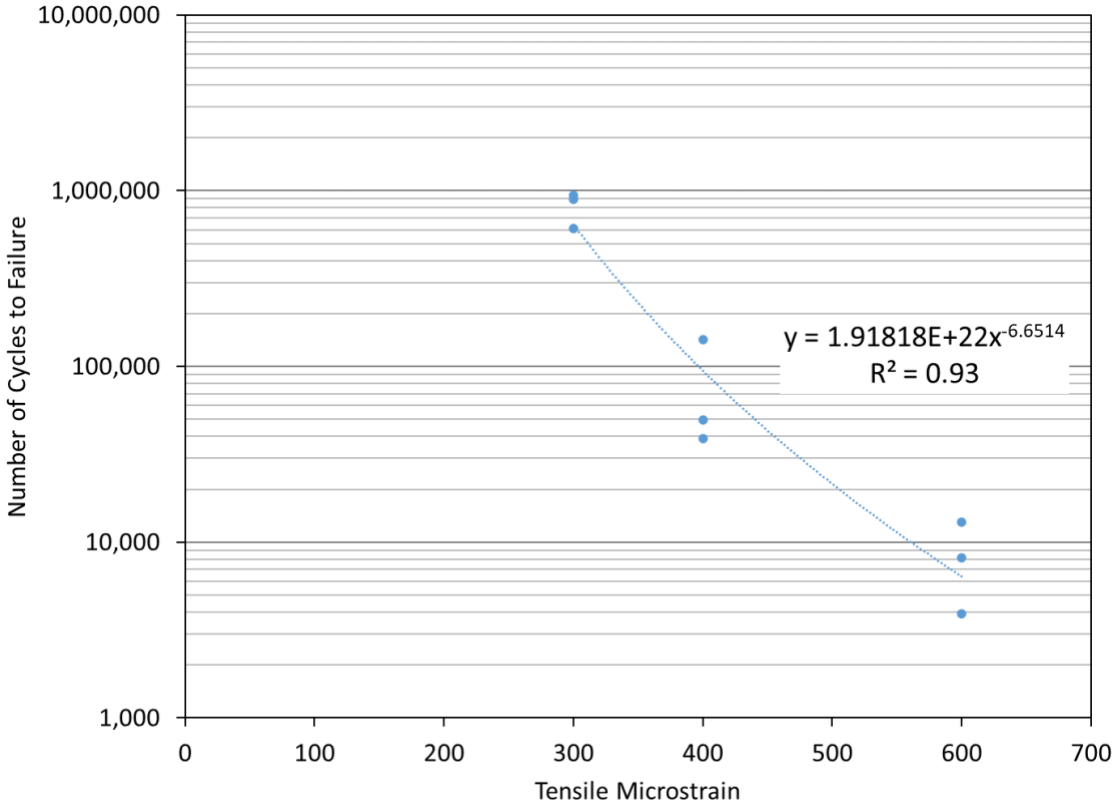

Figure 32. Section S2 Base Mix Bending Beam Fatigue Transfer Function

11.5.3 Ideal CT Testing

Additional cracking tolerance of the surface mix (S2-4) was determined with the IDEAL-CT test following ASTM D8225-19. For this test, six specimens were compacted to a target air void content of 7% and the results are shown in Table 10. The non-sequential sample identification numbers resulted from some specimens not meeting the required specimen volumetrics (i.e., ten samples were created to have six that could be tested).

There is active and ongoing debate regarding minimum CT_{Index} values for use in balanced mix design. One commonly-cited specification from the Virginia DOT requires a CT_{Index} exceeding 70 to avoid surface cracking problems (*8*) and some mixes previously placed on the Test Track with

CT_{Index} values in the 30s also performed well (*9*). However, the CT_{Index} values highlighted in Table 10 are below even this lower threshold, so top-down cracking may become a problem in the next test cycle though it is not evident through the first two years and 10 million ESALs of trafficking.

Table 10. Section S9 Surface Mix Ideal CT Test Data

Sample ID #	2	3	4	5	7	10
Air Voids	7.1	6.7	6.8	6.9	7	7.1
Thickness (mm)	62	62	62	62	62	62
Diameter (mm)	150	150	150	150	150	150
Test Temperature	25C	25C	25C	25C	25C	25C
CT_{Index}	**25.2**	**19.3**	**23.4**	**17.9**	**18.8**	**24.3**
Peak Load (lbs)	4612.5	4731.4	4731.6	4678.7	4809.3	4681.9
Fracture Energy (J/m2)	8429.9	8155.6	8907.9	7949.2	8257.8	8538.1
Post Peak Slope (kN/mm)	7.39	8.486	8.018	8.853	8.556	7.619
Displacement @75% (mm)	3.307	3.015	3.162	2.987	2.918	3.25

Note: Loading rate = 50 mm/min

11.5.4 Hamburg Wheel Track Testing

Rutting susceptibility of the surface mix was measured at 50°C with the Hamburg Wheel Track Testing device according to AASHTO T324-19. Specimens were compacted to a target air void content of 7%. The measured profile data are shown in Figures 33 and 34 with the summary results presented in Table 11. Like IDEAL-CT design criteria, there is a range of published thresholds for acceptable Hamburg test results (*10*). Generally speaking, a mix with an unmodified binder should have less than 12.5 mm of rutting after 10,000 or 15,000 wheel passes. The maximum rutting in Table 11 is well below this threshold. Furthermore, the mixture had no stripping problems as it achieved over 20,000 passes with no stripping evident.

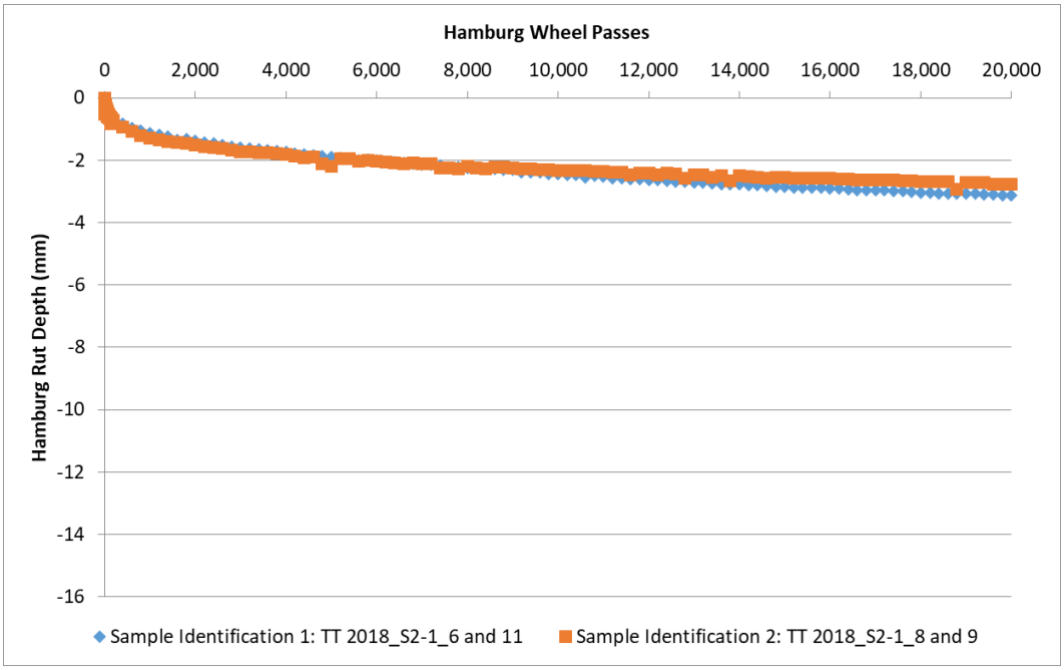

Figure 29. Section S2 Surface Mix Hamburg Wheel Track Testing Minimum Profile Values

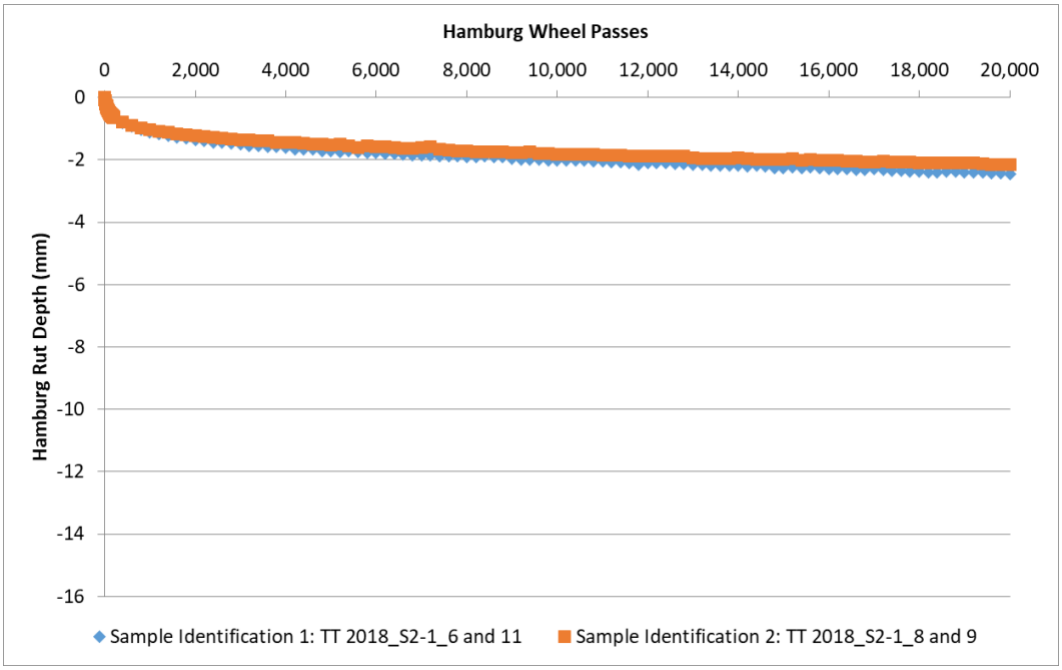

Figure 30. Section S2 Surface Mix Hamburg Wheel Track Testing Center Profile Values

Table 11 Section S2 Surface Mix Hamburg Wheel Track Testing Summary

Parameter	Replicate 1	Replicate 2
Sample 1 ID	6	8
Sample 2 ID	11	9
Sample 1 Va (%)	7.1	7.2
Sample 2 Va (%)	7.1	7.2
Max Rut - 10k Passes (mm)	2.45	2.33
Max Rut - 20k Passes (mm)	3.14	2.78
Passes to 12.5 mm Rut	>20,000	>20,000
Approximate Stripping Inflection Point (passes)	>20,000	>20,000

11.6 Summary, Conclusions, and Recommendations

Section S2 was constructed for the Mississippi DOT to evaluate a flexible pavement with a stabilized foundation. Based on the results presented in this chapter, the following conclusions and recommendations are made:

1. The stabilized foundation section exhibited excellent performance over the 10 million ESALs. Rutting was less than 0.15”, no cracking was observed, and smoothness did not change appreciably over time.
2. Measured vertical stresses were as expected with stresses decreasing with depth and influenced exponentially by temperature. Stresses in the deeper pavement layers were less affected by AC temperature.
3. Strain levels measured at the bottom of the AC were very low (less than 100 microstrain), which was expected from relatively thick AC over a stabilized foundation. Bottom-up cracking is not expected to occur in this section.
4. Decreasing strain levels at the bottom of the AC with increasing temperature (lower AC moduli) was measured under both truck and FWD loading. This trend was opposite to

previous and current trends measured in conventional flexible pavements. A critical AC temperature of 75°F was found where the mode changes from tension to compression. Below 75°F, the primary mode is tensile while above 75°F the bottom of the AC experiences compression.

5. Simulations using the customized MASTIC software confirmed the measured pavement responses and also identified another critical zone at the mid-AC depth where tensile strains could reach a peak level. Repeated tension at this depth could lead to middle-up cracking. Further trafficking of the section should be conducted to evaluate this hypothesis.
6. An in-depth investigation determined that FWD testing on flexible pavements with stabilized foundations may yield deflection basins so small that they prevent obtaining reasonable backcalculated moduli. Eliminating deflection basins where this occurred greatly improved the backcalculation results and is recommended for further backcalculation activities. Furthermore, it is recommended that additional heavier impact loading be added to the FWD testing sequence for S2. Currently, testing is conducted at 6-, 9- and 12-kip loading. Adding 16 kip loading to the sequence could provide more deflection basins that provide reasonable backcalculated moduli.
7. The optimal cross-section for backcalculation was found to be AC over CTB over LTS over MS Subgrade with the AC/CTB interface fully bonded and the other interfaces with a nearly full-slip condition. This cross section yielded reasonable results, as verified by laboratory testing, and would produce the strain inversion phenomenon observed in both measurement and simulation.
8. IDEAL-CT testing indicated that the surface may crack over time as the index values fell below commonly accepted thresholds. Again, additional time and trafficking will evaluate this hypothesis.
9. Surface mix rutting is not expected in this section since the Hamburg rutting data fall well within acceptable limitations.
10. This section will experience another 10 million ESALs during the 2021 Test Track research cycle. During that cycle, surface performance monitoring (i.e., rutting, cracking and ride quality) and subsurface characterization (i.e., stress, strain measurement and FWD testing) will continue. Linkages between the performance measurements and structural characterization will provide needed data sets for M-E analysis and design of stabilized foundation sections.

11.7 References

1. Timm, D. H. *Design, Construction, and Instrumentation of the 2006 Test Track Structural Study*. Report No. 09-01, National Center for Asphalt Technology, Auburn University, 2009.
2. McCarty, C. *Early Characterization and Performance of a Flexible Thick Lift Pavement*. M.S. Thesis, Auburn University, 2019.
3. Nakhaei, M., and D. H. Timm. Middle-Up Cracking Potential in Flexible Pavements with Stabilized Foundations. *Transportation Research Record: Journal of the Transportation Research Board of the National Academies*, Washington, D.C., 2021.
4. Nakhaei, M., *Full-Scale Mechanistic and Performance Investigation of a Flexible Pavement with a Stabilized Foundation*, Doctoral Dissertation, Auburn University, 2021.

5. Taylor, A.J. and D.H. Timm. *Mechanistic Characterization of Resilient Moduli for Unbound Pavement Layer Materials.* Report No. 09-06, National Center for Asphalt Technology, Auburn University, 2009.
6. Tutu, K. and D.H. Timm. Determination of an Optimum Backcalculation Cross-Section for Unconventional Pavement Profiles. *Transportation Research Record No. 2641*, Transportation Research Board, 2017, pp. 48-57.
7. Sullivan, W., *Field Application of the PM Device and Assessment of Early Age Behaviors of Cement Stabilized Pavement Layers*, Doctoral Dissertation, Mississippi State University, 2021.
8. Virginia Department of Transportation. *Special Provision for Balanced Mix Design (BMD) Surface Mixtures Designed Using Performance Criteria*, 2020.
9. West, R. C., D. H. Timm, B. Powell, M. Heitzman, N. Tran, C. Rodezno, D. Watson, F. Leiva, and A. Vargas, *Phase VI (2015-2018) NCAT Test Track Findings*, NCAT Report 18-04, National Center for Asphalt Technology, Auburn University, 2018.
10. West, R. C., C. Rodezno, F. Leiva, and F. Yin. *Development of a Framework for Balanced Mix Design*. National Cooperative Highway Research Program Project 20-07/Task 406, 2018.

12. MISSISSIPPI AND TENNESSEE SPRAY-ON REJUVENATOR EXPERIMENT

Dr. Raquel Moraes

12.1 Background

Asphalt age hardening occurs when an asphalt binder near the pavement surface becomes stiffer and more brittle due to oxidation, leading to surface deterioration such as non-load associated distresses and top-down fatigue cracking. To preserve the functional and structural integrity of asphalt binders from age hardening and subsequent deterioration, spray-on rejuvenators can be applied on existing asphalt pavement surfaces. Designed to penetrate into the asphalt material near the pavement surface to renew the hardened/oxidized asphalt binder, rejuvenators can be combined with emulsified asphalt binders (to produce rejuvenating fog seals) and/or other materials (e.g., polymers) to seal low-severity surface cracks and inhibit raveling.

Spray-on rejuvenators are petroleum- or bio-based oils with chemical and physical characteristics selected to restore properties of aged asphalt binder in the surface layer. For optimal restoration of the aged asphalt binder's properties, consideration should be given not only to the viscosity-reducing capacity of the rejuvenator, but also to its chemical composition. Furthermore, the degree of diffusion of the rejuvenator into the aged binder is of the utmost importance, since it will allow changes in the intermolecular agglomeration and self-assembly of the asphalt polar micelles, affecting the overall performance properties of the aged asphalt mixes. While not meant to soften the underlying asphalt, the newly rejuvenated binder will have lower stiffness than the aged asphalt present on the pavement surface and will protect the underlying surface from further deterioration, especially due to raveling and top-down cracking (*1*).

When rejuvenators are combined with emulsified asphalt binders or other materials such as polymers to treat raveled and aged pavements, these products can delay aging by reducing the infiltration of oxygen into the pavement (*2*). They are considered a viable pavement preservation treatment for rejuvenating and sealing pavement surfaces and can typically be applied every three to four years to prolong pavement life by reducing the stiffness and brittleness of the asphalt binder in the upper 3/8-inch of the surface layer (*1, 2*).

Spray-on rejuvenators should be applied using well calibrated distributors that spread as evenly as possible to achieve optimum coverage and penetration of surface cracks. The rate of application depends on surface texture, level of oxidative aging, degree of cracking, and the product being sprayed. Spray-on rejuvenators, especially when being used with other materials to seal the pavement surface, are not recommended for application to pavements with poor surface texture, large cracks, rutting, shoving, or other structural deficiencies (*1*).

12.2 Research Objective

As part of the 2018 Test Track research cycle, the Mississippi and Tennessee Departments of Transportation both sponsored spray-on rejuvenator experiments. The objective of the study presented herein was to evaluate over time the field performance of four spray-on rejuvenator products commercially available in the United States, including their short- and long-term effectiveness in renewing asphalt surfaces and their effects on surface friction after application.

The rejuvenating capability of each product was solely assessed considering rheological parameters and surface friction measurements obtained before and after the application of the spray-on rejuvenator products.

12.3 Spray-on Rejuvenator Products

For Section S3, two spray-on rejuvenator products were applied over the surface of a 1.5" mill/inlay asphalt pavement section constructed in 2012 after the section experienced around 20 million ESALs of traffic without presenting rutting and cracking distresses (Figure 1). The hot mix asphalt (HMA) of Section S3 was a dense-graded mix with sand and gravel containing 25% reclaimed asphalt pavement (RAP) and an asphalt content of 6.8%. The asphalt binder used in the design was a neat binder with performance grade (PG) 67-22.

Figure 35. S3-A and S3-B Application of Spray-on Rejuvenators

For Section S4, two spray-on rejuvenator products were applied over the surface of a 1.5" mill/inlay asphalt pavement section constructed in 2015 after the section experienced around 10 million ESALs of traffic without presenting rutting and cracking distresses (Figure 2). The HMA was a dense-graded mix with sand and limestone containing 15% fine RAP (F-RAP) and with an asphalt content of 6.2%. The asphalt binder used in the design was a neat binder with PG 67-22.

Figure 36. S4-A and S4-B Application of Spray-on Rejuvenators

The four spray-on rejuvenator products utilized in this study are listed in Table 1. The application rate, water dilution rate, and residual application rate of the applied products were decided by the manufacturer of each product, and this information is listed in the table. The Mississippi DOT, which sponsored the experiment on Section S3, opted for not disclosing the commercial name of the applied products. Thus, the two spray-on rejuvenators of Section S3 will be described in this report as S3-A and S3-B. The Tennessee DOT, which sponsored the experiment on Section S4, opted for disclosing the commercial name of the applied products. The products were CMS-1PF (e-Fog) and Reclamite, and are listed in this report as S4-A and S4-B, respectively.

Table 28. Spray-on Rejuvenator Products and Application Parameters

Section S3	S3-A	Composition:	Not disclosed by the manufacturer
		Use by Manufacturer Recommendation:	Age-regenerating surface treatment
		Application Rate:	0.07 gal/yd^2
		Residual:	20% residual (product was originally 60% residual)
		Dilution Rate:	2:1
		Residual Application Rate:	0.014 gal/yd^2
	S3-B	Composition:	Plant-based rejuvenator
		Use by Manufacturer Recommendation:	Topical rejuvenating seal
		Application Rate:	0.10 gal/yd2
		Residual:	20%
		Dilution Rate:	Undiluted
		Residual Application Rate:	0.020 gal/yd^2
Section S4	CMS-1PF (eFog) (S4-A)	Producer:	Ergon Asphalt & Emulsions, Inc.
		Composition:	Hybrid emulsion, containing polymer-modified asphalt base and rejuvenator
		Use by Manufacturer Recommendation:	Rejuvenating fog seal that can be used to prevent pavement distress and restore essential elements in the existing asphalt (*3*)
		Application Rate:	0.08 gal/yd^2
		Residual:	30%
		Dilution Rate:	Undiluted
		Residual Application Rate:	0.024 gal/yd^2
	Reclamite® (S4-B)	Producer:	Pavement Technology, Inc.
		Composition:	Maltene-based from napthenic crude base
		Use by Manufacturer Recommendation:	Asphalt pavement rejuvenator (*4*)
		Application Rate:	0.08 gal/yd^2
		Residual:	50%
		Dilution Rate:	1:1
		Residual Application Rate:	0.040 gal/yd^2

The layout considering the untreated control and treated areas of Sections S3 and S4 is depicted in Figure 3(a) and 3(b), respectively. For the laboratory rheological evaluation of asphalt binders extracted and recovered from the treated sections, field cores were obtained from either the very beginning or the very end of each subsection.

Figure 3. Test Track Layout of Sections S3 and S4

Figure 4 shows the pavement surfaces of Section S3, including control and treated sections after 1 month and 24 months of application of the spray-on rejuvenator products. For section S3-A, the cores were collected from the diamond ground portion of the section that existed prior to this study. Figure 5 shows the pavement surfaces of Section S4, including control and treated sections after 1 month and 24 months of application of the spray-on rejuvenator products.

Figure 4. Section S3 Pavement Surfaces Before and After 1 Month and 24 Months of Treatment Application

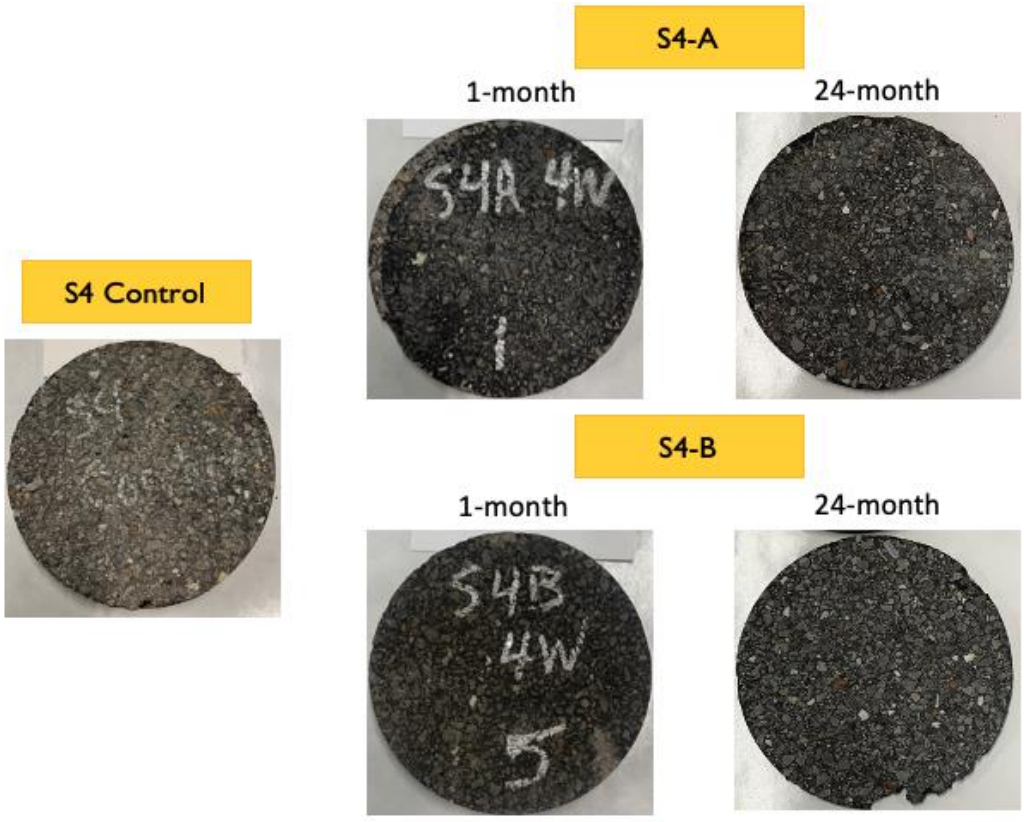

Figure 5. Section S4 Pavement Surfaces Before and After 1 Month and 24 Months of Treatment Application

12.4 Test Methods

A schematic of the testing matrix utilized in this study for the untreated controls and treated sections is shown in Figures 5 and 6, respectively. Descriptions of the test methods considering rheological parameters and surface friction measurements are included below. A modification of the Federal Aviation Administration's (FAA) P-632 (Bituminous Pavement Rejuvenation) specification was used in this experiment. This specification evaluates the rejuvenation capability of spray-on rejuvenator products by rheological parameters [e.g., complex modulus (|G*|) and phase angle (δ) at 60°C] of binders extracted and recovered from the upper 3/8-inch (9 mm) of treated pavement surfaces after one month of product application. Pavement friction characteristics tested between 24 and 96 hours after application of spray-on rejuvenator products and tested at no less than 180 days or greater than 360 days after the application are also included in the FAA P-632 specification.

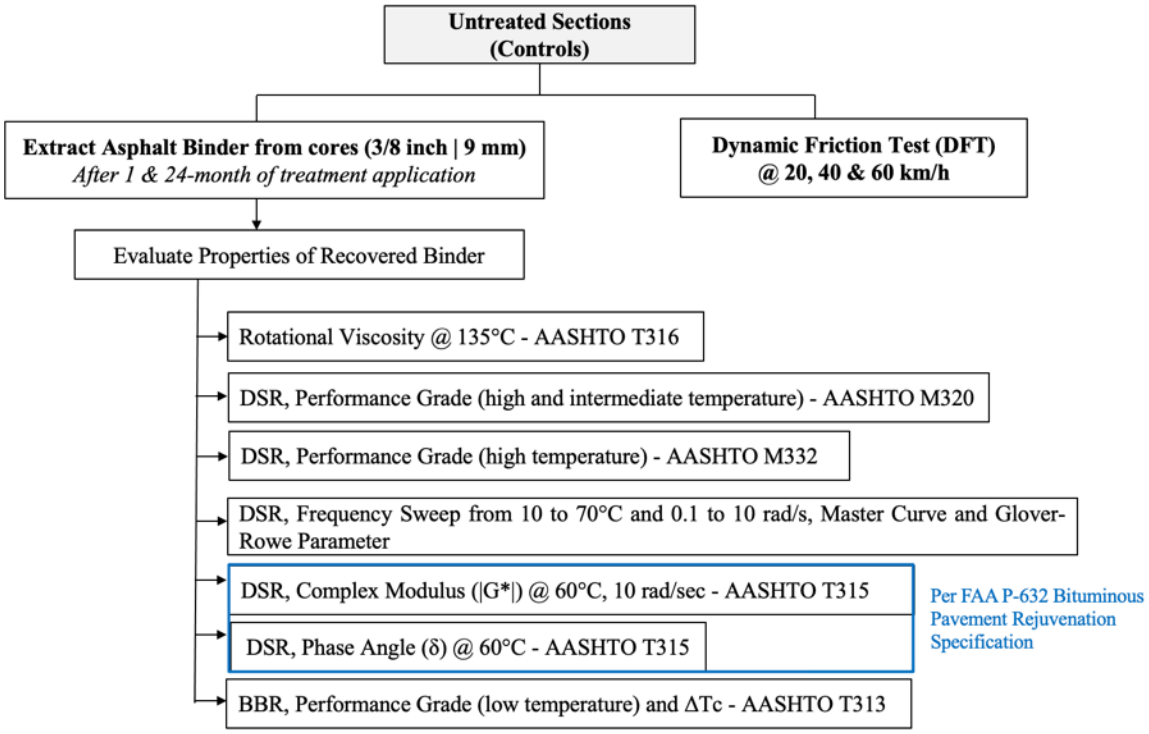

Figure 37. Testing Matrix Performed on Untreated Control Sections

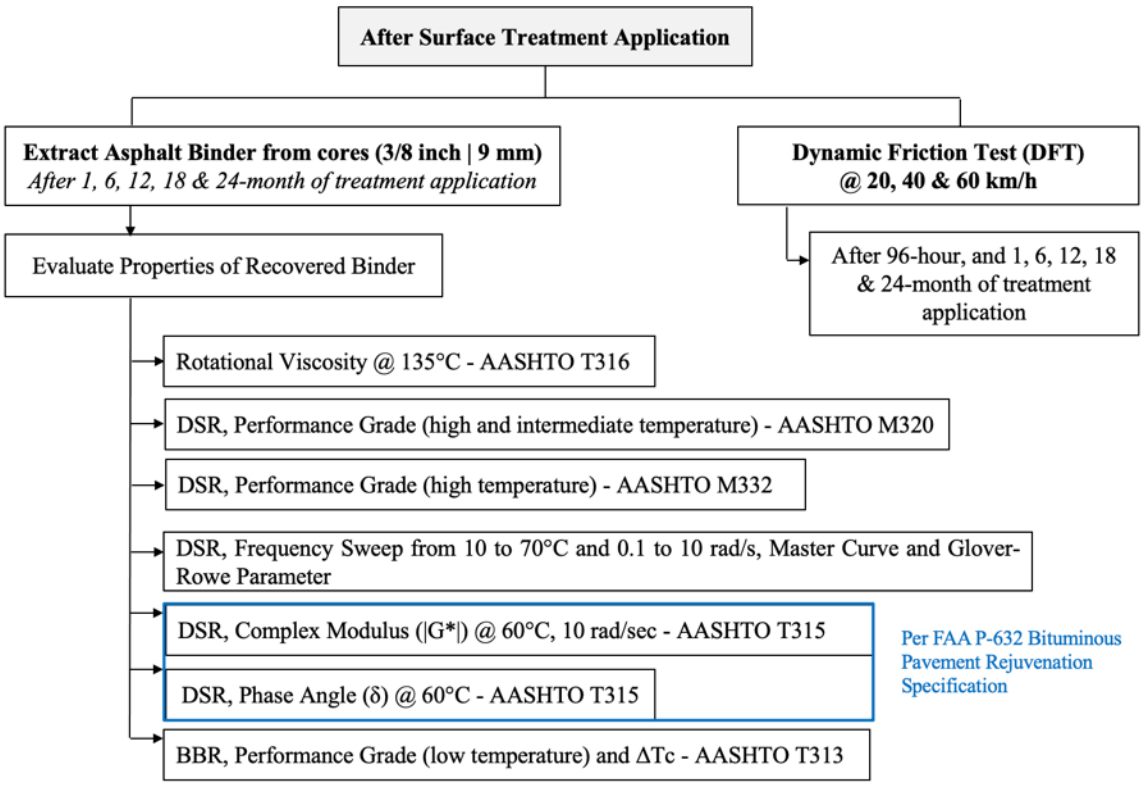

Figure 38. Testing Matrix Performed on Treated Sections

12.4.1 Asphalt Binder Extraction and Recovery

The asphalt binders were extracted per ASTM D2172 (method A) using trichloroethylene and recovered per ASTM D5404 from samples of the upper 3/8-inch (9 mm) of the collected pavement cores. For each treated pavement section, the asphalt binders were extracted and recovered from field cores at several time intervals after application of the spray-on rejuvenator products (i.e., 1 month, 6 months, 12 months, 18 months, and 24 months). For the untreated control sections, due to the short length of the section (Figure 3), the asphalt binders were extracted and recovered from field cores after 1 month and 24 months of the application of the spray-on rejuvenator products on the treated sections.

12.4.2 Rotational Viscosity

In accordance with the FAA P-632 specification, the absolute viscosity (ASTM D2171) at 60°C of asphalt binders extracted and recovered from treated pavement surfaces after one month of product application is a requirement for acceptance of a spray-on rejuvenator product. Due to the oxidized/hard nature of the binders evaluated in this study, the absolute viscosity at 60°C was not possible to be measured. Thus, to obtain information about the flow properties of the binders, the Brookfield rotational viscosity was performed in accordance with AASHTO T316. The rotational viscosity test measures the torque required to maintain a constant rotational speed (20 RPM) of a cylindrical spindle while submerged in the asphalt binder at a constant temperature of 135°C. This torque is then converted to a dynamic viscosity value that is used to ensure that the asphalt binder is sufficiently fluid for pumping and mixing.

12.4.3 Dynamic Shear Rheometer Tests

The dynamic shear rheometer (DSR) was used to characterize the viscous and elastic behavior of asphalt binders per AASTHO T315/ASTM D7175. The DSR measures the viscous and elastic properties of a thin asphalt binder sample sandwiched between an oscillating and a fixed plate. As the force (or shear stress, τ) is applied to the asphalt by the oscillating plate, the DSR measures the response (or shear strain, γ) of the asphalt to the force. The relationship between the applied stress and the resulting strain in the DSR provides the information necessary to calculate two important asphalt binder properties: the complex shear modulus ($|G^*|$) and the phase angle (δ). $|G^*|$ is the ratio of maximum shear stress (τ_{max}) to maximum shear strain (γ_{max}). The lag between the applied stress and the resulting strain is the phase angle (δ). For a perfectly elastic material, the phase angle is zero, and all of the deformation is temporary. For a viscous material, the phase angle approaches 90 degrees, and all of the deformation is permanent. Due to its viscoelasticity, the total response of asphalt binders to load consists of two components: elastic (recoverable) and viscous (non-recoverable).

In accordance with AASHTO M320, the Superpave specification defines and places requirements on a rutting parameter ($|G^*|/\sin(\delta)$) that represent the high temperature viscous component of the overall binder stiffness. $|G^*|/\sin(\delta)$ must be at least 1.00 kPa for the original asphalt binder and a minimum of 2.20 kPa after aging in the rolling thin film oven (RTFO). Binders with values below these may be too soft to resist permanent deformation. The continuous high temperature true grade is then selected as the lowest temperature value when comparing both the unaged and RTFO aged binder. The $|G^*|$ and δ measured with a DSR are also used to evaluate fatigue in asphalt binders at intermediate temperatures, evaluating the asphalt binder after it has been subjected to both RTFO (short-term) and PAV (long-term) aging.

The Superpave specification defines and places requirements on a fatigue parameter (|G*|×sin(δ)) that represents the intermediate temperature binder stiffness. |G*|×sin(δ) must be below a maximum of 5000 kPa; binders with values above this may be too hard to resist fatigue cracking.

Furthermore, in accordance with AASHTO M332, the multiple-stress creep-recovery (MSCR) test was performed on RTFO aged binders at 64°C based on the Alabama climate. The test was conducted by applying two stress levels of 0.1 kPa (for twenty cycles) and 3.2 kPa (for ten cycles). Each cycle consisted of one second of shear creep followed by a recovery period of nine seconds. The MSCR test generates two key parameters that are used to determine the binder grade as per AASHTO M332: non-recoverable creep compliance (J_{nr}) and percent recovery (%R). A binder with high value of recovery may produce less permanent deformation in a pavement. On the other hand, a high J_{nr} value indicates that a binder is more rutting susceptible. The MSCR grading generally categorizes asphalt binders into four grades based on creep compliance (J_{nr}) as measured at 3.2kPa. Also, it is generally required that the J_{nr} difference be less than 75%. This requirement was imposed to rule out additives that reduce creep compliance at low stress levels but fail to work at higher stresses, ultimately leading to pavement damage. The limits for MSCR grades are as follows:

- Standard (S): J_{nr} at 3.2kPa $\leq$ 4.5 kPa^{-1}
- Heavy (H): J_{nr} at 3.2kPa $\leq$ 2.0 kPa^{-1}
- Very Heavy (V): J_{nr} at 3.2kPa $\leq$ 1.0 kPa^{-1}
- Extreme (E): J_{nr} at 3.2kPa $\leq$ 0.5 kPa^{-1}

To investigate the cracking potential of the binders at intermediate temperatures, a 1% strain amplitude was applied using a frequency sweep over the range of 0.1 to 10 rad/s and seven testing temperatures (i.e., 10, 20, 30, 40, 50, 60, and 70°C) in the DSR. The data was used to produce a master curve using the principle of time-temperature superposition and a fit to the Christensen-Anderson (CA) model at a reference temperature of 15°C. The master curves were then utilized to calculate the Glover-Rowe (*G-R*) parameter. The *G-R* parameter (Equation 1) considers both binder stiffness and embrittlement and offers an indication of the cracking potential at intermediate temperature, where the two proposed *G-R* parameter criteria for the onset of block cracking and visible surface cracking are 180 kPa and 600 kPa, respectively (*5*). Regarding the values of the *G-R* parameter, it has been shown that asphalt binders with higher values of *G-R* experience a higher level of oxidative aging than those with lower *G-R* parameter values (*6-8*).

$$G - R = \frac{|G^*|(cos\ \delta)^2}{sin\ \delta}_{(T=15°C,\ \ f=0.005\ rad/s)} \quad (1)$$

Lastly, using the DSR and parallel plate geometry at 60°C and a frequency of 10 rad/s per AASTHO T315/ASTM D7175, the complex shear modulus (|G*|) and phase angle (δ) of the asphalt binders were determined before and after application of the spray-on rejuvenator products. The |G*| is an indicator of the stiffness or resistance of the asphalt binder to deformation under load. The phase angle (δ) is an indicator of the viscous and elastic behavior

of the asphalt binder. At intermediate temperatures, such as 20°C, asphalt binders are said to be viscoelastic (phase angle near 45 degrees).

12.4.4 Bending Beam Rheometer

The bending beam rheometer (BBR) was used to measure rheological characteristics of the binder at low temperatures per AASHTO T313. The test uses engineering beam theory to measure the stiffness of a small asphalt beam under an applied creep load. The creep load is used to simulate the stresses that gradually build up in a pavement when temperature drops. Two parameters are evaluated with the BBR: creep stiffness (S), which is related to stresses in an asphalt pavement due to thermal contraction; and m-value, which is related to the ability of an asphalt pavement to relieve these stresses. The Superpave binder specifications require, at a loading time of 60 seconds, a maximum limit on creep stiffness ($S(60) \leq 300$ MPa) and a minimum limit on m-value ($m(60) \geq 0.3$), where the binder must have some minimum ability to relieve thermal stresses without cracking. Since low-temperature thermal cracking occurs during the service life of the pavement, the specification addresses this distress by evaluating the asphalt binder performance after it has been subjected to both RTFO (short-term) and PAV (long-term) aging. The measurements of creep stiffness and the m-value of binder beams are collected after one-hour isothermal conditioning.

12.4.5 ΔTc

The ΔT_c parameter ($\Delta Tc = Tc,S - Tc,m$) is the difference between the continuous low temperature binder grade measured via BBR creep stiffness (related to thermal stresses in an asphalt pavement due to shrinking) and m-value (related to the ability of an asphalt pavement to relieve these stresses), and targets cracking behavior that is affected by asphalt binder durability related to aging of the binder in an asphalt mixture. It has been suggested that asphalt binders with low (i.e., more negative) ΔT_c have less ductility and reduced relaxation properties than asphalt binders with higher (less negative or positive) ΔT_c (*9*). Initially, the ΔT_c parameter was thought to be principally related to block cracking. However, studies have indicated that fatigue, edge, longitudinal, reflection, and transverse cracking may indirectly be related to the ΔT_c of asphalt binders; where ΔT_c can play a supporting role in the development of these distresses (*10*). A minimum ΔT_c threshold of -5°C after RTFO plus 40 hours of PAV aging has been suggested to minimize the risk of cracking (*10*). Among the ten department of transportation agencies currently adopting the ΔT_c as an asphalt binder specification parameter, five utilize -5°C after RTFO plus 40 hours of PAV aging as the limiting threshold (*10*). Validating the ΔT_c parameter, a field study in Wisconsin has showed that binders with a highly negative ΔT_c had high rates of cracking (*11*).

12.4.6 Dynamic Friction Test

Using the Dynamic Friction Test (DFT), pavement surface frictional properties as a function of speed were measured before and after application of the spray-on rejuvenator products. For the untreated control sections (i.e., S3 and S4 control), the friction measurements were collected over the same period prior to the application of the treatments. For each treated pavement section, the friction measurements were collected from the wheel path of each section at several time intervals after application of the spray-on rejuvenator products (i.e., 96

hours, 1 month, 6 months, 12 months, 18 months, and 24 months). The DFT consists of a horizontal spinning disk fixed with three spring-loaded rubber sliders that contact the pavement surface (Figure 8). A water spray system was used to simulate wet conditions. When the disk was lowered onto the test surface, the DFT measured the torque generated by the sliders' resistive force to calculate the friction coefficient of the asphalt pavement surface. Velocity is also measured to indicate the relationship between coefficient of friction and speed. The DFT is capable of providing a maximum tangential velocity of 90 km/h (55 mph) (*12*). The equipment is interfaced by an external laptop controller, which allows the collected data to be stored for later analysis. In this study, the speeds of 20, 40, and 60 km/h were selected for measurement of the friction properties of the pavement surfaces. Each DFT test included three replicate measurements. The detailed test procedure is described in ASTM E1911.

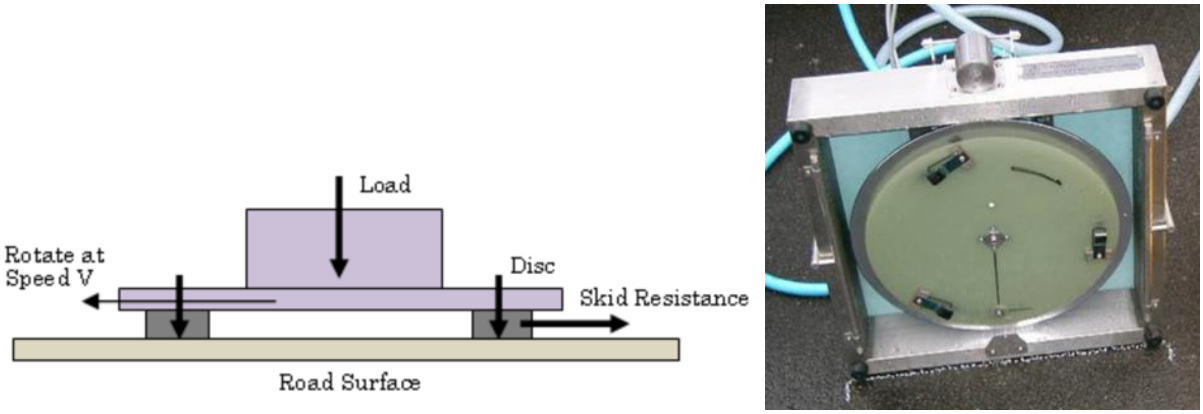

Figure 39. Dynamic Friction Tester (DFT)

12.5 Results

12.5.1 Rotational Viscosity

Viscosity denotes the fluid property of a material and is a measure of its resistance to flow. Figure 9 presents the obtained viscosity results before and at several time intervals after application of the four spray-on rejuvenator products (i.e., 6-month, 12-month, 18-month, and 24-month). The asphalt binders extracted and recovered from the field cores were tested without additional aging using the RTFO and PAV. As expected, field aging increased the viscosity values of the evaluated asphalt binders (i.e., controls and treated binders).

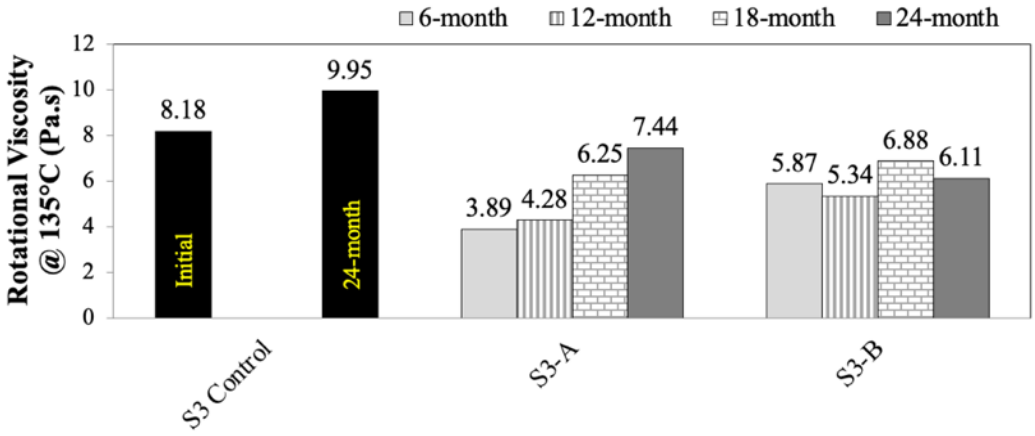

(a) Section S3 Treated with Products S3-A and S3-B

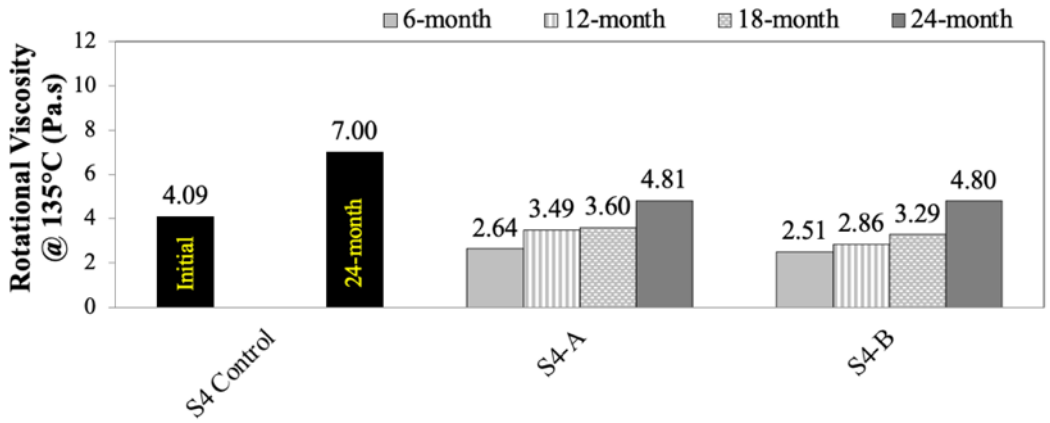

(b) Section S4 Treated with Products S4-A and S4-B

Figure 9. Rotational Viscosity Results at 135°C

As indicated in Figure 9, as the field aging interval increased (i.e., from 6 months towards 24 months of field aging), the viscosity of the controls and treated sections also increased. However, after 24 months of field aging, the treated sections still showed viscosity values smaller than the control at same field aging interval (i.e., 24-month). This decrease in viscosity was found as dependent of the spray-on chemical composition and influenced by the characteristics of the asphalt material present in the surface of each section as well as the date of construction (i.e., Section S3 was constructed in 2012 and Section S4 was constructed in 2015). The variableness among the 12-, 18- and 24-month viscosity readings for S3-B could be related to experimental error and the variability inherited by the extraction and recovery process of the asphalt binders obtained from field cores.

To address the longevity of the effectiveness of the spray-on rejuvenator products in decreasing the viscosity of the asphalt material present in the surface of each section, an aging index was determined per Equation 2 and the results are presented in Figure 10.

$$Rotational\ Viscosity\ Aging\ Index\ @\ 135°C = \frac{Treated\ Section\ (\eta)_{24-month}}{Control\ Section\ (\eta)_{24-month}} \quad (2)$$

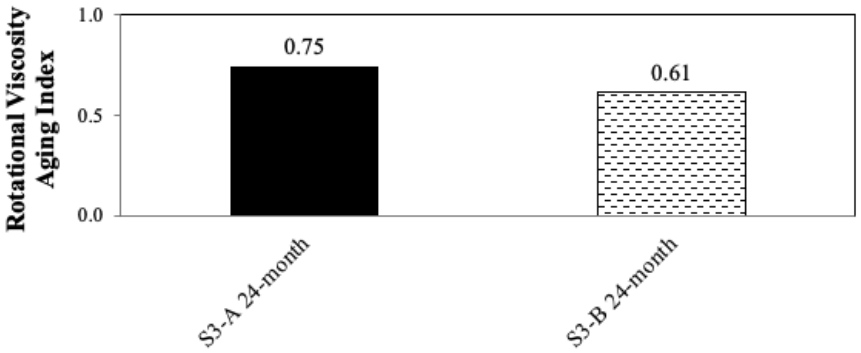

(a) Section S3 Treated with Products S3-A and S3-B

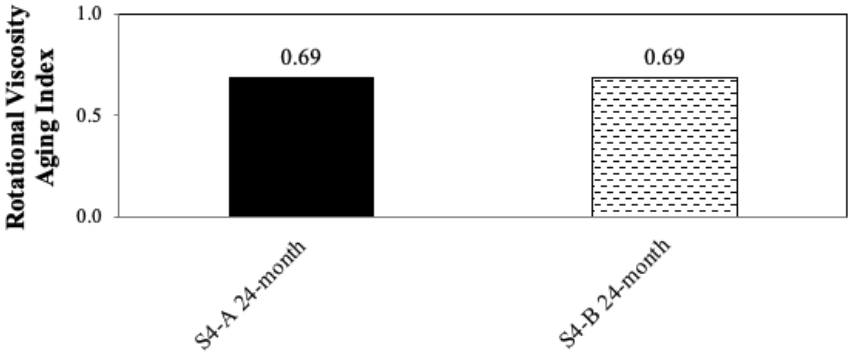

(b) Section S4 Treated with Products S4-A and S4-B

Figure 10. Rotational Viscosity Aging Index

As indicated in Figure 10(a), spray-on rejuvenator products S3-A and S3-B showed rotational viscosity aging index below 1.0 24 months after application, indicating that the viscosity of the binders extracted from the treated sections remained below the viscosity of the S3 control binder measured after 24 months of field aging. When comparing S3-A and S3-B, the product S3-B showed a smaller rotational viscosity aging index (i.e., 0.61) than product S3-A (i.e., 0.75), indicating higher longevity of the effectiveness in decreasing the viscosity of the asphalt material present in the surface of Section S3. As indicated in Figure 10(b), the two spray-on rejuvenator products S4-A and S4-B applied on Section S4 also showed aging index below 1.0 24 months after application, indicating that the viscosity of the binders extracted from the treated sections remained below the viscosity of the S4 control binder measured after 24 months of field aging. Moreover, S4-A and S4-B showed equal rotational viscosity aging index (i.e., 0.69), indicating equal longevity of the effectiveness in decreasing the viscosity of the asphalt material present in the surface of Section S4.

An interesting observation is related to the field exposure time interval where the lowest viscosity values were observed for all treated samples. This point was located at either 6 months (Spring 2019) or 12 months (Fall 2019) after treatment application. As indicated in Figure 11, disregarding experimental error and the variability inherited by the extraction and recovery process of the asphalt binders, the overall trend is that the maximum rejuvenating capability of the applied spray-on rejuvenator products was achieved between 6 and 12 months of treatment application.

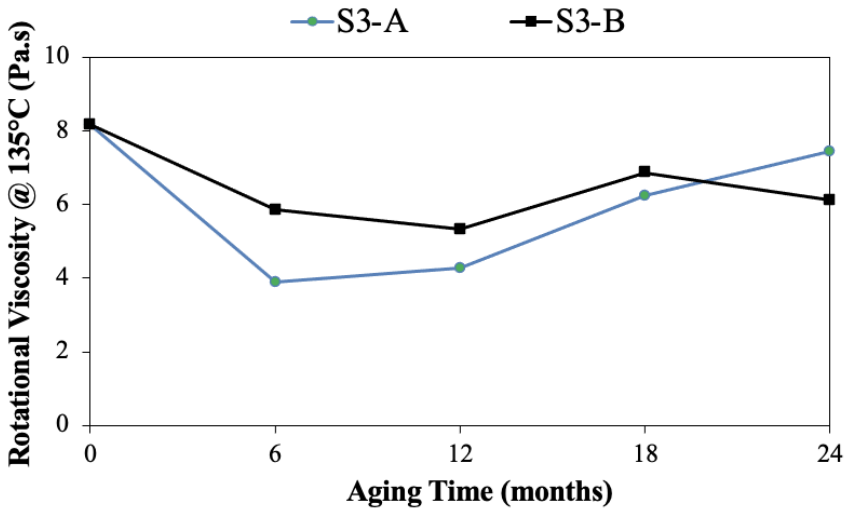

(a) Products S3-A and S3-B

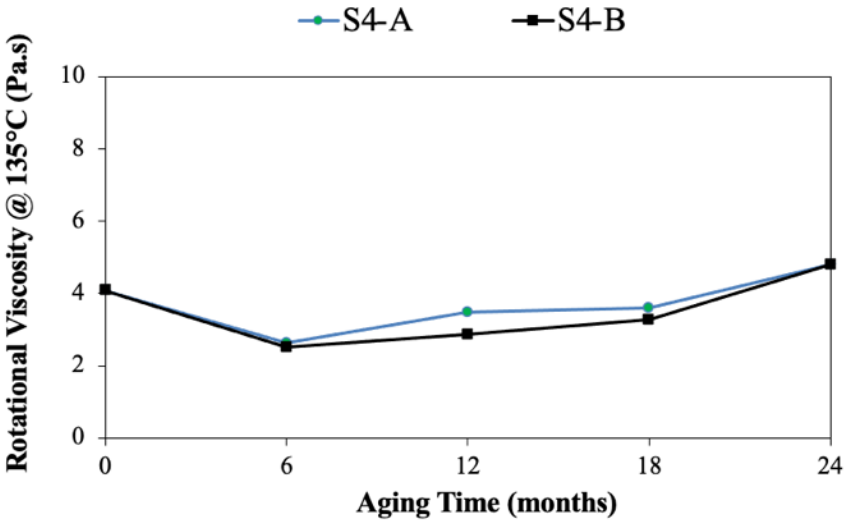

(b) Products S4-A and S4-B

Figure 11. Rotational Viscosity versus Aging Time

12.5.2 Superpave Performance Grade Classification

The final PG classifications of all asphalt binders evaluated in this study are presented in Table 2. In summary, the application of the spray-on rejuvenator products initially decreased the high temperature PG of the asphalt material present in the surface of the sections, but this decrease was dismissed after long-term field exposure. Moreover, the application of treatments positively resulted in a decrease in the temperature at which the limiting fatigue parameter [|G*|.sin(δ)] was satisfied by the control binders after one month of field exposure, based on AASHTO M320. The exception occurred for product S3-B after 12 months of field aging and product S4-A after 24 months of field aging; however, both pass/fail intermediate temperatures remained lower than the control S3 and S4 after 24 months of field aging. An improvement in thermal cracking resistance was observed for the treated sections in comparison to the control

sections, with the exception of product S4-A, which after 24 months provided equal low-temperature PG to the S4 control after 24 months of field aging.

Table 2. Performance Grade Classification of Asphalt Binders

Sample	Field Aging Interval	T_{cont}, High, Unaged °C	T_{cont}, High, RTFO °C	T_{cont}, Intermediate, °C	T_{cont}, Low S, °C	T_{cont}, Low m-value, °C	ΔT_c (°C)	PG HT	PG LT
S3 Control	1-month	107.0	103.9	39.3	-19.4	-4.0	-15.4	100	-4
	24-month	110.0	104.4	41.4	-17.9	-2.9	-15.0	100	2
S4 Control	1-month	100.4	97.0	35.9	-17.5	-7.4	-10.1	94	-4
	24-month	105.1	101.7	39.5	-12.8	-3.2	-9.6	100	2
S3-A	1-month	97.0	94.1	34.0	-19.8	-11.6	-8.2	94	-10
	6-month	98.4	97.8	35.5	-17.5	-9.8	-7.7	94	-4
	12-month	100.5	100.8	35.8	-18.9	-6.4	-12.5	100	-4
	18-month	104.9	101.4	37.5	-15.1	-8.4	-6.7	100	-4
	24-month	105.8	101.9	38.0	-18.7	-7.0	-11.7	100	-4
S3-B	1-month	98.5	97.8	33.3	-18.9	-9.2	-9.7	94	-4
	6-month	103.8	101.6	37.0	-12.4	-6.6	-5.8	100	-4
	12-month	103.1	102.9	39.4	-16.8	-5.9	-10.9	100	-4
	18-month	107.3	102.7	39.1	-19.6	-5.9	-13.7	100	-4
	24-month	102.8	101.4	38.0	-19.1	-5.0	-14.1	100	-4
S4-A	1-month	94.4	93.0	31.2	-29.6	-11.0	-18.6	88	-10
	6-month	94.4	92.2	31.3	-23.1	-11.6	-11.5	88	-10
	12-month	98.5	99.9	35.2	-21.1	-4.6	-16.5	94	-4
	18-month	99.1	101.6	34.3	-23.0	-7.3	-15.7	94	-4
	24-month	103.0	101.4	36.1	-17.3	-3.6	-13.7	100	2
S4-B	1-month	93.3	93.3	33.3	-20.2	-12.1	-8.1	88	-10
	6-month	93.8	94.8	35.1	-22.9	-11.2	-11.7	88	-10
	12-month	97.9	97.5	32.4	-19.9	-5.5	-14.4	94	-4
	18-month	101.8	100.9	34.0	-21.6	-9.1	-12.5	100	-4
	24-month	99.9	102.0	35.4	-19.7	-4.9	-14.8	94	-4

Figure 12 presents the observed change in the continuous high temperature true grade 1 month and 24 months after application of the spray-on rejuvenator products. The change was calculated in comparison to the control binders after 1 month and 24 months of field aging. As indicated in Figure 12(a), the application of product S3-A resulted in a decrease of the high temperature true grade by 9.8 and 2.5°C 1 month and 24 months after application, respectively. Product S3-B resulted in a decrease of the high temperature true grade by 6.1 and 3.0°C 1 month and 24 months after of application, respectively. For Section S4, as indicated in Figure 12(b), for product S4-A the decrease in the high pass/fail temperature was by 4.0 and 0.4°C 1 month and 24 months after application, respectively. While for product S4-B the decrease in the high pass/fail temperature was by 3.7 and 1.8°C 1 month and 24 months after application, respectively.

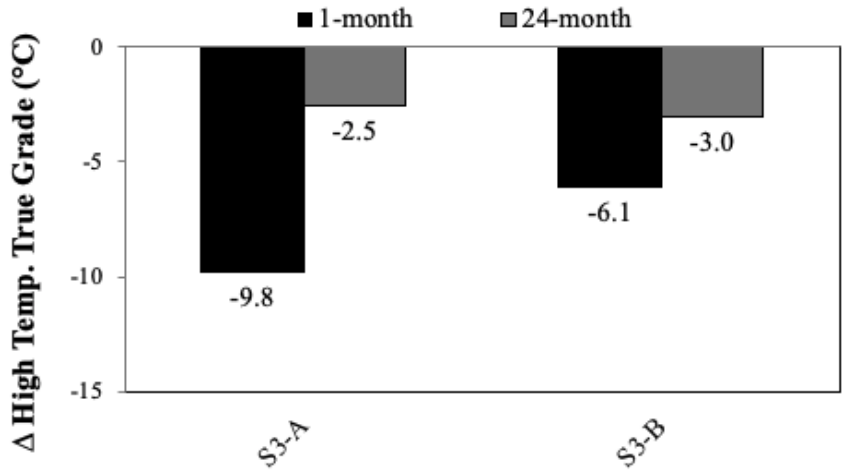

(a) Section S3 Treated with Products S3-A and S3-B After 1 Month and 24 Months

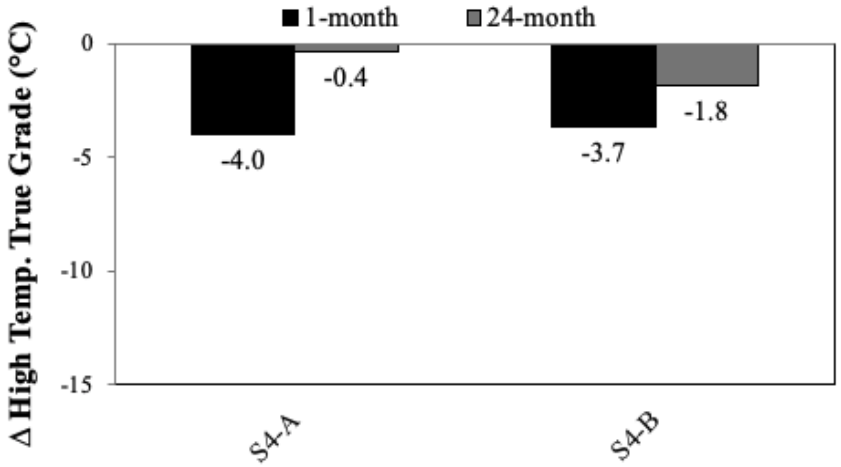

(b) Section S4 Treated with Products S4-A and S4-B After 1 Month and 24 Months

Figure 12. Change in High Temperature True Grade After Treatment Application

Figure 13 presents the observed change in the continuous intermediate temperature true grade 1 month and 24 months after application of the spray-on rejuvenator products. As aforementioned, the change was calculated in comparison to the control binders after 1 month and 24 months of field aging. As indicated in Figure 13(a), 1 month after treatment application, products S3-A and S3-B decreased the intermediate temperature true grade by 5.3 and 6.0°C, respectively, increasing the fatigue resistance of the S3 control binder. 24 months after treatment application, both products behaved in an equal manner and decreased the intermediate temperature true grade by 3.4°C. For Section S4, as indicated in Figure 13(b), for product S4-A the decrease in the intermediate pass/fail temperature was by 4.7 and 3.4°C 1 month and 24 months after application, respectively. Product S4-B decreased the temperature at which the limiting fatigue parameter [|G*|.sin(δ)] was satisfied by 2.6 and 4.1°C 1 month and 24 months after application, respectively, based on AASHTO M320.

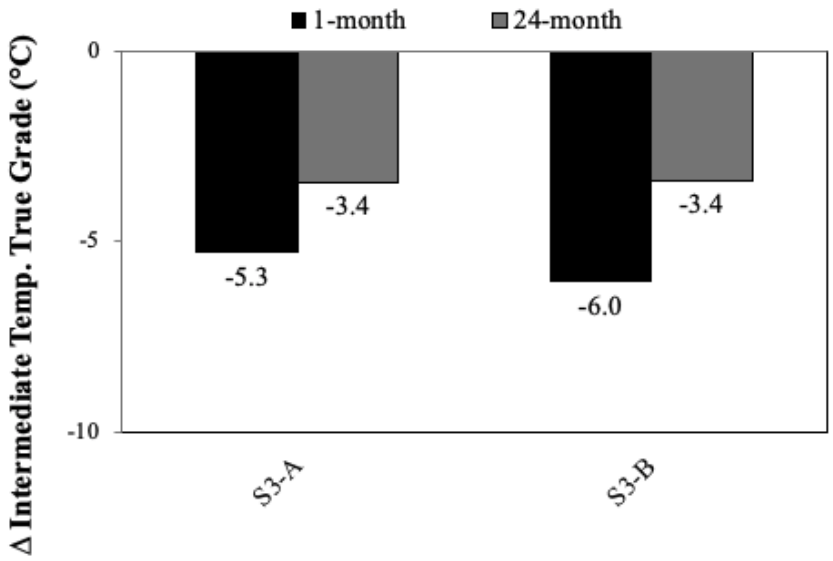

(a) Section S3 Treated with Products S3-A and S3-B After 1 Month and 24 Months

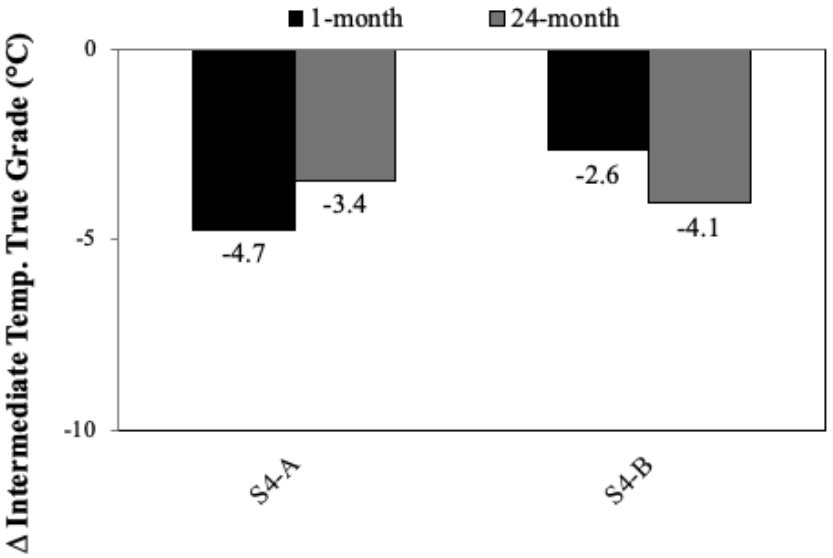

(b) Section S4 Treated with Products S4-A and S4-B After 1 Month and 24 Months

Figure 13. Change in Intermediate Temperature True Grade After Treatment Application

Figure 14 presents the observed change in the continuous low temperature true grade 1 month and 24 months after application of the spray-on rejuvenator products. The change was calculated in comparison to the control binders after 1 month and 24 months of field aging. As expected, the treatments had a positive effect on the low temperature performance of the control binders. As indicated in Figure 14(a), a decrease of the low temperature true grade by 7.6 and 4.1°C was observed 1 month and 24 months after application of product S3-A, respectively. For product S3-B, the decrease of the low temperature true grade 1 month and 24 months after application was by 5.2 and 2.1°C, respectively. As indicated in Figure 14(b), when product S4-A was applied on Section S4, the decrease in the low pass/fail temperature was by 3.6 and 0.4°C 1 month and 24 months after application, respectively; product S4-B decreased

the low temperature true grade by 4.7 and 1.7°C 1 month and 24 months after application, respectively.

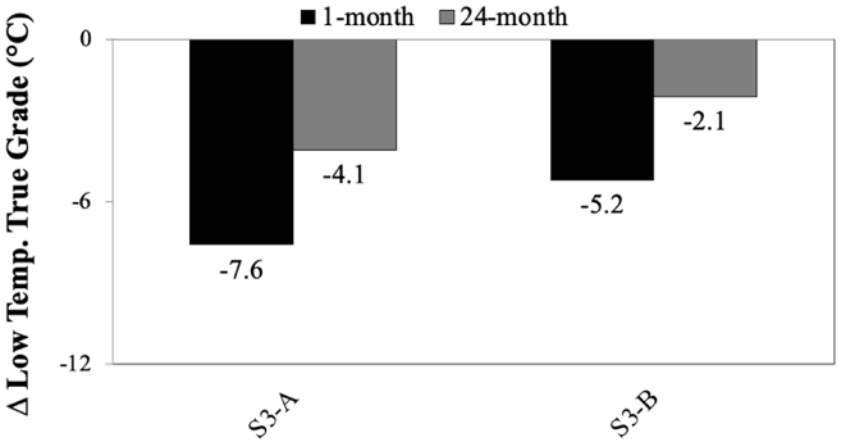

(a) Section S3 Treated with Products S3-A and S3-B After 1 Month and 24 Months

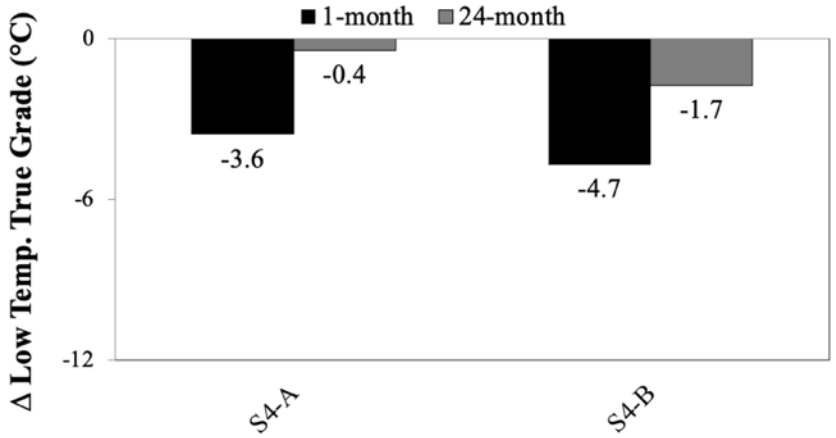

(b) Section S4 Treated with Products S4-A and S4-B After 1 Month and 24 Months

Figure 14. Change in Low Temperature True Grade After Treatment Application

It has been suggested that asphalt binders with low (i.e., more negative) ΔT_c have less ductility and reduced relaxation properties than asphalt binders with higher (less negative or positive) ΔT_c. As indicated in Table 2, the untreated control binders and the treated binders presented ΔT_c values below the threshold of -5°C, regardless of the field aging interval.

Lastly, the effect of the spray-on rejuvenator products was evaluated in terms of changes in the ΔT_c parameter in comparison to the control binders 1 month and 24 months after treatment application. Figure 15(a) indicates that the application of the spray-on rejuvenator product S3-A on Section S3 was beneficial, resulting in a less negative ΔT_c 1 month and 24 months after treatment application with an increase in ΔT_c by 7.2 and 3.3°C, respectively. Product S3-B also increased the ΔT_c parameter by 5.7 and 0.9°C 1 month and 24 months after treatment application, respectively. ΔT_c is intended to provide an indication of loss of ductility, indicating when the asphalt binder cannot relax the stresses fast enough to prevent breaking. Figure 15(b) indicates that the spray-on rejuvenator product S4-A did not improve the ΔTc parameter of the asphalt material present in the surface of Section S4. The application of product S4-A resulted

in a more negative ΔT_c 1 month and 24 months after treatment application with a decrease in ΔT_c by 8.5 and 4.1°C, respectively. On the other hand, the spray-on rejuvenator product S4-B improved the ΔT_c of the control S4 binder after 1 month with an increase of 2.0°C. However, after 24 months of treatment application, this improvement was lost as a decrease in ΔT_c by 5.2°C was observed.

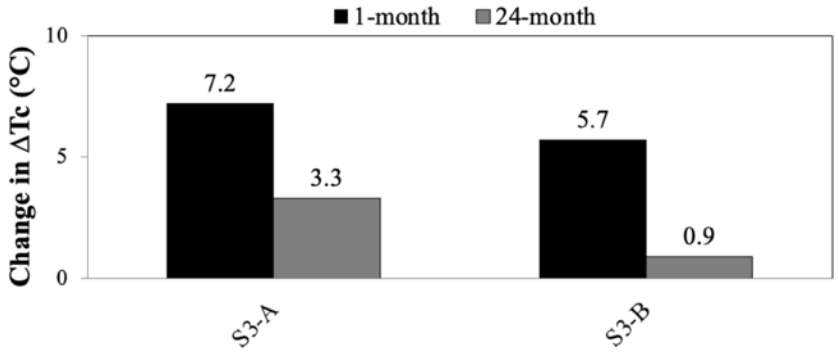

(a) Section S3 Treated with Products S3-A and S3-B After 1 Month and 24 Months

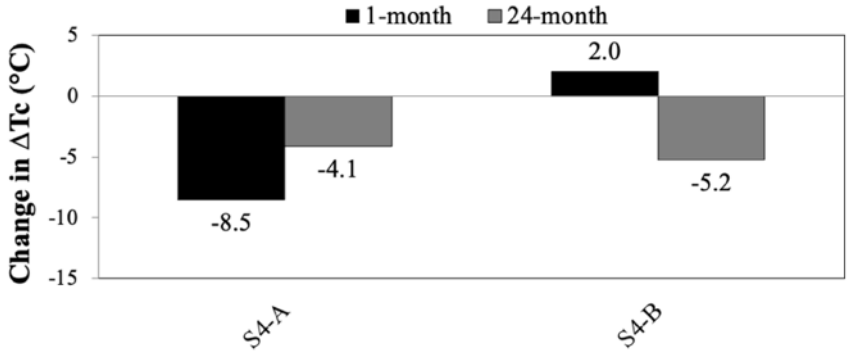

(b) Section S4 Treated with Products S4-A and S4-B After 1 Month and 24 Months

Figure 15. Change in the ΔT_c Parameter After Treatment Application

Results from this study have also indicated that classifying asphalt binders as more or less prone to cracking in terms of the ΔT_c parameter and its threshold can sometimes be misleading, especially when dealing with non-conventional (such as severely aged or polymer modified) asphalt binders since certain features of these binders may have a worsening effect on ΔT_c and therefore make it appear as if they exhibit diminished durability. One example of misleading information obtained from the ΔT_c can be seen when observing the results of the S4 control after 1 month and 24 months of field aging, with ΔT_c values of -10.1 and -9.6°C, respectively. Even though these ΔT_c results are somewhat similar, the values of stiffness and m-value are different, and when analyzed alone for each binder, they indicate that the long-term aging indeed affected the low-temperature performance of the control binder: S=-17.5°C and m-value=-7.4°C after 1 month of field aging; and S=-12.8°C and m-value=-3.2°C after 24 months of field aging.

Figure 16 presents the BBR creep stiffness (related to stresses in an asphalt pavement due to thermal contraction) and m-value (related to the ability of an asphalt pavement to relieve these stresses) at the same testing temperature (i.e., 6°C) for the S3 control and treated binders after

24-month field aging. The ranking from lower to higher stiffness was: S3-B < S3-A ≈ S3 control. However, the ranking from lower to higher m-value was: S3 control < S3-B < S3-A. When considering resistance to thermal cracking, asphalt binders with lower stiffness and higher m-value usually present good overall performance. In accordance with the results presented in Figure 16, after 24 months of field aging, the S3 control binder showed the worst performance for both stiffness and m-value (87 MPa and 0.296, respectively). When comparing among the two spray-on rejuvenators applied in Section S3, product S3-B showed the best performance on decreasing stiffness (73 MPa), while product S3-A showed the best performance on increasing the m-value (0.321).

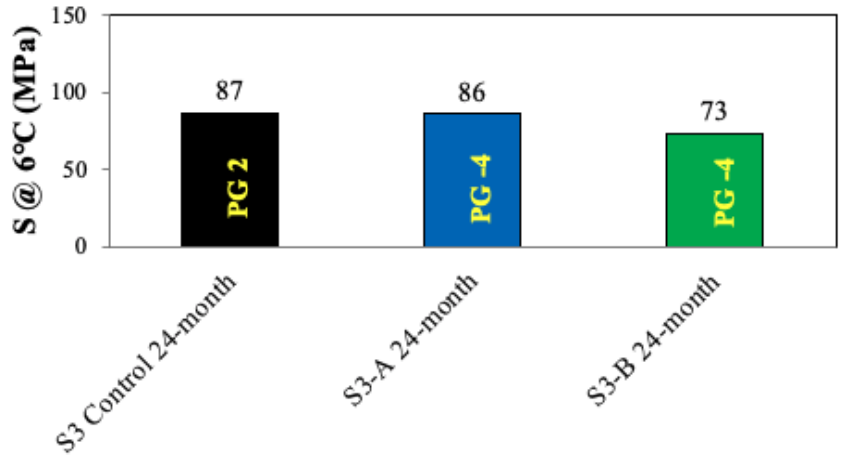

(a)

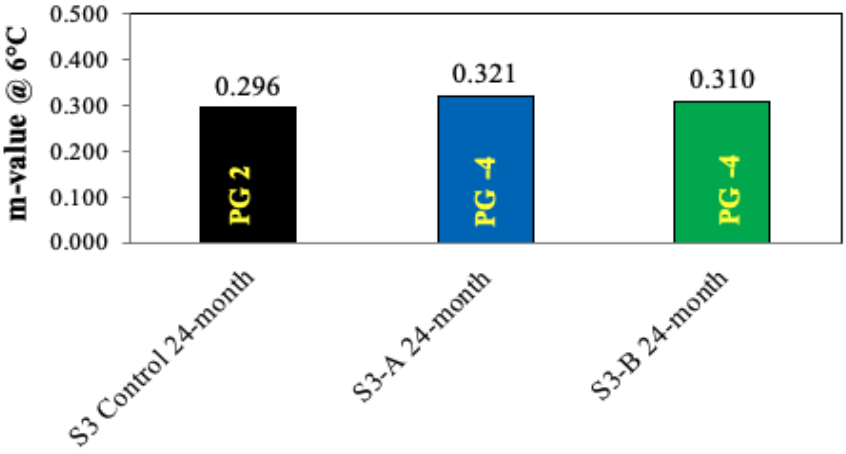

(b)

Figure 16. BBR Data at 6°C After 24 Months of Field Aging for S3 Control and After Treatment with Products S3-A and S3-B: (a) S, (b) m-value

Figure 17 shows the aforementioned analysis of BBR creep stiffness and m-value at 6°C for the S4 control and treated binders after 24-month field aging. The ranking from lower to higher stiffness was: S4-B < S4-A < S4 control. However, the ranking from lower to higher m-value was: S4 control < S4-A < S4-B. In accordance with the results presented in Figure 17, after 24 months of field aging, the S4 control binder showed the worst performance for stiffness and m-value

(96 MPa and 0.292, respectively). Moreover, the combination of lowest stiffness and highest m-value was obtained when Section S4 was treated with product S4-B.

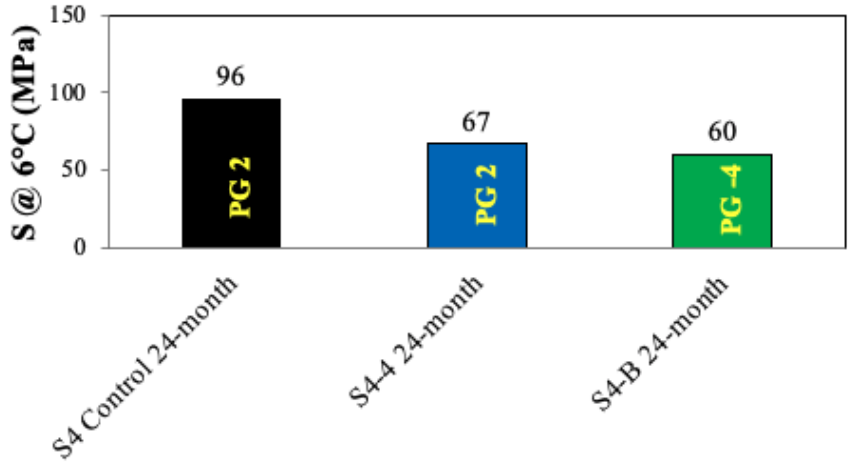

(a)

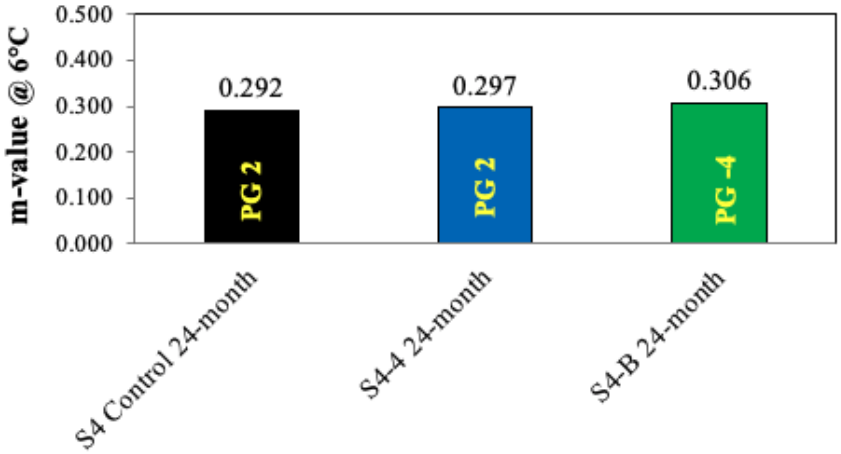

(b)

Figure 17. BBR Data at 6°C After 24 Months of Field Aging for S4 Control and After Treatment with Products S4-A and S4-B: (a) S, (b) m-value

12.5.3 Multiple Stress Creep and Recovery (MSCR) Test for High Temperature Performance

Figure 18 presents the MSCR testing parameter J_{nr} at 3.2 kPa for: control S3 and S4 binders after 1 month and 24 months of field aging [Figure 18(a)]; Section S3 treated with products S3-A and S3-B after 1 month, 6 months, 12 months, 18 months, and 24 months of field aging [Figure 18(b)]; and Section S3-4 treated with products S4-A and S4-B after 1 month, 6 months, 12 months, 18 months, and 24 months of field aging [Figure 18(c)]. Overall, despite experimental error and the variability inherited by the extraction and recovery process of the asphalt binders obtained from field cores, the creep compliance decreased as field aging exposure increased, and all asphalt binders were classified as Extreme (E). Figure 18(b) and (c) indicates that the four spray-on rejuvenator products seemed to have an effect on the overall magnitude of J_{nr},

increasing it; this increase was observed with up to 18 months of field aging, and after 24 months the J_{nr} values of controls and treated sections became similar.

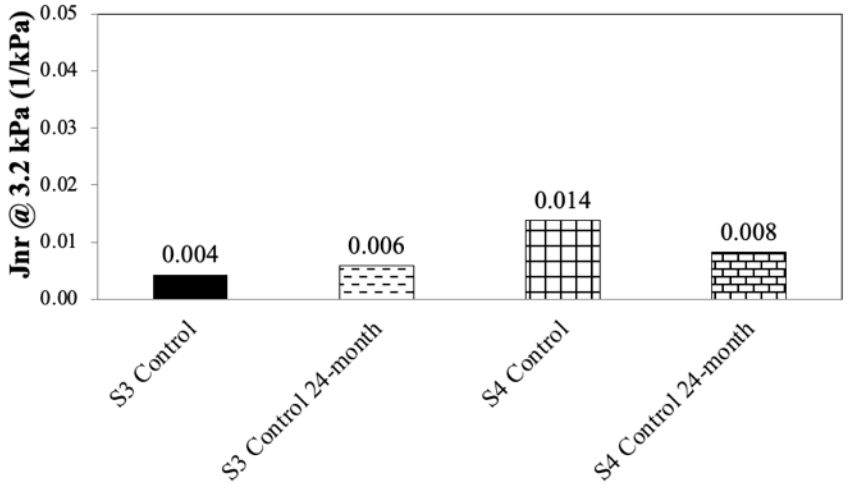

(a) S3 Control and S4 Control

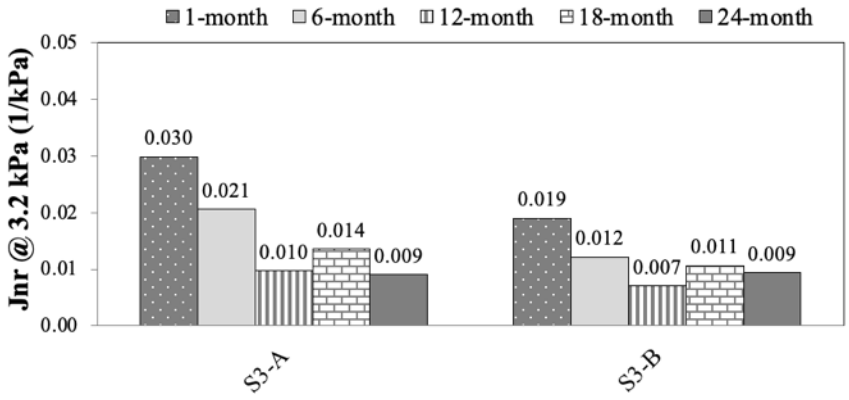

(b) S3 After Treatment with Products S3-A and S3-B

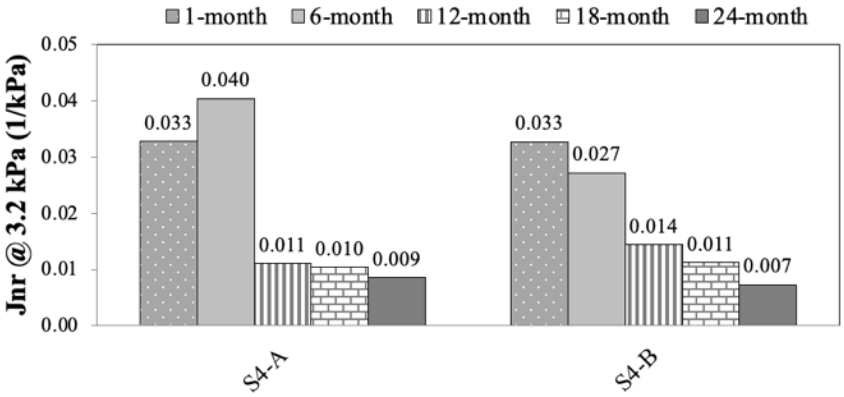

(c) S4 After Treatment with Products S4-A and S4-B

Figure 18. Effect of Field Aging on J_{nr} at 3.2 kPa and 64°C

Figure 19 shows that the behavior of the MSCR %Recovery parameter was found to be highly influenced by the creep compliance J_{nr} of the binders, regardless of the presence of polymer.

For example, overall, the %Recovery of the section treated with product S4-A was similar to the section treated with product S4-B, when it is known that product S4-A contained a polymer-modified asphalt base and product S4-B did not (each product information is listed in Table 1). Thus, the high %Recovery value of the binders was due to the extremely low J_{nr} of the materials. Furthermore, as a result of aging, it is known that a decrease in phase angle of asphaltic materials allows for a decrease in the ratio of energy stored to energy dissipated; hence, the binders become more elastic.

When evaluating among products, Figure 19(b) indicates that the spray-on rejuvenator products S3-A and S3-B decreased the %Recovery of the S3 control section up to 24 months after treatment application. As indicated in Figure 19(c), the spray-on rejuvenator products S4-A and S4-B decreased the %Recovery of the S4 control section only up to 6 months after treatment application.

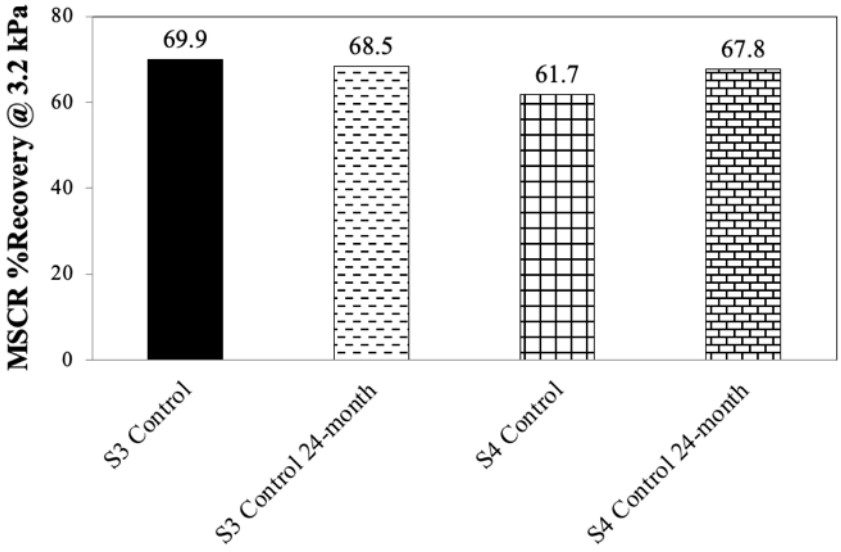

(a) S3 Control and S4 Control

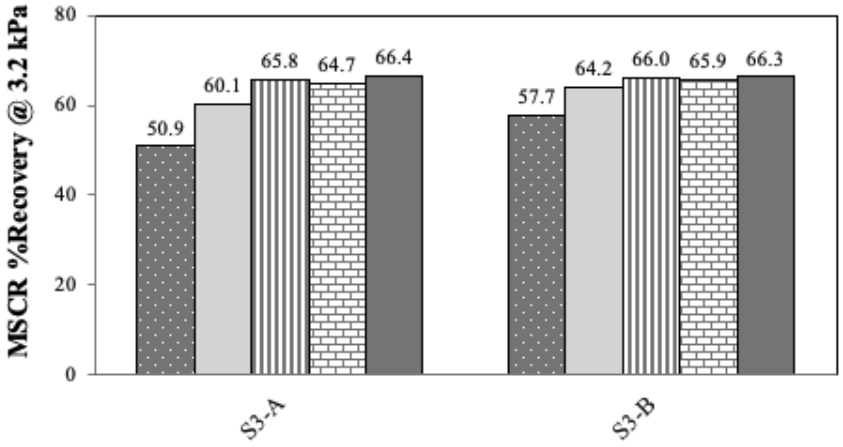

(b) S3 After Treatment with Products S3-A and S3-B

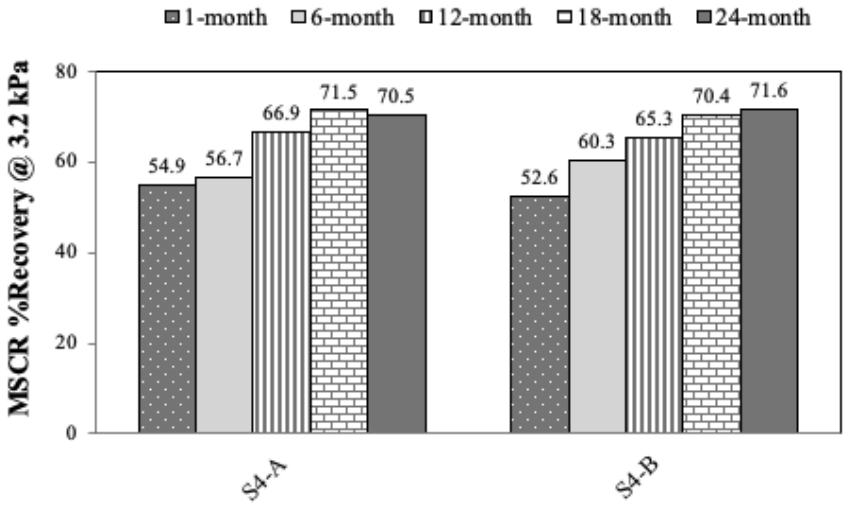

(c) S4 After Treatment with Products S4-A and S4-B

Figure 19. Effect of Field Aging on %Recovery at 3.2 kPa and 64°C

Figure 20 illustrates the aforementioned relationship between J_{nr} and %Recovery, where %Recovery for a given binder is associated to the J_{nr} of the binder. Moreover, it can be seen that base binder type and spray-on rejuvenator product type and dosage played a role in the overall MSCR results of the binders.

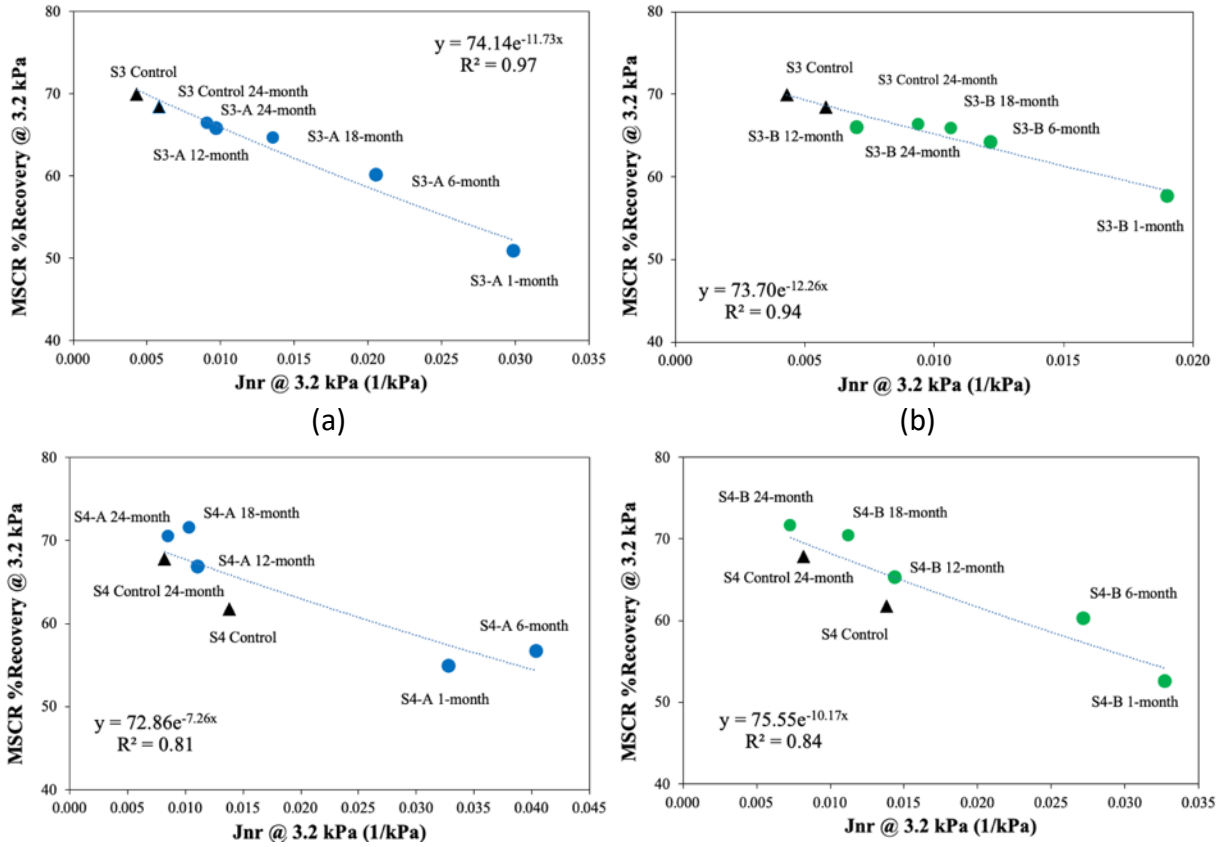

Figure 20. J_{nr} versus %Recovery at 3.2 kPa and 64°C for: (a) S3 Control and After Treatment with Product S3-A, (b) S3 Control and After Treatment with Product S3-B, (c) S4 Control and After Treatment with Product S4-A, (d) S4 Control and After Treatment with Product S4-B

12.5.4 Complex Modulus (|G|) and Phase Angle (δ) at 60°C*

As asphalts age, they harden; this results in a progressive increase in the stiffness modulus of the asphalt and a reduction in its stress relaxation capability. The increase in binder stiffness is not detrimental to rutting or other plastic deformation resistance but can be detrimental for fatigue and thermal cracking at intermediate and low-temperatures, respectively. Application of spray-on rejuvenator products should counterbalance these negative effects of aging. For the testing results presented in this section, the asphalt binders extracted and recovered from the field cores were tested without additional aging using RTFO and PAV.

Figure 21 presents the |G*| at 60°C and 10 rad/s [representing higher temperatures and the shearing action corresponding to a traffic speed of about 55 mph (90 km/h)] of all binders evaluated in this study. As indicated in Figure 21(a), the S3 control binder showed an increase of 30.1% (i.e., from 367.7 to 478.5 kPa) on its stiffness during the 24-month field aging interval. The application of the spray-on rejuvenator products S3-A and S3-B decreased the S3 control binder stiffness, and as the field aging interval increased (i.e., from 6 months towards 24 months of field aging), the stiffness of the treated sections also increased. However, after 24 months of field aging, the treated sections still showed complex modulus values smaller than

the S3 control before treatment application (i.e., 367.7 kPa): product S3-A showed a decrease in |G*| of 14.9% while product S3-B showed a decrease of 21.4%. Figure 21(b) shows that the S4 control binder showed an increase of 7.9% (i.e., from 252.5 to 272.5 kPa) on its stiffness during the 24-month field aging interval. After 24 months of field aging, the treated sections still showed stiffness values smaller than the S4 control before treatment application (i.e., 252.5 kPa): product S4-A showed a decrease in |G*| of 16.8% while product S4-B showed a decrease of 11.5%.

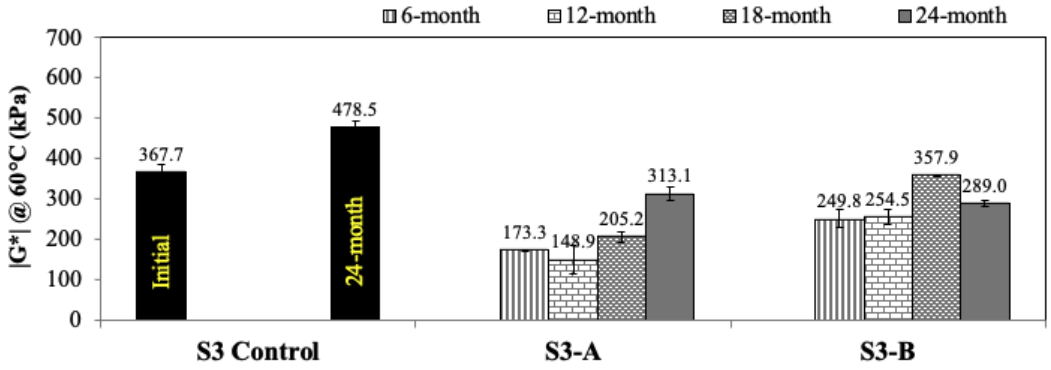

(a) S3 Control and After Treatment with Products S3-A and S3-B

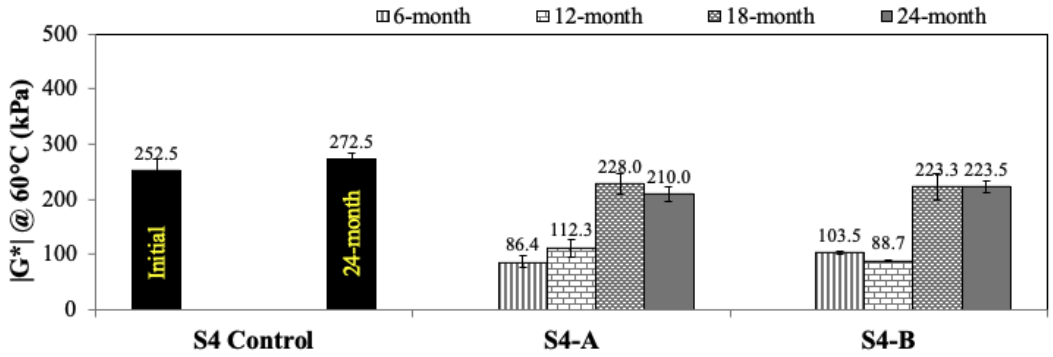

(b) S4 Control and After Treatment with Products S4-A and S4-B

Figure 21. Effect of Field Aging on |G*| at 60°C and 10 rad/s

As indicated in Figure 22(a), this NCAT field study has shown that the restoration capacity of a spray-on rejuvenating treatment increases rapidly after application as a result of the decrease in asphalt binder stiffness, but then begins to slowly decrease with oxidative aging as a result of the embrittlement of the binder. Therefore, the one-month (four-week) aging time proposed in the FAA P-632 procedure, which was described in Section 12.3.2 of this report, can be misleading for the assessment of a spray-on rejuvenator product's long-term effectiveness. By using the DSR, the rheological evaluation of asphalt binders extracted and recovered from field cores have shown that, in most cases, a minimum 18 months of field aging is required to observe clear indication of a product's effectiveness.

When comparing the two products applied over Section S3, which was an eight-year-old pavement containing 25% RAP, products S3-A and S3-B started to differentiate in terms of effectiveness on reducing |G*| 18 months after application [Figure 22(b)]. For Section S4,

which was a five-year-old pavement containing 15% fractionated RAP, the two applied products S4-A and S4-B reached a plateau in terms of effectiveness on reducing |G*| 18 months after application [Figure 22(c)]. Disregarding experimental error and the variability inherited by the extraction and recovery process of the asphalt binders obtained from field cores, the overall trend is that the maximum rejuvenating capability of the applied spray-on rejuvenator products was achieved between 6 and 12 months of treatment application. Moreover, the decrease in stiffness was found to be product dependent and was influenced by the characteristics of the asphalt material present in the surface of each section as well as the construction date of each section (i.e., Section S3 was constructed in 2012 and Section S4 was constructed in 2015).

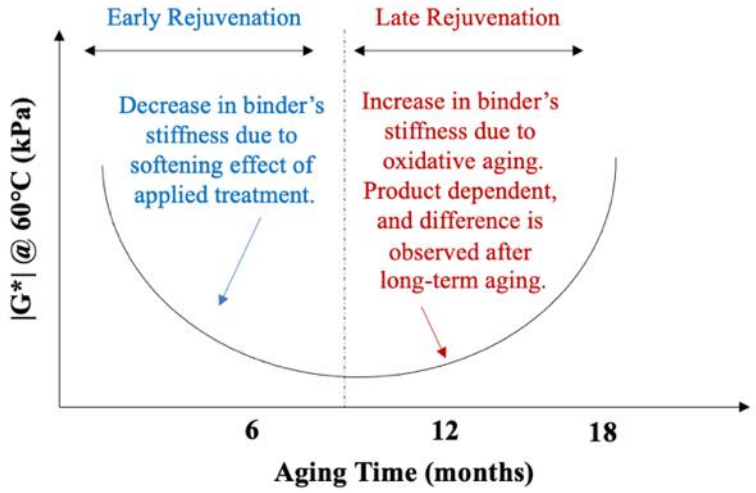

(a)

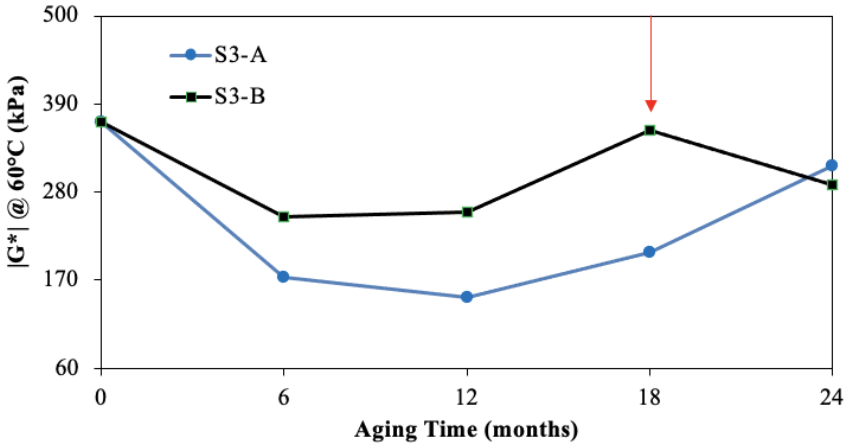

(b)

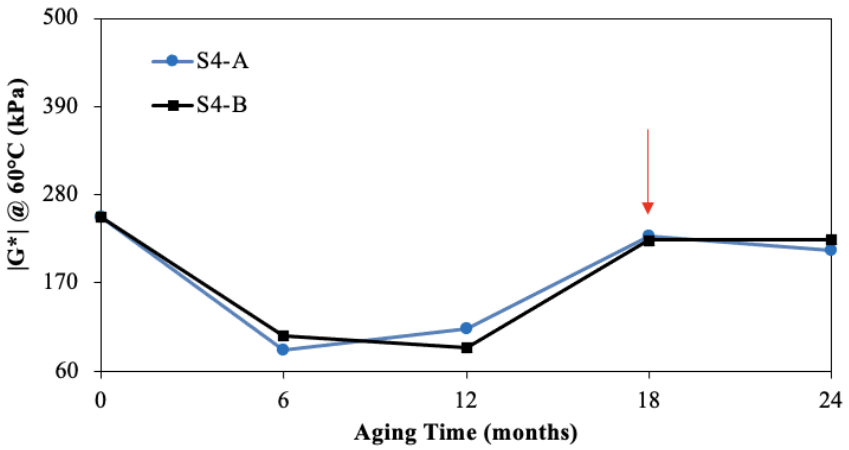

(c)

Figure 22 (a) Hypothesized Behavior of Spray-on Rejuvenator Products; (b) Effect of Field Aging on |G*| at 60°C and 10 rad/s for Section S3 After Treatment with Products S3-A and S3-B; (c) Effect of Field Aging on |G*| at 60°C and 10 rad/s for Section S4 Control and After Treatment with Products S4-A and S4-B

Figure 23 presents the phase angle (δ) at 60°C and 10 rad/s of all binders evaluated in this study. With aging, for a given temperature, δ decreases as the asphalt binder stiffens. As indicated in Figure 23, this behavior was observed for the control and treated binders as the field aging interval increased (i.e., from 6 months towards 24 months of field aging). When the spray-on rejuvenator products were applied to the surface of Sections S3 and S4, lowering the stiffness of the control binders, an increase in the phase angle of the resulting materials was observed at a given temperature (i.e., 60°C). This increase in phase angle was observed up to 18 months after treatment application, with the exception of product S4-B for which the increase in phase angle was observed up to 12 months after application. After 24 months of application, the four spray-on rejuvenator products presented phase angles similar to the controls exposed to 24-month field aging. When considering product S4-A, a spray-on rejuvenator product that also has an elastomeric polymer in its composition, it is possible that the rejuvenated binder's δ decreased due to increased elastic response of the material. This behavior is highly dependent on the overall stiffness of the composite material as well as the temperature at which the rheological response is tested.

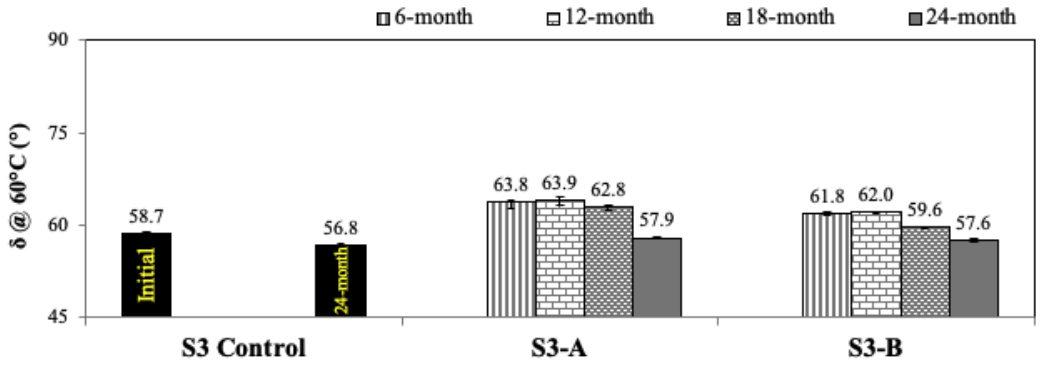

(a) S3 Control and After Treatment with Products S3-A and S3-B

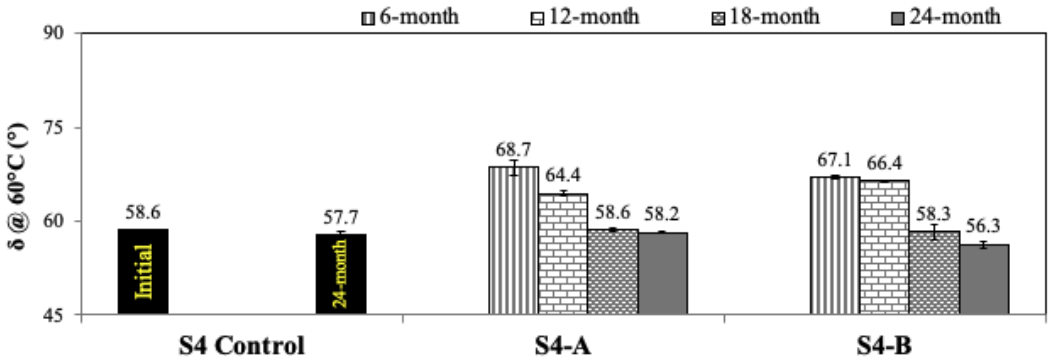

(b) S4 Control and After Treatment with Products S4-A and S4-B

Figure 23. Effect of Field Aging on δ at 60°C and 10 rad/s

12.5.5 Glover-Rowe Parameter and Black Space Diagram

The Glover-Rowe (*G-R*) parameter considers both binder stiffness and embrittlement and offers an indication of the cracking potential at intermediate temperature (*5*). Table 3 presents the |G*| and δ at 15°C and 0.005 rad/s as well as the *G-R* parameter results before and at several time intervals (i.e., 1 month, 6 months, 12 months, 18 months, and 24 months) after application of the four spray-on rejuvenator products. For the testing results presented in this section, the asphalt binders extracted and recovered from the field cores were tested without additional aging using RTFO and PAV.

As the field aging interval increased (i.e., from 1 month towards 24 months), the *G-R* parameter of the control and treated sections also increased. However, the treated sections consistently showed *G-R* values smaller than the controls. For Section S3, 24 months after treatment application of products S3-A and S3-B, the obtained *G-R* values of the treated sections were smaller than the S3 control after either 1 month or 24 months of field aging. For Section S4, product S4-A showed *G-R* values smaller than the S4 control after either 1 month or 24 months of field aging. Product S4-B showed *G-R* values smaller than the 1-month S4 control up to 18 months after application; 24 months after treatment application, the obtained *G-R* result was higher than the 1-month S4 control but remained smaller than the 24-month S4 control.

Table 3. |G*| and δ at 15°C and 0.005 rad/s, and G-R Parameter Results of Asphalt Binders

Sample	Field Aging Interval	15°C, 0.005 rad/s (unaged)		
		|G*| (kPa)	δ (°)	G-R (kPa)
S3 Control	1-month	5400.1	43.0	4234.8
	24-month	5881.0	41.7	4936.8
S4 Control	1-month	1680.2	48.3	997.6
	24-month	3294.8	44.5	2388.3
S3-A	1-month	1333.8	52.9	607.3
	6-month	1809.1	50.7	936.0
	12-month	1501.7	48.3	888.2
	18-month	2647.1	47.7	1624.9
	24-month	3835.7	44.0	2851.7
S3-B	1-month	2009.6	47.0	1280.0
	6-month	2480.9	47.8	1509.5
	12-month	2058.1	47.7	1258.8
	18-month	3628.4	45.0	2565.8
	24-month	3081.9	44.4	2245.4
S4-A	1-month	930.3	53.1	419.9
	6-month	1075.4	51.0	547.4
	12-month	1003.8	48.6	584.7
	18-month	2572.7	44.3	1888.2
	24-month	2697.2	44.2	1991.3
S4-B	1-month	937.7	53.2	420.4
	6-month	1123.3	50.8	580.6
	12-month	923.7	50.2	493.1
	18-month	1193.4	49.9	648.9
	24-month	2567.9	44.1	1904.3

Figure 24 presents the *G-R* parameter results on a Black Space diagram for Sections S3 and S4, where the binder's |G*| at 15°C and 0.005 rad/s is plotted on the y-axis versus δ at the same condition on the x-axis. As aging increased for each binder, the |G*| and δ data migrated from the lower right corner [i.e., low stiffness (|*G**|) and high ductility (δ)] to the upper left corner [i.e., increased stiffness (|*G**|) and increased brittleness (δ)] of the Black Space diagram. The dashed and bold curves in the figure represent the two preliminary *G-R* parameter criteria of 180 kPa and 600 kPa for the onset of block cracking and visible surface cracking, respectively.

As can be seen, all asphalt binders exceeded the preliminary *G-R* parameter criterion of 180 kPa for the onset of block cracking. For Section S3, at all field aging intervals, the S3 control (eight-year-old pavement containing 25% RAP and treated with products S3-A and S3-B) were above the *G-R* 600 kPa limit that relates to visible surface cracking [Figure 24(a) and 24(b)].

For Section S4, the S4 control (five-year-old pavement containing 15% F-RAP) exceeded the preliminary *G-R* parameter criterion of 600 kPa at all field aging intervals. After application of the spray-on rejuvenator products S4-A and S4-B, the *G-R* parameter criterion of 600 kPa was only exceeded at the 18-month field aging interval [Figure 24(c) and 24(d)], and thus the binders extracted and recovered from treated sections after 1-month, 6-month, and 12-month field aging were located within the cracking damage zone.

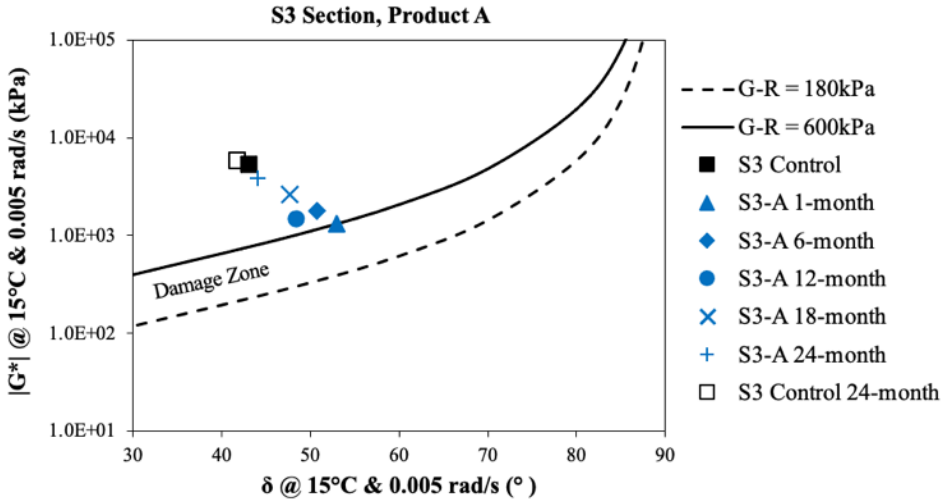

(a) S3 Control and After Treatment with Product S3-A

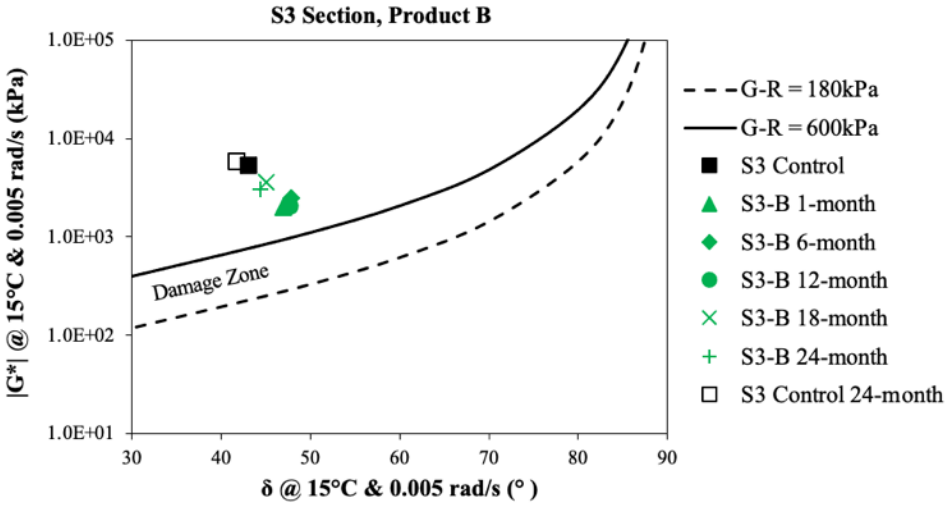

(b) S3 Control and After Treatment with Product S3-B

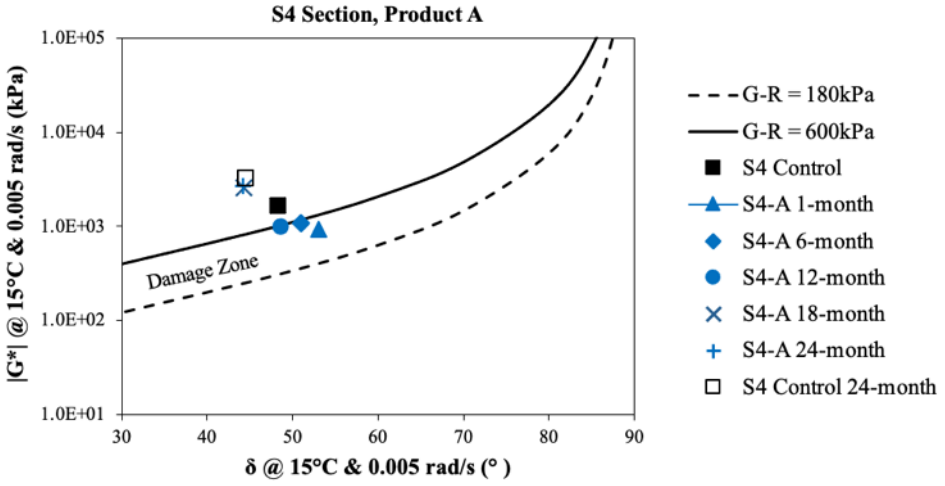

(c) S4 Control and After Treatment with Product S4-A

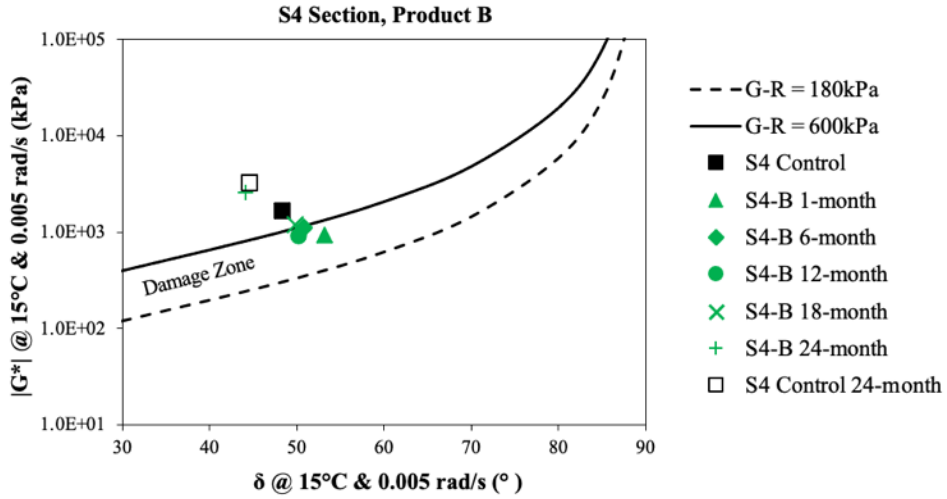

(d) S4 Control and After Treatment with Product S4-B

Figure 24. $|G^*|$ and δ Results on a Black Space Diagram

When investigating the potential binder rejuvenation of the four products, it was observed that the application of the surface treatments decreased the stiffness of both S3 control and S4 control, regardless the field aging interval (i.e., from 1 month towards 24 months of field aging). Moreover, for products S3-A and S3-B, it can be seen that this decrease in stiffness was followed by an increase in the phase angle (δ) [Figure 24(a) and (b)]. For products S4-A and S4-B, the decrease in stiffness was followed by an increase in the δ up to the 12-month field aging interval [Figure 24(c) and (d)]. When comparing the performance of the four spray-on rejuvenator products after long-term field aging (i.e., 24 months), it was observed that all of the treated sections were located above the cracking damage zone on the Black Space diagram. This indicates that, after long-term field aging (i.e., 24 months), all treated sections exceeded the preliminary *G-R* parameter criterion of 600 kPa that relates to visible surface cracking.

12.5.6 Complex Modulus |G| Aging Indexes at 10°C and 50°C*

In order to investigate the relationship between oxidative aging and the potential binder rejuvenation of the spray-on rejuvenator products, a complex modulus aging index was calculated using |G*| at 10°C and 10 rad/s (representing lower temperatures or higher traffic speed) and at 50°C and 0.1 rad/s (representing higher temperatures or lower traffic speed). The aging indexes were calculated in accordance with Equation 3. For the testing results presented in this section, the asphalt binders extracted and recovered from the field cores were tested without additional aging using RTFO and PAV. Table 4 presents the |G*| results after 1 month and 24 months of field aging.

$$\text{Aging Index } (|G^*|) = \frac{Treated\ Section\ (|\mathbf{G}^*|)_{1-\text{month, 24-month}}}{Control\ Section\ (|\mathbf{G}^*|)_{1-\text{month, 24-month}}} \quad (3)$$

Table 4. |G*| at 10°C and 10 rad/s and at 50°C and 0.1 rad/s of Asphalt Binders

Sample	Field Aging Interval	|G*| (kPa)	
		10°C, 10 rad/s	50°C, 0.1 rad/s
S3 Control	1-month	127,000	87
	24-month	122,000	96
S4 Control	1-month	62,900	26
	24-month	91,000	56
S3-A	1-month	70,800	16
	24-month	102,000	57
S3-B	1-month	68,200	31
	24-month	81,400	52
S4-A	1-month	50,800	13
	24-month	75,800	43
S4-B	1-month	54,700	12
	24-month	71,000	48

As indicated in Figure 25(a), both spray-on rejuvenator products S3-A and S3-B showed complex modulus aging index below 1.0 after 1 month of application, indicating that the stiffness of the binders extracted from the treated sections remained below the stiffness of the S3 control binder measured after 1 month of field aging. At 10°C and 0.1 rad/s (representing lower temperatures or higher traffic speed), product S3-B showed a marginally smaller complex modulus aging index (i.e., 0.54) than product S3-A (i.e., 0.56) after 1 month of application; and after 24 months of application, S3-B also showed a smaller complex modulus aging index (i.e., 0.67) than product S3-B (i.e., 0.84), indicating higher longevity of the effectiveness in decreasing the stiffness of the asphalt material present in the surface of Section S4. When comparing S3-A and S3-B at 50°C and 0.1 rad/s (representing higher temperatures or lower traffic speed), product S3-A showed a smaller complex modulus aging index (i.e., 0.18) than product S3-B (i.e., 0.36), after 1 month of application; and after 24 months of application, product S3-B showed a slightly smaller complex modulus aging index (i.e., 0.55) than product S3-A (i.e., 0.59).

Figure 25(b) indicates that the two spray-on rejuvenator products S4-A and S4-B applied on Section S4 also showed |G*| aging index below 1.0 after either 1 month or 24 months of application, indicating that the stiffness of the binders extracted from the treated sections remained below the stiffness of the S4 control binder. When comparing S4-A and S4-B at 10°C and 10 rad/s, product S4-A showed a slightly smaller complex modulus aging index (i.e., 0.81) than product S4-B (i.e., 0.87) after 1 month of application; and after 24 months of application, S4-B showed a slightly smaller complex modulus aging index (i.e., 0.78) than product S4-A (i.e., 0.83). At 50°C and 0.1 rad/s, product S4-B showed a marginally smaller complex modulus aging index (i.e., 0.44) than product S4-A (i.e., 0.49) after 1 month of application; and after 24 months of application, S4-A showed a smaller complex modulus aging index (i.e., 0.77) than product S4-B (i.e., 0.86), indicating higher longevity of the effectiveness in decreasing the stiffness of the asphalt material present in the surface of Section S4.

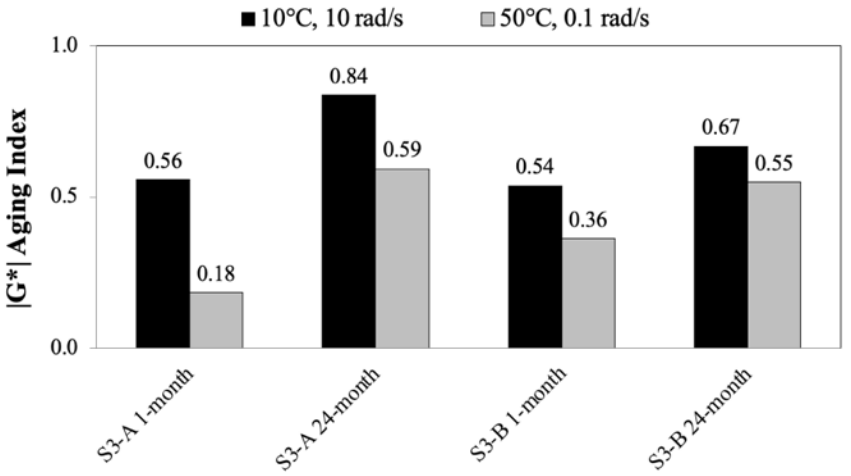

(a) Section S3 Treated with Products S3-A and S3-B

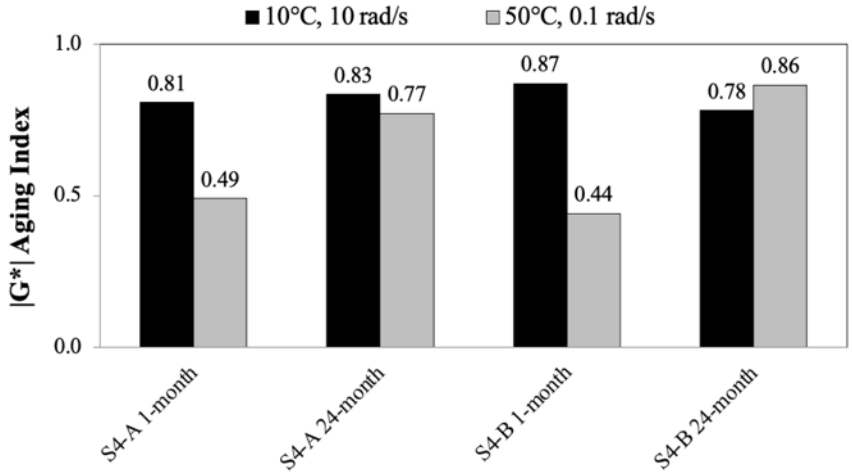

(b) Section S4 Treated with Products S4-A and S4-B

Figure 25. |G*| Aging Index at 10°C and 10 rad/s and at 50°C and 0.1 rad/s

12.5.7 Dynamic Friction Tester (DFT)

In this study, three DFT measurements were performed at 20, 40, and 60 km/h for evaluation of the pavement surface friction properties at several time intervals after application of the four spray-on rejuvenator products (i.e., 72 hours, 96 hours, 2 weeks, 1 month, 6 months, 12 months, 18 months, and 24 months). For the S3 and S4 untreated control sections, the friction measurements were collected over the same period prior to the application of the treatments. Heitzman and Moore indicated that the speed that produces the most repeatable measure in the DFT is 40 km/h (*13*). Therefore, this speed was used for detailed analysis.

Figure 26 shows the average friction number (F_n) at 40 km/h before and at several time intervals after application of the four spray-on rejuvenator products. For all of the evaluated products, it can be seen that the friction of the pavement surface decreased after treatment application, but the friction results improved with time. For Section S3, between pretreatment and 96 hours of treatment application, product S3-A showed the highest decrease in friction (29.6%), while product S3-B showed the smallest decrease in friction (3.7%) [Figure 26(a)]. For

Section S4, the decrease in friction was sharp after application of the surface treatments, which might be a safety concern if the treated sections are exposed to traffic. The initial drop in friction of products S4-A and S4-B was similar when considering pretreatment and 72 hours of treatment application: product S4-A showed the highest decrease in friction (66.6%), while product S4-B showed the smallest decrease in friction (62.7%) [Figure 26(b)]. The initial time intervals of 96 hours and 72 hours for Sections S3 and S4, respectively, for collecting the friction values were different due to weather conditions that made it difficult to collect the field data. Two weeks after application, products S3-A and S3-B showed friction values equal (0.27) and higher (0.30) than the S3 control section, respectively. For Section S4, product S4-B showed friction values higher (0.52) than the S4 control section two weeks after application, while product S4-A showed friction value higher (0.62) than the control section only after 18 months of application. For the four evaluated spray-on rejuvenator products, the long-term test results indicated that the applied products did not show adverse effects on the friction of the pavement when comparing with the friction of the control sections.

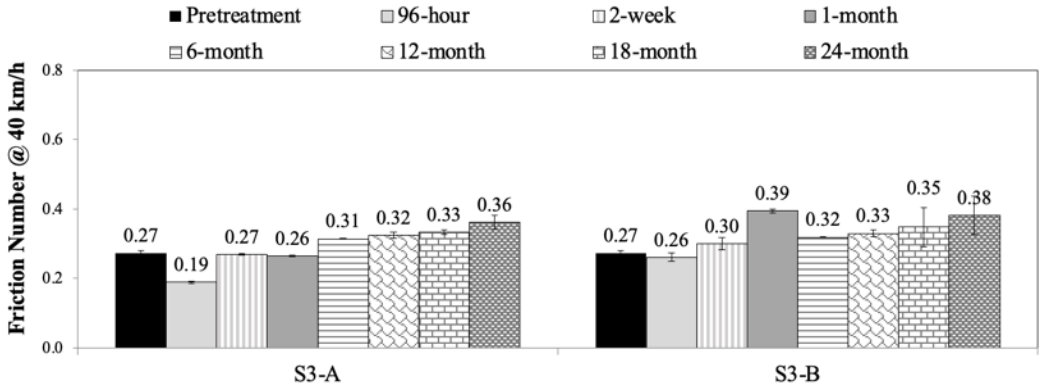

(a) Section S3 Treated with Products S3-A and S3-B

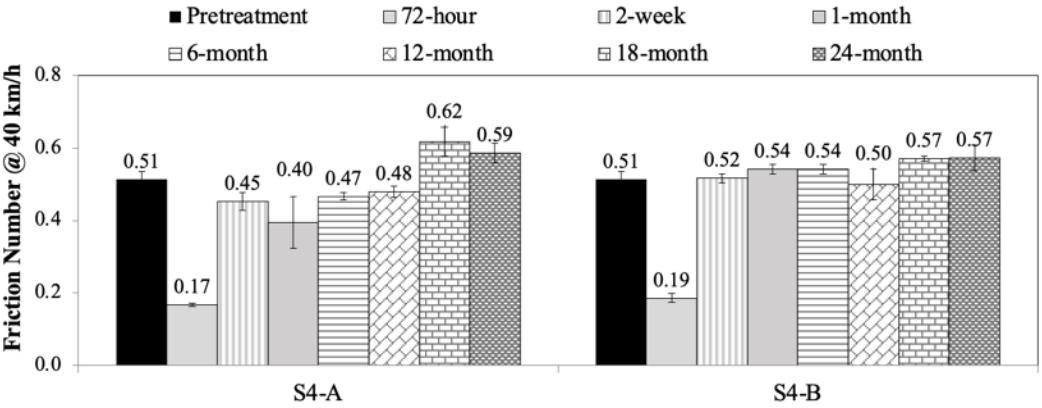

(b) Section S4 Treated with Products S4-A and S4-B

Figure 26. Average Fn at 40 km/h at Several Time Intervals

Overall, Section S4 (a five-year-old dense-graded mix with sand and limestone containing 15% F-RAP) showed higher friction values in comparison to Section S3 (eight-year-old dense-graded mix with sand and gravel containing 25% RAP).

12.6 Field Performance

Due to the length restriction of both S3 and S4 control sections (Figure 3), it was not possible to evaluate the field performance of the untreated sections using an automated pavement condition survey vehicle. However, the treated sections were evaluated for rutting, cracking, smoothness, and surface texture on a weekly basis using an automated pavement condition survey vehicle.

This report is representative of the field data up to 10 million ESALs of heavy truck traffic for the 2018-2021 research cycle. As indicated previously, the S3-A and S3-B spray-on rejuvenator products were applied after Section S3 was subjected to a total of ≈20.0 million ESALs of traffic since construction, without rutting and cracking distresses. The S4-A and S4-B spray-on rejuvenator products were applied after Section S4 was subjected to a total of ≈10.0 million ESALs of traffic since construction without rutting and cracking distresses.

12.6.1 Rutting Evaluation

Figure 27 compares rut depth versus traffic ESALs for the S3 and S4 sections treated with the spray-on rejuvenator products. As can be seen in Figure 26(a), the average rut depth of the section treated with product S3-A was 5.36 mm for around 9.9 million ESALs of traffic. For the same applied traffic, the average rut depth of the section treated with product S3-B was 3.52 mm. Figure 27(b) shows that the obtained average rut depth of the section treated with product S4-A was 3.03 mm for around 9.9 million ESALs of traffic, while for the section treated with product S4-B, the average rut depth was 2.66 mm. For all four treated sections, the obtained field rut values were smaller than the rut depth limit of 12.5 mm, which is commonly considered failing. Therefore, the treated sections have shown no significant rutting thus far. These results agree with the MSCR binder data presented in this report, which indicated adequate rutting resistance of these materials.

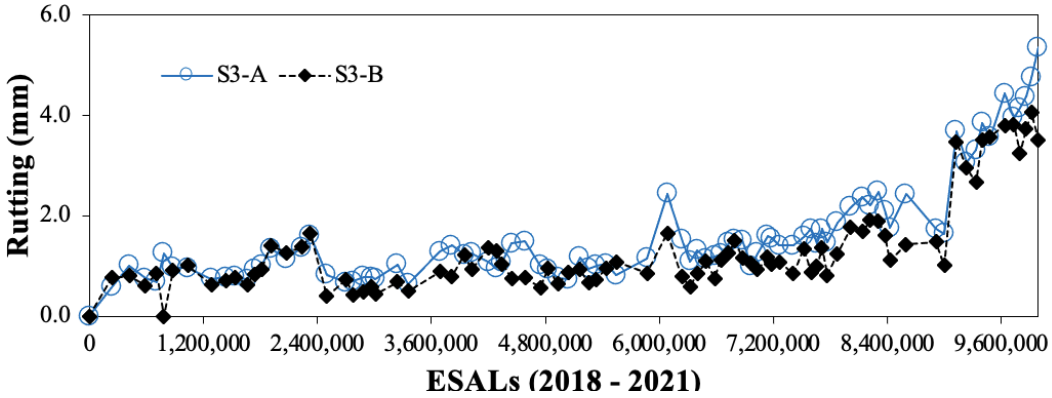

(a) Section S3 Treated with Products S3-A and S3-B

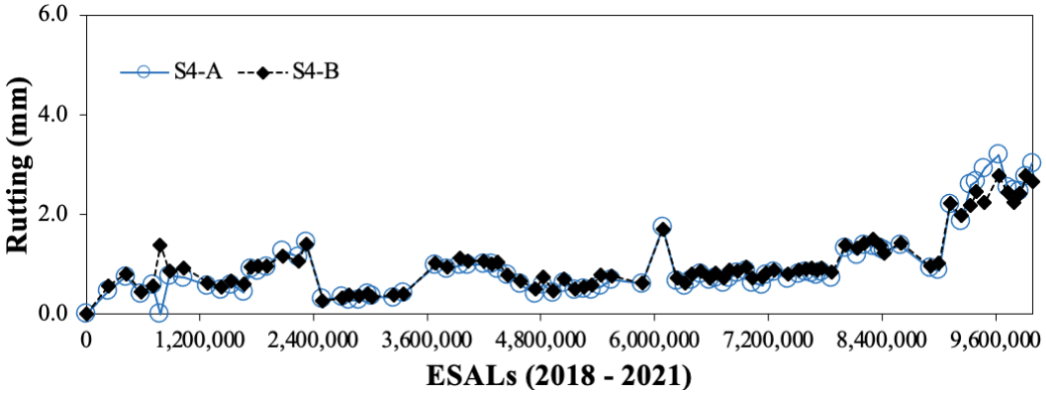

(b) Section S4 Treated with Products S4-A and S4-B

Figure 27. Field Performance - Rut Depth versus ESALs

12.6.2 Cracking

Figure 28 presents the surface cracking data versus ESALs where cracking is expressed as the percentage of lane area cracked. As can be seen in Figure 28(a), for Section S3 treated with product S3-A, the first cracks started after around 584,084 ESALs (≈20.6 million ESALs since 2012) and ≈2 months after treatment application, with 0.1% of lane area cracked; for Section S3 treated with product S3-B, the first cracks started after around 3,581,376 ESALs (≈23.6 million ESALs since 2012) and ≈9 months after treatment application, with 0.2% of lane area cracked. After around 10.0 million ESALs of traffic (total of ≈30.0 million ESALs since 2012) and ≈28 months after treatment application, the section treated with product S3-A and the section treated with product S3-B exhibited similar cracking performance with 2.0 and 1.7% of lane area cracked, respectively. Figure 28(b) indicates that for Section S4, the first cracks started after around 584,084 ESALs (≈10.6 million ESALs since 2015) and ≈2 months after treatment application, with 0.3% of lane area cracked for products S4-A and S4-B. After around 10.0 million ESALs of traffic (total of ≈20.0 million ESALs since 2015) and ≈28 months after treatment application, the section treated with product S4-A and the section treated with product S4-B exhibited similar cracking performance with 0.7 and 0.8% of lane area cracked, respectively. Thus, the S3 and S4 treated sections were far from exceeding the maximum lane area cracked limit of 20%. The type of cracking observed for the four treated sections was classified as early block cracking.

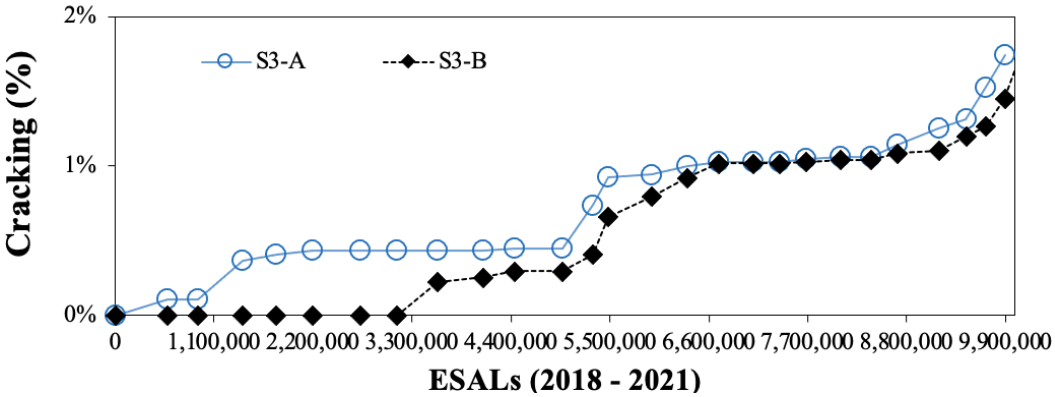

(a) Section S3 Treated with Products S3-A and S3-B

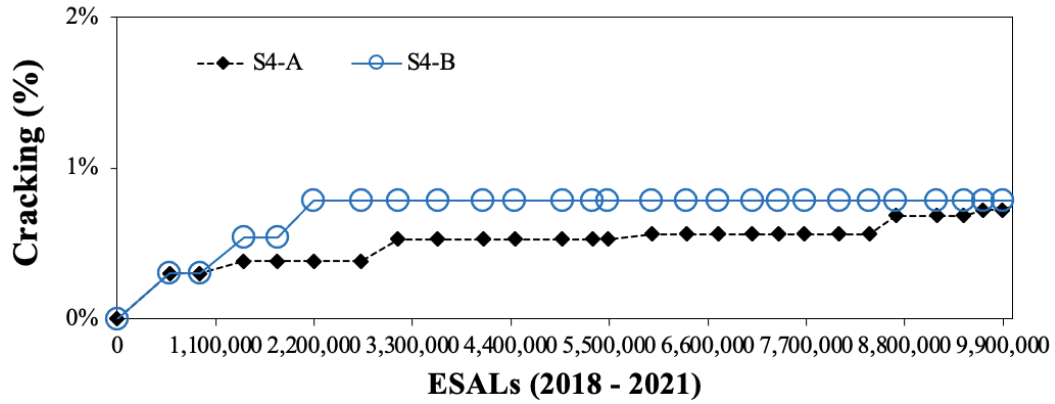

(b) Section S4 Treated with Products S4-A and S4-B

Figure 28. Field Performance - Cracking versus ESALs

Table 5 presents a summary of the ΔT_c and *G-R* binder cracking parameters and the cracking field performance for the four treated sections. As can be seen, after 1 month of application of the four spray-on rejuvenator products, the treated sections presented ΔT_c values below the minimum threshold of -5°C, but no cracking was observed in the field sections. However, as the field aging progressed towards 24 months of field aging, the ΔT_c values became more negative and cracking was observed in the four treated sections. Regarding the *G-R* parameter threshold for visible surface cracking (i.e., 600 kPa), it can be seen that S3-A after 1 month of treatment application, and S3-B after 1 and 6 months of treatment application, presented *G-R* values above 600 kPa and no cracking was observed in the field. Furthermore, both S4-A and S4-B after 6 and 12 months of treatment application presented *G-R* values below 600 kPa and cracking was observed in the field. As the field aging progressed towards 24 months, the *G-R* values increased above the threshold for visible surface cracking (i.e., 600 kPa) and cracking was observed in the four treated sections.

Table 5. Laboratory and Field Results of Treated Sections: ΔT_c and G-R Binder Cracking Parameters, Cracking Performance and ESALs

Sample	Field Aging Interval	ΔT_c (°C)	G-R (kPa)	Cracking (%)	ESALs	
					2018 – 2021	Construction - 2021
S3-A	1-month	-8.2	607.3	0.0	329,764	20,385,012
	6-month	-7.7	936.0	0.4	2,196,281	22,251,529
	12-month	-12.5	888.2	0.4	4,971,971	25,027,219
	18-month	-6.7	1624.9	1.0	7,097,968	27,153,216
	24-month	-11.7	2851.7	1.3	9,156,176	29,211,424
S3-B	1-month	-9.7	1280.0	0.0	329,764	20,385,012
	6-month	-5.8	1509.5	0.0	2,196,281	22,251,529
	12-month	-10.9	1258.8	0.3	4,971,971	25,027,219
	18-month	-13.7	2565.8	1.0	7,097,968	27,153,216
	24-month	-14.1	2245.4	1.1	9,156,176	29,211,424
S4-A	1-month	-18.6	419.9	0.0	329,764	10,339,221
	6-month	-11.5	547.4	0.4	2,196,281	12,205,738
	12-month	-16.5	584.7	0.5	4,971,971	14,981,428
	18-month	-15.7	1888.2	0.6	7,097,968	17,107,425
	24-month	-13.7	1991.3	0.7	9,156,176	19,165,633
S4-B	1-month	-8.1	420.4	0.0	329,764	10,339,221
	6-month	-11.7	580.6	0.8	2,196,281	12,205,738
	12-month	-14.4	493.1	0.8	4,971,971	14,981,428
	18-month	-12.5	648.9	0.8	7,097,968	17,107,425
	24-month	-14.8	1904.3	0.8	9,156,176	19,165,633

12.6.3 Pavement Roughness

Pavement roughness was quantified using the International Roughness Index (IRI). Figure 29(a) indicates that, despite slight fluctuations in the smoothness of the pavement of Section S3, the overall IRI of the section treated with product S3-A was 90.1 in/mile, while for product S3-B was 56.1 in/mile. Increases in roughness are commonly associated with pavement distresses. On Section S3, a fleet accident resulted in the need for a wrecker to remove a damaged trailer set. During the removal process, one of the trailers overturned, impacting Section S3-A. Therefore, the higher overall IRI measured for Section S3 treated with product S3-A is likely due to the higher area of lane cracking observed from the aforementioned accident. Note that the cracking originated from this accident was not accounted in the field cracking results presented in Figure 28(a). As can be seen in Figure 29(b), the change in roughness over time for Section S4 treated with product S4-A was 52.2 in/mile, while for the product S4-B was 35.8 in/mile.

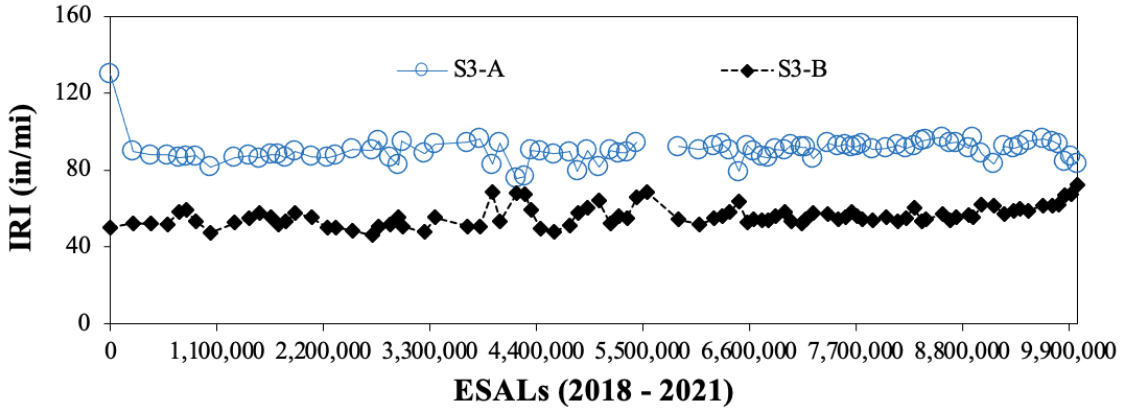

(a) Section S3 Treated with Products S3-A and S3-B

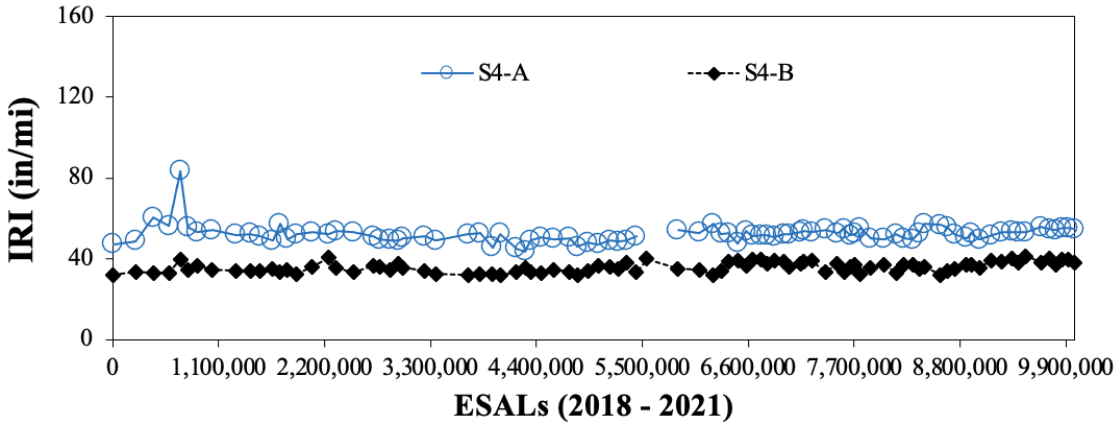

(b) Section S4 Treated with Products S4-A and S4-B

Figure 29. Field Performance - Roughness versus ESALs

12.6.4 Surface Texture

Figure 30(a) indicates that the mean texture depths (MTD) after application of products S3-A and S3-B were 0.61 and 0.65 mm, respectively. As can be seen in Figure 30(b), the MTD values after application of products S4-A and S4-B were 0.38 and 0.33 mm, respectively. Nevertheless, for both Sections S3 and S4, the applied spray-on rejuvenator products showed similar MTD results.

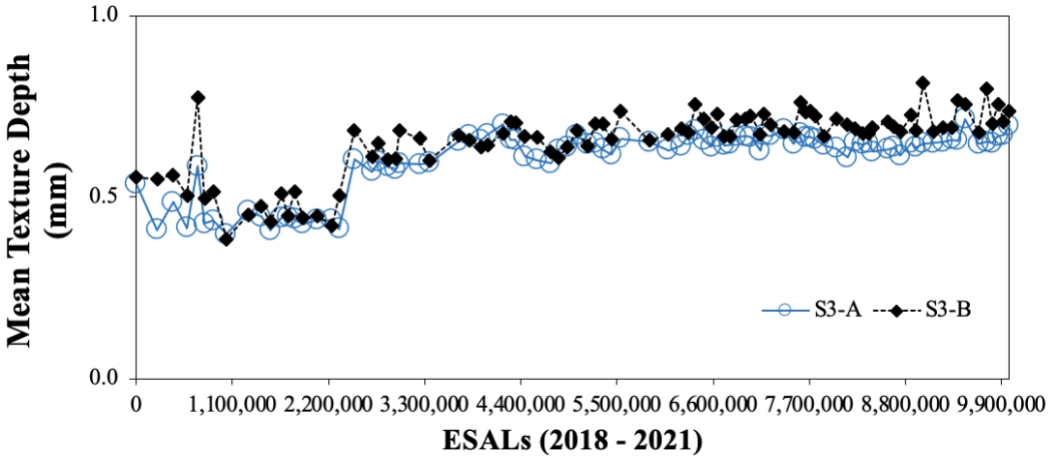

(a) Section S3 Treated with Products S3-A and S3-B

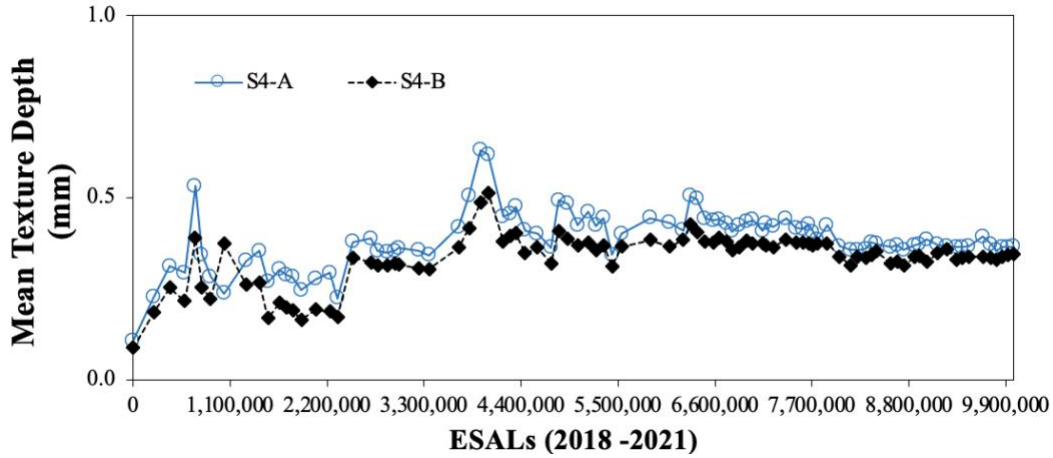

(b) Section S4 Treated with Products S4-A and S4-B

Figure 30. Field Performance - Mean Texture Depth versus ESALs

12.7 Conclusions and Recommendations

Efforts were placed on the evaluation of the short- and long-term field performance of four spray-on rejuvenator products. The long-term evaluation allowed a better assessment of each product's effectiveness, since a longer aging time was observed as necessary to differentiate between stiffness and relaxation properties of different spray-on rejuvenator technologies and base asphalts. The rheological changes observed with aging are not linear, and thus, depending on the product utilized, cannot be fully captured when only considering short-term aging. Based on the findings presented in this chapter, the following conclusions and recommendations were made.

- The NCAT field study has shown that the restoration capacity of a spray-on rejuvenating product can be separated into early rejuvenation and late rejuvenation. During early rejuvenation, the restoration capacity increases rapidly as a result of the decrease in asphalt binder stiffness but then begins to slowly decrease with oxidative aging as a result of the embrittlement of the binder (late rejuvenation). Moreover, during late

rejuvenation, the restoration capacity is product-dependent and can only be fully captured after long-term aging. Therefore, the one-month (four-week) aging time proposed in the FAA P-632 procedure can be misleading for the assessment of a spray-on rejuvenator product's long-term effectiveness. The laboratory rheological evaluation of asphalt binders extracted and recovered from field cores have shown that, in most cases, 18 months of field aging is required to differentiate among products and to observe a sufficient indication of a product's effectiveness.

- The application of the spray-on rejuvenator products initially decreased the high temperature PG of the asphalt material present in the surface of the sections, but this decrease was dismissed after the long-term field exposure. With respect to the intermediate-temperature performance grade, an improvement in the fatigue resistance of control binders was observed. Exceptions occurred for product S3-B after 12 months of field aging and product S4-A after 24 months of field aging; however, both pass/fail intermediate temperatures remained lower than the control S3 and S4 values after 24 months of field aging. An improvement in low temperature performance was observed for the treated sections in comparison to the control sections, with exception of product S4-A, which after a 24-month period provided a low-temperature PG equal to the S4 control after 24 months of field aging.
- After 24 months of the application of the spray-on rejuvenator products on Section S3 (an eight-year-old pavement containing 25% RAP) and Section S4 (a five-year-old pavement containing 15% F-RAP), the asphalt binder properties of the treated sections are still improved in comparison to the control sections. This improvement was found as product dependent, and was influenced by the characteristics of the asphalt material present in the surface of each section as well as the construction time of each section.
    - Rotational viscosity aging index calculated 24 months after application indicated that the viscosity of the binders extracted from the treated sections remained below the viscosity of the control binders measured after 24 months of field aging. Moreover, the time interval where the lowest viscosity values were observed for all treated samples was located at either 6 months or 12 months after treatment application.
    - Complex modulus aging index, calculated at 10°C and 10 rad/s (representing lower temperatures or higher traffic speed) and at 50°C and 0.1 rad/s (representing higher temperatures or lower traffic speed), indicated that the stiffness of the binders extracted from the treated sections remained below the stiffness of the control binders.
    - Glover-Rowe (*G*-*R*) parameter results showed that the treated sections consistently presented *G*-*R* values smaller than those of the controls. However, after long-term field aging (i.e., 24 months), all treated sections exceeded the preliminary *G*-*R* parameter criterion of 600 kPa that relates to visible surface cracking. The field cracking data confirmed that the treated sections presented early block cracking after 24 months of application of the spray-on rejuvenator products.
- To ensure safety, the coefficient of friction of the existing pavement surface should be measured before and after the application of the spray-on rejuvenators. For Section S3,

between pretreatment (i.e., friction of the control untreated section) and 96 hours of treatment application, the observed decrease in friction was 29.3% for product S3-A, and 3.7% for product S3-B. For Section S4, the initial drop in friction was sharp when considering pretreatment and 72 hours of treatment application: 66.6% and 62.7% for S4-A and S4-B, respectively. Two weeks after application, products S3-A and S3-B showed friction values equal or higher than the S3 control section, while product S4-B showed friction value higher than the S4 control section. Product S4-A showed friction value higher than the control section only after 18 months of application. The long-term friction test results indicated that the four applied products did not show adverse effects on the friction of the pavement when comparing with the friction of the control sections.

- Surface cracking data after 10.0 million ESALs of traffic (2018-2021 research cycle) indicated that, after treatment with the spray-on rejuvenator products, Section S3 (total of ≈30.0 million ESALs since 2015) and Section S4 (total of ≈20.0 million ESALs since 2015) were far from exceeding the maximum lane area cracked limit of 20%. The section treated with product S3-A and section treated with product S3-B exhibited 2.0 and 1.7% of lane area cracked, respectively. The section treated with product S4-A and section treated with product S4-B exhibited 0.7 and 0.8% of lane area cracked, respectively. The type of cracking observed for the four treated sections was classified as early block cracking.

In summary, spray-on rejuvenator products are a good option for preventing or retarding the surface deterioration of pavements, practical in use since they do not require specialized equipment, and can be effective for restoring the surface condition of an existing pavement. Both sections are recommended for traffic continuation in the next research cycle to further monitor and evaluate the long-term performance of the applied products, indicating the time interval where these products will lose effectiveness.

12.8 References

1. Hanson, D., G. King, M. Buncher, J. Duval, P. Blankenship, and M. Anderson. *Techniques for Prevention and Remediation of Non-Load Related Distresses on HMA Airport Pavements (Phase I)*. Airfield Asphalt Pavement Technology Program, 2009.
2. Estakhri, C., and H. Agarwal. *Effectiveness of Fog Seals and Rejuvenators for Bituminous Pavement Surfaces*. Research Report 1156-1F, Research Study 2-18-87-1156, Texas State Department of Highways and Public Transportation, 1991.
3. Ergon Asphalt & Emulsions, Inc. eFog Rejuvenating Fog Seal. https://ergonasphalt.com/storage/2162/EA&E-Product-Handouts-September-2019---eFog.pdf
4. Pavement Technology, Inc. Reclamite Asphalt Pavement Rejuvenator. https://www.pavetechinc.com/wp-content/uploads/2017/11/Reclamite_PTI_Full-Page.pdf
5. Rowe, G. M. Prepared Discussion for the AAPT paper by Anderson et al.: Evaluation of the Relationship between Asphalt Binder Properties and Non-Load Related Cracking. *Journal of the Association of Asphalt Paving Technologists*, Vol. 80, 2011, pp. 649-662.

6. Rodezno, C., R. Moraes, M. Fortunatus, and F. Yin. *Recycled Asphalt Binder Study*. WisDOT Final Report ID no. 0092-19-04, 2021.
7. Kaseer, F., L. Cucalon, E. Arámbula-Mercado, A. Epps Martin, and J. Epps. Practical Tools for Optimizing Recycled Materials Content and Recycling Agent Dosage for Improved Short- and Long-Term Performance of Rejuvenated Binder Blends and Mixtures. *Journal of the Association of Asphalt Paving Technologists*, 87, 2018.
8. Zhou, F., S. Im, D. Morton, R. Lee, S. Hu, and T. Scullion. Rejuvenator Characterization, Blend Characteristics, and Proposed Mix Design Method. *Journal of the Association of Asphalt Paving Technologists*, Vol. 84, pp. 675-704, 2015.
9. Anderson, M., G. N. King, D. I. Hanson, and P. B. Blankenship. Evaluation of the Relationship between Asphalt Binder Properties and Non-Load Related Cracking. *Journal of the Association of Asphalt Paving Technologists*, Vol. 80, 2011, pp. 615-664.
10. Asphalt Institute. State-of-Knowledge: Use of DeltaTc Parameter to Characterize Asphalt Binder Behavior, 2019.
11. Reinke, G. *The Relationship of Binder Delta T_c to Mixture Fatigue*. Southeastern Asphalt User Producer Group, Jacksonville, Florida, 2017.
12. Vollor, T., and D. Hanson. *Development of Laboratory Procedure for Measuring Friction of HMA Mixtures – Phase I*. NCAT Report 06-06, National Center for Asphalt Technology at Auburn University, 2006.
13. Heitzman, M., and J. Moore. *Evaluation of Laboratory Friction Performance of Aggregates for High Friction Surface Treatments*. NCAT Report 17-01, National Center for Asphalt Technology at Auburn University, 2017.

13. OKLAHOMA BALANCED MIX DESIGN EXPERIMENT

Dr. Fan Yin

13.1 Background

The Oklahoma Department of Transportation (ODOT) began moving forward with the development and implementation of balanced mix design (BMD) in 2017. The first draft of ODOT's provisional specification on BMD required the use of the Hamburg Wheel Tracking Test (HWTT) (AASHTO T 324) and the Illinois Flexibility Index Test (I-FIT) (AASHTO TP 124) for the evaluation of mixture rutting resistance and cracking resistance, respectively. Furthermore, the Cantabro test was required for mix design testing to evaluate mixture durability, but the result was for informational purposes only. To allow contractors to add more asphalt binder in the mix for improved cracking resistance and durability, ODOT relaxed the design air voids from 4% to a range of 3.0 to 4.0%. ODOT allowed up to 15% reclaimed asphalt pavement (RAP) binder replacement in surface mixes designed with the BMD approach while RAP was not previously permitted in the Superpave mix designs.

In 2019, ODOT decided to adopt the Indirect Tensile Asphalt Cracking Test (IDEAL-CT) instead of the I-FIT as the mixture cracking test for the implementation of BMD in Oklahoma. This decision was made based on the findings of several research studies suggesting that both tests were able to discriminate asphalt mixes with different cracking resistance (*1, 2*), but IDEAL-CT was simpler and quicker and thus, more suitable for quality control and acceptance testing during production. Furthermore, ODOT eliminated the requirement of Cantabro testing for mix design.

ODOT's most recent provisional specification for BMD uses the *Performance-Modified Volumetric Design* approach to design asphalt mixtures that meet the BMD performance requirements but not necessarily the Superpave volumetric requirements. The design air voids content is 3.0 to 4.0% at a design gyration (N_{design}) of 50, 65, and 80 for mixtures containing a PG 64-22, PG 70-28, and PG 76-28 binder, respectively. The minimum VMA criteria vary from 12.5 to 16.5% as a function of aggregate nominal maximum aggregate size (NMAS). The mixture performance tests used are the HWTT and IDEAL-CT. The HWTT criteria are based on the number of passes to 12.5 mm rut depth at 50°C, where a minimum threshold of 10,000, 15,000, and 20,000 passes is required for mixtures containing a PG 64-22, PG 70-28, and PG 76-28 binder, respectively. The IDEAL-CT is conducted at 25°C and its criterion is a minimum cracking tolerance index (CT_{Index}) of 80 for all mixtures regardless of virgin binder grade. Both test criteria are based on short-term aged specimens for four hours at 135°C per AASHTO R 30. Production acceptance is purely based on mixture volumetric properties with no requirements on the HWTT and IDEAL-CT results at this time. Trial projects and field mixture testing are currently being conducted to set a baseline of production data.

13.2 Objective and Scope

In the 2018 research cycle, ODOT sponsored Sections N9 and S1 for evaluation on the NCAT Test Track (Figure 1). The overall objective of the experiment was to support ODOT with the implementation of mixture performance testing and criteria for BMD. Both sections were built as mill-and-inlays using asphalt mixtures designed with a BMD approach. Section N9 was placed as a 1.5-inch layer while S1 was placed in two layers with a total thickness of 5.0 inches. The key

question that ODOT sought to answer from this experiment was: are the proposed performance criteria in the BMD provisional specification sufficient, or do they need to be adjusted to achieve good rutting and cracking performance in the field?

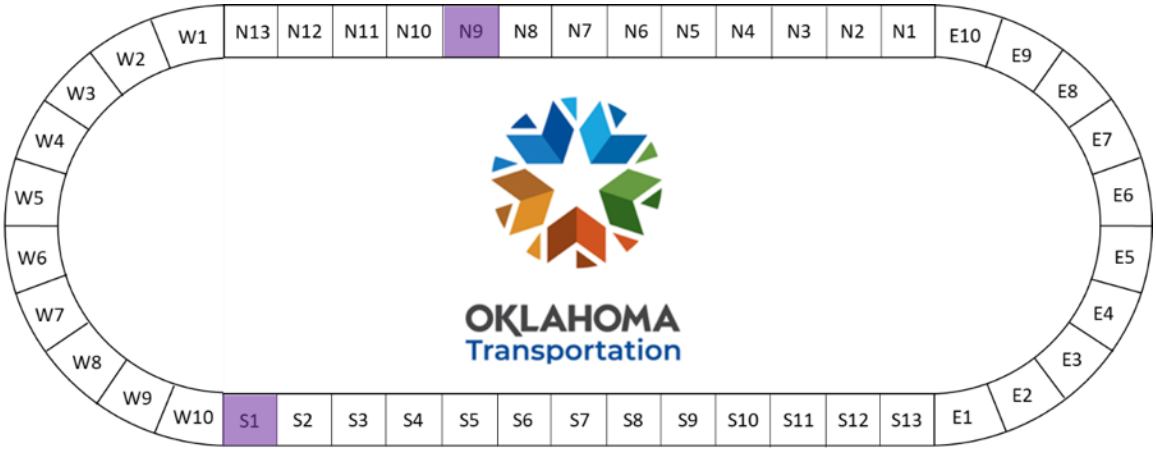

Figure 1. Layout of ODOT's Sections N9 and S1 on the NCAT Test Track

13.3 Existing Pavement Conditions

The existing pavement of Section N9 was constructed in 2006 with an overall research focus on the perpetual pavement concept. The pavement was constructed with 14 inches of asphalt mix over 9.6 inches of graded aggregate base and a soft subgrade that was representative of the soil in Oklahoma. The pavement had excellent field performance through three research cycles from 2006 to 2015. It had no cracking after being trafficked for 20 million equivalent single axle loads (ESALs) but started to show top-down cracking along the left wheel path in the third research cycle starting in 2012. Figure 2 presents the crack map generated in October 2014, which showed approximately 10% of lane area cracked.

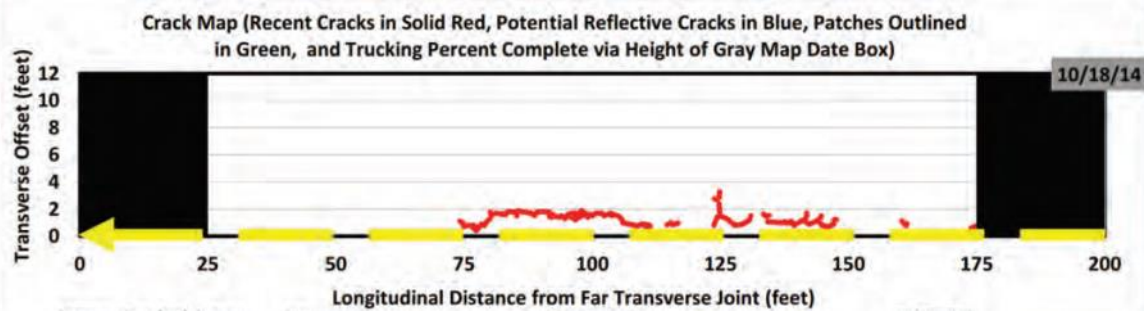

Figure 2. Crack Map of Section N9 in October 2014

In the 2015 research cycle, Section N9 was converted to an open-graded friction course (OGFC) study for ODOT to evaluate the friction performance of OGFC mixes using locally available aggregates. The section was divided into two sub-subsections, which were milled and inlaid with 0.75 inches of sandstone OGFC mixes with two tack coat rates. In May 2018, the top 1.5 inches of the OGFC and underlying mixes were milled off for the preparation of the 2018 research cycle, as shown in Figure 3(a).

(a) (b)

Figure 3. Existing Pavements after Milling in (a) Section N9 and (b) Section S1

The existing pavement of Section S1 has supported numerous surface layer experiments since the original Test Track construction. The overall thickness of the section includes 24 inches of asphalt mixes. In May 2018, the top 5.0 inches were milled off for the preparation of the 2018 research cycle, as shown in Figure 3(b).

13.4 Mix Design

Table 1 presents the job mix formula (JMF) of the N9, S1 surface, and S1 base mixes provided by two contractors in Oklahoma. The N9 mix was an ODOT S5 mix with a 9.5 mm NMAS. The mix used a PG 76-28 SBS modified binder, a blend of granite and sand, and 15% RAP by weight of the mix. The mix had an optimum binder content (OBC) of 5.6%, design air voids of 4.0%, and VMA of 15.5% at 80 gyrations. The resultant RAP binder replacement of the mix was 14.0%. The mix was designed using the *Volumetric Design with Performance Verification* approach described in AASHTO PP 105-20, where the OBC was determined based on the Superpave volumetric analysis and then verified with HWTT and I-FIT to ensure compliance with the rutting and cracking test requirements. Figure 4 presents the performance diagram of the N9 mix based on the mix design testing results provided by the contractor and ODOT. As shown, the mix passed ODOT's HWTT and the previous I-FIT requirements [i.e., a maximum rut depth of 12.5 mm at 20,000 passes and a minimum flexibility index (*FI*) of 8.0, respectively] and was expected to have balanced performance between rutting resistance and cracking resistance. The mix fell within the "sweet zone" of the performance diagram in Figure 4.

Table 1. Mix Design and Quality Control (QC) Data of N9, S1 Surface, and S1 Base Mixes

Sieve (in.)	Job Mix Design			Quality Control		
	N9	S1 Surface	S1 Base	N9	S1 Surface	S1 Base
25 mm (1”)	100	100	100	100	100	100
19 mm (3/4”)	100	100	98	100	100	99
12.5 mm (1/2")	100	94	89	100	94	89
9.5 mm (3/8”)	97	88	83	97	90	84
4.75 mm (#4)	77	63	62	76	68	63
2.36 mm (#8)	50	37	42	48	41	42
1.18 mm (#16)	34	24	28	33	28	28
0.60 mm (#30)	25	17	19	26	20	19
0.30 mm (#50)	18	10	12	18	13	12
0.15 mm (#100)	10	5	7	9	7	7
0.075 mm (#200)	6.5	4.5	5.7	6.0	5.4	5.2
Design Gyration	80	65	65	80	65	65
NMAS (mm)	9.5	12.5	19	9.5	12.5	19
OBC (%)	5.6	5.8	5.2	5.6	5.5	5.1
Virgin Binder	76-28 SBS	70-28 SBS	64-28 SBS	76-28 SBS	70-28 SBS	64-28 SBS
RAP Binder Ratio (%)	14	11	30	15	11	31
Air Voids (%)	4.0	3.4	3.4	2.1	2.3	2.7
Blend G_{sb}	2.642	2.619	2.633	2.663	2.632	2.614
G_{mm}	2.462	2.410	2.450	2.478	2.432	2.459
G_{mb}	2.364	2.329	2.367	2.427	2.377	2.392
VMA (%)	15.5	16.2	14.0	14.0	14.7	13.1
V_{be} (%)	11.5	12.8	10.6	11.9	12.4	10.4
VFA (%)	74	79	76	85	85	79
Dust Proportion	1.3	0.8	1.3	1.2	1.0	1.2

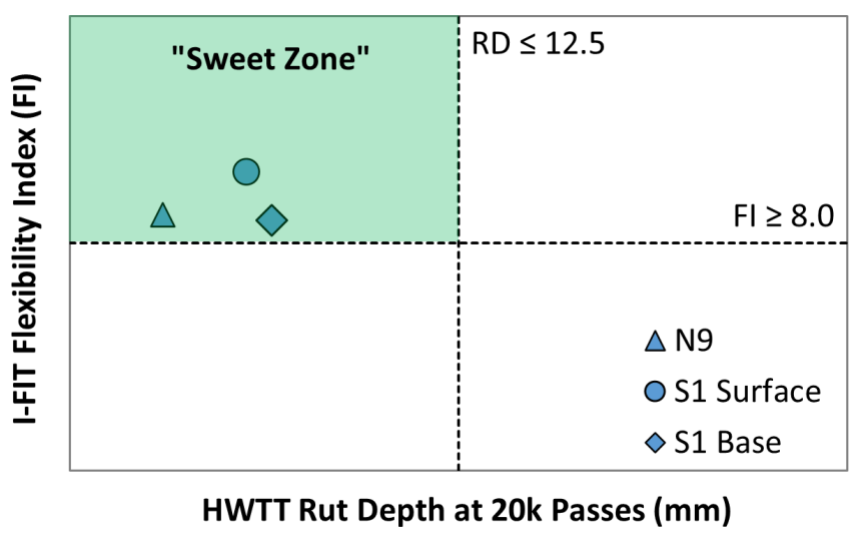

Figure 4. Performance Diagram from Mix Design Testing

The S1 surface mix was an ODOT S4 mix with a NMAS of 12.5 mm. The mix used a PG 70-28 SBS modified binder, a blend of granite, chat, and sand, as well as 12% RAP. The mix had an OBC of 5.8%, design air voids of 3.4%, and VMA of 16.2% at 65 gyrations. The S1 base mix was an ODOT S3 mix with a NMAS of 19 mm. The mix used a PG 64-28 SBS modified binder, a blend of granite

and sand, and 30% RAP. Because of the high RAP content, a tall-oil based recycling agent (RA) was added to improve the durability and cracking resistance of the mix at a dosage of 3.1% by weight of the virgin binder. The mix had an OBC of 5.2%, design air voids of 3.4%, and VMA of 14.0% at 65 gyrations. Both the S1 surface and base mixes were designed using the *Performance Modified Volumetric Design* approach as described in AASHTO PP 105-20, where an initial OBC was determined based on the Superpave volumetric analysis but then adjusted according to the mixture performance test results. At their final OBCs, both mixes passed ODOT's HWTT and the previous I-FIT requirements, which included a maximum rut depth of 12.5 mm at 15,000 passes (for the S1 surface mix) and 10,000 passes (for the S1 base mix), and a minimum *FI* of 8.0 for both mixes. As shown in Figure 4, the two mixes fell within the "sweet zone" of the performance diagram and were expected to have good rutting resistance and cracking performance.

13.5 Mix Production and Construction

Section N9 was built as a 1.5-inch mill-and-inlay on a 14-inch asphalt pavement. The mix was produced and placed on September 10, 2018 with a 24-hour high temperature of 84°F, a low temperature of 73°F, and less than 0.1 inch of 24-hour rainfall. With ODOT's approval, the mix was produced with a virgin binder at the same PG grade but from a different source than what was used by the contractor in Oklahoma for the mix design. The aggregates and RAP used for production were the same as mix design. As shown in Table 1, quality control testing of the production mix hit the target total binder content and gradation from the JMF. However, the production mix had 2.1% air voids and 14.0% VMA. Although these changes were outside ODOT's production tolerance, the performance test results of the production mix (which will be discussed later) indicated good rutting and cracking resistance. Given that the mix was designed using a BMD approach, ODOT agreed to relax the volumetric requirements for production and leave the mix in-place for performance evaluation on the Test Track. The mix had an average production temperature of approximately 325°F and in-place density of 96.4%. Figure 5 shows the mix laydown and compaction for Section N9.

Figure 5. Construction of Section N9

Section S1 was built as a 5.0-inch mill-and-inlay. The inlay was constructed in two layers; the bottom layer was the 19.0 NMAS mix constructed at 3.0 inches in thickness, while the 12.5 mm NMAS surface layer was constructed to 2.0 inches. Similar to the N9 mix, both the S1 surface and base mixes were produced with virgin binders at the same PG grades but from different sources as those used by the contractor in Oklahoma for mix design. The S1 base mix was produced and placed on September 20, 2018 and the surface mix was produced and placed on the next day. The climate conditions were ideal for paving with a 24-hour high temperature of 92°F, a low temperature of 73°F, and no rainfall.

As shown in Table 1, QC testing of the S1 base mix indicated a slight reduction in the total binder content from 5.2% in mix design to 5.1% at production but no significant changes in the combined aggregate gradation from the JMF. Although the mix had a reduction in air voids from 3.4% in mix design to 2.7% at production and a reduction in VMA from 14.0% to 13.1%, these differences were within ODOT's production tolerance. The S1 base mix had an average production temperature of approximately 305°F and in-place density of 94.6%. Figure 6 shows the laydown and compaction of the base mix for Section S1.

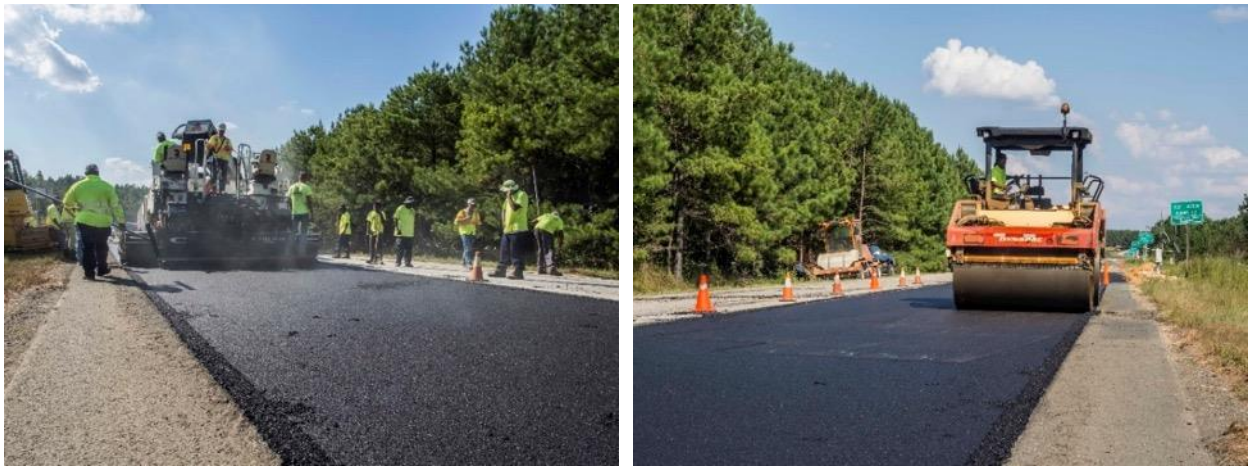

Figure 6. Construction of the Base Layer of Section S1

QC testing of the S1 surface mix showed a reduction in the total binder content from 5.8% in mix design to 5.5% at production but no significant changes in the combined aggregate gradation from JMF. Furthermore, the mix had a notable reduction in air voids from 3.4% in mix design to 2.3% at production and a reduction in VMA from 16.2% to 14.7%, but these changes were within ODOT's production tolerance. The S1 surface mix had an average production temperature of approximately 325°F and in-place density of 96.1%. Figure 7 shows the laydown and compaction of the surface mix for Section S1.

Figure 7. Construction of the Surface Layer of Section S1

13.6 Laboratory Testing and Data Analysis

During construction of the two sections, plant mixes were sampled from the Test Track and transported back to the NCAT lab, where they were reheated to fabricate plant-mixed, lab-compacted (PMLC) specimens for performance testing. HWTT and I-FIT were conducted to evaluate the rutting and cracking resistance, respectively, of the three plant-produced mixes and determine their compliance with ODOT's criteria. In addition, IDEAL-CT and Cantabro tests were conducted to explore their feasibility as surrogate cracking tests for BMD production testing. To consider the effect of asphalt aging on mixture durability and cracking resistance, the I-FIT, IDEAL-CT, and Cantabro tests were conducted on both reheated and critically aged PMLC specimens for the N9 and S1 surface mixes. The critical aging (CA) protocol used in the experiment was loose mix aging for eight hours at 135°C, which is expected to simulate a critical field aging condition of 70,000 cumulative degree days where top-down cracking starts to develop after four to five years in-service in Alabama (*3, 4*).

13.6.1 Production Test Results of N9 Mix

Figure 8 presents the HWTT and I-FIT results of the reheated PMLC specimens of the N9 mix on a performance diagram. The mix design testing results of short-term aged lab-mixed, lab-compacted (LMLC) specimens provided by the contractor in Oklahoma and ODOT are also presented for comparison purposes. As shown, the reheated PMLC specimens of the N9 mix had similar *FI* from the I-FIT testing, but significantly higher total rut depth (*TRD*) at 20,000 passes in HWTT than the LMLC specimens. The reheated PMLC specimens failed HWTT with 12.5 mm rutting at approximately 15,000 passes and a stripping inflection point of 11,786 passes. The HWTT rut depth curve in Figure 9(a) exhibited an apparent stripping phase, which indicated the occurrence of stripping failure during the test. Visual observation of the HWTT specimens after testing, shown in Figure 9(b), also confirmed the stripping of asphalt binder from the aggregate. Because of the stripping failure, the N9 production mix failed ODOT's HWTT criteria and fell outside the "sweet zone" of the performance diagram, as shown in Figure 8.

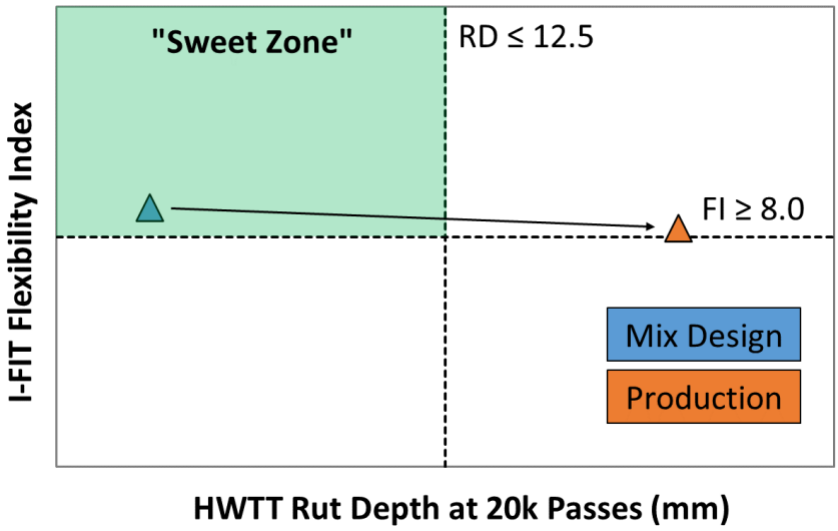

Figure 8. Performance Diagram of N9 Mix from Mix Design and Production Testing

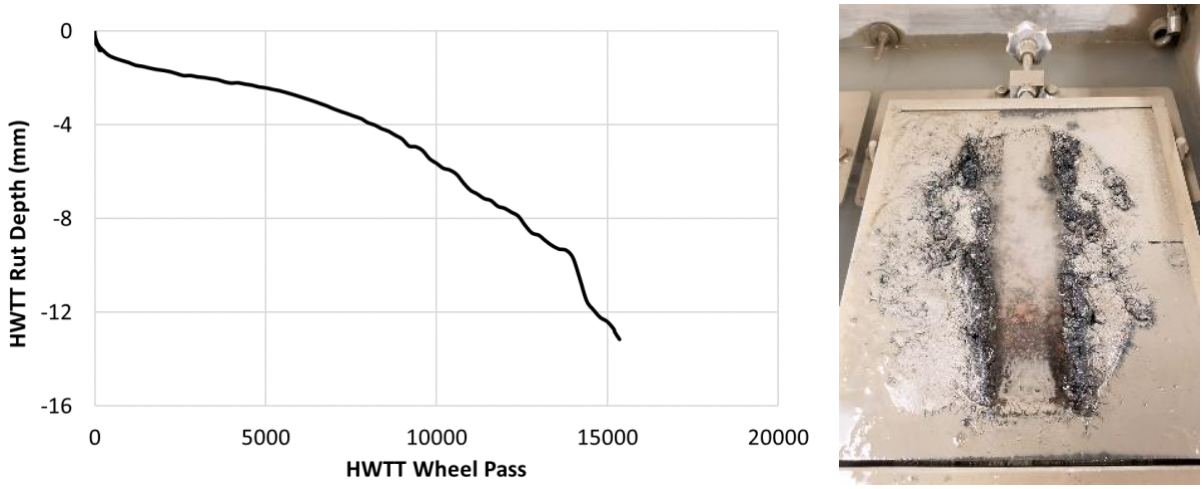

(a) (b)

Figure 9. HWTT Results of N9 Reheated PMLC Specimens; (a) Rut Depth Curve, (b) Specimens after Testing

The significant difference in HWTT results between the reheated PMLC and short-term aged LMLC specimens in Figure 8 may be attributed to several possible factors, including a change in binder source, changes associated with plant production, and between-lab variability associated with sample preparation and testing. For example, these two sets of specimens used virgin binders with the same PG grade (i.e., PG 76-28) but from different sources. Furthermore, the reheated PMLC specimens were prepared from the plant-produced mix while the LMLC specimens were prepared from the lab-produced mix. Finally, these two sets of specimens were tested at different laboratories. To investigate the effect of each individual factor on the HWTT results, two additional sets of LMLC specimens were prepared and tested in the HWTT at the NCAT lab. The first set was produced following the JMF and using the same PG 76-28 virgin binder as the contractor in Oklahoma for mix design, while the other set was prepared

following the JMF but using the PG 76-28 virgin binder sampled from the production of the N9 mix for Test Track construction.

Figure 10 presents the HWTT results of LMLC versus PMLC specimens for the N9 mix. The blue curve in the figure corresponds to the mix design specimens prepared by the contractor in Oklahoma and tested at the ODOT central lab. The orange curve corresponds to the mix design specimens prepared and tested at the NCAT lab. The grey curve corresponds to the mix design specimens using the virgin binder sampled from the production of the N9 mix for Test Track construction that were prepared and tested at the NCAT lab. Finally, the green curve corresponds to the reheated PMLC specimens prepared and tested at the NCAT lab. Comparison of these curves indicated that the significant difference in the HWTT results from the mix design and production testing in Figure 8 was mainly due to the between-lab variability associated with sample preparation and testing and changes associated with plant production. Changing binder source, however, did not have a significant impact on the HWTT results of LMLC specimens prepared and tested at the NCAT lab.

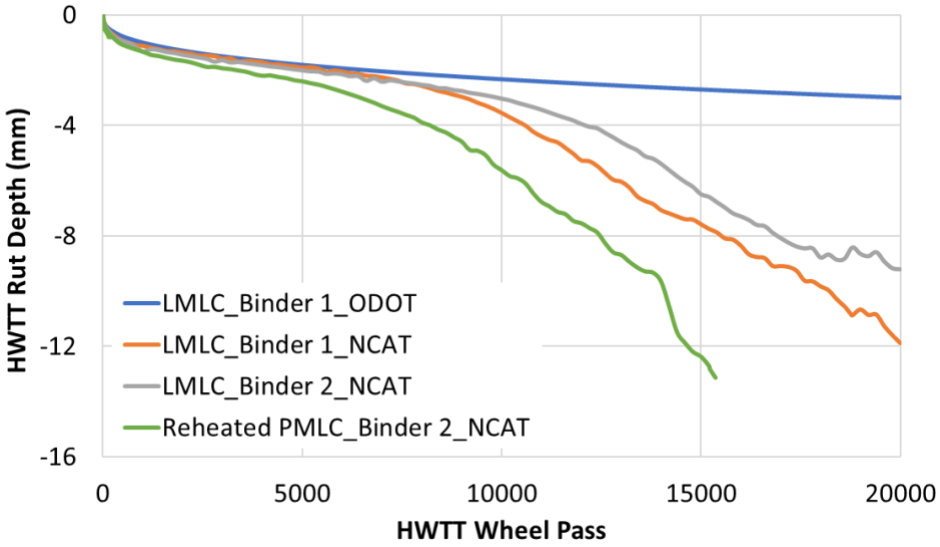

Figure 10. HWTT Curves of LMLC Versus Reheated PMLC Specimens for N9 Mix

To assess the rutting resistance of the N9 production mix, the HWTT results were analyzed with an alternative data analysis method based on a rutting parameter called the corrected rut depth (*CRD*). *CRD* is a simplified version of the viscoplastic strain increment parameter proposed by Yin et al. (*5*). Compared to the traditional HWTT rutting parameter of *TRD*, *CRD* isolates the rut depth caused by permanent deformation of the mix from stripping and thus, is expected to provide a more accurate indication of rutting resistance. Furthermore, *CRD* has shown to have a better correlation with the field rutting data on the NCAT Test Track than *TRD* (*6*). Based on the alternative HWTT analysis, the reheated PMLC specimens had a *CRD* of 3.5 mm at 20,000 passes, which indicated that the production mix had satisfactory rutting resistance and was not expected to have a rutting failure on the Test Track. Similar findings were also obtained in the High-temperature Indirect Tensile (HT-IDT) test and the Indirect Tensile Asphalt Rutting Test (IDEAL-RT) results, where the reheated PMLC specimens had an

average HT-IDT strength of 36.4 psi and rutting tolerance index (RT_{index}) of 110.8 when tested at 50°C. Although the criterion development of these two tests is still at an early stage, the preliminary HT-IDT test criterion used by the Alabama DOT is a minimum HT-IDT strength of 20 psi. For IDEAL-RT, Zhou has recommended a minimum preliminary RT_{index} of 60, 65, and 75 for mixes containing a PG 64-xx, PG 70-xx, and PG 76-xx (or higher) binder, respectively, via email correspondence. Therefore, the HT-IDT and IDEAL-CT results confirmed the excellent rutting resistance of the N9 production mix.

Although the HWTT results shown in Figures 9 and 10 indicate that the N9 production mix was highly susceptible to moisture damage, the Tensile Strength Ratio (TSR) test results provide a different conclusion. The reheated PMLC specimens had an average conditioned strength of 128.6 psi and an average unconditioned strength of 146.1 psi, which yielded a TSR of 88.0%. These results passed ODOT's TSR requirement for Superpave mix designs. The discrepancy in the HWTT and TSR results is likely attributed to the different moisture conditioning procedures used in the two tests. This discrepancy is a concern to state highway agencies for the evaluation of moisture resistance in BMD and warrants further research investigation.

13.6.2 Production Test Results of S1 Surface and Base Mixes

Figure 11 presents the performance diagram of the reheated PMLC specimens for the S1 surface and base mixes, where the I-FIT results are plotted on the y-axis against the HWTT results on the x-axis. The mix design testing results of short-term aged LMLC specimens provided by the contractor in Oklahoma and ODOT are also presented for comparison purposes. As shown, for both mixes, the reheated PMLC specimens had similar HWTT *TRD* but significantly reduced I-FIT *FI* results than the LMLC specimens. The reheated PMLC specimens of the S1 surface and base mixes had an average *FI* of 5.5 and 3.2, respectively, which failed ODOT's previous criterion of a minimum *FI* of 8.0 for mix design approval. Therefore, the reheated PMLC specimens of both mixes fell outside the "sweet zone" of the performance diagram, as shown in Figure 11.

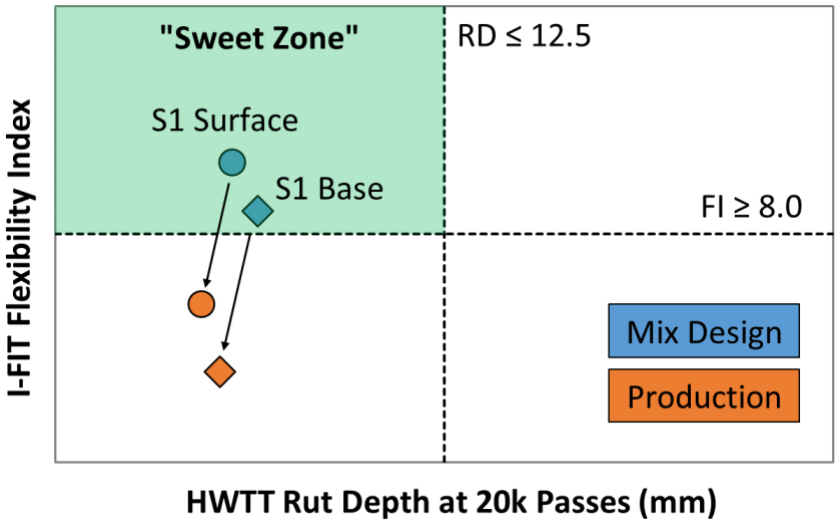

Figure 11. Performance Diagram of S1 Surface and Base Mixes from Mix Design and Production Testing

Similar to the previous discussions about the HWTT results of the N9 mix, the difference in the I-FIT results from mix design versus production testing for the S1 surface and base mixes (Figure 11) could be caused by several possible factors, including a change in binder source, changes in the mix associated with plant production, and between-lab variability associated with sample preparation and testing. To determine the effect of each individual factor, two sets of LMLC specimens were prepared for the S1 surface mix following the JMF but using different virgin binders from the contractor's mix design and the production of plant mix for Test Track construction, respectively, and tested for I-FIT at the NCAT lab.

Figure 12 presents the I-FIT results of different LMLC versus reheated PMLC specimens for the S1 surface mix. The blue bar corresponds to the mix design specimens prepared by the contractor in Oklahoma and tested at the ODOT central lab, orange corresponds to the mix design specimens prepared and tested at the NCAT lab, grey corresponds to the mix design specimens prepared with the virgin binder sampled from the production of plant mix for Test Track construction that were prepared and tested at the NCAT lab, and green corresponds to the reheated PMLC specimens prepared and tested at the NCAT lab. As shown, the significant reduction in the *FI* results from the mix design testing at the ODOT central lab to the production testing at the NCAT lab was mainly due to changes in the mix associated with plant production and possibly different mix aging conditions of mix design and production samples as indicated by the difference between the grey and green bars. On the other hand, between-lab variability and changing binder source did not have significant impacts on the I-FIT results of LMLC specimens.

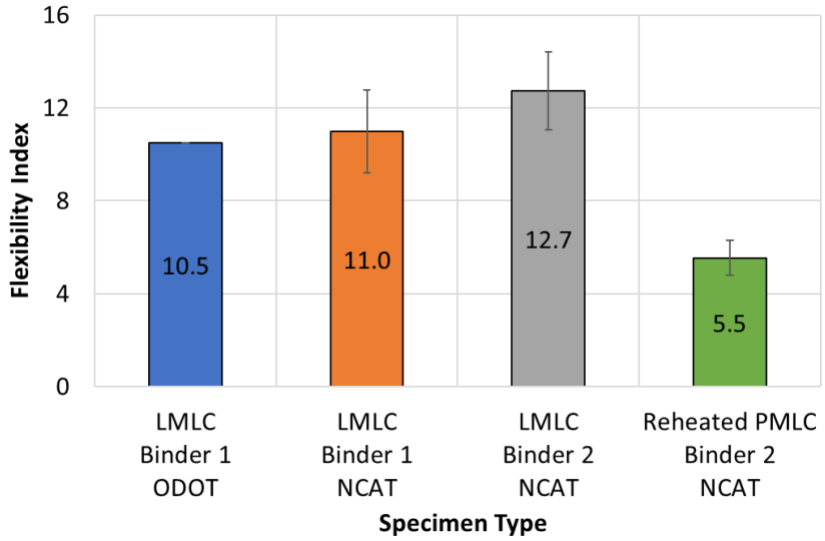

Figure 12. I-FIT Results of LMLC Versus Reheated PMLC Specimens for S1 Surface Mix

13.6.3 Impact of Critical Aging on Mixture Cracking Test Results

Figures 13 through 15 present the I-FIT, IDEAL-CT, and Cantabro test results of reheated versus critically aged PMLC specimens, respectively. Although critical aging is appropriate for surface mixes only, the S1 base mix was also tested in the I-FIT, IDEAL-CT, and Cantabro tests at both reheated and critically aged conditions to assess its aging susceptibility. For all three mixes

tested, the critically aged PMLC specimens showed consistently reduced cracking resistance and durability compared to the reheated PMLC specimens, as indicated by reduced *FI* and CT_{Index} results and increased Cantabro mass losses. To quantify the susceptibility of different mixes to critical aging, the absolute percentage change in the cracking test results after critical aging was determined; the results are summarized in Table 2. As shown, regardless of the cracking tests, the S1 base mix showed the highest absolute percentage change and thus, was expected to be most susceptible to aging, followed by the N9 mix and the S1 surface mix, respectively. The higher aging susceptibility of the S1 base mix was likely attributed to the use of a softer PG 64-28 virgin binder and a recycling agent. As previously noted, critical aging of non-surface mixes is considered unnecessary at this point.

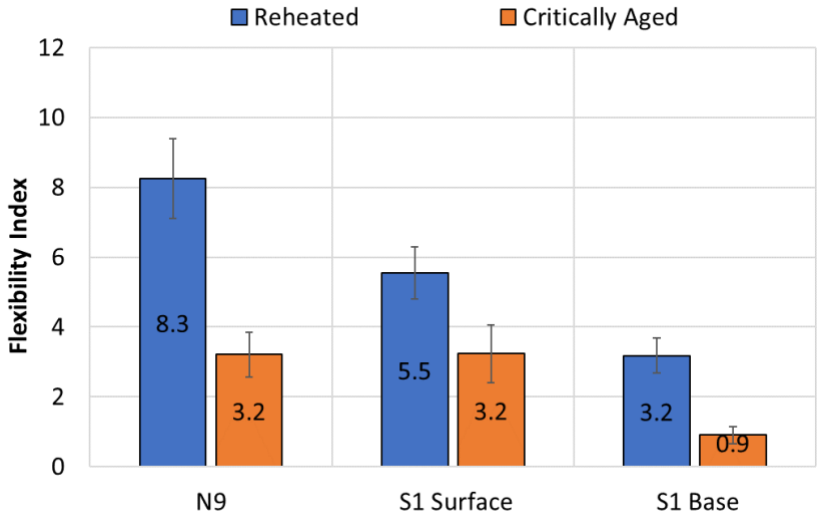

Figure 13. I-FIT Results of Reheated Versus Critically Aged PMLC Specimens

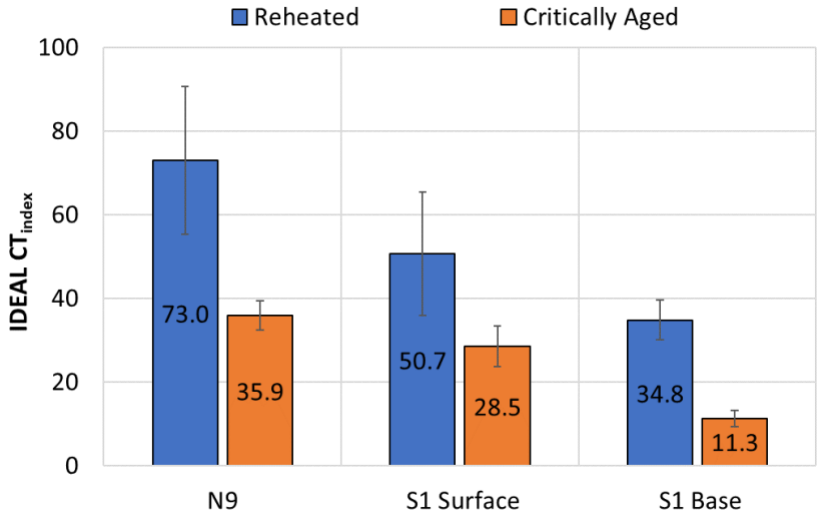

Figure 14. IDEAL-CT Results of Reheated Versus Critically Aged PMLC Specimens

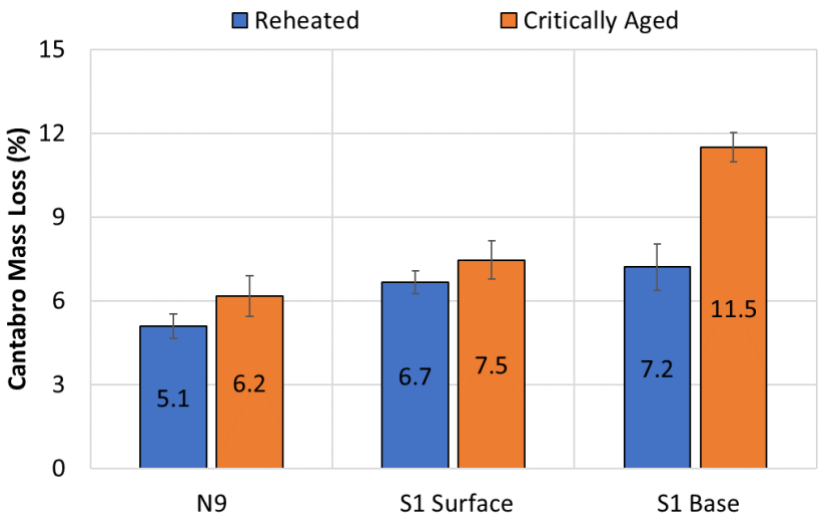

Figure 15. Cantabro Test Results of Reheated Versus Critically Aged PMLC Specimens

Table 2. Absolute Percentage Change in Cracking Test Results after Critical Aging

Mix ID	I-FIT *FI*	IDEAL CT_{Index}	Cantabro *Mass Loss*
N9	61.1%	50.9%	21.0%
S1 Surface	41.7%	43.7%	12.1%
S1 Base	71.6%	67.6%	59.6%

13.6.4 Correlation between I-FIT, IDEAL-CT, and Cantabro Test Results

Figures 16 and 17 present the correlations between the I-FIT, IDEAL-CT, and Cantabro test results. In this study, the I-FIT was used as the mixture cracking test for mix design testing while the IDEAL-CT and Cantabro tests were evaluated as two candidate surrogate tests for production testing. The N9 and S1 surface mixes were tested with three sets of specimens: the short-term aged LMLC specimens prepared with the virgin binder sampled from plant production, the reheated PMLC specimens, and the critically aged PMLC specimens. The S1 base mix was tested with the reheated and critically aged PMLC specimens only.

As shown in Figure 16, there was a very strong linear correlation (R^2 = 0.9814) between the I-FIT and IDEAL-CT results among the three mixes, where the *FI* and CT_{index} parameters were positively correlated to each other. A strong linear relationship (R^2 = 0.7779) was observed between the I-FIT and Cantabro results in Figure 19, but the *FI* and Cantabro mass loss showed a negative correlation. These results highlighted the potential of using the IDEAL-CT and Cantabro test as surrogate performance tests to I-FIT for BMD production testing. However, the strong correlations observed in Figures 16 and 17 were based on three mixes only and thus, should be interpreted with caution. Previous studies have indicated that the I-FIT and IDEAL-CT results do not always correlate to each other, depending on the mixture type, aggregate gradation, virgin binder grade, and recycled materials content, among other factors (*7, 8, 9*). Therefore, it is not advisable for state highway agencies to utilize a "universal" correlation to determine production criteria for IDEAL-CT based on mix design criteria using I-FIT. Mix-specific correlations, however, may exist between the two cracking tests and need further investigation.

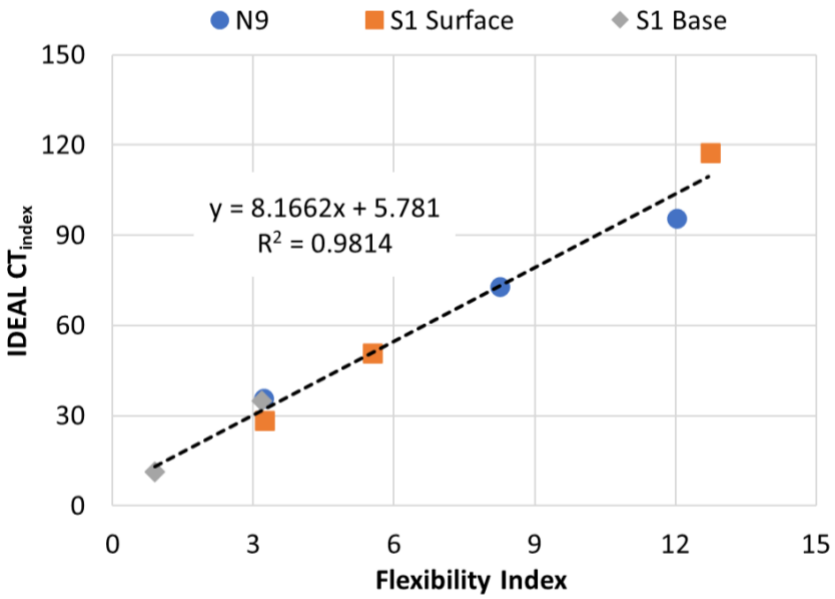

Figure 16. Correlation Between I-FIT and IDEAL-CT Results

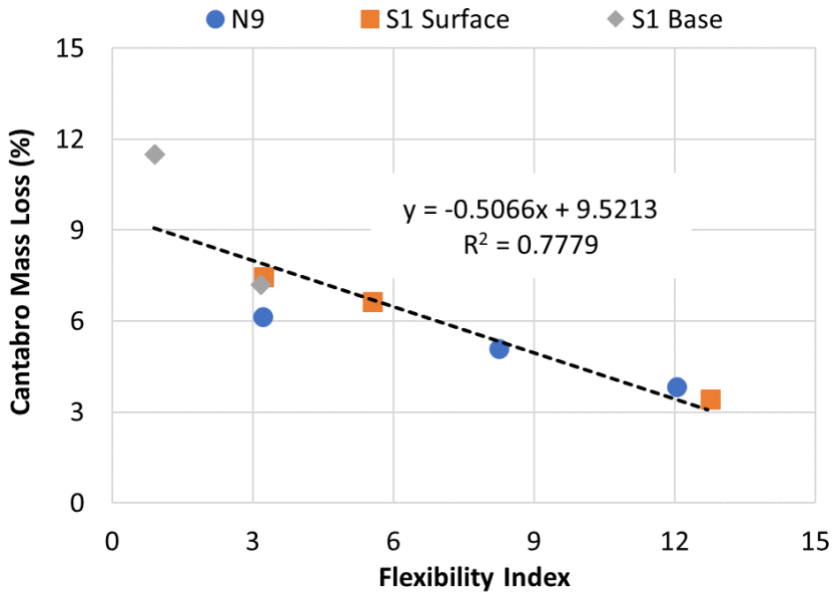

Figure 17. Correlation Between I-FIT and Cantabro Test Results

13.7 Field Performance

Heavy traffic loading of the two sections on the NCAT Test Track started on October 10, 2018. As of February 24, 2021, 10 million ESALs of heavy truck traffic had been applied. Throughout trafficking of the test sections, surface cracking, rutting, smoothness, and surface texture were monitored on a weekly basis using an automated pavement condition survey vehicle. Additionally, surface friction was measured every month using a locked-wheel friction trailer.

Figure 18 presents the field rutting data. Both sections have performed very well in terms of rutting resistance. Section N9 had almost no measurable rutting after 10 million ESALs. Section S1 had approximately 0.30 inches of rutting with most occurring in the summer of 2019. The

field rutting performance of N9 is consistent with the HWTT *CRD*, HT-IDT, and IDEAL-RT results of the reheated PMLC specimens, which indicated that the production mix had satisfactory rutting resistance although it failed ODOT's HWTT requirements due to stripping failure. No signs of moisture damage are evident in either Section S1 or N9.

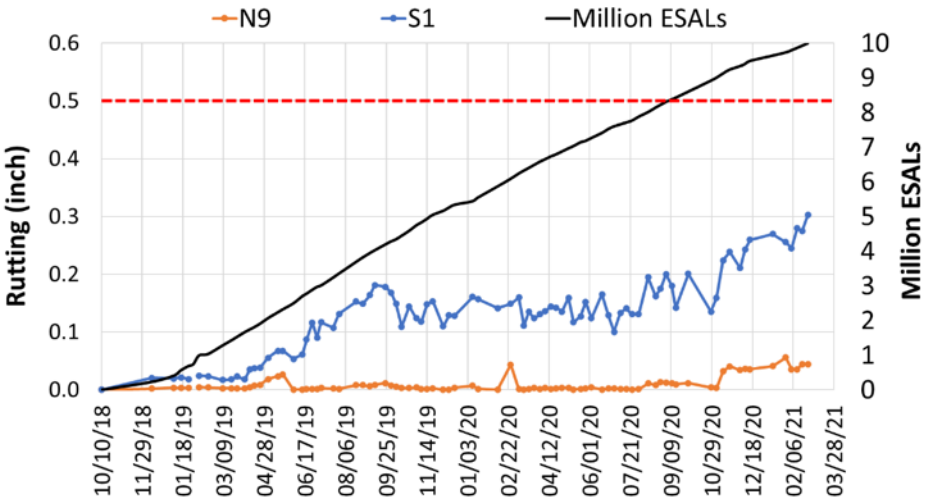

Figure 18. Field Rutting Data

Figure 19 presents the surface cracking data of sections N9 and S1, where cracking is expressed as percent of lane area cracked. Both sections showed excellent cracking performance after 10 million ESALs. Although the reheated PMLC specimens of the S1 surface and base mixes failed ODOT's previous I-FIT criteria and current IDEAL-CT criteria, Section S1 had no cracking as of February 24, 2021. Section N9 had only 3.3% of lane area cracked, with the first cracking observed along the left wheel path in January 2020. Coring of the cracked area confirmed that this cracking was caused by the reflection of previously existing cracking in the underlying layer, as shown in Figure 20.

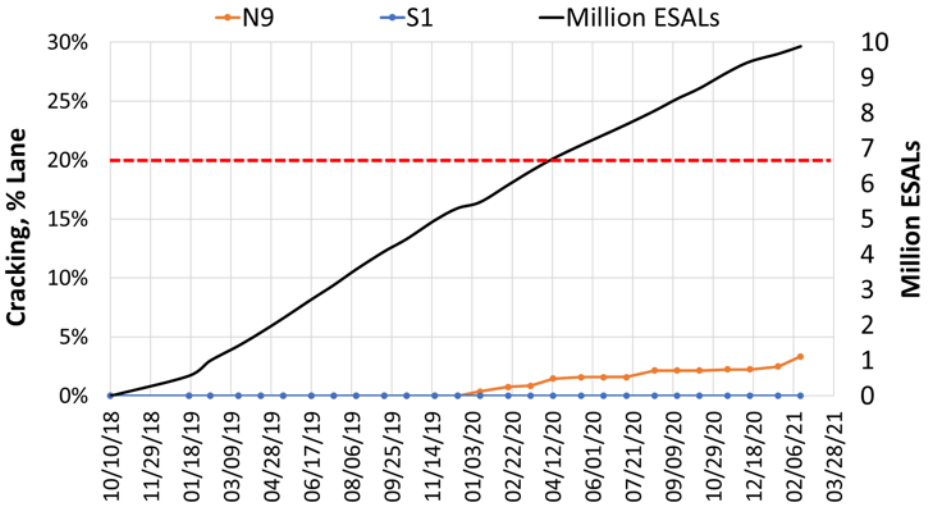

Figure 19. Field Cracking Data

Figure 20. Field Core from Cracked Area in Section N9

Figures 21 through 23 present the smoothness, texture, and friction data. Both sections showed no significant changes in the international roughness index (IRI) and mean texture depth (MTD) results after being trafficked for 10 million ESALs. The skid number results in Figure 23 show slight reductions over time but are well above the general threshold of 25.

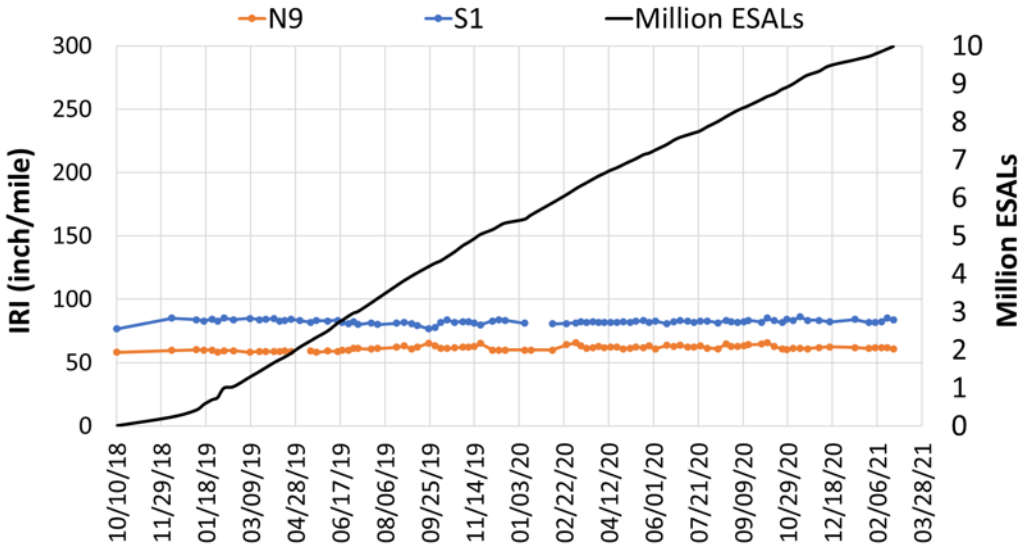

Figure 21. Field Smoothness Data

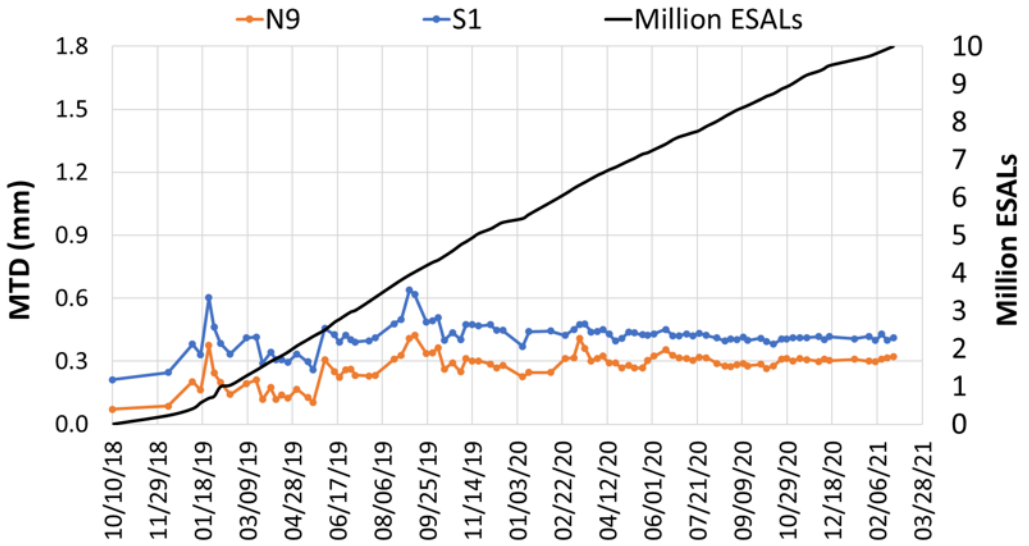

Figure 22. Field Texture Data

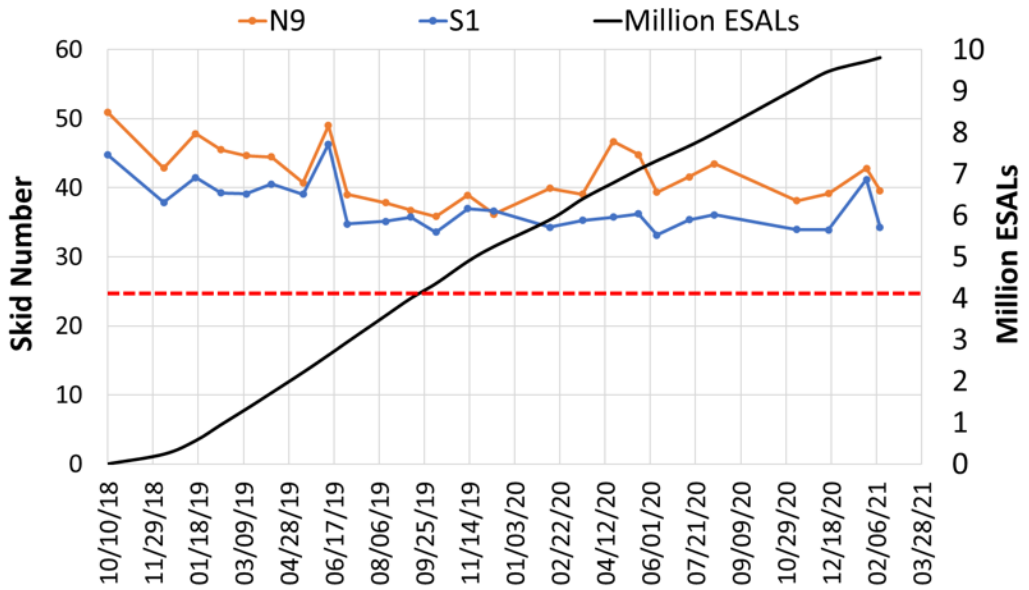

Figure 23. Field Friction Data

13.8 Conclusions and Recommendations

Based on the laboratory test results and field performance data collected after 10 million ESALs, the following conclusions and recommendations are made.

- The N9 production mix had similar I-FIT but significantly reduced HWTT results than the design mix prepared by the contractor in Oklahoma. The production mix failed ODOT's HWTT criterion due to stripping failure and thus, fell outside the "sweet zone" on the BMD performance diagram.
- The significant reduction in HWTT results between the N9 production mix and the design mix was mainly caused by the between-lab variability associated with sample

preparation and testing as well as changes the in the mix associated with plant production. Changing binder source did not have a significant impact on the HWTT results of LMLC specimens prepared and tested at the NCAT lab.

- Although the N9 production mix failed HWTT due to stripping failure, the alternative data analysis using the *CRD* parameter indicated that the mix had satisfactory rutting resistance and was not expected to have a rutting failure on the Test Track. Similar findings were also obtained based on the HT-IDT test and IDEAL-RT results.
- The HWTT and TSR results of the N9 production mix provided different conclusions regarding the evaluation of moisture resistance. This discrepancy is likely attributed to the different moisture conditioning procedures associated with the two tests and warrants further research investigation. No signs of moisture damage have been evident in the field for Section N9, which indicates a potential false positive HWTT stripping failure of the production mix.
- For the S1 surface and base mixes, the production mix had similar HWTT but significantly lower I-FIT results than the design mix prepared by the contractor in Oklahoma. Both production mixes failed ODOT's previous I-FIT criterion and thus, fell outside the "sweet zone" of the BMD performance diagram.
- The significant reduction in I-FIT results between the production versus design mix for the S1 surface and base mixes was mainly caused by changes in the mix associated with plant production and possibly different mix aging conditions of mix design and production samples. Between-lab variability and changing the binder source did not have significant impacts on the I-FIT results of LMLC specimens.
- The critical aging protocol of aging loose mix for eight hours at 135°C significantly reduced the cracking resistance and durability of the N9, S1 surface, and S1 base mixes. Although the S1 base mix was found to be most susceptible to critical aging, which was likely due to the use of a softer virgin binder and a recycling agent, aging of the base layer in the field is not expected to be a significant concern.
- Strong linear correlations were observed between the I-FIT, IDEAL-CT, and Cantabro test results, which indicated the potential of using the IDEAL-CT and Cantabro test as surrogate cracking tests to I-FIT for BMD production testing. However, these correlations were established based on three mixes only, and thus, should be interpreted with caution.
- Sections N9 and S1 performed very well with minimal rutting and cracking after 10 million ESALs. Neither section had significant changes in roughness or texture. The skid number results showed slight reductions over time, but they were well above the general threshold from a safety perspective.
- Although the N9 production mix failed ODOT's production tolerance for volumetric properties (i.e., air voids and VMA), it had excellent field performance on the Test Track after 10 million ESALs. This indicates a lack of correlation between mix volumetrics and field performance. Therefore, it is recommended for ODOT to consider further relaxing the volumetric requirements for mix design approval and production acceptance of BMD mixes provided that the performance test requirements are met.

- Because the reheated PMLC specimens of the S1 surface and base mixes failed ODOT's previous I-FIT and current IDEAL-CT criteria, it is recommended to leave section S1 for traffic continuation in the next research cycle to further monitor its long-term performance on the Test Track. This longer-term cracking performance data will be highly valuable for ODOT to assess the robustness of their current IDEAL-CT criteria for the implementation of BMD in Oklahoma.

13.9 References

1. Al-Qadi, I.L., H. Ozer, J. Lambros, A. El Khatib, P. Singhvi, T. Khan, J. Rivera-Perez, and B. Doll. *Testing Protocols to Ensure Performance of High Asphalt Binder Replacement Mixes Using RAP and RAS*. Illinois Center for Transportation/Illinois Department of Transportation, 2015.
2. Zhou, F., S. Im, L. Sun, and T. Scullion. Development of an IDEAL Cracking Test for Asphalt Mix Design and QC/QA. *Road Materials and Pavement Design*, 18(sup4), 2017, pp. 405-427.
3. Chen, C., F. Yin, P. Turner, R. C. West, and N. Tran. Selecting a Laboratory Loose Mix Aging Protocol for the NCAT Top-Down Cracking Experiment. *Transportation Research Record: Journal of the Transportation Research Board, No. 2672,* Transportation Research Board of the National Academies, Washington, D.C., 2018, pp.359-371.
4. Chen, C., F. Yin, A. Andriescu, R. Moraes, D. Mensching, N. Tran, A. Taylor, and R. West. Preliminary Validation of the Critical Aging Protocol for NCAT Top-down Cracking Experiment. *Journal of the Association of Asphalt Paving Technologists*, Vol. 89, 2020.
5. Yin, F., E. Arambula, R. Lytton, A. E. Martin, and L. G. Cucalon. Novel Method for Moisture Susceptibility and Rutting Evaluation Using Hamburg Wheel Tracking Test. *Transportation Research Record: Journal of the Transportation Research Board, No. 2446,* Transportation Research Board of the National Academies, Washington, D.C., 2014, pp.1-7.
6. Yin, F., C. Chen, R. West, A. E. Martin, and E. Arambula-Mercado. Determining the Relationship Among Hamburg Wheel-Tracking Test Parameters and Correlation to Field Performance of Asphalt Pavements. *Transportation Research Record: Journal of the Transportation Research Board, No. 2674,* Transportation Research Board of the National Academies, Washington, D.C., 2020, pp.281-291.
7. Moore, N. *Update on Cracking Group Experiments*. 2019 MAAPT Conference, December 5, 2019.
8. Al-Qadi, I.L. *Illinois Flexibility Index Test (I-FIT): Theory, Variability, & Field Validation*. AASHTO COMP Technical Subcommittee 2d – Proportioning of Asphalt-Aggregate Mixtures Meeting, August 4, 2020.
9. Yin, F., A. J. Taylor, and N. Tran. *Performance Testing for Quality Control and Acceptance of Balanced Mix Design*. NCAT Report 20-02. National Center for Asphalt Technology at Auburn University, Auburn, Ala., 2020.

14. PROACTIVE PAVEMENT PRESERVATION

Dr. Adriana Vargas

14.1 Background

Pavement preservation refers to "a program employing a network level, long-term strategy that enhances pavement performance by using an integrated, cost-effective set of practices that extend pavement life, improve safety and meet motorist expectations" (*1*). By applying preservation treatments at the right time, it is possible to keep good roads good with minimal investments instead of performing costly rehabilitation treatments later in a pavement's life when the structure has deteriorated (*2*).

Micro surfacing is a popular pavement preservation treatment that consists of a mixture of polymer-modified asphalt emulsion, graded aggregates, mineral filler, water, and other additives. The mixture is made by a specialized machine and placed on a continuous basis by mixing the materials simultaneously in a pug mill. This treatment is capable of addressing minor surface defects, protecting the pavement structure from moisture, and extending overall pavement life when applied to structurally sound pavements (*3, 4*).

As with other preservation treatments, performance of treated sections depends on many factors, including climatic conditions, traffic volumes, existing pavement condition, material quality, mixture design, and construction quality (*5*). Estimates for pavement life extension typically range from three to seven years; however, the criteria for defining performance varies among sources (*6*). Service life extension is usually estimated based on rutting or roughness; nonetheless, micro surfacing has also shown to slow the progress of reflective cracking (*7*).

Micro surfacing has been successful on high-volume roads across the United States, where good performance has been achieved on Interstate routes subjected to heavy traffic (*8*).

14.2 Objective and Scope

The objective of this study was to evaluate the field performance of a micro surfacing test section subjected to full-scale accelerated pavement testing. The treatment was placed on half of Section N6 on the NCAT Test Track and its performance was compared to the remaining untreated section.

14.3 Test Sections

Section N6 was identified as a suitable candidate for pavement preservation. Originally constructed in 2009, the pavement consisted of 7 inches of asphalt concrete over 4.8 inches of aggregate base and had started to show signs of deterioration (mainly rutting and weathering) after receiving over 17.5 million equivalent single axle loads (ESALs) in 2014, but was in overall good condition. The wearing surface was a fine-graded 9.5 mm nominal maximum aggregate size Superpave mixture containing a PG 76-22 polymer-modified binder (*9*).

The 200-ft section was split into two subsections, leaving one untreated and placing a Type II micro surface on the other. This provided an opportunity for direct comparison and assessment of treatment benefits.

14.4 Micro Surfacing Treatment

A Type II micro surfacing treatment was designed following the recommendations outlined in the International Slurry Surfacing Association (ISSA) A143 guidelines (*10*). The aggregate type used was granite with a gradation as shown in Table 1. In addition, the mineral filler used was Portland cement, and the asphalt emulsion was a CSS-1HP grade with properties as shown in Table 2. The mix design yielded an optimum emulsion content of 12% and a 1% cement content.

The choice of a Type II micro surface (a finer mixture compared to the Type III alternative) was made to match other test sections previously constructed on an open roadway as part of the same research study, which were not subjected to accelerated testing.

Table 1. Aggregate Gradation

Sieve Size	% Passing	Specification*
3/8"	100	100
#4	98	90-100
#8	74	65-90
#16	49	45-70
#30	33	30-50
#50	21	18-30
#100	15	10-21
#200	11.3	5-15

*As outlined by the ISSA guidelines (*10*)

Table 2. Emulsion Properties

Property		AASHTO Test Method	Result	Specification
Viscosity, Saybolt Furol, SFS	50°C	T 59	29	20-100
Particle charge			Positive	Positive
Sieve Test, %			0.02	0.1 max
Residue by distillation, %			63.8	62.0 min
Penetration (100 g, 5 sec.), dmm	25°C	T 49	64	40-90
Softening point, °F		T 53	158.5	135 min
Solubility in TCE, %		T 44	99.25	97.5 min

The micro surfacing treatment was applied on April 28, 2014 on the first 100 ft of the test section (N6A). Prior to construction, the equipment was calibrated to ensure the specified amounts of materials were being used. A trial application was conducted to ensure that adequate workmanship, aesthetics, and cure time of the mixture were achievable when applied on the test section. The trail application was performed under similar conditions as those expected during actual application.

A plastic strip was placed at the stopping point to ensure a sharp, uniform edge. The treatment was applied to the clean pavement surface with a variable width spreader box equipped with augers and a secondary strike off at a rate of 24 lbs/yd^2. Due to various maintenance activities being conducted at the Track during that time, fleet operations were suspended from April 26 to May 2, 2014. Cones were placed around the section as a precaution to protect it from light traffic and construction equipment until it had properly cured. However, vehicles were unlikely

to drive on the test section as the inside lane is typically used during maintenance and construction activities. Normal traffic operations resumed on May 2 without any issues. Figures 1 and 2 show the treatment application on N6A.

Figure 1. Micro Surfacing Application on Section N6A

Figure 2. Plastic Strip at Stopping Point

14.5 Performance Measurement

Performance data were obtained weekly using a data collection vehicle equipped with an inertial profiler, laser systems, and high-resolution cameras. The inertial profiler collected the longitudinal profile of the pavement surface for both wheel paths. These profiles were used to

measure the roughness of the pavement in terms of the international roughness index (IRI). Laser rut and mean texture depth (MTD) measurements were also obtained. The images obtained with the high-resolution cameras were processed to assess the extent of detected cracking. In addition, friction was measured monthly with a locked-wheel skid trailer using a ribbed tire at 40 mph on a wet surface according to ASTM E274.

Three of the measurements obtained (cracking, rutting, and IRI) were used to assign condition categories based on the performance criteria established by the Federal Highway Administration, as shown in Table 3 (*11*). These criteria are used by state departments of transportation to develop and implement transportation asset management plans and therefore were included in this research as a means of evaluating the effectiveness of the treatment.

Table 3. Pavement Condition Categories (*11*)

Condition Rating	Cracking, %	Rutting, in	IRI, in/mi
Good	< 5%	< 0.2	< 95
Fair	5 – 20%	0.2 – 0.4	95 – 170
Poor	> 20%	> 0.4	> 170

14.6 Initial Condition

At the time of treatment application in April 2014, the existing pavement had been in place for approximately five years and had been subjected to 17,534,537 ESALs. Although this represents moderately heavy traffic loading, the section was in relatively good condition, as seen in Table 4.

Table 4. Initial Pavement Condition

Indicator	Section Average	Condition Category
Cracking, %	1.8	Good
Rut depth, in	0.33	Fair
IRI, in/mi	62.6	Good
MTD, mm	0.66	Not Applicable
Skid number	43.2	Not Applicable

It should be noted that the amount of cracking presented in Table 3 refers to the percentage of the total lane area. The rutting, IRI, MTD, and friction measurements were uniform across the test section; however, once the section was split into subsections N6A and N6B, the resulting cracking percentages were 2.3 and 1.4%, respectively. Although slightly different, both amounts were considered minimal and representative of “good” cracking performance. Section N6A was selected as the pavement preservation section and received a Type II micro surface, while Section N6B was left untreated and used as a control.

14.7 Field Performance

Following treatment application, traffic operations were resumed and carried out through the end of Phase VII in February 2021. Since its original construction in 2009, the pavement section has been subjected to a total of 39.1 million ESALs. The treated surface portion of the section has accumulated 21.6 million ESALs since its application in 2014.

It should be noted that the untreated portion (section N6B) did not survive until the end of the research cycle and had to be milled and inlaid in May 2020 due to the amount and severity of distress observed, including rutting and depressions that compromised the safety of traffic operations. Figure 3 shows a timeline along with accumulated traffic for the test section. Due to traffic diversions resulting from work performed on or around the test section, the accumulated ESALs for Phase VII was under the target 10 million set for each phase.

The following sections provide a comparison of the two subsections at two points in time that clearly highlight the effect of pavement preservation: prior to micro surfacing application and when rehabilitation was required in the control section.

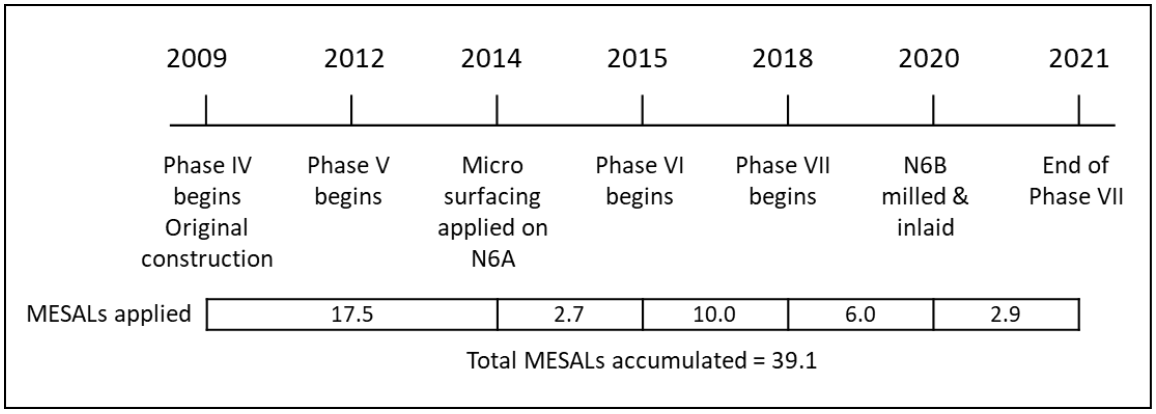

Figure 3. Section Timeline and Traffic

14.7.1 Cracking

The total cracking percentages are shown in Figure 4. Although micro surfacing is not considered a crack mitigating treatment, it is evident that cracking performance was significantly improved in the treated section. While both sections exhibited similar amounts of cracking at the time of treatment, the control section developed approximately 1.7 times more cracking than the treated surface before it had to be repaired. By May 2020, the control section had reached the “poor” condition category, while the micro surfacing section was still in “fair” condition.

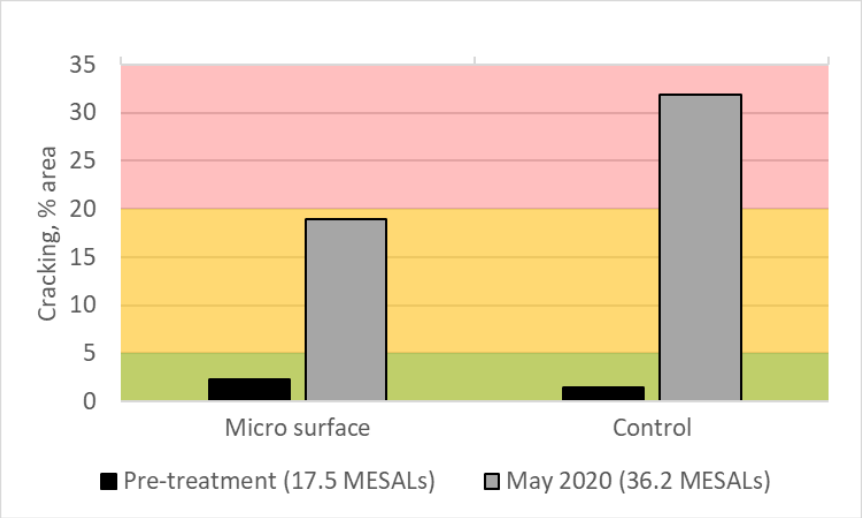

Figure 4. Cracking Performance

It should be noted that the type of cracking observed was mostly low severity fatigue cracking, manifested as longitudinal cracking with a few interconnected cracks along the wheel paths and widths under 10 mm. However, in the control section, some cracking areas were also accompanied by pumping and depressions (Figure 5), which accelerated the deterioration of the pavement compared to the micro surfaced section.

Figure 5. Cracking and Depressions in Untreated Section

14.7.2 Rutting

Prior to treatment application, the section exhibited moderate amounts of rutting, between 0.2 and 0.4 inches. As shown in Figure 6, micro surfacing reduced the average rut depth in more

than half to a range that can be considered in “good” condition, while in the untreated section, rut depths continued to increase under traffic, reaching more than 0.4 inches and falling into the “poor” condition category before being repaired.

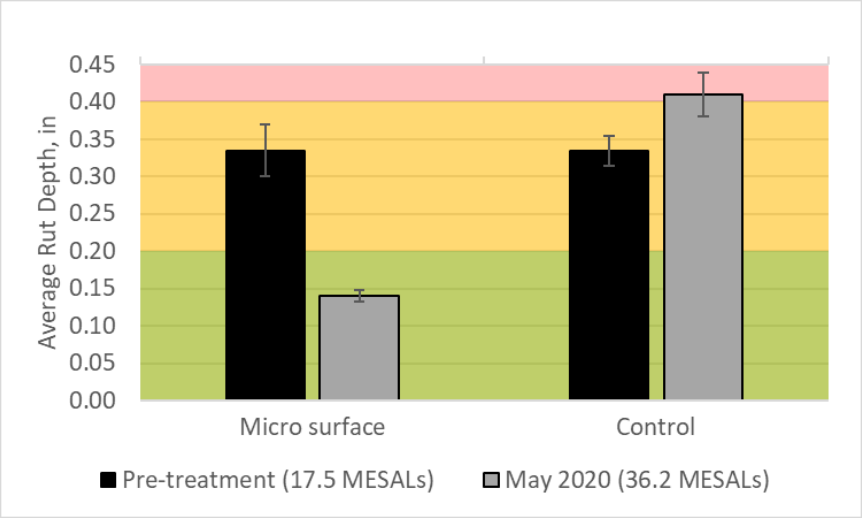

Figure 6. Rutting Performance

14.7.3 Roughness

At the time of treatment, ride quality (measured by means of IRI) was considered in “good” condition with values under 95 in/mi. Since then, IRI values increased as part of the normal deterioration process. However, while the treated section remained just below the 95 in/mi threshold, the control section deteriorated to the “fair” condition category as seen in Figure 7.

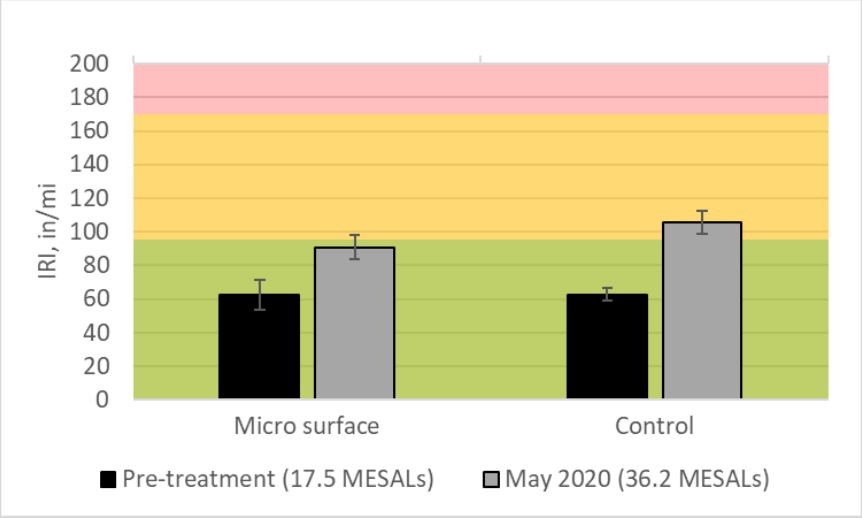

Figure 7. Roughness Performance

14.7.4 Macrotexture and Friction

In general, surface characteristics such as macrotexture and friction have shown little variation since the test section was divided in 2014. The only significant change observed was an increase

in mean texture depth (MTD) in the control section, associated with weathering and raveling of the original surface (Figures 8 and 9).

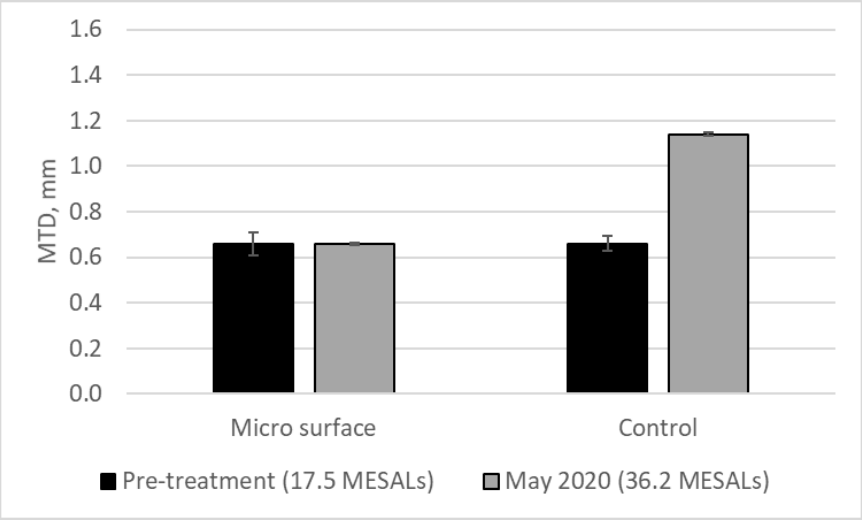

Figure 8. Macrotexture Comparison of Test Sections

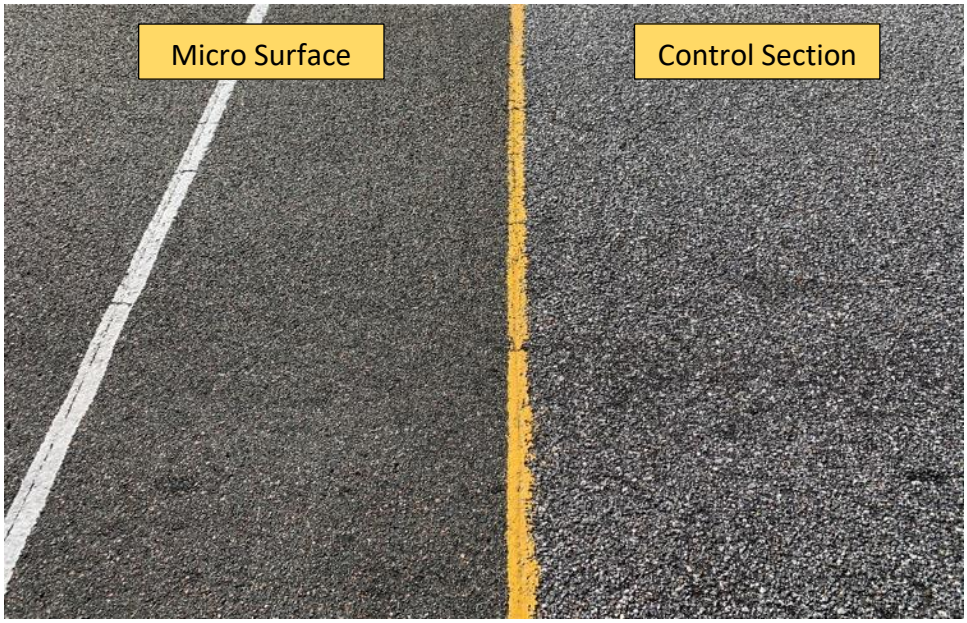

Figure 9. Surface Condition of Test Sections

Friction is monitored along with distress data to ensure the safety of traffic operations. While there is no official threshold for minimum skid number, the values observed in each section both before and after treatment application (Figure 10), are well above what various state highway agencies have established as the trigger value for intervention, which ranges from 25 to 37 for ribbed-tire friction (*12*). The increase in the skid number of the control section may be related to the rougher texture mentioned above.

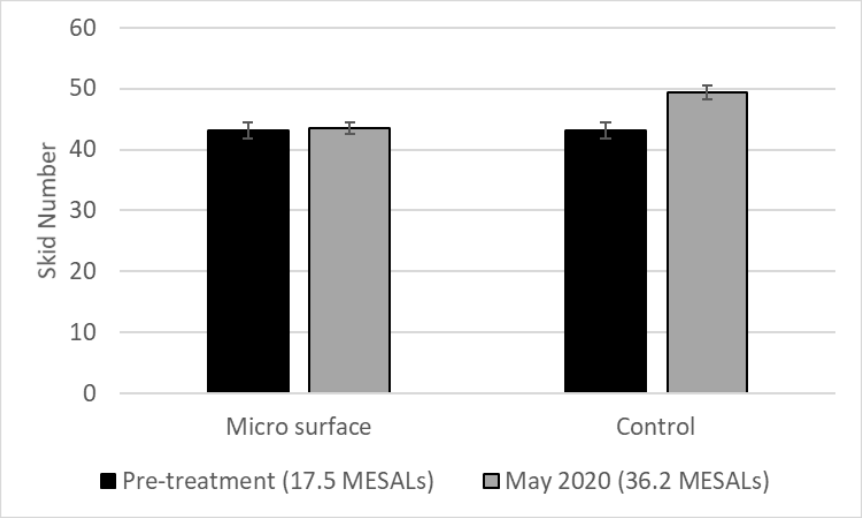

Figure 10. Friction Comparison of Test Sections

14.7.5 End of Cycle

As mentioned, the treated section outlasted the control and remained in place until the end of the research cycle, accumulating an additional 3 million ESALs. By February 2021, when traffic operations were completed at the Test Track, the micro surfaced section still maintained a better condition than the control at the time milling was conducted. Table 5 summarizes the measured performance indicators in the micro surfacing section at the end of the research cycle. It can be observed that after being subjected to 21.6 million ESALs since treatment application, the pavement remained in fair condition in terms of rutting and friction while slightly surpassing the poor condition threshold for cracking and was able to provide functionality and safety of traffic operations through the entire testing period.

Table 5. Pavement Condition of Micro Surfacing Section at End of Cycle

Indicator	Section Average	Condition Category
Cracking, %	22.3	Poor
Rut depth, in	0.28	Fair
IRI, in/mi	106.2	Fair
MTD, mm	0.68	Not Applicable
Skid number	43.5	Not Applicable

Figure 11 shows a general view of the treated section. Micro surfacing application was effective in restoring the pavement surface and correcting rutting while maintaining safe frictional characteristics. The treatment was able to withstand heavy traffic loading without wearing off, contributing to extending the life of the existing pavement. These observations agree with NCAT's research findings from full-scale test sections that are located in open roadways and subjected to live traffic. Long-term monitoring of these off-track sections has shown that micro surfacing is capable of improving cracking performance over time, correcting minor rutting and maintaining ride quality and pavement integrity (*13, 14*).

Figure 11. Overview of Micro Surfacing Test Section

14.8 Conclusions

This work evaluated the field performance of a micro surfacing full-scale test section subjected to accelerated pavement testing compared to a similar untreated pavement section. Based on the results obtained through seven years and over 21 million ESALs, treatment application resulted in better pavement condition in terms of cracking, rutting, roughness, and surface wear.

Since the treatment was able to withstand trafficking comparable to interstate highway traffic, micro surfacing appears to be a feasible option for preserving major roadways in a cost-effective manner. These results are in agreement with NCAT's research findings from off-track full-scale test sections subjected to live traffic, where micro surfacing application has resulted in extended pavement life.

14.9 References

1. Geiger, D. R. *Pavement Preservation Definitions*. Memorandum dated September 12, 2005, FHWA Office of Asset Management.
2. Proctor, G. D., S. Varma, and S. Varnedoe. *Asset Sustainability Index: A Proposed Measure for Long-Term Performance*. No. FHWA-HEP-12-046, 2012.
3. Gransberg, D. *Microsurfacing. A Synthesis of Highway Practice. NCHRP Synthesis 411*. Transportation Research Board, Washington, D.C., 2010.
4. Labi S., G. Lamptey and S. Kong S. Effectiveness of Microsurfacing Treatments. *Journal of Transportation Engineering*, 133(5), 298-307, 2007. doi: 10.1061/(ASCE)0733-947X(2007)133:5(298).

5. Morian, D.A. *Cost Benefit Analysis of Including Microsurfacing in Pavement Treatment Strategies & Cycle Maintenance.* Report No. FHWA-PA-2011-001-080503, Pennsylvania Department of Transportation, 2011.
6. Cuelho, E., R. Mokwa and M. Akin. *Pavement Maintenance Treatments of Flexible Pavements: A Synthesis of Highway Practice.* Report No. FHWA/MT-06-009/8117-26, 2006.
7. Ji, Y., T. Nantung, B. Tompkins and D. Harris. Evaluation for Microsurfacing as Pavement Preservation Treatment. *Journal of Materials in Civil Engineering*, 25(4), 540-547, 2013. doi: 10.1061/(ASCE)MT.1943-5533.0000568.
8. Peshkin, D., K.L. Smith, A. Wolters, J. Krstulovich, J. Moulthrop and C. Alvarado. *Preservation Approaches for High-Traffic-Volume Roadways.* Washington, DC: The National Academies Press, 2011. doi: 10.17226/14508.
9. West, R., D. Timm, R. Willis, B. Powell, N. Tran, D. Watson, M. Sakhaeifar, R. Brown, M. Robbins, A. Vargas-Nordcbeck, F. Leiva-Villacorta, X. Guo and J. Nelson. *Phase IV NCAT Test Track Findings*. NCAT Report 12-10, Auburn, AL., 2012.
10. International Slurry Surfacing Association. *Recommended Performance Guideline for Microsurfacing*. ISSA A143, Annapolis, MD., 2010.
11. Federal Highway Administration. *National Performance Management Measures; Assessing Pavement Condition for the National Highway Performance Program and Bridge Condition for the National Highway Performance Program*. Federal Register, Vol. 82, No. 11, 2017.
12. Hall, J.W., K.L. Smith, L. Titus-Glover, J.C. Wambold, T.J. Yager and Z. Rado. *Guide for Pavement Friction. NCHRP Web-Only Document 108*. National Cooperative Highway Research Program, 2009. doi: 10.17226/23038.
13. Vargas-Nordcbeck, A. 6-Year Study on Micro Surfacing Performance. *Airfield and Highway Pavements 2019: Design, Construction, Condition Evaluation, and Management of Pavements*. Reston, VA, American Society of Civil Engineers, 189-197, 2019. doi: 10.1061/9780784482452.019.
14. Vargas-Nordcbeck, A. *Field Performance of Micro Surfacing Treatments for Pavement Preservation*. Proceedings of the 7th Eurasphalt & Eurobitume Congress v1.0, first published 1st July 2020, ISBN: 9789080288461.

15. SOUTH CAROLINA DEPARTMENT OF TRANSPORTATION FULL-DEPTH RAPID REBUILD

Dr. David Timm

15.1 Introduction

The asphalt concrete (AC) layer of a flexible pavement is typically comprised of multiple lifts paved in succession with tack bonding the lifts together. This method takes advantage of using various AC mix designs, binder grades, and lift thicknesses to optimize the pavement structure and maximize the economy of the cross-section. However, this approach has disadvantages in some situations. First, the time of construction can prove problematic when placing multiple lifts, and potential drop-offs between lanes can create an operational hazard during construction. Additionally, slippage failures can occur even when tack is applied. Methods of more rapid construction using single thick-lift construction are therefore needed to mitigate these problems.

The South Carolina DOT (SCDOT) has been investigating using thick-lift construction in high-traffic areas where relatively short lane closures are more conducive to maintaining higher levels of service to the public. Projects in South Carolina using up to 5 inches in a single lift have been successfully completed where a pavement section is milled and inlaid with new material in a relatively short timeframe (i.e., overnight). On select projects, SCDOT has paved two thick lifts in a single night achieving total depths of 8 to 12 inches (*1*). While this practice has been successful, there is a desire to mill and inlay to even greater depths in a single lift, but questions regarding in-place density, rutting, cracking performance, and as-built smoothness necessitate accelerated pavement testing before attempting on high volume roadways in South Carolina. To that end, the SCDOT sponsored a section in the 2018 Test Track research cycle that was paved 8 inches thick in one pass. Section S9, the so-called "thick-lift" section, was meant to answer the following questions:

1. Could thick-lift AC be adequately compacted?
2. How long will a lift 8 inches thick take to reach a temperature at which it can be subjected to traffic after paving?
3. Could a thick-lift pavement achieve sufficient smoothness during construction?
4. Will a thick-lift pavement perform well under heavy trafficking? Of particular concern was rutting that could occur if the mix was not adequately compacted. Additionally, if sufficient compaction was not achieved, premature cracking could occur.
5. Will a thick-lift pavement behave like conventional multi-lift pavement in terms of pavement response (i.e., stress, strain, deflection) under loading?

To answer these questions, the thick-lift section was designed and built in the summer of 2018 under the guidance and at the direction of the SCDOT. The section used a mix design developed by the SCDOT, featured embedded instrumentation to measure pavement responses, and was subjected to regular performance evaluation to determine rutting, ride quality, and cracking performance. Routine laboratory tests were also conducted to determine fundamental and expected performance properties to assist the field evaluation.

15.2 Construction and Instrumentation of Section S9

Preparation of Section S9 for paving included removal of the old AC through milling. The remaining substructure consisted of approximately 6 inches of crushed granite aggregate base over the native Test Track A-4 (0) soil. Figure 1 shows the prepared surface prior to placing the AC.

Figure 1. Section S9 Prior to Paving

Preparation of instrumentation prior to paving has been documented by McCarty (*2*) and followed well-established Test Track procedures (*3*). A schematic of the gauge array is shown in Figure 2. The asphalt strain gauges (ASGs) for measuring bending at the bottom of the AC and earth pressure cells (EPCs) for measuring vertical compressive stress at the AC/aggregate base interface were placed just prior to paving as depicted in Figure 3. Figure 3a shows the twelve ASGs aligned in the direction of travel, and the center line of four gauges was in the center of the outside wheelpath. The other two rows of four gauges were offset 2 feet to the left and right of the center of the outside wheelpath, respectively. The two EPCs were placed before and after the array of ASGs in the center of the outside wheelpath.

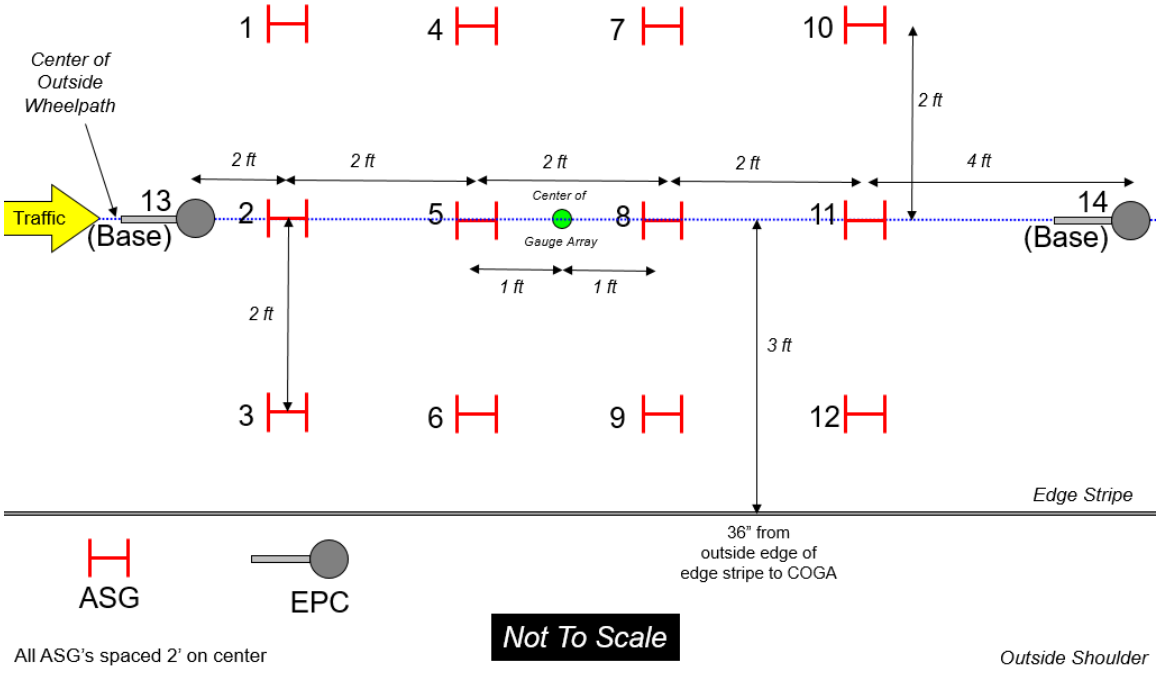

Figure 2. Gauge Array Schematic

a) Pre-Placement of Instrumentation

b) Gauges Covered with Sieved Mix Before Paving

Figure 3. Instrumentation Prior to Paving

As documented by McCarty, Section S9 was paved on August 24, 2018 beginning at 10:00 AM (*2*). On the day of construction, the high temperature was 85°F and the low temperature was 67°F. The AC was classified as an SCDOT "Type B Intermediate Special" which is used for rehabilitation repairs, interstates, and high-volume primary routes. The mix was a dense graded 12.5 mm NMAS mix with a PG 64-22 binder and 25% RAP. The target mix design air voids are usually around 2.5 to 3.0% for these mixes to make them easier to compact in the field (*1*). This particular mix was designed for 2.5% air voids with 75 design gyrations. The resulting asphalt content was 5.75% of which 4.37% was new binder and 1.38% came from the RAP. The AC layer was placed in a single 8" lift on top of the existing granular base. The materials in the mix were considered local to the Test Track but matched closely to the gradation and volumetrics of South Carolina's Asphalt Intermediate Course Type B mixture described above. The plant configuration settings and mix design are listed in Table 1. The plant configuration for this mix design adds up to 106% because East Alabama Paving Company operates their plant based on aggregate weight instead of on the total mixture weight. This results in 100% for total aggregate as shown in Table 1. Furthermore, the Evotherm M1 additive is based on the weight of the binder instead of on the weight of mixture or aggregate (*2*). The thick-lift section was produced as a warm mix asphalt (WMA) delivered by seven truckloads with an average temperature of 248°F. The mix was transferred from trucks into a material transfer vehicle, then loaded into the Roadtec paver pictured in Figure 3b.

Table 1. S9 Plant Configuration (*2*)

Material	% Setting
Binder Content	5.5
Shorter Sand	14
78 Granite	25
89 Granite	36
EAP -1/2 RAP	25
Evotherm M1	0.5

Compaction of S9 was accomplished using the same equipment and similar rolling patterns as the other sections built during the same Test Track reconstruction cycle. The compaction equipment included by static and vibratory steel wheel rollers in addition to a pneumatic tire roller. One obvious concern when laying and compacting AC of this thickness is achieving adequate compaction. This was a non-issue, as 95% of maximum density was achieved with no density gradient with depth, which was determined through testing of sliced cores. The density testing consisted of three cores sliced into thirds in conjunction with eight non-destructive core-corrected nuclear density tests in backscatter mode. The average density of the top 1/3 of the cores was 93.4% of maximum, the middle 1/3 average was 95.1% of maximum, and the bottom 1/3 average density was 92.3%. The non-destructive nuclear density tests determined the overall section wide average density of 95%.

Cooling of the thick-lift pavement in comparison to standard construction practices was the next concern in S9. The major benefit of thick-lift paving is opening the pavement to traffic quickly since multiple paving passes with tack between layers is not needed. A cooling analysis was performed using in-situ measurements and a surface monitoring thermal imaging system. Section S9 required 5 hours and 50 minutes to cool from 242°F to 175°F at mid-depth. From

paving additional trial sections ahead of S9, it was determined that time of day had a major impact on cooling time. As expected, paving at night minimized the cooling time (less than two hours) while the longest time (nearly six hours) was achieved when starting mid-morning, which was the case for S9. It was also observed that only using surface temperature devices (e.g., infrared gun) to monitor cooling would be highly misleading, since the mid-depth temperatures changed much more slowly. It was suggested that monitoring future thick-lift paving could easily be done with an embedded thermal probe to monitor temperatures deeper in the section. Further details regarding the cooling, monitoring, and analysis have been documented by McCarty (*2*).

After construction, the design and as-built parameters were documented and compared for quality control. Table 2 and Figure 4 show the aggregate gradations. The as-built gradation was considered within acceptable deviation from the target gradation.

Table 2. S9 Target and As-Built Gradations (*2*)

Sieve Size, mm	Percent Passing, %	
	Target	As-Built
25	100	100
19	99	100
12.5	95	98
9.5	83	92
4.75	54	67
2.36	35	37
1.18	26	29
0.6	18	21
0.3	13	12
0.15	8	7
0.075	4	4.5

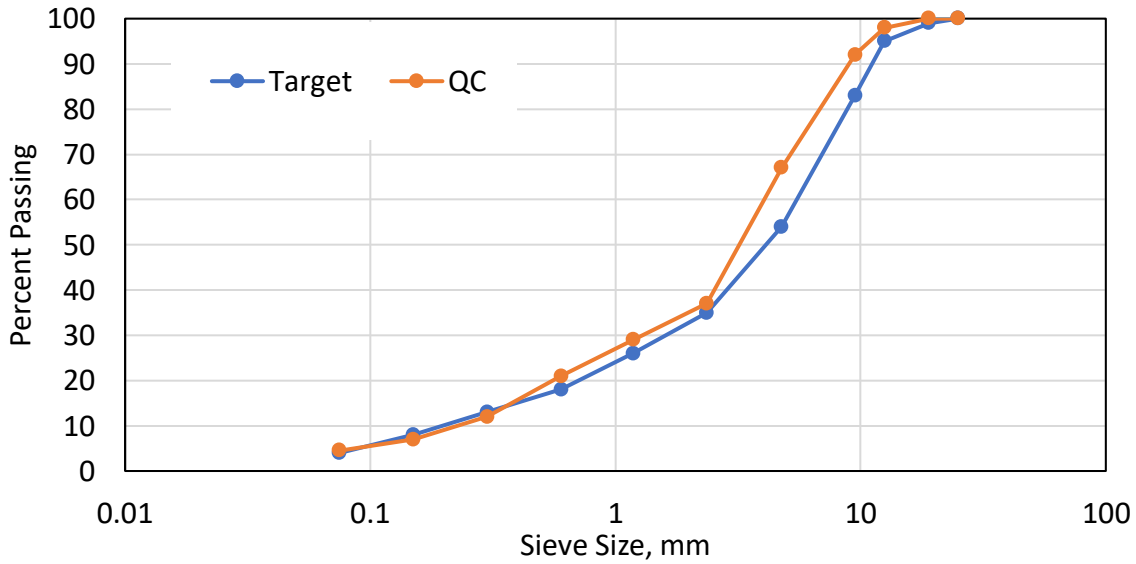

Figure 4. S9 Target and As-Built Gradations (*2*)

Mix sampled at the time of paving was also used to determine as-built laboratory properties and compare back to the target mix design properties for quality control. Table 3 shows the pertinent values, which were all deemed within acceptable tolerance for acceptance by the SCDOT.

Table 3. S9 Volumetric Targets versus In-Place (*2*)

Volumetric Property	Mix Design Target	As-Built
Rice Gravity (Gmm)	2.426	2.461
Bulk Gravity (Gmb)	2.364	2.402
Air Voids (Va), %	2.5	2.4
Aggregate Gravity (Gse)	2.642	2.678
VMA, %	15.7	15.2
VFA, %	84	84

As stated above, in-place density exceeded 95% of maximum theoretical density, so adequate compaction was not a problem. However, another major concern with single thick-lift constructability was controlling pavement smoothness. Based on past experience with this issue, the SCDOT has used diamond grinding or a top surface layer or open graded surface course to improve ride quality (*1*). As expected, the pavement had high roughness after paving as shown in Table 4, which contains the measured International Roughness Index (IRI) from both the right (R) and left (L) wheel paths and the mean IRI after paving and after the diamond grinding. Clearly, achieving smoothness with thick-lift paving is a challenge, which was addressed in this case with diamond grinding. Some would consider the post-grinding IRI also to be fairly high, but it was deemed acceptable by the SCDOT to proceed with trafficking. Additional experience in paving thick-lift sections should improve the initial roughness values if the practice gains wider use. Figures 5 and 6 show the finished section after paving and after grinding, respectively.

Table 4. S9 IRI Before and After Diamond Grinding (*2*)

Condition	L, IRI (in/mile)	R, IRI (in/mile)	Mean, IRI (in/mile)
After Paving	457.3	335.5	396.4
After Grinding	79.3	122.5	100.9

Figure 5. Section S9 After Paving

Figure 6. Section S9 After Grinding

The final sensor installation occurred after grinding to achieve smoothness. To monitor in situ temperatures, a bundle of four thermocouples was installed to measure temperatures at the top, middle, and bottom of the AC layer, and 3 inches into the aggregate base. A vertical hole was drilled into the pavement just outside the edge stripe that was deep and wide enough to accommodate the four thermocouples, with the top one flush to the pavement surface. Figure 7 shows the installation, with a slotted trench containing the thermocouple cables running to the shoulder before everything was covered and sealed with roofing asphalt (Figure 8).

Construction of the thick-lift section in S9 demonstrated that adequate compaction was possible in an 8-inch lift. The final average AC thickness, as determined through total station measurements at twelve locations in the section, was 8.05 inches. No special rolling equipment or patterns were needed to reach 95% of maximum density, though roughness was an issue that was addressed through grinding of the section. Cooling of the AC took nearly six hours; as cooling is dependent on the time of day and time of year of paving, consideration should be given to these factors in future thick-lift paving operations. The following sections address the field performance and structural response aspects of thick-lift paving.

Figure 7. Installed Thermocouple Bundle Prior to Covering with Roofing Asphalt

Figure 8. Covering Thermocouple Bundle with Roofing Asphalt

15.3 Field Performance

As with all of the other Test Track sections, the thick-lift section was measured frequently for rutting and roughness and inspected for cracking during the two-year research cycle. The following sections document the field performance in terms of both time and traffic application, expressed as equivalent single axle loads (ESALs). Though ESALs are a convenient expression of traffic, they were applied by five triple-trailer trucks traveling at 45 mph with steer axles weighing approximately 11 kips, drive tandem axles weighing approximately 40 kips and 5 trailing single axles weighing approximately 20.5 kips. These axle weights and groups resulted in a truck factor of approximately 10 ESALs/truck.

15.3.1 Rutting

Rutting progression for the thick-lift section is presented in Figure 9. Rutting increased primarily during the first spring/summer (April 2019 through September 2019) up to about 0.15 inches. At that point, it leveled off and did not experience increased rutting through the second summer, maintaining rut depths around 0.15 inches. The increase at the very end of the test cycle from 0.15” to 0.25” is believed to be related to a change in the data acquisition software rather than a true increase in rutting, as this jump was not evident in manual methods of rut depth measurement. In either case, rutting did not exceed 0.25” after the application of 10 million ESALs and most likely leveled off at 0.15” after primary rutting occurred during the first summer. Since rutting failure is defined as exceeding 0.5”, rutting performance of the section through the first 10 million ESALs is excellent. This is a critical finding, since a concern expressed

by SCDOT engineers with thick-lift paving is the potential for excessive rutting, which did not occur.

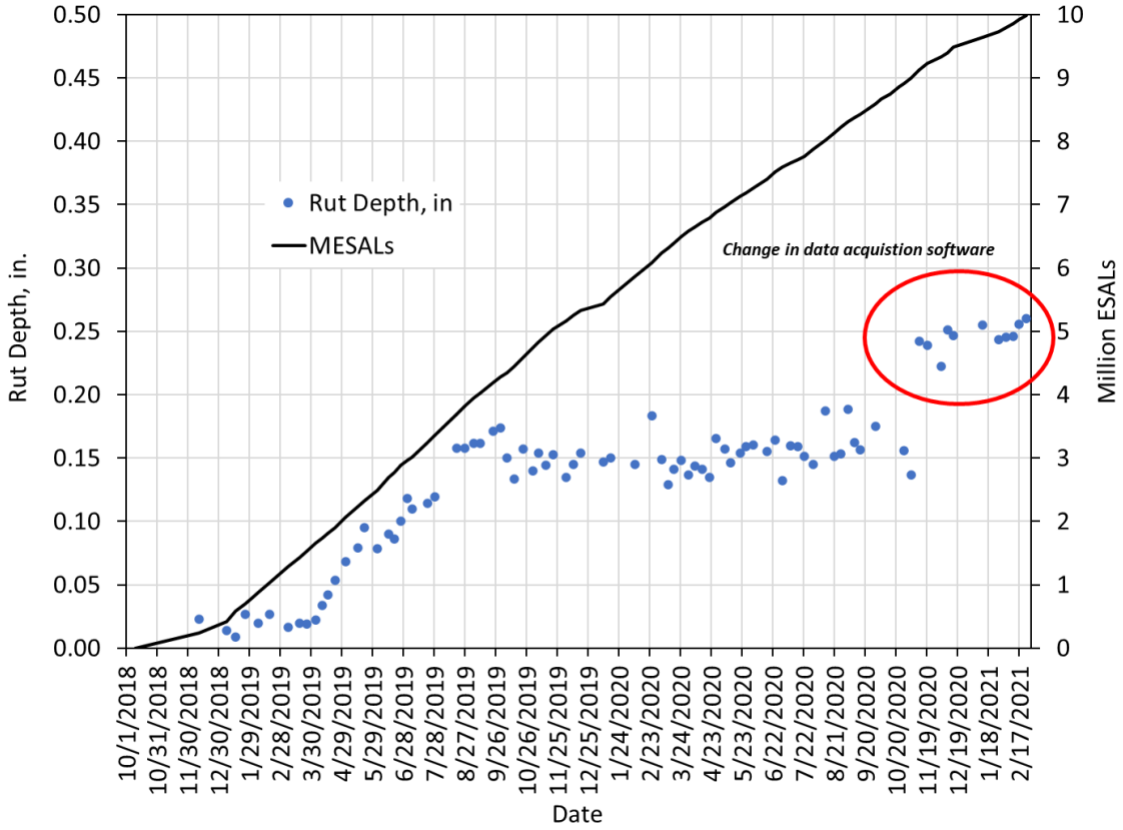

Figure 9. Section S9 Lift Rutting Performance

15.3.2 Cracking

A small amount of cracking was observed in the section, first observed in mid-December 2020 after approximately 9.4 million ESALs. The hairline cracks were aligned in the direction of travel and were at the edges of the wheelpath. At the end of trafficking, the cracking represented a total of 0.7% of the lane area or 1.1% of the wheelpath area. One crack was located at the edge of the outside wheelpath near the gauge array, while another crack was further along the section at the edge of the outside wheelpath. Figures 10 and 11 show the two cracks lightly highlighted for easier identification, and traffic moves in the vertical direction in each photo.

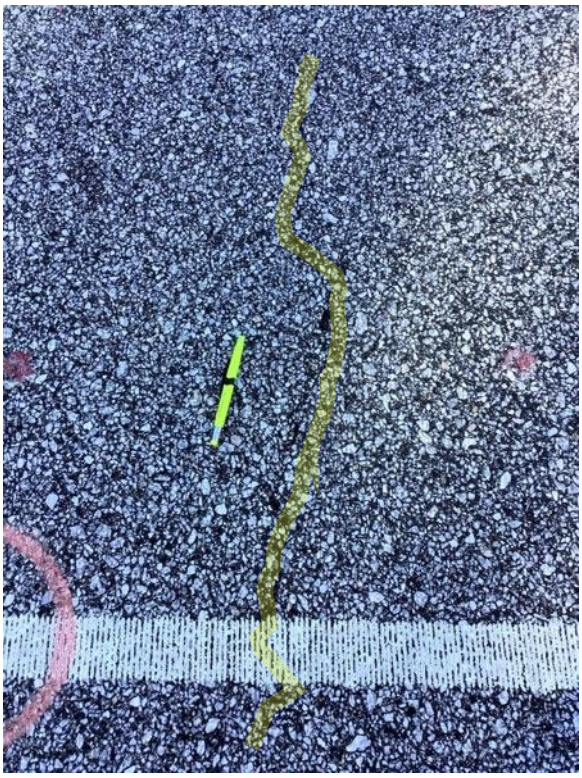

Figure 10. Section S9 Longitudinal Crack at Edge of Outside Wheelpath

Figure 11. Section S9 Longitudinal Crack at Edge of Inside Wheelpath

At this time, given the magnitude, amount, and orientation of the cracking, it seems that it is likely top-down. As will be presented in the structural characterization section, the stress, strain, and backcalculated modulus data also support this assertion. Future destructive forensic coring and/or trenches will be done to check this hypothesis.

15.3.3 Ride Quality

Though the initial roughness was higher than optimal for this section, the ride quality did not change over time and application of traffic. Figure 12 shows remarkably steady IRI data from throughout the experiment, which is consistent with little rutting and almost no cracking. Presumably, a section built with a lower starting IRI would also experience little to no change in ride quality under similar conditions.

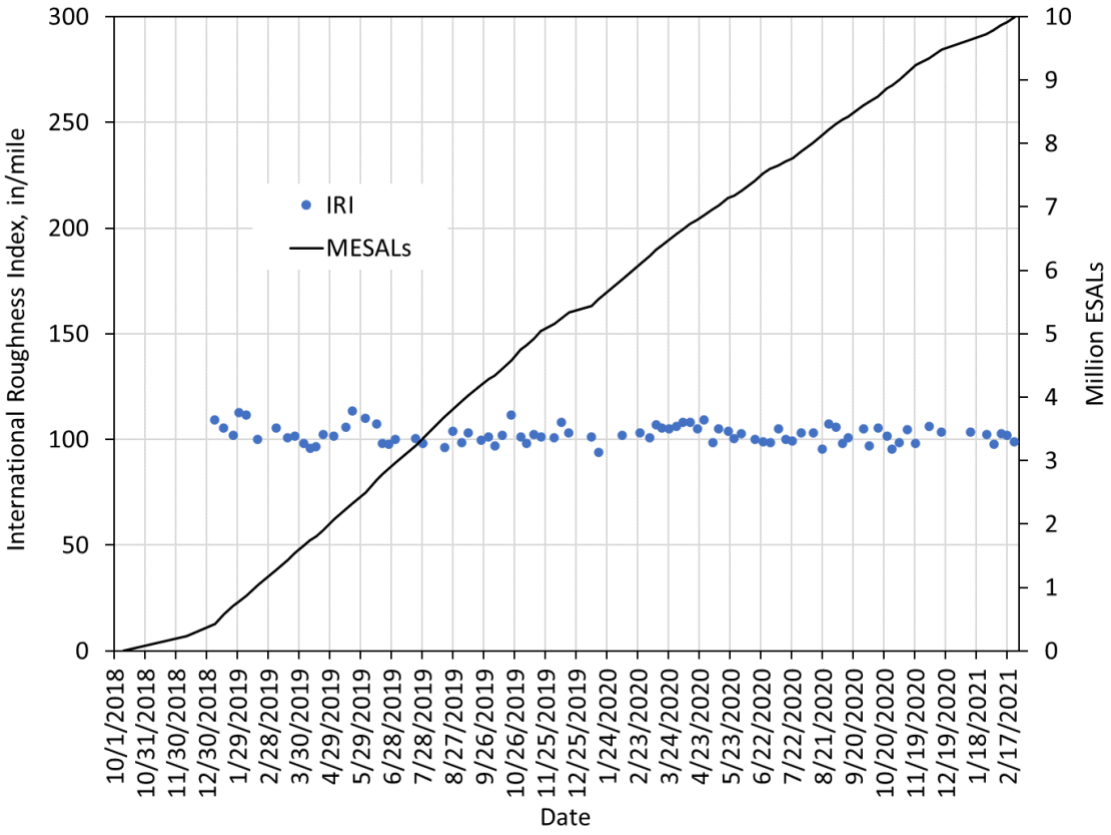

Figure 12. Section S9 Smoothness Data

15.4 Structural Response Characterization

The construction and performance data indicated that a thick-lift section could be successfully built and exhibit excellent performance through 10 million ESALs. The next portion of this investigation was to characterize the structural response through direct measurement under truck loading and falling weight deflectometer testing.

15.4.1 Structural Responses Measured with Embedded Instrumentation

Structural response measurements were made on a weekly basis during the experiment using the ASGs and EPCs embedded during construction. Response measurements consisted of at

least 15 truck passes, from which the 95th percentile highest measurement was used to represent the “best hit” on that collection day. Trucks were traveling at approximately 45 mph during each measurement, and though all axles were measured, only single axle responses are presented herein for brevity. There was some variation among all the single axles, but they typically weighed approximately 20,000 lb with dual tires.

Measured tensile strain response versus time is plotted in Figure 13, which displays the strong influence time of year has on bending of the section. Peak strain levels are achieved in the warmer summer months, while lower strains are measured at the cooler times of the year. The short-term cycling observed in the data stems from collecting data alternatingly in the mornings and afternoons on a week-to-week basis. Figure 13 matches well with other multi-lift sections measured in this fashion at the Test Track.

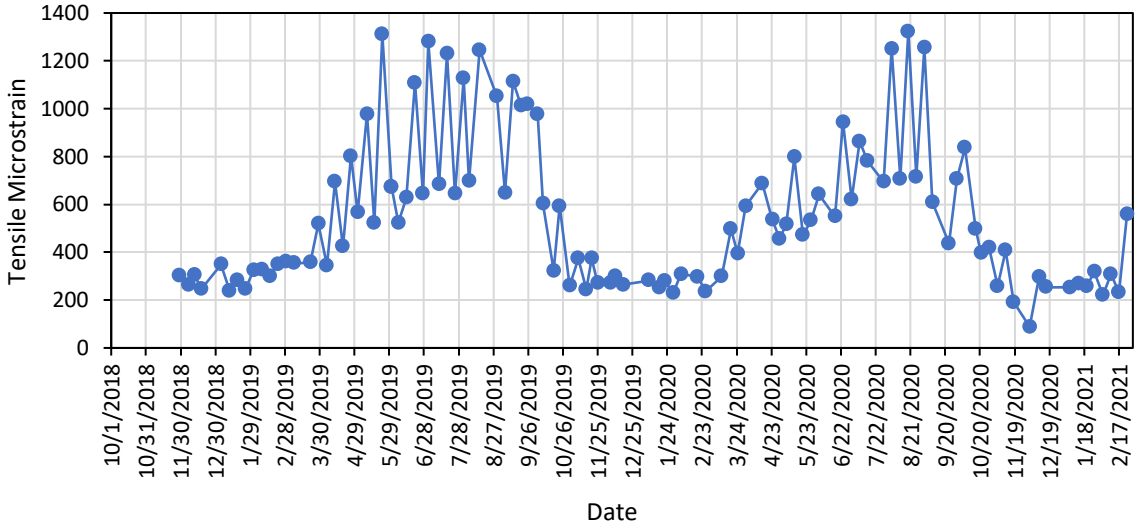

Figure 13. Section S9 Tensile Strain versus Time

The strain readings from Figure 13 were plotted against the mid-depth temperature at the time of measurement, as depicted in Figure 14. The strong influence of temperature seen in Figure 13 is quantified in Figure 14 with the exponential trendline fitted to the data. The relatively high R^2 (exceeding 0.94) means the variation in measured strain response is due almost entirely to changes in temperature, with some scatter possibly due to wheel wander and other random variations.

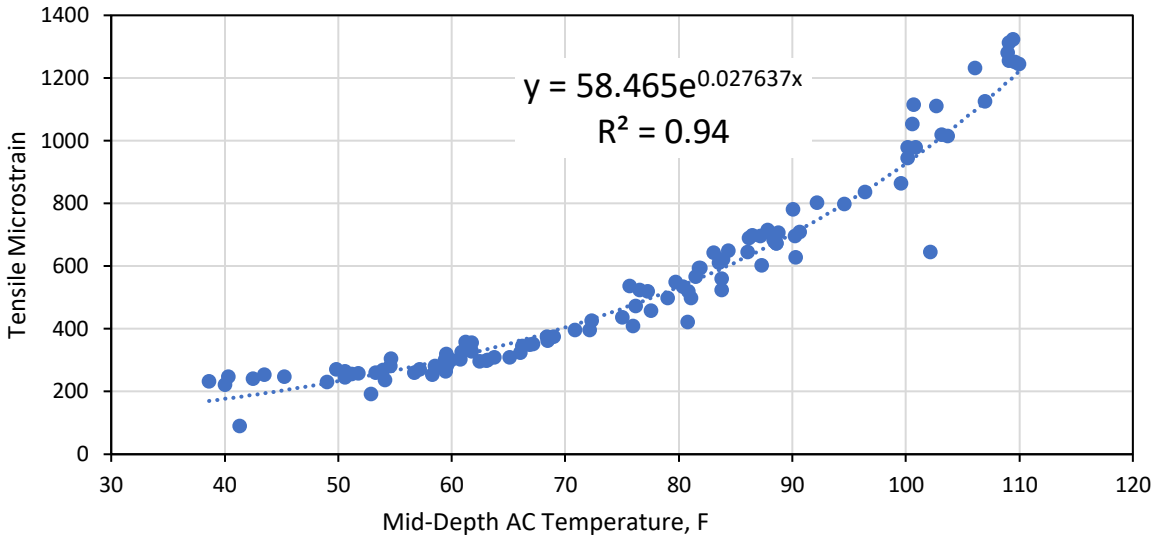

Figure 14. S9 Tensile Strain versus Temperature

The regression equation from Figure 14 was used to normalize the strain data to a reference temperature, following well-established Test Track procedures as documented by McCarty (*2*). The normalized tensile strain at 68°F is plotted versus time in Figure 15, where the relative stability of the measurements indicates good structural health. Had the recently observed cracking been more severe, or bottom-up, strain levels would have been expected to increase over time.

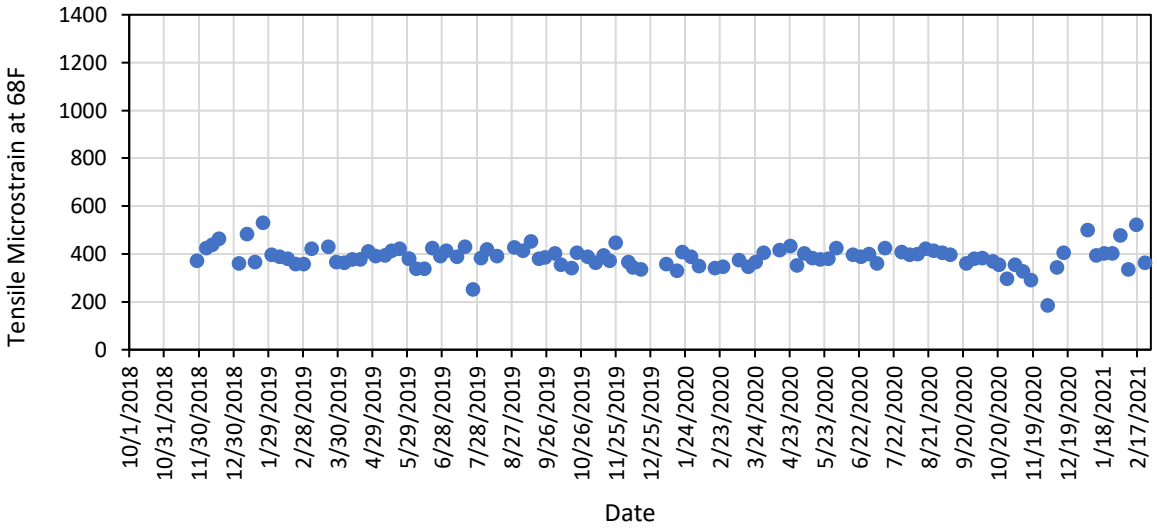

Figure 15. Section S9 Tensile Strain at 68°F versus Date

Similar graphs (Figures 16, 17, and 18) were constructed using the base pressure measurements. The data closely mimic the strain data in the importance of pavement temperature on the measured response (Figure 16). The exponential function fitted to the data (Figure 17) again quantifies the strong influence of temperature, and the pressures normalized

to 68°F (Figure 18) show steady if not slightly declining pressure over time. Like the strain data, these measurements indicate good structural health and are consistent with measurements made in other multi-lift sections at the Test Track.

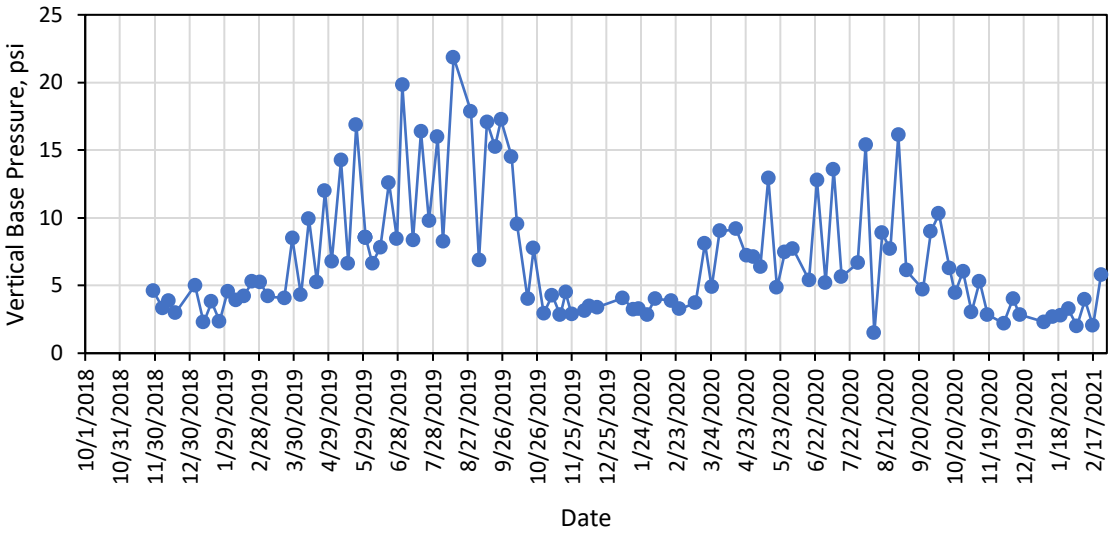

Figure 16. Section S9 Compressive Stress versus Time

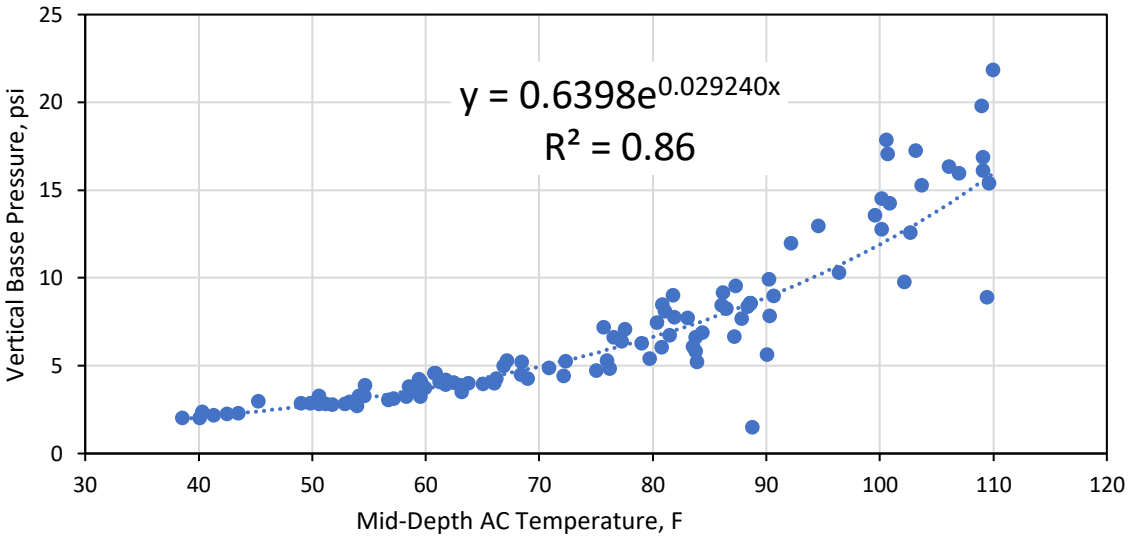

Figure 17. Section S9 Compressive Stress versus Temperature

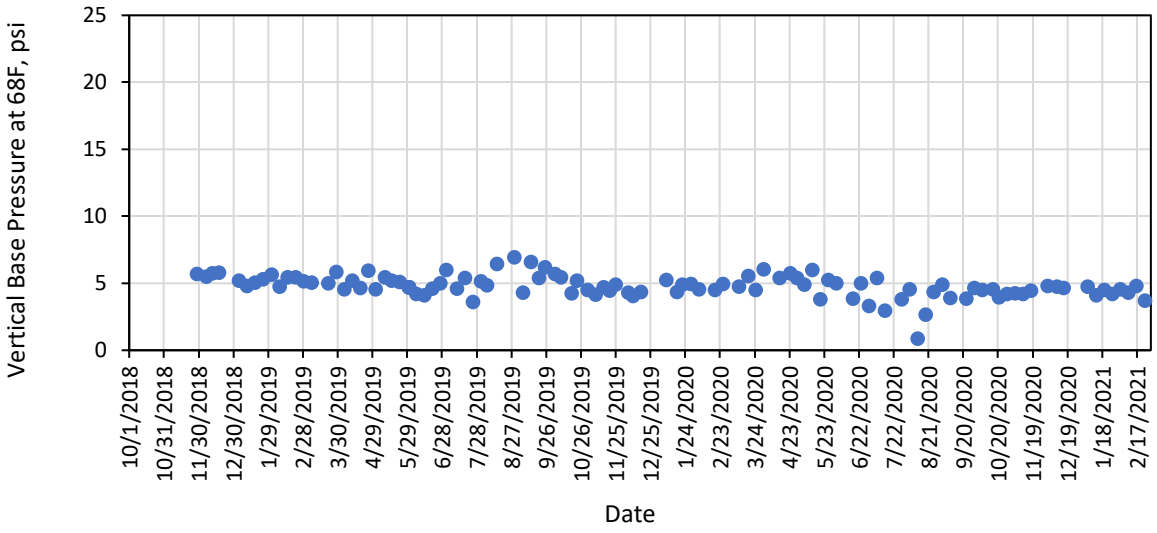

Figure 18. Section S9 Compressive Stress at 68°F versus Date

15.4.2 Falling Weight Deflectometer (FWD) Testing and Backcalculation

FWD testing was conducted several times per month during the two-year trafficking cycle using a Dynatest 8000 FWD with nine sensors using standard spacing at 0, 8, 12, 18, 24, 36, 48, 60, and 72 inches from the load center. Testing was conducted at four random locations in the section with three lateral offsets (inside wheelpath, outside wheelpath, and between wheelpaths) at each location. Each FWD test consisted of two seating drops followed by three replicate drops at 6,000, 9,000 and 12,000 lb, respectively. The data presented below pertains only to the 9,000 lb loading.

Backcalculation of the deflection basins was conducted using EVERCALC 5.0, with the cross-section depicted in Figure 19. A previous study had shown the need for combining the aggregate base layer with 16 inches of the Test Track subgrade to yield more accurate backcalculation results and was used for this study (*4*). Note that Figure 19 shows the average as-built thicknesses, but the surveyed depths from each of the 12 FWD test locations was used on a location-by-location basis for backcalculation. Only AC modulus values resulting in less than 3% root mean square error between measured and predicted deflection basins are presented.

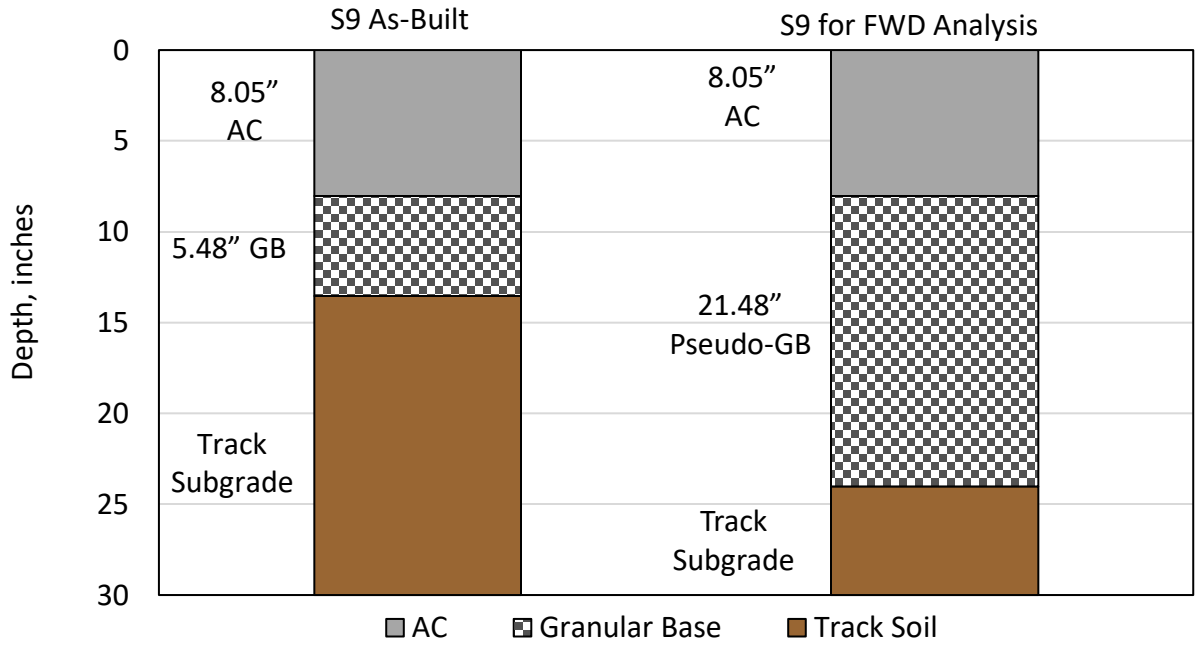

Figure 19. Section S9 As-Built and Backcalculation Cross-Sections

Figure 20 plots the backcalculated AC moduli versus test date, where the seasonal effects are readily apparent, much like the measured strain and stress responses presented above and similar to observations of other multi-lift sections at the Test Track. The AC modulus changes by about an order of magnitude from summer to winter. This profound influence of season, and therefore temperature, on the modulus is why the other measured responses are so dramatically affected as well. The vertical spread of the data on any given date represents the spatial variability across the section (random locations and wheelpath offset).

The backcalculated AC moduli were then plotted against the corresponding measured mid-depth temperature (Figure 21) where, much like the strain and pressure data, the influence of temperature is very strong ($R^2 > 0.95$) and follows an exponential trendline. Following the same temperature normalization process used with the strain and pressure data, the AC modulus corrected to 68^{o}F were plotted against time in Figure 22. The remarkable stability of the data over time again indicates a structurally healthy section since one would expect modulus to start decreasing if AC cracking was becoming a problem.

A histogram of the data presented in Figure 22 was generated and plotted in Figure 23. The distribution appears normal with a mean of 802 ksi and standard deviation of 128 ksi, which translates to a coefficient of variation of 16%. These values are comparable to other mixtures produced and placed at the NCAT Test Track.

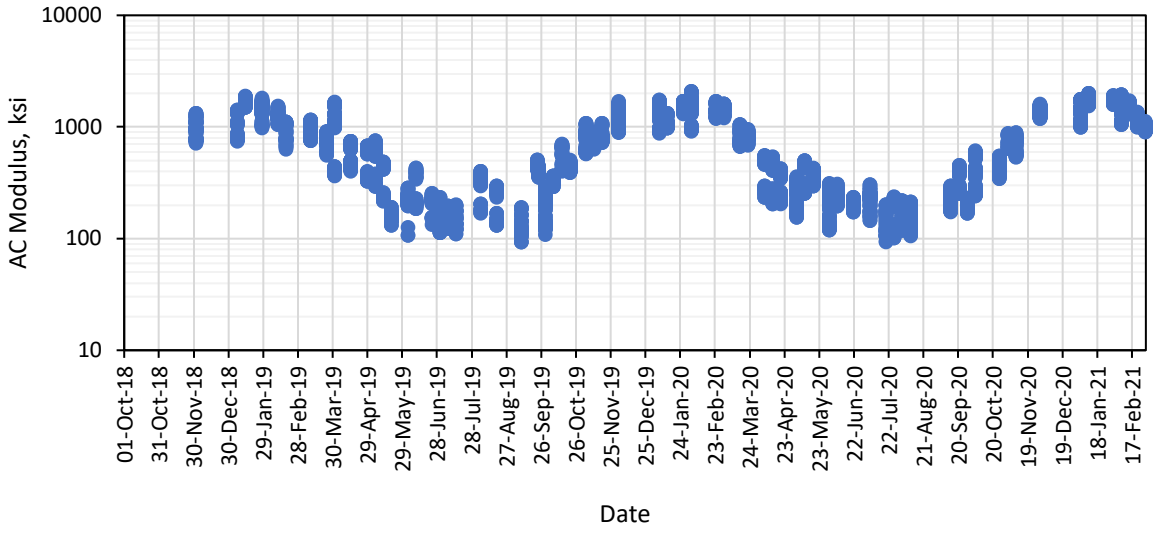

Figure 20. Section AC Modulus versus Date

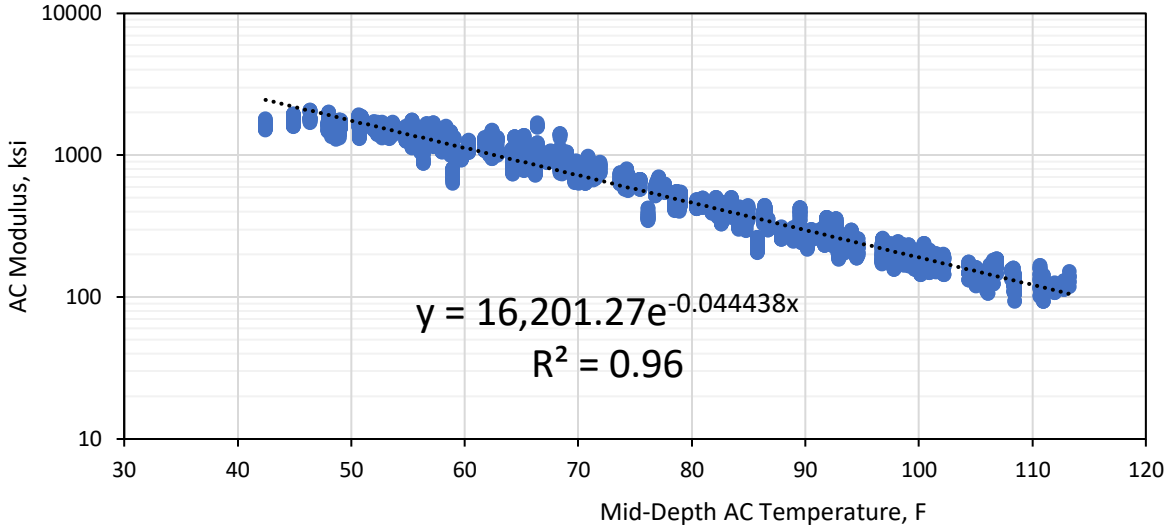

Figure 21. Section S9 AC Modulus versus Temperature

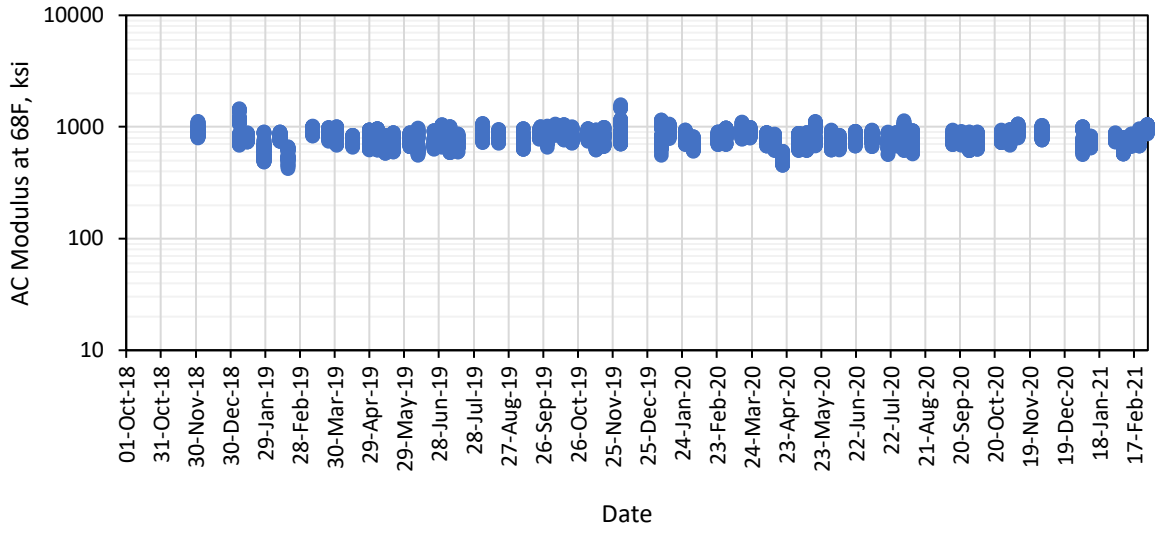

Figure 22. Section S9 AC Modulus versus Date at 68°F

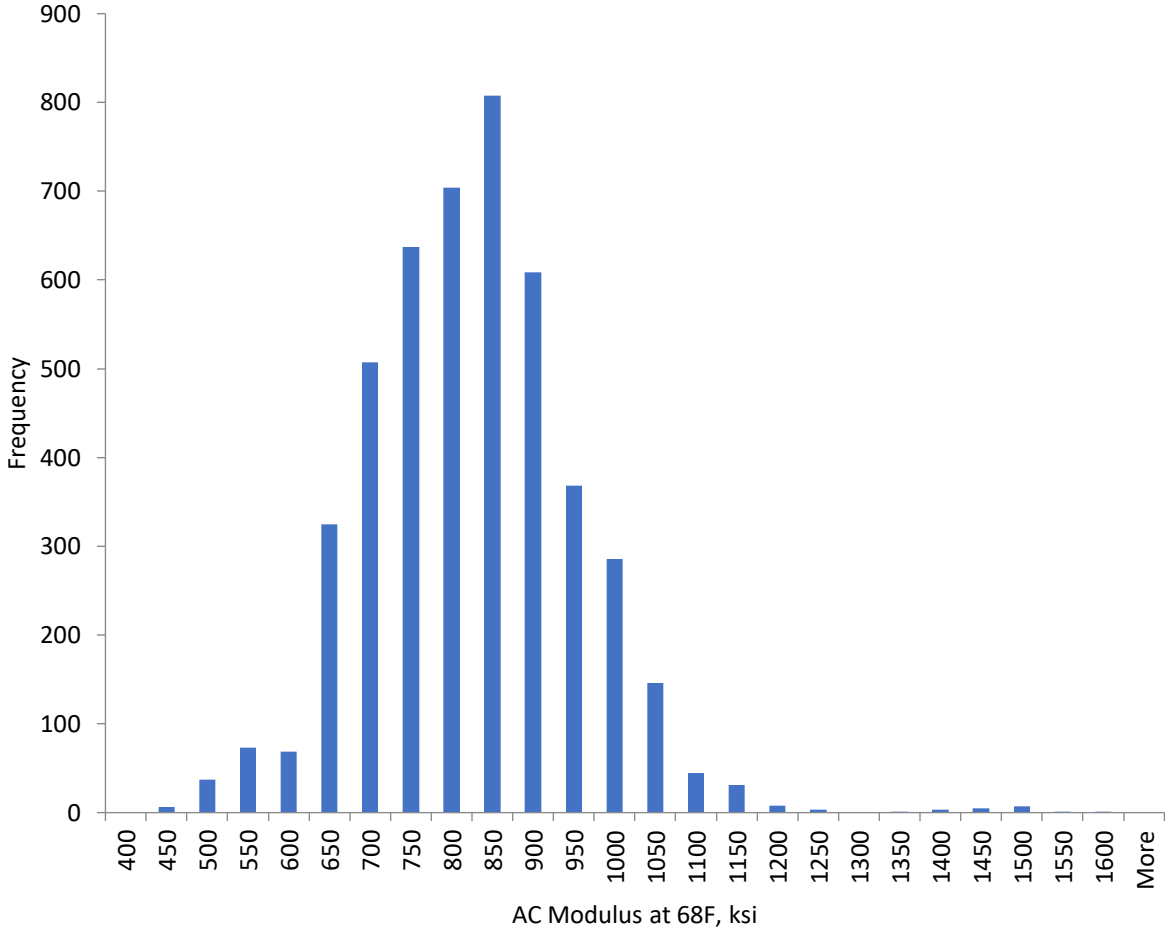

Figure 23. Section S9 AC Modulus Distribution at 68°F

15.5 Laboratory Testing

Fundamental material property and performance tests were conducted on plant-produced, lab-compacted specimens as part of routine testing conducted on Test Track structural sections. The following sections present the test results from Dynamic Modulus, Fatigue (both bending beam and cyclic), Ideal-CT, and Hamburg Wheel Tracking testing.

15.5.1 Dynamic Modulus

Small geometry dynamic modulus (E*) specimens were prepared according to AASHTO PP 99-19 and tested according to AASHTO TP 132-19. Specimens were compacted to a target air void content of 5% to match in situ conditions. Table 5 tabulates the data at the three temperatures and frequencies used in the testing, while Figure 24 illustrates the master curve generated from the test data following AASHTO R 84-17. While these data may be used in mechanistic-empirical modeling, it is also useful to compare E* to backcalculated moduli determined through FWD testing as shown in Figure 25. This figure indicates good agreement between lab and field-generated modulus values, particularly at an E* frequency of 1 Hz.

Table 5. S9 Dynamic Modulus Test Data

Temp (°C)	Temp (°F)	Freq (Hz)	Dynamic Modulus	
			MPa	ksi
4	39	10	16,062	2,330
4	39	1	12,431	1,803
4	39	0.1	8,931	1,295
20	68	10	8,281	1,201
20	68	1	5,078	737
20	68	0.1	2,720	394
40	104	10	2,345	340
40	104	1	978	142
40	104	0.1	376	55

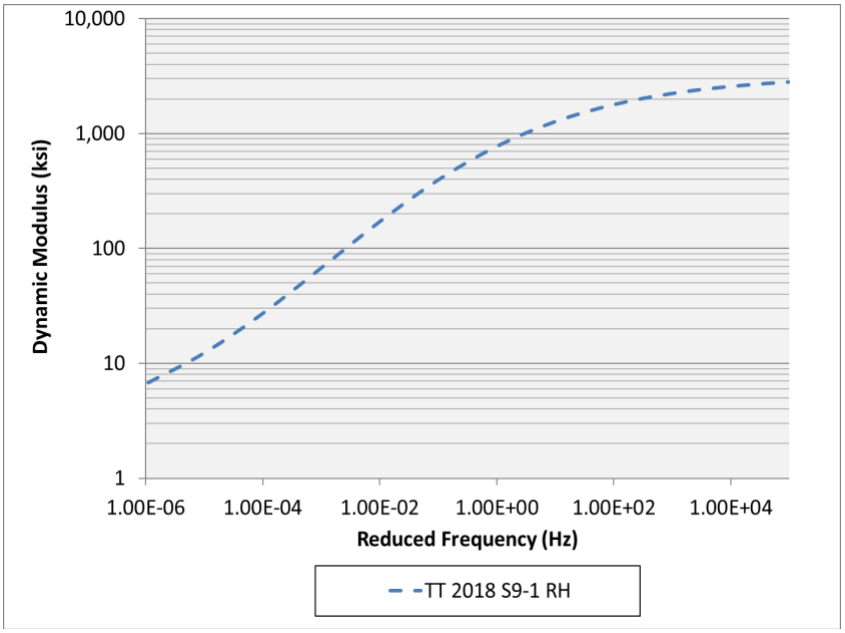

Figure 24. S9 Dynamic Modulus Master Curve

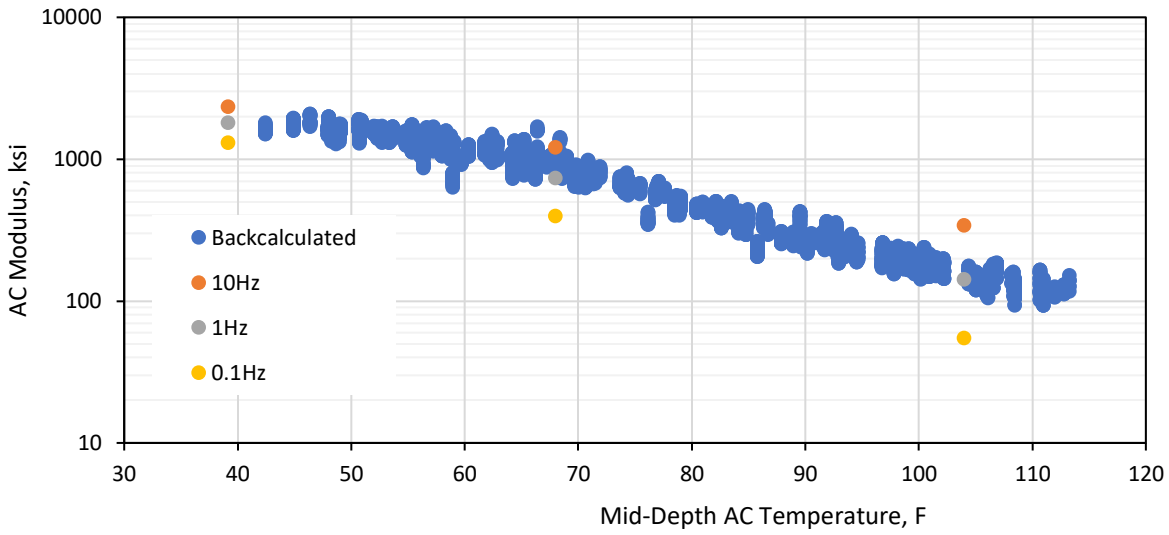

Figure 25. S9 Comparison between E* and Backcalculated Moduli

15.5.2 Fatigue Testing

Two types of fatigue testing were conducted on the S9 asphalt concrete. Bending Beam Fatigue Testing (BBFT) followed AASHTO T 321-17 with specimens again compacted with target air voids of 5% to match field conditions. Small sample cyclic fatigue testing using an AMPT followed AASHTO TP 133-19 with air voids again targeted at 5%.

The results from BBFT, with three replicates at three strain levels, are shown in Table 6 and Figure 26. The C-S curve determined from cyclic fatigue testing is shown in Figure 27, with its corresponding derived transfer function shown in Figure 28. It is difficult to derive meaning from the transfer functions without control mixtures for comparison. However, it is useful to compare the two modes of testing, as depicted in Figure 29, where the transfer functions share similar curvature but vastly different orders of magnitude. The mode of loading (i.e., bending versus direct tension) dictates the difference, with direct tension being the more destructive testing mode. Also, recall that the average measured tensile strain under loading was approximately 400 microstrain at 68°F. Using this value in the respective transfer functions results in the following predicted number of cycles to failure:

- Bending Beam Fatigue Cycles to Failure = 514,049
- Cyclic Fatigue Cycles to Failure = 368

Since the section has experienced 10 million ESALs during the research cycle with no apparent bottom-up cracking, the transfer functions need calibration once or if bottom-up fatigue occurs. Further trafficking may offer that opportunity in the next test cycle.

Table 6. Section S9 Bending Beam Fatigue Test Data

Sample ID	Sample Air Voids (%)	Initial Beam Stiffness (MPa)	Initial Beam Stiffness (ksi)	Cycles to Failure (Peak Mod x Cycles)	Peak-to-Peak On-Specimen Microstrain
2	5.0	6,004	871	689,181	400
4	6.0	6,181	896	721,661	400
12	5.3	6,138	890	296,255	400
5	5.4	5,987	868	22,646	600
6	5.4	5,965	865	63,826	600
8	5.0	5,829	845	69,582	600
9	5.0	5,788	839	7,747	800
10	5.0	5,553	805	11,681	800
11	5.7	5,662	821	10,471	800

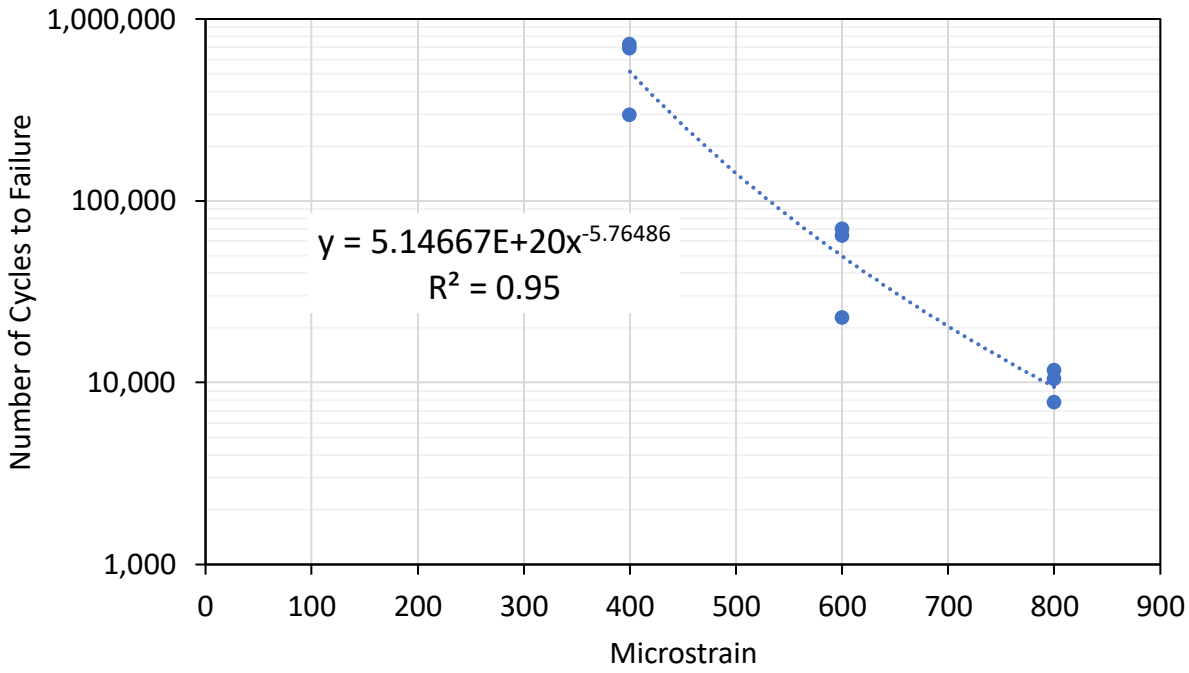

Figure 26. Section S9 Bending Beam Fatigue Transfer Function

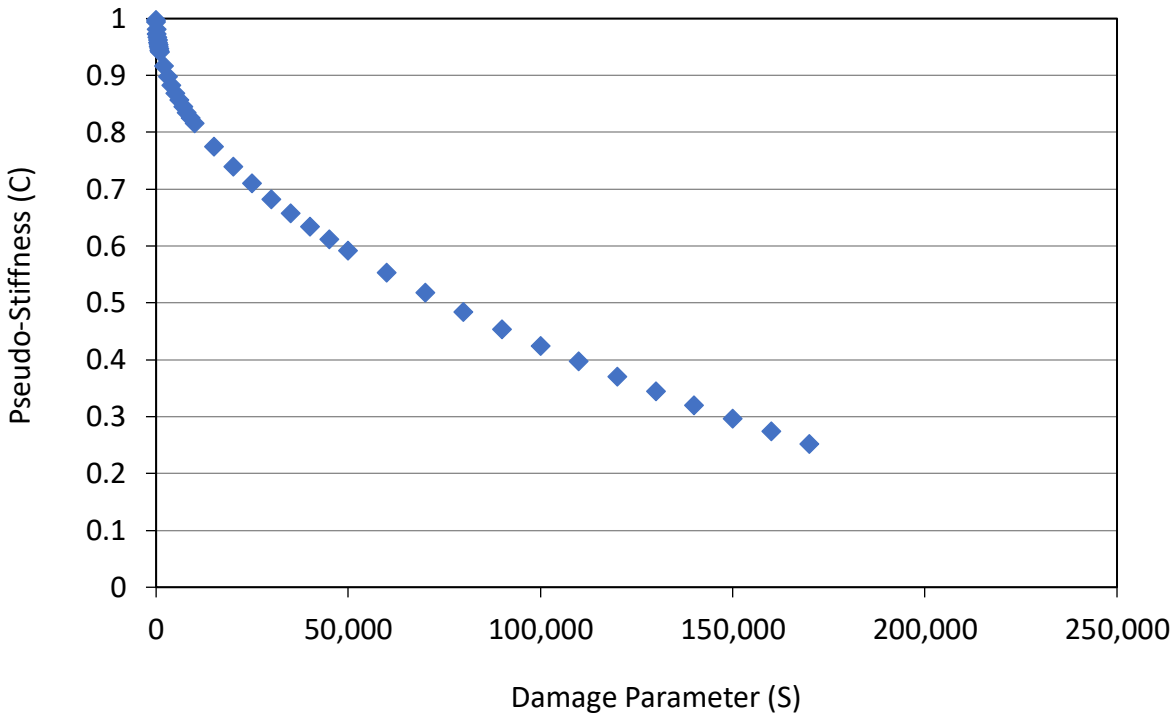

Figure 27. Section S9 C versus S Cyclic Fatigue Curve

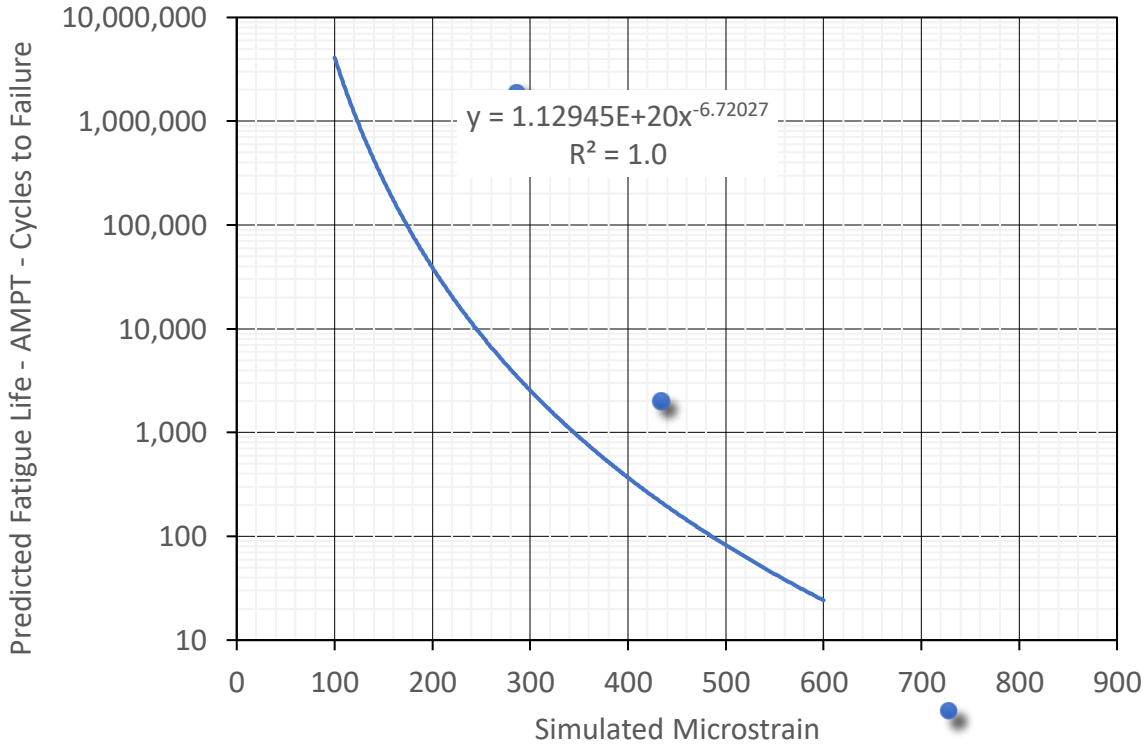

Figure 28. Section S9 Cyclic Fatigue Transfer Function

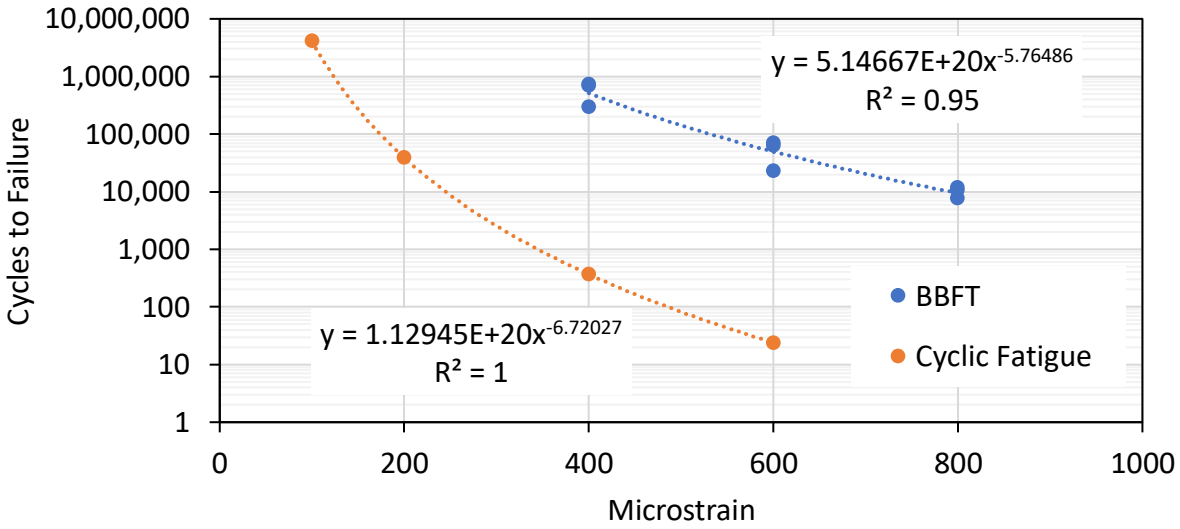

Figure 29. Section S9 BBFT and Cyclic Fatigue Transfer Functions

15.5.3 IDEAL-CT Testing

Additional cracking tolerance was determined with the IDEAL-CT test following ASTM D8225-19. For this test, six specimens were compacted to a target air void content of 7%, and the results are shown in Table 7. There is active and ongoing debate regarding minimum CT_{Index} values for use in balanced mix design. One commonly cited specification from the Virginia DOT requires a CT_{Index} exceeding 70 to avoid surface cracking problems (*5*). However, some mixes previously placed on the Test Track with CT_{Index} values in the 30s also performed well (*6*). Since significant differences between the SCDOT mix for this experiment and those used in other studies and specifications exist, caution should be exercised when trying to infer performance from these threshold values. However, given that the mix in S9 survived two years of accelerated trafficking and environmental conditions with minimal cracking, it is suggested that the CT_{Index} values in Table 7 are acceptable.

Table 7. Section S9 IDEAL-CT Test Data

Sample ID #	2	3	5	6	7	9
Air Voids	7.0	6.7	7.1	7.0	7.1	7.3
Thickness (mm)	62.0	62.0	62.0	62.0	62.0	62.0
Diameter (mm)	150.0	150.0	150.0	150.0	150.0	150.0
Test Temperature	25C	25C	25C	25C	25C	25C
CT Index	**64.5**	**50.0**	**58.8**	**55.2**	**59.2**	**57.5**
Peak Load (lbs)	3536.2	3690.7	3603.7	3498.6	3565.3	3415.5
Fracture Energy (J/m²)	8405.9	8554.00	8702.2	8250.3	8624.6	8332.9
Post Peak Slope (kN/mm)	3.915	4.8	4.361	4.3	4.1	4.272
Displacement @75% (mm)	4.506	4.2	4.42	4.3	4.2	4.418

Note: Loading rate = 50 mm/min

15.5.4 Hamburg Wheel Track Testing

Rutting susceptibility of the mix was measured with the Hamburg Wheel Track Testing device according to AASHTO T324-19. Specimens were compacted to a target air void content of 7%. The measured profile data are shown in Figures 30 and 31, with the summary results presented in Table 8.

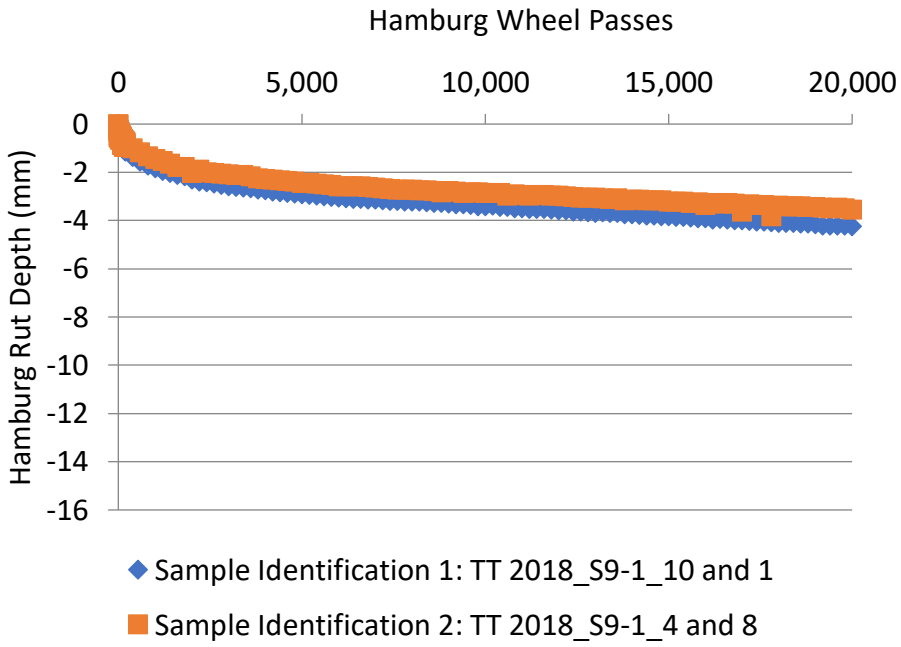

Figure 30. Section S9 Hamburg Wheel Track Testing Minimum Profile Values

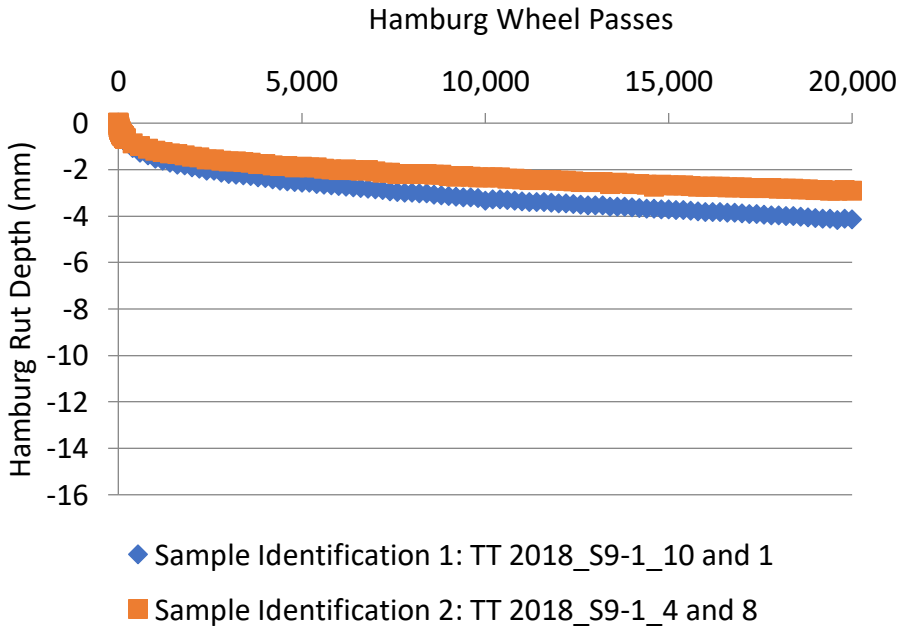

Figure 31. Section S9 Hamburg Wheel Track Testing Center Profile Values

Table 8. Section S9 Hamburg Wheel Track Testing Summary

Parameter	Replicate 1	Replicate 2
Sample 1 ID	10	4
Sample 2 ID	1	8
Sample 1 Va (%)	6.8	6.8
Sample 2 Va (%)	6.8	6.8
Max Rut - 10k passes (mm)	3.40	2.86
Max Rut - 20k passes (mm)	4.24	3.54
Passes to 12.5 mm Rut	>20,000	>20,000
Approximate Stripping Inflection Point (passes)	>20,000	>20,000

Like Ideal-CT design criteria, there is a range of published thresholds for acceptable Hamburg test results (*7*). Generally speaking, a mix with an unmodified binder should have less than 12.5 mm of rutting after 10,000 or 15,000 wheel passes (*7*). The maximum rutting in Table 8 is well below this threshold. Furthermore, the mixture had no stripping problems as it achieved over 20,000 passes with no evident stripping.

15.6 Summary, Conclusions, and Recommendations

Section S9 was constructed for the SCDOT as a single thick-lift pavement to evaluate the constructability, performance, and structural characteristics of this rapid reconstruction technique. Based on the results presented in this chapter, the following conclusions and recommendations are made:

- The construction of a single 8-inch lift is viable. Care should be taken regarding the cooling time needed to open to traffic, but it can be controlled somewhat by selecting the time of year and time of day for paving. In practice, the SCDOT has found that nighttime placement in cold weather months is optimal while paving in weather above 70^{o}F creates longer cooling times and subpar smoothness (*1*).
- Achieving density with an 8.05-inch lift was a non-issue. Density exceeding 95% of the theoretical maximum was accomplished with standard rollers and roller patterns. No specialized processes or equipment were needed.
- As-built smoothness may be an issue with thick-lift paving and certainly was with this section. The problem was rectified somewhat with diamond grinding. It is anticipated that paving crews, given more opportunities to pave thick-lifts, could greatly improve as-built smoothness. In practice, the SCDOT has found that having an additional lane to stage material transfer vehicles, trucks, and rollers is beneficial to minimize dips in the longitudinal pavement profile (*1*).
- The thick-lift section exhibited excellent performance over the 10 million ESALs. Rutting was less than 0.25”, very little cracking (likely top-down) developed, and smoothness did not change. Premature or excessive rutting, which was a potential liability for this construction technique, was not evident and should not be a problem provided that adequate compaction is achieved during construction. Further, the Hamburg test results confirm that rutting of the mix should not be a problem in this experiment.
- The thick-lift section behaved in much the same fashion as other conventional multi-lift sections with respect to measured mechanistic response and backcalculation of

deflection basins. The influence of pavement temperature was evident, and expected, in the measured pavement responses and backcalculated AC moduli. The temperature-corrected data were remarkably consistent over time, indicating good structural health despite the small amount of cracking observed in the section.

- Laboratory determination of dynamic modulus produced data consistent with backcalculated moduli. Either data set could be used for future mechanistic modeling of the test section.
- The bending beam and cyclic fatigue tests produced vastly different transfer functions, but both require calibration, as using the functions with measured tensile strain in the section at 68^{o}F predicts relatively short fatigue life compared to the 10 million ESALs applied to the section with no observed bottom-up cracking.
- Depending on the specification applied, the Ideal-CT may indicate that top-down cracking could be a problem. Since only minor cracking has been observed through 10 million ESALs, further monitoring will help determine an acceptable threshold.
- One area not yet explored with this section is the possible advantage of single lift construction not having lift interfaces that could suffer slippage and loss of structural integrity. This feature is inherent to the method of construction and could help alleviate this type of distress in addition to providing for a more rapid rebuild of the cross-section.

15.7 References

1. Selkinghaus, C., *Personal Communication*, South Carolina Department of Transportation, May 14, 2021.
2. McCarty, C. *Early Characterization and Performance of a Flexible Thick Lift Pavement*. M.S. Thesis, Auburn University, 2019.
3. Timm, D. H. *Design, Construction, and Instrumentation of the 2006 Test Track Structural Study*. Report No. 09-01, National Center for Asphalt Technology, Auburn University, 2009.
4. Tutu, K. and D.H. Timm, "Determination of an Optimum Backcalculation Cross-Section for Unconventional Pavement Profiles," Transportation Research Record No. 2641, Transportation Research Board, 2017, pp. 48-57.
5. Virginia Department of Transportation. *Special Provision for Balanced Mix Design (BMD) Surface Mixtures Designed Using Performance Criteria*, 2020.
6. West, R. C., C. Rodezno, F. Leiva and F. Yin. *Development of a Framework for Balanced Mix Design*, National Cooperative Highway Research Program, Project 20-07/Task 406, 2018.
7. West, R. C., D. H. Timm, B. Powell, M. Heitzman, N. Tran, C. Rodezno, D. Watson, F. Leiva, and A. Vargas. Phase VI (2015-2018) NCAT Test Track Findings. NCAT Report 18-04, National Center for Asphalt Technology, Auburn University, 2018.

16. TEXAS DEPARTMENT OF TRANSPORTATION BALANCED MIX DESIGN EXPERIMENT

Dr. Fan Yin

16.1 Background

The Texas Department of Transportation (TxDOT) has a long history of using mixture performance tests for asphalt mix design and is one of the leading agencies in the development and implementation of balanced mix design (BMD). In 2018, TxDOT developed a special specification for BMD that requires the use of the Hamburg Wheel-Tracking Test (HWTT) (Tex-242-F) for the evaluation of mixture resistance to rutting and moisture damage and the Overlay Test (OT) (Tex-248-F) for the assessment of mixture cracking resistance. The HWTT temperature is 50°C and the criterion is based on the number of passes to 12.5mm rut depth, where a minimum threshold of 10,000, 15,000, and 20,000 passes is required for mixtures containing a PG 64 (or lower), PG 70, and PG 76 (or higher) virgin binder, respectively.

Historically, TxDOT had been using the Cycles to Failure (N_f) as the OT cracking parameter, which is defined as the number of cycles corresponding to a 93% reduction of the initial peak load. Although this parameter has proved effective in discriminating asphalt mixtures with different cracking potential, it has high variability with an average reported coefficient of variance between 30 and 50%. To overcome this limitation, TxDOT recently adopted two new OT parameters of Critical Fracture Energy (G_c) and Crack Resistance Index (*CRI*) based on a research study conducted by the University of Texas at El Paso (UTEP) (*1*). G_c is defined as the energy required to initiate a crack on the bottom of the specimen at the first loading cycle, which characterizes the fracture properties of the specimen during the crack initiation phase. *CRI* is defined as the reduction in load required to propagate cracking under cyclic loading conditions, which characterizes the flexibility and fatigue properties of the specimen during the crack propagation phase. TxDOT's current OT test criteria for surface mixtures includes a minimum threshold of 1.0 in.-lb/in.^{2} for the G_c parameter and a maximum threshold of 0.45 for the *CRI* parameter. In addition to the HWTT and OT requirements, the most recent BMD special specification also includes requirements on the Delta T_c (ΔT_c) parameter of asphalt binder (i.e., greater than or equal to -6.0°C after 20-hour PAV aging) as well as the maximum allowable reclaimed asphalt pavement (RAP) and recycled asphalt shingles (RAS) contents, and recycled binder ratios for surface mixtures.

16.2 Objective and Scope

In the 2018 research cycle, TxDOT sponsored Sections S10 and S11 for evaluation on the NCAT Test Track (Figure 1). The overall objective of the experiment was to compare the field performance of asphalt mixtures designed using a BMD approach versus the traditional volumetric approach. Both sections were built as 2.5-inch mill-and-inlays on top of 4.5-inch existing asphalt pavements. Section S10 was constructed with a BMD mix while Section S11 used a dense-graded volumetric mix. The two questions that TxDOT sought to answer from this experiment were: 1) Will the BMD mix have a potential rutting issue? 2) Are the current OT test criteria sufficient or do they need to be adjusted to ensure satisfactory cracking performance?

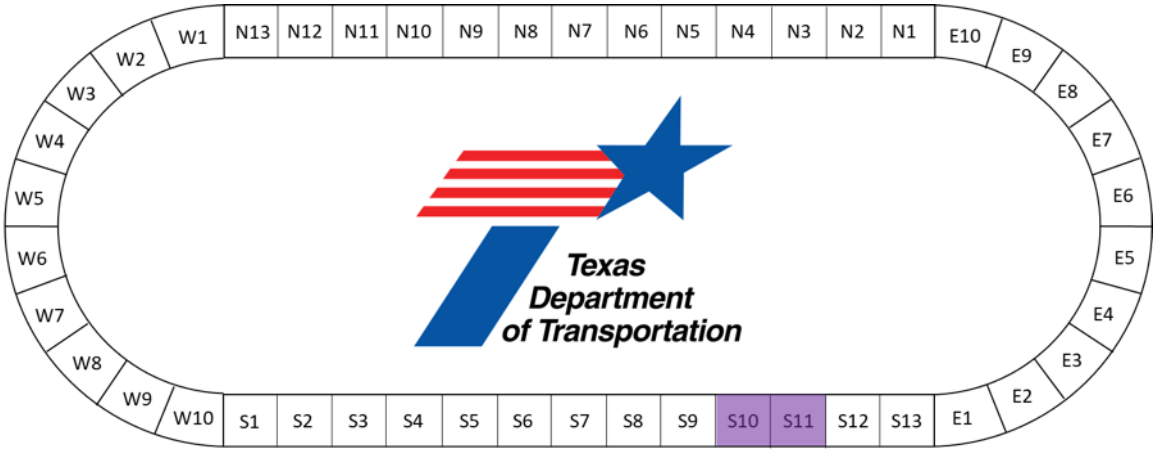

Figure 1. Layout of TxDOT's Sections S10 and S11 on the NCAT Test Track

16.3 Existing Pavement Conditions

The existing pavements of Sections S10 and S11 were constructed in 2009 as part of the Green Group Experiment. Both sections were constructed with 7 inches of asphalt mix over 6 inches of graded aggregate base and a stiff subgrade (approximately 30 ksi). The sections had approximately 15 to 20% of the lane area cracked after being trafficked for 14 million equivalent single axle loads (ESALs) through April 2014, when at that point, they were converted to the Pavement Preservation Experiment. Section S10 was divided into two sub-sections and treated with scrub cape and scrub seal, respectively. Section S11 was also divided into two sub-sections, with one treated with chip seal and the other left untreated as a control section. In May 2018, the top 2.5 inches of both sections were milled off for the preparation of the 2018 Test Track research cycle. Figure 2 shows the fatigue cracking in the underlying pavement of sections S10 and S11 after milling. These two sections allowed TxDOT and NCAT to determine if a BMD mix would still outperform a volumetric mix in terms of cracking resistance with a challenging underlying pavement condition.

Figure 2. Fatigue Cracking in Underlying Pavement of Sections 10 and S11 after Milling

16.4 Mix Design

Table 1 presents the job mix formula of S10 BMD and S11 volumetric mixes. Note that the table also includes the quality control data which will be discussed later in the report. Both mixes were designed by UTEP by adjusting a TxDOT approved 12.5 mm SP-C surface mix design. The two mixes used the same component materials, including a PG 70-22 styrene butadiene styrene (SBS) modified binder, fractionated RAP, and a blend of granite and dolomitic limestone. The S10 BMD mix had a RAP content of 18.1%, which is higher than that of the S11 volumetric mix (i.e., 16.0%). Despite this difference, the two mixes had the same RAP binder replacement ratio of 20%. Both mixes were designed with 4.0% air voids at 50 design gyrations. The S11 volumetric mix had an optimum binder content (OBC) of 4.7% and 15% voids in mineral aggregate (VMA) (calculated using aggregate G_{se} per TxDOT specifications). The S10 BMD mix was designed with a slightly coarser gradation, a higher OBC of 5.5%, and a higher VMA (G_{se}) of 16.6%, which was expected to provide improved mixture durability and cracking resistance.

Table 1. Mix Design and QC Data of S10 BMD and S11 Volumetric Mixes

Sieve (in.)	Job Mix Design		Quality Control	
	S10 Mix	S11 Mix	S10 Mix	S11 Mix
25 mm (1”)	100	100	100	100
19 mm (3/4”)	100	100	100	100
12.5 mm (1/2")	93	92	93	95
9.5 mm (3/8”)	82	81	78	82
4.75 mm (#4)	52	53	46	55
2.36 mm (#8)	30	34	27	37
1.18 mm (#16)	21	24	19	25
0.60 mm (#30)	16	17	14	17
0.30 mm (#50)	11	12	11	12
0.15 mm (#100)	7	7	8	8
0.075 mm (#200)	4.9	4.8	5.2	5.7
Design Gyration (N_{design})	50	50	50	50
NMAS (mm)	12.5	12.5	12.5	12.5
Total Binder Content (%)	5.5	4.7	5.3	4.4
Virgin Binder Grade	PG 70-22 (SBS)	PG 70-22 (SBS)	PG 70-22 (SBS)	PG 70-22 (SBS)
RAP Binder Ratio (%)	20	20	19	20
Air Voids (%)	4.0	4.0	2.4	3.6
Blend G_{se}	2.668	2.656	2.660	2.651
G_{mm}	2.450	2.470	2.451	2.475
G_{mb}	2.353	2.370	2.393	2.387
VMA (G_{se}) (%)	16.6	15.0	14.8[#]	14.0[#]
V_{be} [calculated with VMA (G_{se}), %]	12.6	11.0	12.4*	10.4*
VFA [calculated with VMA (G_{se}), %]	76	73	84	74
Dust Proportion	0.9	1.0	1.0	1.3
Extracted Binder Grade	-	-	PG 82-16	PG 82-16

Notes:

[#] VMA calculated using NCAT-measured G_{sb} of post-extraction aggregate blend from the production mix was 12.6% (S10) and 11.9% (S11).

* V_{be} calculated using VMA (G_{sb}) instead of VMA (G_{se}) was 10.3% (S10) and 8.3% (S11).

The S10 BMD mix was designed with the *Volumetric Design with Performance Verification* approach as described in AASHTO PP 105-20, where the optimum binder content was determined based on the Superpave volumetric analysis and then verified with HWTT and OT to ensure compliance with the rutting and cracking test requirements. Figure 3 presents the performance diagram from mix design testing where the HWTT results in terms of the total rut depth at 15,000 passes plotted on the x-axis versus the OT *CRI* results on the y-axis. The two dashed lines represent TxDOT's performance test criteria. As shown in the figure, the S10 BMD mix fell within the "sweet zone" of the performance diagram (by passing both the HWTT and OT criteria) and thus, was expected to have balanced rutting and cracking resistance. The S11 volumetric mix, on the other hand, passed the HWTT requirement but failed the OT *CRI* requirement, and thus, was located outside the "sweet zone" of the performance diagram.

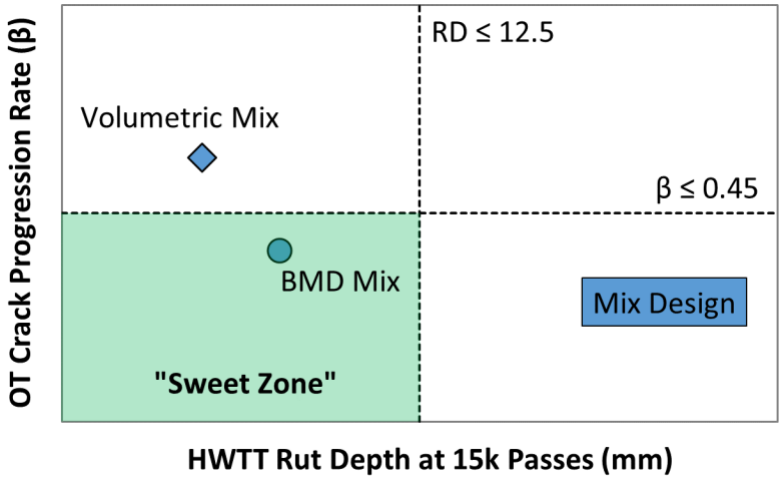

Figure 3. Performance Diagram from Mix Design Testing

16.5 Mix Production and Construction

The S10 BMD mix was produced and placed on September 18, 2018, with a high temperature of 91°F, a low temperature of 73°F, and no rainfall. As shown in Table 1, quality control (QC) testing of the plant mix showed a reduction in the total binder content from 5.5% in mix design to 5.3% at production, as well as slight changes in the 3/8", #4, #8, and #50 fractions. The production mix had 2.4% lab-molded air voids and 14.8% VMA (G_{se}) at 50 gyrations (N_{design}), and 4.0% lab-molded air voids and 16.2% VMA (G_{se}) at a reduced N_{design} of 35 gyrations. The production mix met TxDOT's specifical specification for *Superpave Mixtures – Balanced Mix Design*, except that the %passing on the #8 sieve size was 1% lower than the allowed master gradation limits. The extracted binder of the mix was graded to be PG 82-16. The mix had an average production temperature of approximately 305°F and in-place density of 95.9%. Figure 4 shows the laydown and compaction of the BMD surface mix for Section S10.

Figure 4. Construction of Section S10 with a BMD Mix

The S11 volumetric mix was produced and placed on September 18, 2018, with a high temperature of 93°F, a low temperature of 72°F, and no rainfall. As shown in Table 1, QC testing of the plant mix showed a reduction of asphalt content from 4.7% in mix design to 4.4% at production and slight changes in the 1/2", 3/8", #16, and minus #200 fractions. The plant mix had 3.6% lab-molded air voids and 14.0% VMA (G_{se}) at 50 gyrations (N_{design}), which met TxDOT's specification for Item 341, *Dense-Graded Hot-Mix Asphalt*. The extracted binder of the mix was graded to be PG 82-16, which was the same as that of the S10 BMD mix. The S11 mix had an average production temperature of approximately 300°F and had in-place density of 95.4%. Figure 5 shows the laydown and compaction of the volumetric mix for Section S11.

Figure 5. Construction of Section S11 with a Volumetric Mix

16.6 Laboratory Testing and Data Analysis

During construction of the test sections, plant mix was sampled from the Test Track and transported back to the NCAT laboratory, where it was reheated to fabricate plant-mixed, lab-compacted (PMLC) specimens for performance testing. HWTT and OT were conducted to evaluate the rutting and cracking resistance, respectively, of the two plant-produced mixes and determine their compliance with TxDOT's performance test criteria. In addition, the High-temperature Indirect Tensile (HT-IDT) test and Indirect Tensile Asphalt Cracking Test (IDEAL-CT)

were conducted to explore their feasibility as surrogate tests to HWTT and OT, respectively, for BMD production testing. To consider the effect of asphalt aging on mixture cracking resistance, the OT and IDEAL-CT tests were conducted on both reheated and critically aged PMLC specimens. The critical aging (CA) protocol used in the experiment was loose mix aging for eight hours at 135°C, which is expected to simulate a critical field aging condition of 70,000 cumulative degree days where top-down cracking starts to develop after four to five years in service in Alabama (*2, 3*).

Figure 6 presents the HWTT and OT results of the reheated PMLC specimens on a performance diagram. The mix design testing results of short-term aged lab-mixed, lab-compacted (LMLC) specimens provided by UTEP are also presented for comparison purposes. As can be seen, the two sets of specimens showed the same trend, where the S10 BMD mix fell within the "sweet zone" of the performance diagram while the S11 volumetric mix fell outside the "sweet zone". As compared to the S11 volumetric mix, the S10 BMD mix had lower OT *CRI* values and higher HWTT rut depths, which indicated better cracking resistance but reduced rutting resistance, respectively. The S10 BMD mix met both TxDOT's HWTT and OT criteria and therefore, was expected to have balanced rutting and cracking resistance.

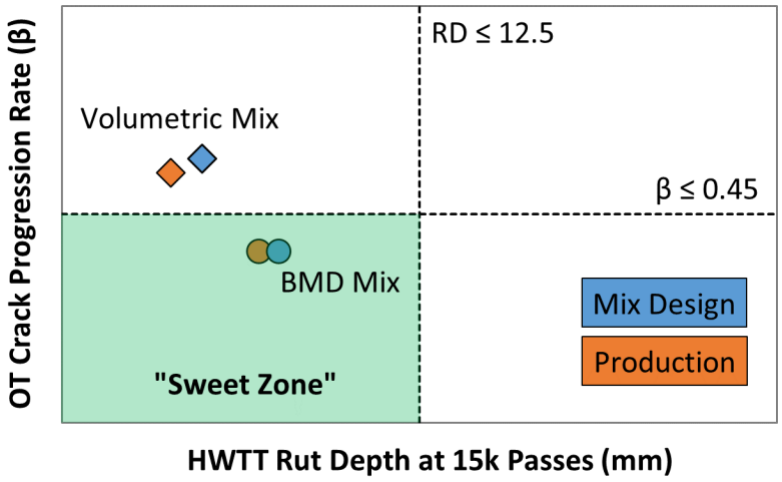

Figure 6. Performance Diagram from Mix Design and Production Testing

Figure 7 presents the OT results of short-term aged LMLC, reheated PMLC, and critically aged PMLC specimens for S10 BMD versus S11 volumetric mixes. Note that the LMLC specimens were tested at UTEP while the reheated and critically aged PMLC specimens were tested at NCAT. Despite the difference in volumetric properties (Table 1), the LMLC specimens and reheated PMLC specimens of both mixes had statistically equivalent *CRI* results. The CA protocol of loose mix aging for eight hours at 135°C yielded a significant increase on the *CRI* results, which indicated reduced cracking resistance possibly due to increased mix embrittlement and reduced relaxation properties. At both the reheated and critically aged conditions, the S10 BMD production mix had lower *CRI* results and thus, were expected to have better cracking resistance than the S11 volumetric mix.

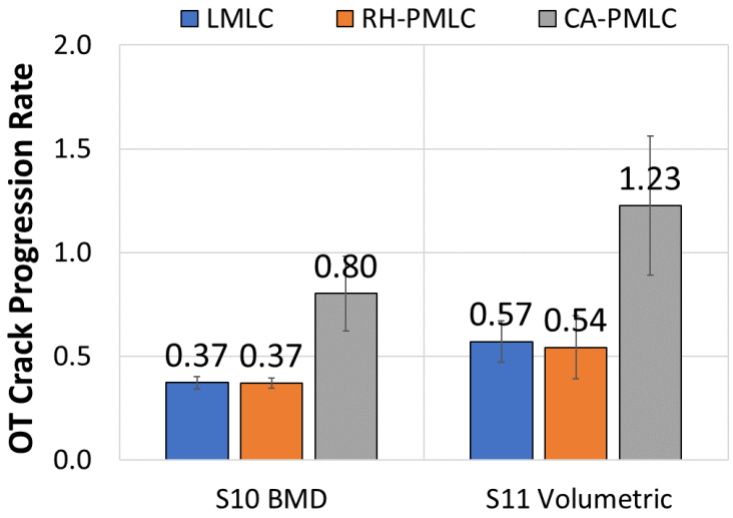

Figure 7. OT *CRI* Results of Short-term Aged LMLC, Reheated PMLC, and Critically Aged PMLC Specimens

Figure 8 presents the IDEAL-CT results of reheated and critically aged PMLC specimens. At both aging conditions, the S10 BMD mix showed significantly higher CT_{Index} results, indicating better cracking resistance than the S11 volumetric mix. These results agreed with the OT results in Figure 8 and highlighted the potential of using IDEAL-CT as a surrogate test to OT for BMD production testing. As shown in Figure 9, there was no strong correlation between the limited IDEAL CT_{Index} and OT *CRI* results, which agreed with a previous NCAT study (*4*). Mix-specific correlations, however, may exist between these two tests and warrant further investigation.

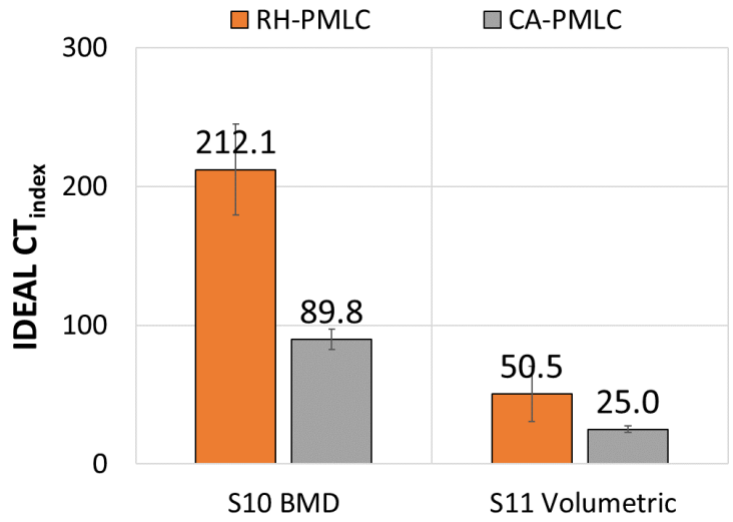

Figure 8. IDEAL CT_{Index} Results of Reheated and Critically Aged PMLC Specimens

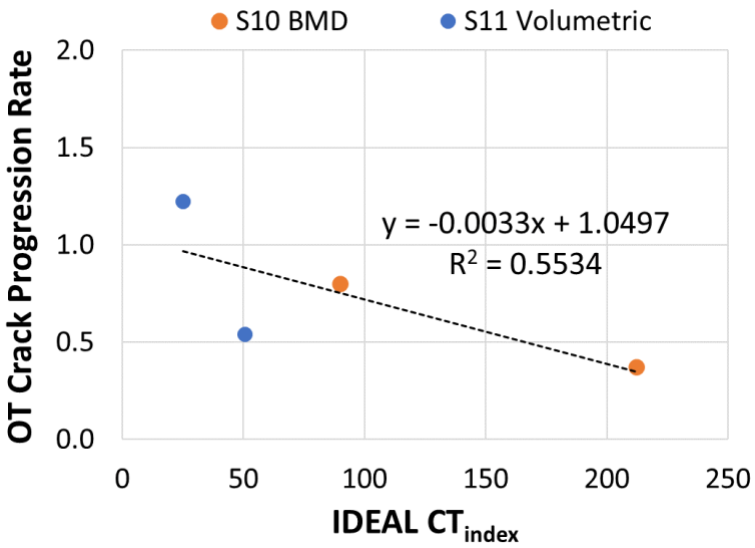

Figure 9. Correlation between IDEAL *CT$_{Index}$* and OT *CRI* Results of Reheated and Critically Aged PMLC Specimens

Figure 10 presents the HT-IDT test results of reheated PMLC specimens. As shown, the S10 mix had a lower HT-IDT strength and thus, was expected to have a reduced rutting resistance than the S11 volumetric mix. These results agreed with the HWTT rut depth results in Figure 6 and highlighted the potential of using the HT-IDT test as a surrogate to HWTT for BMD production testing. However, the correlation between these tests could not be determined due to the limited data availability in the study.

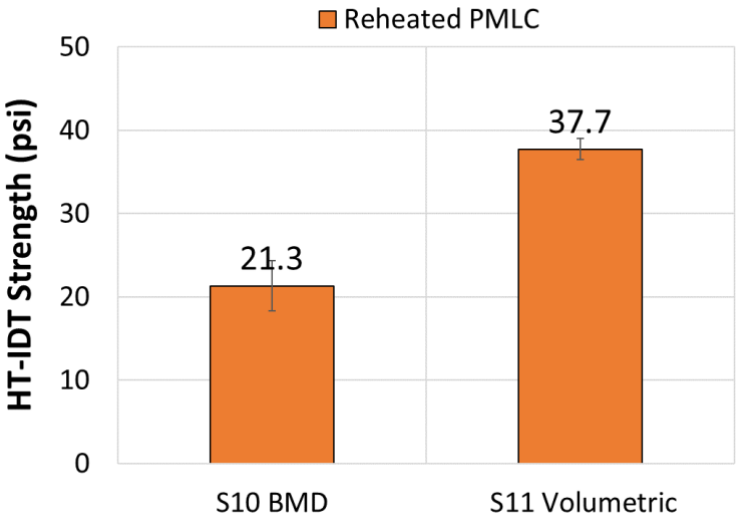

Figure 10. HT-IDT Strength Results of Reheated PMLC Specimens

16.7 Field Performance

Heavy traffic loading of the two sections started on October 10, 2018. As of February 24, 2021, 10 million ESALs of heavy truck traffic had been applied. Throughout the trafficking of the test sections, surface cracking, rutting, smoothness, and surface texture were monitored on a

weekly basis using an automated pavement condition survey vehicle. Additionally, surface friction was measured every month using a locked-wheel friction trailer.

Figure 11 presents the field rutting data. Section S10 had 0.3 inches of rutting after 9.6 million ESALs, which was approximately 30% higher than that of section S11 (i.e., 0.23 inches). For both sections, most of the rutting occurred in the summer of 2019 and then began to level off. Although Section S10 rutted more than Section S11, it was far from exceeding the maximum rutting threshold of 0.5 inches. The field rutting data in Figure 11 agreed with the HWTT and HT-IDT results, which indicated reduced but adequate rutting resistance of the S10 BMD mix compared to the S11 volumetric mix.

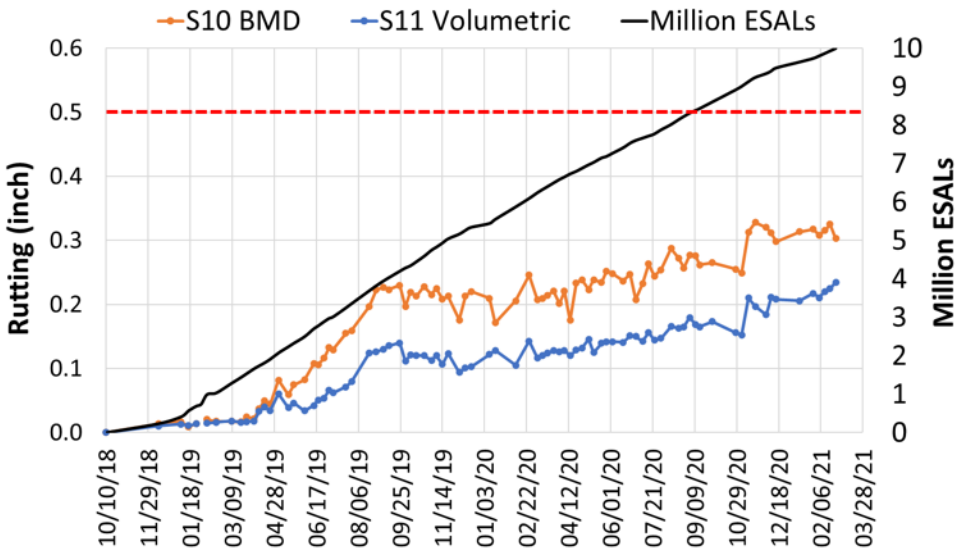

Figure 11. Field Rutting Data

Figure 12 presents the surface cracking data, where cracking is expressed as percentage of lane area cracked. As can be observed, Section S10 exhibited superior cracking performance with only 1.4% of cracked lane area after 10 million ESALs, while section S11 had an 8.5% of cracked lane area, which was approximately six times higher than section S10. These data agreed with the laboratory OT and IDEAL-CT results, which indicated that the S10 BMD mix had better cracking resistance than the S11 volumetric mix. Cracking in Section S11 was first observed in mid-November 2019, which was later confirmed to be caused by the reflection of previously existing cracking in the underlying layer. Despite the notable difference in the field cracking data, both sections were far from exceeding the maximum lane area cracked limit of 20%.

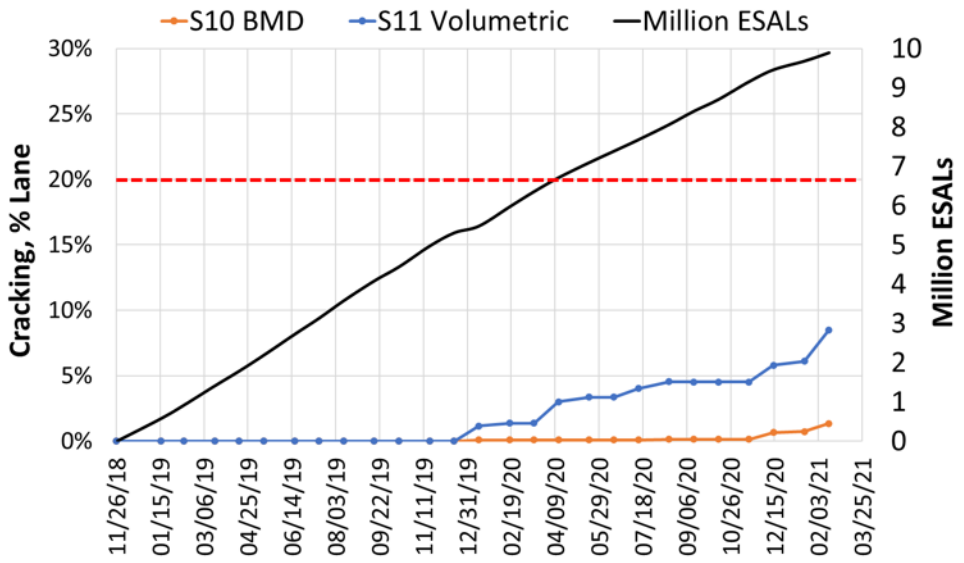

Figure 12. Field Cracking Data

Figures 13 through 15 present the international roughness index (IRI), mean texture depth (MTD), and skid number (tested with ribbed tire) results. As shown, the two sections had similar and acceptable smoothness, texture, and friction data after 10 million ESALs. Neither section had significant changes in the IRI through mid-February 2020. At that time, maintenance patches were applied in the transition areas of the test sections, which caused a steep increase in the IRI. After that, the IRI started to decrease gradually over time. Section S10 had a higher initial MTD than Section S11, which was likely attributed to the coarser gradation of the mix. Nevertheless, the two sections had similar MTD results after September 2020. Finally, the skid number of both sections reduced from approximately 40 after construction to 30 after 10 million ESALs, but they still met the general skid number threshold of 25 for Test Track sections.

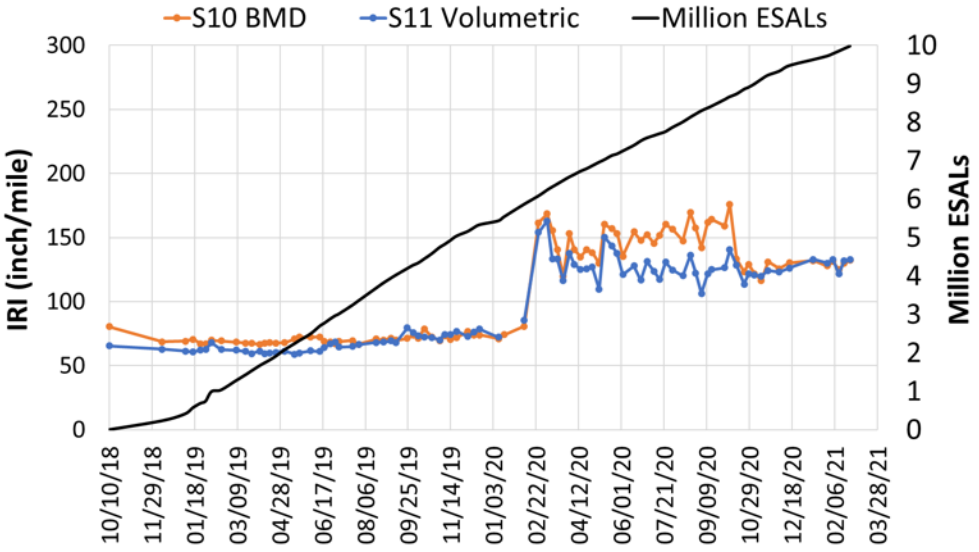

Figure 13. Field Smoothness Data

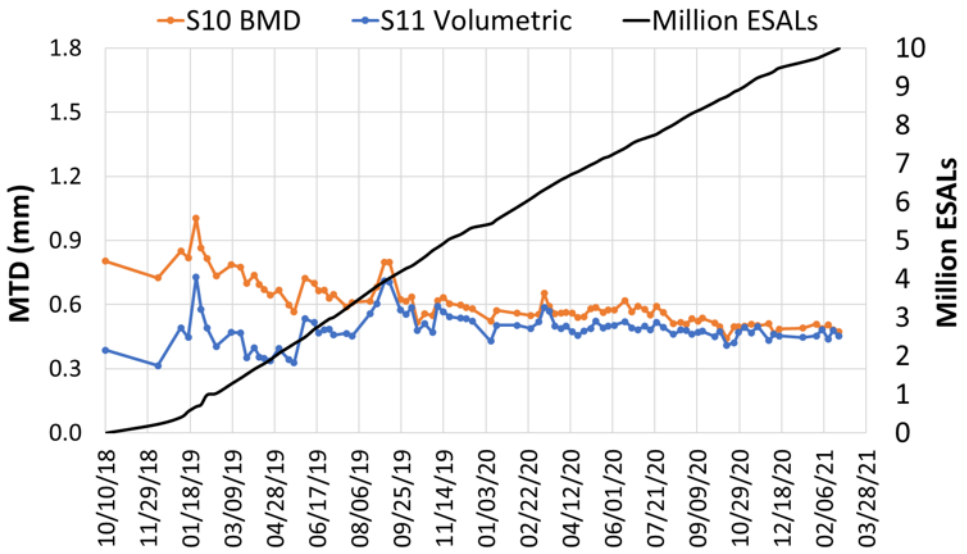

Figure 14. Field Texture Data

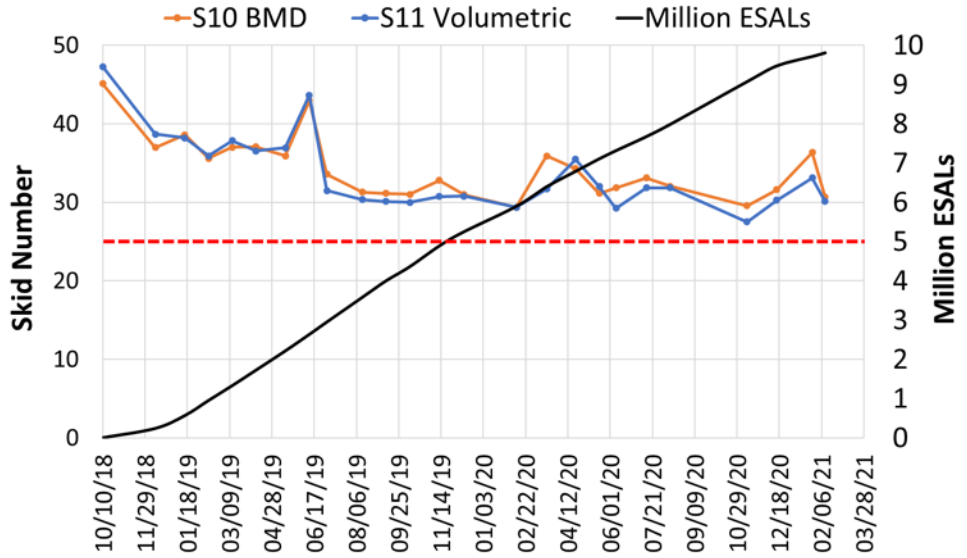

Figure 15. Field Friction Data

16.8 Conclusions and Recommendations

Based on the laboratory test results and field performance data collected after 10 million ESALs, the following conclusions and recommendations were made.

- As compared to the S11 volumetric mix, the S10 BMD mix was designed with a slightly coarser gradation but significantly higher OBC and VMA to achieve improved mixture durability and cracking resistance.
- The OT and HWTT testing of both mix design and production samples indicated that the S10 BMD mix had better cracking resistance but reduced rutting resistance than the S11 volumetric mix. The S10 BMD mix passed TxDOT's OT and HWTT requirements and thus,

was expected to have balance performance between cracking and rutting resistance while the S11 volumetric mix failed the OT requirement.

- The critical aging protocol of aging loose mix for eight hours at 135°C had a significant impact on reducing the cracking resistance of both S10 BMD and S11 volumetric mixes. Nevertheless, the S10 BMD production mix significantly outperformed the S11 volumetric mix in OT and IDEAL-CT at both reheated and critically aged conditions.
- The IDEAL-CT and HT-IDT tests showed a consistent trend in terms of the performance evaluation for S10 BMD versus S11 volumetric mixes as the OT and HWTT tests, respectively, which indicated that they have potential for being used as surrogate tests to OT and HWTT for BMD production testing.
- Both sections performed well after 10 million ESALs. Section S10 had more rutting but less cracking than Section S11, which agreed with the laboratory test results. Possibly because of the coarser gradation, Section S10 had higher MTD than Section S11 after construction, but the difference was significantly reduced over time. Finally, the two sections showed similar smoothness and friction characteristics through the research cycle.
- Both sections are recommended for traffic continuation in the next research cycle to further monitor and evaluate their long-term performance on the Test Track. This longer-term performance data will be highly valuable for TxDOT to verify the benefits of implementing BMD in extending the service life of asphalt pavements in Texas.

16.9 References

1. Garcia, V. M., Miramontes, A., Garibay, J., Abdallah, I., Carrasco, G., Lee, R., & Nazarian, S. (2017). Alternative methodology for assessing cracking resistance of hot mix asphalt mixtures with overlay tester. Road Materials and Pavement Design, 18(sup4), 388-404.
2. Chen, C., Yin, F., Turner, P., West, R. C., & Tran, N. (2018). Selecting a laboratory loose mix aging protocol for the NCAT top-down cracking experiment. Transportation Research Record, 2672(28), 359-371.
3. Chen, C., Yin, F., Andriescu, A., Moraes, R., Mensching, D., Tran, N., Taylor, A., & West, R. (2020). Preliminary Validation of the Critical Aging Protocol for NCAT Top-down Cracking Experiment. Journal of the Association of Asphalt Paving Technologists.
4. Yin, F., Taylor, A., & Tran, N. (2020). Performance Testing for Quality Control and Acceptance of Balanced Mix Design. NCAT Report 20-02.

17. BIO-POLYMER MODIFIED ASPHALT MIXTURE

Dr. Nam Tran

17.1 Introduction

The need for more durable pavements with better performance and longer service life has led to an increasing use of modified asphalt binders, as they can meet the requirements for a wider Superpave performance grade (PG) range (*1*). Different modifiers, such as polymers and oils, have been used for asphalt binder modification (*2, 3, 4, 5*). Polymers used in asphalt paving materials have been traditionally made from petroleum-based products, but they can now be made from bio-based feedstocks.

Iowa State University has developed a bio-derived polymer produced from the transesterification of glycerol from the triglycerides in epoxidized soybean oil by using benzyl alcohol. This bio-polymer, which includes epoxidized benzyl soyate (EBS), is thought to also improve the resistance of asphalt binders to oxidative aging as the epoxide rings within the EBS react to form crosslinks and block nucleophilic sites where asphalt oxidation occurs.

Preliminary laboratory work has shown that the EBS could be used to restore the performance properties of heavily aged asphalt binders and maintain the performance characteristics after long-term aging. Further evaluation of EBS in a full-scale accelerated field experiment was needed to verify previous laboratory test results and support the adoption of this bio-polymer product by state highway agencies.

17.2 Research Objective and Scope

The objective of this experiment was to evaluate the impacts of the new bio-polymer on asphalt binder, plant-produced mixture, and its field performance on the NCAT Test Track. The bio-polymer modified asphalt binder was blended at an asphalt terminal and delivered to East Alabama Paving's plant in Opelika, Alabama. The bio-polymer asphalt mixture was then produced and paved in the surface layer of Section W10 at the NCAT Test Track.

The laboratory and field performance of the bio-polymer modified binder and mixture was compared with that of a conventional styrene-butadiene-styrene (SBS) polymer binder and its mixture placed in Section E5A. Both sections (i.e., W10 and E5A) were constructed in 2018 and evaluated under the same heavy truck traffic loading conditions at the NCAT Test Track. During construction, samples of asphalt binder and loose mix were taken for laboratory testing to assist the field performance evaluation. This chapter summarizes the laboratory evaluation of asphalt binders and mixtures placed in Sections E5A and W10 and their field performance at the end of the 2018 research cycle in February 2021.

17.3 Experimental Plan

The structure of Sections W10 and E5A was originally built for the 2000 research cycle. It was designed with sufficient thickness to ensure that no structural damage would occur during testing. Surface distresses, including rutting and surface (or near surface) cracking, have been only those observed in the original pavement sections at the NCAT Test Track. In 2018, the surface layers of these sections were milled and replaced with new mixtures for this field performance evaluation. In the following subsections, the compositions of the surface mixtures

are first discussed, followed by an experimental plan for evaluating the binders and mixtures sampled during construction.

17.4 Asphalt Mixtures

The new surface mixtures used in Sections W10 and E5A were produced based on the same mix design except for the new (virgin) asphalt binders used. The surface mixture for Section W10 was produced using an asphalt binder modified with EBS bio-polymer, while the control surface mixture in Section E5A was produced utilizing an asphalt binder modified with SBS polymer. These binders were modified from two base binders provided by different suppliers. The aggregate gradation used in the mix design was a 12.5 mm nominal maximum aggregate size (NMAS) blend of 1/2" processed reclaimed asphalt pavement (RAP) with a binder content of 5.5%, granite 78s, granite 89s, and a local sand. Table 1 shows the properties of the aggregates used in the mix design. Table 2 provides a summary of the mix design parameters for Sections W10 and E5A.

Table 1. Aggregate Properties

Property	RAP	GRN 78s	GRN 89s	Sand
Cold feed percentage (%)	20	38	24	18
Bulk specific gravity (G_{sb})	2.624	2.627	2.570	2.716
Apparent specific gravity (G_{sa})	2.678	2.682	2.650	2.745
Absorption (%)	0.8	0.8	1.2	0.4

Table 2. Summary of Mix Design Volumetric Parameters

Property	Value
Design Air Voids (VTM), %	4.0
Total Combined Binder (Pb), %wt	5.3
Effective Binder (P_{be}), %	4.9
Dust Proportion (DP)	1.0
Maximum Specific Gravity (G_{mm})	2.466
Voids in Mineral Aggregate (VMA), %	15.3
Voids Filled with Asphalt (VFA), %	73.7

17.5 Laboratory Testing Plan

Figures 1 and 2 show plans for evaluating the asphalt binders and mixtures, respectively. For each test section, representative samples of the virgin binders and plant produced asphalt mixtures were collected. The representative binder samples were taken from the tankers when the binders were delivered. The representative loose mix samples were obtained by diverting mix from the conveyor of the material transfer machine going into the paver onto a flatbed truck. The flatbed then brought the mix to the rear of the Test Track laboratory where the mixes were shoveled into five-gallon buckets and labeled. A total of 16 buckets of each mixture were sampled for this study.

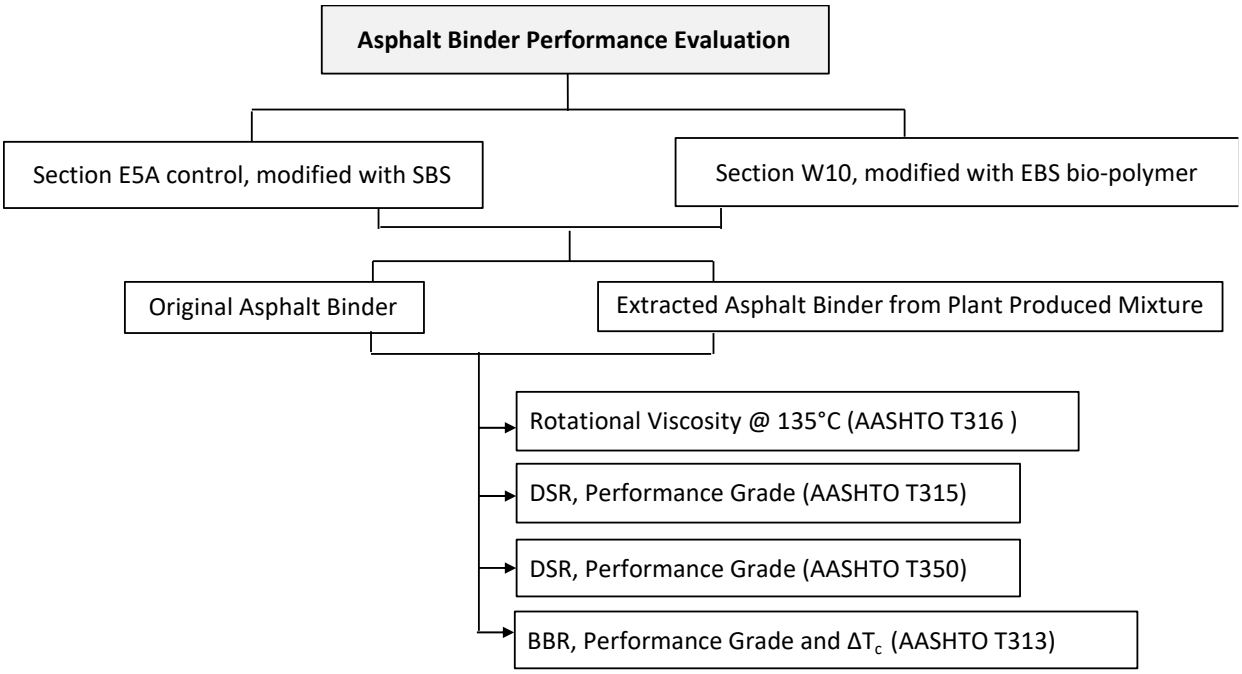

Figure 40. Testing Plan Performed for Asphalt Binder Evaluation

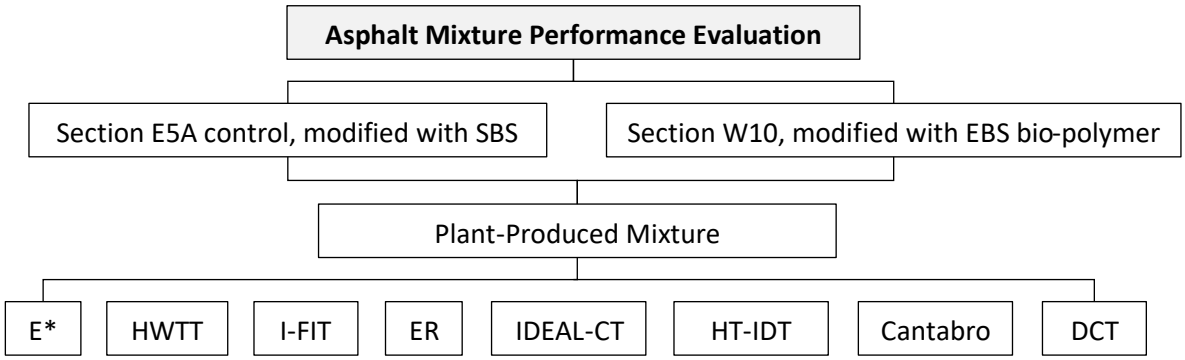

Figure 41. Testing Plan Performed for Asphalt Mixture Evaluation

For the laboratory mixture performance evaluation, the plant produced mix was heated (RH PMLC) in an oven at 150°C (compaction temperature) for two hours, then was reduced to testing size by following the quartering method described in AASHTO R47. The theoretical maximum specific gravity test was performed on both mixes in accordance with AASHTO T209, and the results were 2.478 and 2.491 for the E5A and W10 mixes, respectively. AASHTO T166 was followed to obtain the bulk specific gravity of the mixes. The target air voids of the specimens for mixture performance testing (after either cutting or coring when applicable) were 6.5%, which was selected based on the in-place densities achieved in the two test sections. A description of each test method is given below.

In addition to testing the virgin binders, asphalt binders were also extracted from the plant produced mixtures per ASTM D2172 (method A) using trichloroethylene and recovered per ASTM D5404. For both sections (E5A and W10), the rheological evaluation of the recovered

binders was performed in comparison with the virgin binders sampled at the asphalt plant during production.

17.6 Asphalt Binder Performance Results

17.6.1 Rotational Viscosity

Viscosity is a measure of fluid's resistance to flow and is indicative of asphalt binder handling properties. The rotational viscosity test was performed at 135ºC in accordance with AASHTO T316. Figure 3 shows rotational viscosity values of the asphalt binders utilized in Sections E5A (control, modified with SBS) and W10 (modified with EBS bio-polymer). As expected, there was an increase in asphalt binder viscosity with the addition of RAP (i.e., results of the binders extracted and recovered from plant produced mixes), especially for the bio-polymer modified binder. The Superpave Brookfield rotational viscosity value limit for asphalt binders at 135ºC is 3 Pa.s, and all tested binders, with and without the addition of aged RAP binder, showed viscosity values below the specification limit.

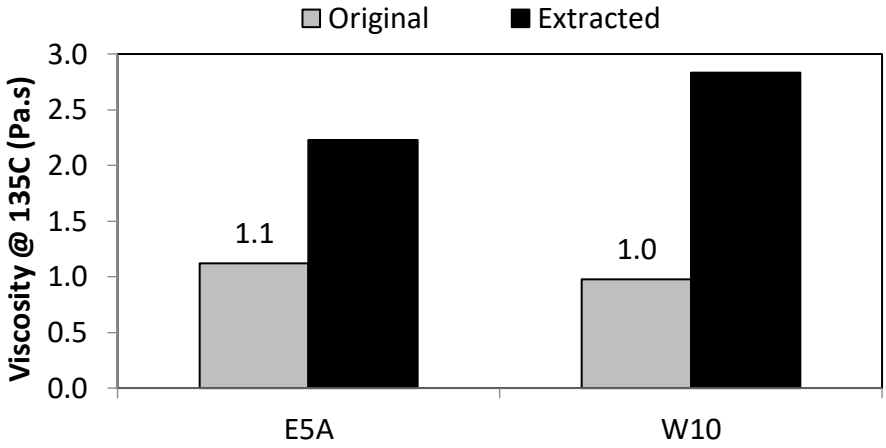

Figure 3. Rotational Viscosity at 135ºC

17.6.2 Performance Grading (PG) and ΔTc

Table 3 shows the high, intermediate, and low pass/fail temperatures, as well as the ΔT_c of the asphalt binders utilized in Sections E5A and W10. The results were obtained by conducting the following tests:

- The Dynamic Shear Rheometer (DSR) per AASTHO T315 was used to characterize the viscous and elastic behavior of unaged, rolling thin film oven (RTFO) aged, and pressure aging vessel (PAV) aged binders.
- The Bending Beam Rheometer (BBR) per AASHTO T313 was used to measure the rheological characteristics of PAV aged binders at low temperatures.

As indicated in Table 3, the asphalt binder extracted and recovered from both the E5A and W10 plant produced mixtures had a higher continuous grade temperature than the original asphalt binders. Furthermore, the addition of the RAP binder (i.e., results of the binders extracted and recovered from plant produced mixes) had a slightly higher effect on the properties of the W10

binder, resulting in a slightly larger increase in the continuous grade temperature before and after short-term aging. At an intermediate temperature, the W10 original binder showed higher intermediate continuous grade temperature than the E5A original binder. At the low temperature, for both stiffness and m-value, the W10 original binder showed warmer low continuous grade temperature in comparison to the E5A original binder. As indicated by the initial BBR stiffness and m-value results, the E5A original and extracted and recovered asphalt binders presented better low temperature cracking resistance than the W10 binder. As shown in Table 3, both virgin control and virgin W10 binders resulted in acceptable $\Delta T_{c.}$ After addition of RAP (i.e., results of the binders extracted and recovered from plant produced mixes), the stress relaxation of binders changed significantly, lowering ΔT_c (i.e., it become more negative). A lesser cracking susceptibility was observed for the binder modified with the extracted bio-polymer ($\Delta T_{c=}$ -6.6) in comparison to the extracted SBS-control binder ($\Delta T_{c=}$ -7.3). All binders, before and after mixture production, were found to be "m-controlled" (i.e., failure potentially controlled by inadequate stress relaxation).

Table 3. ΔT_c, High, Intermediate and Low Pass/Fail Temperatures of Binders

Sample	T_{cont} High unaged (°C)	T_{cont} High RTFO (°C)	T_{cont} Intermediate (°C)	T_{cont} Low S (°C)	T_{cont} Low m-value (°C)	ΔT_c
E5A Virgin	76.3	77.2	22.6	-27.3	-24.7	-2.6
E5A Extracted	89.7	88.4	25.2	-26.6	-19.2	-7.3
W10 Virgin	73.6	75.7	24.6	-24.6	-21.6	-3.0
W10 Extracted	92.0	89.1	29.8	-22.6	-16.0	-6.6

Table 4 presents the final PG of the asphalt binders before and after the production of the mixtures containing RAP. Typically, asphalt binders with a broader PG range (i.e., useful temperature interval - UTI) are thought to provide better pavement performance under a given traffic and environmental condition.

Table 4. PG and Useful Temperature Interval of Binders

Sample	PG High Temp. (°C)	PG Low Temp. (°C)	UTI (°C) (PG High Temp. - PG Low Temp.)
E5A Virgin	76	-22	98
E5A Extracted	88	-16	104
W10 Virgin	70	-16	86
W10 Extracted	88	-16	104

As shown in Table 4, the addition of RAP increased the stiffness of the total binder in both the E5A and W10 asphalt mixes. An increase in true PG was observed for both E5A and W10 binders with the low PG of the extracted E5A binder changing from -22°C to -16°C. However, no difference in the useful temperature interval (UTI) of binders was observed for the extracted asphalt binders blended with SBS and EBS bio-polymer.

17.6.3 Multiple-Stress Creep-Recovery (MSCR) Test

The Multiple-Stress Creep-Recovery (MSCR) test was conducted at 64°C in accordance with AASHTO T350 to measure the non-recoverable creep compliance (J_{nr}) and percent recovery (%R) of RTFO aged binders. The MSCR results are presented in Table 5 and indicate that the E5A virgin binder containing SBS has lower non-recoverable creep compliance (J_{nr}) over the W10

virgin binder containing the EBS bio-polymer, having a MSCR grading of PG 64E-22 (Extremely Heavy) in comparison to the PG 64V-16 (Very Heavy) of the W10 binder.

Table 5. MSCR High Temperature PG Classification of Asphalt Binders at 64°C

Sample	J_{nr} @ 3.2, kPa^{-1}	% diff J_{nr}	%R @ 3.2, kPa^{-1}	High Temp. PG (°C)
E5A Original	0.33	33.4	59.9	64E
E5A Extracted	0.09	5.7	58.7	64E
W10 Original	0.65	33.4	29.5	64V
W10 Extracted	0.09	16.6	59.9	64E

Furthermore, as shown in Figure 4, the E5A virgin binder showed higher percent recovery (i.e., 59.9%) in comparison to the W10 original binder (i.e., 29.5%), indicating higher resistance to pavement permanent deformation. All modified binders, before and after addition of the RAP binder, passed the J_{nr} percent-difference parameter, indicating no negative effect on stress susceptibility.

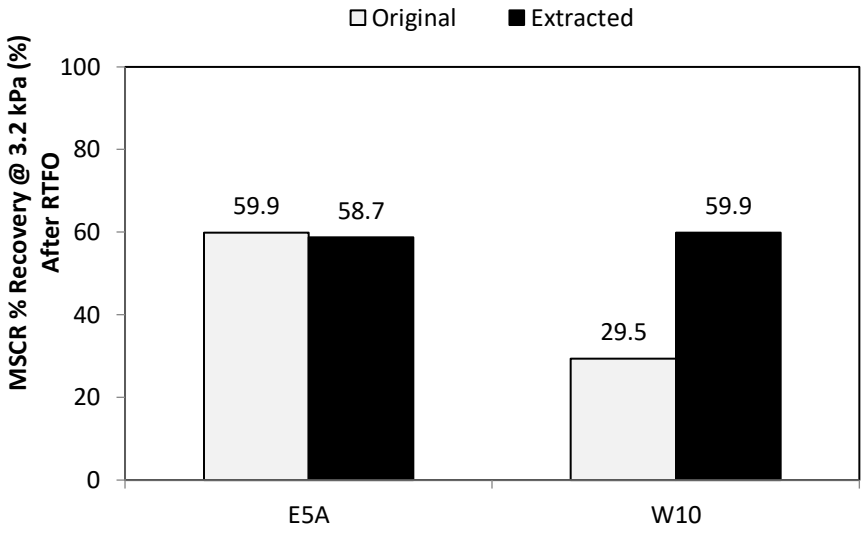

Figure 4. MSCR Percentage Recovery at 64°C

Figure 5 indicates that, for the extracted and recovered binders, the addition of the oxidized RAP binder resulted in a reduction of J_{nr}. Therefore, the improvement in the %R parameter for the W10 extracted binder can be attributed to the aged binder coming from the RAP. Evaluation of the binder properties after exposure in the field will allow a better understanding of the influence of the bio-polymer in the overall performance of the asphalt binder.

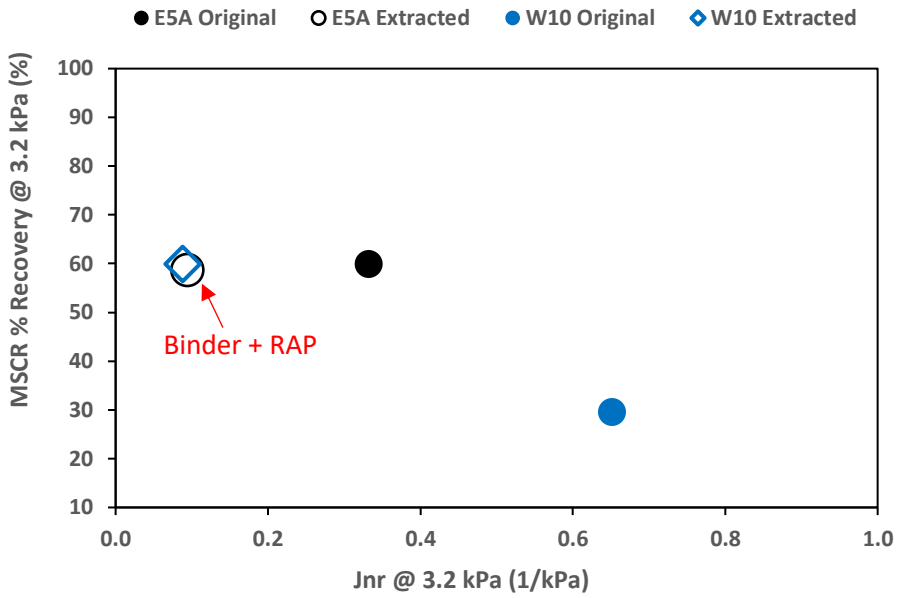

Figure 5. MSCR Percentage Recovery Versus Jnr at 3.2 kPa and 64°C

17.7 Mixture Performance Testing Results

17.7.1 Dynamic Modulus Test

Dynamic Modulus (E*) testing was performed for each mixture in accordance with AASHTO T 378-17 using an Asphalt Mixture Performance Tester (AMPT) on three 38 mm diameter x 110 mm tall asphalt specimens that met the target air voids. Specimens were tested at three temperatures (4, 20, and 40°C) and three loading frequencies (10, 1, and 0.1 Hz) at each of these temperatures. Specimens were additionally tested at 0.01 Hz at the 40°C test temperature. The data collected facilitated the construction of the E* master curve for each mix so that the relative stiffness of the two mixtures could be examined across a wide range of temperatures and loading rates.

The Dynamic Modulus master curves for the E5A (control) and W10 mixtures are shown in Figure 6. The results show that the two mixtures had comparable stiffness at higher loading rates and lower temperatures (right-hand side of the curve), but the mixture with the EBS bio-polymer binder was stiffer than the SBS modified control mixture across the remainder of the curve with higher temperatures and slower loading rates (left-hand side of the curve).

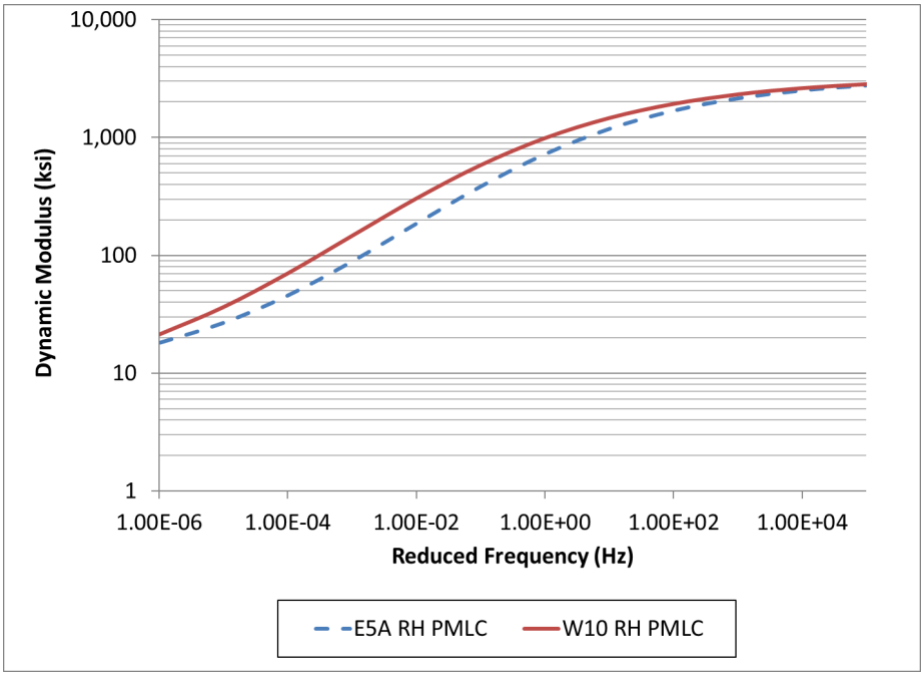

Figure 6. Dynamic Modulus Master Curves

17.7.2 Hamburg Wheel Tracking Test

The Hamburg Wheel Tracking Test (HWTT) was conducted in accordance with AASHTO T324 on specimens submerged in 50°C water to evaluate both rutting resistance and moisture susceptibility of the asphalt mixtures. The HWTT results of the E5A control and W10 mixtures are summarized in Table 6. As can be seen, both mixes presented rut depths of less than 2 mm at 10,000 and 20,000 passes. This rut depth was significantly less than the common threshold criteria of 12.5 mm at 20,000 passes (*6*). Neither mixture exhibited signs of stripping in the Hamburg test.

Table 6. Hamburg Wheel Tracking Results Summary

Mix	Rut Depth at 10,000 passes (mm)	Rut Depth at 20,000 passes (mm)	Rut Depth of 12.5 mm (# passes)	Stripping Inflection Point (# passes)
E5A	1.28	1.51	>20,000	>20,000
W10	1.48	1.68	>20,000	>20,000

17.7.3 Illinois Flexibility Index Test (I-FIT)

The Illinois Flexibility Index Test (I-FIT) was conducted per AASHTO TP124 at 25°C to evaluate the mixture resistance to intermediate temperature cracking. The I-FIT results are shown in Figure 7. The E5A control mix showed an average flexibility index (FI) result of 4.5 while the W10 bio-polymer mix showed an FI of 2.0. A two-sample t-test conducted at a significance level of 5% showed that the E5A control mix had statistically higher FI than the W10 bio-polymer mix (p-value = 4.9e-5 < α). Based on this result, the SBS-control mix was found to be more resistant to cracking than the W10 EBS-modified mix based on the I-FIT test.

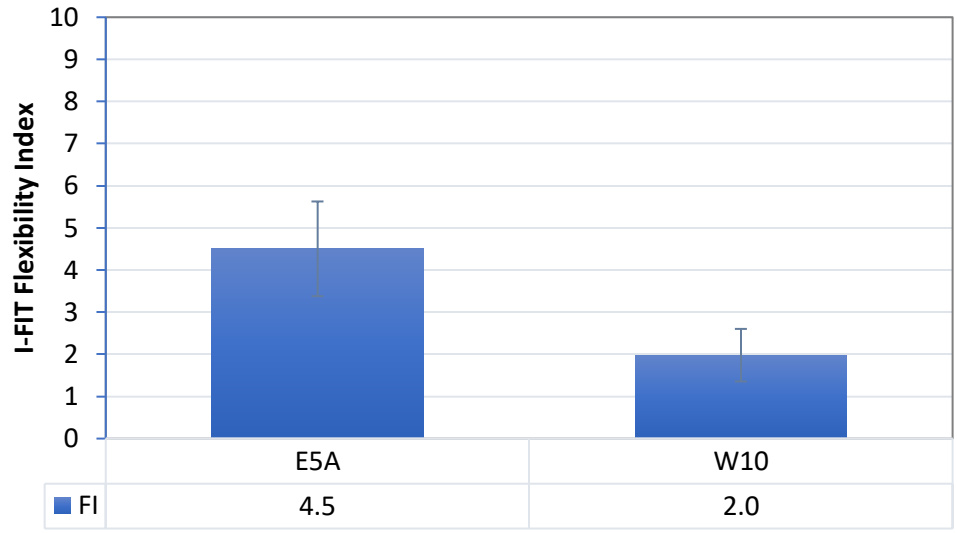

Figure 7. I-FIT Flexibility Index Results

17.7.4 Energy Ratio

The evaluation of asphalt mixtures using Energy Ratio (ER) was conducted to assess the susceptibility of the mixtures to top-down cracking by performing three indirect tension tests on the same mixture specimens. Testing was performed on IDT specimens trimmed to 50 mm thick and instrumented with both horizontal and vertical strain gauges. These tests are resilient modulus (ASTM D7369), creep compliance (AASHTO T322), and indirect tensile strength (ASTM D6931). The ER is the ratio of dissipated creep strain energy threshold of the mixture (DCSEHMA) and the minimum dissipated creep strain energy required to resist top-down cracking (*7*). The dissipated creep strain energy is the energy required beyond the elastic region to initiate cracking. The higher the ER, the more the mixture should be resistant to top-down cracking.

Table 7 shows the summary of the Energy Ratio analysis. At the ER test temperature of 10°C, both mixtures appeared to have similar properties in the three component tests (resilient modulus, creep compliance, and fracture energy). This resulted in both mixes having a similar ER, with the control having an ER of 4.3 and the W10 mix having an ER of 4.8.

Table 7. Energy Ratio Results

Mix	Resilient Modulus (GPa)	Creep Compliance Rate	IDT Fracture Energy (kJ/m^3)	DCSE$_{HMA}$ (kJ/m^3)	ER
E5A	13.14	3.586 E-06	3.2	2.97	4.3
W10	12.96	3.290 E-06	3.6	3.27	4.8

17.7.5 Indirect Tensile Asphalt Cracking Test (IDEAL-CT)

The Indirect Tensile Asphalt Cracking Test (IDEAL-CT) was conducted per ASTM D8225 at 25°C to evaluate the mixture's resistance to intermediate temperature cracking. The IDEAL-CT test data were used to determine the CT_{index} values for the two mixtures, as shown in Figure 8. The W10 mix showed an average CT_{index} of 17.2 with a standard deviation of 4.3, while the E5A

mixture showed an average CT_{index} of 26.3 with a standard deviation of 6.4. A two-sample t-test was conducted at a 95% confidence interval to determine the statistical significance difference of the means assuming equal variances. The t-test showed that the W10 bio-polymer mixture had a statistically lower CT_{Index} as compared to the E5A control mix (p-value = 0.024 < α = 0.05). Therefore, the bio-polymer mixture is less resistant to cracking in comparison to the SBS-control mixture based on the IDEAL-CT test results.

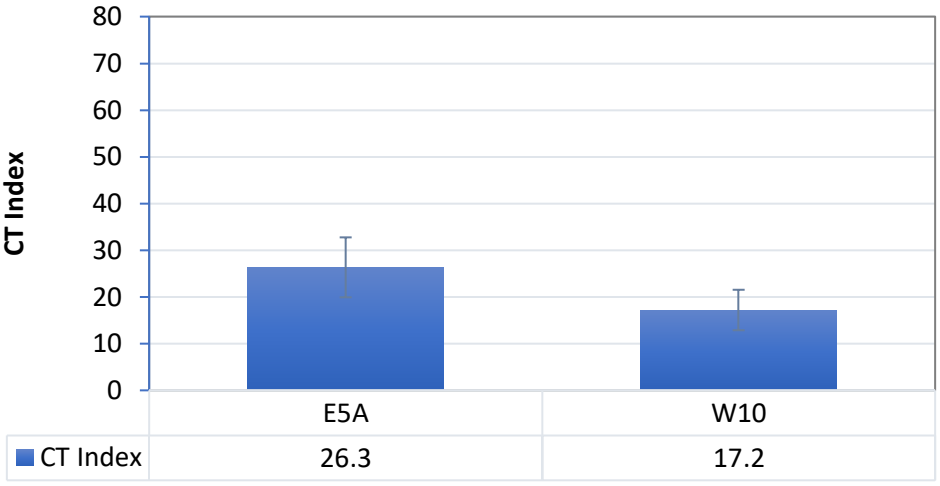

Figure 8. IDEAL-CT Results

17.7.6 High Temperature Indirect Tensile Test

The High Temperature Indirect Tensile Test (HT-IDT) was conducted in a similar manner as the IDEAL-CT except that the test temperature was at 50.2°C. The test was conducted to evaluate the rutting susceptibility of the mixes. A higher IDT strength at high temperatures would be generally indicative of better relative rutting resistance.

As shown in Figure 9, the average IDT strength for the W10 bio-polymer and the E5A control mixes were 69.5 psi and 49.3 psi, respectively. Individual specimen results are summarized in Appendix A. The standard deviation of the bio-polymer sample was 14.2 psi while the control was 5.2 psi. A two-sample t-test showed that the IDT strength of the EBS-modified mixture was statistically higher in comparison to the SBS-control mix (p-value = 0.036 < α = 0.05). These results indicate that the bio-polymer asphalt mixture is more resistant to rutting in comparison to the control mix in the High Temperature IDT test.

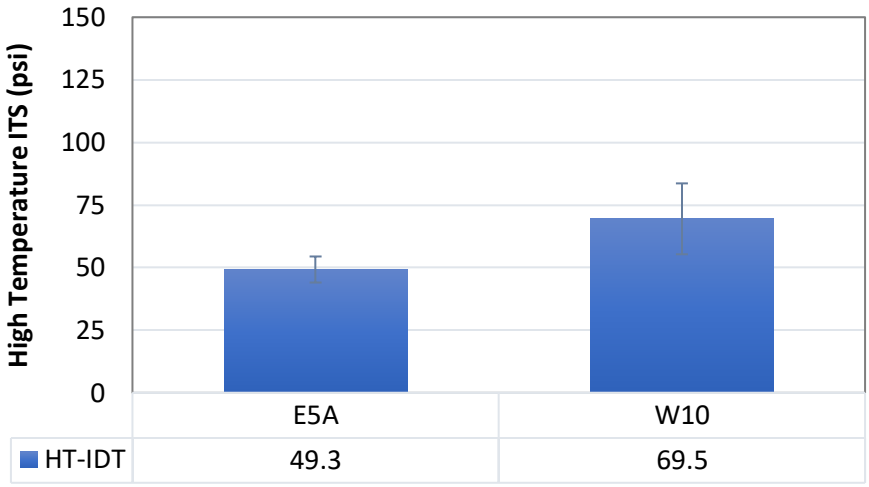

Figure 9. High Temperature Indirect Tensile Test Results

17.7.7 Cantabro Percentage Loss

The Cantabro test was performed to assess the raveling potential of the asphalt mixtures in accordance with AASHTO TP108-14. The Virginia Department of Transportation is currently proposing to use a maximum Cantabro Mass Loss of 7.5% for specimens compacted to N_{design} for their BMD surface mixes (VDOT, 2019).

Figure 10 summarizes the Cantabro mass loss and specimen air voids for the specimens compacted to N_{design}. A Cantabro percentage mass loss of 12% and an average air voids content of 4.8% was observed for the W10 mixture containing the EBS bio-polymer. For the E5A control mixture, a mass loss of 9.8% and an average air voids content of 3.9% was observed. A two sample t-test showed that while the W10 mix had a statistically higher mass loss than the control mix at N_{design} (p-value = 0.02 < α = 0.05), the W10 mix had statistically higher air voids than the control mix at N_{design} as well (p-value = 0.003 < α = 0.05).

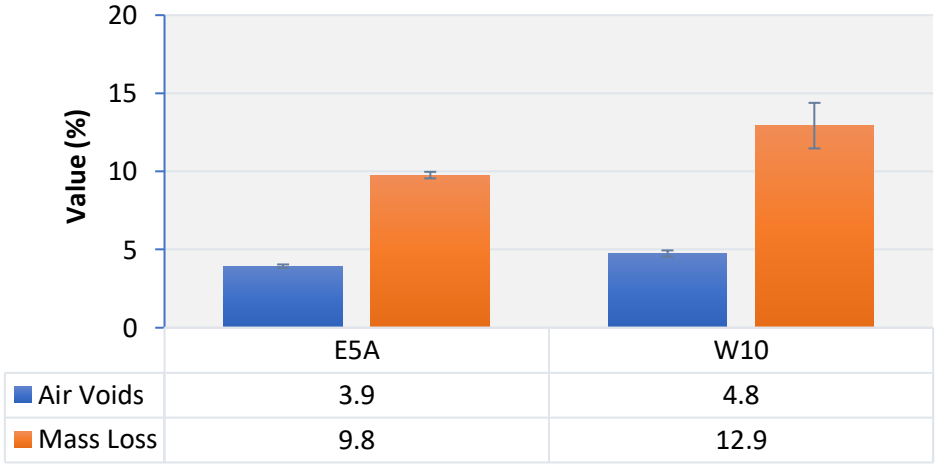

Figure 10. Cantabro Mass Loss – N_{design} Specimens

Figure 11 shows the Cantabro loss based on the target air voids content (6.5±0.5%). As can be seen, the percentage mass loss was 11.3% for the mixture containing the EBS bio-polymer and 10.1% for the mixture containing SBS. A two-sample t-test conducted on the mass loss values showed that the average mass loss was not statistically significantly different among the control and W10 mixtures (p-value = 0.072 > α = 0.05).

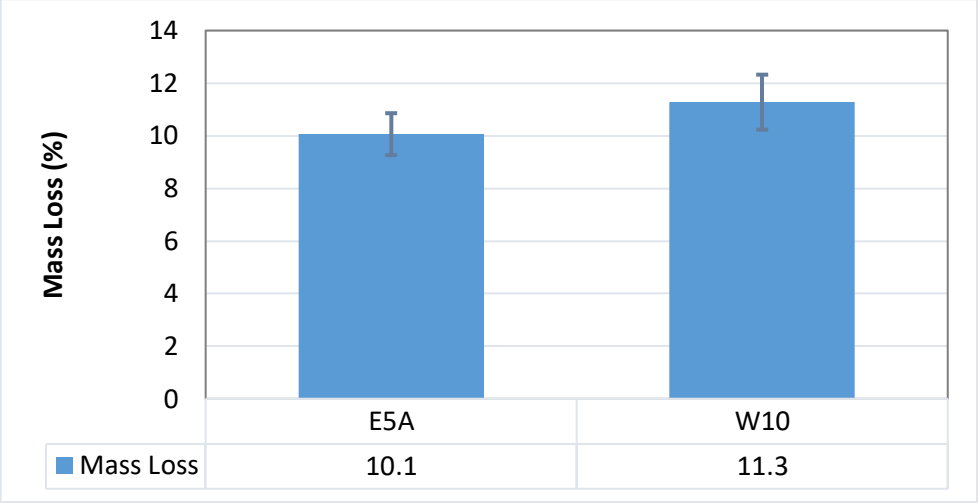

Figure 11. Cantabro Mass Loss – Specimens Compacted to 6.5 +/- 0.5 Percent Air Voids

17.7.8 Disk Shaped Compact Tension (DCT) Test

The low temperature cracking resistance of the study mixes was assessed using the Disk-Shaped Compact Tension (DCT) test. Testing was performed in accordance with ASTM D7313-13 at a test temperature of -12°C.

Figure 12 shows the DCT fracture energy (FE) (J/m^2) for the mixtures tested in this study. The E5A mix had an average FE of 604.5 J/m^2 with a standard deviation of 56.8 J/m^2 (CV of 9.4%) while the W10 mix had an average FE of 510.3 J/m2 with a standard deviation of 81.7 J/m^2 (CV of 16.0%). A two-sample t-test conducted on the DCT FE values showed that the E5A mix had a statistically greater fracture energy than the W10 mixture (p-value = 0.043 < α = 0.05). Therefore, the bio-polymer mixture is less resistant to low temperature cracking in comparison to the SBS-control mixture based on the DCT test results. Also, based on the fracture energy criteria proposed in a previous study (Marasteanu et al., 2012), both mixtures can provide satisfactory performance for a moderate traffic level (10 to 30 million ESALs).

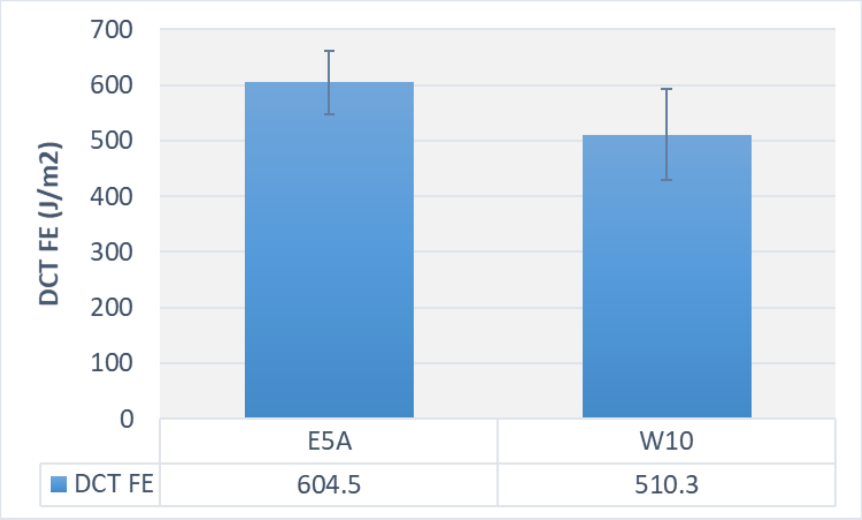

Figure 12. DCT Fracture Energy Results

17.8 Field Performance

Sections E5A (control, SBS modified) and W10 (modified with EBS bio-polymer) were evaluated for rutting, cracking, roughness, and macrotexture at the NCAT Test Track for 10 million equivalent single axle loads (ESALs), as shown in Figure 13. Figure 13a compares rut depth measurements for the SBS-control E5A and the EBS-bio-polymer W10 sections. The average rut depth of the bio-polymer section was 4.7 mm after 10 million ESALs in 2021. For the same applied traffic, the average rut depth of the control section was 2.4 mm. These values are smaller than the rut depth limit of 12.5 mm, which is commonly considered failing. Therefore, both mixes have shown no significant rutting thus far.

Figure 13b compares cracking measurements for the two test sections. The first crack was observed in Section E5A on November 20, 2020. At the end of the trafficking cycle on February 28, 2021, low-severity cracking measured in Section E5A was 0.4% of lane area. No cracking has been observed in Section W10 thus far.

For each section, pavement roughness was quantified using the International Roughness Index (IRI). Increases in roughness are commonly associated with pavement distresses. As can be seen in Figure 13c, the change in roughness over time for the E5A control and W10 sections was similar, especially towards the end of the trafficking cycle. Despite slight fluctuations in the smoothness of the pavement, the overall IRI of Section W10 was 102 in/mile, while 112 in/mile roughness was obtained for Section E5A.

The final assessment of field performance was surface macrotexture. Section W10 showed higher macrotexture at the beginning of the research cycle. However, the change in surface macrotexture over time for the two test sections was almost identical. The sections will continue to be monitored for rutting, cracking, roughness, and macrotexture in the next (2021) Test Track research cycle.

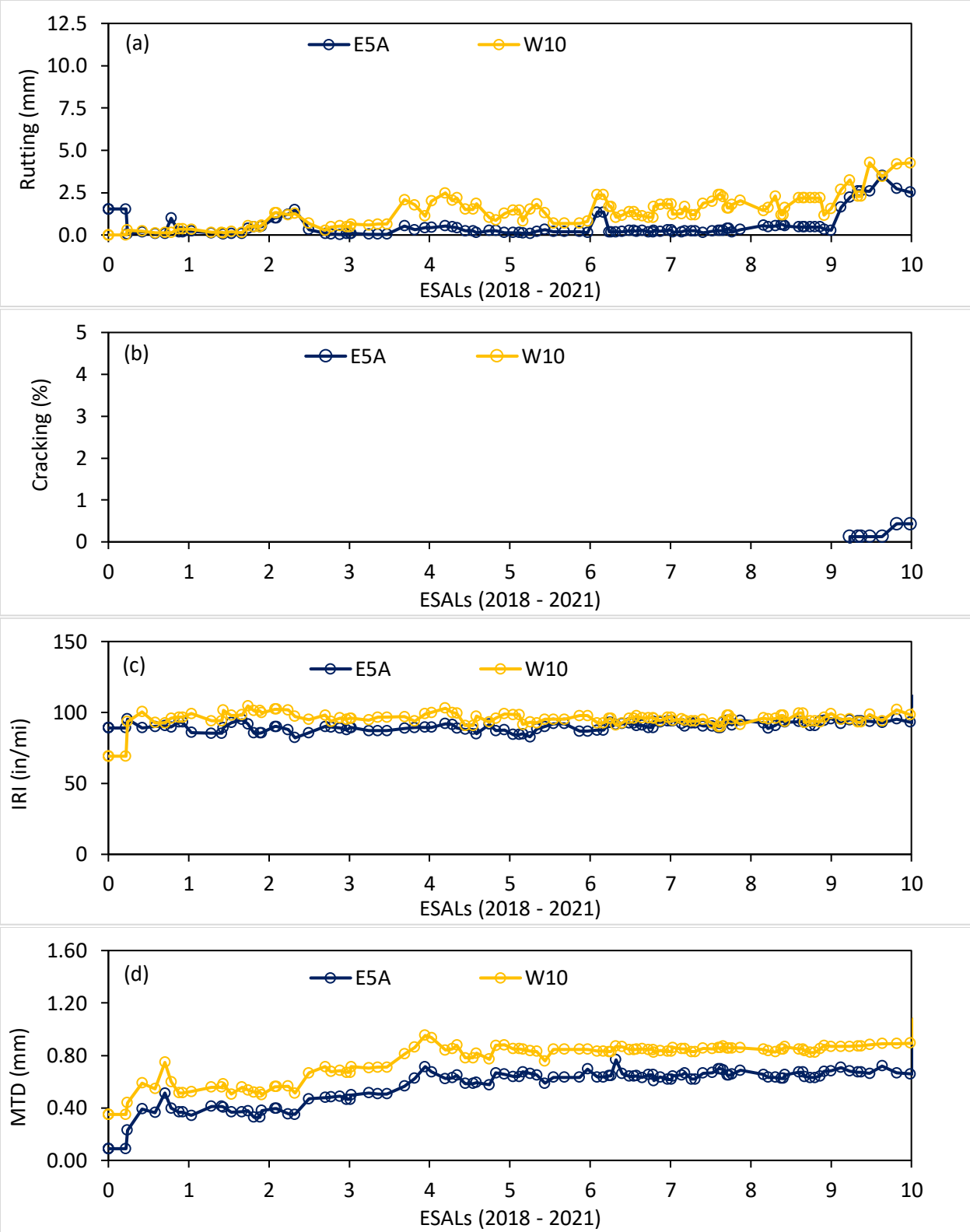

Figure 13. Field Performance of Sections E5A and W10

17.9 Summary and Conclusions

The surface layer of Section W10 was milled and paved with a new asphalt mixture containing an EBS bio-polymer binder. The section was tested as part of the 2018 Test Track research cycle and was compared against a control section (E5A). The surface layer of E5A was paved with an asphalt mixture produced based on the same mix design but utilizing a standard SBS modified PG 76-22 binder. A comprehensive suite of laboratory binder and mixture tests was performed on materials sampled during construction, and the test sections were continuously monitored for texture, rutting, and cracking performance. This section summarizes the results of the laboratory study along with the field performance data collected in the 2018 Test Track research cycle.

The following observations were made regarding the laboratory binder characterization.

- The high temperature stiffness of the EBS-modified binder (W10) was lower than the SBS-modified binder (E5A). Higher stiffness at high temperatures may indicate increased resistance to rutting.
- The high temperature grade of the EBS-modified binder in section W10 was more affected by the incorporation of the RAP binder in comparison to the SBS-modified binder in section E5A, with the asphalt binder from the W10 plant produced mixture being stiffer than that from the E5A mixture.
- At intermediate temperature, the stiffness of the EBS-modified binder (W10) was higher than the SBS-modified binder (E5A). Increased intermediate temperature stiffness may indicate decreased resistance to load related cracking. The addition of RAP binder further increased the intermediate-temperature stiffness of asphalt binder for both mixtures. As with the high temperature stiffness, the asphalt binder from the EBS modified plant mix had a higher increase in stiffness at intermediate temperature.
- At low temperature, both original binders were found to be m-controlled and presented similar negative values of ΔT_c (i.e., -2.6 for E5A and -3.0 for W10). After the addition of RAP binder (i.e., results of the binders extracted and recovered from plant produced mixes), a ΔT_c of -7.3 and -6.6 was obtained for E5A and W10, respectively.

The following observations were made based on the mixture performance testing on the re-heated plant-produced mixtures.

- The Dynamic Modulus (E*) test generally showed the W10 mixture to be stiffer than the control SBS mixture across the majority of temperatures and frequencies tested. This observation was consistent with the majority of the other laboratory test results for rutting, cracking, and durability.
- Both mixtures rutted less than 2 mm in the Hamburg test with no evidence of stripping. The W10 mixture had a higher IDT strength than the control at the 50.2°C. However, neither mixture is expected to show significant rutting on the NCAT Test Track.
- Both the I-FIT and IDEAL-CT cracking tests (conducted at 25°C) showed the control (E5A) mix to have better cracking resistance than the W10 mixture. The Energy Ratio test (conducted at 10°C) showed the mixtures to have comparable cracking resistance. The DCT test for low temperature cracking resistance (conducted at -12°C) showed that the

control (E5A) mix may have better low temperature cracking resistance than the W10 mixture.

- The Cantabro test for mixture durability showed the W10 mix to have a higher mass loss (less durability) at Ndesign than the control mix. However, this mixture also had a higher air void content at mix design, which may have been a contributing factor. The two mixtures did not show statistically different Cantabro mass loss values for specimens compacted to the same target air void content.

The test sections have undergone 10 million ESALs of trafficking at the NCAT Test Track and have shown comparable field performance thus far. Both sections showed good rutting with final rut depths below 5.0 mm. No cracking was observed in Section W10 with the EBS-modified mixture while low severity cracks were recorded for 0.4% of lane area in Section E5A with the SBS-modified mixture.

These sections will be kept in place for continued trafficking for another 10 million ESALs in the 2021 Test Track research cycle, which will be important to evaluate the long-term performance of the bio-polymer modified asphalt against the conventional SBS modified asphalt.

17.10 References

1. Bahia, H. U., D. I. Hanson, M. Zeng, H. Zhai, M. A. Khatri, and R. M. Anderson. *NCHRP Report 459: Characterization of Modified Asphalt Binders in Superpave Mix Design.* TRB, National Research Council, Washington, D.C., 2001.
2. Li, Y., R. Moraes, E. Lyngdal, and H. U. Bahia. Effect of Polymers and Oils Modification on the Aging Susceptibility of Asphalt Binders. *Transportation Research Record: Journal of the Transportation Research Board*, No. 2574, Vol. 1, Transportation Research Board of the National Academies, Washington, D.C., 2016, pp. 28-37.
3. Moraes, R., and H. U. Bahia. Effect of Mineral Fillers on the Oxidative Aging of Asphalt Binders: A Laboratory Study Using Mastics. *Transportation Research Record: Journal of the Transportation Research Board*, No. 2506, Transportation Research Board of the National Academies, Washington, D.C., 2015, pp. 19-31.
4. Golalipour, A. *Investigation of the Effect of Oil Modification on Critical Characteristics of Asphalt Binders.* University of Wisconsin–Madison, 2013.
5. Ruan, Y., R. R. Davison, and C. J. Glover. Oxidation and Viscosity Hardening of Polymer-Modified Asphalts. *Energy and Fuels,* Vol. 17, 2003, pp. 991-998.
6. Bonaquist, R. *NCHRP Report 673: A Manual for Design of Hot Mix Asphalt with Commentary.* NCHRP, Washington, D.C., 2011.
7. Roque, R., B. Birgisson, C. Drakos, and B. Dietrich. Development and Field Evaluation of Energy-Based Criteria for Top-Down Cracking Performance of Hot Mix Asphalt (with discussion). *Journal of the Association of Asphalt Paving Technologists*, Vol. 73, 2004.

18. LONG TERM PERFORMANCE OF COLD CENTRAL PLANT RECYCLED ASPHALT FLEXIBLE PAVEMENTS

Dr. David Timm, Dr. Benjamin Bowers

18.1 Introduction

The Virginia Department of Transportation (VDOT) initiated an experiment at the Test Track in 2012 to study the use and viability of cold central plant recycled (CCPR) asphalt mix as a base course in a flexible pavement cross section under heavy traffic conditions. The original experiment featured three test sections and complimented a study that began in 2011 on I-81 in Virginia featuring a range of recycling techniques. The sections constructed at the Test Track used reclaimed asphalt pavement (RAP) obtained from the I-81 project and were meant to characterize the field performance and quantify the structural characteristics under accelerated trafficking. As described below, the sections exceeded their performance expectations during the first test cycle (2012 to 2014) totaling 10 million equivalent single axle load (ESAL) applications. The sections were left in place for another test cycle (2015 to 2017), again performing well to a total of 20 million ESALs. At that point, VDOT elected to continue trafficking into a third cycle (2018 to 2021) on the two sections at structural extremes (i.e., thickest and thinnest overall cross sections) while taking the third section out of service. At the conclusion of the third test cycle, 30 million ESALs had been applied to these two test sections and one of the sections may, in fact, be perpetual. This chapter documents the performance of the three sections in contrast with sections built earlier at the Test Track that were confirmed as perpetual pavements.

18.2 Test Sections

The sections in this investigation include the three VDOT CCPR sections and two older sections built in 2003 as part of the first structural study at the Test Track. Figure 1 shows the cross-sections where the first three sections on the left (Sections N3, N4, and S12) were the CCPR sections built in 2012 while last two sections on the right (N3-2003 and N4-2003) were part of the 2003 study. As previously documented, the total thickness of asphalt bound materials (including CCPR) was comparable between the sections, ranging from 8 to 10 inches over the foundation layers (*1*). The naming conventions for the CCPR sections in Figure 1 indicate the AC thickness (4 inches or 6 inches) over the CCPR and an additional label for the stabilized foundation base (SB) in Section S12. The design depth of CCPR in each section was 5 inches, with as-built depths shown in Figure 1. The older perpetual pavement sections are labeled according to their section number with the year they were built, 2003. They were designed to have 9 inches of asphalt concrete (AC) with the as-built depths very close to that as shown in Figure 1. N3-2003 used a locally-available performance grade (PG) 67-22 binder while N4-2003 had a styrene-butadiene-styrene (SBS) modifier that graded to a PG 76-22.

Each section was built on the same Test Track subgrade classified as an AASHTO A-4 soil. Except for S12, the sections were also built on the same crushed granite aggregate base. Additional information on these materials has been extensively documented previously (*2*). Section S12, as part of the CCPR experiment, used the same crushed granite but was stabilized in place with 4% Type II cement using a full-depth reclamation (FDR) process. The in-place stabilization also included the top 2 inches of the Test Track subgrade. Tables 19.1 and 19.2 contain properties of

the materials used in each layer for the 2012 CCPR sections and the 2003 dense graded sections, respectively. Though the AC mixtures were designed under different specifications with nine years between them, they arrived at similar binder contents and compacted densities. It should also be noted that the 2012 CCPR sections (Table 1) included RAP in the surfacing mixtures while the 2003 dense graded section surface mixtures (Table 2) did not. It should also be noted that the binder grades listed at the top of Table 2 were the same through the depth of each section, respectively (i.e., N3 was unmodifed while N4 was modified). Since these sections were not meant to be part of the same experimental design, these differences are not unexpected but should be considered when comparing the two sets of sections (*1*).

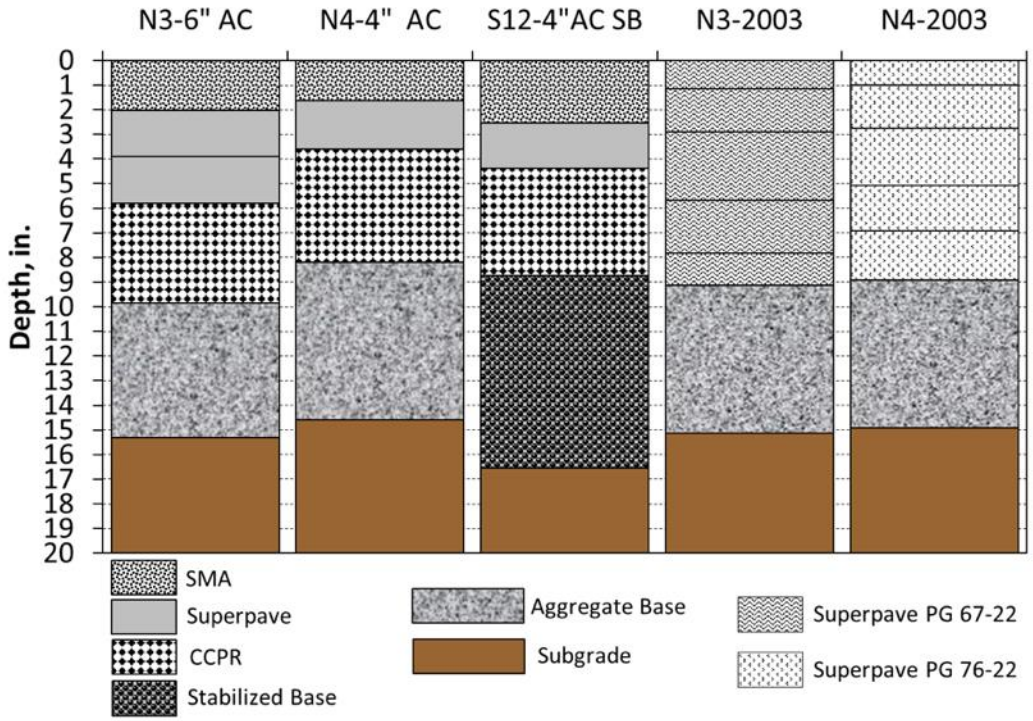

Figure 1. CCPR Average As-Built Thicknesses and Depth of Instrumentation (*1*)

Table 1. As-Built Layer Properties for 2012 CCPR Sections (*3*)

Section	N3-6"AC	N4-4"AC	S12-4"AC SB
Layer Description	Lift 1-12.5 mm NMAS SMA with 12.5% RAP and PG 76-22 binder		
Binder Content, %	6.1	6.0	6.1
In Place Air Voids, %	4.3	4.7	4.2
Layer Description	Lift 2-19 mm NMAS Superpave with 30% RAP and PG 67-22 binder		
Binder Content, %	4.6	4.6	4.7
In Place Air Voids, %	7.1	7.4	6.7
Layer Description	Lift 3-19 mm NMAS Superpave with 30% RAP and PG 67-22 binder		
Binder Content, %	4.4	*Sections N4 and S12 did not have 3rd AC lift*	
In Place Air Voids, %	6.4		
Layer Description	CCPR-100% RAP with 2% Foamed 67-22 and 1% Type II Cement		
Layer Description	Crushed granite aggregate base	6" Crushed granite aggregate base and 2" subgrade stabilized in-place with 4% Type II cement	
Layer Description	Subgrade – AASHTO A-4 Soil		

Table 2. As-Built Layer Properties for 2003 Perpetual Sections (*1*)

Section	N3-2003 (PG 67-22)	N4-2003 (PG 76-22)
Layer Description	Lift 1-9.5 mm NMAS Superpave	
Binder Content, %	6.1	6.1
Air Voids, %	5.7	5.5
Layer Description	Lift 2-19 mm NMAS Superpave	
Binder Content, %	4.3	4.3
Air Voids, %	4.7	4.7
Layer Description	Lift 3-19 mm NMAS Superpave	
Binder Content, %	4.5	4.4
Air Voids, %	3.1	3.3
Layer Description	Lift 4 – 19 mm NMAS Superpave	
Binder Content, %	4.3	4.7
Air Voids, %	5.1	3.0
Layer Description	Layer 5 – 19 mm NMAS Superpave	
Binder Content, %	4.6	4.4
Air Voids, %	4.0	4.5

18.3 Performance

The 2012 CCPR sections were built in the summer of 2012 with trafficking beginning on October 23, 2012. The older perpetual pavement sections were built during the summer of 2003 with traffic beginning on October 21, 2003. The seasonal similarity when traffic began for each set of sections (October) helps mitigate the disparity in overall time differences between the test sections as they began and were subjected to very similar climate conditions during their respective experimental durations. The 2003 dense graded sections were subjected to three cycles of trafficking, totaling 30 million ESALs. Section N4 and S12 of the 2012 CCPR sections were also subjected to three test cycles (30 million ESALs), while N3 was reassigned to another experiment after the first two cycles and was subjected to only 20 million ESALs. Each section was monitored on a weekly basis for cracking, rutting, and ride quality as described below.

18.3.1 Cracking

Each section was inspected weekly during its respective traffic cycle for cracking. No cracks were observed in N3-6”AC (20 million ESALs) or S12-4”AC SB (30 million ESALs). However, minor cracking was observed in N4-4”AC near the end of the third test cycle on January 25, 2021, after the application of 29.6 million ESALs. Cracking was confined to the outside wheelpath, primarily transverse to the direction of travel (though there were some interconnecting longitudinal cracks), and spread evenly along the length of the section. The cracks were relatively tight and there was no evidence of pumping or fines at the surface. Figure 2 shows some of the cracks with highlighting. It should be noted that the pavement surface was wet during this particular visual inspection. Subsequent inspections on later dates revealed much less cracking, which did not appear to progress or worsen during the last 400,000 ESAL applications. As of February 15, 2021 (29.9 million ESALs) there was 0.5% of the lane area cracked and 0.1% of the wheelpath area cracked as determined from inspection of high-resolution crack mapping images. Both values are quite low and do not indicate a pavement experiencing cracking failure. It is also curious that the lane area had more reported cracking than the wheelpath, which indicates more cracking outside of the wheelpaths than inside. This may be indicative of top-down

cracking rather than bottom-up. Future forensic investigations will reveal the nature of the cracking, but at this point it is recommended to leave N4-4" AC in place to better capture cracking progression with the application of more traffic in the next test cycle.

The older perpetual pavement sections did experience some cracking near the completion of 30 million ESALs. However, it was localized to a very small area and, through forensic trenching, the cracks were determined to be top down (N4-2003) or related to the presence of instrumentation (N3-2003). In the case of the N3-2003 section, the one bottom up crack that was observed was directly over a pressure plate installed at the top of the aggregate base. None of the 2003 dense graded sections experienced bottom-up fatigue cracking, which would qualify them for perpetual status (*1*).

Figure 2. Sample Cracking in N4-4"AC on 1/25/2021 (29.6 Million ESALs)

18.3.2 Rutting

Figure 3 contains all of the rutting data gathered over the three test cycles for the 2012 CCPR sections. Overall, each section performed extremely well with rutting generally less than 0.3 inches. The N3-6"AC series stops after the second test cycle since it was taken out of service. The increase in rutting at the end of the third test cycle in the other two sections is believed due to a software change in the data acquisition system rather than an actual increase in rutting. Regardless, the sections were well short of the Test Track failure threshold of 0.5 inches after 30 million ESALs.

Figure 4 compares the 2012 CCPR rutting performance to the 2003 perpetual pavement sections. In this plot, the x-axis is million ESALs to place each section on the same scale and the series represent 4-point (i.e., monthly) moving averages. Recall that the sections began their trafficking in October, so the seasonal changes are approximately the same between all sections. Similar performance was noted between all the sections: an initial increase in rutting followed by little additional change with all sections below 0.3 inches of rutting at the

completion of traffic. Again, the apparent increase toward the end of the CCPR data sets is believed due to a software change in the data collection system.

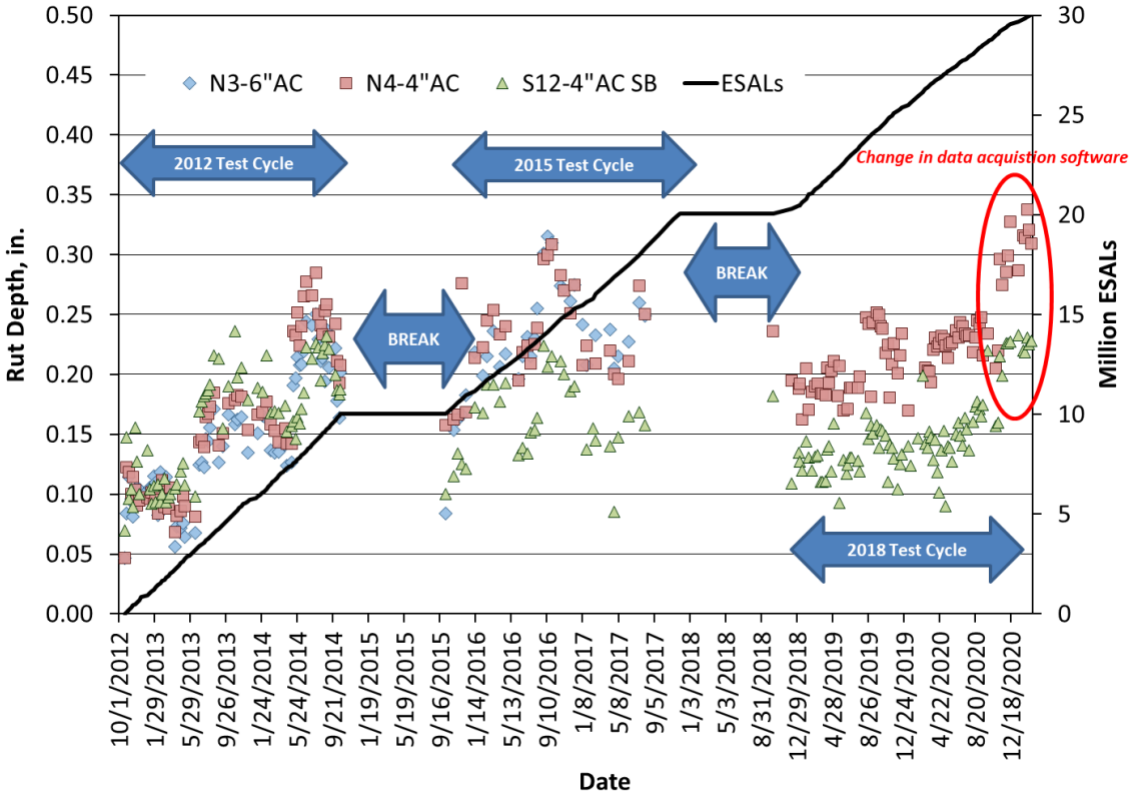

Figure 3. CCPR Rutting Performance

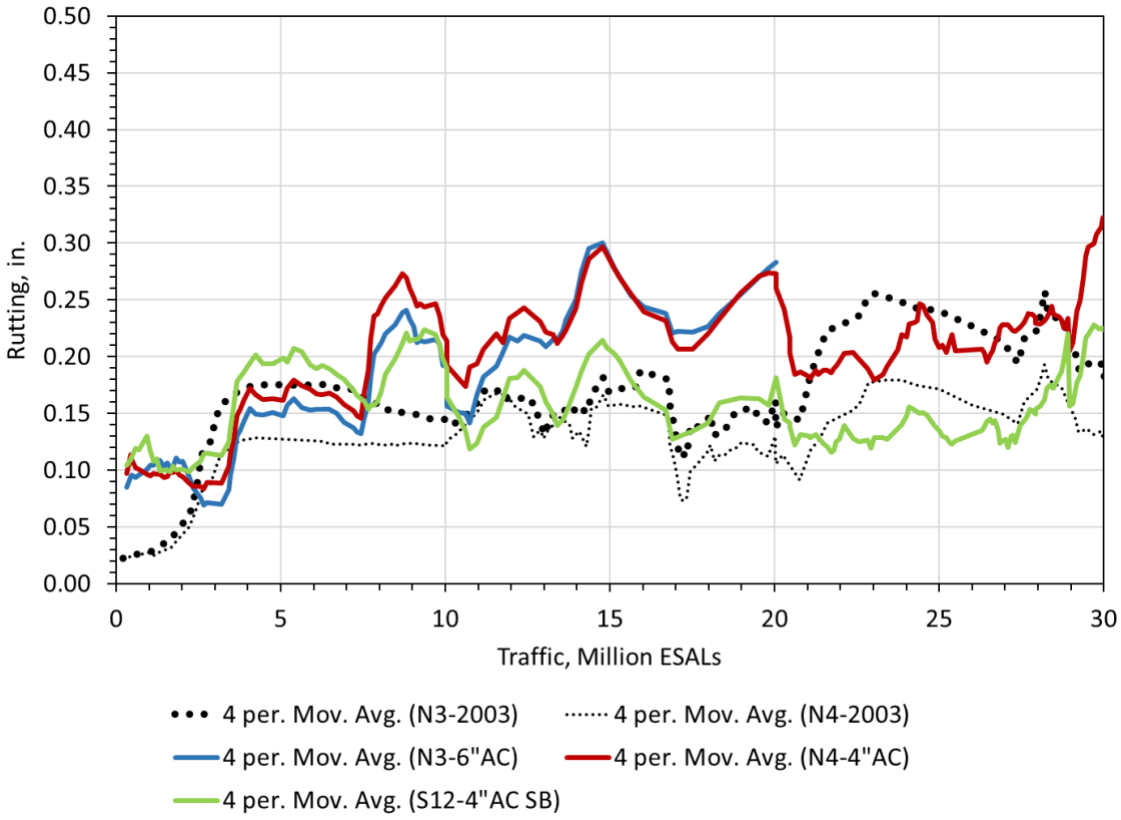

Figure 4. CCPR and Perpetual Pavement Rutting Performance

18.3.3 Ride Quality

Figure 5 contains ride quality data, expressed as the International Roughness Index (IRI) for the CCPR sections. Given the excellent rutting performance and little to no cracking, it is not surprising that the ride quality values are so steady over time and traffic application. Section S12 had notably higher overall roughness. However, as documented previously, this section had a localized area near the beginning of the section that had very high roughness (*4*). Despite the rough area, the section was left in place for the first 10 million ESALs after which grinding was conducted to improve the roughness, which explains the drop in IRI at 10 million ESALs. The following 20 million ESALs did not change the IRI appreciably.

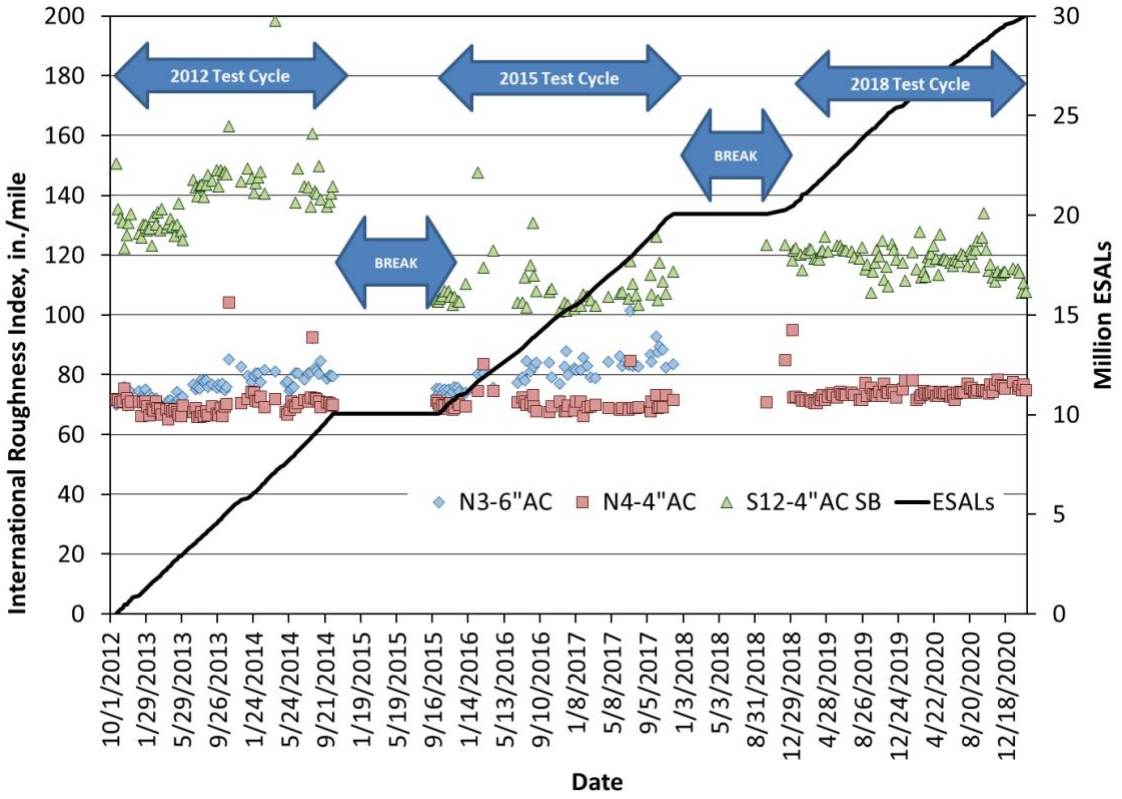

Figure 5. CCPR Ride Quality

Figure 6 contains four-point (monthly) moving averages of all five sections and shows that the 2003 dense graded sections were built smoother and maintained low IRI values through 30 million ESALs. Despite the CCPR sections having higher as-built roughness, they appeared to have the same relative steadiness in ride quality over time with the exception of S12-4”AC SB, which was explained above. To better compare the sections relative to their respective initial roughness values, the data in Figure 6 were normalized by subtracting the initial IRI data, obtained after construction but before trafficking began, from the remaining measurements as shown in Figure 7. It should be noted that the S12 data, after the first 10 million ESALs, was renormalized to account for the grinding that occurred between the first and second test cycles. Though the data shows fluctuation for each test section, it is notable that the net change at the end of traffic was less than a 15 in/mile increase, which was again considered excellent performance consistent with perpetual pavement performance expectations.

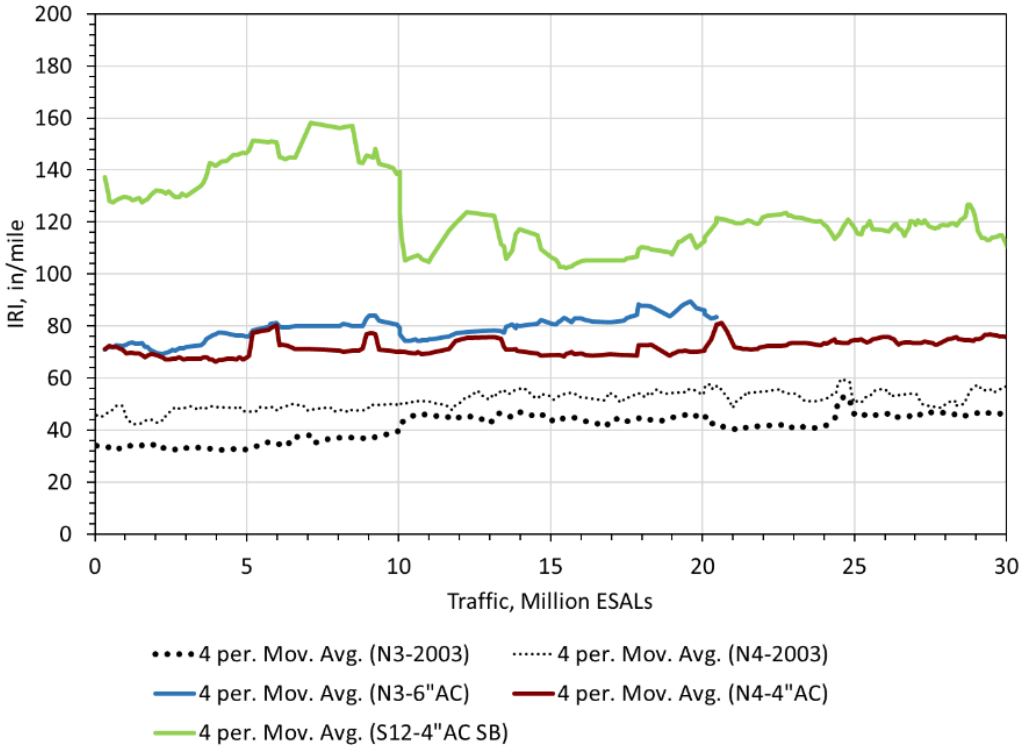

Figure 6. CCPR and Perpetual Pavement Ride Quality

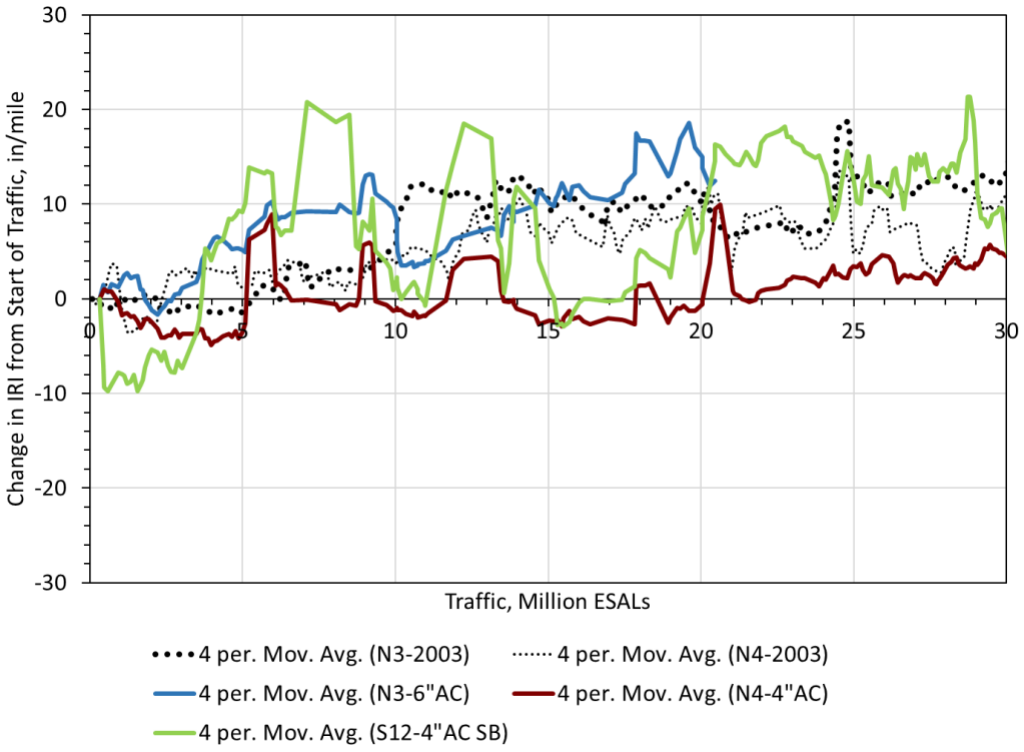

Figure 7. CCPR and Perpetual Pavement Change in Ride Quality

18.4 Structural Characterization

The CCPR and perpetual pavement sections were instrumented with strain gauges and earth pressure cells to measure in situ pavement responses under truck loading. The strain gauges were positioned to measure horizontal tensile strain at the bottom of the CCPR layer in the VDOT sections and at the bottom of the AC in the perpetual section and are the focus of the investigation in the next subsection. Additionally, each section was subjected to frequent falling weight deflectometer (FWD) testing and backcalculation that will also be discussed below.

18.4.1 Measured Strain Responses

Figure 8 depicts measured tensile strain responses in the longitudinal direction (i.e., with traffic) made at the bottom of the CCPR layer in each of the CCPR sections. Due to lack of extensive strain data and differences in how strains were measured in the 2003 sections, their strain data are not included in Figure 8. The figure clearly shows the impact of seasonal temperatures on the measured strain responses, with the CCPR N3 and N4 sections behaving very similarly while S12 appears to be much less affected by changing temperatures, likely due to the stabilized base layer. The strong influence of temperature was expected due to the viscoelastic nature of the asphalt-bound materials and has been often observed in other Test Track studies (*5, 6*). Sections N3 and S12 do not appear to have appreciably changed over their test cycles while N4 may have higher strain levels during the third cycle, which could have been a precursor to the small amount of damage observed at the surface in 2021.

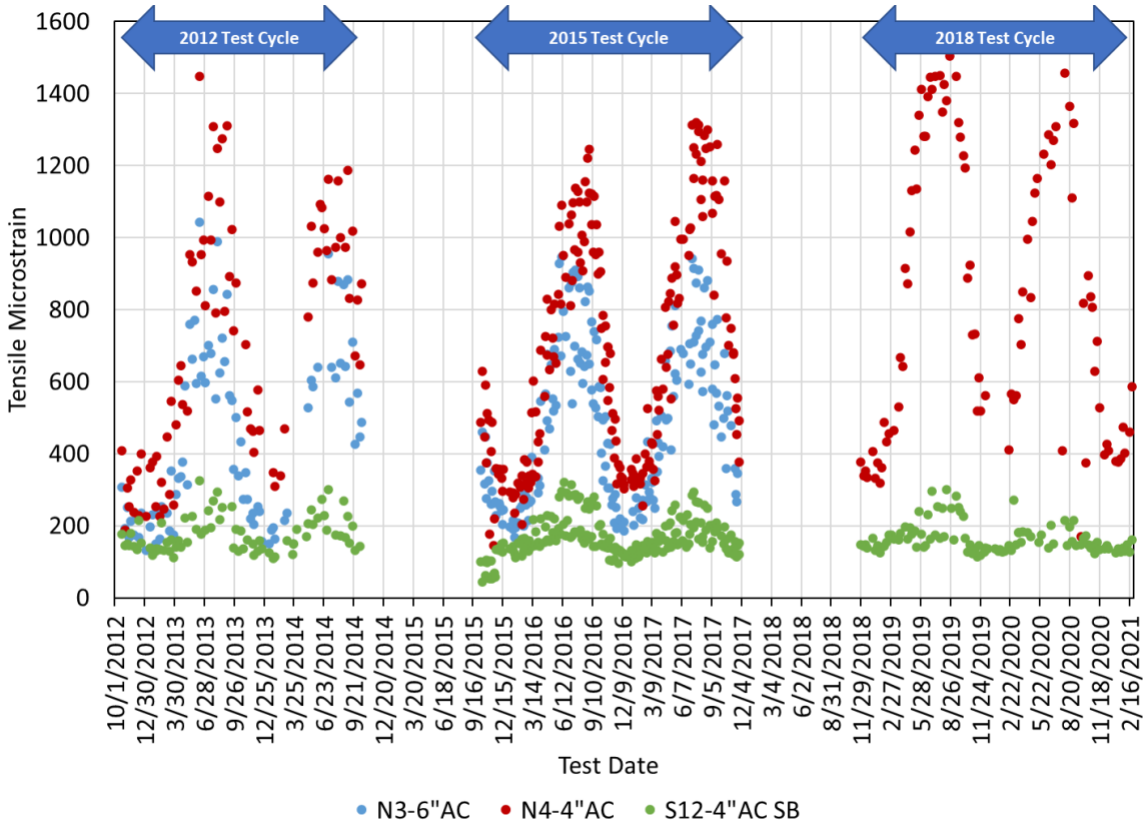

Figure 8. CCPR Measured Strain Responses

The measured strain responses in Figure 8 were plotted against their corresponding mid-depth AC temperature at the time of measurement as shown in Figure 9. The strong influence of temperature is clearly evident with exponential trendlines fitted to each data set. The effect of the stabilized base in S12 greatly reduced the temperature sensitivity of the tensile strain while the other two sections had very similar trends with temperature. The difference observed in the N3 and N4 trendlines results primarily from the extra 2 inches of AC in section N3. Furthermore, N4 had much more scatter versus the trendline and was subdivided by test cycle in Figure 10, which shows an upward trend in strain level from the original test cycle (2012) into the second test cycle (2015) and finally the last test cycle (2018) with higher strain levels and much more scatter in the data. Interestingly, the trendline for the intermediate cycle (2015) appears to link between the other two test cycles matching the 2012 cycle at low temperatures and the 2018 cycle at higher temperatures. Close examination of the 2012 and 2018 trendlines indicates strain levels increasing, on average, by 100 to 165 microstrain across the temperature spectrum. It is also important to note that this increase was observed for the entire 2018 test cycle, while cracking was not observed until the very end, so subsurface cracking may have been occurring. Future forensic investigation will evaluate this hypothesis.

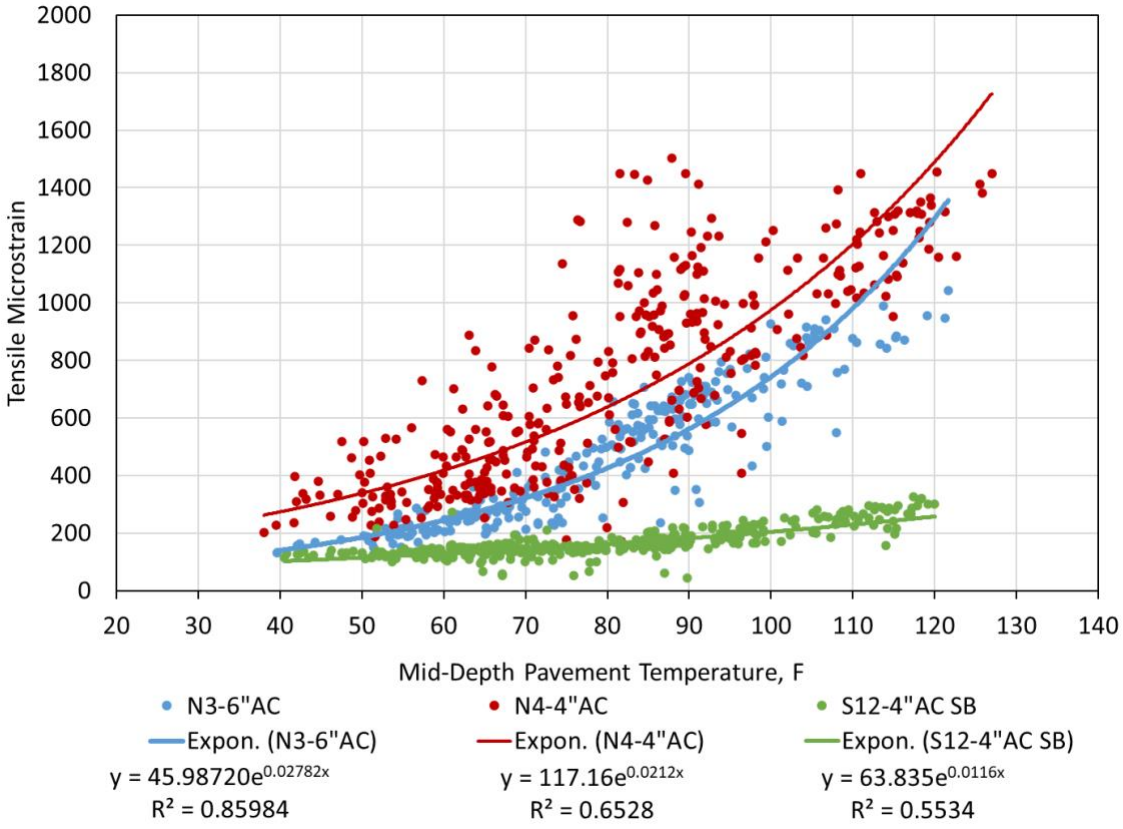

Figure 9. CCPR Measured Strain versus Mid-Depth Pavement Temperature

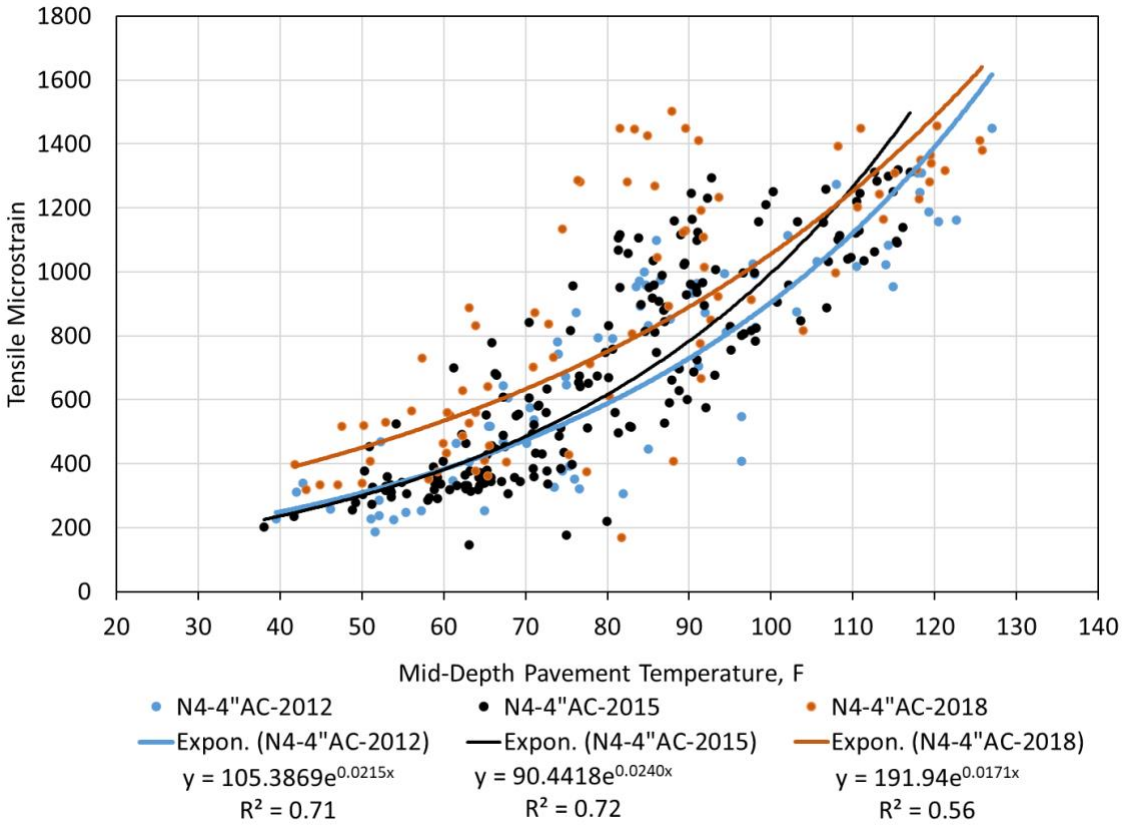

Figure 10. Section N4-4”AC Measured Strain versus Mid-Depth Pavement Temperature by Test Cycle

A final strain comparison between the CCPR and perpetual pavement sections is shown in Figure 11 where cumulative strain distributions are shown for the 2012 CCPR sections along with the so-called Willis Limit for perpetual pavement design (*5, 6*). The Willis Limit was based on the 2003 dense graded sections and expressed a strain upper bound for conventional flexible pavements to prevent bottom-up fatigue cracking. The limit was validated with perpetual pavement award winners from around the U.S. and serves as a trial benchmark for the CCPR sections (*7, 8*). Note that S12, with the stabilized foundation, is less than the limit (i.e., to the left) above the 40th percentile. Application of the criteria to this section indicates it should not experience bottom-up cracking. The other two CCPR sections, however, are well to the right of the limit and experience has shown from the Test Track that these should have exhibited bottom-up cracking with less than 20 million ESALs (*5, 6*). The fact that N3 did not crack after 20 million ESALs and N4 lasted until 29.6 million ESALs indicates prolonged fatigue life and that CCPR materials may exhibit fundamentally different fatigue behavior. Since it was taken out of service, it will remain unknown whether N3-6”AC would have ever cracked with enough ESAL applications, but it is unlikely that S12-4”AC SB would crack since its strain distribution is below the Willis Limit and is most likely perpetual.

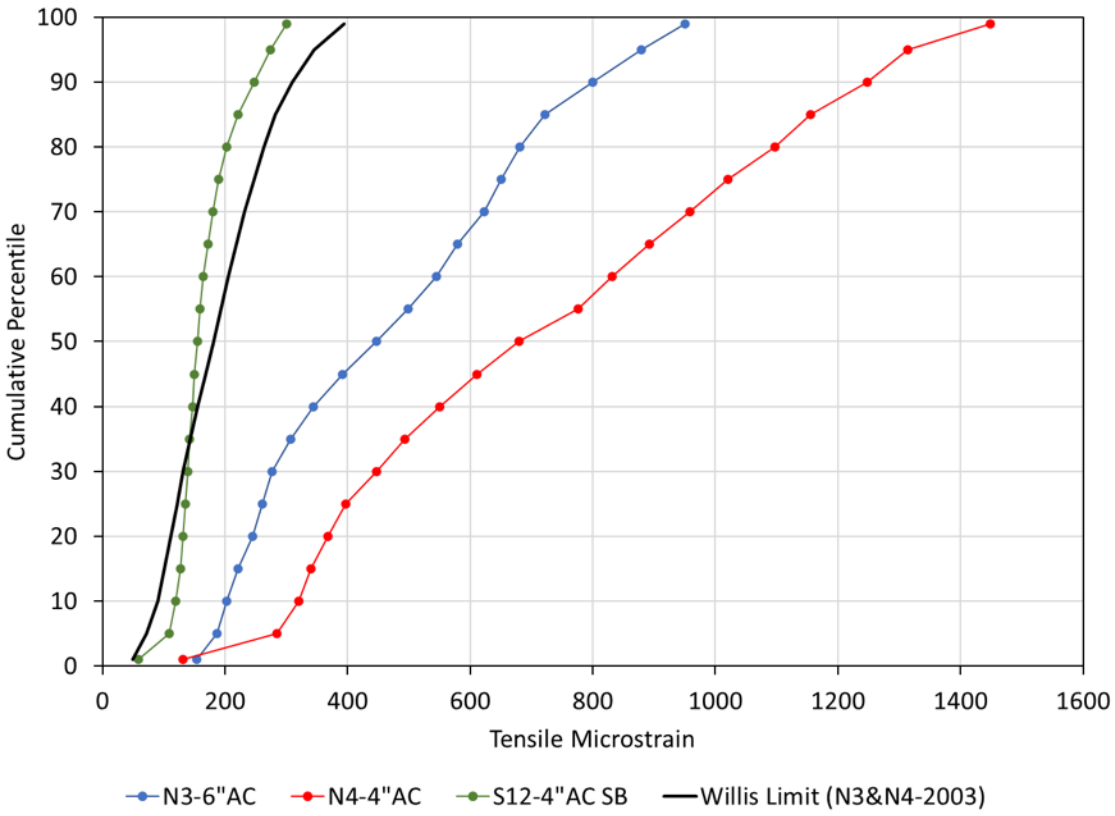

Figure 11. Cumulative Strain Distributions for CCPR and Perpetual Pavement Sections

18.4.2 FWD Testing and Backcalculated AC Moduli

Falling weight deflectometer (FWD) testing was conducted frequently on each section followed by multi-layer backcalculation to determine layer properties. As previously documented, the 2012 CCPR sections were tested several times per month during each cycle using a Dynatest 8000 Falling Weight Deflectometer with the standard nine-sensor arrangement (*1*). The same FWD device and testing frequency was used on the 2003 dense graded sections in their second and third test cycles, but the testing during the first cycle was done on only a monthly basis using a seven-sensor arrangement. Testing was conducted at multiple longitudinal stations in each section representing 50-foot subsections as well as in the middle of the instrumentation array. At each station, both wheelpaths and between wheelpaths were tested. Though multiple drop heights were used, only data pertaining to the 9,000 lb loading is included in this analysis. Mid-depth temperatures using embedded temperature probes were recorded at the time of testing. Backcalculation of the deflection basins was accomplished with EVERCALC 5.0 and a root mean square error limited to less than 3% was used to ensure reliable results. All analyzed sections were treated as three-layer structures for backcalculation purposes. For the 2003 sections, this meant combining all five AC lifts into the first layer, followed by the aggregate base and then subgrade. For the CCPR sections, the AC and CCPR were combined into one layer. This decision was based on laboratory |E*| testing where a master curve was successfully developed for CCPR materials, indicating it acts more like an asphalt concrete material than an

aggregate base (*3, 9*). The base and subgrade layers were the subsequent layers in the CCPR backcalculation models.

Figure 12 plots the backcalculated AC or AC/CCPR modulus in the outside wheelpath with the x-axis representing days since opening to traffic. Since the two experiments began trafficking within days of each other in late October in their respective construction years, the long-term seasonal trends due to temperature changes are remarkably aligned and obvious. Sections N4 and S12 appear to run longer than the 2003 sections since it took longer to reach another 10 million ESALs in the final test cycle due to loss of trucking efficiency associated with the COVID-19 pandemic.

The short-term cycling in Figure 12 represents daily temperature fluctuations and the vertical spread on any given day represents spatial variability within the section. The breaks between test cycles represent the forensic/reconstruction phases at the Test Track where no data was gathered. It appears that each section in Figure 9, with the exception of CCPR N4-4”AC, experienced steady or even slightly increasing modulus over time. During the last test cycle, N4-4” AC appears to have declining modulus, which could correspond to the higher strain levels depicted in Figures 8 and 10 and may have been indicative of cracking developing but not seen at the surface until the very end of the test cycle.

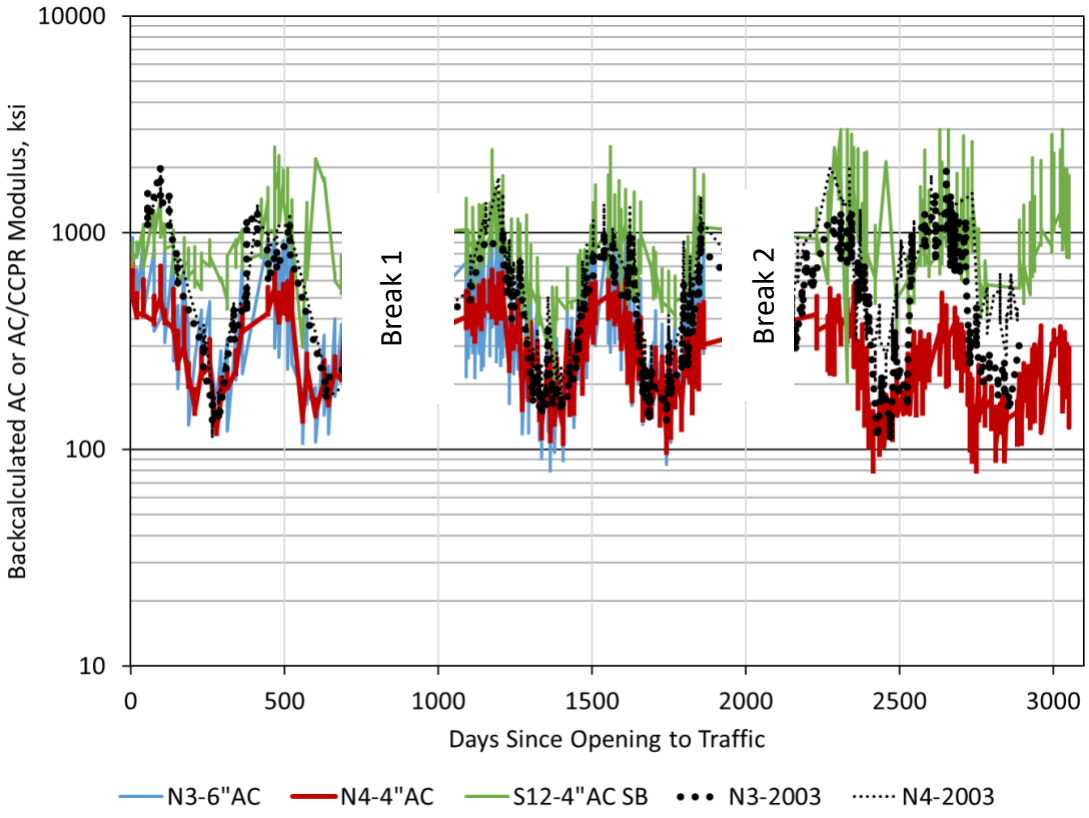

Figure 12. Backcalculated AC or AC/CCPR versus Days Open to Traffic

To better understand the trend in the N4-4” AC section, the data from Figure 12 were plotted against their corresponding temperatures and subdivided according to test cycle in Figure 13.

This was similar to what was done with the strain data presented above. The first and second cycles were nearly identical, with no practical difference between the trendlines. However, the third cycle (2018) exhibited a distinct shift downward (softening) which, again, is an indication of pavement damage. Though damage may be occurring, as discussed with the strain data investigation, the section has survived far longer than expected with excellent performance. The following section discusses the sections in terms of their economics and sustainability.

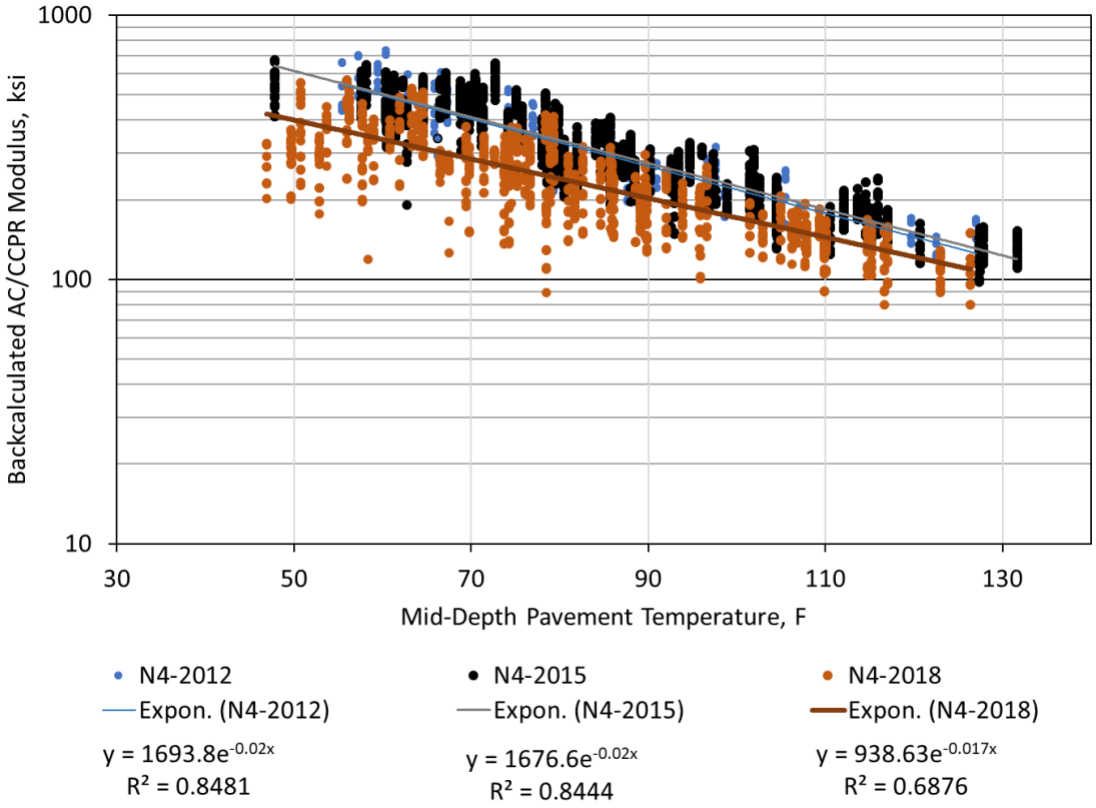

Figure 13. Section N4-4”AC Backcalculated AC/CCPR Modulus versus Mid-Depth Pavement Temperature by Test Cycle

18.5 Economic and Environmental Impact

To compare the economic impact of the cold recycled sections, recent average statewide unit costs (materials and placement), within 3 years of publication, were collected from VDOT. These data included costs for stone matrix asphalt (SMA), dense graded asphalt base, CCPR, FDR, and aggregate base. All costs, along with an assumed density for economic impact estimation, are included in Table 3.

Table 3. Material Unit Costs and Assumed Densities (*1*)

Material	Unit	Unit Cost, $	Assumed Density, lbs/ft³	VDOT Structural Layer Coefficient *(10)*
Asphalt surface (SMA)	Tons	106	146	0.44
Asphalt base (dense graded)	Tons	95	146	0.44
CCPR	Tons	45	136	0.35
FDR	Square Yard	8	Not applicable	0.25
Aggregate Base	Tons	20	152	0.12

Table 4 provides the economic analysis of each as-built section when applying the unit costs described in Table 3. Each pavement section was converted to square yards to account for the different densities of the materials. The pavement section cost from lowest to highest cost was N4-4" AC ($37.04/SY), S12-4" AC SB ($44.20/SY), N3-6" AC ($48.90/SY), N4-2003 ($55.37/SY), and N3-2003 ($56.52/SY). Interestingly, all of the CCPR cross sections are lower in cost than a traditional asphalt concrete section, with Section S12-4" AC SB (second lowest cost) having a higher structural number (SN) than any of the sections. The typical layer coefficients used by VDOT were used to calculate the SN for each section (*10*).

Also shown in Table 4, the SY cost was divided by the SN to normalize the cost since each section has a varied thickness, a key step since it is unknown how long these sections may perform. The cost per SY per SN resulted in nearly the same order as the cost per SY with the exception that S12-4" AC SB was the least expensive of all options at $8.18/SY/SN, saving 31% over the 2003 dense graded asphalt sections. The remaining two CCPR sections yielded greater than 10% savings over the 2003 dense graded asphalt sections, showing that CCPR can be used with or without a stabilized base/FDR layer and still result in a lower overall cost.

Table 4. Results of Economic Analysis Based on Materials Costs (Table 3) and As-Built Thickness

Layer Thickness, inch					
	N3-6" AC	**N4-4" AC**	**S12-4" AC SB**	**N3-2003**	**N4-2003**
AC	5.8	3.6	4.4	9.1	8.9
CCPR	4.0	4.6	4.3	-	-
Agg Base	5.5	5.2	-	6.0	6.0
FDR	-	-	7.8	-	-
Pavement Section Cost, $/SY					
	$48.90	$37.04	$44.20	$56.52	$55.37
Structural Number (SN)					
	4.62	3.80	5.40	4.74	4.64
Structure Normalized Pavement Section Cost, $/SY/SN					
	$10.57	$9.74	$8.18	$11.93	$11.93
Estimated Savings Based on Normalized Pavement Section Cost, %					
	11%	18%	31%	-	-

It is important to consider not just economics, but also environmental impact. As discussed in Timm et al., the percentage of recycled materials by weight used in each of the CCPR sections was estimated and a weighted average of recycled material per inch was calculated (*1*). It is important to note that the 2003 dense graded asphalt sections did not contain any recycled

materials. In the CCPR sections, the SMA layer contained 11% RAP, intermediate layer contained 30% RAP, CCPR contained 97% RAP (2% was recycling agent and 1% cement), and FDR layer contained 96% recycled materials (4% portland cement). Overall, N3-6" AC contained 54% recycled material per inch when considering only the bound layers (i.e., not the aggregate base), N4-4" AC contained 62% recycled material per inch when considering only the bound layers, and S12-4" AC SB contained 76% recycled material. A life cycle assessment was not conducted as a part of this study, though it should be noted that other cold recycling projects have been documented to reduce energy demand by 50 to 70% and Global Warming Potential (emissions) by 40 to 70% compared to a more conventional dense graded asphalt design (*11*).

18.6 Conclusions and Recommendations

This investigation featured five pavement sections built at the NCAT Test Track that were not originally part of a common experimental design but were instructive in exploring perpetual pavement concepts related to flexible pavements having no recycled materials versus those that contain much higher levels of recycled pavement. Based on the findings presented in this chapter, the following conclusions and recommendations are made:

- All five sections exhibited excellent performance over their respective test cycles after applying 20 to 30 million ESALs. Final rut depths did not exceed 0.3 inches and ride quality did not change by more than 15 inches/mile. Some minor cracking appeared in the CCPR Section N4-4"AC at 29.6 million ESALs. It was minor and contained to the outside wheelpath, but the effects were apparent in the strain and backcalculated modulus values. Despite the occurrence of cracking in this section, all sections exhibited excellent cracking performance through their respective trafficking cycles.
- The strain data in two of the 2012 CCPR sections (N3-6" AC and S12-4" AC SB) were steady over their test cycles indicating good structural health with no signs of pavement distress. Conversely, section N4-4" AC had increased strain during the third test cycle corresponding to crack development. Increasing the asphalt thickness or stabilizing the foundation would be expected to improve the performance of the design used in Section N4.
- Comparing cumulative strain distributions among the sections showed that the non-stabilized base CCPR sections far exceeded the limit derived from the 2003 sections which should correspond to eventual bottom-up cracking. Cracking did occur in N4-4" AC, though the exact nature of the cracking will not be known until a full forensic investigation is completed. Since N3-6" AC was taken out of service after 20 million ESALs, it is impossible to conclude with 100% certainty whether it would experience cracking, but the data suggest good structural health. Since other NCAT Test Track sections experienced bottom-up cracking within 20 million ESALs with strain distributions less extreme than N3-6" AC and N4-4" AC, it is possible new criteria will be needed for perpetual design of pavements using CCPR.
- The cumulative strain distribution for S12-4" AC SB fell below the limit for perpetual design and met the same performance criteria (i.e., no cracking, limited rutting and no significant change in ride quality after 30 million ESALs) to be classified as perpetual. The low strain levels largely derived from the relatively stiff stabilized base layer.

- Backcalculated AC and AC/CCPR moduli showed relative consistency over time for each test section, with the exception of the CCPR section, N4-4" AC, which supported the observations and conclusions made from the measured strain data. The apparent decline in AC/CCPR modulus for N4-4" AC during the last test cycle was consistent with the increase in strain and correspond to the cracking damage.
- The economic analysis showed that the 2012 CCPR pavement sections had lower average structural normalization costs by 11% (N3-6" AC), 18% (N4-4" AC), and 31% (S12-4" AC SB) when compared to the 2003 dense graded asphalt sections. Therefore, inclusion of CCPR in a pavement section can result in significant cost savings.
- Section N3-6" AC contains 54% recycled material per inch, Section N4-4" AC contains 62% recycled material per inch, and Section S12-4" AC SB contains 76% recycled material per inch. Excellent performance can be achieved at a very high recycled material content even for high truck traffic roadways.
- Section S12-4" AC SB is an example of a perpetual pavement having a very high recycled material content.
- It is recommended that a pavement life cycle assessment be conducted on all sections presented herein to capture the energy and greenhouse gas savings, accounting for the fact that S12-4" AC SB is a perpetual pavement.

18.7 References

1. Timm, D.H., B.K. Diefenderfer, B.F. Bowers and G. Flintsch, "Utilization of Cold Central Plant Recycled Asphalt in Long-Life Flexible Pavements," Transportation Research Record, Transportation Research Board, under review, 2021.
2. Taylor, A. J., and D. H. Timm. *Mechanistic Characterization of Resilient Moduli for Unbound Pavement Layer Materials*. NCAT Report No. 09-06. National Center for Asphalt Technology, Auburn, Ala., 2009.
3. Timm, D.H., Diaz-Sanchez, M. and B. Diefenderfer. Field Performance And Structural Characterization of Full-Scale CCPR Pavements. Presented at 94th Annual Meeting of the Transportation Research Board, Washington, D.C., 2015.
4. Diefenderfer, B.K., M.A. Diaz-Sanchez, D.H. Timm and B.F. Bowers. *Structural Study of Cold Central Plant Recycling Sections at the National Center for Asphalt Technology (NCAT) Test Track.* Final Report VTRC 17-R9, Virginia Transportation Research Council, 2016.
5. Willis, J.R. and D.H. Timm. Field-Based Strain Thresholds for Flexible Perpetual Pavement Design. Report No. 09-09, National Center for Asphalt Technology, Auburn University, 2009.
6. Willis, J.R. and D.H. Timm. Development of Stochastic Perpetual Pavement Design Criteria. Journal of the Association of Asphalt Paving Technologists, 2010. 79: 561-596.
7. Tran. N., M.M. Robbins, D.H. Timm, J.R. Willis and C. Rodezno. *Refined Limiting Strain Criteria and Approximate Ranges of Maximum Thicknesses for Designing Long-Life Asphalt Pavements*. Report No. 15-05, National Center for Asphalt Technology, Auburn University, 2015.
8. Castro, A.J., N. Tran, M.M. Robbins, D.H. Timm and C. Wagner. Further Evaluation of Limiting Strain Criteria for Perpetual Asphalt Pavement Design. *Transportation Research Record: Journal of the Transportation Research Board*, 2017. 2640: 41-48.

9. Diefenderfer, B.K. and S.D. Link. Temperature and Confinement Effects on the Stiffness of a Cold Central-Plant Recycled Mixture. Proceedings of the 12th International Society for Asphalt Pavements Conference, Raleigh, NC, 2014.
10. Virginia Department of Transportation. Manual of Instructions, Materials Division, Richmond, 2018.
11. Federal Highway Administration. In-Place and Central-Plant Recycling of Asphalt Pavements in Virginia. FHWA-HIF-19-078, Washington, DC, 2020.

19. WEST VIRGINIA FRICTION STUDY FOR ASPHALT SURFACE MIXTURE WITH ALTERNATIVE AGGREGATES

Dr. Fan Gu

19.1 Background

Although frictional aggregates are effective in enhancing pavement friction, material cost must also be considered in the selection of aggregates. From an economic perspective, locally available aggregates are preferred for producing asphalt mixtures. However, for regions that have a large amount of highly polishable aggregates but a limited amount of frictional aggregates, balancing friction performance and material cost is crucial. To maintain adequate friction and acceptable construction costs, state highway agencies in the U.S. typically limit the amount of highly polishable aggregates (e.g., dolomite) in asphalt surface mixtures. For example, West Virginia Division of Highways (WVDOH) requires that dolomite shall not exceed 50% of the coarse aggregates in an asphalt surface mixture if the projected traffic is greater than 3.0 million equivalent single axle loads (ESALs). To reduce material costs, highway agencies are interested in increasing the amount of highly polishable aggregates in asphalt surface mixtures while still maintaining an appropriate threshold without sacrificing friction performance.

In 2018, WVDOH sponsored two test sections (W4 and W5, which are the 4th and 5th sections in the west curve) on the NCAT Test Track to investigate how an increase in the amount of dolomite impacts the friction characteristics of an asphalt surface mixture. In West Virginia, sandstone can be used as frictional coarse aggregate in asphalt surface mixtures. In this study, Section W4 used a surface mixture containing 70% dolomite and 30% sandstone as coarse aggregates, and W5 had 90% dolomite and 10% sandstone as coarse aggregates. Both sections had a 50 mm thick (2 inch) surface course.

Trafficking of the sections started in November 2018. Their performance was closely monitored in terms of surface friction, texture, and roughness, as well as cracking and rutting. Based upon the performance results, this study aimed to develop a friction-based framework to evaluate the feasibility of using more highly polishable aggregates in asphalt surface mixtures.

19.2 Materials and Experimental Plan

The asphalt surface mixture job mix formulas are shown in Table 1. The design traffic level was 3 to 30 million equivalent single axle loads (ESALs). Note that WVDOH defines coarse aggregates as the particles retained on sieve No. 4 (4.75 mm). Both W4 and W5 asphalt surface mixtures had the same amounts of asphalt binder and fine aggregates; the only difference was the coarse aggregate proportion. The W4 mixture had 28% dolomite and 12% sandstone as coarse aggregates, while the W5 mixture contained 36% dolomite and 4% sandstone. These proportions were equal to 70% dolomite in coarse aggregates for the W4 mixture and 90% dolomite in coarse aggregates for the W5 mixture. Figure 1 presents the blended aggregate gradations, both of which met the requirements of WVDOH. The nominal maximum aggregate size of these mixtures was 12.5 mm. Table 2 shows the properties of dolomite and sandstone coarse aggregates that were measured by the Aggregate Imaging System (AIMS) (*1*). Compared

to sandstone aggregate, dolomite aggregate has slightly higher angularity but much lower texture.

Table 1. Mixture Composition of Asphalt Surface Mixtures for WVDOH Study

Mixture Composition		Mixture Type	
		W4	W5
Coarse Aggregate Content[1]	Dolomite	28%	36%
	Sandstone	12%	4%
Fine Aggregate Content[2]	Limestone	44%	44%
	RAP	15%	15%
	Baghouse Fines	1%	1%
Binder Type		PG 76-22	PG 76-22
Binder Content[3]		5.6%	5.6%
Liquid Anti-strip Additive Content[4]		0.5%	0.5%

Note: [1] Coarse aggregate content is by weight of aggregates; [2] Fine aggregate content is by weight of aggregates; [3] Binder content is by weight of asphalt mixture; [4] Liquid anti-strip additive content is by weight of asphalt binder

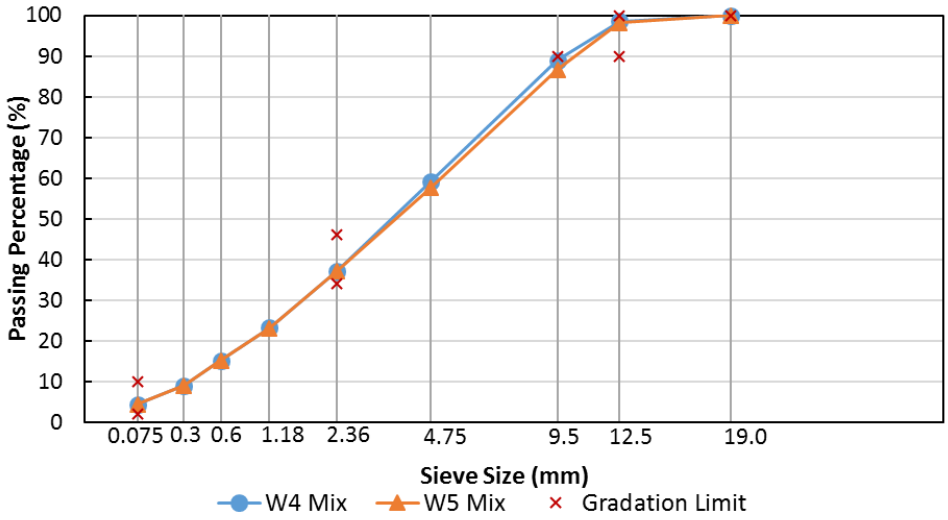

Figure 1. Blended Aggregate Gradations of Asphalt Surface Mixtures

Table 2. Results of Aggregate Imaging System Test for Dolomite and Sandstone Aggregates

Aggregate Properties	Aggregate Type		Specified Range		
	Dolomite	Sandstone	Low	Medium	High
Angularity	3100.1	2882.9	≤3300	3300-6600	6600-10000
Texture	183.8	349.4	≤260	260-550	550-1000
Sphericity	0.60	0.63	≤0.3	0.3-0.7	0.7-1.0

The experimental plan of this study is presented in Figure 2, which includes friction evaluation of laboratory-compacted asphalt slabs, field test sections, and one field friction treatment applied to the sections after 6 million ESALs of trafficking. The laboratory friction evaluation focused on the quantification of the friction performance of asphalt surface mixtures containing various percentages of dolomite aggregates. The field friction evaluation was conducted to validate the findings from the laboratory tests. The experimental methods used in this study

included the three-wheel polishing device (TWPD) surface conditioning, dynamic friction tester (DFT) test, circular texture meter (CTM) test, and locked-wheel skid trailer (LWST) test.

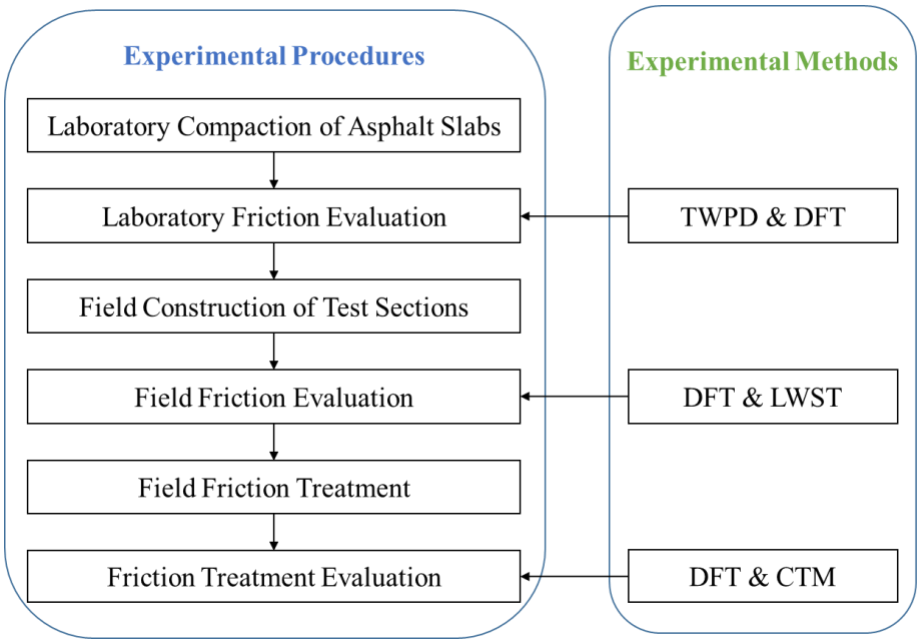

Figure 2. Experimental Plan of This Study

19.3 Laboratory Friction Performance of Asphalt Mixtures

In the laboratory, dolomite and sandstone aggregates were blended in different proportions to fabricate asphalt mixture slabs. The TWPD was used to simulate the polishing of field traffic to the surface of asphalt mixtures. The DFT test was conducted at the 5,000th, 20,000th, 50,000th, and 100,000th cycles to characterize the deterioration trend of asphalt surface friction.

Figure 3 shows the effect of dolomite content on the DFT friction coefficient of asphalt mixtures. It is not surprising to see that the asphalt mixture containing dolomite had a slightly higher peak friction coefficient at 5,000 polishing cycles than the mixture containing only sandstone. This is because dolomite has slightly higher angularity than sandstone, which is important for the initial friction of asphalt mixtures. From 5,000 to 20,000 polishing cycles, all asphalt mixtures containing dolomite aggregate experienced more rapid reduction in friction coefficients than those without, which is because sandstone typically has better polishing resistance. From 20,000 to 50,000 polishing cycles, the friction coefficients continued decreasing but the deterioration rates were slow. After 50,000 cycles, the friction curves tended to be flat, indicating that traffic polishing no longer had a significant impact on the asphalt mixtures friction. To compare the friction performance of asphalt mixtures, the deterioration rates of friction coefficient from 5,000 to 20,000 polishing cycles were calculated using Equation 1.

$$Friction\ Deterioration\ Rate = \frac{Reduction\ of\ Friction\ Coefficient}{Number\ of\ Polishing\ Cycles} \quad (1)$$

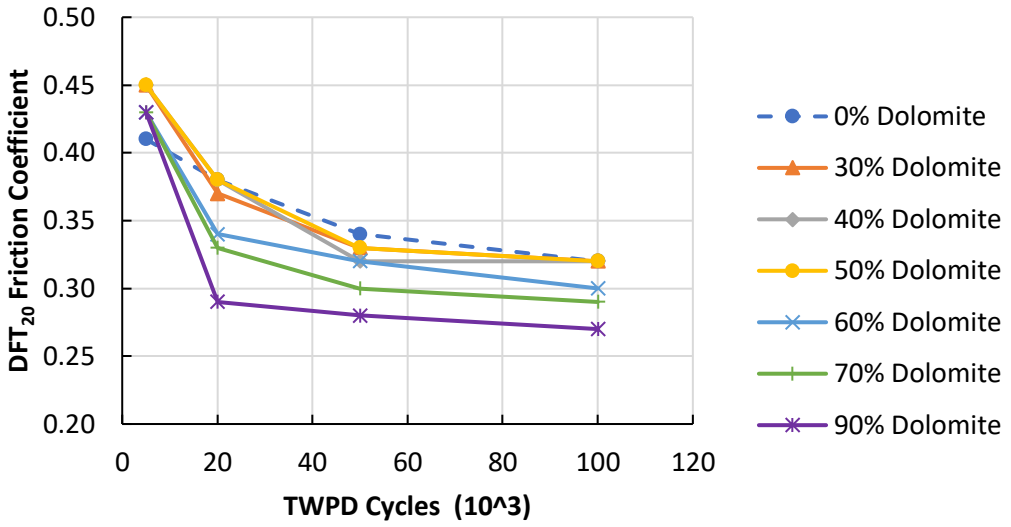

Figure 3. Effect of Dolomite Content on DFT Friction Coefficient of Asphalt Mixtures

Figure 4 shows that the friction deterioration rate from 5,000 to 20,000 polishing cycles had a good linear correlation with dolomite content. Increasing dolomite content resulted in a faster deterioration rate of friction at the early polishing stage (5,000 to 20,000 cycles). This implies that asphalt surface mixtures containing more dolomite aggregates would enter into the terminal friction stage much faster.

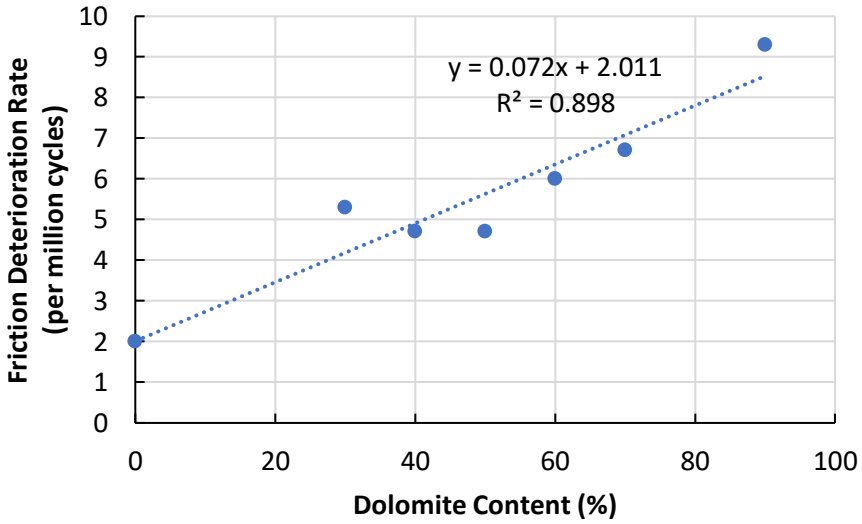

Figure 4. Correlation Between Friction Deterioration Rate and Dolomite Content

Figure 5 illustrates how dolomite content affected the terminal friction coefficient (measured at the end of 100,000 polishing cycles). It is shown that the terminal friction remained constant when dolomite content increased from 0% to 50%, but decreased linearly as dolomite content increased from 50% to 90%. The terminal friction coefficients of asphalt mixtures containing 70% and 90% dolomite aggregates reduced to 0.29 and 0.27, respectively, which were less than the NCAT's minimum threshold of DFT friction coefficient (i.e., friction coefficient = 0.30).

Therefore, limiting dolomite content to no greater than 50% ensures an adequate terminal friction coefficient for West Virginia asphalt surface mixtures, which validates why WVDOH requires that dolomite shall not exceed 50% of coarse aggregate in asphalt surface mixtures for high traffic volume applications. According to the historic experience at NCAT, the terminal friction coefficient typically ranges from 0.35 to 0.45 for dense-graded asphalt surface mixtures, which is higher than the terminal friction coefficients of West Virginia asphalt mixtures measured in this study. This could be explained by the AIMS test results that both dolomite and sandstone aggregates had relatively low angularity and texture, and high sphericity.

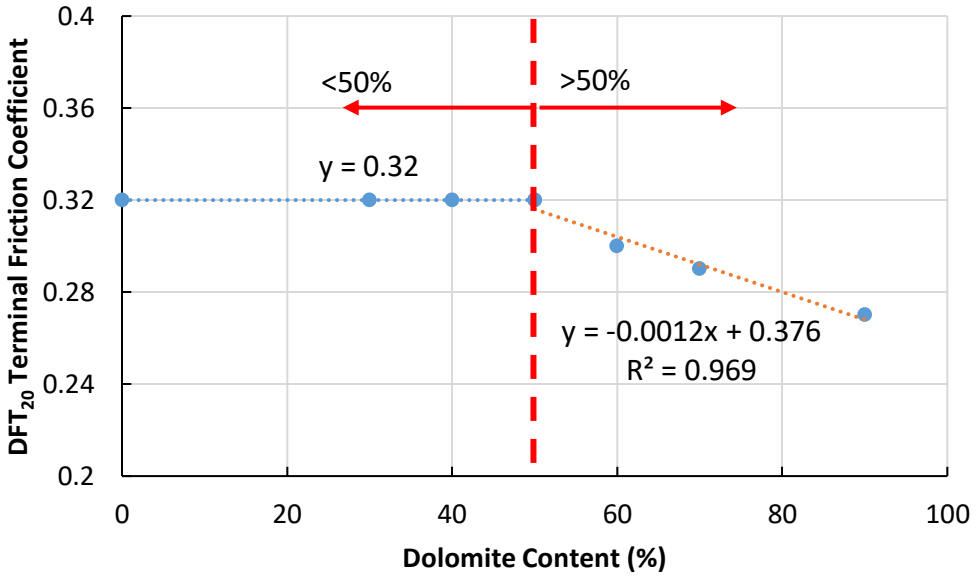

Figure 5. Relationship Between Terminal Friction Coefficient and Dolomite Content

19.4 Field Friction Performance of Asphalt Mixtures

Sections W4 and W5 were trafficked by five heavy trucks each pulling three loaded trailers. The LWST was used to monitor the skid resistance of the sections on a monthly basis. Figure 6 presents the LWST test results of sections W4 and W5. It is shown that the skid resistance of both sections dropped rapidly after being trafficked for 1.0 million ESALs and continued degrading from 1.0 to 3.0 million ESALs of traffic. When the accumulated traffic reached 3.0 million ESALs, the skid resistance (SN40R) of W4 and W5 sections dropped to 26.4 and 22.8, respectively, which were lower than the minimum safety threshold at the Test Track (i.e., skid number = 30). This is consistent with the finding from laboratory friction evaluation. After 3.0 million ESALs of accumulated traffic, the traffic polishing had a negligible influence on pavement friction. Compared to section W4, section W5 generally had a lower skid resistance due to the higher dolomite content. It is also noted that the skid number of both sections slightly increased when the accumulated traffic was beyond 4.3 million ESALs. Considering that these sections could not regain skid resistance without any treatment, the increase in skid number is attributed to the influence of test temperature on the LWST measurement. For the same pavement surface, the skid number measured in winter is typically greater than that measured in summer due to the lower test temperature.

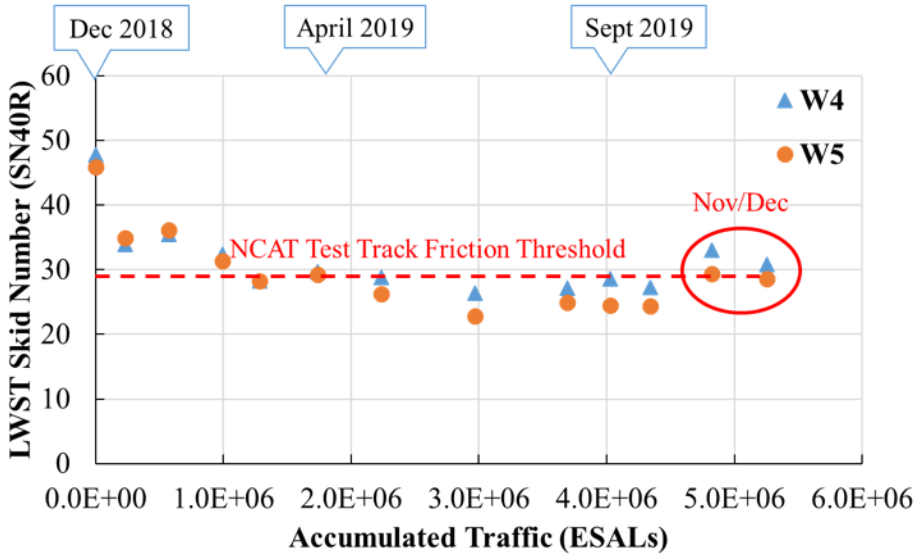

Figure 6. LWST Test Results for NCAT Test Track Sections W4 and W5

In addition, DFT was used to measure the friction coefficient of Sections W4 and W5. Figure 7 shows the DFT test results of these two sections. Similar to the LWST test results, both sections showed low friction performance after 1.5 million ESALs of traffic. This confirms that the asphalt surface mixtures containing 70% and 90% dolomite aggregates do not provide adequate friction coefficients if the projected traffic volume is greater than 3.0 million ESALs. It is also shown that Section W5 had a lower friction coefficient than Section W4 in general, which is consistent with the finding from the LSWT test.

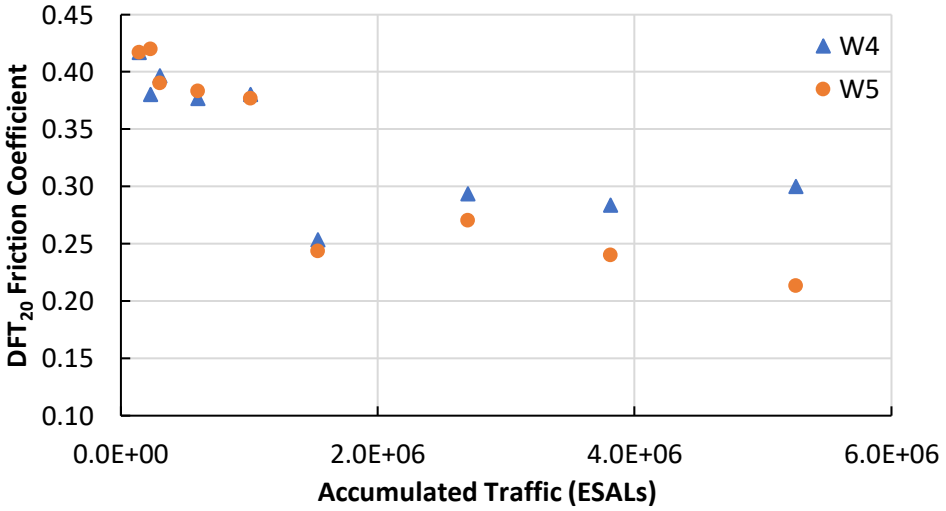

Figure 7. DFT Test Results for NCAT Pavement Test Track Sections W4 and W5

19.5 Influence of Shotblasting Treatment on Surface Friction

When sections W4 and W5 continued showing DFT friction coefficients lower than 0.3, there was an urgent need to apply a friction treatment to address roadway safety concerns. Due to the ease of application and low cost, the shotblasting treatment was selected and applied after

5.3 million ESALs of accumulated traffic. The details of shotblasting treatment can be found in Sarkar et al. (*2*). Figure 8a illustrates a typical shotblasting system, including an operating room, a shotblasting apparatus, a shot recycler, and a dust collector. The shotblasting apparatus is an essential unit that consists of a shot propeller, vacuum system, magnetic separator, brush, and broom. Figure 8b shows the shotblasting treatment at the NCAT Pavement Test Track. The shotblasting train ran at a speed of 28.3 m/min (92.8 ft/min) with a treatment width of 1.8 m (5.9 ft).

(a) Shotblasting System (b) Treatment at Test Track

Figure 8. Shotblasting Treatment at NCAT Test Track

Figure 9 compares the DFT friction coefficient and surface texture of Sections W4 and W5 before and immediately after shotblasting treatment. As shown in Figure 9a, the shotblasting treatment improved the friction coefficient of both sections. This is primarily because shotblasting abraded the asphalt pavement surface, which created more angular aggregate faces exposed to traffic, thereby increasing the microtexture of pavement surface. Figure 9b shows that the pavement sections had much higher mean profile depth (MPD) values after shotblasting. This demonstrates that the shotblasting treatment substantially enhanced the macrotexture of the asphalt pavement surface, which also contributed to the friction gain.

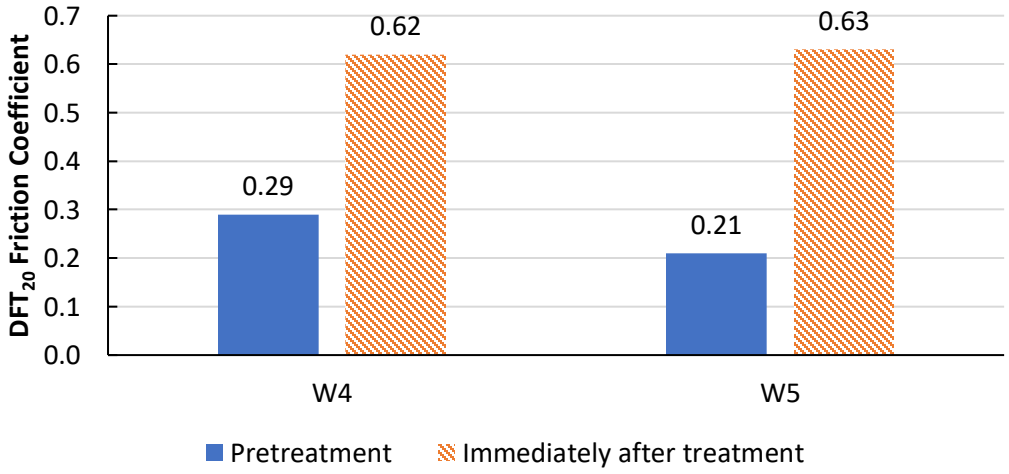

(a) Friction Coefficient

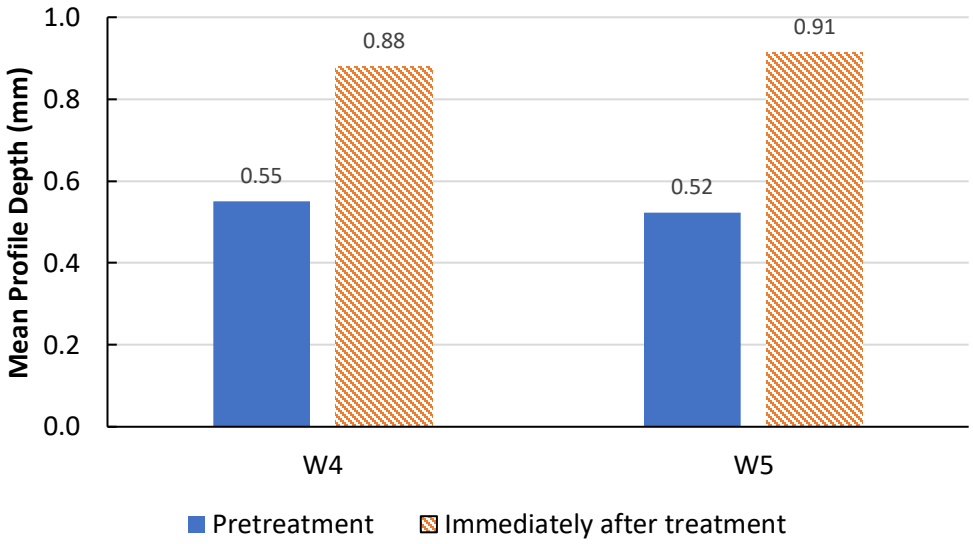

(b) Surface Texture

Figure 9. Comparison of Friction Coefficient and Surface Texture of Pavement Sections before and after Shotblasting Treatment

Figure 10 shows the influence of traffic polishing on the friction performance of shotblasted pavement sections. As presented, the friction coefficient of Sections W4 and W5 significantly increased during the first 0.1 million ESALs of traffic, which was attributed to the wearing of coated asphalt binder on the exposed aggregate surface. However, the friction coefficient of both sections sharply reduced from 0.1 to 0.2 million ESALs of traffic, indicating that the improved aggregate surface microtexture was worn off during this period. After that, the friction deterioration rate tended to be extremely low. Due to the increased surface macrotexture, both sections held friction coefficients above 0.30 after being trafficked for more than 2.0 million ESALs. Based on these friction performance curves, the improved microtexture was quickly reduced by traffic polishing, but the improved macrotexture provided extended the friction benefit. Note that shotblasting provides an immediate improvement in aggregate surface microtexture, but aggregate polish resistance is controlled by aggregate geology. Overall, the shotblasting treatment was effective in improving long-term friction performance. Figure 11 presents the influence of traffic polishing on macrotexture of shotblasted pavement sections. It is confirmed that the enhanced surface macrotexture by shotblasting treatment was negligibly affected by traffic polishing, which explains why the shotblasting treatment provided the long-term friction gain.

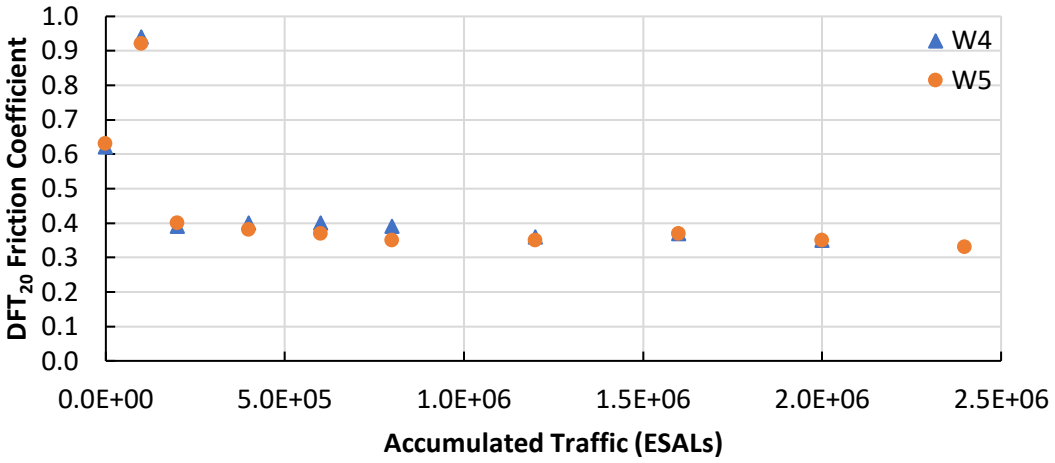

Figure 10. Influence of Traffic Polishing on Friction Performance of Shotblasted Pavement Sections

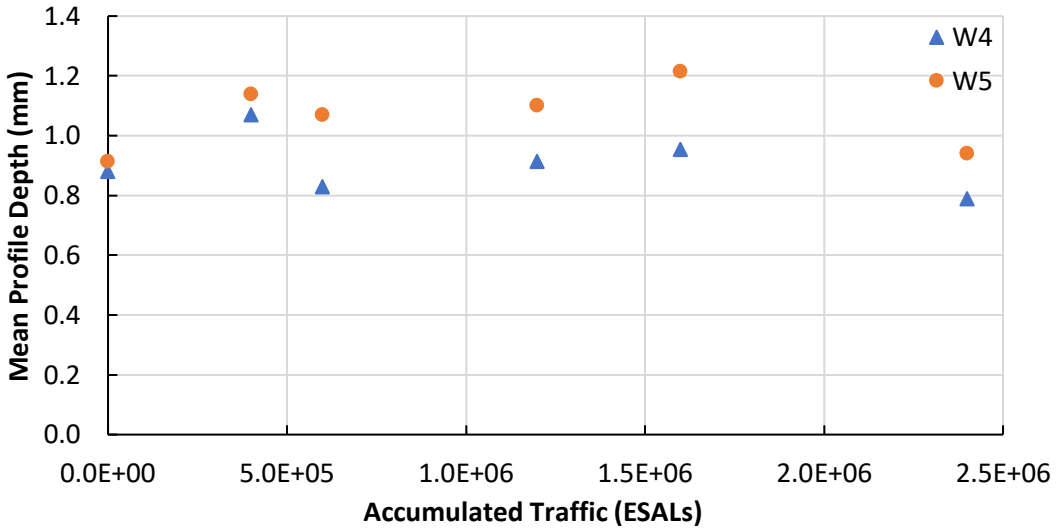

Figure 11. Influence of Traffic Polishing on Macrotexture of Shotblasted Pavement Sections

Since the friction benefit provided by the shotblasting treatment was promising, one question remaining was whether this treatment brought any detrimental impact on pavement performance. This study investigated the performance of Sections W4 and W5 before and after shotblasting treatment in terms of international roughness index, rut depth, and cracking percent. After being trafficked for 10 million ESALs, neither sections exhibited any cracking distress. Figure 12 shows the results of international roughness index and rut depth of sections W4 and W5. As presented, international roughness index and rut depth values remained stable on both sections before and after shotblasting treatment. This indicates that the friction treatment had no adverse effect on pavement performance. In addition, both sections showed great smoothness and extremely low rut depth, which implies that the friction results obtained from this study were not impacted by pavement distresses.

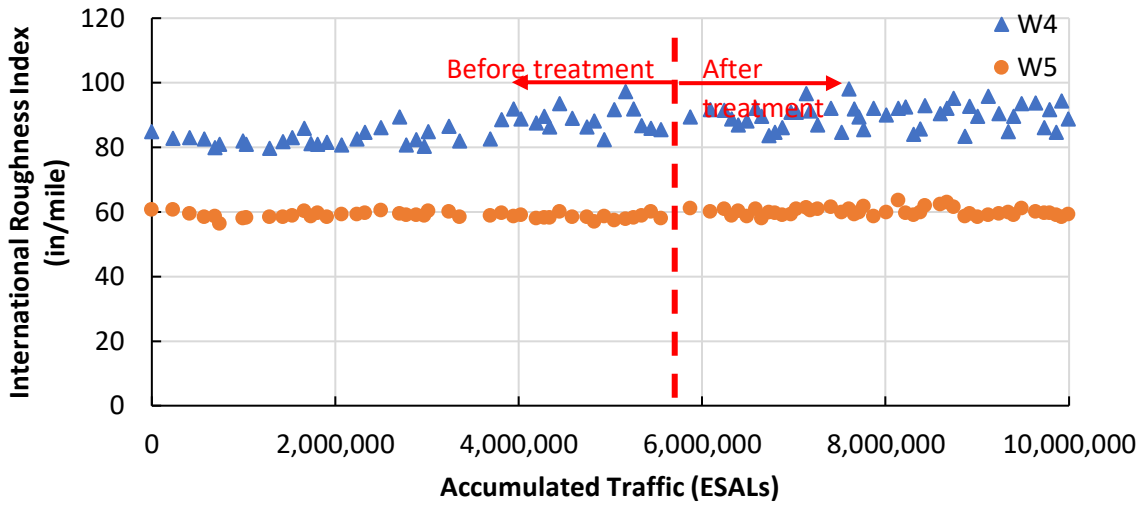

(a) International Roughness Index

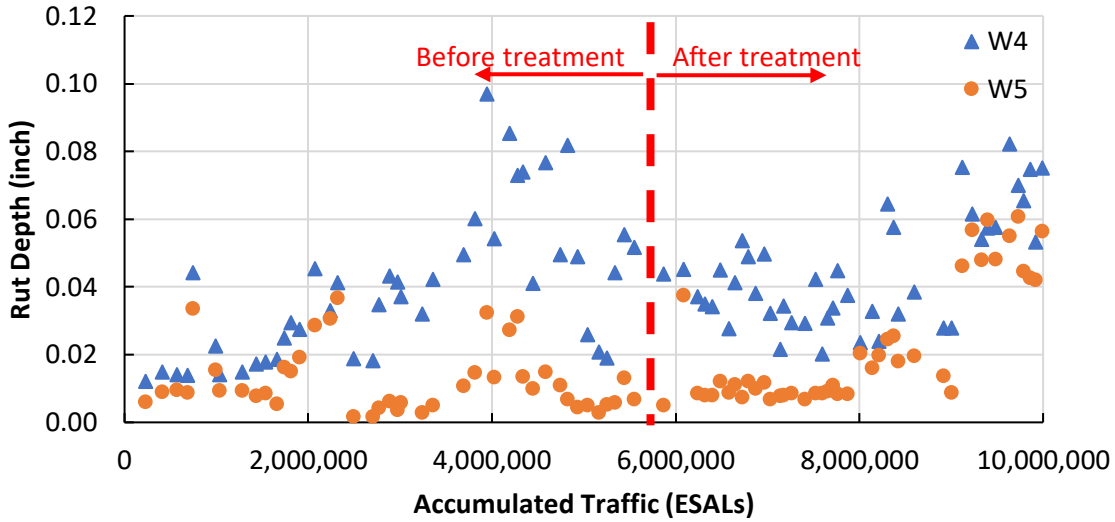

(b) Rut Depth

Figure 12. Influence of Shotblasting Treatment on International Roughness Index and Rut Depth of Pavement Sections

19.6 Summary and Conclusions

This study evaluated the feasibility of using an increased amount of dolomite in asphalt surface mixtures, which involved both laboratory and field friction experiments. The dynamic friction tester (DFT) was employed to determine the friction coefficient of the laboratory-compacted asphalt slabs that were abraded by the three-wheel polishing device (TWPD). The locked-wheel skid trailer and DFT tests were performed to measure the skid resistance of two test sections at the NCAT Test Track that were polished by heavy trucks. The major findings of this study are summarized as follows.

- Increasing dolomite content in asphalt surface mixtures led to a faster deterioration rate of friction at the early polishing stage.

- Both laboratory and field test results indicated that the asphalt surface mixtures containing 70% and 90% dolomite coarse aggregates provided terminal friction coefficients less than 0.30.
- Asphalt surface mixture containing no more than 50% dolomite coarse aggregate had an adequate terminal friction coefficient. This validated why WVDOH specification requires that dolomite shall not exceed 50% of coarse aggregate in an asphalt surface mixture if the projected traffic volume is greater than 3.0 million ESALs.
- The comparison of laboratory and field friction results verified that the TWPD was capable of simulating traffic polishing in the field.
- Due to the increased surface macrotexture, shotblasting treatment improved both short- and long-term friction performance of asphalt pavements and had no detrimental impact on pavement performance in terms of cracking, rutting, and surface roughness.

19.7 References

1. Masad, E. A. (2005). Aggregate Imaging System (AIMS): Basics and Applications. Final Report No. FHWA/TX-05/5-1707-01-1, Texas A&M Transportation Institute, College Station, Texas.
2. Sarkar, M., Gu, F., Heitzman, M., and Powell, B. (2021). Using Shotblasting Treatment to Improve Asphalt Pavement Friction at the NCAT Test Track. ASCE International Airfield & Highways Pavements Conference Proceedings, 332-344.

20. IMPLEMENTATION SYNOPSES

20.1 Cracking Group Experiment

For a couple of decades, pavement engineers across the U.S. have expressed concerns about the durability of asphalt pavements. Although the Superpave system effectively solved rutting issues, many new pavements and overlays have not performed well regarding cracking and raveling. Highway agencies began exploring ways to increase asphalt contents of mixes by tweaking volumetric requirements, adjusting compactive efforts, and tightening down on policies related to aggregate testing. At the same time, efforts were being made to increase recycled asphalt materials contents for economic and sustainability reasons. A number of states initiated research studies with their local universities to develop new tests to identify mixtures that were prone to premature cracking. After another 10 years of these efforts, only a few states had made any progress toward implementation. A variety of new cracking tests had been recommended by researchers, but most of the tests lacked field validation and there was no consensus on which test (or tests) were suitable for day-to-day usage.

In 2015, NCAT and MnROAD began a partnership to address national research needs that the two organizations are uniquely suited to handle. One of those needs is field validation experiments for balanced mix design cracking tests. NCAT built test sections to focus on top-down, load-related cracking. MnROAD's experiment has focused on thermal cracking. Ten state DOTs and FHWA funded the experiment that has taken two cycles to complete.

The importance of in-service aging on the development of top-down cracking was evident at the end of the first cycle when hairline cracking was observed on just a few of the seven NCAT test sections. However, the additional investment and effort paid off. Through the second cycle, a range of cracking was documented in the test sections. Two sections had so much cracking distress by 4½ years that they had to be milled and overlayed to complete trafficking of the other test sections. One section ended with no cracking and two others only had about one percent cracking. The sixth test section had a low extent of relatively minor cracking, and the last section had a moderate amount of low-severity cracking. This range of performance was ideal for validating the laboratory cracking tests.

Seven laboratory cracking tests were selected for evaluation by the sponsors for the top-down cracking experiment: energy ratio (ER), Texas overlay (OT-TX) test, NCAT modified overlay test (OT-NCAT), Louisiana semi-circular bend test (SCB-LA), Illinois flexibility index (I-FIT) test, IDEAL cracking test (IDEAL-CT), and the asphalt mixture performance tester (AMPT) cyclic fatigue test.

Another deliverable of this experiment was the development of the NCAT critical-aging procedure to simulate the first few years of in-service aging of surface layers. Analysis of rheological and chemical binder properties from a limited number of mixtures in Alabama, Washington, and Michigan indicate loose-mix aging for eight hours at 135°C is similar to five days of loose-mix aging at 95°C. NCAT has referred to the loose-mix aging at 135°C for eight hours as the "critical-aging" protocol.

Selecting the best tests for balanced mix design is the first major step toward improving pavement performance and opening the door to a wide range of innovations that cannot be adequately evaluated with Superpave binder and mix specifications. Based on the results of the

NCAT top-down cracking experiment, the following findings and recommendations were provided:

- Energy ratio results did not match the field performance for top-down cracking. This test also lacks practicality for routine use due to the complexity and time to complete the three parts of the test, so it is not recommended for implementation.
- The new β parameter from the OT-TX test is a very good indicator of a mixture's resistance to top-down cracking. It is a much more discerning indicator than cycles to failure. For OT-TX tests on critically-aged mixtures, a β value of 1.75 separated mixtures with moderate top-down cracking resistance from mixtures with very good performance. However, the OT-TX test is not a practical cracking test for day-to-day use in BMD and testing for quality assurance due to the time required to prepare specimens and the cost of the equipment.
- The NCAT-modified version of the overlay test is a very good indicator of resistance to top-down cracking. A maximum β value of 0.37 is recommended as a preliminary criterion for critically-aged mixtures based on the plant mix results of this experiment. The NCAT-OT has a lower coefficient of variation than the OT-TX procedure and the testing time is faster. However, like the OT-TX, the test lacks practicality due to time to prepare specimens and high equipment cost.
- The Louisiana SCB test did not provide a suitable correlation with the top-down cracking performance of the mixtures in this experiment. Two of the mixtures that performed very well on the track had results very similar to those of mixtures with moderate cracking. Other disadvantages of the SCB-LA are the time and cost of preparing notched semi-circular specimens, and that standard methods of variability analysis cannot be applied to the results.
- The flexibility index from the I-FIT procedure had a good correlation with top-down cracking observed for the test sections. However, due to high variability of *FI* for several mixtures, the critically-aged, plant mix results were not statistically distinguishable among some good and moderately performing mixtures or between good and poor performing mixtures. Like the SCB-LA test, a disadvantage of the I-FIT is the time and cost of preparing specimens. Also, *FI* results are affected by specimen air void contents in an incorrect manner. Specimens with lower air voids have lower *FI* results, which is counter to the field cracking performance as evidenced by the performance of test sections N1 versus N2 in this experiment.
- The CT_{Index} from the IDEAL-CT method is a very good indicator for resistance to top-down cracking. It has strong correlations to the field performance of the NCAT test sections and the results are statistically discernable from mix to mix. For critically-aged samples, a minimum CT_{Index} of 15.0 is recommended as a preliminary criterion for good resistance to top-down cracking. As with the *FI*, CT_{Index} results are affected by specimen air void contents in an incorrect manner. Until this issue is corrected, it is recommended that the test only be conducted on specimens compacted to 7.0±0.5%. The IDEAL-CT method is the most practical of the evaluated cracking tests and is well suited to everyday use in BMD and quality assurance testing.

- The AMPT cyclic fatigue test index parameter, S_{app}, correlated well with the observed top-down cracking for the test sections for this experiment. The results also support North Carolina State University's recommended minimum S_{app} criterion of 30 for short-term aged mixture samples for Very Heavy traffic pavement applications. However, the S_{app} results for the asphalt rubber mixture appear to be lower than what they should be based on excellent field performance on the Test Track and the results of other cracking tests in this study. This may indicate that the cyclic fatigue test or its criteria need to be adjusted for this mixture type. Disadvantages of this test are the time and cost to prepare specimens, cost of the equipment, and complexity of data analysis. For these reasons, it is not well suited for routine use in BMD or quality assurance testing.

20.2 Alabama Long Term Evaluation of OGFC

Open graded friction course (OGFC) mixtures are used as the final riding surface on many roadways as they offer benefits such as reducing hydroplaning, reducing splash and spray behind vehicles for improved driver visibility, improving wet pavement friction, and reducing surface reflectivity during wet-weather conditions. Despite these benefits, the use of OGFC has diminished over the years due to durability and service-life issues.

A typical OGFC mix in Alabama consists of a 12.5-mm nominal maximum aggregate size (NMAS), 0.3% cellulose fiber, and 6% PG 76-22 asphalt modified with styrene-butadiene-styrene (SBS), which usually exhibits premature distresses (e.g., raveling) after approximately six or seven years in service. Therefore, there is a need to change the current OGFC mix design to improve mix durability.

In 2012, ALDOT sponsored three test sections (E9A, E9B, and E10) to evaluate potential mix design changes to improve the durability of OGFC mixtures in Alabama. The following changes for an OGFC mixture were evaluated.

1. A finer 9.5-mm NMAS gradation (instead of a typical 12.5-mm NMAS gradation) was designed with a cellulose fiber and SBS-modified asphalt binder for the OGFC mixture in Section E9A.
2. A synthetic fiber (instead of a cellulose fiber) was utilized in the OGFC mix design for Section E9B with a typical 12.5-mm NMAS gradation and SBS-modified asphalt binder.
3. A ground tire rubber (GTR) modified binder was used in place of SBS-modified binder for the OGFC mixture in Section E10 with a typical 12.5-mm NMAS gradation but without cellulose fiber.

The OGFC mixtures were designed prior to the construction of the three test sections based on a 12.5-mm OGFC mix design previously approved by ALDOT. These mixtures were designed with a design compaction effort of 50 gyrations to have minimum air voids of 15%, a maximum Cantabro loss of 15%, and a minimum conditioned splitting tensile strength of 50 psi.

Sections E9A, E9B, and E10 were milled and inlaid with the OGFC mixtures in 2012. All the mixes were placed 0.75-inches thick with in-place air voids immediately after construction at approximately 20%. Except for the changes made in the mix designs, the sections were paved following common construction practices for OGFC mixtures in Alabama. While a state-approved OGFC mix design was referenced when designing the three mixtures, it was not paved

on the Test Track, as previous in-service pavements on a nearby portion of Interstate 85 were considered the control for this experiment.

After 30 million ESALs of trafficking from 2012 through 2021, these test sections showed consistent roughness, and excellent rutting and cracking resistances. Compared to the three experimental OGFC mixtures, the state-approved OGFC mixture that was previously paved on Interstate-85 lasted less than 20 million ESALs. In addition, the 9.5 mm mixture in Section E9A exhibited a greater field permeability and lower rate of permeability degradation compared to the 12.5 mm mixes in Sections E9B and E10. Compared to Sections E9A and E10, Section E9B containing synthetic fiber showed no cracking distress after 30 million ESALs. Based on the field evaluation performance, adjustments made in the three modified OGFC mixtures including using smaller NMAS, synthetic fiber, and additional asphalt binder can potentially improve the long-term field performance of OGFC mixtures in Alabama.

20.3 Evaluation of BMD Mixture with High RAP and Anova^{TM} Asphalt Rejuvenator

One concern of high RAP mixtures is related to the recycled asphalt binder, as it is often oxidized and stiffer than the virgin binder used in the asphalt mixture. Increasing the RAP content may make the asphalt mixture stiffer and more susceptible to various modes of cracking.

To minimize the effect of oxidized asphalt binder on the quality of asphalt mixtures produced with high RAP contents, especially their resistance to cracking, several approaches have been evaluated over the years. One of these approaches is to use a rejuvenator to help achieve a desired performance grade (PG) of the total binder blend. In addition, the optimum contents of rejuvenator and virgin binder can be determined based on a balanced mix design (BMD) approach to improve overall mixture resistance to rutting and cracking. Based on this concept, the objective of this study was to determine the use of Cargill's Anova^{TM} asphalt rejuvenator in balancing cracking and rutting performance of high RAP mixtures within the BMD framework.

The control asphalt mixture had 30% RAP with no rejuvenator, and it was placed in the surface layer of Section N3A. The experimental asphalt mixture had 45% RAP with Anova asphalt rejuvenator and was paved in the surface layer of Section N3B. The same PG 64-22 binder was used in both mixtures. Sections N3A and N3B, each 100 feet long, were trafficked for 10 million ESALs from October 2018 through February 2021. Their field performance, including rutting, cracking, ride quality, and surface macrotexture, was monitored on a weekly basis. The experimental mixture was also produced without rejuvenator for laboratory testing only. The three plant-produced mixtures were tested using several performance tests, and the data were analyzed to assist the field evaluation at the Test Track.

Prior to Test Track construction, two asphalt mix designs were conducted following the Virginia Department of Transportation (VDOT) BMD provisional specification. The provisional BMD specification is comprised of three laboratory tests to evaluate asphalt mixture susceptibility to rutting, cracking, and raveling, including Asphalt Pavement Analyzer (APA) with a maximum rut depth of 8.0 mm after 8,000 cycles, Indirect Tensile Asphalt Cracking Test (IDEAL-CT) with a minimum CT_{index} of 70, and Cantabro abrasion test with a maximum mass loss of 7.5%.

The control (30% RAP) and experimental (45% RAP and Anova rejuvenator) mixtures were first designed based on VDOT's volumetric mix design criteria. Several dosages of Anova were tested to select the most appropriate one for the experimental mixture. The two volumetric mix designs for the control and experimental mixtures had the same binder content of 5.2% and showed similar APA rut depths and CT_{Index} results. Their APA rut depths met the VDOT maximum rut depth threshold of 8 mm, but their CT_{index} values did not meet the VDOT minimum CT_{Index} criterion of 70. To meet the VDOT minimum CT_{Index} threshold, the binder contents of the two volumetric mix designs were increased. The control mixture met the CT_{Index} requirement at a total binder content of 5.5% while the experimental mixture met the requirement at 5.8% total binder content with CT_{Index} and APA rut depth results being almost the same. Both mixtures met the VDOT maximum Cantabro loss threshold of 7.5%.

Both BMD mixtures were produced, placed, and compacted to achieve good in-place density (i.e., 96.2% for N3A and 96.8 for N3B) on the Test Track. Based on the laboratory performance test results of reheated plant mixtures, the control and experimental mixtures would have similar rutting and cracking resistance. The difference in cracking test results for the experimental mixtures produced with and without Anova showed the positive impact of Anova on the cracking resistance of the reheated plant mixtures. However, after critical aging for four hours at 135°C, which is representative of four to five years of field aging at the Test Track, the cracking test results of the three plant mixtures reduced significantly and were similar to each other.

Field performance data collected from Sections N3A and N3B on the NCAT Test Track showed similar performance for the two sections in terms of rutting, ride quality, and surface macrotexture. While there were some signs of near surface cracking initiation observed in the last week of truck trafficking in February 2021, they may disappear due to the hot summer at the Test Track. Thus, Sections N3A and N3B have performed well with no cracking reported in this research cycle.

Key takeaways from the research include the following:

- The BMD approach can be followed to design a high RAP mixture with rejuvenator for improving its resistance to cracking and raveling without causing a detrimental effect to its resistance to rutting.
- Both sections showed good and almost identical field rutting performance, which also agreed with the APA and HWTT results for the reheated plant-produced mixtures sampled during construction.
- Both sections exhibited good cracking performance in the 2018 research cycle. However, the laboratory cracking test results suggested a significant decrease in I-FIT, OT, and IDEAL-CT test results after critical aging, which is representative of four to five years of field aging at the Test Track. Thus, it is important to continue monitoring the cracking performance of these test sections in the future.
- The transition area of Section N3A was repaired due to an issue not related to the control mixture, affecting the ride quality measurement for Section N3A. Otherwise, both sections showed good ride quality and almost identical, consistent surface macrotexture measurements throughout the research cycle.

- When comparing the experimental mixtures produced with and without the rejuvenator, the effect of the rejuvenator on the cracking test results was more profound on the reheated plant-produced mixtures and less on the critically aged plant mixes.

In summary, Anova asphalt rejuvenator can be used to improve the cracking resistance of a high RAP mixture within the BMD framework without affecting the mixture's resistance to rutting. Sections N3A and N3B will be kept in place for traffic continuation in the next research cycle to allow for a thorough field performance evaluation.

20.4 Evaluation of High RAP Mixture with Delta S Rejuvenator

Several methods have been investigated to reduce the potential adverse effect of RAP binder on the field performance of asphalt mixtures. One method is to use rejuvenators to restore some rheological properties of oxidized asphalt binders in RAP mixtures. These rejuvenators can be petroleum-based or bio-based materials that have been formulated to restore the balance of maltenes that were lost or transformed to asphaltenes in the oxidized RAP binder.

One of the bio-based rejuvenators commercially available is Delta S, which was developed by the Warner Babcock Institute for Green Chemistry and later commercialized by Collaborative Aggregates, LLC for use in recycled asphalt mixtures. This bio-based rejuvenator was used to produce asphalt mixtures with high recycled contents that were placed in the surface layer of Section N7, and the test section has been trafficked for field performance evaluation on the NCAT Test Track since 2015. The control section for this experiment is Section N1, which has a similar pavement structure with a surface mixture containing 20% RAP.

The surface layer of Section N7 was originally built on August 6, 2015, using a 9.5 mm mixture with 20% RAP and 5% RAS. After 1.4 million ESALs, cracking in Section N7 was first noted on January 31, 2016. The original surface mixture later showed severe surface cracking and interlayer delamination caused by the incomplete interaction between Delta S and the recycled binder, especially in the RAS, leaving a higher proportion of Delta S in the virgin binder than originally intended.

Section N7 was rebuilt by removing all asphalt layers and repaving from the aggregate base up on May 12, 2016. The surface layer of the rebuilt section was paved using a 35% RAP surface mixture with only 5% Delta S. To give Delta S rejuvenator time to interact with the aged binder in the RAP, the mixture was stored in a silo for two hours before being transported to the Test Track.

At the end of the 2015 research cycle in December 2017, the two surface mixtures in Sections N1 and N7 showed good ride quality and rutting performance. The area of cracking observed in the surface mixture of Section N7 was approximately 21.3% while the area of cracking in Section N1 was recorded at 10.3%. The cracks in both sections were very tight (less than 1 mm opening) near-surface cracks.

Fleet operations for the 2018 research cycle started in October 2018. Cracking grew sharply in spring (around March and April) and fall (around October) seasons and gradually in other months. For Section N1, cracking was recorded at 11.5% in March 2020. It jumped to 37.4% in

April and then gradually increased up to 45.8% at the end of the research cycle in February 2021. For Section N7, cracking increased gradually in 2019 and reached 33.1% in February of 2020. While the cracks observed in Section N7 were low severity, the cracks became connected in some areas, and fines could be seen along some of the connected cracks. Field cores were then extracted from the areas with the connected cracks. The cracks found on the field cores appeared to develop from the bottom of Section N7 and propagate to the surface, affecting the performance of the surface layer in this study.

Delta Mist spray-on rejuvenator was applied to the distressed surface of Section N7 at a 0.08 GSY rate on February 21, 2020 to evaluate if the spray-on rejuvenator could help extend the life of asphalt pavements with bottom-up fatigue cracking. However, cracking progressed significantly the week after Delta Mist was applied. The surface layer was milled and inlaid in May 2020 at which cracking was recorded at 53.4%. The addition of Delta Mist presumably softened the distressed asphalt structure and accelerated the rate of failure.

Lessons learned from the research include the following:

- Delta S should not be used with southeastern post-consumer RAS without an adequate reaction time during production. Without an adequate reaction time with aged binder, Delta S may excessively soften the virgin binder, potentially leading to premature failures.
- The Texas overlay and Illinois flexibility index tests suggested similar cracking performance for the 35% RAP mix with Delta S and the control mix with 20% RAP. However, cracking appeared to progress slightly quicker for the 35% RAP mix with Delta S at the Test Track.
- Connected cracks were observed in some locations within Section N7, and the cores extracted from these areas showed these cracks initiated from the bottom layer and propagated to the top, affecting the cracking performance of the 35% RAP mix with Delta S.
- A spray-on rejuvenator is intended to remedy near surface distresses supported by a sound pavement structure. Thus, applying the Delta Mist spray-on rejuvenator to Section N7, when distresses had propagated from the bottom to the asphalt surface, accelerated failure.
- The average rut depths measured in Section N7 were below 5.0 mm, indicating good rutting performance prior to the bottom-up cracking failure. Section N7 also showed good ride quality (IRI) and similar increasing trends in macrotexture compared to Section N1.

20.5 Florida DOT Increased RAP Study

The purpose of this study was to determine if increased levels of RAP above 20% could be used in mixtures containing polymer-modified PG 76-22 binder without a loss in performance. The use of a polymer-modified softer binder, PG 64-28, was also evaluated in one of the two sections with 30% RAP.

To evaluate their options under consideration, FDOT sponsored four subsections that were resurfaced with approximately two inches of four FC-12.5 Superpave mixtures. The four surface

mixtures were designed with a design compaction effort (N_{des}) of 100 gyrations. The main differences between these mixtures was the amount of RAP used and base binder's performance grade (PG 64-28 and PG 58-28). The quality control data showed 20.0% RAP for E7A mix, 23.9% RAP for E7B, 28.9% RAP for E8A, and the same PG 76-22 polymer-modified binder was used in the three mixtures. The E8B surface mix had 28.8% RAP, similar to the E8A mix, but had a softer polymer-modified PG 64-28 binder.

The four subsections were trafficked for two years to evaluate their field performance. In addition, laboratory testing was conducted on plant mix and asphalt binder to determine if additional testing can be specified during mix design to evaluate the rutting and cracking performance of FC-12.5 Superpave mixtures with more than 20% RAP. Load application was extended for one more cycle to complete 20 million equivalent single axle loads (ESALs) to achieve the level of damage suitable for comparisons and statistical analyses.

All sections showed slight variations in IRI values from the beginning up to 10 million ESALs, and after this point three sections grouped at a similar IRI level (100 to 125 in/mi), while one section (E8B) showed a small increase at the beginning of the second cycle and stayed constant until the end of trafficking. On the other hand, a small steady increase in the mean texture depth was observed after 5 million ESALs. Almost no rutting was reported between 0 and 18 million ESALs with rut depths below 2 mm. After 18 million ESALs, a sharp increase in rutting was measured in all sections. However, all field sections had less than ¼" total rutting after 20 million ESALs of traffic. A change in the measuring equipment was perform after 18 million ESALs, which may be the cause of the elevated results at the end of the cycle.

The 25% RAP, PG 76-22 mixture was the first to crack in the field (E7B). However, cracking after 10 million ESALs was the highest for the 20% RAP, PG 76-22 mixture (E7A) and the lowest cracking was reported for the 30% RAP, PG 76-22 mixture (E8A), which also was the last mix to crack. At the end of the study, Section E7A showed 19.3% cracking followed by Section E7B with 19.2% cracking. Cracking severity stayed low until the end of the study for Sections E8A and E8B. It was observed that after 5 million ESALs, cracks did not change much in length but increased in severity for Sections E7A and E7B to the point of being classified as medium severity cracks. At the end of trafficking, cracking was classified as low severity for all sections.

Each section had roadway core samples taken from the wheel paths every three months during the first 10 million ESALs and one or two samples taken during the second cycle. Density tended to increase over time during the first cycle and reached a maximum density near the end of the cycle. This was expected due to additional consolidation under traffic loading. On all the sections but E8B, a decrease in density was observed during traffic loading of the second cycle. This could be due to cracking and loss of fines/binder in the wheel paths, which was seen by the steady increase in texture. No correlations between field performance measurements and density were obtained. However, it can be seen that Section E7B, with the lowest (91.6% of Gmm) initial density, had the most cracking of all four sections at 20 million ESALs.

The amount and variability of in-place cracking prior to construction could also be considered a confounding factor. Section E7A had the lowest cracking extension but at the end of the study it was one of the two sections with the highest cracking percent. On the other hand, section E8B

was significantly damaged with extensive fatigue cracking, but at the end of the study this section showed the lowest cracking percent.

Cracking maps developed prior to construction and after trafficking were compared to help stablish the type of crack: reflective or new. For Section E7A, the majority of cracking seems to be newly developed and not reflective cracking since there are only a few cracks that can be matched. For the remaining sections, these maps do not provide enough evidence to conclude that cracking can be categorized as reflective. For Section E7B, there were small differences in the location of the cracks on both longitudinal and transverse directions, but overall cracking shapes and patterns matched well enough to be considered reflective cracking. This is the only case where reflective cracking was identified.

The results of this study support the following conclusions.

- Field cracking did not follow the expected trend with regards to RAP content. Sections E7A and E7B with the 20 and 25% RAP, respectively, showed the highest amount of cracking compared to the other sections with 30% RAP.
- The use of a softer modified binder did not show significant differences in field performance (Section E8B with a softer binder compared to E8A).
- After 20 million ESALs of traffic, the percentage of field cracking showed good correlation with Cantabro loss and fair correlation with Energy Ratio.
- After visual inspection of the crack maps, it seems that a great number of measured cracks for these sections can be characterized as reflective for Section E7B. There is not enough evidence to conclude if the measured cracks are reflective for the remaining sections.
- After 20 million ESALs of traffic, field performance for these sections was good overall in terms of roughness (relatively constant through the study and below 125 in/mi) and permanent deformation (below 5 mm).

Increasing the amount of RAP in mixtures containing PG 76-22 binder responsibly has merit. There may be some durability issues in surface mixtures with higher amounts of RAP and PG 76-22 binder. The use of softer polymer modified binders when using higher levels of RAP needs to be studied further for Florida conditions but shows promise for increased levels of RAP.

The results of this study along with other research has already resulted in a specification change allowing increased amounts of RAP in mixtures containing PG 76-22 binder below the surface.

20.6 Florida DOT Density Study

The objective of this experiment was to evaluate the effect of density level on pavement performance. A secondary objective of this work was to characterize the mixtures' properties and performance in the laboratory utilizing the same density level achieved in the field. To complete this research, one asphalt mixture containing 20% reclaimed asphalt pavement (RAP) and a polymer modified binder was placed and compacted in four 100-foot test strips in Sections E5 and E6 during the 2018 reconstruction of the NCAT Test Track.

Unless otherwise specified, laboratory performance tests for this study were performed on samples made from re-heated plant-produced mix. Performance testing samples were

compacted to the following density targets: 6.5% air voids for E5A, 8.0% air voids for E5B, 12.0% air voids for E6A, and 10.0% air voids for E6B. Target air voids for laboratory specimens after all necessary saw trimming was ±0.5%. The mixtures were evaluated for cracking potential, rutting potential, and durability using seven different tests: energy ratio, Illinois Flexibility Index Test (I-FIT), dynamic modulus test (E*), Indirect Tensile Asphalt Cracking Test (IDEAL-CT), Cantabro Mass Loss, Hamburg Wheel Tracking Test (HWTT), and high-temperature indirect tensile (HT-IDT).

All mixtures had energy ratios above 1.95 and $DCSE_f$ values higher than 0.75 kJ/m^3. Therefore, this mixture is expected to sustain over one million equivalent single axle loads (ESALs) per year at the four air void levels studied in this project. All mixtures had FI values below the preliminary Illinois criterion, but significant differences were observed. Section E6B-1 with 10.1% air voids was statistically the top performer, followed by sections E6A-1 and E5A-1 and lastly, as bottom performer, section E5B-1 with 8.1% air voids. Air voids content increased as the CT_{index} increased. Statistical analysis indicated that the top performer was Section E6A-1 with 11.9% air voids and the bottom performer was Section E5A-1 with 6.3% air voids. However, no statistical differences between Sections E6A-1 and E6B-1 or between Sections E6B-1 and E5B-1 were obtained. Cantabro test results indicated that the mass loss of the mixture compacted for Section E6A-1 was statistically different (higher) from the rest of the sections. On the other hand, mass loss of Section E5A-1 was statistically different from Sections E6B-1 and the N_{des} sample. Section E5B-1 showed the lowest mass loss of all sections. Other than these results, there is no evidence of difference between other sets of sections. The mixtures did not show any signs of stripping; therefore, it is not expected that any of the mixtures will be susceptible to moisture damage. Additionally, all four mixtures showed good resistance to rutting, as 12.5 mm is a common threshold for this test. As expected, an increase in rutting was obtained with an increase in air voids. A good correlation between HT-IDT strength results and rut depths measured with the Hamburg wheel-tracking device was obtained.

Field performance evaluations for roughness (International Roughness Index, IRI), mean texture depth (MTD), rutting (rut depth), and cracking (expressed as a percentage of the lane) are included for all sections from 0 to 10 million ESALs of traffic (as a function of millions of ESALs). Most sections showed slight variations in IRI values from the beginning, but this value remained almost constant in all cases. On the other hand, a small steady increase in mean texture depth was observed through 4 million ESALs. After that, texture has remained almost constant in all cases. Almost no rutting was reported before 9 million ESALs with rut depths below 2.0 mm. At the end of the cycle, a significant increase in rutting was measured. However, rut depths for all sections were below 5.0 mm (¼ inches) at the conclusion of 10 million ESALs of traffic. Despite the low density and potential high permeability of Section E6A, no evidence of moisture damage such as weathering or raveling were found after 10 million ESALs of trafficking and 2.5 years in place. Section E6A, with the lowest overall density, was the first to crack. Section E5A, with the highest overall density, was the last one to crack at around 9 million ESALs. All of the quantified cracks in these sections were low severity cracks at the end of trafficking. Total cracking in all sections was less than 5% of the lane after 10 million ESALs of traffic.
The results of this study support the following conclusions.

- Laboratory cracking test results did not exhibit expected trends in terms of density or air voids. However, a reversed trend for the I-FIT and IDEAL-CT tests with respect to density was expected based on past experience. There was no consensus among parameters to define a top performer.
- All mixtures, regardless of density level, are expected to sustain over one million equivalent single axle loads (ESALs) per year based on Energy Ratio criteria.
- Mixtures were not susceptible to rutting in the laboratory regardless of the density levels used in this study based on HWTT results. No evidence of moisture damage was observed in the HWTT. This agrees with the observations of minimal rutting and no moisture damage seen in the field through the first cycle of traffic for these sections.
- Section E5A had dynamic moduli significantly higher than the rest of the sections at all tested temperatures and frequencies. That significant separation from the lower density mixtures was also reflected in the HWTT and HT-IDT rutting test results.
- At the end of trafficking, field performance was good with cracking at less than 5% of the lane in each section with no changes in roughness, little permanent deformation, and no significant changes in texture.
- At the end of trafficking, observed cracking in the test sections was classified as low severity.

An additional round of trafficking will be needed to fully determine the effects of density on performance. This was expected and is consistent with other recent studies FDOT has funded at the NCAT Test Track when evaluating cracking performance. The lowest density section has begun exhibiting cracking.

FDOT is considering revisions to its current density specification for both the minimum allowable density and the target density. Once this study is complete, the data will be used to refine their specifications accordingly.

20.7 Mississippi DOT Stabilized Foundation Pavement

The Mississippi DOT (MDOT) primarily constructs semi-rigid pavements that often include both a cement or lime stabilized subgrade layer and a cement stabilized material (CSM) base layer. When MDOT began developing a plan to locally calibrate the performance models in the Mechanistic-Empirical Pavement Design Guide (MEPDG), neither the damage nor distress transfer functions related to this pavement type had been calibrated at the national level. Therefore, there was a need to build a section at the Test Track that would reasonably replicate conditions in Mississippi to provide Level 1 inputs with well documented structural and performance data sets to enable future design and analysis of these pavement types using the MEPDG. To that end, MDOT sponsored Section S2, which was constructed for the 2018 research cycle.

The construction of MDOT's section began by excavating approximately 5.5 ft of existing Test Track materials from Section S2. Soil classified as AASHTO A-6 (20) was imported from Mississippi and placed in eight lifts totaling approximately 56 inches. The top 6 inches of the soil were treated and mixed in place with dry hydrated lime, now called the lime treated soil (LTS) layer. Several weeks later, a silty-sand base material, also imported from MS and classified as

AASHTO A2-4, was placed on top of the lime-stabilized soil. This material was treated and mixed in place with cement and was allowed to cure for several more weeks and is now called the cement treated base (CTB) layer. Once the LTS and CTB layers were sufficiently cured, paving of the asphalt layers began. Four Superpave lifts were placed achieving a total asphalt concrete (AC) depth of 9.25". During construction, earth pressure cells, asphalt strain gauges, and temperature probes were installed to provide mechanistic response and environmental condition data during the two years of trafficking.

The surface performance of the stabilized foundation pavement has been excellent. Total rutting after 10 million ESALs was less than 0.15", no cracking was observed at the surface, and smoothness did not change appreciably over time. Structural health monitoring through frequent falling weight deflectometer testing and backcalculation, stress measurements, and strain measurements show no significant changes over time indicating good structural health.

Measured vertical stresses in the section under truck loading were as-expected with stress decreasing with depth and increasing exponentially with temperature of the asphalt concrete. Stresses deeper in the structure were less affected by temperature.

Strain measurements made at the bottom of the AC were very low (less than 100 microstrain in tension), which was expected given the thickness of the AC resting on the stabilized foundation. The very low tensile strain levels suggest that bottom-up fatigue cracking of the AC should not occur in this section. However, a surprising trend was observed where the tensile strain decreased with increasing temperature, which is opposite of more conventional flexible pavements having unstabilized foundation layers. A critical AC temperature of 75^{o}F was found where the mode changes from tension to compression. Below 75^{o}F, the primary mode is tensile while above 75^{o}F the bottom of the AC experiences compression. Simulations using the customized MASTIC software that follows layered elastic theory confirmed the measured pavement responses and identified another critical zone at the mid-AC depth where tensile strains could reach a peak level. Repeated tension at this depth could lead to middle-up cracking. Further trafficking of the section should be conducted to evaluate this hypothesis.

An in-depth investigation determined that FWD testing on flexible pavements with stabilized foundations may yield deflection basins so small that they prevent obtaining reasonable backcalculated moduli. Eliminating deflection basins where this occurred greatly improved the backcalculation results and is recommended for further backcalculation activities. Furthermore, it is recommended that additional heavier impact loading be added to the FWD testing sequence for S2. Currently, testing is conducted at 6-, 9- and 12-kip loading. Adding 16 kip loading to the sequence could provide more deflection basins that provide reasonable backcalculated moduli. The optimal cross-section for backcalculation was found to be AC over CTB over LTS over MS Subgrade with the AC/CTB interface fully bonded and the other interfaces with a nearly full-slip condition. This cross section yielded reasonable results, as verified by laboratory testing, and would produce the strain inversion phenomenon observed in both measurement and simulation.

To further investigate and validate the findings from S2, MDOT is constructing an instrumented test section in Mississippi on State Route 76 that will include asphalt strain gauges located at two intermediate depths within the AC. These measurements will help confirm the theoretical

findings of strain reversal at intermediate depths during hot weather months and investigate the occurrence of mid-level AC cracking in this type of pavement structure. It is anticipated that the findings may result in changes to the approach for designing intermediate lift mixes to consider crack-resistance in these layers.

While the S.R. 76 section is similar to S2, a key difference is that S2 included a lime stabilized subgrade while S.R. 76 includes a cement stabilized subgrade. Similar to S2, S.R. 76 will provide long-term in-situ modulus of both the cement stabilized subgrade and cement stabilized base layers to evaluate current design approaches recommended in the MEPDG. As with S2, this section will be monitored until it requires mill and fill, AC overlay, or other rehabilitation.

20.8 Mississippi and Tennessee Spray on Rejuvenator Experiment

As part of the 2018 Test Track research cycle at NCAT, the Mississippi and Tennessee Departments of Transportation both sponsored spray-on rejuvenator experiments. The spray-on rejuvenator products were applied on existing asphalt pavement surfaces alone or in combination with emulsified asphalt binders and other materials (e.g., polymers) to produce rejuvenating fog seals. The objective of the study was to evaluate, over time, the field performance of four spray-on rejuvenator products commercially available in the United States, including their short- and long-term effectiveness in renewing asphalt pavement surfaces and their effects on surface friction after application.

For Mississippi DOT, the motivation for sponsoring the experiment was to verify how spray-on rejuvenator products perform in the field and how these products can be evaluated in the laboratory, since the number of products being market to the agency has increased over the years. For Tennessee DOT, the motivation for sponsoring the experiment was to evaluate the effectiveness of these products, since most of the data available for the agency was provided by the products' suppliers. Furthermore, the agency expressed safety concerns regarding the potential friction reduction that can occur once these spray-on rejuvenators are applied over a pavement surface.

Section S3, sponsored by Mississippi DOT, was divided into two subsections: one treated with a plant-based topical rejuvenating seal (product S3-A), and the other treated with a proprietary age-regenerating surface treatment (product S3-B). Section S3 was a dense-graded mix with sand and gravel containing 25% RAP and an asphalt content of 6.8%, placed in 2012. The asphalt binder used in the design was a neat binder with PG 67-22. Section S4, sponsored by Tennessee DOT, was also divided into two subsections, with one subsection treated with CMS-1PF e-Fog (product SA-A) and the other treated with Reclamite® (product S4-B), both products from Ergon. Section S4 was a dense-graded mix with sand and limestone containing 15% fine RAP and an asphalt content of 6.2%, placed in 2015. The asphalt binder used in the design was a neat binder with PG 67-22.

The rejuvenating capability of each spray-on rejuvenator product was assessed considering rheological parameters and surface friction measurements. A modification of the Federal Aviation Administration's procedure P-632 (Bituminous Pavement Rejuvenation) was used to evaluate the rheological properties of binders extracted and recovered from field cores at several time intervals after application of the four spray-on rejuvenator products (i.e., 1 month,

6 months, 12 months, 18 months, and 24 months). Pavement surface friction characteristics collected with the dynamic friction tester (DFT) before and after the application of each treatment were also used in the evaluation process.

The NCAT field study has shown that the restoration capacity of a spray-on rejuvenating product can be separated into early rejuvenation and late rejuvenation. During early rejuvenation, the restoration capacity increases rapidly as a result of the decrease in asphalt binder stiffness but then begins to slowly decrease with oxidative aging as a result of the embrittlement of the binder (late rejuvenation). Moreover, during late rejuvenation, the restoration capacity is product-dependent and can only be fully captured after long-term aging. Therefore, the one-month (four-week) aging time proposed in the FAA P-632 procedure can be misleading for assessment of a spray-on rejuvenator product's long-term effectiveness. The rheological evaluation of asphalt binders extracted and recovered from field cores have shown that 18 months of field aging is required to differentiate among products and to observe a finer indication of a product's effectiveness in most cases.

Disregarding experimental error and the variability inherited by the extraction and recovery process of the asphalt binders obtained from field cores, the overall trend when considering complex modulus (|G*|) at 60°C and 10 rad/s (the evaluation parameter proposed in the FAA P-632 procedure) is that the maximum rejuvenating capability of the applied spray-on rejuvenator products was achieved between 6 and 12 months of treatment application. However, after 24 months of the application of the spray-on rejuvenator products on Sections S3 and S4, the asphalt binder properties of the treated sections are still improved in comparison to the control sections. For example, |G*| aging index calculated at 10°C and 10 rad/s (representing lower temperatures or higher traffic speed) and at 50°C and 0.1 rad/s (representing higher temperatures or lower traffic speed), indicated that the stiffness of the binders extracted from the treated sections remained below the stiffness of the control binders. This improvement in stiffness was found as dependent of the spray-on chemical composition (i.e., product type), and was influenced by the characteristics of the asphalt material present in the surface of each section as well as the construction time of each section.

The field experiment has indicated that the coefficient of friction of the existing pavement surface should be measured before and after the application of the spray-on rejuvenators to ensure safety. Depending on the characteristics of each product (i.e., product type, application rate, residual, dilution rate, and residual application rate) as well as the characteristics of the control sections, the observed decrease in friction between pretreatment and 72 to 96 hours of treatment application varied from 3.7% to 66.6%. The recovery in friction value to either equal or higher than the control sections was observed after two weeks or 18 months of application of the spray-on rejuvenator products. The long-term friction test results indicated that the four applied products did not show adverse effects on the friction of the pavement when comparing with the friction of the control sections. Surface cracking data after 10.0 million ESALs of traffic (2018-2021 research cycle) indicated that, after treatment with the spray-on rejuvenator products, Section S3 (total of ≈30.0 million ESALs since 2015) and Section S4 (total of ≈20.0 million ESALs since 2015) were far from exceeding the maximum lane area cracked limit of 20%.

After reviewing the results of the experiment, Mississippi and Tennessee expressed their contentment to the fact that the evaluated spray-on rejuvenator products can be effective for restoring the asphalt binder properties of a treated pavement surface. Furthermore, Tennessee DOT recognized that even though these products can briefly affect the friction characteristics of the pavement after application, they can still be utilized if some precautions are maintained short-term.

With regards to the implementation of this type of pavement preservation and rejuvenation, Mississippi DOT is not ready to implement yet, but will continue to consider how spray-on rejuvenators may fit into its highway maintenance program. Tennessee DOT is currently looking for options to grow the use of spray-on rejuvenators as preventive maintenance treatments.

20.9 Oklahoma Balanced Mix Design

The Oklahoma Department of Transportation (ODOT) began moving forward with the development and implementation of balanced mix design (BMD) in 2017. In the 2018 research cycle, ODOT sponsored a BMD surface experiment consisting of Sections N9 and S1 for evaluation on the NCAT Test Track. The objective of this experiment was to support ODOT with the implementation of mixture performance testing and criteria for BMD. Both sections were built as mill-and-inlays using BMD mixes designed with the Illinois Flexibility Index Test (I-FIT) and Hamburg Wheel Tracking Test (HWTT). Section N9 was placed as a 1.5-inch layer while S1 was placed in two layers with a total thickness of 5.0 inches.

For all three mixes of Sections N9 and S1, the mix design samples passed ODOT's performance test requirements, which indicated that the mixes had good rutting and cracking resistance. For construction of the test sections, the mixes were produced with the same aggregates and RAP using virgin binders with the same performance grades but from different sources as those used in mix design. Quality control testing of the production samples showed that the N9 mix failed ODOT's production tolerance for air voids and voids in mineral aggregate (VMA), while the S1 surface and base mixes met ODOT's specification requirements.

Performance testing of the production samples showed that all three mixes failed ODOT's performance test criteria for mix design approval and thus, fell outside the outside the "sweet zone" of the BMD performance diagram. The N9 mix failed HWTT due to a stripping failure while the S1 surface and base mixes failed I-FIT. Additional analysis of the HWTT results for the N9 production sample as well as the supplementary rutting tests indicated that the mix had satisfactory rutting resistance and was not expected to have a rutting failure on the Test Track. Additional testing of the N9 mix at NCAT indicated that the significant reduction in HWTT results from mix design to production was mainly due to the between-lab variability associated with sample preparation and testing as well as changes associated with plant production, while changing binder source did not have a significant impact on the HWTT results.

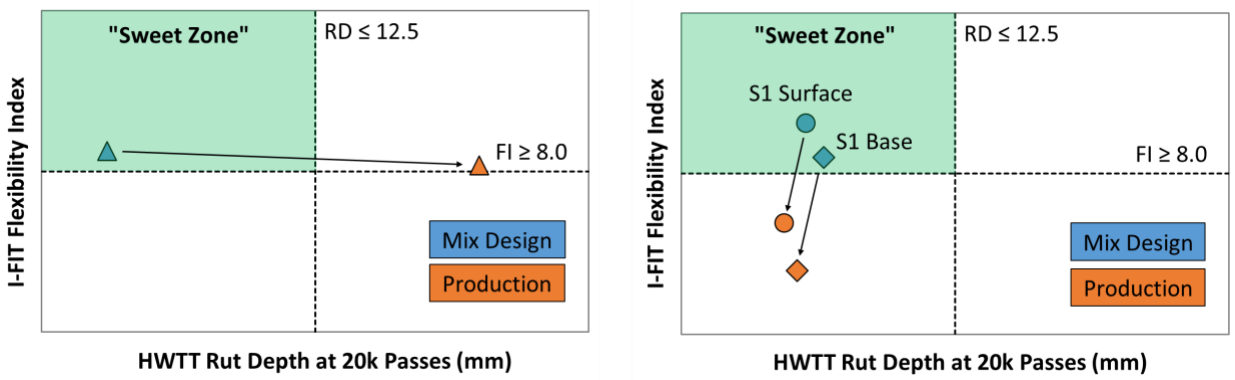

Figure 1. BMD Performance Diagram of N9 (left) and S1 (right) Mixes from Mix Design and Production Testing

For the S1 surface and base mixes, additional I-FIT testing indicated that the different flexibility index results between mix design and production were mainly due to changes in the mix associated with plant production and possibly different mix aging conditions of mix design and production samples. Between-lab variability and changing binder source, on the other hand, did not seem to significantly affect the results.

Critical aging was found to have a significant impact on I-FIT, Indirect Tensile Asphalt Cracking Test (IDEAL-CT), and Cantabro test results for the N9, S1 surface, and S2 base mixes. The mixes after critical aging were more susceptible to cracking and durability related distresses. Furthermore, the S1 base binder was found to be most susceptible to oxidative aging, followed by the N9 mix and the S1 surface mix, respectively. Strong linear correlations were observed between the results of the three mixture cracking tests, which highlighted the potential of using the IDEAL-CT and Cantabro test as surrogate performance tests to I-FIT for BMD production testing. These correlations, however, should be interpreted with caution because they were based on a limited number of mixes and aging conditions.

Both sections N9 and S1 performed very well with minimal rutting and cracking after 10 million ESALs and exhibited steady smoothness and texture results over the three-year research cycle. The skid number results showed slight reductions over time, but they were well above the general threshold from a safety perspective.

Key takeaways of the experiment are:

- Despite the mix design efforts in meeting the performance test criteria, BMD mixes could become “unbalanced” in terms of rutting and cracking resistance during production. Therefore, it is recommended that mixture performance tests be conducted for both mix design approval and production acceptance to ensure good field performance of BMD mixes.
- Between-lab variability has a significant impact on performance test results, which highlights the importance of conducting statewide round robin studies and hands-on training for specimen fabrication and mixture performance testing for the implementation of BMD.

- An asphalt mix could fail HWTT due to rutting failure, stripping failure, or both, which unfortunately cannot be discriminated using the traditional HWTT data analysis approach. Therefore, it is recommended that an alternative data analysis approach based on the corrected rut depth parameter be used to separate the rut depth in HWTT due to permanent deformation of the mix from the stripping of asphalt binder from the aggregate.
- Mixture volumetric properties do not necessarily correlate with the field performance data on the Test Track. Therefore, it is recommended that some of the volumetric requirements for mix design approval and production acceptance for BMD mixes be relaxed provided that the performance test requirements can be met.

20.10 Proactive Pavement Preservation

State and local agencies are constantly looking for ways to maintain or improve their pavement network condition at the lowest annual cost per lane mile. Micro surfacing is a popular pavement preservation treatment that is capable of addressing minor surface defects, protecting the pavement structure from moisture, and extending overall pavement life when applied to structurally sound pavements. The objective of this study was to evaluate the field performance of a micro surfacing test section subjected to full-scale accelerated pavement testing. The treatment was placed on half of Section N6 on the NCAT Test Track and its performance was compared to the remaining untreated section.

As with other preservation treatments, performance of treated sections depends on many factors including climatic conditions, traffic volumes, existing pavement condition, material quality, mixture design, and construction quality. Estimates for pavement life extension typically range from three to seven years; however, the criteria for defining performance varies among sources. Service life extension is usually estimated based on rutting or roughness; nonetheless, micro surfacing has also shown to slow the progress of reflective cracking. Micro surfacing has been successful on high-volume roads across the United States, where good performance has been achieved on Interstate routes subjected to heavy traffic.

Section N6, originally constructed in 2009, was identified as a suitable candidate for pavement preservation. The pavement had started to show signs of deterioration (mainly rutting and weathering) after receiving over 17.5 million equivalent single axle loads (ESALs) in 2014 but was in overall good condition. The 200-ft section was split into two subsections, leaving one untreated and placing a Type II micro surface on the other. This provided an opportunity for direct comparison and assessment of treatment benefits. The Type II micro surfacing treatment was designed following the recommendations outlined in International Slurry Surfacing Association A143 guidelines and consisted of a granite aggregate source, Portland cement as the mineral filler, and a CSS-1HP grade asphalt emulsion. The mix design yielded an optimum emulsion content of 12% and a 1% cement content.

Following treatment application, traffic operations were resumed and carried out through the end of Phase VII in February 2021. Since its original construction in 2009, the pavement section was subjected to a total of 39.1 million ESALs. The treated surface portion of the section accumulated 21.6 million ESALs since its application in 2014. It should be noted that the untreated portion did not survive until the end of the research cycle and had to be milled and

inlaid in May 2020 due to the amount and severity of distress observed, including rutting and depressions that compromised the safety of traffic operations.

Table 1 provides a comparison of the two subsections at two points in time that clearly highlight the effect of pavement preservation: prior to micro surfacing application and when rehabilitation was required in the control section. Figure 1 shows an overview of the two subsections in 2020.

Table 1. Pavement Condition

Indicator	April 2014 (Pre-treatment)		May 2020 (Rehabilitation Required for Control Section)			
	Section Average	MAP-21 Condition Category	Micro Surface Subsection	Condition Category	Control Subsection	MAP-21 Condition Category
Cracking, %	1.8	Good	18.9	Fair	31.9	Poor
Rut depth, in	0.33	Fair	0.14	Good	0.41	Poor
IRI, in/mi	62.6	Good	90.9	Good	105.5	Fair
MTD, mm	0.66	Not Applicable	0.66	Not Applicable	1.14	Not Applicable
Skid number	43.2	Not Applicable	43.5	Not Applicable	49.4	Not Applicable

(a) (b)

Figure 1. Overview of a) Control and b) Micro Surfacing Test Sections

Micro surfacing application was effective in restoring the pavement surface and correcting rutting while maintaining safe frictional characteristics. The treatment was able to withstand heavy traffic loading without wearing off, contributing to extending the life of the existing pavement. These observations agree with NCAT's research findings from full-scale test sections that are located in open roadways and subjected to live traffic. Long-term monitoring of these off-track sections has shown that micro surfacing is capable of improving cracking performance over time, correcting minor rutting and maintaining ride quality and pavement integrity.

While it is evident that performing proactive pavement preservation yields better results than delaying treatment, the cost-effectiveness of this approach needs to be determined on a case-by-case basis as unit costs vary significantly among agencies.

20.11 South Carolina Full-Depth Rapid Rebuild

South Carolina DOT sponsored a full-depth, thick-lift, rapid rebuild section in the 2018 research cycle to further develop a rapid construction method that utilizes reduced lane closure lengths on major highways and primary routes resulting in less traffic disruption. They were also interested in developing a durable, easy-to-compact pavement that could be used as a riding surface that has less risk for failures at individual lift interfaces compared to conventional rebuilds. Developing knowledge of how the deep sections will respond to heavy loading on the Test Track in a short period of time was also of high interest.

The section (S9) was constructed in August 2018 to an asphalt concrete (AC) depth of 8.05" in a single lift on a prepared crushed granite aggregate base. The AC was a dense graded 12.5 mm NMAS mix with a PG 64-22 binder and 25% RAP. The target mix design air voids are usually around 2.5 to 3% for these mixes to make them easier to compact in the field. The AC was produced as a warm mix and mat temperatures were monitored during construction. Paving initiated at 10 AM and it was found that the section required nearly six hours to cool from 242^{o}F to 175^{o}F. Simulations of pavement cooling were conducted with MultiCool, which were not very accurate for such a thick lift, so caution should be exercised making future predictions with MultiCool. However, paving at more advantageous times of day (i.e., early evening or night) will significantly reduce to the cooling time to under two hours. This was confirmed both through simulation and measurements of a similar trial section placed at the Test Track.

Achieving density with an 8-inch lift was a non-issue. Density exceeding 95% of the theoretical maximum was accomplished with standard rollers and roller patterns. No specialized processes or equipment were needed. However, as-built smoothness may be an issue with thick-lift paving and certainly was with this section. The problem was rectified somewhat with diamond grinding. It is anticipated that paving crews, given more opportunities to pave thick-lifts, could greatly improve as-built smoothness. In practice, the SCDOT has found that having an additional lane to stage material transfer vehicles, trucks, and rollers is beneficial to minimize dips in the longitudinal pavement profile.

The thick-lift section exhibited excellent performance over the 10 million ESALs. Rutting was less than 0.25", very little cracking (likely top-down) developed, and smoothness did not change. Premature or excessive rutting, which was a potential liability for this construction technique, was not evident and should not be a problem provided that adequate compaction is achieved during construction. Further, Hamburg test results of the AC confirm that rutting of the mix should not be a problem in this experiment.

The thick-lift section behaved in much the same fashion as other conventional multi-lift sections. The expected influence of pavement temperature was evident in the measured pavement responses (i.e., stress and strain) and backcalculated AC moduli. The temperature-corrected data were remarkably consistent over time, indicating good structural health despite the small amount of cracking observed in the section.

Laboratory determination of AC dynamic modulus produced data consistent with backcalculated moduli. Either data set could be used for future mechanistic modeling of the test section. Cracking tests using the bending beam and cyclic fatigue tests produced vastly

different transfer functions, but both require calibration, as using the functions with measured tensile strain in the section at 68°F predicts relatively short fatigue life compared to the 10 million ESALs applied to the section with no observed bottom-up cracking. Additional trafficking and cracking development will be required for calibration. Depending on the specification applied, the Ideal CT may indicate that top-down cracking could be a problem. Since only minor cracking has been observed through 10 million ESALs, further monitoring will help determine an acceptable threshold.

One area not yet explored with this section is the possible advantage of single lift construction not having lift interfaces that could suffer slippage and loss of structural integrity. This feature is inherent to the method of construction and could help alleviate this type of distress in addition to providing for a more rapid rebuild of the cross-section.

SCDOT has used thick lift paving on the order of 4.5” to 6” of AC on several projects over the past few years. Project selection for this type of rapid rehabilitation involves looking for roads that can be reconstructed using thick lift paving in lieu of other rehabilitation methods that often take longer to construct and provide a reasonable cost, and in turn, provide an adequate pavement design. Through the first 10 million ESALs, the thick-lift section at the Test Track has shown their special mix design can be placed up to 8 inches and have excellent long-term performance, which means more projects can be considered for this type of rehabilitation.

20.12 Texas DOT Balanced Mix Design Experiment

The Texas Department of Transportation (TxDOT) is one of the leading agencies in the development and implementation of balanced mix design (BMD). In the 2018 research cycle, TxDOT sponsored a BMD surface experiment in Sections S10 and S11 on the NCAT Test Track to compare the field performance of asphalt mixes designed using a BMD approach (S10) versus the traditional volumetric approach (S11). Both sections were built as 2.5-inch mill-and-inlays over an existing asphalt pavement with approximately 15 to 20% cracked lane area to challenge the surface mixes.

The S10 and S11 mixes were designed by adjusting a TxDOT approved 12.5 mm SP-C surface mix design. Both mixes used the same PG 70-22 modified binder, fractionated reclaimed asphalt pavements (RAP), a blend of granite and dolomitic limestone, and had the same RAP binder replacement ratio of 20%. The major differences between the two mixes were the gradation and the resultant optimum binder content (OBC) with 4.0% design air voids. The S10 BMD mix had a slightly coarser gradation and significantly higher OBC and voids in mineral aggregate (VMA) than the S11 volumetric mix. Performance testing of the mix design samples showed that the S10 mix passed both TxDOT’s Overlay Test (OT) and Hamburg Wheel Tracking Test (HWTT) requirements while the S11 mix failed the OT due to lack of cracking resistance.

For construction, the mixes were produced with the same virgin binders, aggregates, and RAP as those in mix design. Performance testing of the production samples yielded highly consistent results as mix design samples. The S10 production mix passed both the OT and HWTT requirements and thus, was expected to have a good balance between rutting and cracking resistance. The S11 production mix passed HWTT but failed OT; as a result, it fell outside the “sweet zone” of the BMD performance diagram (Figure 1). Critical aging was found to have a

significant impact on the OT and Indirect Tensile Asphalt Cracking Test (IDEAL-CT) results for both S10 and S11 mixes. The mixes after critical aging were more susceptible to cracking possibly due to increased mix embrittlement and reduced relaxation properties. Nevertheless, the S10 BMD mix showed significantly better cracking resistance than the S11 volumetric mix after critical aging.

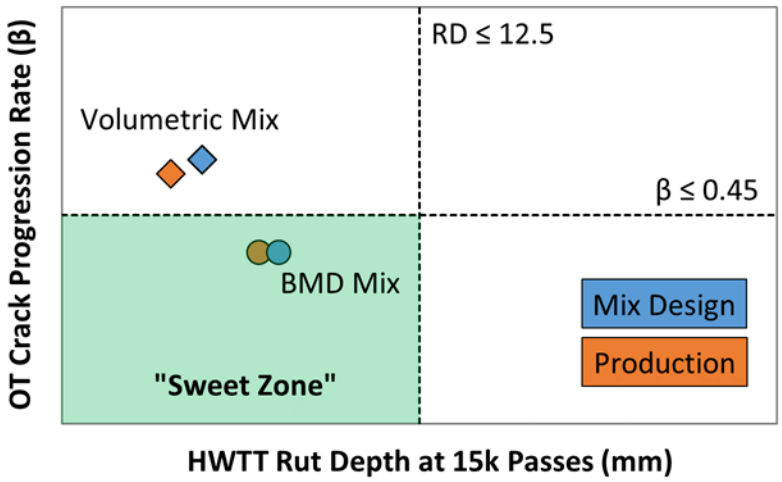

Figure 1. BMD Performance Diagram of S10 BMD and S11 Volumetric Mixes from Mix Design and Production Testing

Both sections performed well after 10 million ESALs. Section S10 exhibited more rutting but considerably less cracking than Section S11, which agreed with the BMD performance test results. The two sections showed similar smoothness and friction characteristics over the three-year research cycle. Section S10 exhibited higher mean texture depth than Section S11 after construction, but the difference was significantly reduced over time.

Key takeaways of the experiment are:

- BMD allows performance enhancement of asphalt mixtures over the traditional mix design approach based on volumetric analysis. By incorporating mixture performance test requirements, BMD can effectively identify and eliminate asphalt mixtures that meet the volumetric requirements but lack in adequate performance properties.
- Mixture performance test results from mix design and production testing are in good agreement with the field pavement of pavement test sections on the NCAT Test Track, which indicates that HWTT, OT, and IDEAL-CT are good candidate tests for mix design approval and production acceptance in BMD.
- BMD mixes have the potential to outperform traditional volumetric mixes in terms of field cracking performance despite the challenging underlying pavement condition.

20.13 Bio-Polymer Modified Asphalt Mixture

Polymers used in asphalt paving materials have been traditionally made from petroleum-based products, but they can now be made from bio-based feedstocks. A new bio-derived polymer has been produced from soybean oil at Iowa State University. The objective of this experiment was to evaluate the new bio-polymer in a field experiment on the NCAT Test Track.

In this study, the bio-polymer modified binder was blended at an asphalt terminal and delivered to East Alabama Paving's plant in Opelika, Alabama. The bio-polymer modified binder was used to produce an asphalt mixture that was then paved in the surface layer of Section W10 at the NCAT Test Track. This test section was compared with Section E5A, which was surfaced with a conventional styrene-butadiene-styrene (SBS) polymer modified mixture. The two surface mixtures were evaluated under the same heavy truck traffic loading conditions. In addition, samples of asphalt binder and loose mix were taken during construction for laboratory testing to assist the field performance evaluation.

The bio-polymer modified binder used in Section W10 was formulated to have a performance grade similar to that of the SBS polymer modified binder used in Section E5A. The true grade of the bio-polymer modified binder was 73.6 – 21.6 with $\Delta T_c = -3.0$ while the true grade of the conventional SBS modified binder was 76.3 – 24.7 with $\Delta T_c = -2.6$.

Dynamic Modulus test results showed that the bio-polymer modified mixture was stiffer than the SBS modified mixture across the majority of temperatures and frequencies tested. This observation was consistent with the other laboratory test results for rutting, cracking, and durability.

Both mixtures rutted less than 2 mm in the Hamburg test with no evidence of stripping, so neither mixture was expected to show significant rutting on the NCAT Test Track. Both the I-FIT and IDEAL-CT cracking tests (conducted at 25°C) showed the SBS modified mix to have better cracking resistance than the bio-polymer modified mixture. In addition, the DCT test for low temperature cracking resistance (conducted at -12°C) showed that the SBS modified mixture may have better low temperature cracking resistance than the bio-polymer modified mixture.

After 10 million ESALs of trafficking at the NCAT Test Track, both test sections have shown good field performance thus far. They show good rutting with final rut depths below 5.0 mm. No cracking was observed in Section W10 with the bio-polymer modified mixture while low severity cracks were recorded for 0.4% of lane area in Section E5A with the SBS modified mixture.

Key takeaways of the experiment are:

- The new bio-polymer can be used by itself or in combination with other modifiers to modify asphalt binders with performance grades that are similar to conventional polymer modified asphalt binders.
- While the laboratory test results suggested that the bio-polymer modified mixture was stiffer and less resistant to cracking, the field performance showed different results. After 10 million ESALs of trafficking at the NCAT Test Track, no cracking was observed for the bio-polymer modified mixture while low severity cracks were recorded for 0.4% of lane area for the SBS modified mixture. Both mixtures showed good rutting with final rut depths below 5.0 mm.

Both sections will be kept in place for another 10 million ESALs of continued trafficking in the 2021 Test Track research cycle, which will be important to evaluate the long-term performance of the bio-polymer modified asphalt mix against the conventional SBS modified asphalt mixture.

20.14 Long Term Performance of Cold Central Plant Recycled Asphalt Flexible Pavements

In 2012, the Virginia Department of Transportation initiated an experiment at the Test Track to evaluate Cold Central Plant Recycled (CCPR) asphalt pavements under three different scenarios: 4 inches of CCPR with a 4-inch overlay over aggregate base, 5 inches of CCPR with a 6-inch overlay over aggregate base, and 5 inches of CCPR with a 4-inch overlay over an 8-inch cement stabilized layer. Just a year prior, VDOT had constructed similar sections on Interstate-81, just outside of Staunton, Virginia. While early performance on I-81 was promising, VDOT wanted to investigate (1) how the sections would perform under heavy traffic loads, (2) understand the stress and strain distribution within the sections (I-81 was not instrumented) (3) see how long the pavement would perform under accelerated loading, and (4) identify the failure mechanism and rate to inform future maintenance and rehabilitation strategies.

After two test cycles (20 million ESALS) all three sections were performing exceptionally well. VDOT decided to continue trafficking on Section N4 (4" overlay on CCPR) and Section S12 (4" overlay on CCPR on cement stabilized layer) and discontinue trafficking on N3 (6" overlay on CCPR). This would allow VDOT to take both sections to the equivalent levels of trafficking to previous perpetual pavement sections to support the notion that the recycled sections are, in fact, performing as perpetual pavements. The comparative sections were N3-2003 and N4-2003, both of which were designed to have 9 inches of AC. N3-2003 used an unmodified asphalt binder, while N4-2003 used a polymer modified asphalt binder. Further, it was agreed that the thinner Section N4 would be the first to deteriorate if deterioration occurred. This occurrence would yield insights into failure mechanisms of CCPR in a high-traffic environment, allowing VDOT to know what to look for and project an expected rate of deterioration for pavement management planning purposes.

At the conclusion of the third test cycle, both N4 and S12 were performing well. The ride quality of the pavement remained steady throughout the cycle. Rutting was measured to generally stay below 0.3 inches, well below the 0.5" failure threshold used by the Test Track. Cracking is another area where the sections fared well, with Section S12 continuing to perform without any cracking. Section N4 experienced slight cracking after 29.6 million ESALs in the outside wheelpath. The cracking was primarily transverse to the lane of travel and was originally noticed through visual inspection after a rain event. After 29.9 million ESALs, high-resolution crack mapping images indicated that there was 0.1% of the wheelpath area cracked and 0.5% of the lane area cracked, indicating more cracking outside of the wheelpath than within. At the conclusion of the third test cycle, cracking was considered insignificant and there is currently no indication of the type of cracking (i.e., no pumping of fines, etc). With exception to the unknown cause of cracking (i.e., top down or bottom up) in Section N4, both sections track well in comparison to the 2003 perpetual pavement sections.

The structural characterization of the sections provided interesting insights into both the CCPR layer and the impact of the stabilized base. The sections were compared using the so-called Willis Limit for perpetual pavement design, which was based on the 2003 dense graded sections and expressed an upper bound cumulative strain distribution for conventional flexible pavements to prevent bottom-up fatigue cracking. Section S12 was below the Willis Limit, and therefore should not experience bottom-up fatigue cracking, indicating that it is likely

perpetual. Section N3, however, was above the Willis Limit and should have experienced bottom-up fatigue cracking by 20 million ESALs. The fact that N3 did not crack after 20 million ESALs and N4 lasted until 29.6 million ESALs indicates prolonged fatigue life and that CCPR materials may exhibit fundamentally different fatigue behavior. The falling weight deflectometer (FWD) was used to backcalculate the pavement moduli. Like the 2003 dense graded sections, Section S12 maintained a consistent AC/CCPR modulus over all three cycles, only fluctuating with changes in seasons. However, Section N4 experienced a decline in modulus over the third Test Track cycle, indicating pavement damage.

The economic benefit was computed for the recycled sections versus the 2003 dense-graded perpetual sections using VDOT's structural layer coefficients and recent statewide average unit costs (materials and placement) within four years of publication. By normalizing the data to cost (%) per square yard per structural number (SN) for all sections, it was found that the CCPR sections were 11% (N3), 18% (N4), and 31% (S12) less expensive than the 2003 perpetual dense graded sections. Also important are the sustainability implications. The 2003 dense graded sections did not contain any recycled material; however, in the CCPR sections, the SMA layer contained 11% RAP, intermediate layer contained 30% RAP, CCPR contained 97% RAP (2% was recycling agent and 1% cement), and FDR layer contained 96% recycled materials (4% portland cement). Overall, N3-6" AC contained 54% recycled material per inch when considering only the bound layers (i.e., not the aggregate base), N4-4" AC contained 62% recycled material per inch when considering only the bound layers, and S12-4" AC SB contained 76% recycled material.

The study found that all five sections exhibited excellent performance after applying 20 to 30 million ESALS, with Section N3 lasting longer (based on strain readings) than expected and Section S12 exhibiting perpetual behavior. This is an important finding when considering economic and sustainability implications.

For the 2021 test cycle, VDOT has decided to continue trafficking Section N4 so that the deterioration rate can be observed. This, along with data collection and forensic analysis at the conclusion of the test, will provide VDOT with insight on how CCPR materials fail, the rate at which they may fail, and a datapoint that can be used for mechanistic-empirical pavement design.

Because Section S12 is not expected to deteriorate, it will be decommissioned for a new experiment. After the conclusion of forensic investigations (trenching, coring, and materials testing), S12 will be milled and reconstructed. Care will be taken to mill out the CCPR layer independently. The stabilized layer will be completely removed and replaced with the typical test track subgrade. An aggregate base will then be placed, and a section identical to N4 will be placed with two major exceptions: the CCPR layer will be re-recycled CCPR from the original S12 section and only a 2" overlay will be placed on the surface. Once Section N4 reaches a terminal state, the same process will be repeated with a re-recycled CCPR layer, but a 4" overlay will be used to make the new N4 identical to the 2012-present N4. This will make the 2021-N4 a control for 2021-S12 and the thin overlay, as well as an experimental section to compare to 2012-N4 to understand the feasibility of re-recycling CCPR.

20.15 West Virginia Friction Study

Pavement friction is a critical factor in improving roadway safety, especially in wet weather. For asphalt pavements, surface friction (also called skid resistance) is affected primarily by the amount of traffic polishing at the tire-pavement interface, pavement surface macrotexture and microtexture, and the properties of coarse aggregates in the surface mixture. Although frictional aggregates are effective in enhancing pavement friction, material cost must also be considered in the selection of aggregates. From an economic perspective, locally available aggregates are preferred for producing asphalt mixtures. However, for regions that have a large amount of highly polishable aggregates but a limited amount of frictional aggregates, balancing friction performance and material cost is crucial. To maintain adequate friction and acceptable construction costs, U.S. state highway agencies typically limit the amount of highly polishable aggregates (e.g., dolomite) in asphalt surface mixtures. For example, West Virginia Division of Highways (WVDOH) requires that dolomite shall not exceed 50% of coarse aggregate in an asphalt surface mixture if the projected traffic is greater than 3.0 million equivalent single axle loads (ESALs). To reduce material costs, highway agencies always explore the feasibility of using more highly polishable aggregates in asphalt surface mixtures. Meanwhile, there is also a critical need for highway agencies to determine an appropriate threshold for the amount of highly polishable aggregates.

This study aimed to evaluate the feasibility of using more highly polishable aggregates (e.g., dolomite) in asphalt surface mixtures typically used by WVDOH. Asphalt slabs containing different percentages of dolomite coarse aggregates were fabricated in the laboratory and abraded by the NCAT three-wheel polishing device (TWPD). The dynamic friction tester (DFT) was used to measure the friction deterioration of these asphalt slabs. The results indicated that increasing dolomite content in asphalt surface mixtures resulted in a faster deterioration rate at the early polishing stage (i.e., 5,000 – 20,000 polishing cycles). In addition, asphalt surface mixtures containing more than 50% dolomite coarse aggregates had a terminal DFT friction coefficient measured at 20 km/h less than 0.30, which would significantly reduce roadway safety when using for asphalt pavements.

Two Test Track sections were built in 2018 that used 70% and 90% dolomite coarse aggregates in the asphalt surface. DFT and locked-wheel skid trailer (LWST) tests were conducted to determine the friction performance of these two sections and confirmed that replacing sandstone coarse aggregates by 70% and 90% dolomite aggregates resulted in asphalt surface mixtures with fairly low long-term skid resistance. These results validated why the WVDOH requires that dolomite shall not exceed 50% of coarse aggregate in asphalt surface mixture if the projected traffic volume is greater than 3.0 million equivalent single axle loads (ESALs).

Due to safety concern for drivers on the track, a shotblasting treatment was applied to enhance both the microtexture and macrotexture of the sections. After 2.3 million ESALs of traffic, both sections exhibited better friction performance, indicating that the shotblasting treatment was effective in improving the long-term friction performance of asphalt pavements. Meanwhile, through the pavement performance evaluation, the shotblasting treatment was found to have no detrimental impact on cracking, rutting, and surface roughness of asphalt pavements.